

AN INTEGRATED GEOLOGICAL, GEOCHEMICAL,  
ISOTOPIC AND GEOCHRONOLOGICAL STUDY ON THE  
AURIFEROUS SYSTEMS IN THE BOTWOOD BASIN  
AND ENVIRONS, CENTRAL NEWFOUNDLAND

CENTRE FOR NEWFOUNDLAND STUDIES

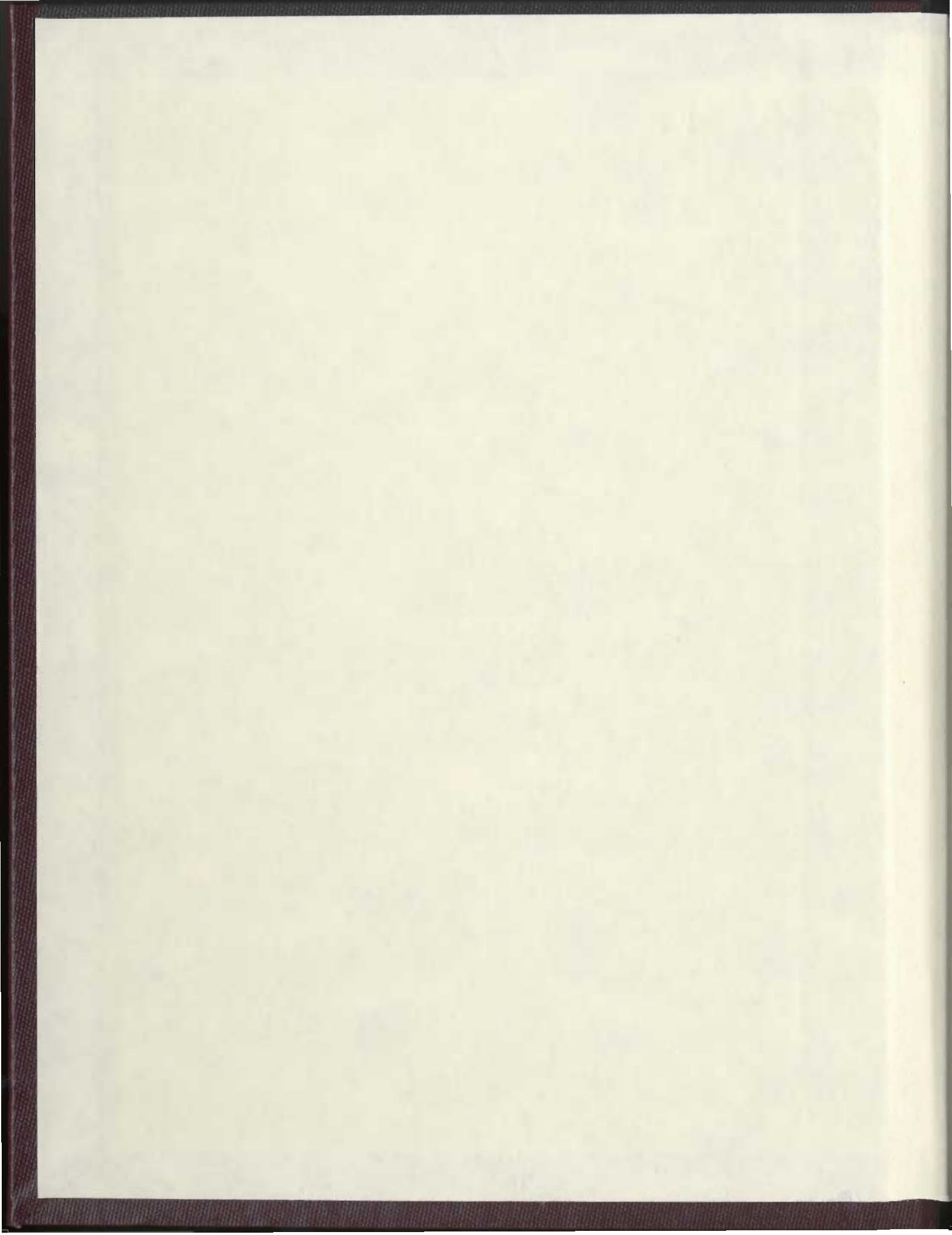
---

**TOTAL OF 10 PAGES ONLY  
MAY BE XEROXED**

(Without Author's Permission)

JACQUELINE MARY O'DRISCOLL









# Memorial

University of New Zealand

An integrated ecological, geomorphological, biological and  
geographical study of the upland ecosystems  
in the Southern Alps and surrounding  
regions, New Zealand

James M. O'Connell, B.Sc. (Hons.)

A thesis submitted to the School of Graduate  
Studies in partial fulfilment of the  
requirements for the degree of

Master of Science

Department of Earth Sciences  
Memorial University of New Zealand  
St John's, New Zealand  
April 2000











# Memorial

University of Newfoundland

**An integrated geological, geochemical, isotopic and  
geochronological study on the auriferous systems  
in the Botwood Basin and environs,  
central Newfoundland**

By:

Jacqueline Mary O' Driscoll, B.Sc. (Hons.)

*A thesis submitted to the school of Graduate  
Studies in partial fulfillment of the  
requirements for the degree of*

***Master of Science***

Department of Earth Sciences  
Memorial University of Newfoundland  
St. John's, Newfoundland  
April 2006





## Abstract



“What lies beneath?”

### Frontispiece

View looking east from Ten Mile Lake Resource Road

“The next best thing to knowing something is knowing where to find it”

-Samuel Johnson



## Abstract

The purpose of this project was to study and compare 20 gold occurrences from within the Botwood Basin and surrounding lithologies. The Botwood Basin is located within the eastern Dunnage Zone of central Newfoundland and encompasses a region comprised of Middle Paleozoic cover sequences deposited upon dominantly Ordovician rocks. The area has been subdivided into two tectonostratigraphic belts that are separated by a major fault (the Dog Bay Line), which has been defined as a major Silurian terrane boundary. The Indian Islands Belt to the southeast of the fault encompasses the deep to shallow marine Davidsville and Indian Islands groups. The Botwood Belt to the northwest of the fault includes the shallow marine to terrestrial Botwood and Badger groups. The large bimodal Mount Peyton Intrusive Suite (MPIS) intruded some of these units during the Late Silurian to Early Devonian in the central Botwood Basin. The MPIS is a composite post kinematic intrusion consisting mainly of gabbro and granite with minor tonalite, diorite and granodiorite phases. The relationship between the gabbro and granite phases, as well as the relationship of the suite to the surrounding sedimentary lithologies, is still poorly understood due to the lack of contact exposures. The auriferous occurrences occur dominantly within the Ordovician Davidsville and Silurian Indian Islands groups and also within intrusive units throughout the region. A key question to be answered was whether regional intrusive suites (granitic to gabbroic) were key components of the ore-forming systems, acting as heat sources driving ore fluids, or just as rheologically contrasting host lithologies.

Reconnaissance mapping confirmed the presence of Indian Island Group rocks to the southeast and resulted in the discovery of new fossiliferous outcrops in the north. These latter localities, at Duder Lake and east of Ten Mile Lake, are significant to regional stratigraphy as they contain Wenlock fossils that are characteristic of the Indian Islands Group. This extends the group to the northwest of the current location of the Dog Bay Line.

Mapping observations along the eastern margin of the MPIS define the relationship between the felsic and mafic phases of the intrusive suite, as well as the relationship of the suite to the Indian Islands Group. Field relationships suggest that the

granite is younger than the gabbro; these include the gabbro's lack of chilled margins and gabbro pieces stopped by the granite suggesting the gabbro was cooled prior to the granite intrusion. Immediately west of Glenwood, a dioritic dyke, which has been correlated with the MPIS, intrudes the Indian Island Group sedimentary rocks. Along Red Rock Brook a faulted relationship is inferred between the granite phase of the MPIS and the Indian Islands Group, and thus, it is possible that the relationship is a fault-modified intrusive contact.

There are different gabbroic intrusive suites in the region as defined by whole-rock geochemistry. Mafic intrusive dykes to the north of the Trans Canada Highway (TCH) are petrographically and somewhat geochemically similar to the mafics of the MPIS. However, these dykes contain slightly higher Ti and less  $\text{SiO}_2$  contents. This may indicate that the dykes are fractionated equivalents of the MPIS, originated from a separate but similar magma source. The intrusive dykes at Duder Lake are petrographically and geochemically distinct from all intrusive bodies examined to the south inclusive of the dykes north of the TCH, the MPIS and the Paul's Pond intrusives. The data also indicate that there is an intermediate phase to the 'bimodal' MPIS. The sedimentary sequences display subtle differences in trace element contents between groups and these differences may be dependant on their locations in the region.

There are wide ranges in sulphur isotope ratios for sulphide mineral separates from different occurrences and the dominant control appears to be the lithological source of the sulphur. That is, occurrences within deep marine sedimentary lithologies are negative in terms of  $\delta^{34}\text{S}$  (‰). Occurrences in proximity to intrusive suites are near 0 ‰. Occurrences in which S was derived from igneous rocks have ratios that are slightly to moderately positive in terms of  $\delta^{34}\text{S}$  (‰).

Trace element compositions of pyrite suggest that different auriferous deposit types have recognizable signatures. For example, several of the pyrite grains from the Mustang Prospect contained the 'toxic suite of elements' characteristic of Carlin-type pyrite. Some pyrite from the Stog'er Tight and Hurricane Prospects contained elevated W and Te recognized in orogenic lode gold occurrences. Pyrite from the Bruce Pond Epithermal Prospect resembles that from low-sulphidation epithermal types of occurrences.

Geochronological data indicate that magmatism in the central to northern Botwood Basin was episodic from the Middle Silurian to Early Devonian. Age data also show that the granitic phase of the MPIS is younger than the gabbroic phase as (LAM-ICP-MS) U-Pb ages of *ca.* 430 Ma and 410 Ma were obtained for the diorite and granite phases of the MPIS, respectively. An intrusive gabbroic dyke to the north of the MPIS and the Charles Cove granodiorite were also dated at *ca.* 430 Ma suggesting that at least some of the magmatism in the northern Botwood Basin corresponded with MPIS magmatism. Thus, the magma may have been more deep-seated and widespread than previously thought. With the recognition that the MPIS granite intruded in Early Devonian time, it is more feasible to recognize the MPIS as a possible heat source for mineralization, at least along its eastern margin. The  $494 \pm 7$  Ma age for the Huxter Lane intrusive in the Botwood Basin basement reveals that auriferous mineralization in the region spans a significant geological time span (494 to 380 Ma).

Inherited zircons were common in both the MPIS and Charles Cove Pluton granites suggesting that Botwood Basin granitoids may have been generated through crustal anatexis of lower crustal material by mantle-derived gabbroic melts. The age of inheritance in both intrusions of *ca.* 1850-1800 Ma suggests that the melts may have sampled either Indian Islands Group rocks, or rocks that were their detritus source, as detrital components from that Group indicate a source region of a similar (1850 Ma) age.

There are several auriferous mineralization styles present in the Botwood Basin including epithermal, orogenic and perhaps Carlin-type. Although these occurrences display similarities in terms of mineralization characteristics, the tectonic and geological disparities throughout the region have led to differences between the occurrences. Thus, a generic model for 'Botwood Basin-type' auriferous mineralization is unrealistic.



## Acknowledgements

First and foremost, thank you to my supervisor Dr. Derek Wilton for accepting me as a student and providing a great study opportunity. I appreciate all the input I received in initializing my fieldwork and carrying out this project. Thank you for answering my questions, providing reassurance and for trusting me to get the work done; such guidance enabled me to complete this thesis.

Thank you to the technical staff on the fifth floor especially Pam King for conducting the XRF analyses and giving instruction when needed in sample preparation, Alison Pye for S-Isotope analysis and Mike Tubrett and Jiggs Diegor for LAM-ICP-MS U-Pb and trace element analyses. Thanks to Michael Shaffer and Danny Mulrooney for helping with electron microprobe imaging and Marc Poujol for showing me how to do Catho-Luminescence, even though my grains were disagreeable in being non-luminescent. Allen Hung crushed some of the samples for geochemistry. Much gratitude also goes to Jeff Pollock for making my life easier by giving me helpful tips on various computer programs on his brief visits back to MUN.

Many thanks to the Newfoundland Department of Natural Resources for making this project possible by providing funding for the project and awarding me the Special Scholarship for Students Pursuing Graduate Studies Related to Resource Development. Fellowship assistance from Memorial University was also greatly appreciated.

I would like to thank Lawson Dickson and Brian O' Brien for leading a field trip around parts of the study area in 2003, introducing me to the regional geology. Also, Lawson Dickson offered further insight into the regional geology and answered my questions after my field season. Thank you to Douglas Boyce for fossil identifications.

Much appreciation goes to Steven Hinchey for enthusiastic field assistance and tin whistle performances and for enduring my driving on the back 'roads' of central Newfoundland. Also, thank you to Darryl Hyde and Sheldon Heulin for stepping up to assist me for a few days when needed.

To my friends at the department, it has been a fun and eventful time, thanks for all of the interesting lunchtime interludes and for introducing me to touch football and all of its craziness (and thank God I'm still in one piece). Also, to my friend and new office mate, Kimberley Janes, whose good company has made these last few months more enjoyable.

Finally and very importantly, thank you to my family for always supporting what seemed like my endless years of student life, and to my husband Patrick McCarthy for giving me the encouragement to keep grinding away at it!!

# TABLE OF CONTENTS

FRONTISPIECE	
ABSTRACT.....	i
ACKNOWLEDGEMENTS.....	iv
TABLE OF CONTENTS.....	v
LIST OF TABLES.....	xii
LIST OF FIGURES.....	xiv
LIST OF PLATES.....	xxii

## CHAPTER 1 INTRODUCTION

1.1 Preamble.....	1
1.2 Location and Access.....	2
1.3 Physiography, Vegetation and Glacial History.....	2
1.4 Previous Work.....	4
1.5 Methods.....	4
1.6 Purpose and Scope.....	6

## CHAPTER 2 GEOLOGICAL SETTING

2.1 Regional Tectonic Setting.....	8
2.2 Geological Development of the Dunnage Zone (Pre and Post Accretion).....	13
2.2.1 Pre-Accretion.....	15
2.2.2 Post-Accretion.....	16
2.3 Geology and Stratigraphy of the Botwood Basin and Environs.....	16
2.3.1 The Mount Cormack Subzone - Spruce Brook Formation.....	18
2.3.2 Pipestone Pond, Coy Pond and Great Bend Complexes.....	19
2.3.3 Gander River Complex.....	19
2.3.4 Duder Complex.....	20
2.3.5 Davidsville Group.....	23
2.3.5.1 Weir's Pond Formation.....	24
2.3.5.2 Hunts Cove Formation.....	25
2.3.5.3 Outflow Formation.....	25

2.3.6 Baie d'Espoir Group (North Steady Pond Formation).....	25
2.3.7 Caradocian Shale.....	26
2.3.8 Badger Group.....	27
2.3.9 Indian Islands Group.....	27
2.3.9.1 Seal Cove Formation.....	29
2.3.9.2 Charles Cove Formation.....	29
2.3.9.3 Horwood Formation.....	29
2.2.10 Botwood Group.....	30
2.3.10.1 Lawrenceton Formation.....	31
2.3.10.2 Wigwam Formation.....	32
2.3.11 Stoney Lake Volcanics.....	33
2.3.12 Ten Mile Lake Formation.....	34
2.3.13 Mount Peyton Intrusive Suite.....	35
2.4 Faults.....	36
2.4.1 Northern Botwood Basin Faults.....	36
2.4.2 Southern Botwood Basin Faults.....	38
2.5 Regional Deformation and Metamorphism.....	38

### **CHAPTER 3 AURIFEROUS OCCURENCES**

3.1 Preamble.....	46
3.2 Northern Botwood Basin.....	47
3.2.1 Duder Lake Prospects.....	47
3.2.1.1 Flirt.....	49
3.2.1.2 Goldstash.....	50
3.2.1.3 Corvette.....	51
3.2.2 Clutha.....	53
3.2.3 Charles Cove.....	53
3.2.4 Knob Hill.....	54
3.2.5 Third Pond.....	56
3.2.6 Jonathan's Pond.....	57
3.2.7 Big Pond.....	59
3.3 Central Botwood Basin: Glenwood-Appleton Region.....	60
3.3.1 Bullet.....	61
3.3.2 Knob.....	62
3.3.3 Bowater.....	63
3.3.4 Dome.....	64
3.3.5 Outflow.....	64
3.4 Central Botwood Basin: Northern Mount Peyton.....	67
3.4.1 Hurricane.....	68



3.4.2 Corsair.....	70
3.4.3 Slip.....	70
3.4.4 Jumper's Brook.....	71
3.5 Southeastern Botwood Basin: Paul's Pond Region.....	72
3.5.1 Hunan .....	73
3.5.2 LBNL.....	74
3.5.3 Goose.....	76
3.5.4 Road Gabbro Showing.....	76
3.5.5 Aztec.....	77
3.5.6 Hornet.....	77
3.5.7 Greens Pond #2.....	78
3.5.8 A-Zone Extension.....	79
3.6 Southern Botwood Basin: Great Bend Region.....	80
3.6.1 Rolling Pond.....	81
3.6.2 Chiouk Brook.....	83
3.6.3 Breccia Pond.....	83
3.6.4 Swan Lake.....	85
3.6.5 Lizard Pond South.....	86
3.6.6 Lizard Pond North.....	88
3.6.7 Huxter Lane.....	89

## CHAPTER 4 REGIONAL MAPPING

4.1 Preamble.....	112
4.2 Duder Lake Area	
4.2.1 Mapping Observations and Petrography.....	113
4.2.2 Paleontology.....	117
4.2.3 Discussion.....	120
4.3 Bellman's Pond Conglomerate	
4.3.1 Mapping Observations and Petrography.....	121
4.3.2 Discussion.....	124
4.4 Twin Ponds to Ten Mile Lake Area	
4.4.1 Mapping Observations and Petrography.....	124
4.4.2 Paleontology.....	128
4.4.3 Discussion.....	130
4.5 Glenwood Appleton Area	
4.5.1 Mapping Observations and Petrography.....	130
4.5.2 Paleontology.....	132

4.6 Salmon River	
4.6.1 Introduction.....	135
4.6.2 Granite-Gabbro Relationships in the Salmon River.....	137
4.6.3 MPIS Granite at Red Rock Brook.....	138
4.6.4 Discussion.....	140
4.7 Careless Brook	
4.7.1 Introduction.....	142
4.7.1 Mapping Observations and Petrography.....	142
4.7.2 Paleontology.....	145
4.7.3 Discussion.....	145
4.8 Coopers Brook	
4.8.1 Introduction.....	146
4.8.2 Mapping Observations.....	148
4.8.3 Discussion.....	148

## CHAPTER 5 WHOLE ROCK GEOCHEMISTRY

5.1 Preamble.....	158
5.2 Igneous Rocks	
5.2.1 Sample Overview.....	160
5.2.2 Trace element discrimination diagrams for rock classification	
5.2.2.1 Introduction.....	163
5.2.2.2 Results.....	164
5.2.3 Harker bivariate plots	
5.2.3.1 Introduction.....	171
5.2.3.2 Results.....	172
5.2.4 Bivariate trace element diagrams for magmatic affinity	
5.2.4.1 Introduction.....	175
5.2.4.2 Results.....	176
5.3 Sedimentary Rocks	
5.3.1 Sample Overview.....	178
5.3.2 Trace element and petrographic discrimination diagrams.....	180
5.4 Discussion	
5.4.1 Igneous Rocks.....	188
5.4.2 Sedimentary Rocks.....	192

## CHAPTER 6 SULPHUR ISOTOPE GEOCHEMISTRY

6.1 Preamble.....	213
-------------------	-----

6.2 Sulphur Isotope Systematics.....	214
6.3 Sulphur Isotope Results.....	216
6.3.1 Isotopically light S-Isotope ratios.....	217
6.3.2 Isotopically intermediate S-Isotope ratios.....	218
6.3.3 Isotopically heavy S-Isotope ratios.....	220
6.4 Discussion.....	221

## **CHAPTER 7 TRACE ELEMENT CONTENT OF PYRITE**

7.1 Preamble.....	227
7.2 Analytical Procedure and Sample Overview.....	229
7.3 Results.....	231
7.4 Discussion.....	233

## **CHAPTER 8 U-Pb GEOCHRONOLOGY**

8.1 Preamble.....	246
8.2 U-Th-Pb Isotope Systematics.....	247
8.3 Sample Overview.....	250
8.4 Results	
8.4.1 Hurricane Diorite.....	253
8.4.2 Corsair Diorite.....	254
8.4.3 Twin ponds Gabbro.....	255
8.4.4 MPIS Granite.....	256
8.4.5 Red Rock Brook Granite.....	257
8.4.6 Charles Cove Pluton.....	258
8.4.7 Huxter Lane.....	259
8.4.8 Contact between Davidsville and Indian Islands Groups.....	260
8.4.9 Bellman's Pond Conglomerate clast.....	261
8.5 Discussion: Geochronology of the MPIS in relation to previous work.....	261
8.6 Significance of dates to regional metallogeny.....	266



## **CHAPTER 9 SUMMARY AND CONCLUSIONS**

9.1 Preamble.....	279
9.2 Principle Results.....	280
9.3 Conclusions.....	290
9.4 Direction for future work.....	294

<b>REFERENCES.....</b>	<b>296</b>
------------------------	------------

<b>APPENDIX 1 PREVIOUS WORK.....</b>	<b>A1-1</b>
--------------------------------------	-------------

## **APPENDIX 2 GOLD DEPOSIT MODELS**

A2.1 Gold Exploration in Dunnage Zone.....	A2-1
A2.2 Overview of applicable Gold Deposit Models.....	A2-3
A2.2.1 Syngenetic.....	A2-3
A2.2.2 Epigenetic	
A2.2.2.1 Orogenic Lode.....	A2-3
A2.2.2.2 Epithermal.....	A2-5
A2.2.2.3 Sediment Hosted Disseminated.....	A2-9

## **APPENDIX 3 ANALYTICAL METHODS**

A2.1 Sample Collection.....	A3-1
A2.2 XRF Geochemical Analysis	
A2.2.1 Introduction.....	A3-2
A2.2.2. Sample preparation and data collection for XRF analysis.....	A3-2
A2.2.3 Precision and Accuracy.....	A3-3
A2.3 Sulfur Isotope Geochemistry	
A2.3.1 Introduction.....	A3-4
A2.3.2 Sample preparation and data collection for S-Isotope analysis...	A3-5
A2.4 Laser Ablation Microprobe-Inductively Coupled plasma-Mass Spectrometry (LAM-ICP-MS) U-Pb Geochronology	
A2.4.1 Introduction.....	A3-6

A2.4.2 Sample preparation and data collection for LAM-ICP-MS analysis.....	A3-7
A2.4.3 Data Reduction.....	A3-9
A2.5 Electron Microprobe	
A2.5.1 Introduction.....	A3-10
A2.5.2 Sample Preparation and Microanalysis.....	A3-11
A2.6 Trace Element Geochemical Analysis of Pyrite via LAM-ICP-MS	
A2.6.1 Introduction.....	A3-12
A2.6.2 Sample preparation and data collection for pyrite chemistry.....	A3-13
<b>APPENDIX 4 COMPILED DATA TABLES.....</b>	<b>A4-1</b>

## LIST OF TABLES

<b>Table A1.1:</b> Brief description of previous work conducted within or adjacent to the Botwood Basin, central Newfoundland (Previous histories of paleontological and geochronological work are listed separately in tables A1.3 and A1.4, respectively).....	A1-1
<b>Table A1.2:</b> Brief descriptions of Botwood Basin auriferous prospects visited for the current study (descriptions modified from Evans (1996), unless otherwise noted).....	A1-26
<b>Table A1.3:</b> Brief description of previous paleontological studies from within the Botwood Basin and environs.....	A1-31
<b>Table A1.4:</b> Brief summary of previous geochronological studies from within the Botwood Basin.....	A1-34
<b>Table A2.1:</b> Generalized Mineral Paragenesis in Carlin Type Gold Deposits. Common alteration types and minerals are in bold and rare minerals are in italics (after Hofstra and Cline, 2000).....	A2-14
<b>Table A3.1</b> List of igneous and sedimentary samples with location and description for XRF analysis.....	A3-14
<b>Table A3.2:</b> Description and location of samples processed for sulphur isotope chemistry.....	A3-18
<b>Table A3.3:</b> Sample location and description for U-Pb Geochronology.....	A3-23
<b>Table A4.1:</b> Paleontological sample location, description and fossil assemblages for samples collected from the Botwood Basin and environs.....	A4-1
<b>Table A4.2:</b> Pressed pellet X-Ray Fluorescence (XRF) data for intrusive and sedimentary rocks from the Botwood Basin.....	A4-3
<b>Table A4.3:</b> Sulphur isotope values for Botwood Basin sulphides.....	A4-11
<b>Table A4.4a:</b> Trace element content of pyrite grains from the Hornet Prospect.....	A4.13
<b>Table A4.4b:</b> Trace element content of pyrite grains from the Goldstash Prospect.....	A4.13
<b>Table A4.4c:</b> Trace element content of pyrite grains from the Outflow Prospect (Piper Zone).....	A4-14



<b>Table A4.4d:</b> Trace element content of pyrite grains from the Jonathon's Pond Prospect.....	A4-14
<b>Table A4.4e:</b> Trace element content of pyrite grains from the Hurricane Prospect.....	A4-15
<b>Table A4.4f:</b> Trace element content of pyrite grains from the Bowater Prospect.....	A4-15
<b>Table A4.4g:</b> Trace element content of pyrite grains from the Outflow Prospect (Mustang Zone).....	A4-16
<b>Table A4.4h:</b> Trace element content of pyrite grains from the Stog'er Tight Prospect.....	A4-16
<b>Table A4.4i:</b> Trace element content of pyrite grains from the Bruce Pond Prospect.....	A4-17
<b>Table A4.5a:</b> Unknown data table for December 19, 2005 U-Pb analysis (Sample JOD21).....	A4-18
<b>Table A4.5b:</b> Unknown data table for March 2, 2004 U-Pb analysis (Sample JOD25).....	A4-19
<b>Table A4.5c:</b> Unknown data table for March 1, 2 and 24, 2004 U-Pb analysis (Sample JOD100).....	A4-20
<b>Table A4.5d:</b> Unknown data table for December 19, 2005 U-Pb analysis (Sample JOD04-17).....	A4-21
<b>Table A4.5e:</b> Unknown data table for March 2, 2004 U-Pb analysis (Sample JOD90A).....	A4-22
<b>Table A4.5f:</b> Unknown data table for March 24, 2004 U-Pb analysis (Sample W03-27).....	A4-23
<b>Table A4.5g:</b> Unknown data table for February 20, 2004 U-Pb analysis (Sample W03-38).....	A4-24
<b>Table A4.5h:</b> Unknown data table for February 25, 2004 U-Pb analysis (Sample JOD08).....	A4-25
<b>Table A4.5i:</b> Unknown data table for February 20, 23 and March 23, 2004 U-Pb analysis (Sample JOD39).....	A4-26
<b>Table A4.6:</b> Known standard data for U-Pb analyses.....	A4-27

## LIST OF FIGURES

<b>Figure 1.1:</b> Map of the island of Newfoundland outlining the study area in blue and illustrating major routes and cities/ towns.....	7
<b>Figure 2.1:</b> Tectonostratigraphic subdivision of the Newfoundland Appalachians. DZ(e)= Dunnage Zone; Exploits subzone; DZ(n)= Dunnage Zone; Notre Dame subzone; GZ= Gander ZoNE; HBF= Hermitage Bay Fault; DF= Dover Fault; RIL= Red Indian Line (from O'Brien <i>et al.</i> 1996).....	40
<b>Figure 2.2:</b> Zonal subdivision of the Newfoundland Dunnage Zone (modified from Williams <i>et al.</i> (1988) and Williams (1995)).....	41
<b>Figure 2.3:</b> Geology of the Dunnage Zone of Newfoundland (modified from Colman-Sadd <i>et al.</i> , 1990).....	42
<b>Figure 2.4:</b> Generalized geology map of the Botwood Basin and environs, and specific locations of auriferous showings sampled for this study (yellow stars) and location of geochronological samples (red circles) from which U-Pb ages were obtained (geology modified from Colman-Sadd and Crisby-Whittle, 2002).....	44
<b>Figure 2.5:</b> Stratigraphic column illustrating the various lithologies and relative ages of the Botwood and Indian Islands Belts, Exploits Subzone (refer to corresponding geology map and legend in figure 2.4).....	45
<b>Figure 3.1:</b> Location map for the Duder Lake, Clutha and Charles Cove Prospects.....	91
<b>Figure 3.2:</b> Major geological units in the Duder Lake area, showing location of the Corvette, Goldstash and Stinger prospects (modified from Churchill <i>et al.</i> , 1993 with geological changes based on Currie, 1995b).....	92
<b>Figure 3.3:</b> Geology in the Tim's Cove Area and location of the quartz vein systems (after Evans, 1996).....	93
<b>Figure 3.4:</b> Central Botwood Basin (Glenwood-Appleton region) prospect location map.....	94
<b>Figure 3.5:</b> Geology of the Jonathon's Pond area (modified from Blackwood, 1982).....	95
<b>Figure 3.6:</b> Geology of the Glenwood-Appleton Area, central Newfoundland (geology from Blackwood, 1982 and Dickson, 1992).....	96

<b>Figure 3.7:</b> Location map for Mount Peyton Prospects, central Botwood Basin.....	97
<b>Figure 3.8:</b> General geology map of the northern Mount Peyton area (geology from Colman-Sadd and Crisby Whittle, 2002).....	97
<b>Figure 3.9:</b> Location map for Southern Botwood Basin Prospects.....	98
<b>Figure 3.10:</b> Geology of the southern Botwood Basin-Paul's Pond region auriferous prospects and the Beaver Brook antimony deposit (Beaver Brook geology examined in more detail in figure 3.11) (geology from Dickson, 1996).....	99
<b>Figure 3.11:</b> Regional geology of the Hunan Line Antimony prospects (modified from Tallman and Evans, 1994).....	100
<b>Figure 3.12:</b> Geology in the Great Bend Region (North of northwest Gander River). The Rolling Pond property is outlined (from Barbour, 1999).....	101
<b>Figure 3.13:</b> Geology of the Rolling Pond property (area outlined in figure 3.12) (modified from Barbour <i>et al.</i> , 1999).....	102
<b>Figure 3.14:</b> General geology and auriferous occurrences of the Great Bend Complex (after Dickson, 1991 and 1996).....	103
<b>Figure 4.1:</b> Block diagram illustrating the internal structure of the tabulate coral <i>Favosites</i> (Late Ordovician to Middle Devonian) (from Stearn and Carroll, 1989).....	118
<b>Figure 4.2:</b> Genera <i>Stictopora</i> , Order <i>Cryptostomata</i> . On the right, complete specimen about natural size; on the left, the surface enlarged to show the zooecia (after Stearn and Carroll, 1989).....	119
<b>Figure 4.3:</b> The living brachiopod <i>Magelania</i> . A) Dorsal view of the shell. B) Side view showing the pedicule and brachial valve and the position of the pedicle (from Stearn and Carroll, 1989). ....	120
<b>Figure 4.4:</b> A) Paleozoic straight nautiloids (arrows indicating centers of gravity and buoyancy respectively). B) A straight nautiloid <i>Armenoceras</i> (Ordovician) with a heavy siphuncle (light colored). The specimen has been cut longitudinally and polished so that the siphuncle is seen in section. The specimen is 16 cm long (from Stearn and Carroll, 1989). ....	134
<b>Figure 4.5:</b> <i>Climagraptus</i> (after Stearn and Carroll, 1989).....	135



<b>Figure 5.1:</b> Symbol key for geochemical diagrams for igneous rocks. All samples in black were analyzed as part of the current study and the samples represented by colored symbols were taken from Churchill (1994) and Dickson (1996) as indicated.....	194
<b>Figure 5.2:</b> Nb/Y vs. Zr/TiO <sub>2</sub> discrimination diagram (Winchester and Floyd, 1977) which illustrates the composition of the igneous rocks from the current study (black) in relation to pre-existing datasets from Duder Lake (Churchill, 1994) [green symbols] and MPIS (Dickson, 1996) [red and blue symbols] (refer to symbol key, figure 5.1).....	195
<b>Figure 5.3:</b> Irvine and Barager (1971) Na <sub>2</sub> O+K <sub>2</sub> O vs. SiO <sub>2</sub> plot illustrating the sub-alkaline nature of the current study, Duder Lake (Churchill, 1994) and MPIS (Dickson, 1996) igneous rocks (refer to figure 5.1 for symbol key).....	196
<b>Figure 5.4:</b> AFM plot of Irvine and Baragar (1971) indicating the chemical affinity of igneous rocks from the current study [black], Duder Lake (Churchill, 1994) [green], and MPIS (Dickson, 1996) [blue] (refer to figure 5.1 for symbol key).....	197
<b>Figure 5.5:</b> Ti-Zr-Y diagram (Pearce and Cann, 1973) illustrating the possible paleotectonic environments for the current [black], Churchill (1994) [green] and Dickson (1996) [blue and red] studies igneous rocks (refer to figure 5.1 for symbol key).....	198
<b>Figure 5.6:</b> Zr vs. Zr/Y diagram (Pearce and Norry, 1979; Pearce, 1983) for igneous rocks from the current study, Dickson's (1996) dataset and Churchill's (1994) dataset illustrating a within plate, continental arc signature (refer to figure 5.1 for symbol key).....	199
<b>Figure 5.7:</b> Tectonic discrimination diagram of Meschede (1986) indicating the tectonic affinity of igneous rocks from the current study [black], Churchill (1994) [green] and Dickson (1996) [red and blue] (refer to figure 5.1 for symbol key).....	200
<b>Figure 5.8:</b> Ti vs. V diagram (Shervais, 1982) for igneous rocks from the current study [black] and Dickson (1996) [red and blue], illustrating a relative enrichment in Ti in the northern region (refer to figure 5.1 for symbol key).....	201
<b>Figure 5.9a:</b> Bivariate plot of SiO <sub>2</sub> vs. FeO illustrating a negative linear trend for the igneous rocks from the current study [black], Dickson (1996) and Churchill (1994) (refer to figure 5.1 for symbol key).....	202



<b>Figure 5.9b:</b> Bivariate plot of SiO <sub>2</sub> vs. MgO illustrating a negative curvilinear trend for the igneous rocks from the current study [black], Dickson (1996) and Churchill (1994) (refer to figure 5.1 for symbol key).....	202
<b>Figure 5.9c:</b> Bivariate plot of SiO <sub>2</sub> vs. K <sub>2</sub> O illustrating a positive linear trend for the igneous rocks from the current study [black], Dickson (1996) and Churchill (1994) (refer to figure 5.1 for symbol key).....	203
<b>Figure 5.9d:</b> Bivariate plot of SiO <sub>2</sub> vs. TiO <sub>2</sub> illustrating a negative linear trend for the igneous rocks from the current study [black], Dickson (1996) and Churchill (1994) (refer to figure 5.1 for symbol key).....	203
<b>Figure 5.10:</b> Zr vs. Al <sub>2</sub> O <sub>3</sub> bivariate plot (after MacLean and Barrett, 1993) illustrating a fractionation trend in the Botwood Basin igneous rocks. The mafic samples collected from the north for the current study either define a separate trend, or have experienced mass gain (refer to figure 5.1 for symbol key).....	204
<b>Figure 5.11:</b> Zr vs. TiO <sub>2</sub> bivariate plot (after MacLean and Barrett, 1993) illustrating a fractionation trend in the Botwood Basin igneous rocks. The mafic samples from the current study have higher Ti values (refer to figure 5.1 for symbol key).....	205
<b>Figure 5.12:</b> Zr vs. Y. diagram (after MacLean and Barrett, 1993) for igneous rocks in the Botwood Basin illustrating the transitional nature of the samples from the current study and the overall transitional to tholeiitic nature of all combined data (refer to figure 5.1 for symbol key).....	206
<b>Figure 5.13:</b> Roser and Korsch (1986) tectonic discrimination diagram for the Botwood basin sedimentary samples from the current study, Churchill (1994) study at Duder Lake in the northern Botwood Basin and O'Reilly (2005) study at the O'Reilly prospect in the central Botwood Basin.....	207
<b>Figure 5.14:</b> Dickinson and Suczec (1979) triangular quartz-feldspar-lithic fragment plot showing relationship between plate tectonics and the Davidsville Group (current study)[Red: JOD15 from central region; yellow: JOD20 from central; purple: JOD39 from central; green: JOD44A from southern region and Indian Islands Group (O'Reilly, 2005) sedimentary rocks [blue].....	208
<b>Figure 5.15a:</b> Zr vs. Nb plot of sedimentary samples from the Botwood Basin (refer to figure 5.13 for symbol key).....	209
<b>Figure 5.15b:</b> Zr vs. Y plot of sedimentary samples from the Botwood Basin (refer to figure 5.13 for symbol key).....	209

<b>Figure 5.15c:</b> Zr vs. $\text{Al}_2\text{O}_3$ plot of sedimentary samples from the Botwood Basin (refer to figure 5.13 for symbol key).....	210
<b>Figure 5.15d:</b> Zr vs. $\text{TiO}_2$ plot of sedimentary samples from the Botwood Basin (refer to figure 5.13 for symbol key).....	210
<b>Figure 5.16:</b> Fralick and Kronberg (1997) $\text{Al}_2\text{O}_3$ - $\text{TiO}_2$ -Zr ration diagram comparing Botwood Basin sedimentary samples with possible volcanic source terrains (refer to figure 5.13 for symbol key).....	211
<b>Figure 5.17:</b> McBride (1963) triangular quartz-feldspar-lithic fragment classification diagram for the Davidsville (circles-see figure 4.14) and Indian Island (blue cross) Group rocks.....	212
<b>Figure 6.1:</b> Sulphur isotope data from Carlin-type gold deposits relative to pertinent references from Ohmoto and Rye (1979) and Kerrich (1989). The isotopic composition of $\text{H}_2\text{S}$ in ore fluids (shaded) was calculated using a temperature of $200^\circ\text{C}$ and isotopic fractionations in Ohmoto and Rye (1979) (from Hofstra and Cline, 2000).....	224
<b>Figure 6.2a:</b> The distribution of sulphur isotope values for common large earth reservoirs (from Ohmoto and Rye, 1979).....	225
<b>Figure 6.2b:</b> Stable isotope composition of sulphur from different Sources (Kyser, 1986; Kerrich, 1989).....	225
<b>Figure 6.3:</b> Compilation of sulphur isotope ratios for sulphide mineral separates from auriferous occurrences of the Botwood basin; data compiled from Churchill (1994), Dalton (1998), Evans and Wilson (1994), D. Evans, unpublished data, 2005), Greenslade (2002), unpublished data from D. Wilton and data from the current study (black) (modified from O' Driscoll and Wilton, 2005).....	226
<b>Figure 7.1a:</b> Plot of As vs. Au illustrating that the Mustang, Hurricane and Hornet Prospect pyrites are elevated in Au and As contents relative to the other samples.....	237
<b>Figure 7.1b:</b> Plot of Hg vs. Au illustrating that the Outflow (Mustang Trend) and Goldstash Prospect pyrites are elevated Hg contents relative to the other samples.....	237
<b>Figure 7.1c:</b> Plot of Sb vs. Au illustrating that the Hurricane and Mustang Prospect pyrites are much more elevated in Sb contents relative to the other samples. The Bruce Pond pyrites has slightly elevated contents (see next chart).....	238

<b>Figure 7.1d:</b> Plot of As vs. Sb (zoomed x-axis) illustrating that some of the Bruce Pond Prospect pyrites are more elevated in Sb contents than all samples except two Hurricane pyrite grains and one Mustang pyrite grain (refer also to figure 7.1c).....	238
<b>Figure 7.1e:</b> Plot of As vs. Pb illustrating that the Mustang Prospect pyrites are elevated in Pb contents relative to the other samples.....	239
<b>Figure 7.1f:</b> Plot of As vs. Pb (zoomed x-axis) illustrating that some pyrite from the Goldstash and Hornet Prospects are also slightly elevated in Pb contents relative to the other samples (refer also to figure 7.1e).....	239
<b>Figure 7.1g:</b> Plot of Te vs. Au illustrating that the Mustang Prospect pyrites are elevated in Te contents relative to the other samples.....	240
<b>Figure 7.1h:</b> Plot of Se vs. Au illustrating that the Bruce Pond Prospect pyrites are elevated in Se contents relative to the other samples.....	240
<b>Figure 7.1i:</b> Plot of W vs. Au illustrating that one Hurricane Pyrite and one Hornet Prospect pyrite are elevated in W contents relative to the other samples. One sample from Jonathon's Pond has slightly elevated content.....	241
<b>Figure 7.2a:</b> Plot of Sb vs. W illustrating that the Jonathon's Pond and Bruce Pond Prospect pyrites are the most elevated in W contents relative to the other samples.....	242
<b>Figure 7.2b:</b> Plot of As vs. Hg illustrating that the Mustang and Goldstash Prospect pyrites are the most elevated in Hg contents relative to the other samples. The Hurricane, Jonathon's Pond, Mustang and Hornet Prospects all have elevated As contents. The Mustang and Goldstash pyrite have elevated Hg contents. It should be noted that the grains from the Mustang that have elevated As do no have elevated Hg and vice versa.....	242
<b>Figure 7.2c:</b> Plot of As vs. Sb illustrating that the Mustang Prospect pyrites Sb content increase with As content. Also, Jonathon's Pond samples plot in two distinct groups indicating a possible element zonation in the pyrite grains.....	243
<b>Figure 7.2d:</b> Plot of As vs. Sb illustrating the elevated content of As and Sb in two of the Hurricane Prospect pyrites. The differences in elevations may indicate that trace elements contents exhibit element zonations.....	243



<b>Figure 8.1:</b> Generalized geology map of the Botwood Basin and environs, and specific locations of auriferous showings sampled for this study (yellow stars) and location of geochronological samples (red circles) from which U-Pb ages were obtained. Obtained ages for magmatic samples are indicated on map. Refer to figure 2.4 for corresponding legend (Geology modified from Colman-Sadd and Crisby-Whittle, 2002).....	268
<b>Figure 8.2:</b> Concordia diagram illustrating the Concordia curve and a line of discordia. Any point along the Concordia curve would produce a concordant or accurate date for the material being tested, whereby discordant points will result from either Pb loss or U loss/gain. Discordant points can be useful if they produce a linear or sublinear discordia as the lower intercept should represent time of formation and an upper intercept should represent the disturbance to the system.....	269
<b>Figure 8.3:</b> Concordia diagram for sample JOD21, Hurricane Prospect; the size of the ellipse represents the error measurement ( $1\sigma$ ) for that particular analysis.....	270
<b>Figure 8.4:</b> Concordia diagram for sample JOD25, Corsair Prospect; the size of the ellipse represents the error measurement ( $1\sigma$ ) for that particular analysis.....	271
<b>Figure 8.5:</b> Concordia diagram for sample JOD100, Twin Ponds gabbro; the size of the ellipse represents the error measurement ( $1\sigma$ ) for that particular analysis.....	272
<b>Figure 8.6:</b> Concordia diagram for sample JOD04-17, MPIS granite; the size of the ellipse represents the error measurement ( $1\sigma$ ) for that particular analysis.....	273
<b>Figure 8.7:</b> Concordia diagram for sample JOD90A, MPIS granite; the size of the ellipse represents the error measurement ( $1\sigma$ ) for that particular analysis.....	274
<b>Figure 8.8:</b> Concordia diagram for sample W03-27, Charles Cove pluton granite; the size of the ellipse represents the error measurement ( $1\sigma$ ) for that particular analysis .....	275
<b>Figure 8.9:</b> Concordia diagram for sample W03-38, Huxter Lane felsic intrusive; the size of the ellipse represents the error measurement ( $1\sigma$ ) for that particular analysis.....	276
<b>Figure 8.10:</b> Histogram of detrital zircon $^{206}\text{Pb}/^{238}\text{U}$ dates for sample JOD39.....	277



**Figure 8.11:** Histogram of zircon  $^{206}\text{Pb}/^{238}\text{U}$  dates for lithic tuff sample JOD08..... 278

**Figure A2.1:** Classification scheme for gold mineralization within the eastern Dunnage Zone. Prospects in red were visited and assessed during the current project and those in blue were visited but have been backfilled since last documentation (modified from Evans, 1993)..... A2-11

**Figure A2.2:** Idealized section of a bonanza epithermal deposit (after Buchanan, 1981)..... A1-12

**Figure A2.3a:** Schematic cross section through a SHDG deposit showing major alteration and mineralization features adjacent to a fluid feeder (after Arehart, 1996)..... A1-13

**Figure A2.3b:** Schematic cross section of northern Nevada and northwest Utah, showing attenuated Archean crust, oceanic crust, overlying stratigraphic sequences and allochthons, fault zones and locations of Carlin-type gold deposits (black) (after Hofstra and cline, 2000)..... A1-13

## LIST OF PLATES

<b>Plate 3.1:</b> a) Looking north towards the northern tip of Duder Lake along the resource road, b) View east from elongate northeast trending ridge. Shear zone outline by valley below and mineralized sandstone and fossil outcrop exposed near vehicle to the west of the shear zone (indicated by arrow) [S. Heulin for scale].....	104
<b>Plate 3.2:</b> a) Grab sample from trenched area exposing Fe-carbonate altered, quartz veined, mineralized sandstone unit (Sample JOD96H). b) Grab sample from Flirt Prospect trench (Sample JOD99). The white mineral is subhedral carbonate, the blue-grey mineral is albite and the green mineral is carbonate [penny for scale].....	104
<b>Plate 3.3:</b> Photomicrograph of a gabbro from the Flirt Prospect exhibiting leuxocene alteration of Fe-Ti Oxides and uraltization of pyroxene. Plagioclase is albitized and contains minor epidote and calcite. Fine-grained calcite and epidote are also present as pinkish flecks in the albite and quartz carbonate veinlets cut the pyroxene [Field of view ~ 7 mm, XP).....	50
<b>Plate 3.4:</b> a) Goldstash Trench (Steve Hinchey for scale). b) Corvette Fe-carbonate altered trench.....	104
<b>Plate 3.5:</b> Photomicrograph of mineralized gabbro from the Goldstash Prospect exhibiting chlorite (Chl), ankerite (Ank) and pyrite (Py). [Field of view ~ 7 mm, PPL and XP).....	51
<b>Plate 3.6:</b> Photomicrographs of mineralized gabbro from the Corvette Prospect exhibiting A) uratitized pyroxene (Ur), pyroxene (Pyr) and leuxocene (Lx) replacement of Fe-Ti oxides and B) albitized plagioclase (Alb) with epidote alteration, quartz and chlorite and [Field of view ~ 7 mm, XP).....	52
<b>Plate 3.7:</b> a) Quartz veins in deformed greywacke at the Knob Hill Prospect, b) Quartz veins in altered greywacke or cherty concretion at the Third Pond Prospect [camera lens for scale, 5 cm wide].....	105
<b>Plate 3.8:</b> Photomicrograph of Davidsville quartzwacke, host to mineralization at the Knob Hill Prospect comprised of moderately sorted quartz, feldspar and Fe-Ti oxides in a fine-grained sericite matrix [Field of view 7mm, PPL and XP].....	55
<b>Plate 3.9:</b> Photomicrograph of carbonate 'concretion' at the Third Pond Prospect. The section is comprised of chlorite (Chl), calcite (Ca) and sericite (Sr) [Field of view 7mm, PPL and XP].....	57

<b>Plate 3.10:</b> a) Quartz float boulder with bladed texture, b) quartz veined, mineralized and talc altered serpentine from Jonathon's Pond Prospect.....	105
<b>Plate 3.11:</b> Sample JOD117-Jonathon's Pond. a) Serpentinized (Sp) and talc altered host exhibiting disseminated blebs of pyrite (py) [field of view 7mm, PPL]. B) Section from quartz carbonate (qtz-cb) vein exhibiting acicular arsenopyrite (asp) [Field of view 2mm, PPL].....	59
<b>Plate 3.12:</b> Bullet Prospect overgrown trench (S. Hinchey for scale).....	105
<b>Plate 3.13a:</b> Sample W90-10A from Davidsville Group host rock to the Bullet Prospect consisting of detrital quartz, minor feldspar, fine-grained mica matrix, platy chlorite, Fe-oxides and pyrite [Field of view 7mm, PPL].....	62
<b>Plate 3.13b:</b> Sample W90-45B of quartz veins in Davidsville Group rocks at the Bullet Prospect. Interstitial fine grains of subhedral quartz occur in clusters as open space filling [Field of view 7mm, XP and PPL].....	62
<b>Plate 3.14:</b> a) Trench at Knob Prospect, northwest of quarry [S. Hinchey for scale], b) Large bull quartz vein containing visible gold in greywacke [hammer for scale].....	106
<b>Plate 3.15:</b> a) the main trench and stripped area of the Dome Prospect [J. O' Driscoll for scale], b) Laminated, stripped outcrop along the 'Appleton Linear' exposing Davidsville slate [utility knife for scale].....	106
<b>Plate 3.16:</b> a) Graphitic, deformed shale north of the trenched area at the Piper Zone, Outflow Prospect, b) View of a trenched area exhibiting silicification and large quartz veins.....	106
<b>Plate 3.17:</b> a) Rusty, silicified and brecciated outcrop at Outflow Prospect [hammer for scale]. b) Quartz brecciated laminated siltstone within the trenched area [camera lens for scale].....	107
<b>Plate 3.18:</b> a,b) Photomicrograph from the Mustang Trend sample W0-49A, Outflow Prospect quartz breccia. Matrix is composed of quartz and carbonate and the fragments are altered to clay [Field of view, 7mm, PPL and XP].....	66
<b>Plate 3.18:</b> c) Photomicrograph exhibiting quartz breccia and quartz veins of sample DW90-50A [Field of View, 7mm, PPL]. d) Close-up of fragment from sample DW90-49A surrounded by radiating carbonate crystals [Field of view 2mm, XP].....	67



<b>Plate 3.19:</b> a) View up the Salmon River with D. Wilton and S. Hinchey at the Hurricane Prospect, b) close-up of Hurricane Prospect (marked by flagging) which is grown over the riverbank [hammer for scale], c) Quartz veined, mineralized diorite from the Hurricane Prospect [penny for scale].....	107
<b>Plate 3.20:</b> Photomicrograph of slightly sericite-altered sample JOD22 from the Hurricane Prospect consisting of hornblende (Hb), plagioclase (Pl), biotite (Bt), pyroxene, apatite, 5% oxides and 10% quartz (note reaction rim with biotite). Dusty alteration is sericite [First photomicrograph has 7mm field of view in PPL and second photomicrograph has 2mm field of view in PPL].....	69
<b>Plate 3.21:</b> Photomicrograph of sample JOD23 from the Hurricane Prospect. The section is comprised of plagioclase, sericite (replaces feldspar), quartz, apatite, Ti-Fe oxides, and pyrite and arsenopyrite. Tiny sulphide veinlets and quartz run through the sample. Sulphides are mainly concentrated along the edges of the quartz veins [Field of view 7mm, PPL and XP].....	69
<b>Plate 3.22:</b> Photomicrograph of sample JOD27B of the Slip Prospect. a) intergrown prismatic quartz (grey) and an carbonate [Field of view 7mm, XP]. b) Granophyric texture [Field of view 7 mm, PPL].....	71
<b>Plate 3.23:</b> a) View along Jumper's Brook where angular mineralized subcrop was observed [backpack for scale], b) close up of mineralized boulder [tack for scale].....	108
<b>Plate 3.24:</b> Photomicrograph of sample JOD118 from Jumpers Brook showing non-orientated grains of chlorite altered hornblende in a sericite-altered, fine-grained matrix of feldspar, quartz [Field of view 2mm, PPL and XP].....	72
<b>Plate 3.25:</b> Photomicrograph of sample JOD45B consisting of a large rhombic arsenopyrite (Ar) grain in a pervasively sericite (Sr) altered leucogranite. Some primary feldspar (Fdspr) exhibiting a granophyric texture remains [Field of view 2mm, PPL]. .....	75
<b>Plate 3.26:</b> a) Large stripped area at the Aztec Prospect exposing a large silica sinter and rusty, mineralized sedimentary rocks. b) Piece of quartz breccia [camera lens for scale].....	108
<b>Plate 3.28:</b> Photomicrograph of sample JOD80A from the Hornet Prospect. a) Very fine grained, pervasively seritized host rock with cubic pyrite grain [Field of view, 7mm PPL]. b) Close-up of k-feldspar grain (fspr) surrounded by carbonate (cb), quartz (qtz) and sericite (sr) [Field of view 2mm, XP].....	78



<b>Plate 3.29:</b> Photomicrograph of section from sample JOD81A from the Greenwood Pond #2 Prospect showing a fine-grained, sericite (Ser) and chlorite altered gabbro with some original quartz, hornblende (Hb) and albite (Ab) preserved. Hornblende is being altered to chlorite and cubic pyrite disseminations are also present [Field of view 2mm, PPL].	79
<b>Plate 3.30:</b> Rolling Pond Prospect. a) Vuggy, well formed quartz crystals [penny for scale], b) Quartz breccia subcrop [pencil for scale].	109
<b>Plate 3.31:</b> View along Chiouk Brook with S. Hinchey standing at the Chiouk Brook Prospect.	109
<b>Plate 3.32:</b> Breccia Pond Prospect. a) Main trench and stripped area, b) Hematite alteration halo around quartz veins in carbonized ultramafic rocks, c) Grab sample from trench 1 exhibiting alteration halo around small quartz vein, d) Red siliceous jasperoid.	110
<b>Plate 3.33:</b> Photomicrograph of sample JOD36B from the Breccia Pond Prospect exhibiting magnesite (Mg) and quartz (Qtz) brecciated hematized serpentinite (Hm-Sp) [Field of view 7mm, PPL].	85
<b>Plate 3.34:</b> Swan Lake Prospect. a) Quartz breccia with dark graphitic fragments. b) 5 cm thick quartz carbonate vein with sulphide staining exposed in trench apparently between a green siltstone unit and a black graphitic unit.	110
<b>Plate 3.35:</b> Lizard Pond South Prospect. a) Main trench and stripped area [J. O' Driscoll and S. Hinchey for scale], b) Large quartz breccia vein [hammer for scale].	111
<b>Plate 3.36a, b:</b> Photomicrograph of magnesite-altered serpentinite ultramafic host to the Lizard Pond South Prospect. Multiple generation of magnesite (Mg-carbonate) veining. Note mesh like texture and oxides from breakdown of igneous minerals. The second section photomicrograph exhibits blotchy pyrite mineralization [Field of view 2mm, PPL and XP].	87
<b>Plate 3.37:</b> Photomicrograph of sample JOD52A from a sample collected from the large stripped area at the Lizard Pond South Prospect [field of view 2mm, PPL]. a) Pyrite mineralization in quartz and magnesite with some serpentinite preserved. b) Mesh like texture of magnesite altered serpentinite with pyrite [Field of view 7mm, PPL].	88
<b>Plate 3.38:</b> Photomicrograph of sample JOD55A illustrating a snakeskin texture common in magnesite (Mg) altered serpentinite (Sp). A grain of chromite is visible in the section [Field of View, 7mm, PPL].	89

<b>Plate 3.39:</b> Huxter Lane Prospect sample consisting of quartz breccia. Brecciated felsic material is mineralized along grain boundaries. The sulphide mineralization is primarily arsenopyrite with minor pyrite.....	111
<b>Plate 3.40:</b> Photomicrograph of sample W03-38 from Huxter Lane illustrating porphyritic fragments in a very fine-grained matrix [Field of view 2mm and 7mm, PPL].....	90
<b>Plate 4.1:</b> Interlayered siltstone and limestone beds with laminations parallel to pencil. A fossiliferous layer where fossils have been weathered out, leaving impressions, is outlined in red.....	150
<b>Plate 4.2:</b> Photomicrograph of sample JOD96K from the Duder Lake transect; note lithic quartz detrital grains in a fine-grained matrix [Field of view 7mm, PPL].....	115
<b>Plate 4.3:</b> Photomicrograph of sample JOD96J from Duder Lake transect. A) Large dolomite crystal [Field of view 2mm, PPL]. B) Epidote alteration around Fe-oxide [Field of view 7mm, PPL] (Dol=dolomite; Ox=Fe-carbonate staining; Ep=epidote).....	116
<b>Plate 4.4:</b> Hand specimen JOD66 from the knobby gabbro exposure north of Duder Lake [penny for scale].....	150
<b>Plate 4.5:</b> Photomicrograph of an altered phaneritic pyroxene gabbro collected north of Duder Lake. Elongate, subhedral pyroxene (augite) crystals exhibit uraltite alteration (Ur) with Ca-plagioclase (Pl) and serpentinite (Sp) occupying spaces between crystals. Minor epidote overprints the minerals and minor biotite is also present [Field of view 7mm, PPL].....	117
<b>Plate 4.6:</b> Sample JOD08 photographed where it was removed from outcrop of the Bellman's Pond Conglomerate (sample is approximately 15 cm in length).....	151
<b>Plate 4.7:</b> Cut section from sample JOD08 left over from removal of the volcanic clast. Several smaller volcanic clasts (red arrow) were identified in this section. The outline of the fragment is also noticeable on the left hand side (blue arrow) [penny for scale].....	117
<b>Plate 4.8:</b> Photomicrograph of sample JOD08, a clast in the Bellman's Pond Conglomerate exhibiting altered feldspar (Fdr) and quartz (Qtz) porphyroblasts in a fine-grained matrix (Mtx) [Field of view 7mm, XP]. This section indicates that a felsic volcanic lithology is present in the conglomerate.....	123
<b>Plate 4.9:</b> Gabbro exposure along Birchy Bay Resource road from which sample JOD57A was collected [Sheldon Huelin for scale].....	152



<b>Plate 4.10:</b> Gabbroic body along Birchy Bay Resource Road (southwest of Duder Lake) as mapped by Evans <i>et al.</i> (1992) and Currie (1995a). A) Rounded, weathered exposure of jointed gabbro [S. Heulin for scale], B) Sub-parallel quartz veins in gabbro [field book and rock hammer for scale].....	152
<b>Plate 4.11:</b> Photomicrograph of sample JOD04-09 collected from an intrusive body west of Ten Mile Lake. The sample comprises hornblende (Hb), plagioclase (Pl), clinopyroxene (Cpx) and Fe-Ti oxides and is classified as an aphanitic gabbro [Field of view 7mm, PPL].....	126
<b>Plate 4.12:</b> Photomicrograph of sample JOD04-13 from an unmapped intrusive body east of Ten Mile Lake. The sample is comprised of plagioclase (Pl), clinopyroxene (Cpx), hornblende (Hb), titanite (Ti), minor Fe-Ti oxides and disseminated sulphides [Field of view 7mm, PPL].....	127
<b>Plate 4.13:</b> Gabbro exposure of elongate ridge near Twin Ponds as mapped by Evans <i>et al.</i> (1992) [field notebook for scale].....	153
<b>Plate 4.14:</b> Photomicrograph of sample JOD100 collected from an intrusive body as mapped by Evans <i>et al.</i> (1992). The sample comprises plagioclase (Pl), hornblende (Hb), and minor clinopyroxene, biotite, chlorite and opaque minerals [Field of view 7mm, PPL].....	128
<b>Plate 4.15:</b> Hand specimen (JOD04-12) bearing re-crystallized fossil casts. A re-crystallized crinoid column is outline in red [pencil for scale].....	153
<b>Plate 4.16:</b> Re-crystallized, deformed limestone outcrop along Ten Mile Lake Resource Road from which sample JOD04-12 was collected [pencil for scale].....	154
<b>Plate 4.17:</b> Polished slab of Lower Carboniferous limestone composed mostly of crinoid columns; view is about 16 cm across (after Stearn and Carroll, 1989).....	129
<b>Plate 4.18:</b> Hand Specimen (JOD04-14) bearing fossils. Re-crystallized crinoid columns are outlined in red [Penny for scale].....	154
<b>Plate 4.19:</b> Ten Mile Lake Resource Road, purple fossiliferous bed from which sample JOD04-14 was collected [GPS for scale].....	155
<b>Plate 4.20:</b> A) Hand sample 120, collected from dark, dense sedimentary interbeds in Davidsville group shale in the Appleton Pit. The sample is cut by a 4 cm wide quartz vein and exhibits sub-parallel quartz filled tension gashes. B) Close up of sample JOD120 showing disseminated sulphide mineralization in altered sediment [tack for scale].....	155

<b>Plate 4.21:</b> Photomicrograph of sample JOD04-20 exhibiting plagioclase (Pl), Hornblende (Hb) and minor pyroxene and biotite [Field of view 7mm, PPL].....	132
<b>Plate 4.22:</b> A-B) Gabbro (Ga)- granite (Gr) contact at Salmon River. The outlined area in A illustrates a piece of gabbro stoped by the intruding granite [rock hammer for scale].....	156
<b>Plate 4.23:</b> Photomicrograph of sample JOD 04-17 which consists of quartz (Qtz), microcline (Mc), Plagioclase (Pl) and minor biotite (Bt) [Field of view 7mm PPL].....	139
<b>Plate 4.24:</b> A) Load casts in Indian Islands Group siltstone [Pencil for scale], B) View upriver, X marks fossil debris flow location, 3) close up of fossil local [Pen for scale], 4) Derek Wilton and Steve Hinchey at contact of Indian Islands Group and Caradoc shale.....	156
<b>Plate 4.25:</b> a) Photomicrograph of sample JOD39A exhibiting subangular quartz grains in a fine-grained matrix. c,d) Photomicrograph of sample JOD39B exhibiting a quartz-carbonate vein [Field of view 7mm, PPL and XP].....	145
<b>Plate 4.26:</b> Cooper Brook exhibiting red and green interbedded siltstone with boudinaged limey beds [rock hammer for scale].....	157
<b>Plate 7.1:</b> BSE image of an ablation pit in a pyrite grain from sample JOD23 collected from the Hurricane Prospect (image ~ 175 µm wide). ....	229
<b>Plate 7.2:</b> Pictures of outcrop at the Bowater Prospect exhibiting multiple quartz veining in Davidsville Group sediment.....	244
<b>Plate 7.3:</b> Siliceous outcrop at the Mustang Zone, Outflow Prospect.....	244
<b>Plate 7.4:</b> Conjugate quartz veining in diorite, approximately 100 m upriver from the Hurricane Prospect.....	244
<b>Plate 7.5:</b> Outcrop at the Stog'er Tight prospect on the Baie Verte Peninsula, representative of orogenic (or mesothermal) lode gold occurrences. Quartz veins in gabbroic host.....	245
<b>Plate 7.6:</b> Photomicrographs of a sample from the Gallery Resources Ltd. Bruce Pond epithermal system. The bladed pyrite crystals in this sample were analyzed as examples of low-sulphidation epithermal systems.....	245



<b>Plate 8.1:</b> a) Row of prismatic zircon grains from sample JOD21 mounted in an epoxy resin puck [Field of view 7mm PPL]. B) Close up of zircon grain from mount exhibiting brownish core [Field of view 2mm, PPL].....	254
<b>Plate 8.2:</b> Backscattered Electron Microprobe images for sample JOD25 of the Corsair Prospect, MPIS diorite. The grains appear to be elongate and homogenous with no apparent zoning.....	255
<b>Plate 8.3:</b> Backscattered electron microprobe images for Sample JOD100. The grains are mostly homogeneous but a few of the grains exhibit oscillatory compositional zoning.....	256
<b>Plate 8.4:</b> Backscattered electron microprobe images for Sample JOD04-17. The grains are very fractured and contain small inclusions.....	257
<b>Plate 8.5:</b> Backscattered electron microprobe images for Sample JOD90A, MPIS granite. Images reveal broken grains with mottled appearance and possible inclusions (the inclusions were not zircon).....	258
<b>Plate 8.6:</b> Backscatter Electron Microprobe images for Sample W03-38, Huxter Lane intrusive.....	260

# CHAPTER 1

## INTRODUCTION

### 1.1 Preamble

Structural and geological studies in central Newfoundland have been ongoing for over a century and through them knowledge of this tectonically complex region continues to evolve. With the development of plate tectonics theories in the 1960's, Newfoundland was quickly recognized as a significant region which exposes a well-preserved geological cross section through the Appalachian Orogen. The section includes remnants of opposing continental terranes, separated by vestiges of the Iapetus Ocean. The rocks and structures of the Eastern Dunnage Zone, central Newfoundland, record a geological history of closing/accreting oceanic tracts which generated geological environments favorable to Au mineralization.

This project is based on the study and comparison of 20 known gold occurrences within the area termed the 'Botwood Basin' of the eastern Dunnage Zone. The term Botwood Basin has been commonly used in press releases and exploration reports and encompasses a region comprised of Middle Paleozoic cover sequences that were deposited upon dominantly Ordovician rocks. Mineral exploration in the 1980-1990's led to the discovery of numerous auriferous vein-hosted orogenic occurrences on the Baie Verte Peninsula (Evans, 2005) and within the Dunnage Zone (Evans, 1996). Several styles of mineralization have been recognized in the Botwood Basin such as epithermal, orogenic (or mesothermal lode), and, more recently, Carlin style has been postulated. In

fact, the suggestion of, and evidence for, Carlin-type gold occurrences created a claim staking rush in central Newfoundland during 2002. With the recognition of the basin as a possible host for gold deposits it has become essential to fully understand the geological history of this area and the relations, if any, between the gold occurrences, host lithologies, and adjacent intrusions and structures.

## **1.2 Location and Access**

The study area is located in central Newfoundland and encompasses areas within several 1: 50,000 NTS map sheets including: 2D/5, 11, 12, 13, 14, and 15 and 2E/2, 3, 7 and 8 in UTM grid Zone 21, NAD 27 (Figure 1.1, p. 7).

Access to the various occurrences is generally good via a large network of forestry access roads owned and operated by Abitibi Consolidated originating from major routes such as the Trans Canada Highway (route 1), the Baie d'Espoir Highway (route 360) and the Gander Bay Highway (route 340). A series of muskeg trails and drill paths which once provided fair access to many occurrences are commonly overgrown since the last documentation (*i.e.*, Evans, 1996) and trenches at some occurrences have been backfilled, preventing observation and sampling in those cases.

## **1.3 Physiography, Vegetation and Glacial History**

As the study area is regionally extensive, these parameters can vary and are generalized here. Commonly, the region has a gently rolling topography with elevations under 200 m dominated by extensive bogs in low lying areas and heavily forested areas at

higher elevations. The most prominent topographic feature in the region is the Mount Peyton Intrusive Suite, which is a 1400 km<sup>2</sup> elliptical body in the center of the map area that has elevations of up to 400 m above sea level.

Central Newfoundland experiences warmer summers and cooler winters than the rest of the island with relatively less summer precipitation and higher evaporation; these conditions lead to enhanced fire frequency. The forested areas are dominated by balsam fir with a good population of black spruce and white spruce in burnt over areas. Due to extensive glacial till cover and vegetation, outcrop exposure is often limited and best observed in ridges or along rivers, ponds and roads.

The region has a variety of ponds, lakes and rivers and only those that are referred to during this study are noted here due to the large extent of the area. The Gander River runs throughout the map area from the Great Bend region of the southern Botwood Basin to Gander Bay in the north. The southern Botwood Basin region contains Great Rattling Brook, Chiouk Brook, Breccia Pond, Swan Lake, Lizard Pond, Greenwood Pond, Paul's Pond, Beavers Brook and Coopers Brook. In the central region, Gander Lake, Twin Ponds and Salmon River are referred to. In the northernmost area Ten Mile Lake, Bellman's Pond, Duder Lake and Rocky Pond are referenced.

Based on examination of the surficial geology in the Comfort Cove-Newstead and Gander River map areas, four ice flow events were defined for the central and northern basin (Scott, 1994). Sediment dispersal was controlled by east to southeastward flow in the central region and by northeastward flow in the north (*op cit.*).



## **1.4 Previous Work**

Evans (1996, 1999) provides the most recent summary with respect to exploration for epigenetic gold occurrences within the Dunnage Zone. He described the various “epigenetic” gold occurrences within the eastern Dunnage Zone through both his own assessments and compilations of previous work.

Table A1.1 is presented as a compilation of past work conducted within the area commonly termed the “Botwood Basin” derived into tectonic, structural, metallogeny, geophysical and miscellaneous sections with a brief description of the objective and relevant results of each study. The table was compiled based on an extensive literature research going back to 1934. It is meant to provide a comprehensive and focused collection of relevant geoscientific work for ease of reference for all future work within the study region.

## **1.5 Methods**

Fieldwork for this project was mainly carried out over five weeks in July-August, 2003. During this period, the author conducted a general overview of the regional geology of the basin, visited and assessed known Au occurrences, and collected samples for petrography and geochemical research. A follow-up re-evaluation of selected areas was conducted in July, 2004. A total of 280 samples were collected from the field area in 2003 and 18 samples in 2004 including: 1) mineralized samples and host rocks (minimum of three samples per showing), 2) regional rock types, 3) samples for geochronology, and 4) fossiliferous samples for paleontological dating. The main foci

for sample collection and mapping were areas of previously recorded gold occurrences or prospects. Sample collection was also aimed towards the intrusive lithologies within the basin and mapping efforts in this area were geared towards the contact relationships where exposed. However, observation of contact relationships proved difficult as exposure is generally limited. Samples were transported to the Department of Earth Sciences, Memorial University of Newfoundland at the end of each field season and catalogued for storage and analysis. Samples were selected for whole rock geochemistry, sulphur isotope chemistry, pyrite trace element chemistry, U-Pb geochronology and petrological research. All samples were prepared and analyzed within the Department of Earth Sciences, Memorial University of Newfoundland.

Polished thin sections were prepared and examined under transmitted and reflected light to ascertain rock type, alteration or mineral assemblages. Major and trace element geochemical analyses were conducted on 40 samples (both sedimentary and igneous in nature), using X-Ray Fluorescence techniques (XRF). The igneous geochemical data were utilized to determine if any relationships exist between intrusive lithologies throughout the study area and the sedimentary geochemical data were used to further define host lithologies by determining possible source rocks and tectonic environments. Sulphur isotopic analyses were carried out on 40 mineralized samples in an attempt to characterize the mineralizing events.  $\delta^{34}\text{S}$  isotope ratios for pyrite, arsenopyrite, galena, and stibnite were analyzed on a VG-PRISM-903 mass spectrometer.

U-Pb geochronological studies were conducted on zircon grains from select lithologies using a Laser Ablation Microprobe-Inductively Coupled Plasma-Mass Spectrometer (LAM-ICP-MS) system to define the ages of host rocks and to determine

the temporal relationship between mineralization and intrusion events. Trace element analyses of pyrite grains from gold occurrences were also conducted on the LAM-ICP-MS to ascertain whether there was a definable distinction between deposit types (refer to Appendix 3 for description of analytical techniques and Appendix 4 for derived analyses).

## **1.6 Purpose and Scope**

Due to the enhanced exploration interest in the Botwood Basin auriferous occurrences, it is imperative to determine the relationships, if any, between the occurrences, host lithologies, adjacent intrusions and structures. Although geological knowledge of the area has evolved significantly with exploration, the vastness and the general lack of exposure throughout the region leave many unanswered questions about the extent of certain units and the contact relationships between each.

This project evaluated the various gold occurrences and associated geological environments within the basin to: 1) review previously defined geological units, specifically those known to host Au mineralization, and contact relationships therein, 2) determine ages of intruding lithologies both adjacent to, and host to, Au mineralization, 3) assess physio-chemical properties of the mineralizing fluids, and 4) determine the relationship, if any, between Au mineralization and adjacent intrusions and structures. These studies will build upon and add to the existing database for Au mineralization in the eastern Dunnage Zone and should provide further insight into the mechanisms of mineralization at this convergent plate boundary.

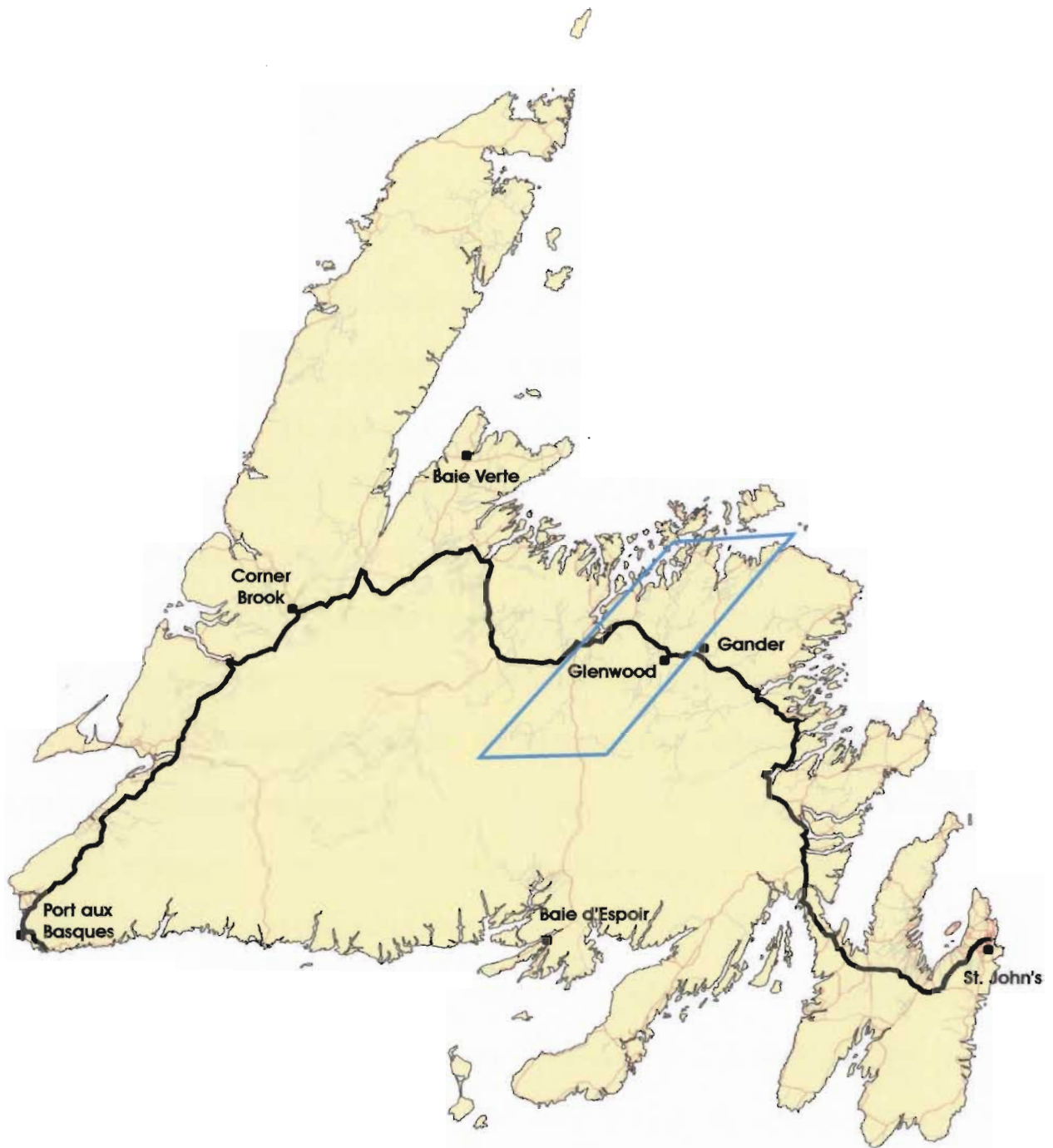


**Figure 1.1:** Map of the island of Newfoundland outlining the study area in blue and illustrating major routes and cities/ towns.



## CHAPTER 2

### GEOLOGICAL SETTING

#### 2.1 Regional Tectonic Setting

The tectonic history of the island of Newfoundland is complex as it represents the northeastern termination of the Appalachian Orogenic Belt, a Late Precambrian to Late Paleozoic mountain belt that extends southward through the Maritime provinces and Quebec into the eastern US to Alabama (Williams *et al.*, 1972; Williams, 1979). The Appalachian Orogen is related to the Caledonian Orogen of Greenland and Western Europe as both systems once formed a continuous mountain belt some 7500 km long prior to the opening of the Atlantic Ocean in Mesozoic time. Examination of the exposed cross section of the orogen that constitutes northeastern Newfoundland led to the interpretation that the Appalachian Belt is a “two-sided symmetrical system” (Williams, 1964) with a threefold division, a western platform, the central volcanic belt and the Avalon platform (Kay and Colbert, 1965).

Williams *et al.* (1972) proposed the first modern subdivision of the Appalachian system within Canada based upon contrasting Ordovician lithologies and structural development. Williams *et al.* (1974) reassessed the nine proposed zones and presented a more detailed description and nomenclature for the zones present in Newfoundland. The result was the subdivision of island geology into four NE trending Late Precambrian to lower Paleozoic tectonostratigraphic zones based on structural, depositional, tectonic, and volcanic-plutonic characteristics. The zones are generally fault bounded (Figure 2.1, p.

40). This more simplified zonal scheme allowed for a better fit into the Appalachian Orogen as a whole (Williams, 1978).

The Humber and Avalon Zones (Williams, 1978), or Humber and Avalon terranes (Williams and Hatcher, 1983), encompass the west and east margins of the system respectively, and represent continental platforms. Between these marginal zones, the central Paleozoic mobile belt (Williams, 1964) is composed of the Dunnage and Gander Zones or terranes (Williams, 1978; Williams and Hatcher, 1983) which represent relicts from the formation, development and subsequent destruction of an Early Paleozoic ocean defined as the “Proto-Atlantic Ocean” (Wilson 1966) or “Iapetus” (Harland and Gayer, 1972). The final closure of Iapetus occurred during the Late Ordovician to Early Silurian and resulted in a westward subduction (van Staal, 1994). This ultimately resulted in the collision of a continentally derived sedimentary wedge (Gander Zone) (van Staal *et al.*, 1996; Whalen *et al.*, 1996) and the previously accreted Exploits arc on the margin of Gondwana with the Laurentian margin (Humber Zone and Notre Dame Arc).

The Humber Zone comprises the ancient North American (Laurentian) continental margin of crystalline basement overlain by Early Paleozoic shelf-facies clastic and carbonate rocks (Whalen *et al.*, 1997). Allochthonous oceanic sedimentary and ophiolitic rocks were uplifted and emplaced upon continental margin rocks during the Ordovician Taconic Orogeny. Thus, this zone represents the development and destruction of an Atlantic-type passive continental margin on the SE margin of Laurentia (Swinden *et al.*, 1988); it is separated from the Notre Dame Arc (Dunnage Zone) by the Baie Verte Brompton Line-Long Reach Fault system (Williams and St. Julien, 1982).

The Dunnage Zone is characterized by Lower Paleozoic rocks, dominated by mafic volcanic rocks, ophiolitic suites, mélanges and associated greywackes, slates, cherts, and minor limestones (Williams, 1995). The zone is comprised of Cambrian to Silurian oceanic volcanic, hypabyssal, and epiclastic rocks that have been interpreted to represent relics of the Iapetus Ocean, which separated the Laurentian and Gondwanan continents (Wilson, 1966; Bird and Dewey, 1970; Harland and Gayer, 1972; Williams *et al.*, 1974; Williams 1979). Pre-Silurian rocks of this zone represent vestiges of the Iapetus Ocean and Cambrian to Middle Ordovician rocks represent accreted island arc-back arc basin systems and mélanges.

The present spatial relationships between the sequences within the zone were originally construed to be indicative of the spatial relationships extant within the Iapetus Ocean prior to accretion (*e.g.*, Bird and Dewey, 1970). The validity of this interpretation has been questioned (*e.g.*, Swinden *et al.*, 1990) based on the argument that the present spatial relationships between the units may result from accretionary processes rather than their position within the Iapetus Ocean. The Dunnage Zone therefore represents remnants from the development, evolution and subsequent destruction of the Iapetus Ocean (Williams, 1979). Williams *et al.* (1988) further subdivided the zone into two subzones, the Notre Dame Subzone and the Exploits Subzone (Figure 2.2, p. 41). The Dunnage Zone rocks are separated from the Gander Zone by the Gander River Ultrabasic Belt, a discontinuous belt of ophiolitic rocks (Jenness, 1958; Blackwood, 1982), now formally renamed the Gander River Complex (O'Neill and Blackwood, 1989).

The Gander Zone is characterized by a variety of metamorphic rocks and granitoid plutons (Kennedy *et al.*, 1982), as well as abundant pre-Silurian quartzose

clastic sedimentary rocks lacking volcanic detritus, which were deposited at or near a continental margin (Colman-Sadd, 1980; Colman-Sadd and Swinden, 1984). The rocks that comprise the Gander Zone are interpreted to lie structurally below the Dunnage Zone lithologies and outcrop in structural windows below the strata of that zone (Colman-Sadd and Swinden, 1984; Williams *et al.*, 1988). Thus, the Gander Zone is interpreted to represent the development and destruction of a continental margin located to the east of the Iapetus Ocean that possessed Celtic affinities (McKerrow and Cocks, 1977, 1986; Wonderly and Neuman, 1984). The zone was further subdivided into the Gander Lake, Mount Cormack, and the North and South Meelpaeg Zones (Williams *et al.*, 1988) and is separated from the Avalon Zone by the Dover Fault-Hermitage Flexure (Blackwood, 1976; Hammer, 1981; Williams, 1982; Holdsworth, 1992).

The Avalon Zone is characterized by Late Precambrian volcanic and sedimentary rocks overlain by Early Paleozoic shallow marine sedimentary sequences (Kennedy *et al.*, 1982; Swinden *et al.*, 1988). During Cambro-Ordovician time, the zone was a stable marine platform of predominantly platformal carbonates and siliciclastics. The zone is representative of either remnants of rifting and opening of Iapetus during the Precambrian (Papezik, 1972) or a subduction cycle that predated the opening of Iapetus (Rast *et al.*, 1976).

The Newfoundland tectonostratigraphic zones have been variably affected or locally deformed by the following events: 1) Precambrian Avalonian Orogeny (Hughes, 1980). 2) Middle Ordovician Penobscot/ Taconic Orogeny (Rodgers and Neale, 1969; Stevens, 1970; Williams, 1975; Colman-Sadd, 1980, 1982), 3) Middle Silurian Salinic Orogeny (Karlstrom *et al.*, 1982; Dunning *et al.*, 1990), 4) Devonian Acadian Orogeny



(Boucot *et al.*, 1964; Williams, 1983) and 5) Carboniferous Alleghanian Orogeny (Bradley *et al.*, 1982; Hyde *et al.*, 1988) (after Churchill, 1994).

Definition of the different zonal divisions within Newfoundland has been further advanced through deep crustal seismic refraction studies across the Newfoundland Appalachians (Keen *et al.*, 1986; Quinlan *et al.*, 1992), which have provided insight on the crustal basement to the zones and the nature of the boundaries that separate them. Keen *et al.*, (1986) suggested that the geophysical surveys revealed the existence of three lower crustal blocks (LCB) to the Newfoundland Appalachians: the western block (otherwise referred to as the Grenville LCB), the central LCB, and the Avalon LCB to the east. The authors inferred that the Grenville and central LCBs extended beneath the Dunnage Zone and shared an apparent sutured contact (Keen *et al.*, 1986). Seismic modeling by Quinlan *et al.* (1992) of the LCBs indicated that two, not three, LCBs are present. The earlier interpretation that the Avalon and central LCBs cut the Moho (Keen *et al.*, 1986) was dismissed. The new modeling indicated that the eastern block, referred to as the Gondwanan plate (correlative with the central and Avalon LCBs of Keen *et al.*, 1986), had been thrust under the western block or Laurentian plate by at least 200 km (correlative with the Grenville LCB of Keen *et al.*, 1986). The seismic data also provided new insight into the boundaries that separate the zones, with particular importance to the bounding structures of the Dunnage Zone. The data indicated that the Baie Verte-Brompton Line and the Gander River Complex cannot be traced to any considerable depth and therefore do not extend deep into the earth's crust. This conclusion supported the suggestion by Colman-Sadd and Swinden (1984) that the Dunnage Zone was

allochthonous upon the rocks of the adjacent zones (Keen *et al.*, 1986; Quinlan *et al.*, 1992).

## **2.2 Geological Development of the Dunnage Zone (Pre and Post Accretion)**

The geological development of the Dunnage Zone had originally been described, based on stratigraphic observations, as a product of subduction and obduction of oceanic crust during the Middle Ordovician (*i.e.*, Williams and Stevens, 1974). This basic model interpreted the ophiolites as representing the Cambrian to Early Ordovician oceanic crust derived from the opening of Iapetus, and the thick Early to Middle Ordovician volcanic/epiclastic sediments as representing arc material deposited during ocean closing. The orogeny was described in terms of two events, an Early to Middle Ordovician Taconian Orogeny wherein oceanic terranes were accreted to Laurentia, and a Silurian to Devonian Acadian Orogeny that represented a period of granitoid plutonism (Colman-Sadd, 1982). However, such a model, which implies that the Dunnage Zone was a single comprehensive unit, was assumed to be an oversimplification by subsequent workers. Geochemical analysis of representative rocks suggested that some of the ophiolites formed in a suprasubduction environment and that some of the volcanic and epiclastic rocks did not originate in arc environments (Coish *et al.*, 1982; Dunning and Chorlton, 1985; Jenner and Fryer, 1980). Furthermore, geochronological work suggested that some of the island arc sequences were older than the oldest known ophiolite sequences (Dunning and Krogh, 1985; Dunning *et al.*, 1991; Evans *et al.*, 1990).

This evidence was used by Williams *et al.* (1988) to subdivide the Dunnage Zone into two subzones, the Notre Dame Subzone and the Exploits Subzone based on contrasts in stratigraphic, geochemical and geophysical relationships. The Red Indian Line, a late rectilinear fault or fault system, separates the two subzones. The Exploits Subzone to the east of the Red Indian Line is mainly composed of Ordovician deep marine sedimentary rocks, Silurian shallow marine to fluvial sedimentary rocks and subaerial volcanics. Silurian-Devonian granitic and gabbroic bodies intruded these rocks. Within and along the south and southeast margins, structural windows expose rocks of inferred Gander Zone affinity (mainly the Mount Cormack and Meelpaeg subzones) (Colman-Sadd and Swinden, 1984) (Figure 2.3, p. 42).

The Notre Dame Subzone lies to the northwest of the Red Indian Line and is characterized by metavolcanic rocks that were intruded by alkalic granitic bodies that differ from those in the Exploits Subzone. These rocks were deposited during the Cambrian to Early Ordovician in intra oceanic island arc and back arc basin environments and were eventually accreted to Laurentia during the Taconic Orogeny (Coish *et al.*, 1982; Williams and Hatcher, 1983; Swinden, 1991).

Building on these new observations, the genesis of most of the Dunnage Zone was shown to be post obduction (Swinden *et al.*, 1990; Colman-Sadd *et al.*, 1992) with a metamorphic and plutonic climax during the Silurian (Currie *et al.*, 1996; Dunning *et al.*, 1990). Structural work promoted these ideas as it was shown that significant deformation and movement occurred between the oceanic terrane and its basement rocks (Cawood, 1989).



As previously stated, the Dunnage Zone rocks represent vestiges of the Iapetus Ocean (Williams, 1979) and its geological history is therefore best described in terms of pre and post accretionary events (Swinden, 1990).

### **2.2.1 Pre-Accretion**

This stage records contemporaneous development of island arcs and back arc basins in the Iapetus Ocean during the Cambrian to Mid-Ordovician or Early Silurian. Distal turbidities were deposited as pre- and syn- accretionary sediments during a lull in Middle Ordovician volcanism forming the Caradocian black shale (Dean, 1977). There was widespread flyschoid sedimentation within fault-bounded basins of the east-central Dunnage Zone during the progressive closure of Iapetus during the Late Ordovician to Early Silurian (Dean, 1978; Kean *et al.*, 1981; Szybinski *et al.*, 1990).

The Davidsville Group (Kennedy and McGonigal, 1972) was deposited as part of these events. It comprises a thick sequence of distal, back-arc turbidities, containing detritus derived from older arc systems to the west, that was “deposited on allochthonous oceanic basement rocks of the Gander River Complex” (Blackwood, 1982). The Exploits Group (Helwig, 1969) was also deposited at this time.

Geological continuity between most of the arc systems has not yet been fully defined (Evans, 1999). The two subzones of the Dunnage Zone were first discriminated based on the differences in pre-Silurian stratigraphy as noted by Williams *et al.* (1988). The Notre Dame Subzone exhibits a widespread sub-Silurian unconformity which separates Early Ordovician rocks from the overlying Early Silurian terrestrial volcanics

and sediments. In contrast, the Exploits Subzone exhibits a somewhat continuous Middle Ordovician to Early Silurian marine sedimentation record (Evans, 1999). Isotopic studies (*e.g.*, Swinden, 1987; Swinden *et al.*, 1988) as well as geochronological studies (*e.g.*, Dunning and Krogh, 1985; Dunning *et al.*, 1986) support the distinctions between the two subzones, further suggesting that the opposing sides of the Red Indian Line represent tectonostratigraphically unrelated, juxtaposed Iapetus terranes.

### **2.2.2 Post-Accretion**

The Iapetus oceanic terranes began to accrete to the Laurentian margin at the end of the Early Ordovician. Crustal thickening resulted in epicontinental style volcanism and fluvatile sedimentation. The accretion of outboard terranes was virtually completed by the Early Silurian as indicated by overlap sequences and stitching plutons (Williams and Hatcher, 1983). Following accretion, the Silurian Botwood (Williams, 1962) and Indian Islands (Baird, 1958) groups were deposited as a result of continued epicontinental-style volcanism (Coyle and Strong, 1987) and shallow marine sedimentation. A period of widespread deformation, plutonism (*i.e.*, Mount Peyton Intrusive Suite, Blackwood, 1981) and metamorphism followed cratonization of the Iapetus tracts during a climatic Silurian Orogeny (Dunning *et al.*, 1990).

## **2.3 Geology and Stratigraphy of the 'Botwood Basin' and Environs**

Murray and Howley (1881) conducted the first geological survey in central Newfoundland. They described the geology along eastern Notre Dame Bay, Gander

River and Gander Lake and reported the first account of gold mineralization in the Dunnage Zone. Snelgrove (1934) reported on chromite occurrences associated with the ultrabasic rocks across Newfoundland. Subsequent studies concentrated on the mapping of coastal outcrops (*e.g.*, Twenhofel and Shrock, 1937; Twenhofel, 1947; Patrick, 1956; and Baird, 1958) during which various units were assigned Ordovician and Devonian ages. During the 1960s, reconnaissance mapping was completed through the region (Williams, 1964, 1970; Anderson and Williams, 1967) at a 1: 50,000 scale and initial stratigraphic correlations were postulated (Williams, 1967). Progressive studies and re-mapping conducted along the coast (*e.g.*, Kay, 1969; Currie *et al.*, 1980; Karlstrom *et al.*, 1982; Williams, 1992) and inland (Blackwood, 1980, 1981; Colman-Sadd, 1981; Colman-Sadd and Russell, 1982) built upon this stratigraphic framework.

This study area lies within the Exploits Subzone of the Dunnage tectonostratigraphic zone as defined by Williams *et al.* (1988). The subzone is primarily composed of Lower to Middle Ordovician sedimentary and volcanic rocks and mélanges. Shale, conglomerates and mafic volcanics dominate the eastern part of the subzone. The areas of interest (here referred to inclusively as eastern Dunnage Zone) lie within the region east of the Reach Fault and Noels Pond Line in the north and south, respectively and west of the Dunnage-Gander Zone boundary. The geology described herein is largely based on previous interpretations and it should be noted that the debate concerning the stratigraphy and its inherent relationships in the northern Botwood Basin is still very much ongoing.

The geology of the eastern Dunnage Zone will be presented in stratigraphic sequence and includes: 1) Cambrian to Ordovician Gander Zone rocks (exposed in the

Mount Cormack tectonic window); 2) Cambrian to Ordovician ophiolitic rocks of the Pipestone Pond, Coy Pond, Great Bend, Gander River and Duder Complexes, encompassing ophiolitic rocks, volcanics and /or sedimentary rocks; 3) Ordovician sedimentary and volcanic rocks (Davidsville and Baie d'Espoir groups and Caradocian shale); 4) Silurian sedimentary and volcanic rocks (Indian Islands, Botwood and Badger groups, Ten Mile Lake Formation and Stoney Lake volcanics); and 5) Siluro-Devonian intrusive rocks (Mount Peyton Intrusive Suite) (refer to Figure 2.4, p. 44 and Figure 2.5, p. 45 for a general geology map and stratigraphic column, respectively).

### **2.3.1 The Mount Cormack Subzone - Spruce Brook Formation (Late Cambrian-Middle Ordovician)**

The Mount Cormack Subzone of the Gander Zone is composed of sedimentary rocks that are exposed as a thrust-bound window beneath the overlying allochthonous Exploits Subzone (Colman-Sadd and Swinden, 1984). The thrusts are outlined by dismembered ophiolitic complexes that were emplaced during the Late Arenig Penobscot Orogeny (Colman-Sadd *et al.*, 1992). The Spruce Brook Formation, Gander Group, is composed of interbedded grey sandstone, siltstone and shale with minor conglomerate and limestone beds. The unit has undergone greenschist and amphibolite facies metamorphism at the Great Bend locality.



### **2.3.2 Pipestone Pond, Coy Pond and Great Bend Complexes (Late Cambrian-Middle Ordovician)**

The Pipestone Pond, Coy Pond and Great Bend Complexes surround the Mount Cormack Inlier (Colman-Sadd and Swinden, 1984; Zwicker and Strong, 1986) which outcrops near the great bend of the Northwest Gander River. The complexes are largely composed of ultramafic rocks and gabbros with local diabase and pillow lavas and sedimentary units; the sedimentary units consist of interbedded black shale and fine-grained sandstone, and conglomerate with mafic volcanic clasts (Colman-Sadd, 1985; Swinden, 1988; Colman-Sadd, 1989).

### **2.3.3 Gander River Complex (Early Ordovician)**

The Gander River Complex (GRC), as defined by O' Neill and Blackwood (1989), contains dismembered ophiolite sequences which were emplaced against the Gander Group by major low to high angle thrust faulting during the Acadian Orogeny. The Davidsville Group was deposited on the GRC. As such, the GRC defines the NE boundary of the Exploits Subzone and is comprised of small mafic-ultramafic rock bodies that look like incomplete ophiolite suites (Blackwood, 1978; Blackwood, 1982).

The GRC forms a narrow linear zone that lies west of, and structurally above, the Gander Group. It is mainly composed of pyroxenite, serpentinite, gabbro, talc, tremolite zones, mafic flows and related volcanoclastics and trondjemite with associated quartz porphyry units (Snow, 1988).

#### 2.3.4 Duder Complex (Early Ordovician-Early Silurian?)

The Duder Complex was postulated to have formed as a result of a significant west-directed Lower Ordovician to Silurian subduction along the Dog Bay Line, defining an accretionary wedge prism on the hanging wall of the subduction zone (Williams *et al.*, 1993; Currie, 1995b). There is an ongoing debate concerning the origin of this unit (*cf.* Currie and Williams, 1995, Currie, 1995b; Currie, 1997; Dickson, 2005). The Duder Group (Currie, 1993) was informally renamed the Duder Complex (Currie, 1994) and it has been suggested that it comprises the basement to the region between the Reach Fault and the Dog Bay Line (Currie, 1995a). The sedimentary rocks that were assigned to the Duder Group were originally identified as part of the Botwood Group (Evans *et al.*, 1992) but were removed based on the presence of intense cleavage and the lack of sedimentary features (Currie, 1993). A section of schist has been mapped in the Duder Lake region and is postulated to underlie two thirds of the Duder Complex. Rare plagioclase porphyry dykes cut the sedimentary units and the gabbroic bodies (Currie and Williams, 1995).

The complex is now defined as an Early Silurian accretionary prism consisting of (Ordovician?) intensively fissile shale and siltstone (Duder Group) and a *mélange* (originally called the Garden Point *Mélange*). Tectonic inclusions of exotic gabbro and basalt as well as sedimentary blocks have been reported (Williams *et al.*, 1993; Currie and Williams, 1995) which range in size from centimeters up to tens to hundreds of meters and strike parallel to cleavage (Currie, 1995a). The gabbroic bodies that host auriferous mineralization at Duder Lake were originally mapped as dykes (Churchill and

Evans, 1992) but were redefined as tectonic inclusions in the Duder Complex by Currie (1994) due to a supposed lack of intrusive relationships both at surface and in drill core (refer to Currie, 1995b). However, Churchill *et al.* (1993) state, “drill core samples of the gabbro bodies that host the Corvette and Goldstash mineralization have chilled margins and host sedimentary rocks are hornfelsed proving the intrusive relationship”. It was also suggested that the gabbroic blocks could be correlatives of the younger gabbroic bodies that cut the Ten Mile Lake Formation to the southwest (Currie and Williams, 1995). The reconnaissance mapping and literature review conducted during the current study does not support the grouping of these gabbroic bodies as tectonic inclusions. For instance, the author observed mappable sedimentary units, which had also been previously interpreted as tectonic blocks, and Churchill *et al.* (1993) observed chill margins in the gabbro in drill core. Furthermore, geochemical and petrographic analyses of the Duder Lake dykes and the intrusive gabbroic dykes to the southwest do not imply a genetic relationship.

The date of formation of the unit is still uncertain as Williams *et al.* (1993) suggested an Ordovician age, whereas Currie (1997) prefers a younger age based on an interpreted Silurian (with the possibility of an older) deformation of the complex. Currie (1997) noted that fossiliferous blocks of limestone in the complex are possibly Indian Islands Group.

Recent work involving the re-mapping of the Indian Islands Group and re-defining its relationships with adjacent units has suggested that much of the area mapped as the Duder Complex (*i.e.*, Currie, 1997) is more likely part of the Indian Islands Group (Dickson, 2005). This interpretation was based on the presence of several fossiliferous

horizons resembling Indian Islands Group lithologies and a preliminary correlation between the fauna. Furthermore, Dickson (2005) found that the assignment of entire islands composed of Indian Islands Group rocks in the north (previously assigned to the Indian Islands Group (Currie, 1995b)) as blocks in the Duder Complex (Currie, 1997)) may have led to an erroneous interpretation of a Silurian age for the Duder Complex (*i.e.*, Currie, 1997). Dickson also concluded that extensive mappable volcanic units within the complex argue against it being a *mélange*. Williams *et al.* (1993) also found that the igneous rocks in the Duder Group were cogenetic. Dickson (2005) suggests that a more acceptable interpretation would be that the Duder Complex is indeed Ordovician, as suggested by Williams *et al.* (1993), and was subsequently deformed along with the Indian Islands Group.

The Duder Complex appears to be conformably overlain by the Ordovician to Silurian Badger and Botwood groups (Currie, 1995a). Currie (1997) also postulated that the Ten Mile Lake Formation conformably overlies the Silurian Indian Islands Group and has conformably overstepped the Duder Complex in certain places. Dickson (2005) argues that such an interpretation with the Ten Mile Formation conformably overlying both the Indian Islands Group and the Duder Complex does not make geological sense if the Indian Islands Group is supposedly younger than the Duder Complex. His findings, coupled with the results from the current study make the case for a possible extension of the Indian Islands Group to the north and west, which would cross the Dog Bay Line (a major terrane boundary). If the group can indeed be extended across the presently defined Dog Bay Line, then either the location for the line is incorrect, or the interpretation of the line as a major terrane boundary is incorrect.



### 2.3.5 Davidsville Group (Ordovician)

The Davidsville Group (Kennedy and McGonigal, 1972) consists of massive, homogeneous, intensely cleaved black shale. The group was subdivided into mappable units, first by Pickerall (1979) who divided the group into six units without defining a formal stratigraphy, and more recently by O' Neill and Blackwood (1989). The latter workers informally divided the group into a lower Weir's Pond Formation, a middle Hunts Cove Formation, and an upper Outflow Formation. Currie (1995a) informally removed the Weir's Pond Formation from the Davidsville Group and defined it as a marine shelf sequence consisting of calcareous quartz sandstone, limestone and limey shale. The name Barry's Pond Formation was introduced to represent the breccia and conglomerate that had been assigned to the Weir's Pond Formation by O'Neill and Blackwood (1989) (Currie, 1992). The proposed redefined stratigraphy would then consist of a basal Barry's Pond Formation (informal), a middle Hunt's Cove Formation and an upper Outflow Formation (Currie, 1995).

The Davidsville Group comprises undivided black slate and/or shale, sandstone, siltstone, greywacke, and argillaceous siltstone of island arc provenance and thinly bedded turbidites and contourites fed by arc systems located to the NW (Blackwood, 1982). The group consists of continentally derived sediment, deposited as fining-upwards-turbidite sequences on a somewhat stable slope. The group exhibits isoclinal folding. The Davidsville Group contains local volcanic lithologies in the north. The volcanics are coarse mafic pyroclastics in massive to thick graded units, pillow lavas, and cherts, all interpreted to be disrupted blocks of Carmenville *mélange* (Pajari *et al.*, 1979)

or erosional remnants of a structural slice above the Carmenville mélange (Williams *et al.*, 1991).

Although the Davidsville Group is considered to be in tectonic contact with the GRC, nonconformable contacts have been reported locally. At Weir's Pond, upper Llanvirn to lower Llandeilo limestone overlies serpentinite (Stouge, 1979; O'Neill, 1987) and elsewhere conglomerates overlie ultramafics (Kennedy, 1975, 1976; Blackwood, 1982). The relationship between the Davidsville Group and the units to the west has had to be reconsidered with the extension of the Indian Islands Group to the south (*i.e.*, Williams, 1993) and the introduction of the Ten Mile Lake Formation to the north (*i.e.*, Currie, 1994). The contact between the Davidsville and Indian Islands (formerly considered Botwood) groups was originally observed to vary from conformable to faulted (Blackwood, 1982). However, the contact between these two units has only been observed along high angle east over west faults. The age of the Davidsville Group is constrained by the Arenig obduction of the Gander River Complex (Colman-Sadd *et al.*, 1992) and the Llandovery deposition of the overlying Indian Islands Group.

#### *2.3.5.1 Weir's Pond Formation (Middle Arenig-Caradoc)*

This lower formation outcrops sporadically along the western margin of the GRC and is an assemblage of fossiliferous limestone, graphitic shale, sandstone and conglomerate that is structurally imbricated with the GRC. The unit contains faunas ranging from Late Arenig-Early Llanvirn to Caradoc (O'Neill and Colman-Sadd, 1993).

#### *2.3.5.2 Hunt's Cove Formation (Caradoc)*

This middle formation has an assumed gradational contact with the Weir's Pond Formation and grades upward from a thickly bedded pebble to cobble conglomerate at the base into sandstone. The sandstone is fine to coarse-grained with local shaley interclasts and is interbedded with grey to black siltstone and slate; the conglomerate beds only form a minor component of the unit. The Hunt's Cove Formation has an abrupt, conformable contact with the Outflow Formation (O' Neill and Blackwood, 1989).

#### *2.3.5.3 Outflow Formation (Caradoc-Ahggill)*

This upper formation comprises the thick shale portion of the Davidsville Group, which includes a wide variety of lithologies ranging from siltstone-mudstone rhythmites through to mudstone rhythmites and finally various shale types and minor conglomerate (O' Neill and Blackwood, 1989). Currie (1995a) suggests that this unit could probably be subdivided in future work.

### **2.3.6 Baie d'Espoir Group (North Steady Pond Formation) (Middle-Late Ordovician)**

The North Steady Pond Formation is exposed in the Great Bend area and is composed of graphitic shale and phyllite, local polymictic conglomerate, and felsic, intermediate and mafic volcanic flows and/or pyroclastic rocks (Colman-Sadd 1980; Colman-Sadd 1985; Swinden 1988; and Dickson, 2000).

### **2.3.7 Caradocian Shale (Late Ordovician)**

The Caradocian shale is a widespread pelagic unit derived from the drowning of Cambro-Ordovician magmatic arc, arc rift and back arc complexes during a high stand of Iapetan sea level. Thus, the deposition of this unit signals the end of deep marine volcanism within the Exploits Subzone (O' Brien, 2003) and the emplacement of the Taconic allochthons (Dean, 1978; Williams and Hatcher, 1982; Williams, 1992). The shales were previously interpreted to have been Middle Ordovician ocean floor muds encased with manganese nodules adjacent to deep-water vents (Kay, 1975). The rocks typically have a cherty base, which was initially thought to indicate deep-water deposition, however, the presence of interbedded shallow water limestone, volcanic rocks and crossbedded sandstones complicated this interpretation (Dean, 1977).

The Caradocian black shale overlies the Dunnage Mélange (Dark Hole Formation) and is also recognized in the adjacent Lawrence Harbour Formation, Exploits Group. These shales are overlain by greywacke of the Point Lemington and Samson formations, respectively. Equivalent argillaceous facies are noted to occur in the slatey rocks of the Davidsville and Indian Islands groups.

Black carbonaceous argillites and argillaceous siltstones occur in the Duder Lake area in fault contact with the Botwood Group (Churchill, 1994) [this has later been reassigned to the Ten Mile Lake Formation by Currie (1994)] and graphitic black shale occurs in the Glenwood-Appleton area in fault contact with the Davidsville Group (Squires, 2005).



### **2.3.8 Badger Group (Late Ordovician-Early Silurian)**

The Badger Group comprises an Upper Ordovician to Lower Silurian marine turbiditic overstep sequence in the Exploits Subzone west of the Dog Bay Line (Williams *et al.*, 1993; Williams, 1995). The sequence grades upwards from a basal unit of greywacke with siltstone and conglomerate interbeds, through a middle conglomerate unit into an upper greywacke and siltstone unit. The group includes the Campbellton Greywacke, the Goldson Conglomerate and the Lewisporte Conglomerate (O' Brien, 2003) and is overlain by the Botwood Group (Williams, 1992). The Badger Group is in stratigraphic contact with the Duder Complex and in regionally conformable, but locally fault modified, contact with the Botwood Group northeast of Duder Lake (Currie, 1993; Williams, 1993). Details of the subunits of this group are not discussed in the context of this study.

### **2.3.9 Indian Islands Group (Silurian)**

The Indian Islands Group (Patrick, 1956; Baird, 1958) spans much of Silurian time and consists of shallow marine deposits grading upwards into terrestrial redbeds (Williams *et al.*, 1993). The unit was first recognized by Twenhofel (1947) east of the Dog Bay Line, northern Botwood Basin. The group was defined to comprise phyllitic slates, quartzite and calcareous sandstones, thin limestone lenses, conglomerate (Baird, 1958) and minor felsic volcanic rocks (Patrick, 1956). It was originally assigned to the Botwood Group and the boundary between the units was described as being faulted (Williams, 1964). Further south, in the Glenwood-Appleton area, units of this group

were also assigned to the Botwood Group (Blackwood, 1982; Boyce *et al.*, 1993), but were later reassigned to the Indian Islands Group based on the overly shaley and calcareous nature of the rocks (Williams, 1993). The group is now defined as isolated sequences along the east side of the Dog Bay Line (Williams *et al.*, 1993)

Along the north coast the group is in unconformable contact with a dark shale unit of the Ordovician Hamilton Sound Group that has been recognized as Caradocian shale (Currie, 1995); this contact was originally interpreted as approximately conformable (Currie, 1993; Williams, 1993). Along much of its eastern boundary, the Indian Islands Group is in contact with the Ordovician Davidsville Group. The contact was previously interpreted as a fault boundary (Williams, 1972) or an unconformity (Currie *et al.*, 1980), but was later reinterpreted as conformable (Wu, 1979; Karlstrom *et al.*, 1982). More recent work (*i.e.*, Williams, 1993; Squires, 2005; O' Driscoll and Wilton, 2005) has suggested that the contact is possibly conformable but fault modified. The group grades upwards into red shale of the Ten Mile Lake Formation (Currie, 1995a).

The Indian Islands Group (1 km thick) represents a Silurian marine shelf assemblage (Williams, 1993) in three formations: the Seal Cove Formation, the Charles Cove Formation and the Horwood Formation. It exhibits a single period of close upright isoclinal folding with the same style as that seen in the Davidsville Group (Currie, 1995a).

#### *2.3.9.1 Seal Cove Formation (Llandovery)*

The Seal Cove Formation encompasses an Early Silurian unit consisting of discontinuous coralline and limestone breccias with *Halysites* (Currie, 1995a). Grey calcareous siltstone with fossiliferous limestone beds occur locally and are overlain by grey to black shale with thin beds of pale buff siltstone; the basal layer is discontinuous and consists of coral-bearing limestone and limestone breccias (Currie and Williams, 1995). This unit is rich in fossiliferous material and contains *Halysites* coral (Llandovery) and brachiopod fauna. The formation is less than 10 m thick and is conformably overlain by the Charles Cove Formation (Currie, 1995a).

#### *2.3.9.2 Charles Cove Formation (Wenlock)*

The Charles Cove Formation is mainly a shallow marine shale and limestone sequence. Greenish-grey, hard calcareous siltstone is present with local fossiliferous limestone lenses ranging from 1-5 cm wide and up to 50 cm long (Currie and Williams, 1995). A Wenlock fossil was collected from this formation by Wu (1979). The minimum thickness of the unit is postulated to be about 600 m and it is conformably overlain by the Horwood Formation (Currie, 1995a)

#### *2.3.9.3 Horwood Formation (Ludlow)*

The Horwood Formation consists of grey to dark grey shale with thin interbeds of pale buff siltstone (Currie and Williams, 1995). The thickness of the unit ranges from 20

to 50 m and it grades upwards into red shale and siltstone, which has been assigned to the Ten Mile Lake Formation (Currie, 1995a).

#### **2.3.10 Botwood Group (Early Silurian-Early Devonian)**

The Botwood Group (Williams, 1964) dominantly consists of subaerial volcanic rocks and sandstones (Dean 1977) and was originally defined to comprise basal conglomerate and mafic volcanics with overlying sedimentary strata. This stratigraphy was subsequently revised by Williams (1972) when he subdivided the group to include only the Lawrenceton and Wigwam formations. The Goldson Formation had originally been assigned as a basal unit to the Botwood Group (Williams 1962, 1972) but was later informally reassigned to the Badger Group (Dean 1977, Williams *et al.*, 1995). The Botwood Group is composed of extensive, thick, subaerial, hematite-rich volcanic rocks of the Lawrenceton Formation overlain by fluvatile red and grey crossbedded sandstone of the Wigwam Formation (Williams, 1993). The group includes an upper polymictic conglomerate unit (Williams *et al.*, 1995) along the western margin. The formations are generally conformable but are fault disrupted in places (Williams, 1993; Williams *et al.*, 1993).

O'Brien (2003) reassigned some rock units from the Wigwam and Lawrenceton formations to the Badger Group and therefore informally redefined the Botwood Group to only include the terrestrial rocks of the Lawrenceton and Wigwam formations. He proposed that the group (1000 m thick) is actually comprised of two formations, a basal terrestrial volcanic unit (Lawrenceton Formation) and an upper red sandstone unit



(Wigwam Formation). The previously interpreted extent of the Botwood Group has been tapered along its eastern margin with the introduction of the Ten Mile Formation in the north (refer to Currie, 1995; Currie, 1997; Dickson, 2005) and the recognition of the Indian Islands Group to the south (refer to Williams 1993; Dickson, 1994; and Colman-Sadd, 1994 for a more detailed description of units).

The Botwood Group subaerial volcanic rocks are interpreted to be in conformable contact with the underlying marine greywacke-conglomerate assemblage (Badger Group) (Patrick, 1956; Baird, 1958; Williams, 1963; Eastler, 1969; McCann and Kennedy, 1974). Locally, unconformities between these two units have been reported (*i.e.*, Change Islands) (van der Pluijm *et al.*, 1989). The unit is overlain by the flat lying Stoney Lake volcanics in the southern study area and is in fault contact with the Duder Complex and Ten Mile Lake Formation to the north.

#### *2.3.10.1 Lawrenceton Formation*

This is the lower unit of the Botwood Group which conformably overlies the conglomerate unit or the Lower Silurian Goldson Formation (Dean, 1977). It comprises subaerial to terrestrial volcanic rocks that are faulted against the Wigwam Formation near Duder Lake. Elsewhere, a gradational contact has been observed between the units (O'Brien, 2003). The subaerial volcanic rocks are purple, red, green to black vesicular and amygdaloidal pillow basalts, breccias and porphyritic flows (Williams, 1995). This contact may have been originally conformable as seen west of Duder Lake, but is fault disrupted locally. The basalt of this formation is grey, fine-grained with amydgules that

are partially calcite-filled (Dickson, 1993). Red, laharic breccia of felsic volcanic rocks, felsic clast conglomerate and felsic tuff to grey basalt with plagioclase-porphyritic, amygdaloidal and massive flows and felsic tuff and minor red sandstone are also characteristic (Dickson, 1994).

The Lawrenceton Formation defines a bimodal mafic-felsic volcanic unit characterized by dominant vesicular basalt flows. Scoriaceous basalt and banded ignimbrite represent subaerial volcanic facies of the formation (O' Brien, 2003).

#### *2.3.10.2 Wigwam Formation*

This unit conformably overlies the Lawrenceton Formation and is characterized by red micaceous sandstone with local conglomerate at its base. It was deposited in a shallow water environment as indicated by cross bedding, ripple marks and mud cracks. Thin volcanic layers indicate that volcanism of the Lawrenceton Formation continued during deposition of the sandstone. The unit was subsequently intruded by Devonian granite and gabbros following the Acadian Orogeny (Dean, 1977).

The sediments consist of thin to medium bedded sandstone and siltstone (Dickson, 1993) and minor polymictic clast-supported conglomerate with felsic clasts typical of the underlying Lawrenceton Formation (Dickson, 1994).

This formation had been mapped as the most prominent unit in the Duder Lake area consisting of undivided micaceous and siliceous, red, brown, grey, and green siltstone, sandstone and shale. A few thin tuffaceous horizons in the Wigwam Formation were also reported east of Duder Lake (Churchill *et al.*, 1993). However, Currie (1995)

notes that this group has not been observed east of the Reach Fault as presumed by other authors (*i.e.*, Evans *et al.*, 1992; Churchill, 1994). The sediments that were originally assigned to the group in that region were reassigned to the Ten Mile Lake Formation. If this interpretation is correct, it would indicate an unconformity between the Wigwam and Lawrenceton formations.

### **2.3.11 Stoney Lake Volcanics (Late Silurian)**

The Stoney Lake Volcanics typically consist of grey to pink flow-banded rhyolites, rhyolitic tuff and agglomerate, porphyritic (feldspar) grey to purple rhyolite, crystal tuff and flow breccia. These lithologies do not resemble volcanic rocks of the Victoria Lake Group to the west or the Botwood Group to the north (Anderson and Williams, 1970). The Stoney Lake Volcanics are thought to unconformably overlie the Botwood Group sandstones because they were not affected by the steep folding observed in that unit. Clasts of Botwood Group have also been reported in the Stoney Lake Volcanics, which would infer them to be younger (Anderson and Williams, 1970). The Stoney Lake Volcanics have been dated at  $423 \pm 3$  Ma by Dunning *et al.* (1990). The inclusion of Botwood Group clasts within the volcanics, combined with structural relationships, therefore suggests that the Stoney Lake Volcanics are younger than the Botwood Group, presenting a possible upper age limit of Late Silurian (Ludlow) for that group.

### 2.3.12 Ten Mile Lake Formation (Late Silurian-Early Devonian)

The Ten Mile Lake Formation outcrops in the northern Botwood Basin and consists of purple to crimson shale interbedded with thin, pink sandstone beds and a few thick, pink to grey-green sandstone beds (Currie and Williams, 1995). The formation was originally considered to be part of the Wigwam Formation, Botwood Group. Williams *et al.* (1993) first recognized that a large area of homogeneous, red, cross-bedded sandstone and siltstone southwest of the Dog Bay Line were not in stratigraphic contact with the Botwood Group. They also suggested that there was a major unconformity between the redbeds and the Duder Group (now known as the Duder Complex) because of observed differences in structural styles (*i.e.*, the redbeds were gently dipping whereas the Duder Group was steeply dipping and very disrupted). The redbeds were officially removed from the Botwood Group by Currie (1995) when he introduced the term Ten Mile Lake Formation to represent them. Pridolian to Lochoulan bivalve fauna have been collected from this formation (Boyce *et al.*, 1993).

The formation conformably overlies the Indian Islands Group from which it has been mapped for up to 10 km to the west (Currie and Williams, 1995; Dickson, 2005). The transitional contact between the two aforementioned units was observed at several localities near Ten Mile Lake and Rocky Pond; some of these localities yielded fauna in limestone interbedded with red sandstone (Dickson, 2005). As previously discussed, the formation appears to be in fault contact with the Botwood Group to the west. This unit has not been mapped south of the TCH.



### 2.3.13 Mount Peyton Intrusive Suite (Middle Silurian-Early Devonian)

This gabbro-granite intrusion was informally named the Mount Peyton pluton by Strong *et al.* (1974). The authors conducted a lithological survey on the northern segment of the pluton and the resulting geochemical data defined the pluton as bimodal with few intermediate silicate phases. It was later suggested that the granite formed from crustal anatexis induced by the intruding gabbro (Strong, 1979; Strong and Dupuy, 1982). The intermediate phases were interpreted to result from magma mixing and/or contamination of the mafic magma by sedimentary country rocks.

The granite is pink and cream, massive, medium to fine-grained, equigranular and contains biotite  $\pm$  hornblende. The gabbro is a grey, massive and dominantly fine-grained, equigranular pyroxene  $\pm$  biotite  $\pm$  hornblende rock (Dickson, 1994).

Thus, the Mount Peyton Intrusive Suite (MPIS) is a composite Silurian post kinematic intrusion consisting of gabbro, tonalite, granodiorite, and diorite (Dickson, 1992) at lower greenschist facies. The relationship between the gabbro and granite phases, as well as the relationship of the suite to the surrounding sedimentary lithologies, is still poorly understood due to the lack of contact exposures. Although the contacts are not well exposed, the intrusive nature of the gabbro portion of the suite is clearly defined by a well-defined metamorphic aureole (within the Exploits Group) and associated mafic dykes and plugs along the western margin (Dickson, 1993). Although no definite evidence exists for a Botwood Group-MPIS relationship, several authors (*i.e.*, Dickson, 1993; Squires, 2005) have implied that a lack of intrusive evidence along the eastern margin may provide the best indication of a faulted contact between the MPIS and Indian

Islands Group. The relationship between the Botwood Group along the southern margin and the Indian Islands Group along the eastern margin of the intrusion is further explored in chapter 4 as part of the current study.

## **2.4 Faults**

Numerous faults cut the study area, ranging from minor to regional scale. These faults have significance to gold exploration because they could provide structural conduits for fluid flow and may localize mineralization events. The structures are discussed here in terms of those north and south of the TCH respectively for ease of reference.

### **2.4.1 Northern Botwood Basin Faults (North of TCH)**

Two major northeast-trending transcurrent faults occur in the northern Botwood Basin of the Exploits Subzone; the Reach Fault (Dean, 1978) and the Dog Bay Line (Williams, 1993). These faults are significant structures in the tectonic evolution of central Newfoundland and may be closely related to the metallogeny of the area. Several smaller faults with comparable geometries also outcrop in the area and appear to represent latest Silurian or younger movement (Churchill, 1994).

The Reach Fault has been defined as a brittle structure with a sinistral sense of shear and displacements of up to 15 km (Currie, 1993). It has long been debated whether this fault represents the final suture plane for the closing Iapetus Ocean (Arnott *et al.*, 1985; McKerrow and Cocks, 1986; Najjarpour and Upadhyay, 1987) and it has been

defined as the western periphery of the Botwood tectonostratigraphic belt (Williams, 1993).

The Dog Bay Line is manifested as a fault zone defined by a series of northeast-trending faults, up to 1 km in width, which exhibit a dominant topographic expression (Churchill, 1994). This complex zone has been described as a major Silurian terrane boundary (Williams *et al.*, 1993) but the suggestion that it represents the suture of the closing Iapetus has been questioned due to the continuity of faunal successions across it (*i.e.*, Williams, 1993). Despite this continuity, there are contrasts in Silurian strata across the line. Thick turbiditic sequences and sub-aerial volcanics west of the Dog Bay Line are not present to the east and marine calcareous rocks are absent to the west of the line. The fault zone has a curvilinear trace and has been mapped from the Indian Islands to Rocky Pond and has been postulated to extend as far southwest as the Mount Peyton Intrusive Suite with dextral transcurrent movement and dip-slip displacement (Williams, 1993).

East-west to northwest-southeast faults cut major northeast-trending features such as the stratigraphy and major faults as previously noted. These secondary faults may have been activated during the Early Devonian or Carboniferous as one of these structures was observed to truncate the Loon Bay Batholith (Churchill, 1994). These findings are in concordance with the work of Lafrance and Williams (1989) who suggested that many of the east-west trending faults in the Notre Dame Bay region may have been initiated in the Silurian but remained active through the Devonian.

Northeasterly-directed thrusts have been documented along the Gander River Complex (GRC). Sub-parallel thrusts cut the Davidsville Group (Tallman, 1990). In the

central-north easternmost Dunnage Zone, a northeasterly trending, westerly dipping structure forms a thrust contact between the GRC to the west and the Gander Group to the east. Also in this area, the Jonathan's Pond fault is a east-west trending structure that has been defined as a large shear zone or tear fault that may have developed syn-tectonically with the main thrusting event (Snow, 1988).

#### **2.4.2 Southern Botwood Basin (South of TCH)**

A brittle, low angle thrust, dipping 30° northwest, is recorded between the Indian Islands (formerly Botwood) and Davidsville groups at the Aztec Showing near Paul's Pond. The fault zone is defined by a graphitic gouge zone and is surrounded by silicified country rock (Tallman, 1990).

In the Great Bend area, numerous northeast-southwest and northwest- southeast trending faults have been mapped. The fault zone that is postulated to separate the Botwood Group and the Spruce Brook Formation coincides with a major northeast trending linear aeromagnetic anomaly and has a moderately plunging lineation to the northeast. Sinistral shear is recorded by southwest striking CS fabrics and the contact between the two units is interpreted to be tectonic rather than unconformable due to these sheared fabrics (Colman-Sadd and Russell, 1985).

### **2.5 Regional Deformation and Metamorphism**

A period of intense plutonism, deformation, metamorphism and reactivation of major fault systems attributed to the Acadian Orogeny occurred during the Late Silurian



to Early Devonian within the eastern Dunnage Zone. A regional northeast-trending penetrative cleavage and axial planar rotated isoclinal folds are observed in rocks of the Botwood and Davidsville groups. Second phase deformation features can be observed in the Davidsville Group as small conjugate kink bands with gently south plunging folds that exhibit  $f_1$  cleavage (Blackwood, 1982). The rocks have been exposed to lower greenschist metamorphism (Evans, 1999).

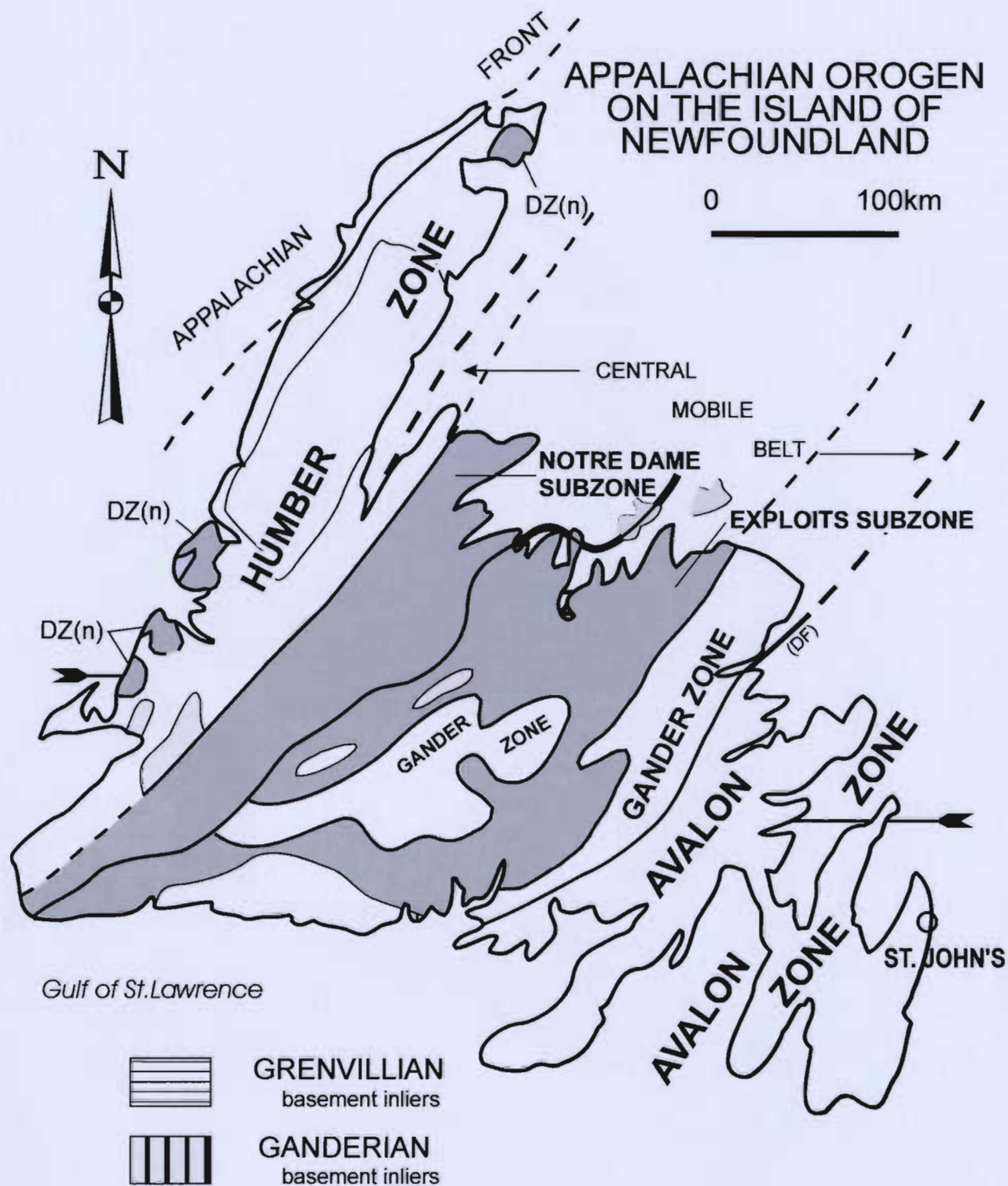


**Figure 2.1:** Tectonostratigraphic subdivision of the Newfoundland Appalachians. DZ(e)= Dunnage Zone; Exploits subzone; DZ(n)= Dunnage Zone; Notre Dame subzone; GZ= Gander Zone; HBF= Hermitage Bay Fault; DF= Dover Fault; RIL= Red Indian Line (from O'Brien *et al.*, 1996)

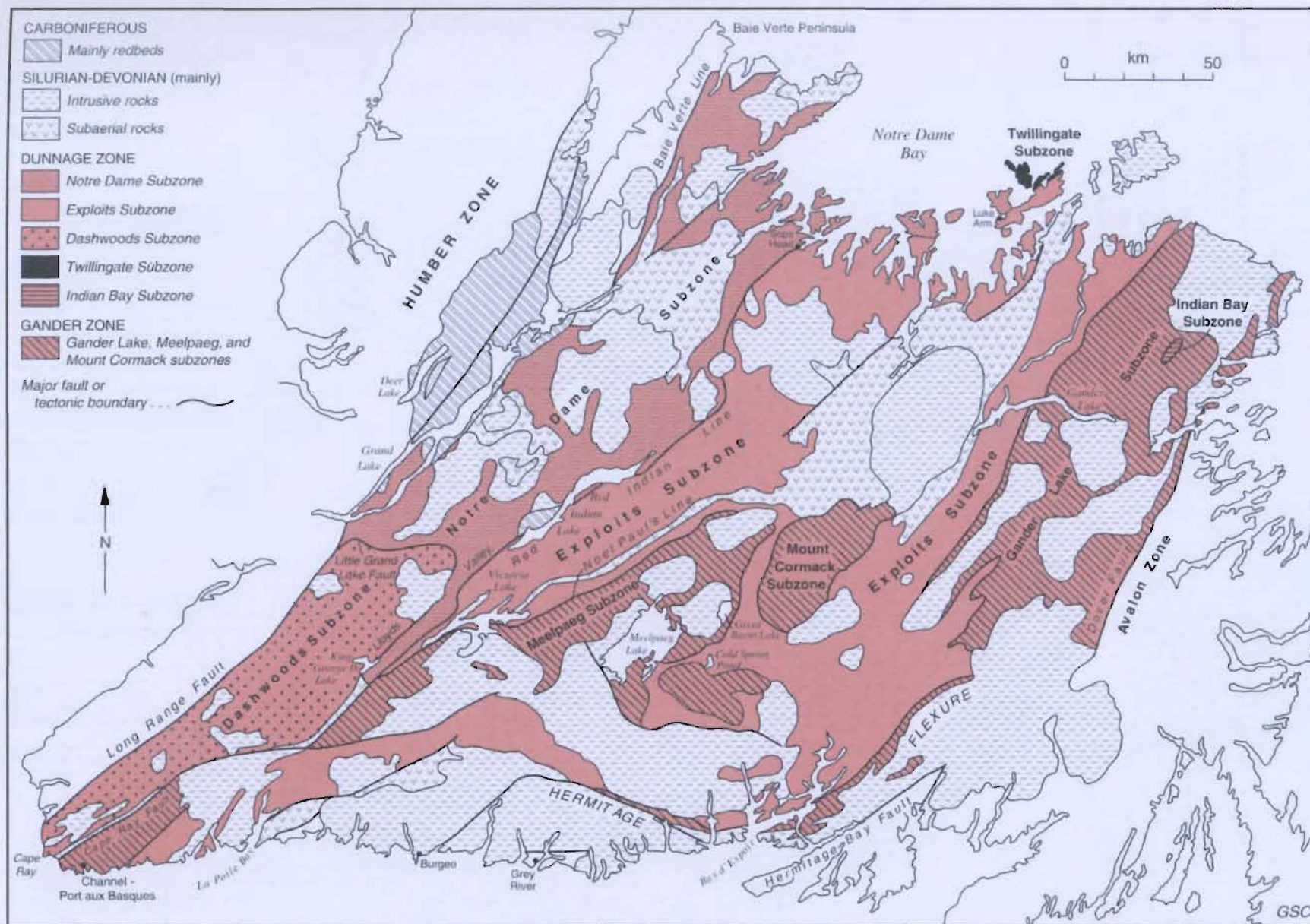


**Figure 2.2:** Zonal subdivision of the Newfoundland Dunnage Zone (modified from Williams *et al.* (1988) and Williams (1995)).



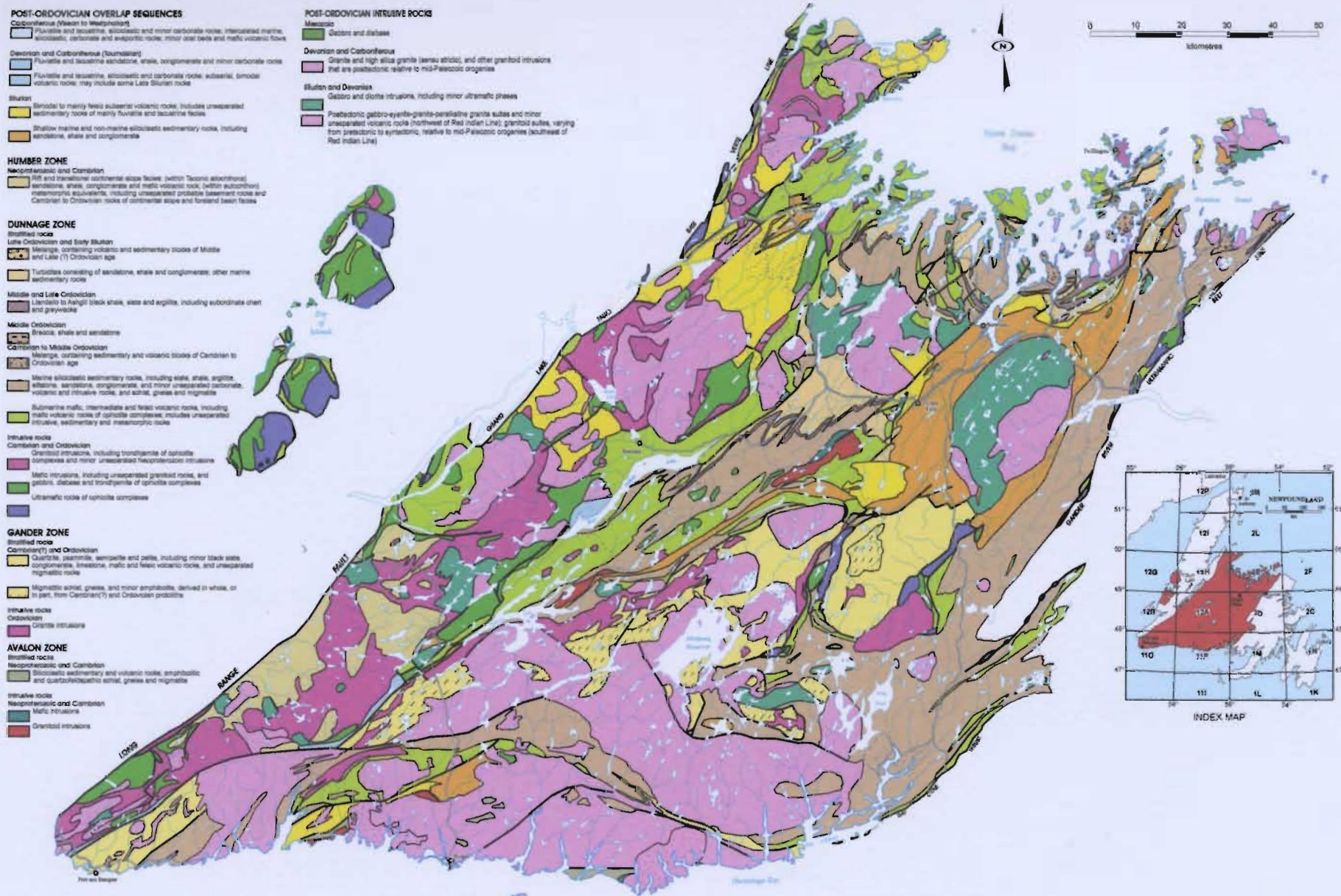


**Figure 2.3:** Geology of the Dunnage Zone of Newfoundland (modified from Colman-Sadd *et al.*, 1990).



# LEGEND

## MOST DEVELOPED DRYLAND WILDLIFE

- Desert Scrub: Areas of yellow scrub, including creosote, sagebrush, and mesquite, which are highly productive for wildlife.
- Desert Scrub: Areas of yellow scrub, including creosote, sagebrush, and mesquite, which are highly productive for wildlife.
- Desert Scrub: Areas of yellow scrub, including creosote, sagebrush, and mesquite, which are highly productive for wildlife.
- Desert Scrub: Areas of yellow scrub, including creosote, sagebrush, and mesquite, which are highly productive for wildlife.

## DESERT ZONE

- Desert Scrub: Areas of yellow scrub, including creosote, sagebrush, and mesquite, which are highly productive for wildlife.
- Desert Scrub: Areas of yellow scrub, including creosote, sagebrush, and mesquite, which are highly productive for wildlife.

Figure 2.4

## DESERT ZONE

- Desert Scrub: Areas of yellow scrub, including creosote, sagebrush, and mesquite, which are highly productive for wildlife.
- Desert Scrub: Areas of yellow scrub, including creosote, sagebrush, and mesquite, which are highly productive for wildlife.

## DESERT ZONE

- Desert Scrub: Areas of yellow scrub, including creosote, sagebrush, and mesquite, which are highly productive for wildlife.
- Desert Scrub: Areas of yellow scrub, including creosote, sagebrush, and mesquite, which are highly productive for wildlife.

## DESERT ZONE

- Desert Scrub: Areas of yellow scrub, including creosote, sagebrush, and mesquite, which are highly productive for wildlife.
- Desert Scrub: Areas of yellow scrub, including creosote, sagebrush, and mesquite, which are highly productive for wildlife.

## DESERT ZONE

- Desert Scrub: Areas of yellow scrub, including creosote, sagebrush, and mesquite, which are highly productive for wildlife.
- Desert Scrub: Areas of yellow scrub, including creosote, sagebrush, and mesquite, which are highly productive for wildlife.

## DESERT ZONE

- Desert Scrub: Areas of yellow scrub, including creosote, sagebrush, and mesquite, which are highly productive for wildlife.
- Desert Scrub: Areas of yellow scrub, including creosote, sagebrush, and mesquite, which are highly productive for wildlife.

## LEGEND

### POST ORDOVICIAN OVERLAP SEQUENCES

#### Silurian



Bimodal to mainly felsic subaerial volcanic rocks; includes unseparated sedimentary rocks of mainly fluvatile and lacustrine facies (Botwood Group; Stoney Lake Volcanics)



Shallow marine and non-marine siliciclastic sedimentary rocks, including sandstone, shale and conglomerate (Botwood Group; Duder Complex?; Ten Mile Lake Formation)



Polydeformed, grey and buff pelite, fine-grained, calcareous and dolomitic sandstone, and thin limestone beds (Indian Islands Group)

### DUNNAGE ZONE

#### Stratified rocks

##### Middle to Late Ordovician



Llandeilo to Ashgill black shale, slate and argillite, including subordinate chert and greywacke (Caradoc Shale)

##### Cambrian to Middle Ordovician



Marine siliciclastic sedimentary rocks, including shale, slate, argillite, siltstone, sandstone, conglomerate and minor unseparated carbonate, volcanic and intrusive rocks and schist, gneiss and migmatite (Davidsville Group; Exploits Group)



Submarine mafic, intermediate and felsic volcanic rocks, including mafic volcanic rocks of ophiolite complexes; includes unseparated intrusive, sedimentary and metamorphic rocks (Gander River Complex, Baie d'Espoir Group, Exploits Group)

### INTRUSIVE ROCKS

#### Cambrian and Ordovician



Mafic intrusions, including unseparated granitoid rocks and gabbro, diabase and trondhjemite of ophiolite complexes



Ultramafic rocks of ophiolite complexes

### POST ORDOVICIAN INTRUSIVE ROCKS

#### Silurian and Devonian



Gabbro and diorite intrusions, including minor ultramafic phases



Granitoid suites, varying from pre-tectonic to syntectonic, relative to mid-Paleozoic orogenies

### GANDER ZONE

#### Stratified rocks

##### Cambrian (?) And Ordovician



Quartzite, psammite, semipelite and elite, including minor black slate, conglomerate, limestone, mafic and felsic volcanic rocks, and unseparated migmatitic rocks

#### Intrusive rocks

##### Ordovician



Granite intrusions

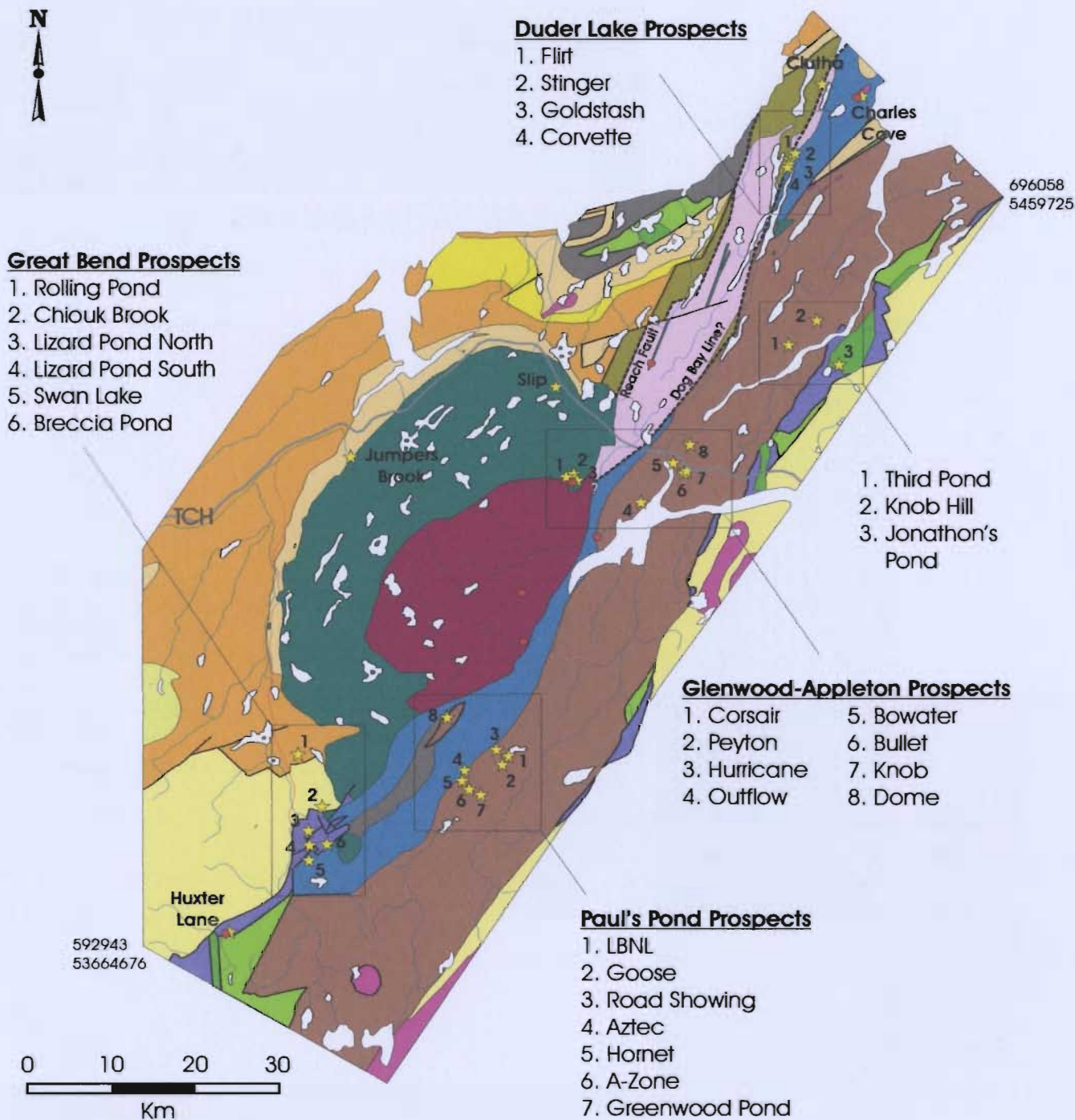


**Figure 2.4:** Generalized geology map of the Botwood Basin and environs, and specific locations of auriferous showings sampled for this study (yellow stars) and location of geochronological samples (red circles) from which U-Pb ages were obtained (geology modified from Colman-Sadd and Crisby-Whittle, 2002).



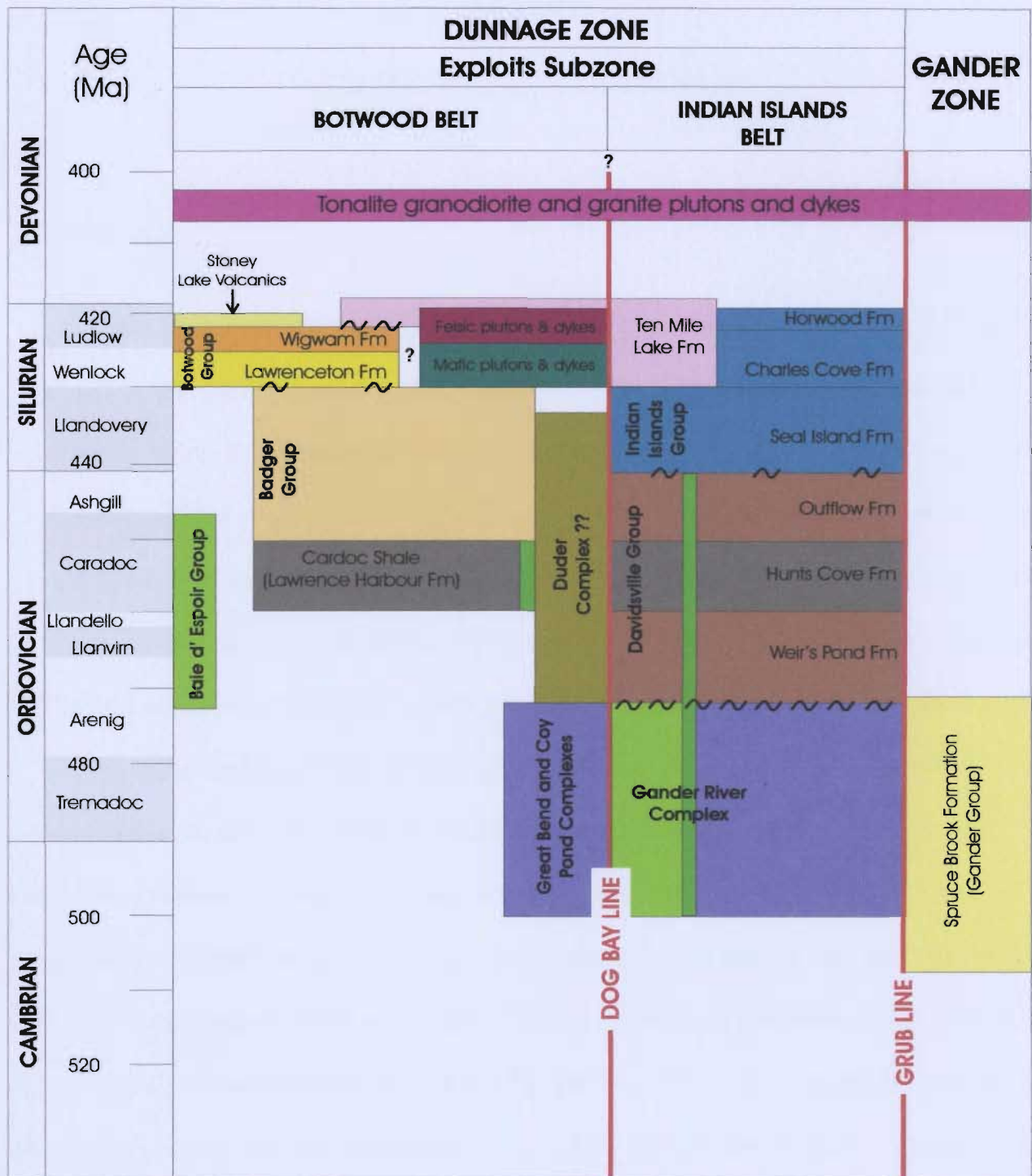


**Figure 2.5:** Stratigraphic column illustrating the various lithologies and relative ages of the Botwood and Indian Islands Belts, Exploits Subzone (refer to corresponding geology map and legend in figure 2.4).



## CHAPTER 3

### AURIFEROUS OCCURENCES

#### 3.1 Preamble

This section describes the gold and antimony occurrences examined for this study in terms of their geological and structural settings. The occurrences were visited and assessed in terms of mineralization, alteration, structure and intrusive relationships. Due to the scope of this project, detailed trench mapping was not conducted. However, where possible, samples were collected of unaltered, altered and mineralized host rocks as well as vein material for assay and petrographical analysis. Petrographical investigations were performed on polished thin sections using a transmitting/reflecting binocular microscope.

A general geology map indicating the location of the occurrences visited for this project within the Botwood Basin and adjacent area is outlined in figure 2.4. Some of these occurrences have previously been described (*i.e.*, Churchill, 1994; Evans; 1996, Evans; 1999) in terms of the deposit models discussed in Appendix 2 and the evidence for those classifications is presented here. A brief overview of the prospects is outlined in table A1.2, along with previously derived assay data. Given that the areal extent of this project is extensive, the occurrences are grouped into regional sections as follows: 1) the Northern Botwood Basin including all of those occurrences that lie to the north of the TCH, 2) the Glenwood-Appleton region which encompass those occurrences adjacent to the towns of Glenwood and Appleton along the TCH, 3) the Mount Peyton group which consist of those occurrences hosted by, or immediately adjacent to, the northernmost

Mount Peyton Intrusive Suite rocks, 4) the Paul's Pond occurrences which comprise those occurrences in the southeastern Botwood basin in the vicinity of Paul's Pond and adjacent to the Northwest Gander River, and 5) the Great Bend occurrences which are present in the southern Botwood Basin and near the Great Bend of the Northwest Gander River adjacent to the Baie d'Espoir Highway.

### **3.2 Northern Botwood Basin**

This section describes those occurrences north of the TCH, east of the Dog Bay Line and west of the Gander Zone and includes the Duder Lake prospects, the Clutha, Charles Cove, Knob Hill, Third Pond and Jonathon's Pond prospects.

#### **3.2.1 Duder Lake Prospects**

The gold showings discussed herein are generally referred to as the Duder Lake occurrences due to their proximity to Duder Lake and are inclusive of the Corvette, Goldstash, Flirt and Stinger prospects. The region lies approximately 8 km east of Birchy Bay (off Highway 331) along a logging resource road, which is in good condition and still in use at the time of this project. The occurrences are located between Duder Lake to the west, Rocky Pond to the east and Ten Mile Lake to the south on NTS map sheet 2E/7 (Figure 3.1, p. 91); outcrop exposure is fair at approximately 25 %. The area has low relief with elongate ridges of gabbro characterizing higher elevations and bogs and marsh typical of low-lying areas (Plate 3.1, p. 104). Structures and lake morphologies generally trend northeast and a till cover ranges from 1.5 to 15 m thick (Churchill, 1994).



The Flirt, Goldstash, and Corvette Au prospects consist of shear-controlled sulphide disseminated (orogenic lode) mineralization restricted to gabbroic dykes and sills (Churchill and Evans, 1992). All three of these occurrences were assessed as part of the present study during the 2003 field season. The Stinger Prospect is hosted in Duder Complex sedimentary rocks that host the gabbros (Figure 3.2, p. 92).

The gabbroic intrusions themselves are generally small, irregular, fine to coarse-grained gabbroic to dioritic dykes and sills (redefined as tectonic blocks by Currie, 1995b) that appear to be elongated in the direction of movement along the major faults in the area. They can be up to 55 m wide and 500 m long with boudinage and stretching parallel to regional cleavage (Green, 1989). Correlation with similar rocks in the Gander Lake region led to the interpretation that the intrusions are Late Silurian to Early Devonian (Churchill and Evans, 1992), however, no absolute determinations have been made as to either the intrusive or deformation ages.

The numerous gabbroic bodies occur along a NE trending fault that cuts the Duder Complex. The fault has been related to movement along the Dog Bay Line (Williams, 1993). The Indian Islands Group lies to the east (Currie and Williams, 1995) and consists dominantly of dark green to black laminated slates and shale with thin interbeds of light green siltstone, greywacke and argillaceous siltstone sequences (Green, 1989).

The style of gold mineralization has been classified as mesothermal hosted by gabbroic and graphitic sedimentary rocks; however, the gabbroic mineralization has been further subdivided into two categories: 1) shear controlled sulphide dissemination in gabbro (Corvette and Goldstash) and 2) shear controlled quartz-carbonate veins with

sulphides and minor gold (Flirt). The sedimentary-hosted occurrence (Stinger) was not examined during this study but has been described as sediment-hosted, shear-controlled quartz vein style of mineralization (Churchill *et al.*, 1993).

#### 3.2.1.1 Flirt

The Flirt gold occurrence occurs in a heavily wooded area adjacent to a bog at UTM coordinates 670596/ 5465115, 1 km due east from the tip of Duder Lake. The occurrence consists of a 15 m wide, brittlely deformed gabbro sill that is cut by quartz-carbonate veins ranging from 1-30 cm wide and containing up to 10% disseminated pyrite and arsenopyrite. The gabbro host is weakly carbonatized and moderately chloritized and has trace pyrite and arsenopyrite locally. The quartz veins have assayed up to 9.29 g/t gold (grab sample) (Green, 1989), however, no significant values have been reported from the gabbro host.

One large, 10 m long trench was examined and the outcrop is comprised of rusty (Fe carbonate alteration), chloritized and slightly brecciated sheared gabbro randomly cut by quartz and quartz-carbonate veins. The host (Plate 3.2b, p. 104) is a fine to coarse-grained, altered gabbro comprised of subhedral white (carbonate and sericite) and blue-grey (albite) minerals and anhedral light green to black (pyroxene) minerals.

Petrographically, the gabbro consists of 30% calcite, 15% pyroxene, 15% uraltite, 10% albite, 10% epidote, 7% leucoxene, 5% chlorite and 5% quartz and 3% pyrite (Plate 3.3, p. 50). Primary igneous phases such as plagioclase and Fe-Ti oxides have been metamorphosed to albite-epidote-calcite and leucoxene. Clinopyroxene is subhedral and



the plagioclase is albitized and altered to epidote and calcite. Fe-rich chlorite (clinochlore) occurs with the albite and leucoxene formed from the break down of primary Fe-Ti oxides. Carbonate alteration occurs through the section and also in small quartz-carbonate veinlets.

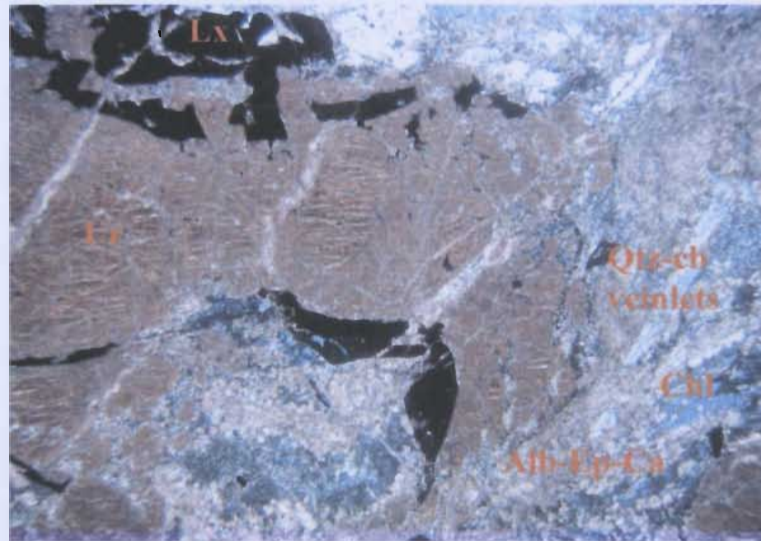


**Plate 3.3:** Photomicrograph of a gabbro from the Flirt Prospect exhibiting leucoxene (Lx) alteration of Fe-Ti oxides and uralitization of pyroxene. Plagioclase is albitized and contains minor epidote (Ep) and calcite (Ca). Fine-grained calcite and epidote are also present as pinkish flecks in the albite and quartz carbonate veinlets cut the pyroxene [Field of view ~ 7 mm, XP].

### *3.2.1.2 Goldstash*

The Goldstash Prospect is located approximately 2 km south of the Flirt Prospect along an old drill path that is essentially overgrown. Several trenches were located during the 2003 field season, however, many were water-filled. The trench at UTM coordinates 670488/ 5464542 has very good outcrop exposure which exposes the contact between altered gabbro and a sedimentary unit (Plate 3.4a, p. 104). The sedimentary unit

is dark grey, shiny and very cleaved and appears to be dark grey slate. The gabbro contains disseminated sulphides and the general trend of schistose gabbro is  $021^{\circ}/90^{\circ}$ .

The mineralized gabbro comprises 30% albite, 20% ankerite, 15% sericite, 10% Fe-Ti oxides, 8% pyrite and 2% arsenopyrite, 5% uralitized pyroxene, 5% leucoxene, and 5% quartz. Fe-carbonate alteration occurs along the grain boundaries of the sulphides (Plate 3.5) and chlorite is associated with sulphides as well as ankerite (ferroan dolomite).

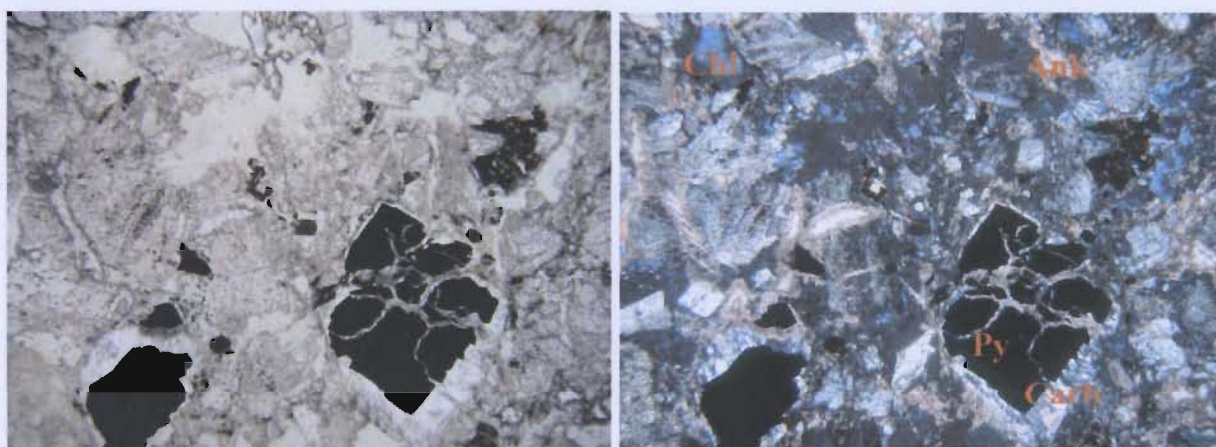


**Plate 3.5:** Photomicrograph of mineralized gabbro from the Goldstash Prospect exhibiting chlorite (Chl), ankerite (Ank) and pyrite (Py). [Field of view  $\sim 7$  mm, PPL and XP].

### *3.2.1.3 Corvette*

The Corvette Prospect is located approximately 800 m along strike to the south of the Goldstash Prospect. Mineralization and alteration at the Corvette are similar to those at the Goldstash, which lie along the same lateral shear zone. Some of the trenches at this prospect were located along the resource road (Plate 3.4b, p. 104), just north of a fossiliferous, Fe-carbonate altered outcrop (see description in chapter 4). Several trenches were noted south of the prospect, although there were no trenches in the



immediate area as indicated on the Newfoundland Department of Mines and Energy (NDME) Mineral Occurrence Database (MOD).

The first trench, at UTM coordinates 670326/ 5463622, exposes a very rusty outcrop of an altered metamorphosed gabbro. Further up the road at UTM coordinates 670357/ 5463793, a fairly large outcrop of unaltered gabbro is exposed, suggesting that alteration and mineralization are local, related to shearing.

Petrographical analysis of sample JOD97B collected from the Corvette trench reveals a slight fabric in one direction. The sample is coarse-grained and the main fabric is defined by quartz and sericite. The section contains 30% leucocene, 20% sericite, 20% uraltite, 15% albite, 10% quartz and 5% pyrite (Plate 3.6, p. 52). The pyroxene is being replaced by uraltite, which appears within cracks in pyroxene and Mg-rich chlorite occurs around the uraltitized pyroxene.

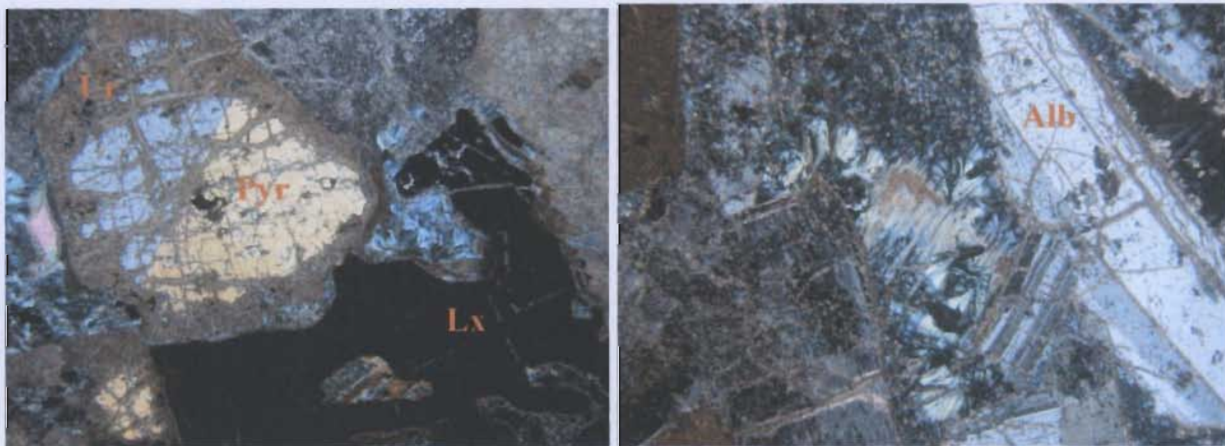


**Plate 3.6:** Photomicrographs of mineralized gabbro from the Corvette Prospect exhibiting A) uraltitized pyroxene (Ur), pyroxene (Pyr) and leucocene (Lx) replacement of Fe-Ti oxides and B) albitized plagioclase (Alb) with epidote alteration, quartz and chlorite and [Field of view ~ 7 mm, XP].

### **3.2.2 Clutha**

The Clutha Prospect is located approximately 4 km south-southwest of the Dog Bay Provincial Park access road from route 331 (Figure 3.1, p. 91) at UTM coordinates 674900/ 5475350 on NTS map sheet 2E/07. An abandoned logging road leads to the prospect and it is only accessible via all terrain vehicles (refer to Evans, 1996 for a description of the Clutha Prospect). The prospect is no longer exposed, as the trenches have been backfilled. Outcrop in the immediate area is sparse and mineralization was not observed.

Immediately west of the prospect location, however, the author noted Indian Island Group-type rocks, which suggests that the group extends further west than currently mapped, as originally proposed by Baird (1958).

### **3.2.3 Charles Cove/ Tim's Harbor**

The Charles Cove Prospect is located in the northeast Botwood Basin at UTM coordinates 681300/ 5475920 on map sheets 2E/07 and 2E/08 (Figure 3.1, p. 91). It is approximately 2 km inland from the coast and can be accessed via a 3 km network of skidder trails from the highway at the community of Rodgers Cove. The topography is generally of low relief consisting of a gentle rise from the coast to a 90 m ridge to the west. The main quartz vein is exposed between the coast and this ridge along a smaller (~30 m asl) ridge. The area between the ridges is swampy and boggy with abundant alders and the ridges are tree covered with good outcrop exposure. The only pond in the vicinity is Charles Pond from which numerous small streams drain into the coast (Wilton



and Taylor, 1999). The author did not visit this prospect; Derek Wilton collected the geochronological sample from the host granodiorite in September 2003.

The prospect consists of an undeformed arsenopyrite-galena-bearing quartz vein hosted by the Silurian Charles Cove granodiorite, which intruded sedimentary rocks of the Ordovician Davidsville Group and Silurian Indian Islands Group (Wilton, 1997) (Figure 3.3, p. 93). This well-exposed quartz vein strikes north-northwest and extends for more than 1 km and varies in width from 2 to 15 m with offshoots extending for 55 m (Wilton and Taylor, 1999).

The prospect exhibits characteristics of both granophile and mesothermal systems. Although a carbon dioxide phase was not present in the Charles Cove quartz vein fluid inclusions, both the temperature range (220-260° C) and the salinity (1 up to 6 equivalent wt% NaCl) may be characteristic of a mesothermal system (Greenslade, 2002). The vein system differs from the other Dunnage Zone mesothermal systems in that it contains W and is hosted by a granodiorite. But the auriferous quartz vein appears to be epigenetic with respect to the granodiorite intrusion (Greenslade, 2002).

#### **3.2.4 Knob Hill**

The Knob Hill Prospect is located at UTM coordinates 674259/ 5445813 on NTS map sheet 2E/2 and is hosted by Davidsville Group greywacke. The prospect was accessed via the Bellman's Pond Resource Road, which is part of a network of roads north of the TCH at Glenwood (Figure 3.4, p. 94). The location as indicated by the MOD

was inaccurate and led to a grassy knoll in an area of cutover; no outcrop was located in the surrounding wooded area.

Some quartz float and outcrop was noted along the sides of the new resource road at UTM coordinates 674259/ 5445813. Coarse-grained, mica-rich Davidsville Group greywacke is cut by quartz veins that are less than 3 cm wide, with no apparent alteration occurring along the margin of the veins (Plate 3.7a, p. 105). The veins cut the structural fabric of the host and exhibit moderately to well-developed quartz crystals, indicating that the veins crystallized post deformation of the greywacke. Evans (1996) noted that the greywacke exhibited chloritic alteration.

Sample JOD15 is composed of 45% very fine-grained muscovite (sericitic alteration), 30% quartz, 8% Fe-oxides, 7% pyrite, 5% feldspar and 5% chlorite (Plate 3.8, p. 55). Some rare perthite twins were observed in the feldspar. Grains are sub-rounded, moderately sorted and are surrounded by ~45% of a fine-grained matrix and therefore this rock is classified as a quartzwacke.

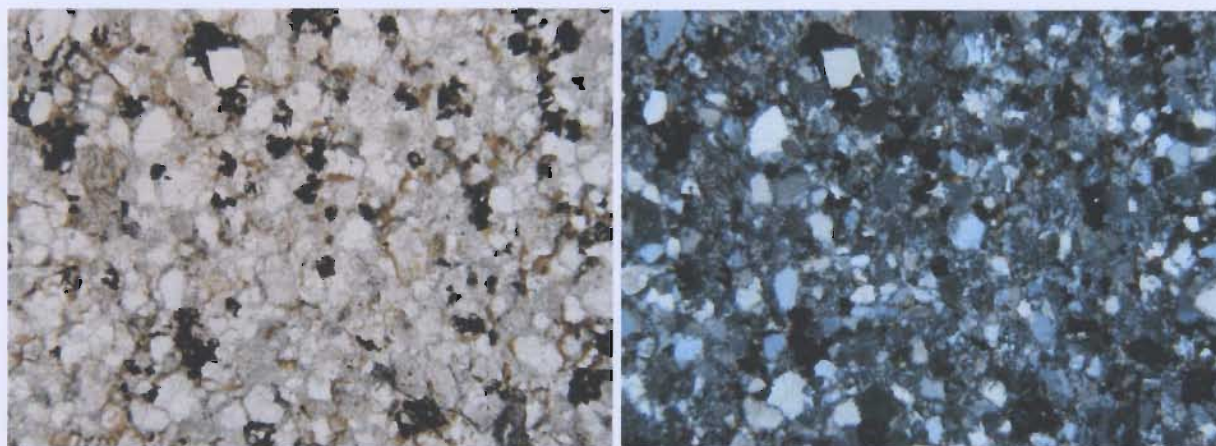


**Plate 3.8:** Photomicrograph of Davidsville quartzwacke, host to mineralization at the Knob Hill Prospect comprised of moderately sorted quartz, feldspar and Fe-Ti oxides in a fine-grained sericite matrix [Field of view 7 mm, PPL and XP].



### 3.2.5 Third Pond

The Third Pond Prospect is located southwest of the Knob Hill Prospect along the Bellman's Pond Resource Road at UTM coordinates 671020/ 5442038 on map sheet 2E/2. The prospect has been described as quartz veins in Davidsville Group slate (Evans, 1996).

At UTM coordinates 671128/ 5442085, a trench exposed two sedimentary units and a large bull vein with very large, euhedral quartz crystals (up to 4 cm long). A 1 x 1.5 m elliptical exposure of what appeared to be a very altered unit (referred to as a cherty concretion in previous descriptions, *i.e.*, Evans (1996)) is apparently interbedded with graphitic shale (Plate 3.7b, p. 105). The wall rock is orange and rusty due to hydrothermal alteration and a small (< 1 cm) alteration halo of coarse-grained chlorite is present along the margin of the veins within the wall rock.

The greywacke consists of 45% sericite, 20% quartz, 10% feldspar, 15% calcite, 5% chlorite and 5% Fe-oxides. The feldspar grains have simple and perthite twins, which are more abundant here than at the Knob Hill Prospect.

The altered 'concretion' comprises 80% platy carbonate (dolomite and chlorite) and 20% sericite (Plate 3.9, p. 57). Concretions are solid mineral inclusions found within shale units that form secondary to the rock-forming processes and are commonly composed of carbonate minerals (American Geological Institute, 1984).

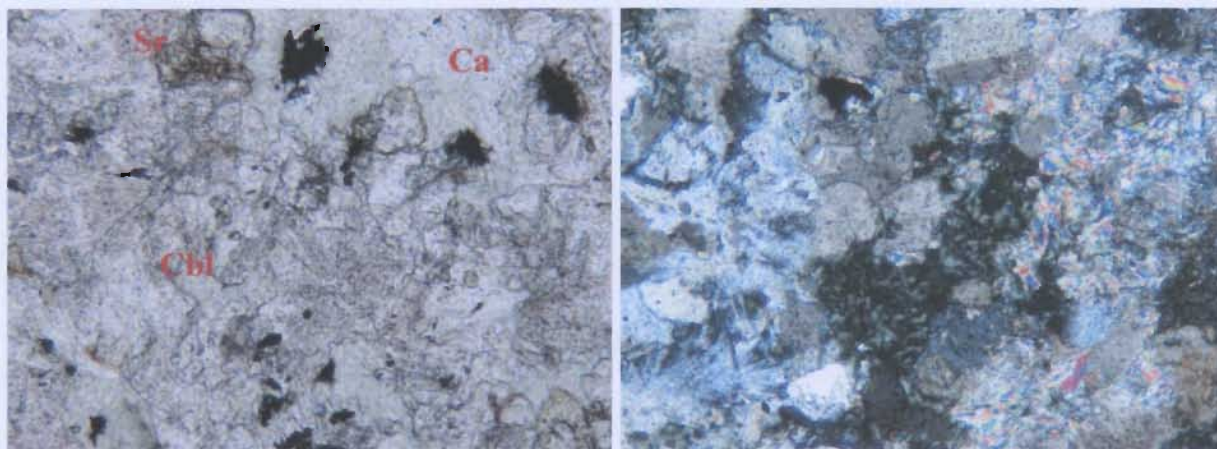


**Plate 3.9:** Photomicrograph of carbonate ‘concretion’ at the Third Pond Prospect. The section is comprised of chlorite (Chl), calcite (Ca) and sericite (Sr) [Field of view 7 mm, PPL and XP].

### 3.2.6 Jonathon’s Pond

The Jonathan’s Pond Prospect is located approximately 15 km north of Gander on the west side of highway 330, NTS map sheet 2E/2, 4 km northwest of the entrance to Jonathon’s Pond Provincial Park (Figure 3.4, p. 94). The prospect can be accessed via an abandoned logging road, which is in poor condition and only suitable for ATVs.

Blackwood (1979, 1982) first recognized Au mineralization in the Jonathon’s Pond area while conducting regional mapping over the Gander River Complex. Geologically the area comprises Lower Ordovician rocks of the GRC that are thrust against older psammitic and pelitic sediments of the Gander Group to the east (Figure 3.5, p. 95). A northeast trending, westerly dipping thrust contact between GRC rocks and Gander Group rocks is the most significant structural feature in the area and has been observed in drill core as 20 m wide, weakly pyritic, chalky serpentinitic gouge (Snow, 1988).



The area surrounding the occurrence was traversed on two separate occasions for this study but the exact location of the prospect was not ascertained as the area indicated by the MOD files did not contain any mineralized outcrop. Generally, this area is heavily forested with some grassy clearances and abundant alders. Ridges of silicified gabbro were located but no mineralization was observed along them. At UTM coordinates 677536/ 5440220, ridges of silicified gabbro were cut by multiple quartz veins up to 5 cm in width. Quartz float at UTM coordinates 677677/ 5440132 in the forested area exhibited an epithermal, interlocking or fibrous texture (Plate 3.10a, p. 105) and the sample was somewhat rounded indicating transport.

Traversing further northwest along the resource road, several trenches were observed which contained sulphide mineralization. The first observed trench at UTM coordinates 676938/ 5441002 consisted of a 2 x 2 m outcrop of a fine-grained, altered, green ultramafic unit cut by quartz veins; sulphide mineralization occurred in and adjacent to the veins. The quartz veins define tension gashes up to 0.75 m long, up to 2 cm wide and trending 110°. The quartz exhibits a very smooth, ribbon like texture; the sulphides (arsenopyrite and pyrite) are semi-massive along the edge of veins and occur as fine disseminations within the host (Plate 3.10b, p. 105). The mafic host rock appears to be very sheared locally.

Traversing east, several trenches of quartz-veined green serpentinite were observed. Approximately 20 m east of the first outcrop, a very large bull quartz vein was observed in a pit within a very sheared serpentinite. At UTM coordinates 677703/ 5440698 an approximately 1 x 0.5 m small trench of magnesite-altered serpentinite, with magnesite veins up to 3 cm wide was observed. A mineralized sample was collected

from the first trench and is comprised of serpentinite, chlorite, quartz, carbonate, arsenopyrite and pyrite (Plate 3.11a and b, p. 59).

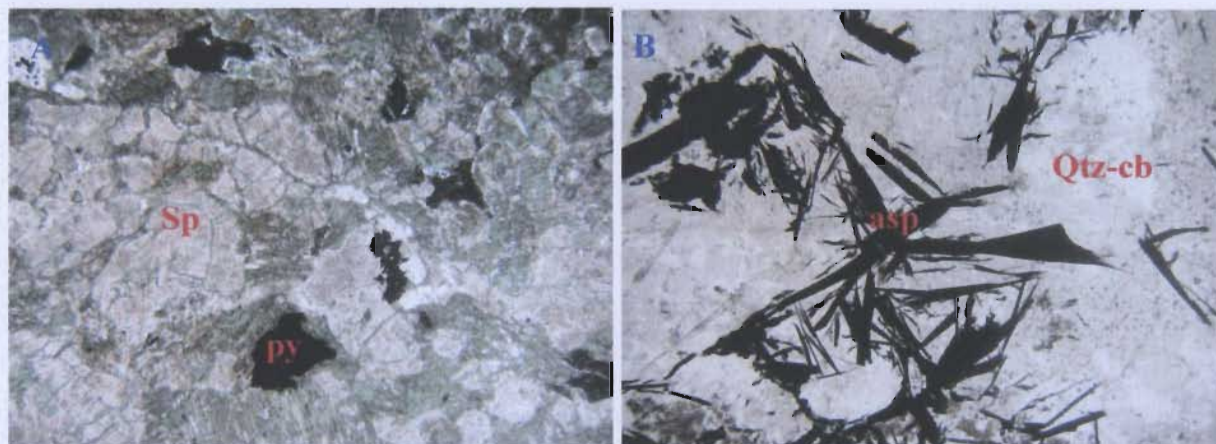


**Plate 3.11:** Sample JOD117-Jonathon's Pond. a) Serpentinized (Sp) and talc altered host exhibiting disseminated blebs of pyrite (py) [Field of view 7 mm, PPL]. B) Section from quartz carbonate (qtz-cb) vein exhibiting acicular arsenopyrite (asp) [Field of view 2 mm, PPL].

According to previous maps (refer to Figure 3.5, Blackwood (1982)), the trenched areas examined should contain mafic flows and the ultramafic lithologies occur further west. This indicates that the mineralization also occurs in ultramafic lithologies in this area and that these units occur further east than previously mapped.

### 3.2.7 Big Pond/ Blue Peter

The area of the Big Pond Prospect can be easily accessed via the North Salmon River Access Road, however, since Evans' (1996) documentation, the trenches have been backfilled. There was no outcrop in the immediate area but trench float was observed. Although the gabbroic host to this prospect was not observed during this study, several silicified ridges of gabbro were examined along the Twin Ponds Resource Road just west of the prospect. Recent reviews of fossil localities and mapping in this vicinity have led



to the supposition that these gabbroic bodies are actually intrusive into the Silurian Indian Islands Group (where it is currently mapped as Ten Mile Lake Formation). A sample from the northeast trending gabbroic body, as mapped by Blackwood (1982), was processed for U-Pb geochronology and the results are presented in Chapter 4.

The prospect reportedly consisted of shallowly dipping, northeast-striking, dilational, gold-bearing quartz veins developed within Fe-carbonate altered, seritized and weakly silicified gabbro (Evans, 1991). The gabbro is fine to medium-grained and intrudes green and maroon siltstone and sandstone of the Botwood Group (Evans, 1991), later redefined as the Ten Mile Lake Formation (Currie, 1995a).

### **3.3 Central Botwood Basin (Glenwood-Appleton Region)**

The central Botwood Basin region as described herein encompasses the area in the immediate vicinity of Glenwood and Appleton, along the TCH and the Gander River outflow and includes the Dome, Bullet, Knob, Bowater and Outflow prospects (Figure 3.4, p. 94). In general, due to the proximity of the occurrences to developed infrastructure, access to all of these prospects is generally good. A low topographic relief dominated by gentle rolling hill slopes and few high points characterizes physiography of this area. A thin, lateral overburden results in poor outcrop exposure. Small streams drain westward into the Gander River Outflow. All of the following prospects have been previously documented as occurring in Davidsville Group rocks (Figure 3.6, p. 96). Thrusting in the region has a northeasterly direction with sub-parallel thrusts cutting the Davidsville Group (Tallman, 1990).

### 3.3.1 Bullet

The Bullet and Knob prospects are located 1 km west of the Glenwood Provincial Park entrance, approximately 0.2 km south from the TCH (Figure 3.4, p. 94). A dirt road leading to a quarry provides access within 100 m of the Bullet Prospect; an overgrown skidder trail, the entrance to which is not visible from the dirt road, leads to the trenched areas which contain abundant quartz float at UTM coordinates 657424/ 5425881.

During this study, several trenches were observed along an overgrown trail, east from the dirt road; outcrop was only observed in two of the trenches, as the others were either overgrown or water-filled (Plate 3.12, p. 105). One trench is approximately 15 m long and trends 282°. It has two small exposures of very cleaved, weathered shale with no quartz or sulphur mineralization. Piles with large pieces of quartz float containing sulphide mineralization were observed in several areas.

Petrographically, samples from the prospect revealed that the host is fine-grained, mainly composed of detrital quartz, minor alkali feldspar, sericite and chlorite, with a defined fabric in one direction (Plate 3.13a, p. 62). Disseminated pyrite occurs throughout as thin veinlets (trending along fabric) and large cubic grains. The host rock is similar to that at the Knob Hill and Third Pond prospects. The quartz veins contain up to 95% quartz and 5% disseminated pyrite with no carbonate (Plate 3.13b, p. 62).



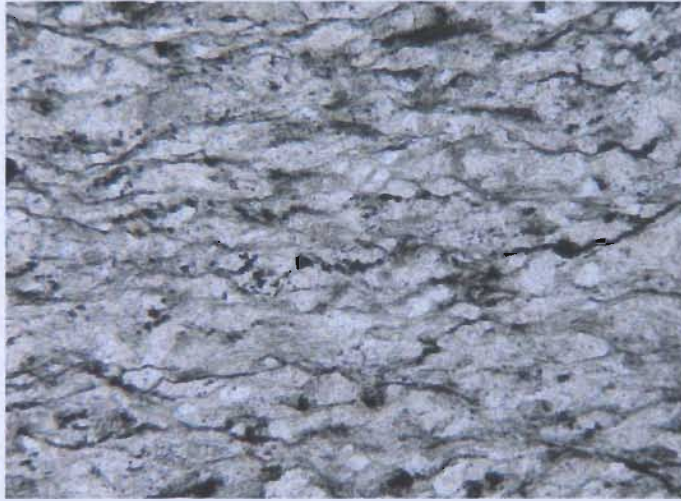


**Plate 3.13a:** Sample W90-10A from Davidsville Group host rock to the Bullet Prospect consisting of detrital quartz, minor feldspar, fine-grained mica matrix, platey chlorite, Fe-oxides and pyrite [Field of view 7 mm, PPL].



**Plate 3.13b:** Sample W90-45B of quartz veins in Davidsville Group rocks at the Bullet Prospect. Interstitial fine grains of subhedral quartz occur in clusters as open space filling [Field of view 7 mm, XP and PPL].

### 3.3.2 Knob

The Knob showing is located just west of the Appleton linear trend, approximately 0.4 km south of the Bullet Prospect at UTM coordinates 657350/ 5425650 and it consists of auriferous quartz veins in black argillites and greywacke.

The discovery outcrop no longer exists because the site is now part of an active quarry. Several trenches are located beyond alders immediately west and northwest of the quarry at UTM coordinates 657181/ 5425631 (Plate 3.14a, p. 106). The trenches expose quartz veins in Davidsville Group greywacke that has been altered to chlorite. Sulphide mineralization is disseminated in the host rock adjacent to quartz. A very small fleck of visible gold (1-2 mm) was observed in quartz float adjacent to a trench and appears to be from an ~ 0.6-1 m wide bull quartz vein (Plate 3.14b, p. 106). The quartz crystals are well formed in places.

In the quarry pit, a contact between greywacke and shale was exposed at UTM coordinates 657285/ 5425642. Quartz veins up to 3 cm wide cut the sediments and a small amount of mineralization was noted in both units and the veins. Also in the quarry, a large bull quartz vein is exposed at UTM coordinates 6573341/ 5425531, which cuts cleaved, chloritized shale; pyrite occurs within the vein and adjacent to it.

### **3.3.4 Bowater**

The Bowater Prospect is located in a gravel pit in the Town of Appleton at UTM coordinates 656026/ 5426826 on map sheet 2D/15, to the west of the Knob Prospect. Although abundant outcrop was observed in the area around the MOD coordinates, the exact location of the showing was not ascertained. Nevertheless, mineralized quartz veins in both greywacke and graphitic shale units are located throughout the area. Quartz veining is dilational and although present in both units, it is more prevalent within the greywacke.

### **3.3.5 Dome**

The Dome Prospect is part of the 'Linear Group' of claims staked in 1998 by Candente Resources Corp., and is located approximately 1 km east of Appleton, north of the TCH at UTM coordinates 658632/ 5428534 on NTS map 2D/15.

The Dome Prospect consists of a very large knob of quartz protruding out of a very large trench (Plate 3.15a, p. 106). In the immediate area to the large vein, pieces of the dark grey sedimentary host unit (Davidsville Group) (Plate 3.15b, p.106) are present in a quartz breccia. The quartz also exhibits open space filling features in places. A very small amount of visible gold was observed to be associated with apple green sericite at the main vein.

### **3.3.6 Outflow**

The Outflow Prospect can be accessed by traveling through the south side of Glenwood along the Gander River outflow. The main road eventually becomes a well-maintained road, which provides easy access within 100 m to the property; skidder trails and grown over drill paths lead directly to the trenched areas. As the Outflow Prospect consists of two large mineralized zones, it is extensive. Trenches were also located by traversing an abandoned logging road off the south Salmon River Resource Road approximately 2 km from Glenwood.

Both the Piper and Mustang zones were examined for this study. Locating the trenches at the Piper Zone was initially time-consuming because there were no signs of trenching activity in the locality defined by the MOD. There was some evidence of



drilling or backfilling in the immediate area of UTM coordinates 653618/ 5422551, but upon much traversing through a thickly wooded area, no outcrop was found. An outcrop of black, very cleaved, quartz veined graphitic shale was located at UTM coordinates 653848/ 5422593 (Plate 3.16a, p. 106).

The first trench or stripped area was located at UTM coordinates 653807/ 5422244 and provided excellent outcrop exposure of a quartz veined, mineralized and altered sedimentary unit (Plate 3.16b, p. 106). Quartz veins cut the sedimentary unit and quartz breccia with rusty staining is well developed (Plate 3.17a and b, p. 107). The brecciated sediment fragments range in size from millimeter scale to 7 cm, are variably silicified and exhibit original laminations. Quartz veins, up to 3 cm wide in places, are smooth to vuggy with well-formed, fine-grained quartz. There was also a single, large 13 cm wide massive, milky, homogeneous quartz vein present which is similar to the veins observed at Jonathon's Pond. Silicification is present in the wall rock adjacent to the quartz veins and excellent comb and fine-grained spectacular quartz textures are present as well. Disseminated pyrite occurs more often in the quartz than in the sedimentary unit and hematite staining is present throughout.

A second, 15 m long trench that trends 134° was observed at UTM coordinates 653624/ 5422060. The trench is mostly grown over, but contains a very small outcrop exposure ~ 2 x 2.5 m of a moderately deformed sediment. The cleaved, fine-grained sandstone exhibits patchy silicification around quartz veins (similar to those observed in trench 1).

Petrographically, the quartz breccia consists of angular, fine-grained sediment clasts altered to clay minerals with disseminated pyrite. The matrix is composed of fine-



grained carbonate and quartz exhibiting interlocking textures (Plate 3.18a and b, p. 66). Vuggy carbonate grains surround sediment fragments and are themselves rimmed by Fe-oxide (Plate 3.18c and d, p. 67).

In 2002, Altius Resources suggested that the Mustang Trend, in particular the Outflow Prospect, exhibited potential Carlin-type Au deposit characteristics based on a variety of evidence that included the presence of dickite, ferroan dolomite alteration, decalcification, barite mineralization, and localized silicification, including jasperoid development. Altius subsequently entered into a joint venture agreement with Barrick Gold on the project which created a staking rush within the Botwood Basin environs. Barrick subsequently dropped the joint venture in 2004.

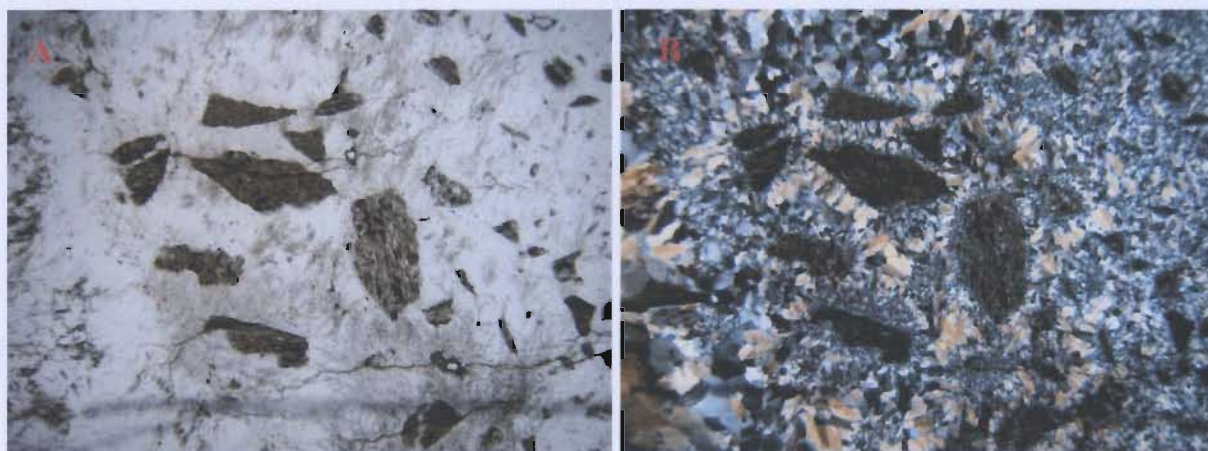


**Plate 3.18:** a,b) Photomicrograph from the Mustang Trend sample W0-49A, Outflow Prospect quartz breccia. Matrix is composed of quartz and carbonate and the fragments are altered to clay [Field of view 7 mm, PPL and XP].

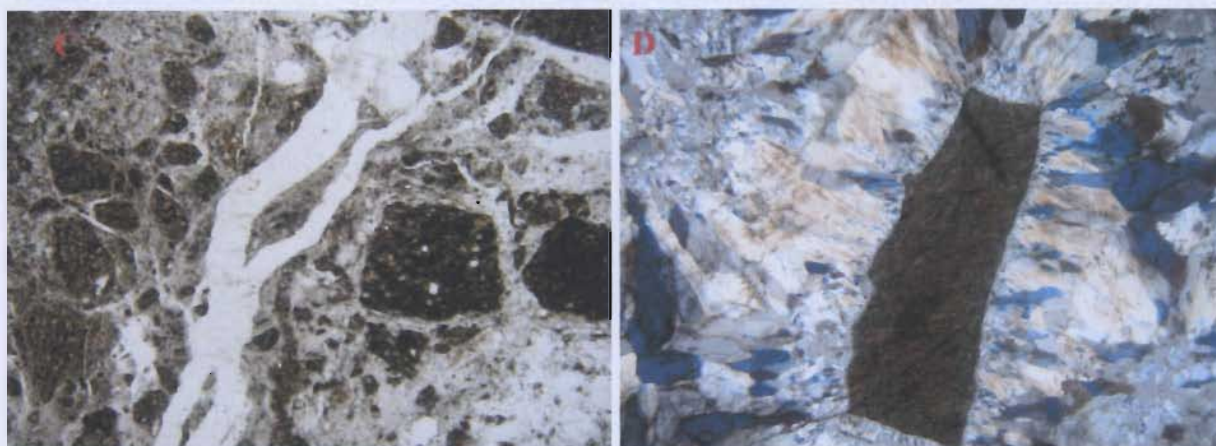


**Plate 3.18:** c) Photomicrograph exhibiting quartz breccia and quartz veins of sample DW90-50A [Field of view 7 mm, PPL]. d) Close-up of fragment from sample DW90-49A surrounded by radiating carbonate crystals [Field of view 2 mm, XP].

### **3.4 Central Botwood Basin (Mount Peyton Prospects)**

The Mount Peyton Prospects as described herein are hosted by, or are immediately adjacent, to the Mount Peyton Intrusive Suite and include the Hurricane, Corsair, Slip and Jumper's Brook prospects on NTS map sheets 2D/14 and 2E/1 (Figures 3.7 and 3.8, p. 97).

Of the five showings along Salmon River, Tallman (1990) identified the Corsair and the Hurricane as the most important and as such, only these two prospects were examined. A fairly poor resource road leading from the southern Salmon River Access Road provides ATV access to the Salmon River. A series of occurrences are located along the Salmon River such as the Hurricane, Corsair, Mount Peyton and Sabre. The Slip and Jumper's Brook prospects are located fairly close to major routes so access is very good.



### **3.4.1 Hurricane Prospect**

The Hurricane Prospect is located approximately 7 km west of Glenwood, along the Salmon River and can be accessed via abandoned logging roads from the South Salmon River Resource Road at UTM coordinates 645161/ 5425138 on NTS map sheet 2D/14.

The prospect is exposed in a small riverbank outcrop (exposure now < 1 x 1 m) along the southwest bank of the river, just down stream from a small island (Plate 3.19a, p. 107). The exposure is mostly grown-over and allows only for a trend of 022° to be estimated (Plate 3.19b, p. 107). The mineralization is hosted in medium-grained diorite of the Mount Peyton Intrusive Suite (Plate 3.19c, p. 107). The host exhibits a white to grey sericitic alteration close to the mineralized zone. The diorite is locally plagioclase porphyritic and sulphides are abundant, occurring as veinlets, patches and disseminations. Two drill collars were found in the boggy area adjacent to the river but transects through the wooded area adjacent the riverbank did not reveal any outcrop or trenches.

Sample JOD22 is comprised of 30% plagioclase, 20% hornblende, 15% sericite, 10% biotite, 10% quartz (reaction rim with biotite), 5% pyroxene, 5% apatite, (with some rare oscillatory zoning) and 5% oxides. The edges of the hornblende are replaced by biotite and rare simple twins are observed in plagioclase. The textures suggest that the pyroxene formed first, followed by hornblende, then biotite and plagioclase (Plate 3.20, p. 69).

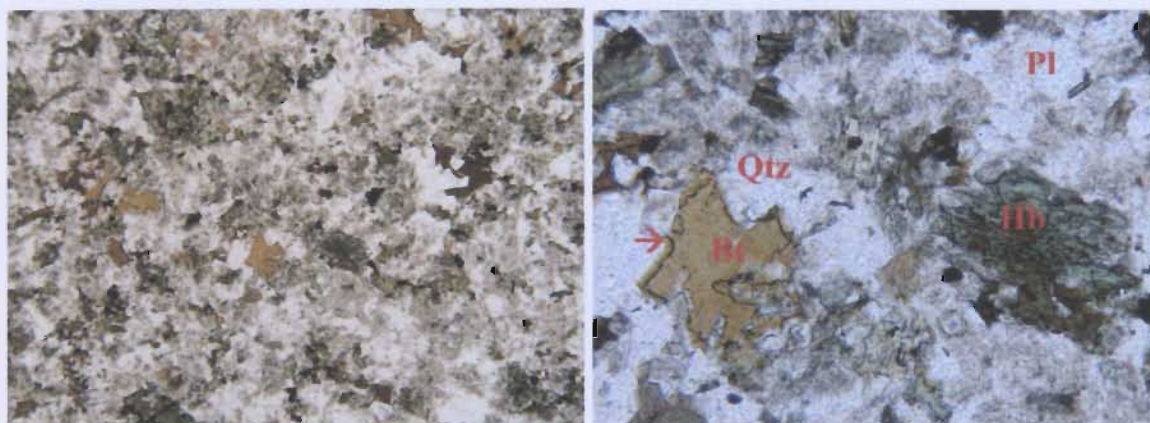


**Plate 3.20:** Photomicrograph of JOD22 from the Hurricane Prospect consisting of hornblende (Hb), plagioclase (Pl), biotite (Bt), pyroxene, apatite, 5% oxides and 10% quartz (note reaction rim with biotite). Dusty alteration is sericite [First photomicrograph has 7 mm field of view in PPL. Second photomicrograph has 2 mm field of view in PPL].

Sample JOD23, an altered and mineralized sample, contains 15% plagioclase, 35% sericite (replaces feldspar), 15% quartz, 5% apatite (occurring in plagioclase), 20% Fe-Ti oxides, and 10% sulphides (Plate 3.21, p. 69). Tiny sulphide veinlets and quartz run through the sample and the sulphides are also disseminated throughout. There is almost complete replacement of original igneous phases in this section indicating that it is severely altered.

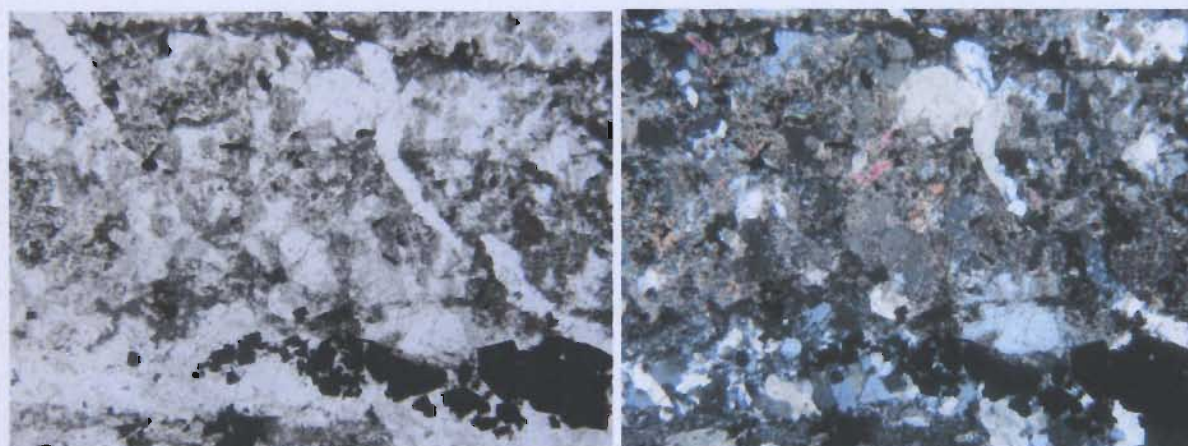


**Plate 3.21:** Photomicrograph of sample JOD23 from the Hurricane Prospect comprised of plagioclase, sericite (replaces feldspar), quartz, apatite, Ti-Fe oxides, pyrite and arsenopyrite. Sulphides are mainly concentrated along the edges of the quartz veins and in tiny sulphide veinlets [Field of view 7 mm, PPL and XP].



### **3.4.2 Corsair Prospect**

The Corsair Showing is located upriver from the Hurricane Prospect at UTM coordinates 644408/ 5425289. The showing outcrops along the riverbank and is partly submerged in the Salmon River. It is ~2 m wide and extends ~ 4 m out into the river. The diorite host exhibits green carbonate and sericite alteration. The outcrop is highly sericitic with very little visible sulphide; however, surficial rusting indicates that sulphides are present.

### **3.4.3 Slip**

The Slip Showing is located in the Neyles Brook quarry at UTM coordinates 643541/ 5438244 on NTS map sheet 2E/03, approximately 15 km west of Glenwood. The quarry began operation in 1995 and is easily accessed via a 500 m dirt road from the TCH. Outcrop is best exposed along blasted pit walls as the glacial till and soil cover in the surrounding area is about 3 m thick (Hoffe, 2003). The Slip Showing consists of mineralization within a miarolitic granitic dyke on the south side of the quarry.

At UTM coordinates 643541/ 5438244 at the back edge of the pit there is a rusty, mineralized zone in the granite containing galena, pyrite and arsenopyrite. Aside from this large mineralized zone in the pit wall, mineralized mylonitic cavities in pegmatite are present near the beginning of the pit at UTM coordinates 643564/ 5438321. Random quartz carbonate veins were also noted throughout the quarry.

Petrographically, sample JOD27B contains 50% alkali feldspar, 30% quartz, 10% carbonate and 10% plagioclase (Plate 3.22, p. 71). The rock is therefore classified as

medium-grained, alkali feldspar granite. A low temperature granophyric texture of intergrown quartz and alkali feldspar is prevalent. The alkali feldspar has undergone sericitic alteration. A large quartz-carbonate vein cuts the sample. Prismatic (euhedral) quartz crystals occur at the edges of the vein, surrounded by anhedral carbonate. The carbonate occurs in one cluster and is not associated with the feldspar.

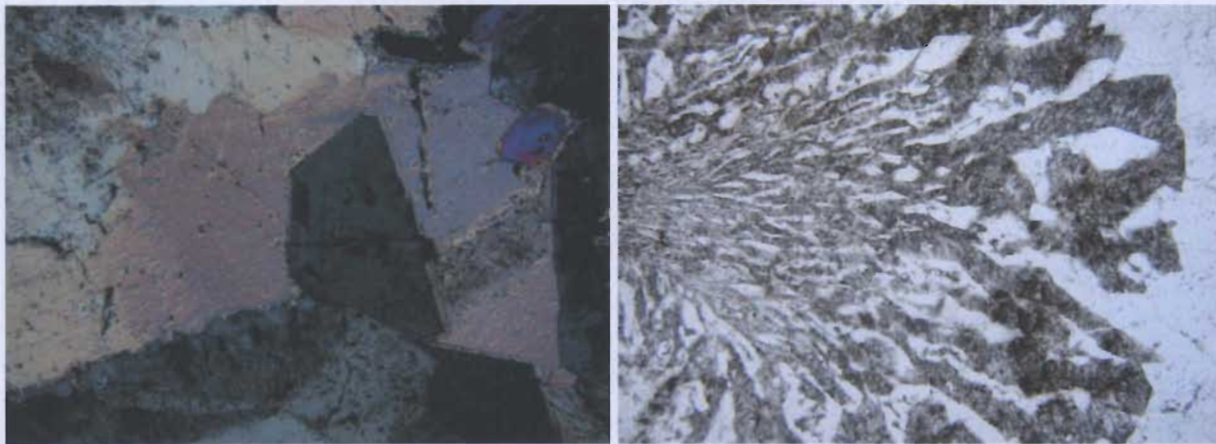


**Plate 3.22:** Photomicrograph of sample JOD27B of the Slip Prospect. a) intergrown prismatic quartz (grey) and carbonate [Field of view 7 mm, XP]. b) Granophyric texture from intergrown quartz and alkali feldspar [Field of view 7 mm, PPL].

#### 3.4.4 Jumper's Brook

The area as indicated by the MOD was traversed extensively. The only outcrop exposure is in the brook as either side of the brook is generally marshy with gently rolling hills littered with abundant boulders of hornfelsed sandstone. The only mineralization located was in subcrop along the brook at UTM coordinates 617185/ 5428579 (Plate 3.23a, p. 108). These boulders are very angular, very fine-grained, silicified hornfels that contain patches and small veinlets of sulphides (Plate 3.23b, p. 108). A vuggy quartz vein cut the hornfels and some mineral banding of mica was observed.



Modal percentages were difficult to determine for sample JOD118 from Jumper's Brook due to alteration. In general, the sample comprised 70% fine-grained matrix (quartz, feldspar and sericite) and 25% non-orientated grains of hornblende, biotite, chlorite and cordierite as well as 5% pyrite veinlets and disseminations (Plate 3.24, p. 72). Hornblende is almost entirely altered to chlorite and plagioclase is altered to sericite. Sub-parallel quartz veins run through the section with sulphide blotches occurring around these veins.

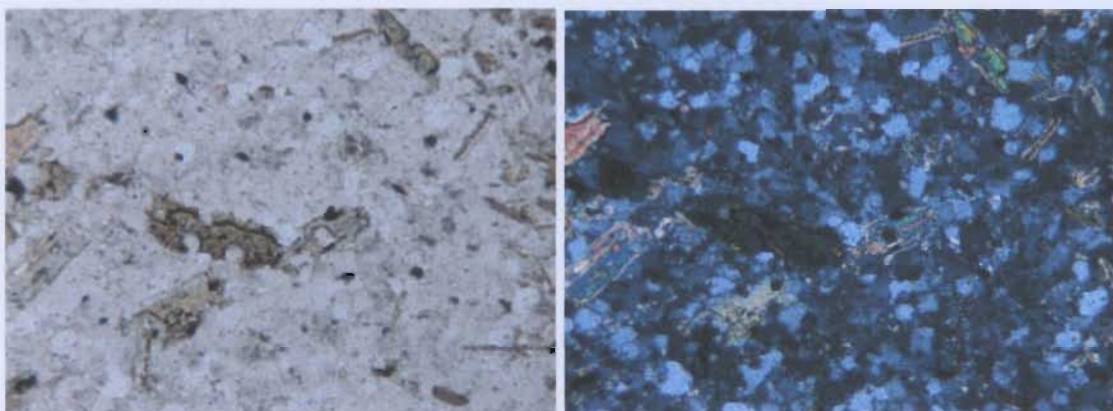


**Plate 3.24:** Photomicrograph of sample JOD118 from Jumpers Brook showing non-orientated grains of chlorite altered hornblende in a sericite-altered, fine-grained matrix of feldspar and quartz [Field of view, 2 mm, PPL and XP].

### **3.5 Southeastern Botwood Basin (Paul's Pond Region)**

With the exception of the Beaver Brook Mine (Hunan Prospect), the following gold occurrences are located in the vicinity of Paul's Pond and include the LBNL, Goose, Road Showing, Aztec, Hornet, Greens Pond #2 and A-zone prospects; all can be accessed via a series of forestry access roads from the steel bridge along the east side of the Northwest Gander River. Many of these roads are no longer in use and are only negotiable via ATVs. Some well maintained trails in the vicinity are kept in good



condition by owners of a nearby hunting lodge. The Hunan Prospect is an antimony occurrence on the west side of the Northwest Gander River and access to this property is excellent along the wide, well maintained Salmon River Access Road (Figure 3.9, p. 98).

The Paul's Pond prospects cover a 20 km<sup>2</sup> area and the property is centered on Paul's Pond and Greenwood Pond on NTS map sheet 2D/11. The prospects occur near the boundary between the Davidsville and Indian Islands groups (Figure 3.10, p. 99). A regional till survey was conducted in this area between 1986-87 but the results were poor due to the thickness of the till cover. A lake bottom survey conducted in 1988 defined a large anomalous area and follow-up prospecting led to the discovery of mineralized outcrops.

### **3.5.1 Hunan (Beaver Brook Mine)**

The Beaver Brook Mine (Hunan Antimony Prospect) is located at UTM coordinates 629855/ 5395490 on NTS map sheet 2D/11, 1 km west of the Northwest Gander River. The mine is ~ 40 km south-southwest of the town of Glenwood and can be accessed by a wide, very well maintained resource road from the TCH. Physiography is characterized by a gentle rise from the Northwest Gander River to the east of the property to the higher ranges of the Mount Peyton to the west. Two northwest trending brooks, Beaver and Cooper Brooks, transect the area, along which outcrop is readily exposed. The prospect consists of fracture-controlled stibnite veins, hosted in lower greenschist facies Silurian metasediments, and has been classified as an Acadian, epithermal style mineralization (Tallman, 1991). The sedimentary host rocks are

currently mapped as part of a thrust slice of Davidsville Group sediments within the Indian Islands Group (figure 3.11, p. 100)

The Hunan Prospect was assessed during the 2003 field season at a trenched and stripped area south of Cooper Brook. The outcrop consists mainly of shale and greywacke beds with abundant quartz veining. The veins appear more linear in the greywacke unit and are slightly sheared at the margins. Movement seems to be enhanced along a contact between the shale and greywacke units. The shale is much more affected by deformation and exhibits brecciation in places. The stibnite mineralization occurs more massively at the boundary between the shale and greywacke and within the quartz veins. Some carbonate veins occur with quartz-filled centers, and some openings have voids where quartz is better formed. The widths of the veins are generally 1 cm wide. Semi massive cubic and disseminated pyrite blebs were noted within quartz veins and the host rock and veins of massive stibnite, up to 4 cm wide, were also noted.

The Beaver Brook Mine was developed between 1994 and 1998 by Roycefield Resource Inc. who erected a 450 ton/ day mill in 1998. A short period of production ensued from 1998-1999, but the world antimony market was flooded by production from China, causing the price to plummet. The site was acquired by Beaver Brook Resources Ltd. in 2002, and in 2003 VVC Exploration Corp. (VVC) acquired all of the mine assets.

### **3.5.2 LBNL**

The LBNL prospect is located at UTM coordinates 636504/ 5391062 and is exposed in a very small outcrop obscured by alders along a trail which veers off an old



resource road. It consists of a very limited exposure of a cherty, fine-grained granitic rock with conjugate tension gashes trending at 074/32 N and 000/70 N. The host rock intrudes Davidsville Group rocks that are exposed just to the northwest and the tension gashes are not observed within the sediments. Pyrite and arsenopyrite are present as disseminations.

Polished thin sections were cut from a sample of mineralized granitic host rock (JOD45B and JOD45B). Sample JOD45B is a sample of pervasively altered, granitic host. The original modal petrography is only estimated due to pervasive alteration, which is dominantly sericitic with some chlorite. The section contains 55% alkali feldspar, 20% quartz, 20 % sericite and 10% sulphides consisting of cubic pyrite and rhombic arsenopyrite (Plate 3.25, p. 75). This rock is classified as fine-grained leucogranite. A low temperature granophyric texture of intergrown quartz and alkali feldspar is preserved where it is not altered to sericite.

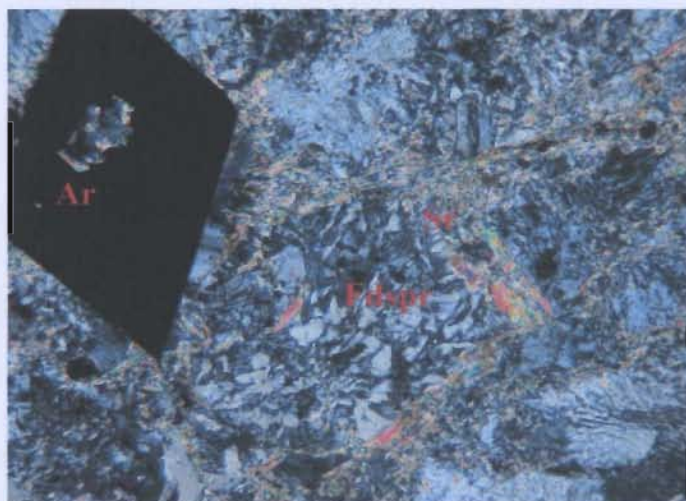


**Plate 3.25:** Photomicrograph of sample JOD45B consisting of a large rhombic arsenopyrite (Ar) grain in a pervasively sericite (Sr) altered leucogranite. Some primary feldspar (Fdspr) exhibiting a granophyric texture remains [Field of view 2 mm, PPL].



### **3.5.3 Goose**

The Goose Prospect is located at UTM coordinates 635743/ 5390002, approximately 1.5 km southwest of Paul's Pond. An overgrown, boggy drill path leads to the prospect, south from the LBNL. The trenches were filled with water, so little outcrop was observed. The samples collected for this study were trench float from along the sides of the trenched areas. Some of the float in the area was mineralized, white granite, as seen at the LBNL Prospect. Other float consisted of mineralized Davidsville Group greywacke in which bedding is sub parallel to cleavage. The greywacke is silicified and exhibits sericitic alteration. Large, randomly orientated, needle-like arsenopyrite grains, up to 0.5 cm long, and elongate pyrite grains, up to 3 mm long, were observed in grab samples.

### **3.5.4 Road Gabbro Showing**

The Road Gabbro Showing is located at UTM coordinates 635216/ 5391238, west of the LBNL Prospect. The trench has been backfilled and is overgrown with alders; outcrop is not visible in the area. A mound of very angular trench material, covered in vegetation, contained mineralized gabbro float with quartz veining. The mineralization consisted of disseminated, fine-grained pyrite and the gabbro was silicified. The prospect has been described as consisting of pyrite-arsenopyrite and quartz veins in silicified and carbonatized gabbro. The gabbroic intrusion cuts Davidsville Group sedimentary rocks (Evans, 1996). The best assay obtained by Noranda from a grab sample at the prospect was 2.24 g/t over 1.0 m (Tallman, 1989).

### **3.5.5 Aztec Prospect**

The Aztec Prospect is located approximately 1 km southwest of Greenwood Pond and 2.2 km east of the Northwest Gander River at UTM coordinates 6306041/ 5388967. It can be accessed via a network of abandoned logging roads. This prospect is exposed in an open area with multiple large trenches and stripped areas (Plate 3.26a, p. 108). The host rock consists of an intensely silicified and seritized breccia. In general, the outcrop appears to be most affected by hydrothermal fluids towards the north-northwest. The sedimentary host unit is heavily jointed with dominant cleavage directions at 111/69S, 126/37N, 047/90, and 167/66W. A large silica sinter, as well as quartz breccia and chalcedonic quartz were exposed at surface (Plate 3.26b, p. 108).

### **3.5.6 Hornet**

The Hornet Prospect is located at UTM coordinates 628844/ 5388101 down a muskeg trail from the Aztec Prospect. There are several large trenches with fairly good outcrop exposure and minor overgrowth. The surrounding, unaltered country rock resembles Indian Island Group sediments, consisting of green-grey silicified siltstone to green micaceous siltstone that weather to a brown color. In general, most of the outcrop is altered and exhibits rusty patches. Veinlets, patches and disseminations of arsenopyrite and pyrite were identified in outcrop and occur within a medium-grained unit (called a felsite in earlier reports (Evans, 1996)), which resembles a K-feldspar granite. The mineralized zone exhibits crosscutting (conjugate), vuggy quartz carbonate veins ranging from 1 to 3 cm wide and trending 158/47 N and 045/30 N (Plate 3.27a, p. 108).



In a polished thin section from sample JOD80A, the sample is pervasively altered to sericite and the original grain boundaries are barely visible making rock identification difficult. The sample contains 30% sericite, 40% K-feldspar, 20% quartz, 10% carbonate, 5% pyrite and Fe oxides (Plate 3.28a, p. 78). A quartz-carbonate vein cuts the unit (Plate 3.28b, p. 78).

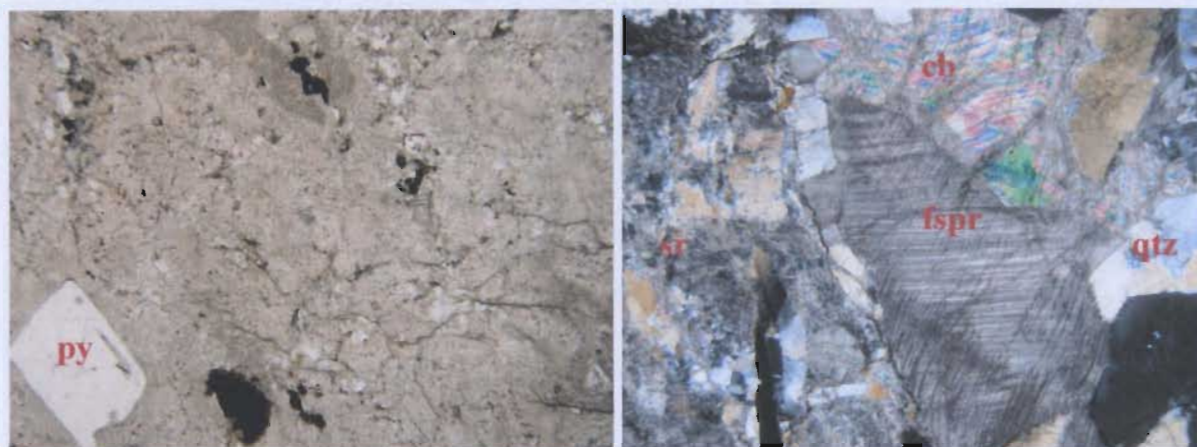


**Plate 3.28:** Photomicrograph of sample JOD80A from the Hornet Prospect. a) Very fine-grained, pervasively seritized host rock with cubic pyrite grain [Field of view 7 mm PPL]. b) Close-up of k-feldspar grain (fspr) surrounded by carbonate (cb), quartz (qtz) and sericite (sr) [Field of view 2 mm, XP].

### 3.5.7 Greenwood Pond #2

The Greenwood Pond #2 Prospect occurs along an ATV trail southeast of the Aztec at UTM coordinates 630400/ 5387150. It consists of a large exposure that has been stripped and/or blasted. The host is a fine-grained gabbro with very large quartz veins that generally trend 045°. The gabbro is intensely Fe carbonate altered and is also rusty from the weathering of sulphides (Plate 3.27b, p. 108).

Sample JOD81A indicates that the lithology is fine-grained with 30% sericite, 20% chlorite, 20% albite, 12% Fe-oxides, 10% quartz, 5% hornblende and 3% sulphides



(Plate 3.29, p. 79). Grain boundaries are not well defined and are aligned in a slight fabric indicating low-grade deformation.

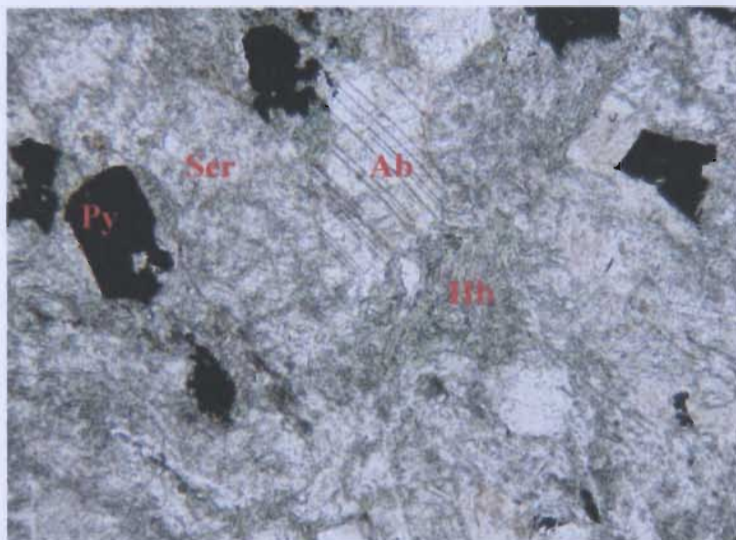


**Plate 3.29:** Photomicrograph of section from sample JOD81A from the Greenwood Pond #2 Prospect showing a fine-grained, sericite (Ser) and chlorite altered gabbro with some original quartz, hornblende (Hb) and albite (Ab) preserved. Hornblende is being altered to chlorite and cubic pyrite disseminations are also present [Field of view 2 mm, PPL].

### 3.5.8 A-Zone Extension

The A-Zone Prospect is located along an ATV trail, just south-southwest of the Hornet Prospect at UTM coordinates 631150/ 5388800. The prospect is exposed in trenches for over 250 m and the gold mineralization is hosted by discontinuous extensional quartz-carbonate veins and veinlets developed within chloritized and potassically altered Davidsville Group greywacke. The greywacke unit occurs as a 15-20 m wide bed within grey-green siltstone. An assay value of 2.60g/t Au over 7.0 m was obtained from this prospect (Tallman, 1989). Two extensively trenched areas were examined which exposed mineralized greywacke with siltstone interbeds. Pyrite and

arsenopyrite occurred in veinlets, up to 0.5 cm wide, and patches and is locally semi-massive near quartz-carbonate veins that are up to 2 cm wide.

### **3.6 Southern Botwood Basin (Great Bend Region)**

This area is referred to as the Great Bend Region because the large bend here in the Northwest Gander River has historically been referred to as the “great bend” (Figure 3.9, p. 98). The region is characterized by gently rolling hills covered by black spruce, scattered bogs and lakes with drainage to the north and is cross-cut by a series of abandoned logging roads. However, outcrop exposure is limited due to a 3-5 m thick till cover. The Rolling Pond and Chiouk Brook prospects occur on the north side of the Northwest Gander River, whereas the Breccia Pond, Lizard Pond and Swan Lake prospects are on the south side.

With the exception of the Rolling Pond, Swan Lake and Huxter Lane prospects, the following properties described herein are underlain by the Great Bend Complex, which occurs adjacent to sedimentary rocks of the Ordovician Spruce Brook Formation (Mount Cormack Subzone), Cambro-Ordovician ophiolitic rocks of the Coy Pond Complex, and Ordovician sedimentary rocks of the Davidsville Group and North Steady Pond Formation (Botwood Group) respectively. The Rolling Pond Prospect occurs within rocks of the North Steady Pond and Spruce Brook formations, the Swan Lake Prospect is hosted within Indian Islands Group sediments, and the Huxter Lane Prospect occurs within the Coy Pond Complex (see Figure 3.9, p. 98 for prospect locations and figure 3.14, p. 103 for geology of the prospects hosted within the Great Bend Complex).

The Great Bend Complex is an ophiolite complex that is in fault contact (possibly overthrust) with the Early Ordovician Spruce Brook Formation (Dickson, 1992) and was tectonically emplaced as a major allocthon (Colman-Sadd and Swinden, 1984).

The best-exposed rocks of the Great Bend Complex are banded or serpentinitized peridotite, magnesite-altered peridotite and sheared serpentinitized peridotite to serpentinite schist and lesser siltstone. Pervasive Fe-carbonate alteration, silicification and talc carbonate alteration with quartz and magnesite veining is characteristic of the Au mineralized areas (Dickson, 1992).

### **3.6.1 Rolling Pond**

The property is located at the boundary between Botwood Group sediments and Spruce Brook Formation metasediments (Dickson, 1991). This interpretation differs from the work of Colman-Sadd and Russell (1988), who mapped the property entirely within Botwood Group rocks; the Spruce Brook Formation was mapped to the south. The MPIS outcrops to the northeast of the property and the Stoney Lake Formation volcanic rocks occur approximately 16 km west of the property (Barbour *et al.*, 1999). A major east-northeast trending fault zone, marked by ophiolitic rocks, that runs through Miquel's Lake, marks the boundary between the Botwood Group and Spruce Brook Formation to the east (refer to Figure 3.12, p. 101) (Colman-Sadd and Russell, 1981). A detailed geology map of the property was presented by Barbour *et al.* (1999) (Figure 3.13, p. 102).



The prospect was accessed via a woodcutting road off the Baie d'Espoir highway, 40 km south of the TCH-Highway 331 junction. A 1999 fieldtrip guidebook (Barbour, 1999) leads to a quartz sinter at UTM coordinates 611423/ 5391239. Here, subcrop of very white quartz, with vugs up to 15 x 7 cm in size, were observed with very well-formed quartz crystals up to 2 cm long (Plate 3.30a, p. 109). Arrays of distinctive epithermal textures are present including cockade textures, quartz rosettes (silica sinter) and silica replaced lattice blades. Approximately 6 m north, there is a large flat outcrop of very massive white quartz, presumably sinter. Quartz-brecciated float is abundant in the area, which increases in amount to the north (Plate 3.30b, p. 109).

At UTM coordinates 611366/ 5391302 subcrop of quartz breccia with a very small outcrop of host rock composed of fine-grained sandstone that is green-grey on fresh surface and brown on the weathered surface is exposed. The host contains some shiny quartz (5%) and exhibits carbonate alteration. At UTM coordinates 611393/ 5391270 there are both outcrop and subcrop exposures consisting mainly of quartz breccia with angular pieces of wallrock. The brecciated fragments consist of a grey, fine to medium-grained, variably silicified sedimentary rock. The fragments vary in size from a few mm to several centimeters and are very foliated. Some of the fragments are red in places, indicating hematite alteration. Trenches, or well-exposed outcrops of host rock, were not located in a radius traversed about the sinter. Along the path to the woodcutting road, a conglomerate outcrop is exposed at UTM coordinates 611171/ 5391587. The conglomerate is foliated and clast-supported with a grey sandy matrix and is interbedded with green/grey fine to medium-grained sandstone.

### **3.6.2 Chiouk Brook**

The Chiouk Brook Prospect is located at UTM coordinates 616099/ 5383976 along Chiouk Brook (Plate 3.31, p. 109) which enters on the north side of the great bend in the Gander River on NTS map sheet 11D/2. It is approximately 6 km east of highway 360 and can be accessed via an old resource road and drill path. Outcrop is very limited and the physiography is characterized by a low relief, gently rolling topography. A large fire swept the area in 1986 so the majority of the land is burnt over making traversing difficult.

The outcrop is mainly exposed along the north-northeast side of the river and consists of a 6 x 3 m zone. The host rock is dark grey, silicified, very fine-grained sandstone that contains disseminated pyrite and arsenopyrite. Down the brook, at UTM coordinates 616144/ 5383959, an outcrop of less silicified, black slate is exposed. This outcrop is very deformed and the main cleavage is sub-parallel to the bedding that trends 026°. The unsuccessfully trenched area was observed along the northeast side of the brook at UTM coordinates 616209/ 5383967 and a very small outcrop of black serpentized material was exposed in close proximity. The Chiouk Brook Prospect is located at the northern margin of the Great Bend Complex.

### **3.6.3 Breccia Pond**

The prospect can be accessed via an abandoned logging road approximately 8 km from the Baie d'Espoir Highway, and is located approximately 3 km south of the resource road at UTM coordinates 616675/ 5380345 and is reachable by traversing

through difficult terrain of thick forest and marsh. An old drill path was noted in the vicinity of the prospect and three trenches were observed between the drill path and Breccia Pond.

The main trench, immediately adjacent to the pond at UTM coordinates 616675/ 5380345, exposes an extremely altered orange to red ultramafic host rock (Plate 3.32a, p. 110). In some places, the host is less altered and exhibits chromite grains ~1 mm in diameter. A few thin quartz veins cut the host rock and range from 0.5- to 1.0 cm wide. Quartz crystallized in fractures following deformation because the crystals are perfectly formed and have not been affected by alteration. There were probably multiple fluid phases as some quartz veins crosscut others. The host rock is very hematized around fractures, forming haloes up to 3 cm wide (Plate 3.32b and c, p. 110). A very minuscule amount of disseminated mineralization was noted in outcrop and a green alteration mineral (possibly malachite) was present. A rosette of yellow and green elongate crystals was noted at one locality and was later identified as an aggregate of tarnished, acicular millerite crystals. Due south, a second trench was found at UTM coordinates 616723/ 5380287. This trench contains the same unit as observed in trench 1, although there is semi massive pyrite present at this locality.

The third trench is located at UTM coordinates 616768/ 5380397 and the outcrop consists of un-mineralized, very red, siliceous jasperoid (Plate 3.32d, p.110). The trench is approximately 40 m in length and exposes abundant outcrop. The outcrop is generally very silica-rich and this area exhibits the most intense alteration at the prospect as indicated by the brecciation and the intense red color of outcrop. In places, the rock



exhibits white coatings of magnesite and beautiful crystalline quartz with very shiny surfaces.

Sample JOD36B was collected from the second trench and is composed of 40% hematite, 30% magnesite, 20% quartz, 5% oxides and 5% serpentinite (Plate 3.33, p. 85). Petrographical analysis revealed that the red alteration mineral was hematite and that quartz occurs as interlocking anhedral crystals in veins that contain sulphides. There are multiple generations of quartz and magnesite veining as indicated by the crosscutting relationships. Thus, this rock consists of silicified and hematized, brecciated serpentinite.

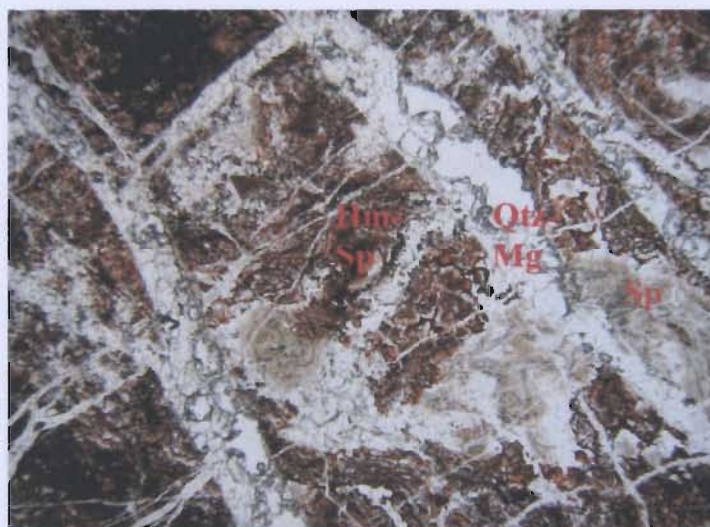


**Plate 3.33:** Photomicrograph of JOD36B exhibiting magnesite (Mg) and quartz (Qtz) brecciated hematized serpentinite (Hm-Sp) [Field of view 7 mm, PPL].

#### 3.6.4 Swan Lake

The Swan Lake Prospect is located along the west side of Swan Lake at UTM coordinates 613387/ 5378508. The prospect was difficult to locate, as the trenched area is located behind the south tree line at the back of a large marsh.

One trench was located during the 2003 field season that was approximately 60 m long with limited outcrop exposure. The south end of the trench is in glacial till,

however, outcrop of green, laminated Indian Islands Group siltstone is exposed. Quartz veins cut through the unit and are up to 2 cm wide, however, no mineralization was found. At the north end of the trench, a black fine-grained slate unit is exposed in a very small outcrop. Abundant quartz breccia float, although not observed in situ, was also found at this end of the trench (Plate 3.34, p. 110). The brecciated pieces consisted of silicified slate and pyrite mineralization was noted in some grab samples. The vegetation cover in this area is extensive and no other outcrop localities were located. The prospect is located within Indian Islands Group sediments near a faulted contact with the Great Bend Complex.

### **3.6.5 Lizard Pond South**

The Lizard Pond South Prospect was discovered by BP Canada in 1989 and is located along the southern end of Lizard Pond at UTM coordinates 614200/ 5379550. It comprises a series of isolated, fault-controlled quartz breccia veins in grey to brown, siliceous, locally brecciated, magnesite-altered serpentinite of the Great Bend Complex.

The large stripped area on the south end of Lizard Pond was examined during the 2003 field season (Plate 3.35a, p. 111). Abundant outcrop was exposed in a very large open trench/ stripped area and the units appeared extremely deformed as indicated by foliation. In general, the main unit is a very altered ultramafic that is cut by quartz veins up to 0.5 m wide (Plate 3.35b, p.111). In places, openings are filled with well-formed quartz crystals and some also contain carbonate that is rimmed by quartz. The original rock appears to have been a serpentinite-altered ultramafic as chromite is still present



locally, however, most of the unit has been altered to magnesite and has been extremely Fe-carbonatized. A dominant, well-exposed quartz breccia vein cuts this altered unit at 067°/ 70° S. The brecciated fragments do not seem to be altered ultramafic and contain sulphides.

A polished thin section of sample JOD50 from a trench at the Lizard Pond South Prospect is composed of 60% serpentinite, 20% magnesite, 10% quartz, 5% chromite, 2% Fe oxides and 3% pyrite. The section is very fine-grained with multiple vein systems. The veins are composed of magnesite and lesser quartz, and one large vein cuts a perpendicular smaller vein, which is offset in several places (Plate 3.36, p. 87). The sample is a magnesite-altered serpentinite with well-preserved serpentinite mesh textures.

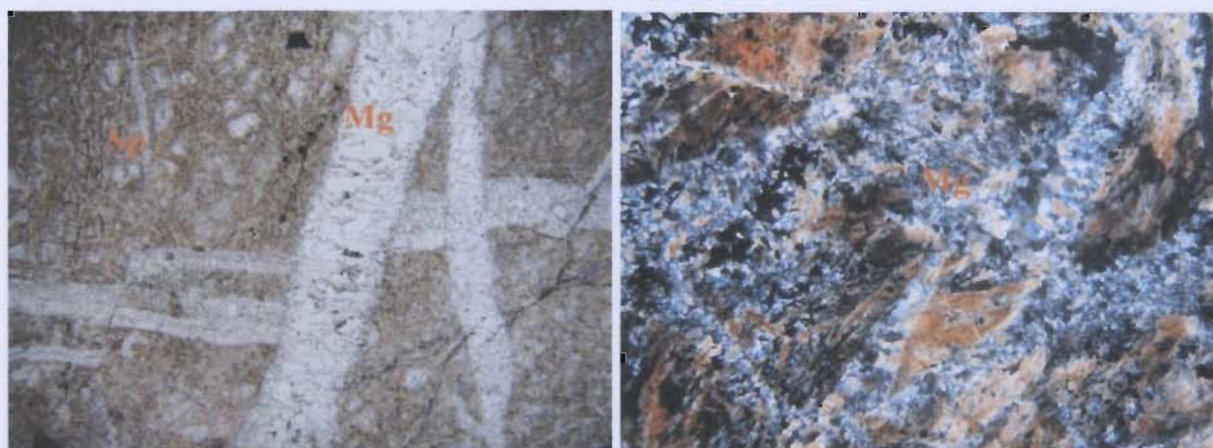


**Plate 3.36a, b:** Photomicrograph of magnesite-altered serpentinite ultramafic host to the Lizard Pond South Prospect. Multiple generations of magnesite (Mg-carbonate) veining. Note mesh like texture and oxides from breakdown of igneous minerals. The second section exhibits blotchy pyrite mineralization [Field of view 2 mm, PPL and XP].

Sample JOD52A from the main trench (Plate 3.37, p. 88) is comprised of 20% serpentinite, 40% magnesite, 20% quartz, 15% acicular pyrite and 5% Fe oxides. The hand specimen was collected from a very siliceous zone of quartz veins with semi massive pyrite.



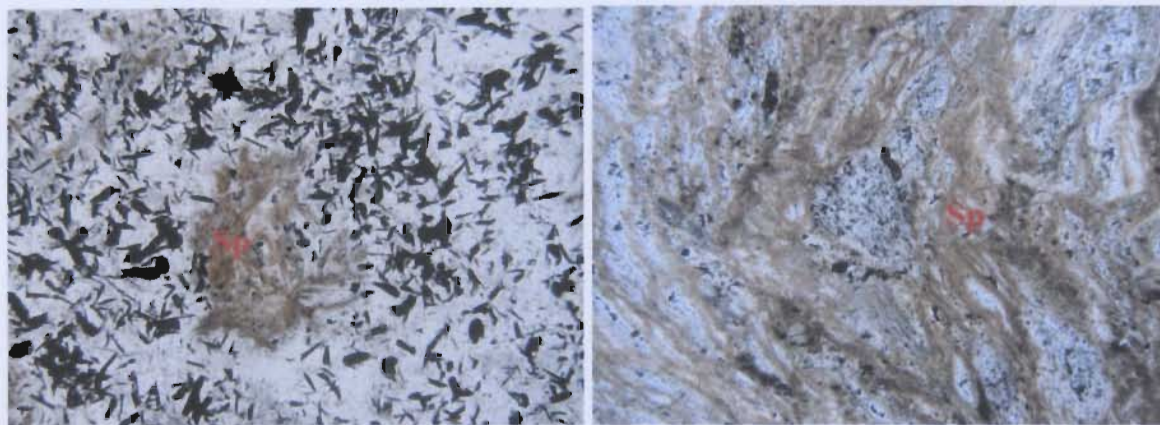


**Plate 3.37:** Photomicrograph of sample JOD52A from a sample collected from the large stripped area at the Lizard Pond South Prospect [Field of view 2 mm, PPL]. a) Pyrite mineralization in quartz and magnesite with some serpentinite preserved. b) Mesh like texture of magnesite altered serpentinite with pyrite [Field of view 7 mm, PPL].

### 3.6.6 Lizard Pond North

The Lizard Pond North Prospect is located at the northwestern tip of Lizard Pond at UTM coordinates 613612/ 5380831 on NTS map sheet 2D/11. The two trenches that were excavated at this prospect were examined. The first trench at UTM coordinates 613612/ 5380831 is large (~15 m long) and has abundant exposure of a greyish blue peridotite. The second trench, approximately 190 m away at UTM coordinates 613471/ 5380697, is only 5-6 m long and exposes a highly talc-carbonate altered zone and an ultramafic shear zone that trends 115/58 N. Disseminated arsenopyrite and pyrite were noted in a magnesite-altered schist.

Sample JOD55A from this prospect is a silicified, light grey ultramafic with 10% green talc and white magnesite. It weathers orange-brown at the surface and still has visible chromite. There are a few small (~2 mm) quartz veins and the rock is very dense.

Petrographically, the sample is comprised of 10% talc, 10% serpentine, 75% magnesite, 3% chromite and 2 % pyrite. The sample is therefore a magnesite-altered serpentinite. The magnesite exhibits a snakeskin texture (Plate 3.38, p. 89).

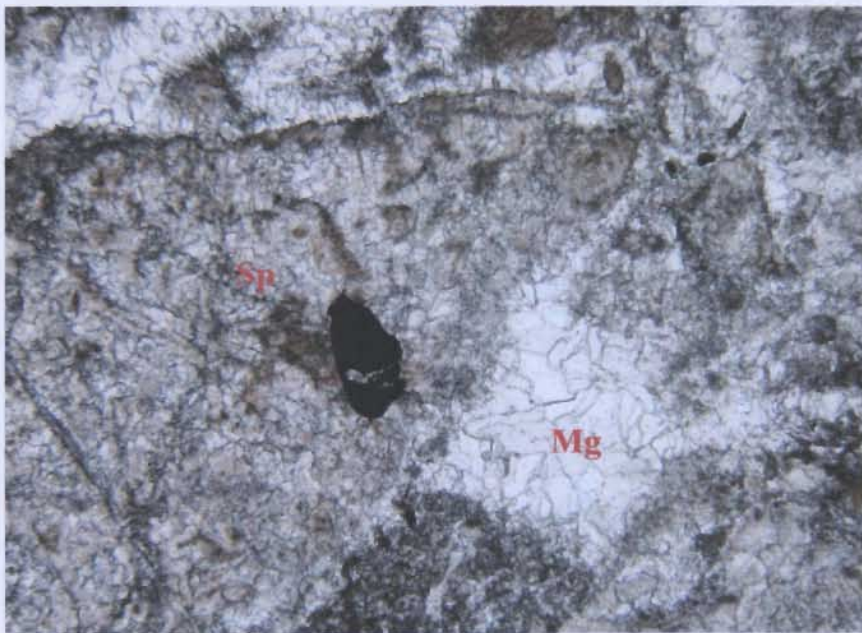


**Plate 3.38:** Photomicrograph of sample JOD55A illustrating a snakeskin texture common in magnesite (Mg) altered serpentinite (Sp). A grain of chromite is visible in the section [Field of view 7 mm, PPL].

### 3.6.7 Huxter Lane

The Huxter Lane Prospect is located in the southern Botwood Basin, approximately 11 km west of the Baie d'Espoir highway and is hosted in intrusive rocks of the Coy Pond Complex at UTM coordinates 603859/ 5367584 within mapsheet 2D/5 (figure 3.9, p. 98). The prospect was discovered in 2002 and is currently under joint venture between Rubicon Minerals Inc. and Meridian gold Inc.. Samples were collected from the prospect by Derek Wilton in 2003 and comprise a light greenish grey porphyritic intrusive cut by quartz breccia veins. The brecciated host contains



disseminated pyrite and arsenopyrite and the rims of the breccia pieces and veins are rimmed in massive arsenopyrite. Disseminated sulphides also occur in the un-brecciated host rock. There is no published information on this prospect. However, a BSc. Honors thesis was conducted by Seymour (2003) on the Reid property, near this prospect, which has similar characteristics. A polished thin section was cut from sample W03-38 (Plate 3.39, p. 111) and comprises 35% plagioclase, 30% quartz, 15% alkali feldspar and 10 % biotite, 5% hornblende and 5% pyrite (Plate 3.40, p. 90). The sample therefore has an intrusive dacitic composition that is further defined by geochemistry (chapter 5).

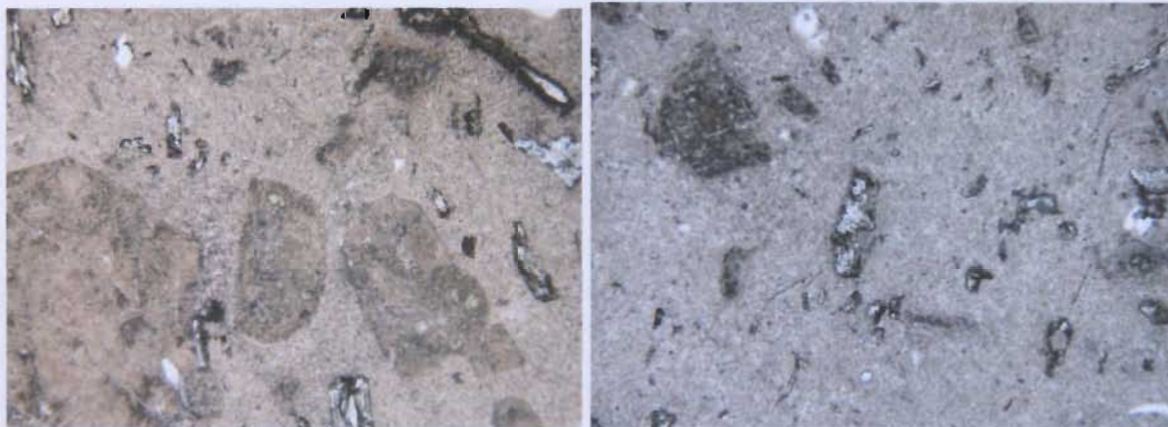


**Plate 3.40:** Photomicrograph of sample W03-38 from Huxter Lane illustrating porphyritic fragments in a very fine-grained matrix [Field of view 2 mm and 7 mm, PPL].



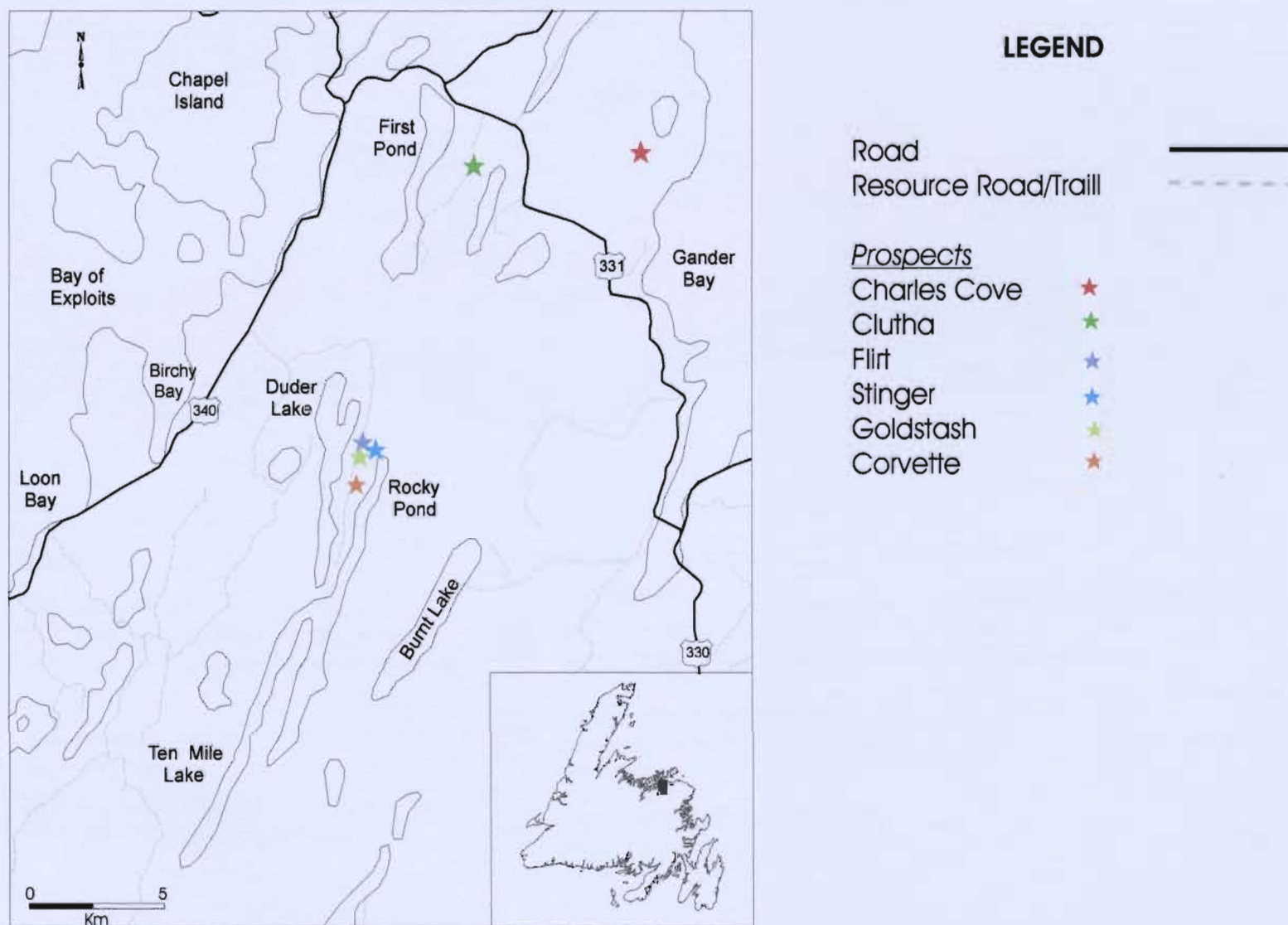
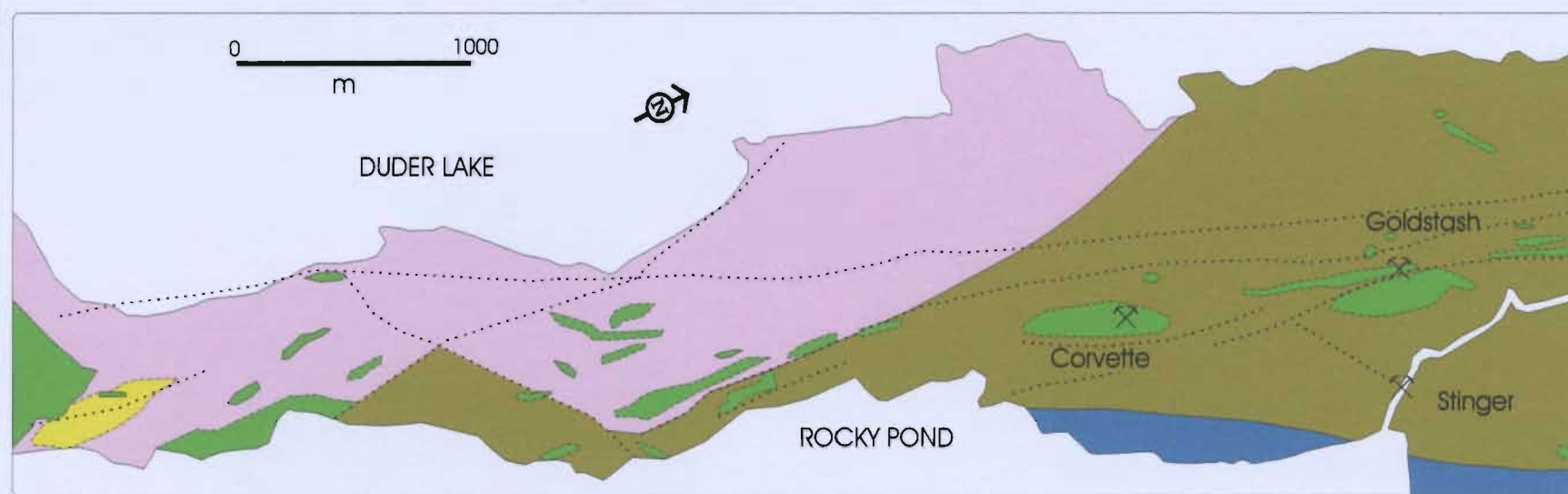


**Figure 3.1:** Location map for the Duder Lake, Clutha and Charles Cove Prospects.



### LEGEND

#### SILURIAN

##### Ten Mile Lake Fm

Red, thin bedded sandstone and shale with intervals of green siltstone

##### Indian Islands Group (Horwood Fm)

Homogeneous grey to black shale with thin buff siltstone beds

#### ORDOVICIAN TO SILURIAN

##### DUDER COMPLEX?

Homogeneous grey shale with disrupted tuff beds, melange

Medium to coarse grained gabbroic, dioritic and diabasic sills

Subaerial purple to black basalt flows and pillows and breccias

Contact (defined, approximate) — — — — —

Faults

Gold Mineralization



**Figure 3.2:** Major geological units in the Duder Lake area, showing location of the Corvette, Goldstash and Stinger prospects (modified from Churchill *et al.*, 1993 with geological changes based on Currie, 1995b).

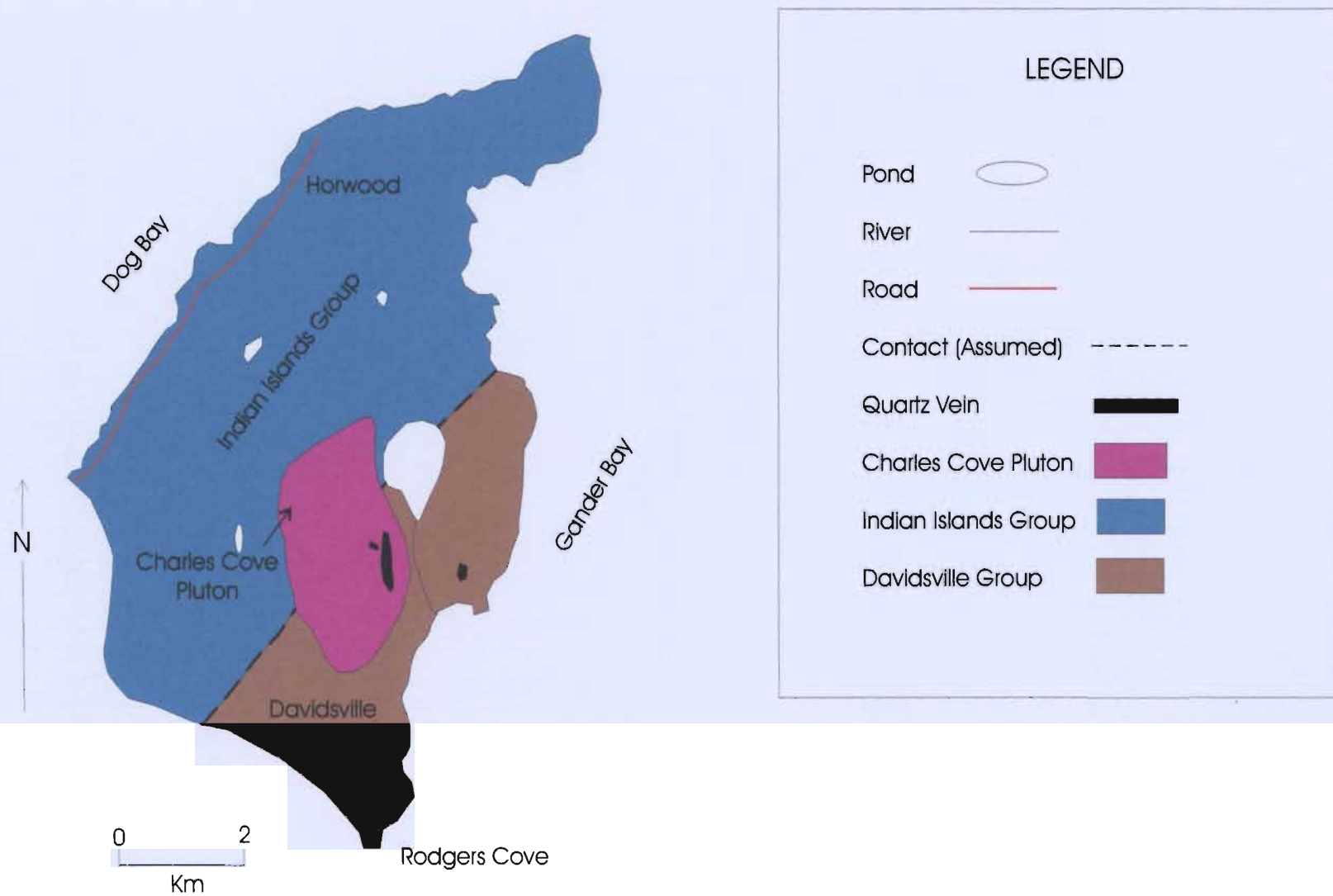


**Figure 3.3:** Geology in the Tim's Cove Area and location of the quartz vein systems (after Evans, 1996).



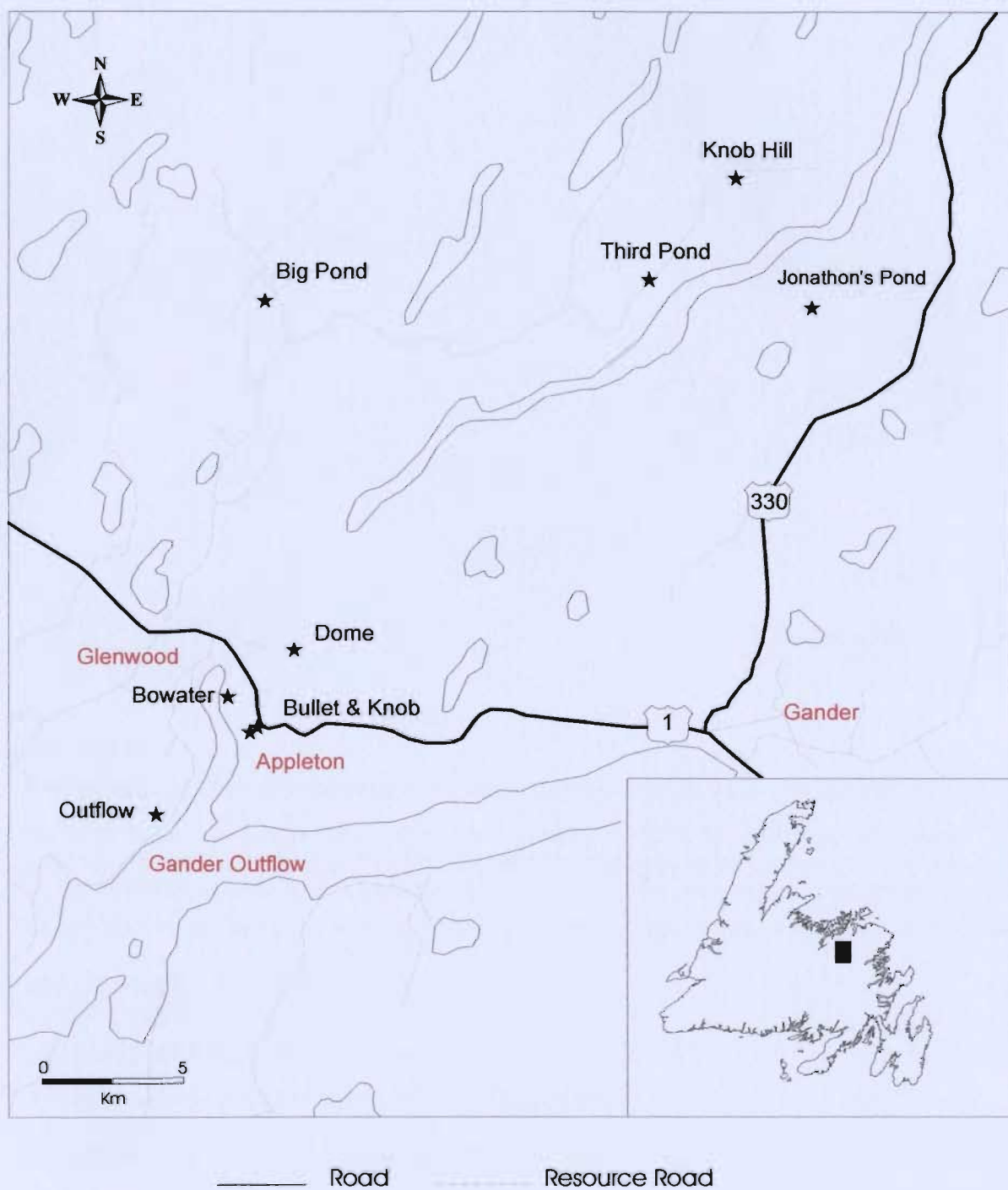
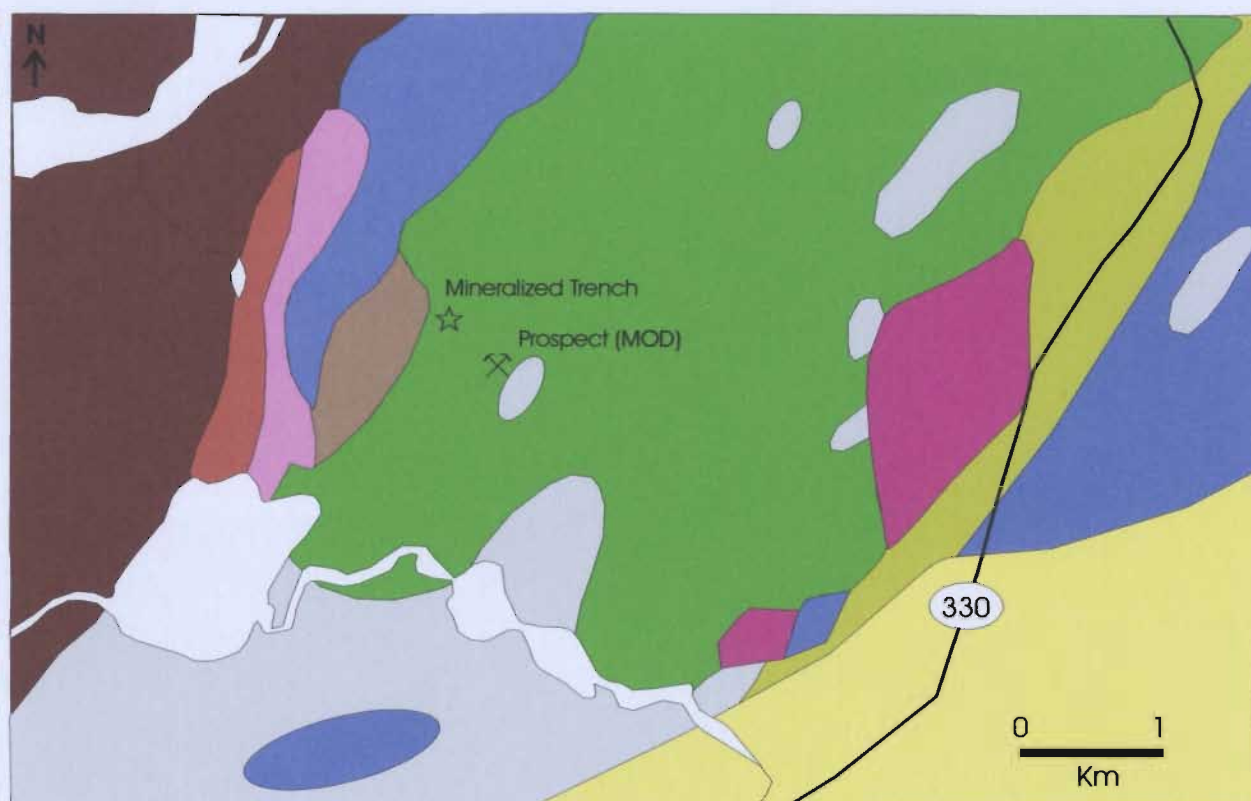


**Figure 3.4:** Central Botwood Basin (Glenwood-Appleton region) prospect location map.



### LEGEND

#### DAVIDSVILLE GROUP

- Hunt's Cove Fm: Grey to black slate and siltstone; minor red slate and minor sandstone
- Weir's Pond Fm: Fine to coarse-grained grey sandstone with pebble lenses, calcareous siltstone; minor red sandstone, limestone, quartzite, and grey to black slate and fine to coarse-grained polymictic (locally olistomictic) conglomerate and minor sandstone
- Fine to coarse grained polymictic (locally olistomictic) conglomerate and minor sandstone

#### EARLY ORDOVICIAN OR EARLIER GANDER RIVER COMPLEX

- Quartz and/or feldspar porphyry, locally brecciated
- Fine to coarse-grained trondjemite, locally brecciated
- Mafic flows; including minor diorite, tonalite and basalt
- Fine to coarse grained gabbro; including minor diorite, tonalite and basalt
- Serpentinite, magnesite and talc tremolite schist; including minor pyroxenite
- Medium to coarse-grained pyroxenite; including minor serpentinite, magnesite, hornblende and gabbro

#### GANDER GROUP

- Psammite and semipelite; including minor mafic tuff bands

**Figure 3.5:** Geology of the Jonathon's Pond area (modified from Blackwood, 1982).

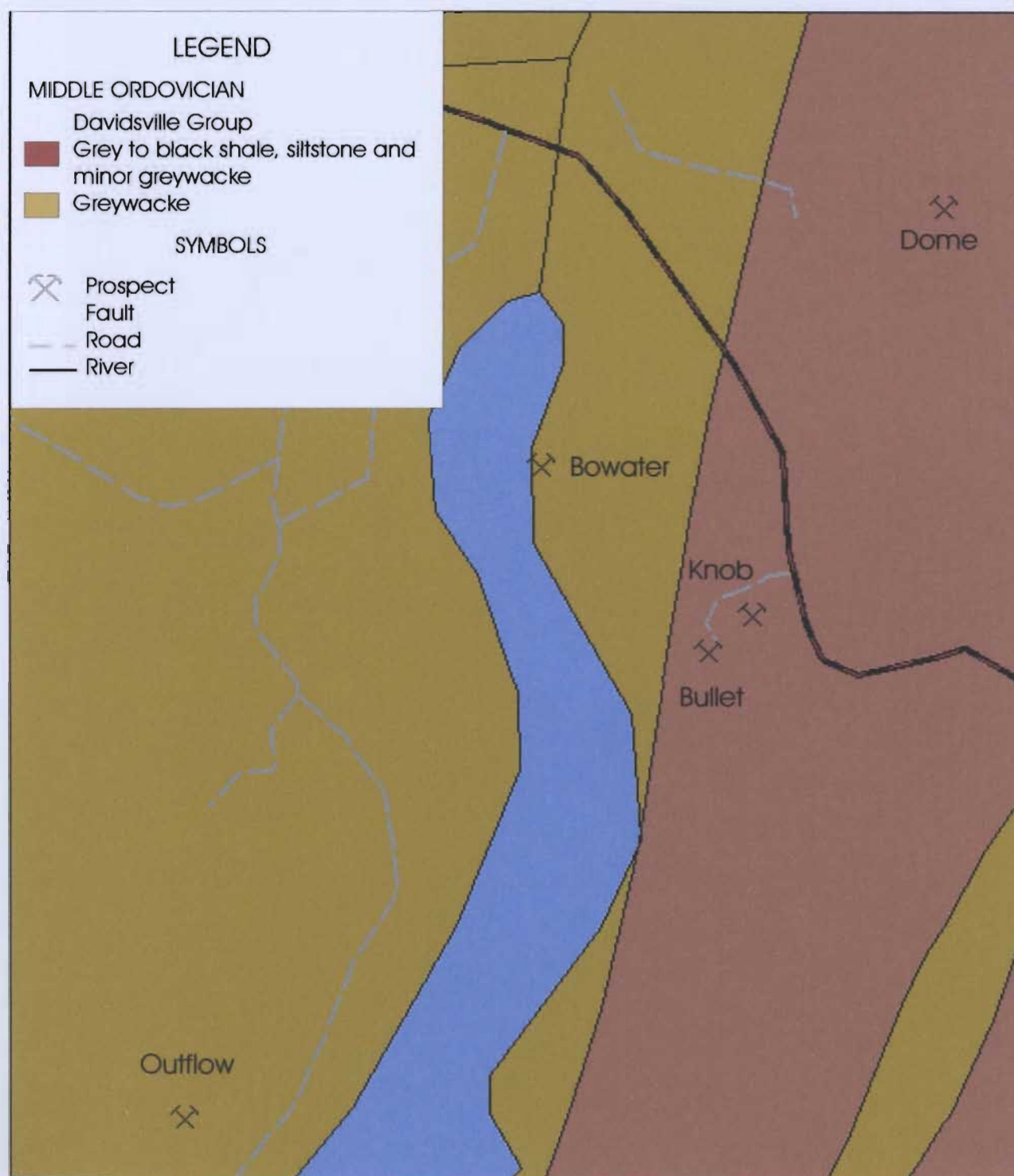


**Figure 3.6:** Geology of the Glenwood-Appleton area, central Newfoundland (geology from Blackwood, 1982 and Dickson, 1992).



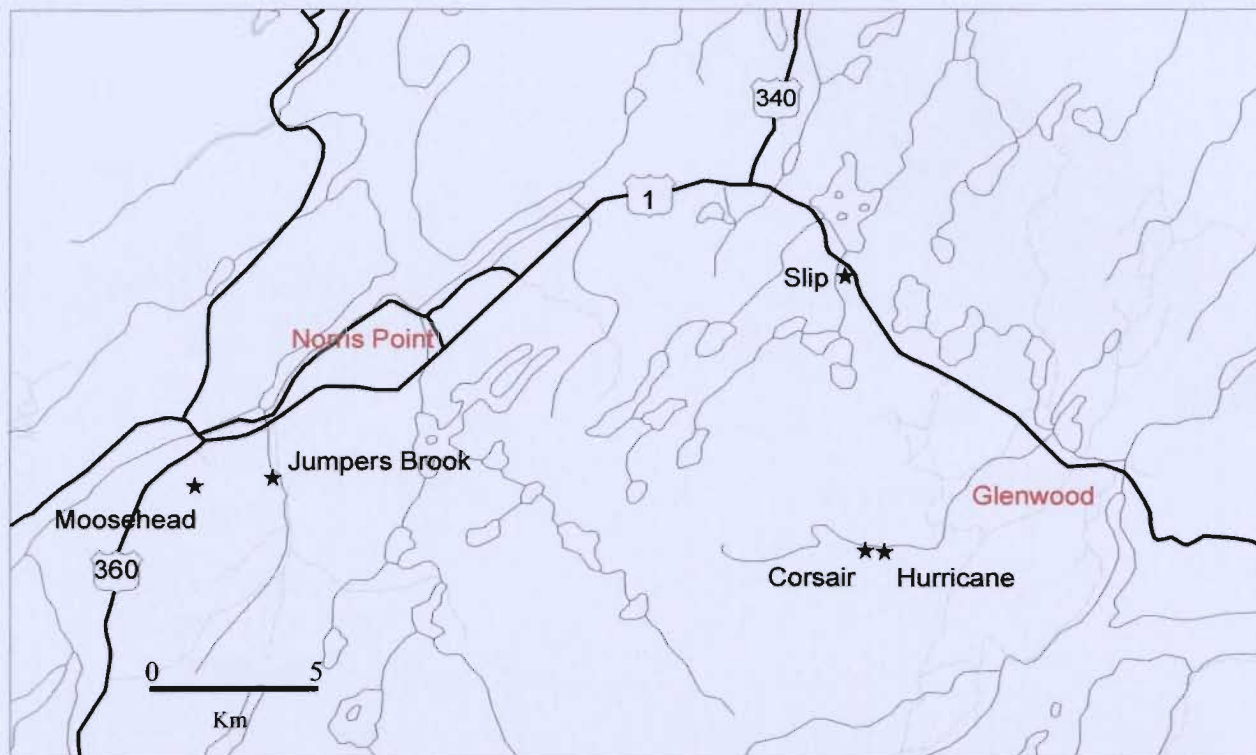


**Figure 3.7:** Location map for Mount Peyton Prospects, central Botwood Basin.



**Figure 3.8:** General geology map of the northern Mount Peyton area (geology modified from Colman-Sadd and Crisby-Whittle, 2002) [refer to figure 2.4 for legend].

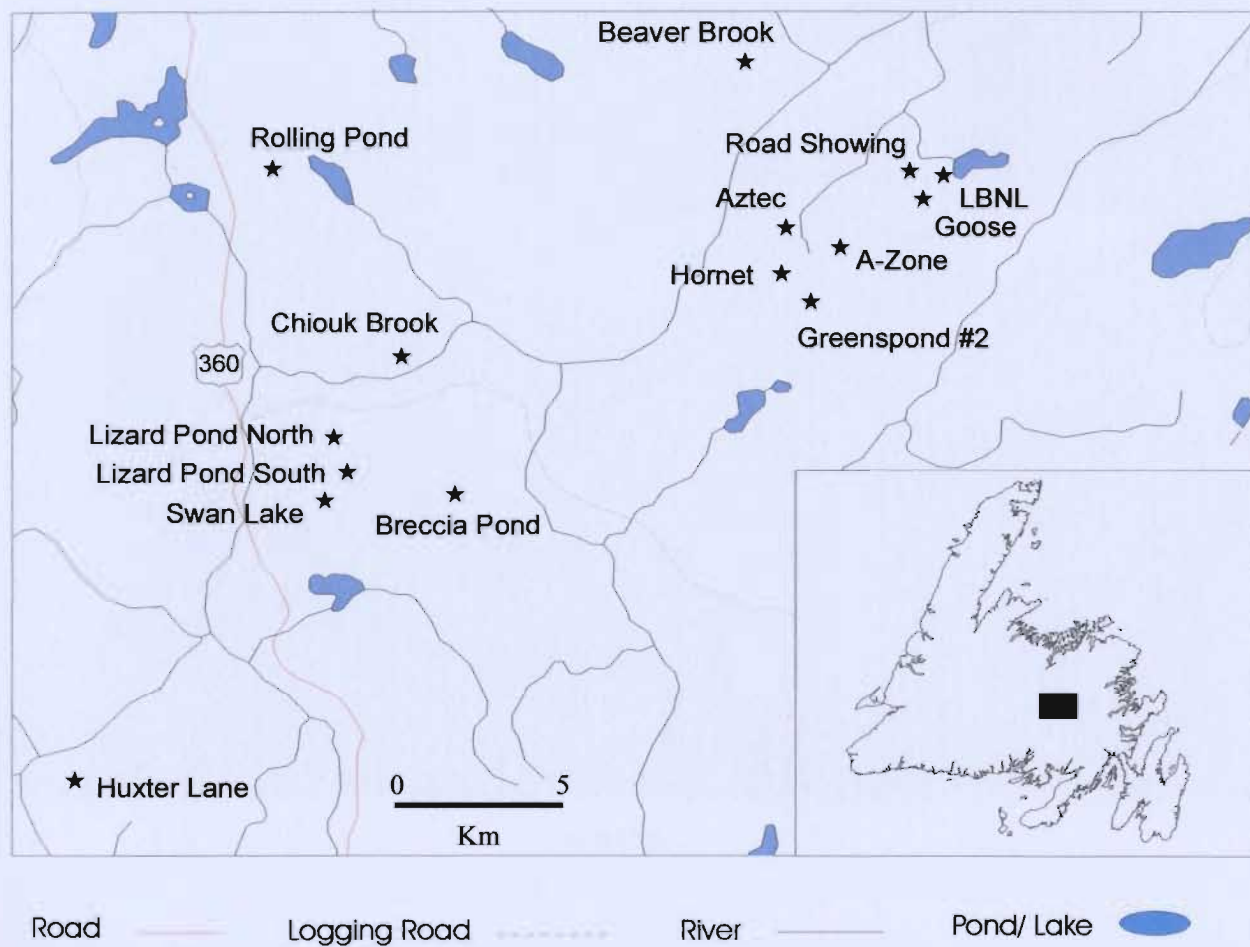
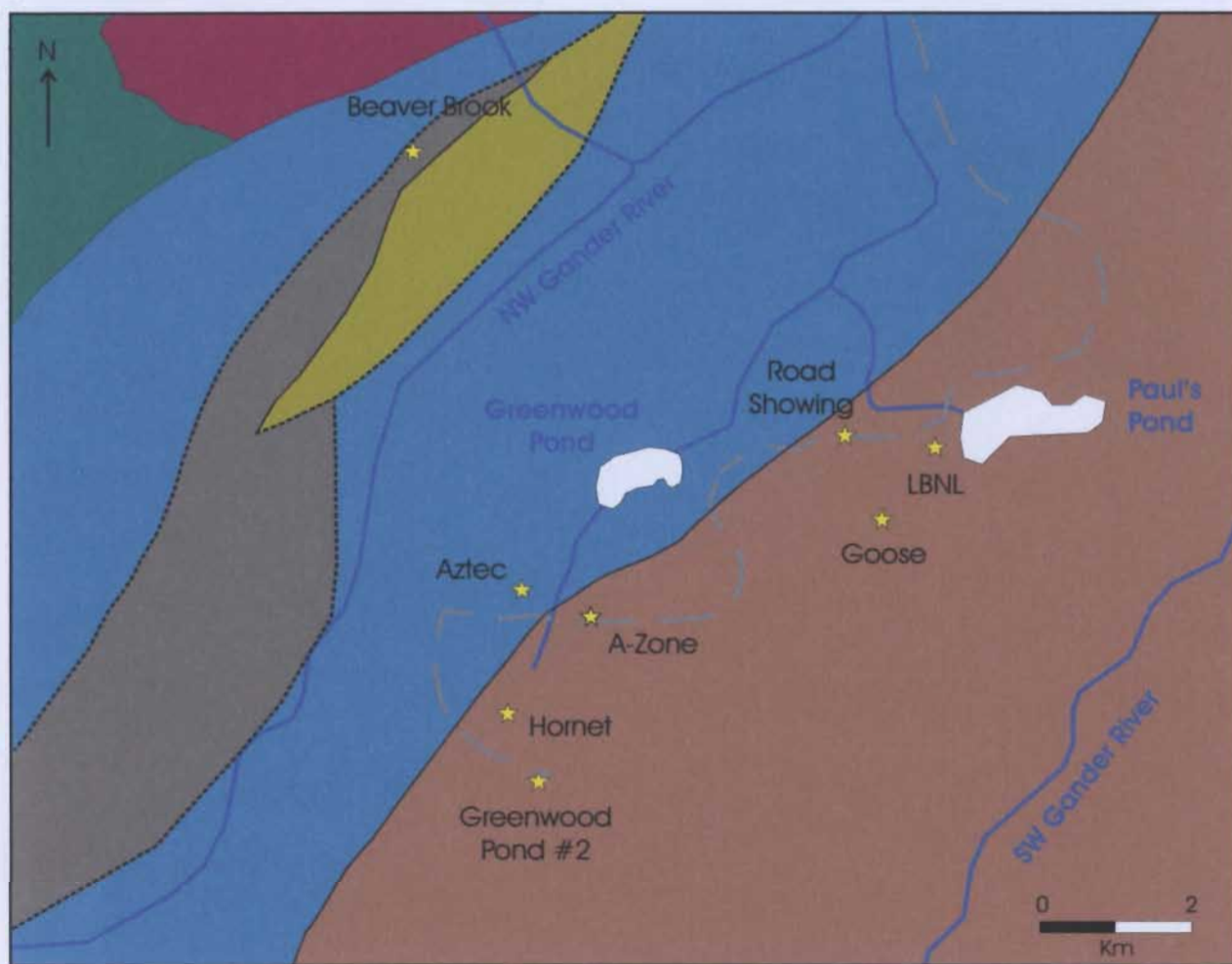


**Figure 3.9:** Location map for Southern Botwood Basin Prospects.



### LEGEND

#### SILURIAN



Mount Peyton Intrusive Suite



Indian Islands Group

#### ORDOVICIAN



Caradocian Shale



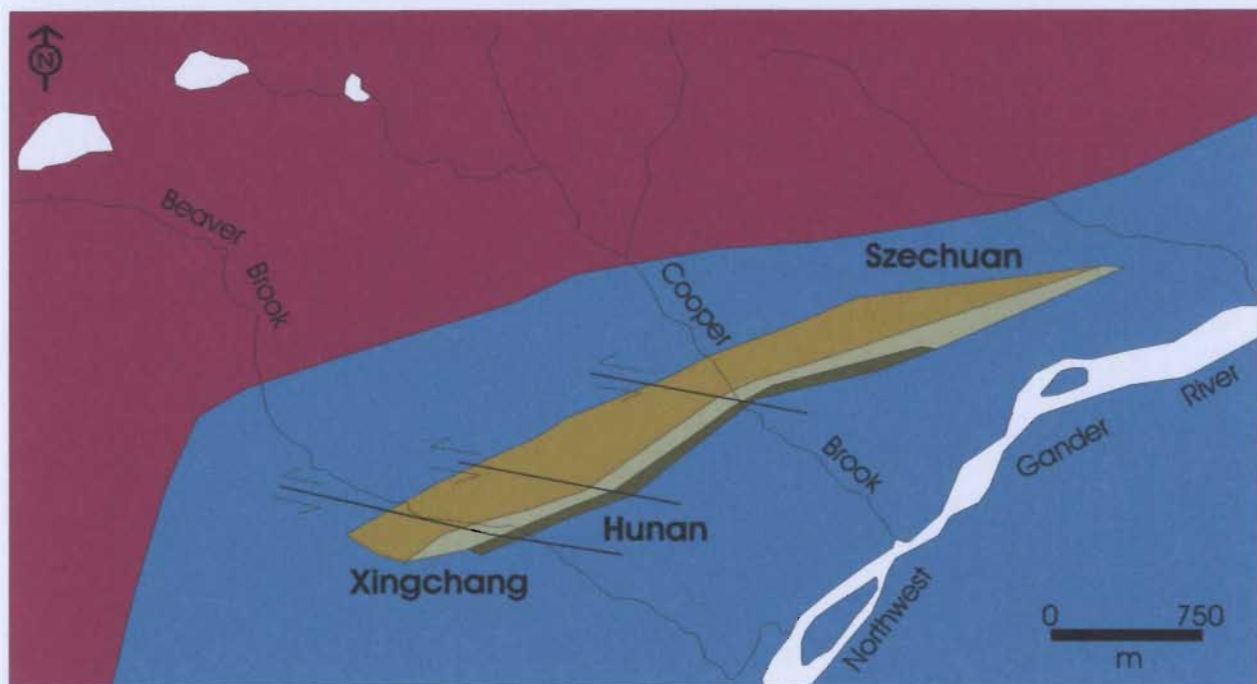
Davidsville Group

#### SYMBOLS

- Fault
- Geological Contact
- River
- Resource Road/ Trail
- ★ Prospect

**Figure 3.10:** Geology of the southern Botwood Basin-Paul's Pond region auriferous prospects and the Beaver Brook antimony deposit (Beaver Brook geology examined in more detail in figure 3.11) (geology from Dickson, 1996).





#### SILURIAN

##### MOUNT PEYTON INTRUSIVE SUITE



Pink and cream massive, medium to fine grained, equigranular biotite +/- hornblende granite

#### INDIAN ISLANDS GROUP



Shallow marine sedimentary rocks consisting of variable rare, massive limestone and calcareous sandstones and siltstones

#### MIDDLE TO LATE ORDOVICIAN DAVIDSVILLE GROUP



Graphitic shale



Pebbly greywacke



Rhythmic bedded siltstone

**Figure 3.11:** Regional geology of the Hunan Line Antimony prospects (modified from Tallman and Evans, 1994 and Dickson, 1996).

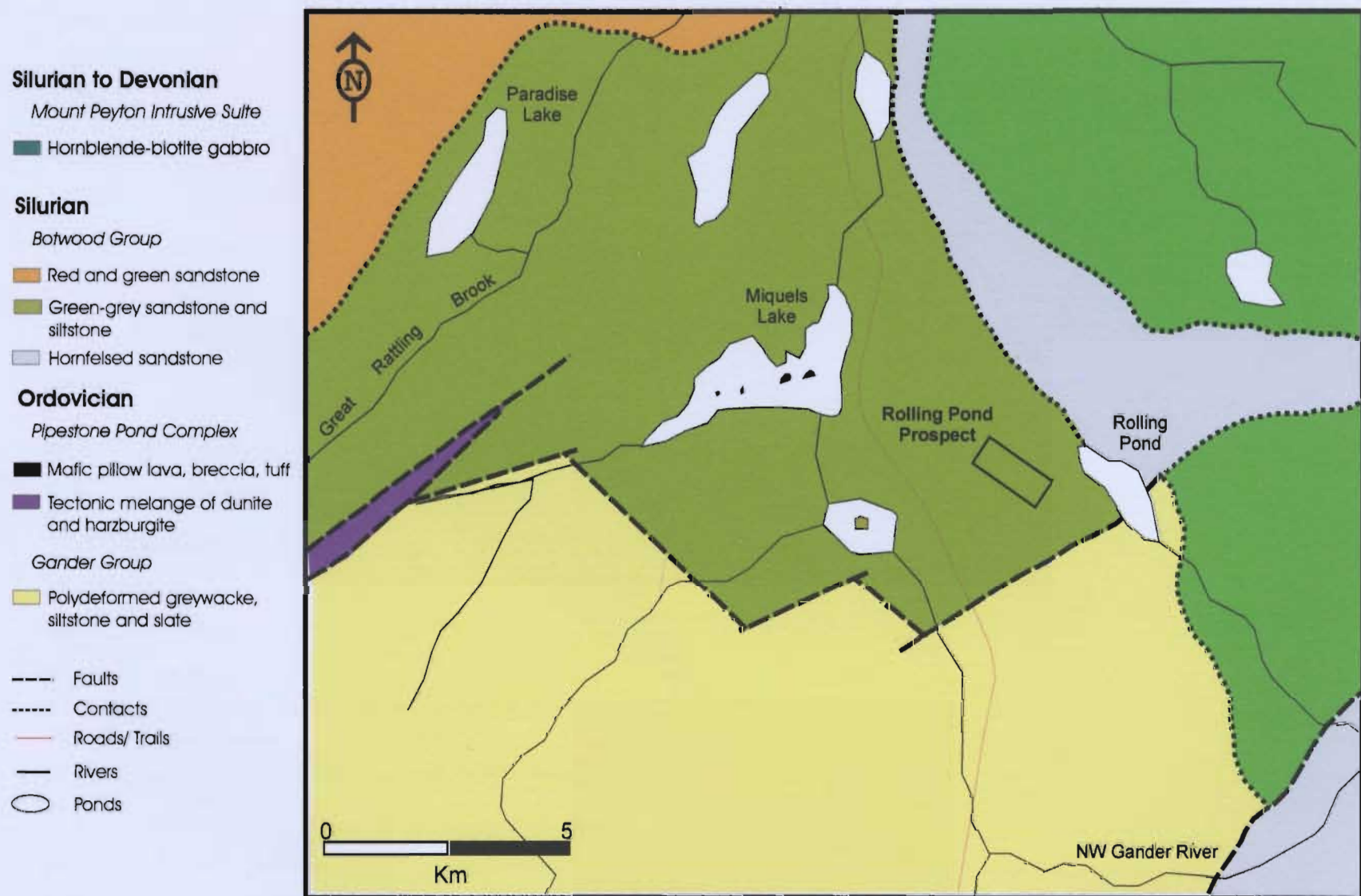


**Figure 3.12:** Geology in the Great Bend Region (north of the Northwest Gander River). The Rolling Pond property is outlined (from Barbour, 1999).

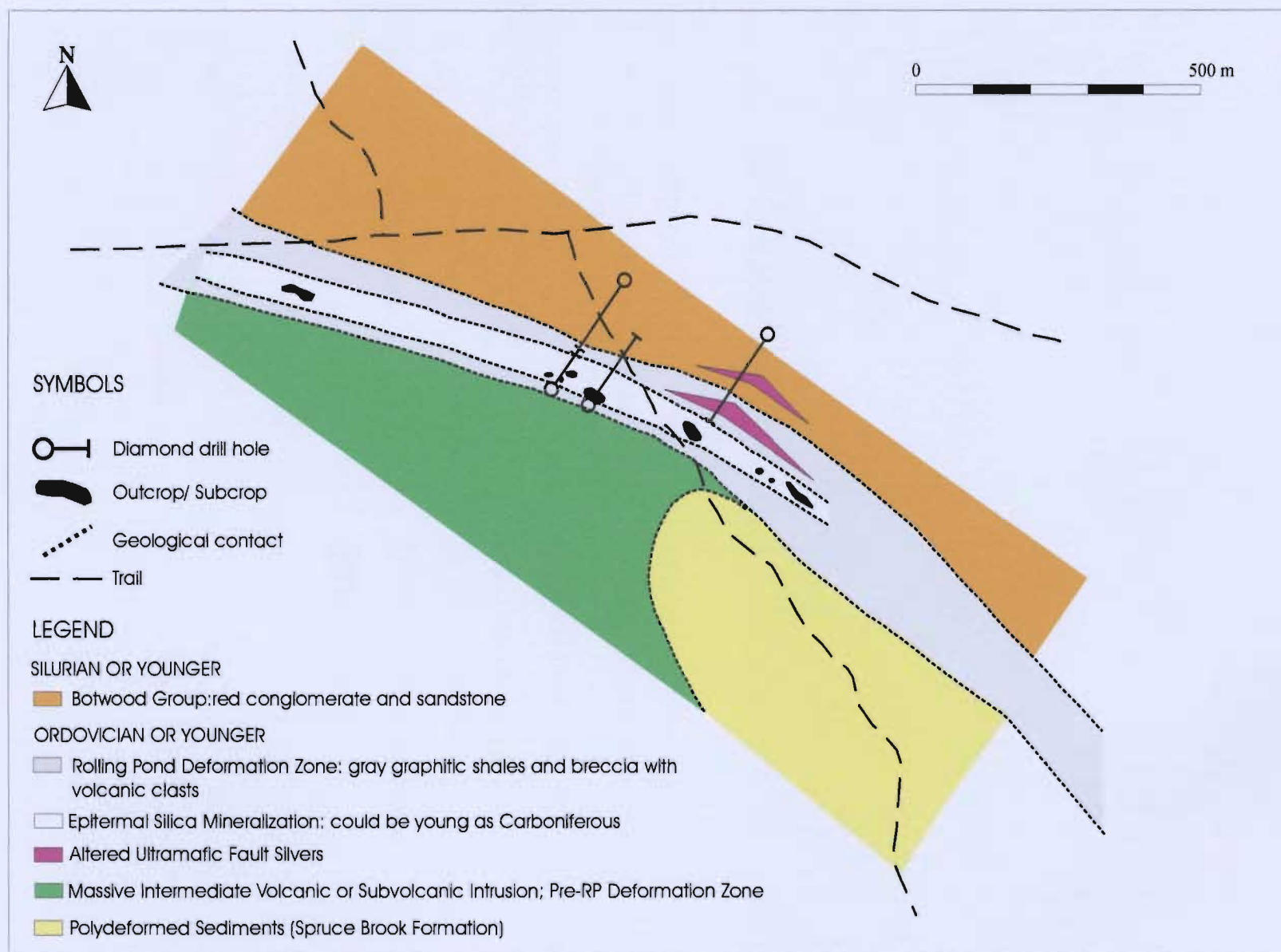
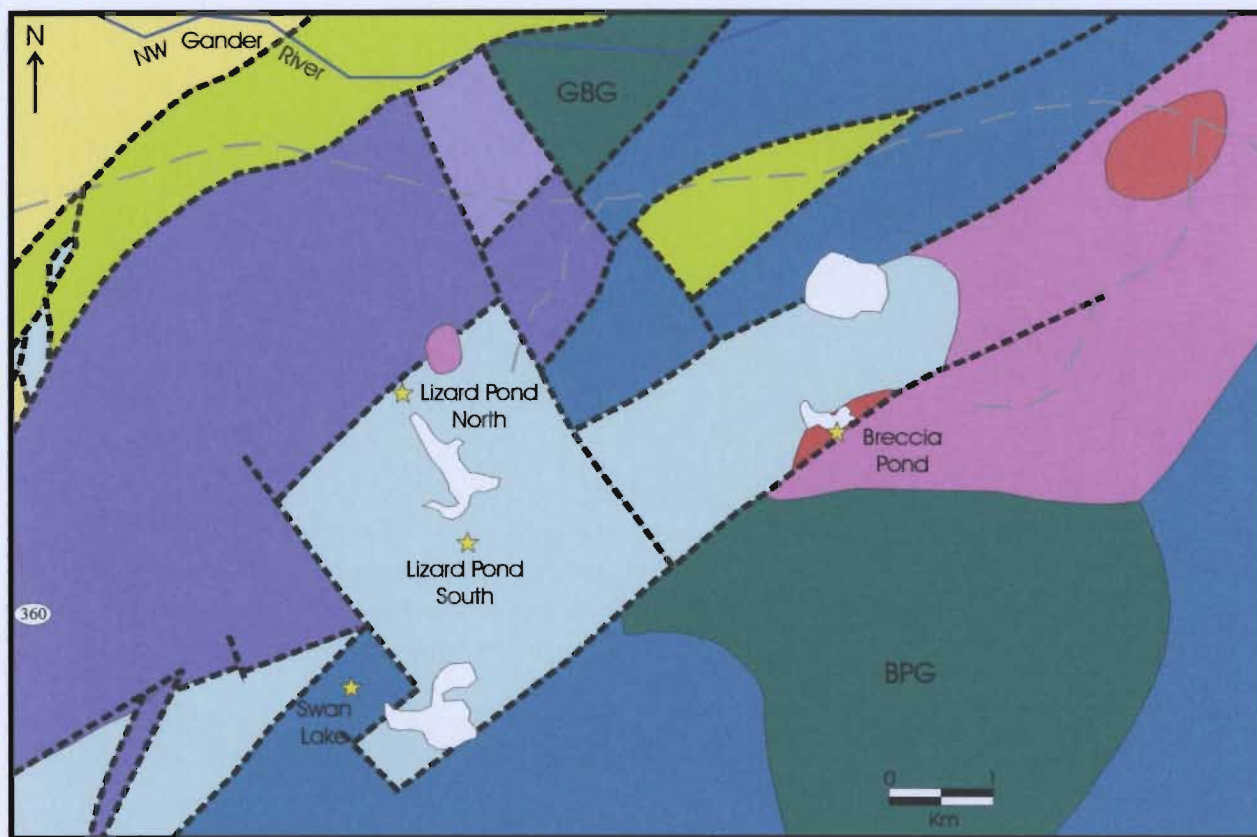


**Figure 3.13:** Geology of the Rolling Pond property (area outlined in figure 3.12) (modified from Barbour *et al.*, 1999).





### LEGEND

#### DEVONIAN OR YOUNGER

Feldspathic sandstone, pebble and cobble conglomerate

#### SILURIAN TO DEVONIAN

Great Bend gabbro (GBG) and Bear Pond gabbro (BPG)

#### SILURIAN

Indian Islands Group?

#### CAMBRIAN TO EARLY ORDOVICIAN

Spruce Brook Formation

Hematized and silicified ultramafic rocks

#### Great Bend Complex

Amphibolite

Schistose Magnesite

Peridotite

### SYMBOLS

Fault.....   
 Geological boundary.....   
 Road.....   
 Pond.....

**Figure 3.14:** General geology and auriferous occurrences of the Great Bend Complex (after Dickson, 1991 and 1996).



**Plate 3.1:** a) Looking north towards the northern tip of Duder Lake along the resource road, b) View east from elongate northeast trending ridge. Shear zone outline by valley below and mineralized sandstone and fossil outcrop exposed near vehicle to the west of the shear zone (indicated by arrow) [S. Heulin for scale].

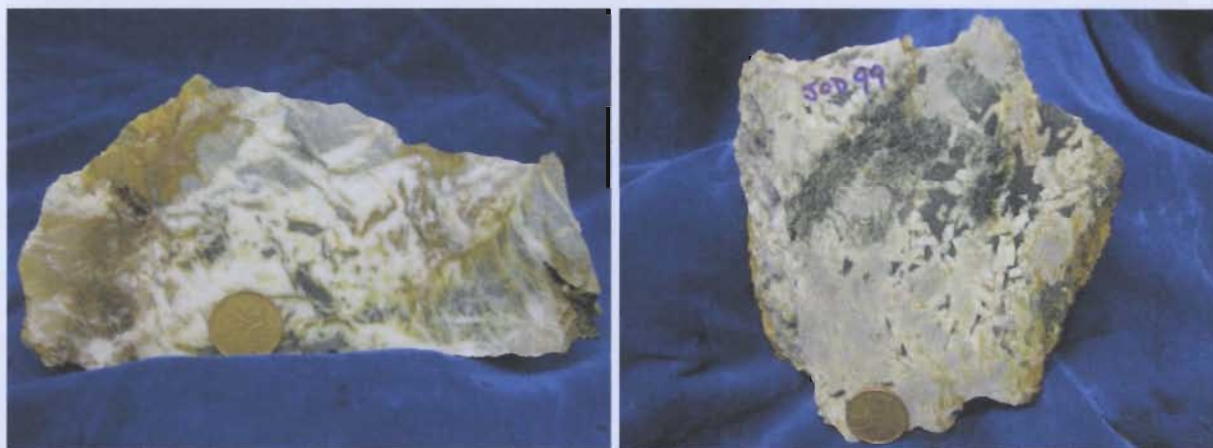


**Plate 3.2:** a) Grab sample from trenched area exposing Fe-carbonate altered, quartz veined, mineralized sandstone unit (Sample JOD96H). b) Grab sample from Flirt Prospect trench (Sample JOD99). The white mineral is carbonate and sericite, the blue-grey mineral is albite and the black mineral is pyroxene [penny for scale].



**Plate 3.4:** a) Goldstash Trench (S. Hinchey for scale). b) Corvette Fe-carbonate altered trench.





**Plate 3.7:** a) Quartz veins in deformed greywacke at the Knob Hill Prospect, b) Quartz veins in altered greywacke or cherty concretion at the Third Pond Prospect [camera lens for scale, 5 cm wide].

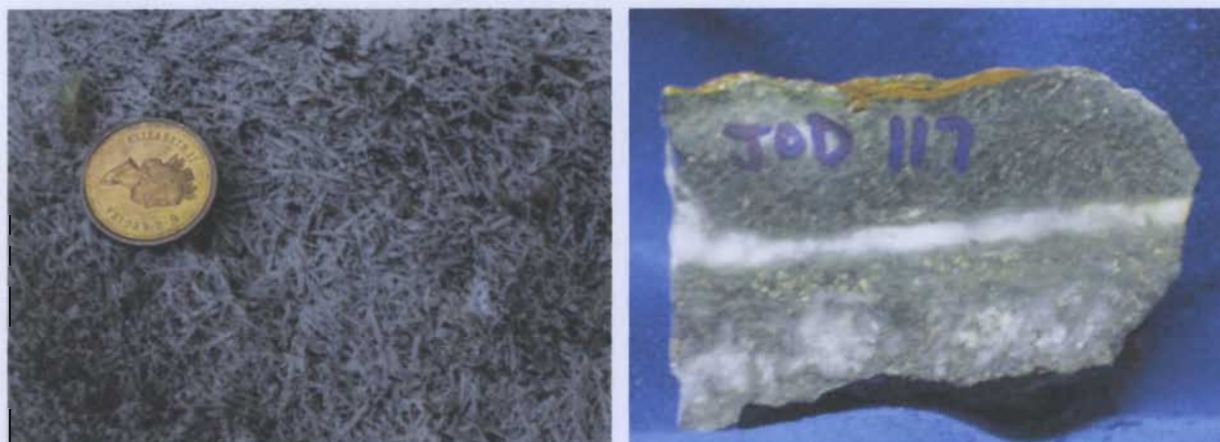


**Plate 3.10:** a) Quartz float boulder with bladed texture, b) quartz veined, mineralized and talc altered serpentine from Jonathon's Pond Prospect.



**Plate 3.12:** Bullet Prospect overgrown trench (S. Hinchey for scale).





**Plate 3.14:** a) Trench at Knob Prospect, northwest of quarry [S. Hinchey for scale], b) Large bull quartz vein containing visible gold in greywacke [hammer for scale].



**Plate 3.15:** a) the main trench and stripped area of the Dome Prospect [J. O' Driscoll for scale], b) Laminated, stripped outcrop along the 'Appleton Linear' exposing Davidsville slate [utility knife for scale].



**Plate 3.16:** a) Graphitic, deformed shale north of the trenched area at the Piper Zone, Outflow Prospect, b) View of a trenched area exhibiting silicification and large quartz veins.





**Plate 3.17:** a) Rusty, silicified and brecciated outcrop at Outflow Prospect [hammer for scale]. b) Quartz brecciated laminated siltstone within the trenched area [camera lens for scale].



**Plate 3.19:** a) View up the Salmon River with D. Wilton and S. Hinchey at the Hurricane Prospect, b) close-up of Hurricane Prospect (marked by flagging) which is grown over [hammer for scale], c) Quartz veined, mineralized diorite from the Hurricane Prospect [penny for scale].





**Plate 3.23:** a) View along Jumper's Brook where angular mineralized subcrop was observed [backpack for scale], b) close up of mineralized boulder [tack for scale].



**Plate 3.26:** a) Large stripped area at the Aztec Prospect exposing a large silica sinter and rusty, mineralized sedimentary rocks. b) Piece of quartz breccia [camera lens for scale].



**Plate 3.27:** a) Conjugate quartz veins in felsite at the Hornet Prospect [camera lens for scale], b) massive quartz veins in hydrothermally altered and mineralized gabbro at the Greenwood Pond #2 prospect [backpack for scale].



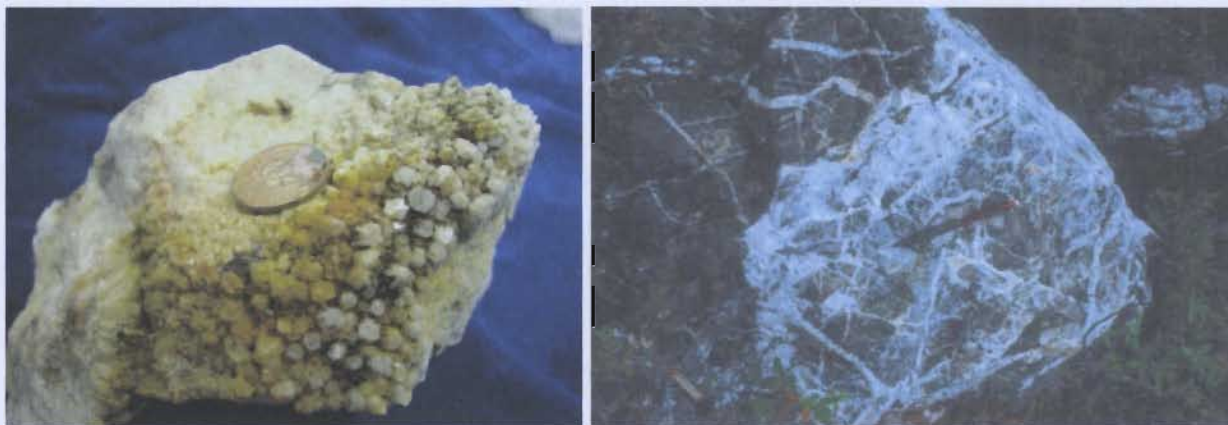


**Plate 3.30:** Rolling Pond Prospect. a) Vuggy, well formed quartz crystals [penny for scale], b) Quartz breccia subcrop [pencil for scale].



**Plate 3.31:** View along Chiouk Brook with S. Hinchey standing at the Chiuok Brook Prospect.



**Plate 3.32:** Breccia Pond Prospect. a) Main trench and stripped area, b) Hematite alteration halo around quartz veins in carbonized ultramafic rocks, c) Grab sample from trench 1 exhibiting alteration halo around small quartz vein, d) Red siliceous jasperoid.



**Plate 3.34:** Swan Lake Prospect. a) Quartz breccia with dark graphitic fragments. b) 5 cm thick quartz carbonate vein with sulphide staining exposed in trench apparently between a green siltstone unit and a black graphitic unit.





**Plate 3.35:** Lizard Pond South Prospect. a) Main trench and stripped area [J. O' Driscoll and S. Hinchey for scale], b) Large quartz breccia vein [hammer for scale].



**Plate 3.39:** Huxter Lane Prospect sample consisting of quartz breccia. Brecciated felsic material is mineralized along grain boundaries. The sulphide mineralization is primarily arsenopyrite with minor pyrite.



## **CHAPTER 4**

### **REGIONAL MAPPING**

#### **4.1 Preamble**

This project involved mapping and lithological sampling along a series of transects across the Davidsville-Botwood boundary and locally into the Mount Peyton Intrusive Suite. The rationale was that the regional geological framework of the Botwood Basin and environs requires greater definition, especially with respect to the metallogeny of the numerous gold occurrences and prospects present in the basin. Regional mapping in the northern portion of the current study area substantiates previous work which suggested that the contact zone between the Davidsville and Botwood groups is complicated with an extensive shallow marine shale and limestone sequence, the Indian Islands Group, present between the two groups. This chapter outlines mapping, petrographic and paleontological observations of the regional lithologies, mainly in the northern and central portions of the basin.

A number of fossiliferous samples were collected during the fieldwork, some of which had identifiable faunal assemblages (Douglas Boyce of the NLDNR made the paleontological identifications). The distinctly different faunal assemblages in the deep marine (Caradocian) Davidsville Group shale vs. the shallow marine Indian Islands Group, combined with regional stratigraphic correlations, provide the most definitive means of distinguishing between those units. Several previously reported fossil localities were re-evaluated and several new localities were discovered. Samples with definable

fossils are listed in table A4.1 and previous paleontological work conducted in the region is outlined in table A1.3.

Mapping transects were undertaken at various localities throughout the basin including: 1) the Duder Lake area, 2) the Bellman's Pond area, 3) the Twin Ponds to Ten Mile Lake area, 4) the Glenwood-Appleton area, 5) Salmon River, 6) Red Rock Brook, and 7) Careless Brook. The observations made are of a reconnaissance nature, hence a more detailed and systematic mapping program may be needed to better define the overall regional stratigraphy. Conclusions derived herein are based on interpretation of previous work in conjunction with the observations made during the current study.

## **4.2 Duder Lake Area**

### *4.2.1 Mapping Observations & Petrography*

Reports on the geology of this area are contradictory (*i.e.*, Churchill, 1994; Currie, 1994; Currie, 1997; Dickson, 2005). The main lithologies previously mapped in the Duder Lake area include the Ten Mile Lake Formation, Duder Complex and Davidsville Group [refer to chapter 2]. The gabbroic hosts to auriferous mineralization had been previously mapped as dykes, intrusive to the Botwood Group (Churchill and Evans, 1992; Evans *et al.*, 1992; Churchill, 1994). Later studies removed the Botwood Group from the local stratigraphic column and defined the Duder Complex as comprising intensely cleaved sedimentary rocks which formed the matrix to variably sized tectonic blocks, including the gabbroic bodies previously mapped as dykes (*cf.* Currie, 1994; Currie, 1995; Currie, 1997). Based on mapping observations and a review of previous

literature, the author supports the definition of these bodies as intrusive to this area [refer to chapter 2]. During this study, the author noted several new fossiliferous localities that had been uncovered as a result of trenching; these fossiliferous horizons, combined with mapping observations may have implications for the redefinition of the stratigraphy in this region.

At UTM coordinates 670020/ 5462754, a trenched area exposes laminated siltstone and interlayered fossiliferous limestone beds (sample JOD96E) (Plate 4.1, p. 150); the fossils present in this sample are described below in section 4.2.2. Overall the outcrop weathers white and brown with cherty green, silty layers in some exposures. Bedding laminations are very fine, striking at  $\sim 346^\circ$  with near vertical dips. Pyrite is disseminated in the siltstone layers. Approximately 6 m north, the beds appear to be less carbonaceous and fossils were not observed in hand specimen; here the predominantly silty beds strike at  $344^\circ/ 85^\circ$  E and exhibit subparallel cleavage. The sedimentary lithologies are variably silicified.

Further north, at UTM coordinates 669996/ 546281, an outcrop of poorly sorted sandstone with quartz veins and visible sulphides is interbedded with laminated siltstone. The 0.2 to 1 cm wide quartz-filled tension gashes were only observed in the coarse-grained layer, although outcrop of the siltstone beds is limited. At one locality, the sedimentary unit is in contact with a sheared foliated unit. The fabric of the deformed material strikes northeast, parallel to the general trend of the contacts in the region. Detritus within the sandstone unit becomes coarser-grained towards the contact with the sheared lithology. The sandstone unit contains abundant pyrite associated with quartz-



filled tension gashes near the shear, suggesting that sulphide mineralization may have been related to the shearing event.

The sandstone unit also contains vesicle-like holes that may represent weathered out fossiliferous material, although no fossil impressions are observed in outcrop.

Bedding trends  $015^{\circ}/85^{\circ}$  E, whereas the shear zone trends  $017^{\circ}/90^{\circ}$ , approximately parallel to the bedding.

Petrographic thin sections were cut from samples JOD96K and JOD96J of the siltstone layer and the sheared unit, respectively. Sample JOD96K (Plate 4.2, p. 115) is an un-deformed, moderately sorted sedimentary rock. Most of the lithic material was too fine-grained to be identified. The larger fragments in thin section are predominantly quartz.

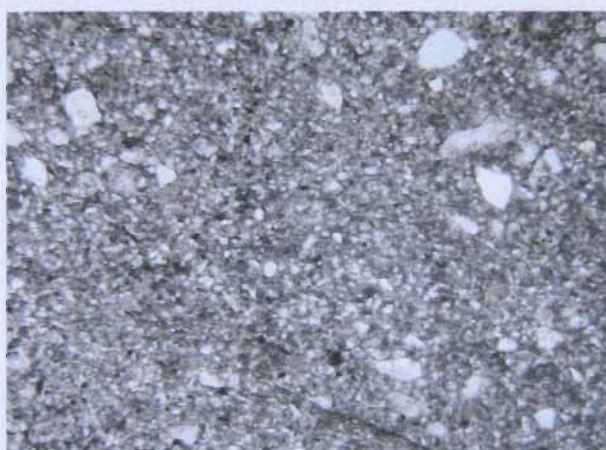


**Plate 4.2:** Photomicrograph of sample JOD96K from the Duder Lake transect; note lithic quartz detrital grains in a fine-grained matrix [Field of view 7mm, PPL].

Sample JOD96J (Plate 4.3, p. 116) is likewise a sedimentary rock which, in this case, consists of 40% dolomite, 30% epidote and 30% Fe-oxides. The minerals are slightly aligned in one direction suggesting that the sample had undergone a small degree of strain or deformation, which is consistent with the observations made at the outcrop.

The protolithology was probably a limestone; hence the unit would belong to the Indian Islands Group as opposed to either the Davidsville or Botwood groups.

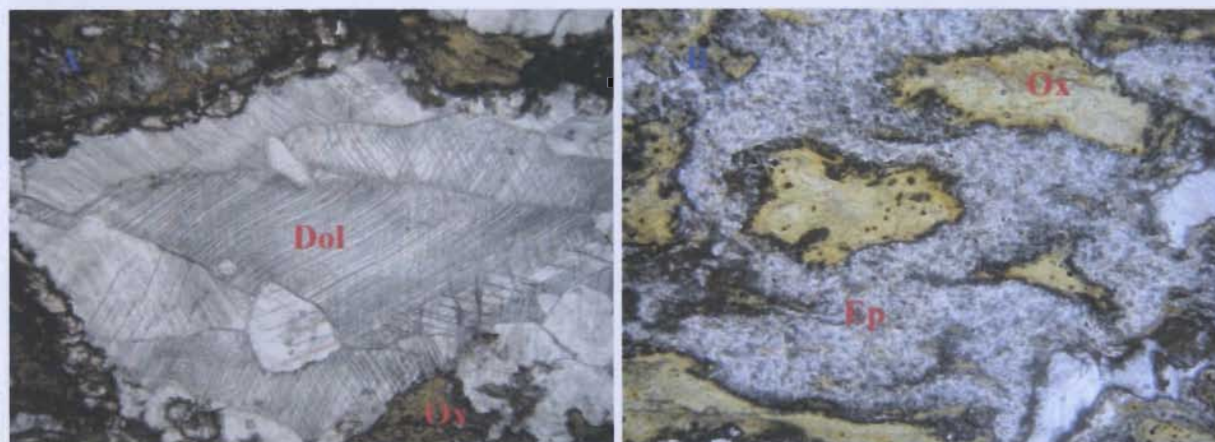


**Plate 4.3:** Photomicrograph of sample JOD96J from Duder Lake transect. A) Large dolomite crystal [Field of view 2mm, PPL]. B) Epidote alteration around Fe-oxide [Field of view 7mm, PPL] (Dol=dolomite; Ox=Fe-carbonate staining; Ep=epidote).

Directly east of this outcrop, a trenched area exposes a very small outcrop from which fossiliferous sample JOD96I was collected. The fossils present in this sample are described below in section 4.2.2.

Sample JOD71B, from a trench at Duder Lake that was not previously mapped, consists of fine-grained sandstone with disseminated pyrite and local, large pyrite cubes. The trench exposes an interlayered coarse and fine-grained sedimentary unit. Randomly orientated quartz veins, ranging from 1 mm to 1 cm wide, cut both types of layers.

At UTM coordinates 669658/ 5468720, an unaltered and unmineralized ridge of gabbro (previously mapped as part of Duder Complex mélange by Currie and Williams, 1995) was sampled for geochronological and petrographical studies (sample JOD66A) (Plate 4.4, p. 150). The ridge comprises medium-grained gabbro with distinctive white, chaulky weathering at the surface. This unmineralized gabbroic body occurs within



cleaved, slightly micaceous, grey-green siltstone which has been previously mapped as part of the Duder Complex by Currie (1995). Petrographically this gabbro is composed of 45% uralitized pyroxene, 30% serpentinite, 10% plagioclase, 5% epidote, 5% biotite and 5 % Fe-oxides (Plate 4.5, p. 117). Augite is altered to uralite (*i.e.*, hornblende pseudomorphs pyroxene). Thus, this rock is classified as an altered phaneritic pyroxene gabbro.



**Plate 4.5:** Photomicrograph of an altered phaneritic pyroxene gabbro collected north of Duder Lake. Elongate, subhedral pyroxene (augite) crystals exhibit uralite alteration (Ur) with Ca-plagioclase (Pl) and serpentinite (Sp) occupying spaces between crystals. Minor epidote overprints the minerals and minor biotite is also present [Field of view 7mm, PPL].

#### 4.2.2 Paleontology

Sample JOD-096E was collected from a limestone bed that was interlayed with cherty siltstone (Plate 4.1, p. 150) near the Duder Lake auriferous occurrences at UTM coordinates 670020/ 5462754. The sample was slightly deformed and the fossils



identified include *Anthozoa\_Tabulata\_Favosites* (sp. undet.) and *Bryozoa\_Stictopora\_Scalpellum* (Lonsdale) (branching stick forms).

The tabulata is an extinct group of colonial corals composed of tubes with prominent tabulae and poorly developed septa. The largest sub order is the Favositida and the typical genus is *Favosites* (Figure 4.1, p. 117). The name is derived from the Latin word *favus* (honeycomb), as the corallites are closely packed and hexagonal, resulting in the honeycomb skeletal appearance. The Favositids are the most common corals of mid-Paleozoic reefs and grew with diameters of up to several meters. The corallites connect by wall openings and septal spines projecting from the walls may be present (6 or 12 in number). Numerous complete horizontal tabulae are usually present. The geologic time range for the *Favosites* is Upper Ordovician to Middle Devonian (Stearn and Carroll, 1989).

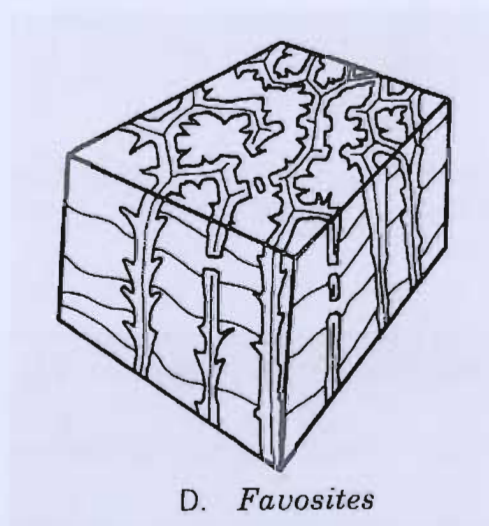


**Figure 4.1:** Block diagram illustrating the internal structure of the tabulate coral *Favosites* (Late Ordovician to Middle Devonian) (from Stearn and Carroll, 1989).

The Byrozoa have a geologic time range of Ordovician to Recent. The most common byrozoan members grew in shallow water environments and had massive

calcareous skeletons and grew in thick branching, hemispherical and encrusting colonies of the order Trepostomata (Stearn and Carroll, 1989). The bryozoan fossils from sample JOD96E have been identified as *Stictopora Scalpellum* (Lonsdale) (branching stick form) (Figure 4.2, p. 119). The genera *Stictopora* consist of erect or straplike colonies of bryozoans with boxlike zooecia openings on both sides and belong to the order *Cyrtostomata* (Stearn and Carroll, 1989). This species is common in Wenlock (Middle Silurian) limestone.

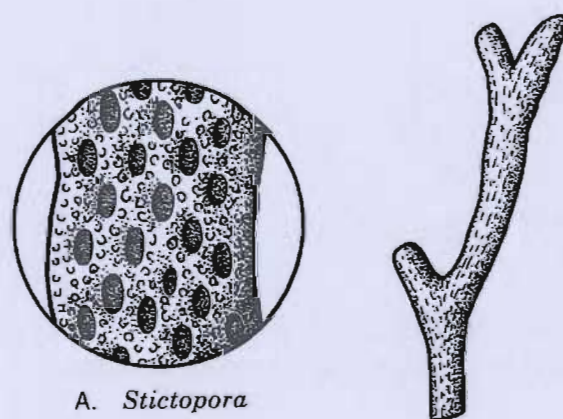


**Figure 4.2:** Genera *Stictopora*, Order *Cryptostomata*. On the right, complete specimen about natural size; on the left, the surface enlarged to show the zooecia (after Stearn and Carroll, 1989).

Sample JOD-096I was also collected from the vicinity of the Duder Lake occurrences, north of the aforementioned fossiliferous outcrop. This sample consists of deformed limestone and due to the greater deformation (shearing) at this locality, only a small, badly warped fossil was found within a large cobble. The fauna were identified as *Brachiopoda\_Articulata* (Gen. et sp (p)). Although an order was not identified, it was determined that the articulate brachiopod is not *Orthambonites*, the most common Late Arenig to Early Llanvirn genera in central Newfoundland.

During the Early Ordovician there was a brachiopod explosion as these calcareous brachiopods increased in both abundance and diversity. Articulate brachiopods are the largest class and valves are composed of calcium carbonate with interlocking teeth and sockets along the hinge (Figure 4.3, p. 120). The geologic time range for articulate brachiopods is Lower Cambrian to Recent.

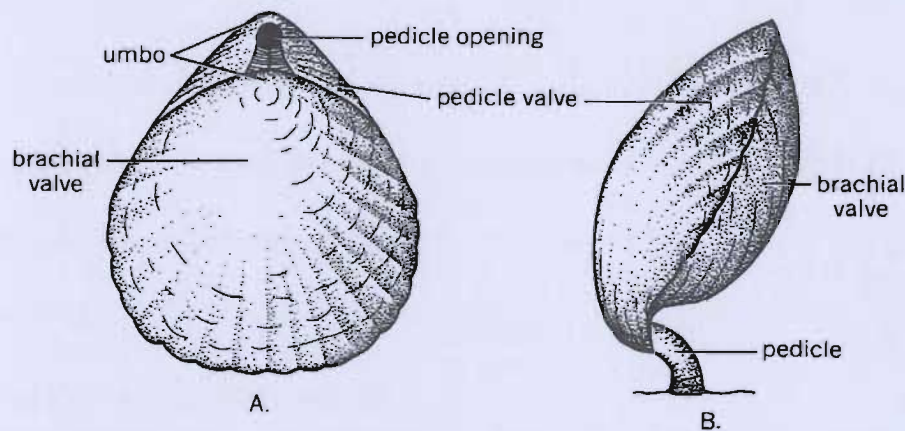


**Figure 4.3:** The living brachiopod *Magelania*. A) Dorsal view of the shell. B) Side view showing the pedicel and brachial valve and the position of the pedicle (from Stearn and Carroll, 1989).

#### 4.2.3 Discussion

The exposed fossiliferous beds contain Silurian fauna, thus providing evidence for the existence of a shallow marine Silurian unit in the Duder Lake area. Although the fossil identifications are broad, correlation of the green micaceous siltstone units as well as limestone and fossiliferous beds in this region with those in the Glenwood area, suggests that the Indian Islands Group is present east of Duder Lake where rocks have previously been mapped as part of the Duder Complex (Currie, 1995b). Currie (1995b) does note the existence of possible Indian Island Group sediments within the Duder Complex and explains their presence as tectonic inclusions. This interpretation is



problematic in that interbeds within the group appear continuous throughout a broad area. If the observed outcrops are from several included tectonic blocks, one would expect to observe different orientations in the bedding planes, and if they are indeed from one large tectonic block it would then have to be quite extensive. Dickson (2005) re-evaluated the area and suggests that observed interbeds of fossiliferous Indian Island Group sediments may indicate a possible extension of the group to the west of its currently mapped position. In order to do so, the position and significance of the Dog Bay Line would need to be revisited. A more detailed study on a local scale is recommended for the area to unravel the existing stratigraphic enigma.

### **4.3 Bellman's Pond Conglomerate**

#### *4.3.1 Mapping Observations and Petrography*

A small sliver of conglomerate crops out along the eastern shoreline of Bellman's Pond, northern Botwood Basin, within shale-siltstone mapped as part of the Outflow Formation, Davidsville Group (Blackwood, 1982). The conglomerate has been variously mapped as a thrust slice of Davidsville Group (Evans *et al.*, 1992) and as a separate Devonian unit (Currie, 1995). It was assumed that definition of the age and lithotectonic affinity of the conglomerate would aid in unraveling the structural history of the Davidsville -Indian Islands group contact. As a result, some time was spent mapping the unit and an attempt was made to date a volcanic tuffaceous clast (see Chapter 8). Although the contact was not exposed, the conglomerate is assumed to be in contact with

interbedded sandstone and siltstone of the Davidsville Group, which was mapped to the northeast of the outcrop.

The Bellman's Pond conglomerate crops out at UTM coordinates 670052/ 5447120, extending approximately 90 m northeast along the Bellman's Pond shoreline, and contains clasts ranging from 2 mm to 15 cm in diameter. The clasts are rounded to sub-rounded and the conglomerate varies locally from matrix-supported to predominately clast-supported. The clasts consist mainly of red and green siltstone, red sandstone, and possibly limestone and volcanics in a red sandstone matrix. At the start of the outcrop, the conglomerate has a general strike of 040°. Bedding generally runs northeast and foliation runs north-south with foliation becoming more dominant to the southwest.

Several features were noted in mapping this conglomerate unit, including: 1) deformed, laminated green, black siltstone beds that appear to have been ripped up in a debris flow, 2) a load clast from a conglomerate interbed into siltstone, indicating a top direction towards the east, 3) an oval clast with a weathered rind, indicating that the clast had been weathered prior to incorporation within the conglomerate, 4) round depressions, presumably resulting from the weathering out of carbonate material, and 5) large clasts of presumably volcanic material with abundant sulphide.

The presumed volcanic fragments were only noted on the south end of the outcrop where foliation was more prevalent. A large clast (JOD08, diameter=15 cm) of volcanic material was collected at UTM coordinates 670009/ 5447133 (Plate 4.6, p. 151). Any remaining conglomerate material that was attached to the clast was carefully removed before the sample was processed for U-Pb geochronology. When these edges were cut by saw, the clast was revealed to have an abundance of porphyritic igneous grains (Plate



4.7, p. 151). Zircons from the igneous sample were dated by LAM-ICP-MS in an attempt to define the age and possible source of detritus, and hence the correct unit designation (refer to chapter 8). As well, sulphide separates from this sample were analyzed for their sulphur isotope ratios (refer to chapter 6).

A polished thin section was cut from the igneous fragment to help ascertain the lithology. The section is comprised of 45% fine-grained matrix (epidote and quartz replacing glass fragments), 35% quartz and plagioclase (anhedral, interlocking perthite), 10% chlorite and 10% Fe-oxides and sulphide minerals (Plate 4.8, p. 123). Thus, this clast was derived from a very altered aphanitic igneous lithic tuff.

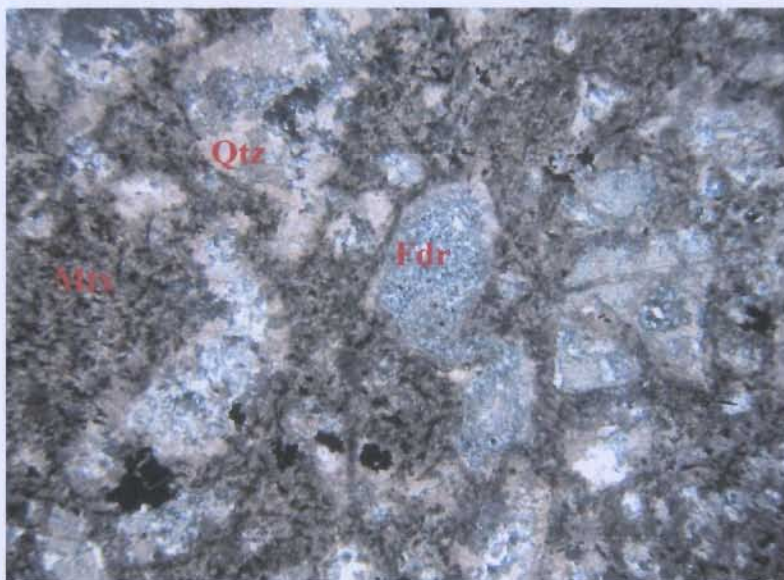


**Plate 4.8:** Photomicrograph of sample JOD08, a clast in the Bellman's Pond Conglomerate exhibiting altered feldspar (Fdr) and quartz (Qtz) porphyroblasts in a fine-grained matrix (Mtx) [Field of view 7mm, XP]. This section indicates that a felsic volcanic lithology is present in the conglomerate.

Along the shoreline at UTM coordinates 670065/ 5447353, a shiny black, fibrous limestone clast was removed from a subcrop conglomerate boulder. This clast, JOD09, although slightly deformed and re-crystallized was sent to D. Boyce for fossil analysis.



No macro-fossils were identifiable due to the deformation and re-crystallization of the specimen, however, the sample might contain conodont fossils.

#### *4.3.2 Discussion*

Based on the mapping conducted during this study, it appears that the Bellman's Pond conglomerate is actually an interbed in the Ordovician Davidsville Group. This agrees with Evans *et al.* (1992) interpretation but is at odds with the interpretation that the unit is a thrust slice (Evans *et al.*, 1992) or a later Devonian unit (Currie, 1995). The conglomerate was likely deposited at the base of a continental slope, which would account for the presence of limestone and weathered clasts and also its relationship with the deep marine Davidsville Group slate and siltstone. The presence of a lithic tuff clast may help to confirm the source of detritus of the Davidsville Group (refer to Chapter 8).

### **4.4 Twin Ponds to Ten Mile Lake Area**

#### *4.4.1 Mapping Observations and Petrography*

The most prominent geological features in this area are gabbros mapped by Evans *et al.* (1992) north of the Trans Canada Highway (TCH), along forestry resource roads. Several gabbro samples (JOD57A, JOD100, JOD101, JOD102 and JOD04-09) were collected from various outcrops for this study. At various localities throughout this paper, these intrusive bodies are referred to as the 'linear' gabbros based on their NE trending linear expression on the map produced by Evans *et al.* (1992). The gabbro

represented by sample JOD57A, from UTM coordinates 662766/ 5450790 (along the resource road that leads to Birchy Bay) (Plate 4.9, p. 152), intruded green siltstone with thin, brown and limey interbeds. Based on these interbeds, these sedimentary rocks are interpreted to be correlatives of the Indian Islands Group; they had previously been mapped as Ten Mile Lake Formation (Currie, 1995a). Bedding in the siltstone is  $354^{\circ}/23^{\circ}$  E and there are multiple cleavage directions at  $061^{\circ}/90^{\circ}$ ,  $098^{\circ}/50^{\circ}$  S, and  $154^{\circ}/52^{\circ}$  W. As multiple joints also cut the gabbro, it is assumed that deformation in both units postdated the intrusive event itself. The cleavage and joint directions are different due to the different properties of both lithologies. The contact with the gabbro is not exposed, but the sedimentary rocks do not appear to have been affected by the gabbro intrusion. The gabbro is cut by small (1 to 3 cm thick) K-feldspar veins as well as joints at  $090^{\circ}/33^{\circ}$  S and  $077^{\circ}/76^{\circ}$  S.

Sample JOD04-09 was collected from a gabbroic dyke 100 m southeast of the previous location at UTM coordinates 662775/ 5450772 (Plate 4.10, p. 152); it is presumably the same dyke previously discussed. The outcrop exposure is limited and consists of a flat gabbroic body, which was uncovered by excavation of the resource road. Petrographically the gabbro comprises 35% dusty feldspar, 25% hornblende, 20% clinopyroxene (augite), 14% Fe oxides, 2% sulphides, and 5% biotite; hence it is classified as an aphanitic hornblende-pyroxene gabbro (Plate 4.11, p. 126).

Sample JOD04-13 is of an unmapped gabbroic body along the Ten Mile Lake Resource Road, to the east of the previously described gabbroic units and Ten Mile Lake at UTM coordinates 667551/ 5456465. This knobby exposure intrudes a green, fine-grained sedimentary unit in which fossiliferous interbeds are present.

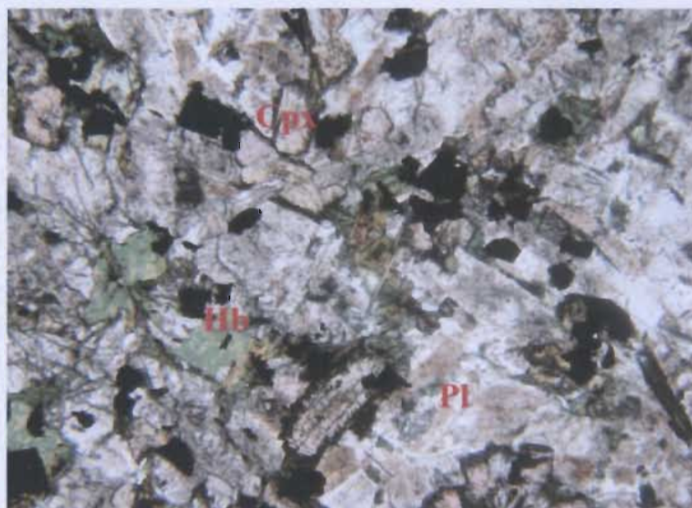


**Plate 4.11:** Photomicrograph of sample JOD04-09 collected from an intrusive body west of Ten Mile Lake. The sample comprises hornblende (Hb), plagioclase (Pl), clinopyroxene (Cpx) and Fe-Ti oxides and is classified as an aphanitic gabbro [Field of view 7mm, PPL].

Thus, it is thought to intrude Indian Island Group rocks. Petrographically the gabbro is composed of 40% plagioclase feldspar, 15% clinopyroxene (augite), 15% titanite, 15% hornblende and 12% Fe oxides and 3% sulphides (some apicular) (Plate 4.12, p. 127). This aphanitic gabbro is similar in composition to the intrusive on Birchy Bay Resource Road; however, it is finer grained, contains elongate titanite grains, less pyroxene and amphibole, and no biotite. Thus, this rock is classified as an aphanitic hornblende-pyroxene gabbro. The presence of titanite may indicate a possible correlation to the gabbroic bodies at Duder Lake as Churchill and Evans (1992) had defined melanocratic type gabbros that were characterized by an enrichment in Ti.

Several samples were collected north of Twin Ponds, approximately 15 km southeast of sample JOD57A, from a second elongate gabbro dyke mapped by Evans *et al.* (1992). Disseminated sulphides were observed in the gabbroic outcrops and the



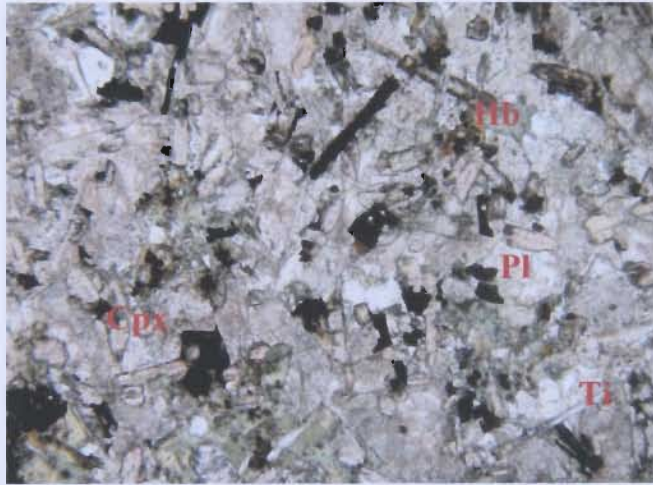


**Plate 4.12:** Photomicrograph of sample JOD04-13 from an unmapped intrusive body east of Ten Mile Lake. The sample is comprised of plagioclase (Pl), clinopyroxene (Cpx), hornblende (Hb), titanite (Ti), minor Fe-Ti oxides and disseminated sulphides [Field of view 7mm, PPL].

surrounding sedimentary rocks (green siltstone) are intensely silicified. Quartz veining was not observed so it is assumed that the siltstone was saturated with replacement silica. In general, the silicified siltstone is somewhat similar to the green siltstones of the Indian Islands Group, however, it was mapped as the Ten Mile Lake Formation by Currie (1995a).

Gabbro sample JOD100 was collected from an outcrop at UTM coordinates 652973/ 5438288 (Plate 4.13, p. 153). Petrographically this gabbro comprises 30% altered plagioclase (simple and lamellar twins), 40% anhedral hornblende (interstitial growth between colorless grains), 5% biotite, 5% chlorite and 12% Fe-oxides and 3% sulphide minerals, and thus would be classified as a phaneritic hornblende gabbro (Plate 4.14, p. 128).

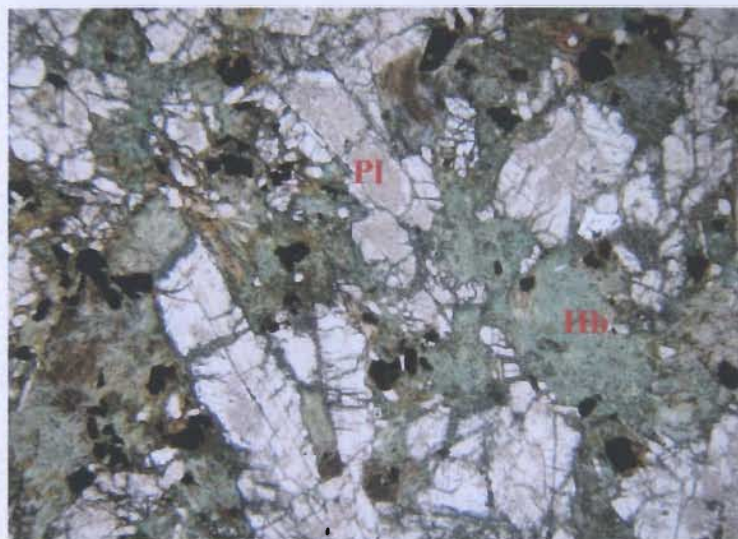


**Plate 4.14:** Photomicrograph of sample JOD100 collected from an intrusive body as mapped by Evans *et al.* (1992). The sample comprises plagioclase (Pl), hornblende (Hb), and minor clinopyroxene, biotite, chlorite and opaque minerals [Field of view 7mm, PPL].

#### 4.4.2 Paleontology

Sample JOD04-12 (Plate 4.15, p. 153) was collected from a re-crystallized fossiliferous limestone outcrop exposed along the Ten Mile Lake Resource Road as a significant area of slightly deformed pink and white rock (Plate 4.16, p. 154). The fossils in this sample were identified as *Echinodermata (P)-Crinozoa(SP)-Crinoidea (C)* (Gen. Et sp (p). undet.) (Douglas Boyce, personal communication) which consist of re-crystallized columnals. Crinoidea were abundant in the Palaeozoic, living in shallow water and attached to the seafloor by a stalk. Crinoids have a cup-shaped head (the calyx), which are attached to long, branching arms. The calyx is usually connected to the bottom via a stem (which is generally preserved in the fossil record) (Plate 4.17, p. 129, after Stearn and Carroll, 1989).





**Plate 4.17:** Polished slab of Lower Carboniferous limestone composed mostly of crinoid columns; view is about 16 cm across (after Stearn and Carroll, 1989).

Sample JOD04-14 (Plate 4.18, p. 154) was collected from a 1 x 1 m purple fossiliferous outcrop or subcrop that has been identified as medium to coarse-grained pebbly sandstone or conglomerate (Plate 4.19, p. 155). It contains several identifiable fossils including: 1) *Brachiopoda-Articluata* (Gen et sp. undet.-heavily ribbed form), 2) *Byrozoa* (Gen et sp. undet.), *Cnidaria-Anthozoa-Zoantharia-Tabulata-Favosites* (Gen et sp (p). undet.) and 3) *Echinodermata-Crinoidea* (Gen et sp(p) undet.-columnals). The fossils were poorly preserved, possibly due to proximity to a large shear zone (the previously defined location of the Dog Bay Line). The Brachiopoda, Byrozoa, and Cnidaria Phylums have been discussed in section 4.2.2 and the Echinodermata has been described above.

Sample JOD04-15 was collected from a large fossiliferous bed interlayer in red siltstone or mud. It contains *Stictopora* Bryozoans of Wenlock age. The stictopora are discussed in section 4.2.2.



#### *4.4.3 Discussion*

This transect crossed several gabbroic bodies south of Duder Lake in the northern Botwood Basin. These gabbros vary slightly in grain size and modal mineral percentages; pyroxene was less common in the gabbros towards the south. Reconnaissance work on the economic potential of these gabbros may be warranted due to the proximity of the bodies to auriferous occurrences, the presence of disseminated sulphides within the gabbros and silica saturation of the adjacent country rock. In general, all of these bodies intrude Ten Mile Lake Formation sedimentary rocks (Currie, 1995a) that resemble Indian Island Group rocks.

Several new fossil localities to the east of Ten Mile Lake, *i.e.*, west of the Dog Bay Line, contain Silurian fauna. The faunal identification is broad due to the deformation of the samples and further work with a more detailed sampling program will be required to obtain more precise ages for the fossiliferous units (such a program was initiated by the NDME in 2005; refer to Dickson (2005)). The samples were collected just to the west of the Dog Bay Line, which may account for the observed deformation.

### **4.5 Glenwood-Appleton Area**

#### *4.5.1 Mapping Observations and Petrography*

A large gravel pit located on the south side of the town of Appleton, along the Gander River, exposes a contact between shale and a sandstone unit of the Davidsville Group at UTM coordinates 655978/ 5426930. The Davidsville Group greywacke sits on

top of Bagder Group Caradocian shale and as such, the Davidsville Group was thrust upon the Badger Group.

The Caradocian shale is quite distinct with black-blue color and a very rich graptolite assemblage at the top edge of the cliff face. Disseminated sulphides were concentrated in shale around quartz veining. One vuggy quartz vein appears to run along, or quite close to, the general trend of contact and the shale appears to be brecciated and cemented by quartz near the contact. Below the contact exposure, there was abundant blasted float of mineralized, altered Davidsville greywacke with vuggy quartz veins (Plate 4.20, p. 155). Greywacke is also exposed above the pit and appears to be silicified with a general cleavage direction of 047°.

The Bowater Prospect occurs within 10 m of the pit, and although the actual trenches could not be located, a portion of the prospect was observed as a large (up to 6 cm wide) vuggy vein, with euhedral quartz crystals, hosted in greywacke. The vein trends 135°/ 70° NE but seems to fill a large tension gash.

Gerry Squires (personal communication, 2003) reported a very altered, brown, 22 cm wide dyke striking along the bedding plane at UTM coordinates 656077/ 542977 and a ~4-5 cm dyke 5 m down hill with some sulphides at UTM coordinates 656078/ 5426975. Two samples, JOD120A and JOD120B, were collected from these dykes. Subsequent geochemical analyses revealed that the exposures were actually Mn-rich interbeds. These interbeds contain disseminated sulphides and small quartz veins.

A gravel pit, just west of Glenwood off of the Salmon River Access Road, was also examined. The pit exposes what appears to be a gabbroic dyke intruding Indian Islands Group sedimentary rocks. Petrographically, sample JOD04-20, collected from



the intrusion (Plate 4.21, p. 132), comprises 50% plagioclase, 25% altered hornblende, 10% pyroxene (augite), 8% Fe oxides, 5% biotite and 2% sulphides associated with the amphibole. This is therefore an aphanitic hornblende gabbro. This dyke has been previously correlated to the MPIS by Dickson (1996) and the significance of this is further explored in section 4.6.2.

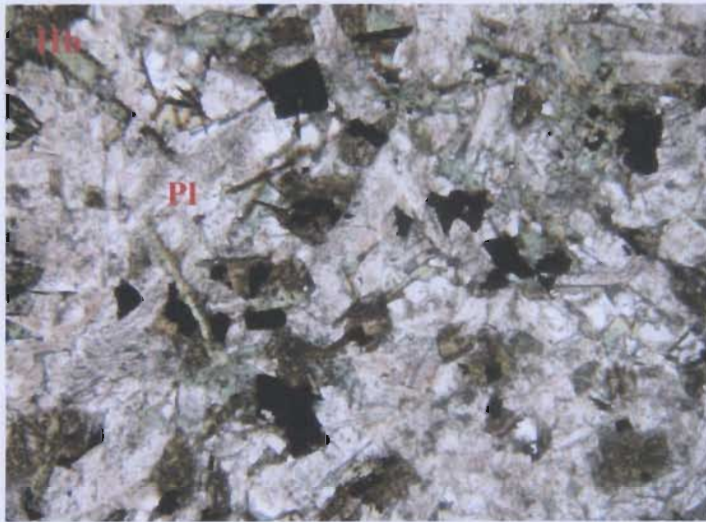


**Plate 4.21:** Photomicrograph of sample JOD04-20 exhibiting plagioclase (Pl), hornblende (Hb) and minor pyroxene and biotite [Field of view 7mm, PPL].

#### *4.5.2 Paleontology*

Two fossil localities, originally described by Blackwood (1982) were examined along the Salmon River Resource Road, just north of the TCH. Fossils were collected from these localities for comparison with the fauna from the new localities further north. The fossils were identified by Doug Boyce and are described below.

The first locality is in a woodcutting pit at UTM coordinates 654920/ 5430998. The pit has minimal outcrop exposure as it was mostly filled with sawdust, but at the far end of the pit a fossiliferous outcrop of grey siltstone is exposed. The siltstone is cleaved,



foliated and crosscut by randomly oriented thin quartz-carbonate veins. A conjugate set of quartz veins is orientated at 140°/ 50°S and 005°/ 55° NE. The fossils are contained in limey brown beds, interbedded with slightly silicified green siltstone and some of the fossil casts are re-crystallized.

Another exposure at the beginning of the pit (UTM coordinates 654875/ 5431010) consists of Indian Islands Group micaceous siltstone with brown and black laminations. Bedding is 210°/90° and the rocks become more micaceous and less limey to the west. No fossils were observed here.

Sample JOD-113 was collected from a small fossiliferous outcrop within interbedded limey and non-limey siltstone located at the back of the pit. The rocks are readily identifiable as Indian Islands Group based on the presence of abundant *Bryozoa* (gen. et sp. undet. ) (branching stick forms), abundant *Echinodermata - Crinoidea* (gen. et sp. undet.) and *Mollusca - Cephalopoda?* (gen. et sp. undet.) (straight form).

The Bryozoa and Echinodermata fossils have been discussed in sections 4.2.2 and 4.4.2 respectively. The Mollusca Phylum is subdivided into eight classes of unsegmented, coelmate metazoans. The Class Cephalopods can be further subdivided into three subclasses and occur from Late Cambrian to Recent. Early Paleozoic cephalopods are generally nautiloids and the shells of these early cephalopods are commonly straight or lightly curved and can be up to 9 m long (Figure 4.4, p. 134). Nautiloid cephalopods have smoothly curved septa, which produce simple, straight sutures (Stearn and Carroll, 1989).

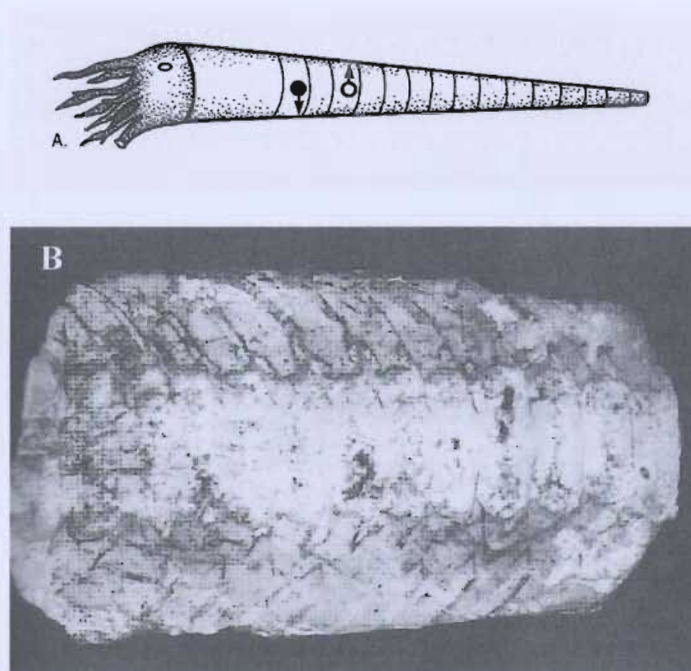


**Figure 4.4:** A) Paleozoic straight nautiloids (arrows indicating centers of gravity and buoyancy respectively). B) A straight nautiloid *Armenoceras* (Ordovician) with a heavy siphuncle (light colored). The specimen has been cut longitudinally and polished so that the siphuncle is seen in section. The specimen is 16 cm long (from Stearn and Carroll, 1989).

The second fossil bed is located 1 km further to the south in a overgrown gravel pit (UTM coordinates 654515/ 543003) on the west side of the resource road as mapped by Blackwood (1982). The outcrop consists of grey, fine-grained, somewhat silicified sandstone. The protruding outcrop is ~ 4 m x 2 m, fossiliferous and cut by 2 to 3 cm wide, randomly orientated, quartz-carbonate veins.

Sample JOD-114 was collected from this locality, and this limey siltstone contains *Anthozoa* *Tabulata* - ?*Favosites* (sp. undet.), *Bryozoa* (gen. et sp. undet.) (branching stick forms), and *Echinodermata* - *Crinoidea* (gen. et sp. undet.). All of these phylums have previously been discussed in this chapter; this sample is therefore, also a representative of the Indian Islands Group.

Sample JOD-086D, from the gravel pit at the south end of the main Appleton Pit, is a black slate. It contains (P) *Chordata*-(SP)*Hemichordata*\_(C) *Graptolithina* - *Climacograptus bicornis* (Hall), a distinctive Caradoc fauna (Ordovician) and *Hemichordata Graptolithina Climacograptus* sp (p) (Figure 4.5, p. 135). This unit, thus, is definitively Caradocian shale.



**Figure 4.5:** *Climacograptus* (after Stearn and Carroll, 1989).

## 4.6 Salmon River and Red Rock Brook

### 4.6.1 Introduction

The Mount Peyton Intrusive Suite (see description in chapter 2) has been studied and mapped by several authors (*i.e.*, Dickson, 1992, 1993, 1996; Hynes and Rivers, 2002; Hoffe, 2003). However, the relationship between the gabbro and granite phase, as well as the relationship of the suite to the surrounding sedimentary lithologies, is still poorly understood due to the lack of contact exposures. Thus, an attempt to locate and examine the contact along the eastern margin of the suite was made during this study.

Two areas of contact were observed. The first, along Salmon River was encountered while walking upriver between the Hurricane and Corsair auriferous



prospects. Here, there is an exposed contact relationship between the mafic and felsic phases of the MPIS. Dickson (1993) reported several contact relationships in the vicinity of Salmon River including exposed contacts between the main felsic and mafic phases of the suite 1.5 km to the south of the Salmon River and plugs of granite (same lithology as main phase of MPIS granite) intruding the gabbro to the northwest. Along Salmon River pink, fine-grained biotite granite was reported to have partially assimilated gabbro, producing a buff-colored fine-grained granodiorite that is exposed for 200 m along the river. Pink medium-grained granite dykes cut these intermediate rocks, as well as the main mafic unit. The intermediate unit, referred to as a hybrid of the main gabbro and granite phases by Dickson (1993), is the host to the Corsair and Hurricane prospects and has been mapped as a diorite in several metallogenic studies (*i.e.*, Tallman, 1990, 1991; Evans, 1996). To the south, granitic dykes containing very large blocks of angular gabbro with small granite veinlets are present along the contact (Dickson, 1993). Observations made along Salmon River during the current study do not support the hybridization theory for the formation of the intermediate phase that hosts the auriferous occurrences.

The second contact locality was located along Red Rock Brook where a granite phase of the MPIS is juxtaposed against sedimentary rocks. Although the actual contact is not directly exposed (the two units outcrop ~60 m apart), evidence of the relationship between the two units was ubiquitous. The sedimentary rocks and their relationship to the granite at this locality were first described by Dickson (1993). He had tentatively assigned the sedimentary rocks to the Indian Islands Group following Currie (1992) (see section 4.7.1) and described them as highly folded and reverse faulted, medium bedded.

brown sandstone. The contact was also re-visited by Squires (2005), who suggested a brittle-fault contact because the granite was heavily brecciated and locally sheared near it.

#### *4.6.2 Granite-Gabbro Relationships in the Salmon River*

At UTM coordinates 645092/ 5425251 along the Salmon River between the Corsair and Hurricane prospects, a relative chronological relationship was observed with a granite phase intruding a gabbro phase of the MPIS batholith (Plate 4.22, p. 156). The granite is interpreted to be a plug of the main granite phase of the batholith. Small pieces of the gabbro had been stooped along fractures by the granite and no chill margins were observed in the gabbro, suggesting that it had formed prior to the granite intrusion.

Further upriver, at UTM coordinates 644887/ 5425295, multiple fractures and three cleavage directions (conjugate joint set) were observed in gabbro. The main cleavage was at  $006^{\circ}/57^{\circ}$  SE with strong Fe-carbonate and epidote alteration. Quartz and carbonate crystallized in the  $\sim 2$  mm joints with a black alteration halo extending  $\sim 2$ -3 cm in width around it. A second cleavage is at  $291^{\circ}/90^{\circ}$  and both of those cleavages are cut by later vein systems.

The relationship at this locality further supports the findings of Dickson (1992) that “intrusive relationships indicate that the granitic rocks are younger than the gabbroic rocks”. However, the diorite host to the auriferous prospects along Salmon River must have formed as an intermediate phase before the formation of the granite rather than by hybridization as the granite would not have been of a sufficient temperature to assimilate the gabbro. The granite would only have been able to stope off pieces of the gabbro and



contain blocks as inclusions as partially observed along the Salmon River during the current study and as reported by Dickson (1993) to the south. Age data presented chapter 8, provides additional support to this interpretation.

#### *4.6.3 MPIS Granite at Red Rock Brook*

Along Red Rock Brook, pink granite of the MPIS batholith and a sedimentary unit (grey, micaceous sandstone and siltstone), possibly part of the Indian Islands Group (Squires, 2005), are exposed. There is a gap of 60 m between the granite and siltstone and sandstone unit. The siltstone and sandstone beds are extremely convoluted in the outcrop nearest to the contact and exhibit a strong cleavage at  $052^{\circ}/47^{\circ}$  SE. The sediment is also intensely weathered to a brown orange color, whereas it is grey on fresh surfaces. Further to the east, the sandstone is less deformed and the cleavage is sub-parallel to bedding at  $134^{\circ}/47^{\circ}$  SE. The granite is extremely jointed along the river. Thus, the contact appears to be structural as suggested by the deformation observed in the granite and sedimentary units and the lack of an alteration halo. This conclusion agrees with the interpretations of Dickson (1993) and Squires (2005).

Sample JOD90B was collected at the first exposed outcrop of granite along the river at UTM coordinates 641210/ 5408962 and JOD90A was collected approximately 100 m upriver. Geochemically (Chapter 5) the granite exhibits no unusual chemistry due to interaction with the sedimentary unit and the granite collected closest to the contact does not differ from granite collected away from the contact.



During the 2004 field season, a third sample of the granite was collected approximately 4 km southwest of the aforementioned location at UTM coordinates 638577/ 5412140. Sample JOD04-17 (Plate 4.23, p. 139) is comprised of 25% anhedral quartz, 60% subhedral perthitic k-feldspar (microcline) intergrown with quartz, 5% plagioclase, 5% minor biotite and 5% opaque minerals. The K-feldspar is coated by secondary hematite. The rock is classified as a micrographic alkali feldspar granite.

Although the granite was jointed in outcrop, no deformation is evident in thin section. Dickson (1993) suggested that the fact that the granite near the contact zone was fine-grained and micrographic could lead to an interpretation of a chill margin in the granite. However, he also notes that these properties extend for several kilometers, as also indicated by this study, and the existence of such a large chill margin would be unlikely.

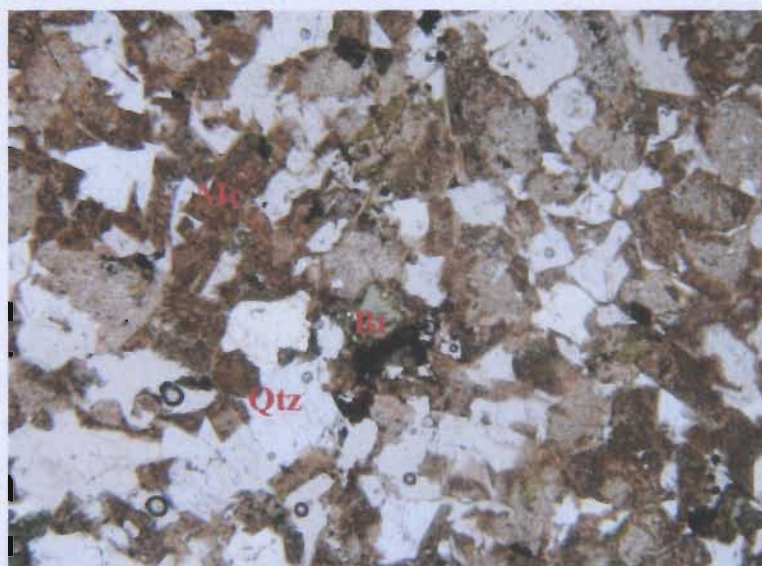


**Plate 4.23:** Photomicrograph of sample JOD 04-17 which consists of quartz (Qtz), microcline (Mc), plagioclase (Pl) and minor biotite (Bt) [Field of view, 7mm PPL].

#### 4.6.4 Discussion

Tallman (1990) noted that the red and green siltstones presumed at that time to be part of the Botwood Group were slightly hornfelsed adjacent to the northeast quadrant of the intrusive. This is important to regional mapping because relationships between the Mount Peyton Intrusive Suite and the sedimentary unit along its eastern margin are poorly understood. Dickson (personal communication, 2005) has not identified any definite intrusive relationships between these two units on the eastern side of the MPIS; however, he noted that in a previous season he identified hornfelsed sandstone just northwest of the Beaver Brook Mine.

An intrusive relationship has been postulated for the MPIS and the Badger Group sediments along the western margin of the intrusion based on the observed extensive metamorphic aureole. The Badger Group ranges from Late Ordovician to Early Silurian and is conformably overlain by the Silurian Botwood Group. The relationships between the Botwood Group and Indian Islands Group to the MPIS are poorly understood.

The lack of intrusive evidence along the eastern margin may provide the best indication of a faulted contact. Several authors have implied such a contact, and it has been even suggested that the faulted contact along the eastern edge of the MPIS might represent the southern extension of the Dog Bay Line (*i.e.*, Dickson, 1993; Squires, 2005).

Williams *et al.* (1993) also proposed that the Dog Bay Line might extend to the southwest, but suggested that the structure may be actually truncated by the MPIS rather than cutting it in the central Botwood Basin. These authors trace the structure from the



north to the TCH where it separates grey siltstone of the Indian Islands Group from red micaceous sandstone of the Botwood Group.

No definite evidence was available to extend the line to the southwest of the MPIS, but it was suggested that it might follow the deformed Ordovician mafic volcanics there as it does at Dog Bay and that the lack of surface expression may be due to a terrestrial sandstone cover that has been assigned to the Botwood Group. To the extreme southwest it was assumed that the Dog Bay Line lies between the Botwood Belt and Noel Paul's Line, or the Gander-Dunnage Zone boundary (Williams *et al.*, 1993).

If in fact the contact along the eastern margin of the MPIS is a continuation of the Dog Bay Line, the geochronological data presented in this study could aid in constraining the timing of movement along the fault as movement would be post plutonic.

Geochronological data for the MPIS, coupled with structural studies to better define the faulted contact along the eastern margin could help provide a better definition on the relationship between the MPIS and adjacent units in the central map area and could have important implications on constraining the timing of Au mineralization and delineating a possible driving heat source (refer to chapter 8).

In terms of the relationship between the MPIS and the Indian Islands Group, the presence of the intrusive dyke in the pit west of Glenwood, reported in section 4.5.1, would suggest an original intrusive relationship as Dickson (1996) correlated this dyke to the MPIS. Recent work by Lake and Wilton (2006) also supports an intrusive relationship as these authors present evidence for an intrusive contact between the MPIS granite and the Indian Islands Group along the southeast quadrant of the intrusion. These findings



cannot disprove the presence of a fault along the eastern margin of the pluton, rather they imply that perhaps the relationship is a fault-modified intrusive contact.

## **4.7 Careless Brook**

### *4.7.1 Introduction*

Careless Brook is located about 13 km southwest of Glenwood and is accessed via the Salmon River Access road. The sedimentary rocks in this area had originally been assigned to the Silurian Botwood Group (*i.e.*, Blackwood, 1982; Dickson, 1992) but subsequent workers have re-assigned the rocks to the Indian Islands Group. The suggestion to extend the Indian Islands Group to this locality was first made by Dickson (1993) when he extrapolated the work of Currie (1992) and Williams (1993) from the north. These other authors found that the Botwood Group did not actually extend as far east into map areas 2E/2 and 2D/15 as hypothesized by previous workers (*i.e.*, Blackwood, 1982; Evans *et al.*, 1992). Dickson (1993) tentatively assigned the exposed rocks to the west of the Northwest Gander River to the Indian Islands Group as defined by Currie (1992). Previous fossil collections from Careless Brook have been described by Williams (1993) and Boyce *et al.* (1993, 1994) (refer to table A1.3).

### *4.7.2 Mapping Observations and Petrography*

The streambed is underlain by laminated, brown and black Indian Islands Group siltstone. In general, the bedding trends  $175^{\circ}/75^{\circ}$  SE with bedding tops upriver as

indicated by sedimentary features such as burrows and crossbedding (Plate 4.24a). Conjugate cleavage sets have directions at 188°/ 61° SE, 032°/ 70° NW and 177°/ 67° SE and are filled with quartz and carbonate. The outcrops become more fossiliferous downriver towards a contact with another sedimentary unit.

At UTM coordinates 647447/ 5418287, a 3-5 cm wide quartz carbonate vein was sampled which cuts bedding at 149°/ 70° W. The vein locally cements brecciated pieces of laminated Indian Islands Group. The vein pinches and swells and appears to have carbonate along its edges.

Further down river, a fossiliferous debris flow? (L. Dickson, pers. comm., 2003) was sampled (JOD37A) for fossil analysis (Plate 4.24b and c, p. 156). As described below the fossils are Silurian.

Further down river, a contact between the Indian Islands Group and shale of either the Davidsville Group or Caradocian shale is implied (Plate 4.24d, p. 156). Williams (1993) collected graptolite fossils from this shale, which he dated at Cardoc-Ashgill age. He described the unit as silty shale from a 'rather coarse, non-fissile, siliceous mudstone'. Although Caradocian shale is typically associated with the Lawrence Harbor Formation, such a rock type is atypical of that formation. He suggested that it either represents the top of a black shale unit passing gradationally into sandstone or is an argillite lens in a coarser sandstone unit. Either of these conclusions is feasible and evidence can be presented for both. Williams *et al.* (1993) included this Caradocian shale as the top unit of the Davidsville Group, which grades up into limestone, siltstone, shale and redbeds of the Indian Islands Group. The contact has not been observed but is assumed to be conformable where not structurally modified.

Squires (2005) also visited the fault-bounded Caradocian shale along Careless Brook, which he stated were related to the structural complexity of the area. Fault-bounded lenticular shales of Caradocian affinity have also been mapped by Dickson (1993) and Williams *et al.* (1993) at two localities to the southwest, near the Beaver Brook Mine.

Although the actual contact was not observed, a graphitic fault gouge zone was present, which would seem to imply that the contact here is faulted and therefore not conformable, further supporting the case for a fault bounded wedge of shale. However, brown silty layers from the Indian Islands Group were observed to be interbedded with the shale unit near the fault zone during this study, suggesting that the contact between the units was initially gradational. This supports the interpretation that Caradocian shale is the top of the Davidsville Group, which is both conformable and fault modified with the Indian Islands Group along Careless Brook. The fault gouge would have been caused by a later event (possibly movement along the Dog Bay Line), which would be expected to exploit this zone of weakness, resulting in wedges of Caradocian shale.

Two samples (JOD39A and JOD39B) were collected from a 0.6 m wide outcrop of the dark, dense shale unit. In thin section (Plate 4.25, p. 145) the shale consists of a 30% fine-grained matrix of clay, quartz and feldspar, 30% quartz (subhedral porphyroblasts), 10% feldspar and 8% dolomite, 2% sulphides, 10% lithic fragments and 10% Fe oxides. The sample is well sorted with subangular grains, hence would be classified as a lithic arkose. The arkose is cut by minute, randomly orientated quartz-carbonate veins which probably resulted from fluid movement along the fault.





**Plate 4.25:** a) Photomicrograph of sample JOD39A exhibiting subangular quartz grains in a fine-grained matrix. b,c) Photomicrograph of sample JOD39B exhibiting a quartz-carbonate vein [Field of view 7mm, PPL and XP].

#### 4.7.3 Paleontology

Sample JOD-037A, from Careless Brook consisted of a micaceous, fine-grained, dark grey calcareous sandstone. Fossils within the sample have been identified as *Anthozoa* *Tabulata* - ?*Favosites* (sp. undet.) (Silurian age) and *Echinodermata* - *Crinoidea* (gen. et sp. undet.). As such this unit would be classified as Indian Islands Group. Boyce *et al.* (1993) had previously identified a latest Silurian to earliest Devonian bivalve fauna (*Cuneamya arata* (Hall, 1860)) upstream from this area.

#### 4.7.4 Discussion

Caradocian graphitic chert has been mapped at Careless Brook by Williams (1993) and to the southwest, near Beaver Brook, by Dickson (1991, 1992) and Williams (1993). Previous workers have identified the Caradocian unit as a fault bounded lenticular unit (*i.e.*, Squires, 2005) and the fault gouge observed during this study supports this supposition. However, the presence of what have been defined as interbeds during this study, provides evidence for a gradational contact between the Davidsville

and Indian Islands groups in the central Botwood Basin. If the contact was gradational, a fault caused by a later movement could have exploited the Caradocian shale, present as the upper unit of the Ordovician Davidsville Group.

The presence of interlayered brown siltstone and black Caradocian shale along Careless Brook supports the previous interpretation of Williams *et al.* (1993) that the contact between the Davidsville and Indian Islands Group is conformable, yet also locally fault-modified. The identification of Silurian fauna in Careless Brook concurs with the ages reported for previous collections and indicates the presence of the Indian Islands Group in this area and further adds to the paleontological database for Silurian fossils of central Newfoundland.

## **4.8 Coopers Brook**

### *4.8.1 Introduction*

Blackwood (1981) first discovered Middle Ordovician (Caradocian) graptolites in a graphitic shale horizon along Beavers Brook (southwest of Coopers Brook). He interpreted the horizon to be a discontinuous thrust wedge of Ordovician Davidsville Group strata in Botwood Group sediments. The thrust wedge was extended to the southwest based on the discovery of additional Caradoc-Ashgill fossils by Dickson (1992). In addition to this extension of the unit, the pebble greywacke host to the Hunan prospect was reinterpreted to be a similar fault block of Devonian or younger material based on the observation of poorly observed bedding. Dickson (1996) inferred that the sediments along the southeastern contact with the MPIS, previously interpreted as

Silurian Botwood Group (*i.e.*, Anderson and Williams, 1970; Blackwood, 1981; Dickson, 1992) were actually part of the Indian Islands Group. Mapping observations from this study provide further evidence for the extension of this group to the south.

An attempt to redefine the stratigraphy in this area based on fossil evidence was made by Williams and Tallman (1995). These authors did not agree with the interpretation that the Early to Middle Ordovician sequence was a fault-bounded wedge (Blackwood, 1981; Dickson, 1992). Rather, they proposed that the sequence youngs to the southeast and is a continuation from the east of the Davidsville Group or its equivalents.

Additional fossils were collected from the Beaver Brook locality of Blackwood (1981) by Williams and Tallman (1995) and the Caradocian age was confirmed. They correlated this unit with the Lawrence Harbour Formation that Williams (1995) says is widespread in the Exploits Subzone. Williams and Tallman (1995) collected additional graptolites along Coopers Brook, 1 km to the east-northeast and dated them as Late Arenig (Early Ordovician), in disagreement with Dickson (1992) who dated the fossils as Caradocian. This new interpretation suggested that several graphitic shale horizons were present in this vicinity.

The problem with this interpretation was that the fossil ages indicated that the succession youngs to the southeast which conflicts with regional stratigraphic relationships. The authors postulated that Coopers Brook is entirely underlain by Ordovician lithologies that extend from the Northwest Gander River to the MPIS, which excluded the presence of the Indian Islands Group in the vicinity as implied by Dickson (1992). However, they did not provide an explanation for the conflict that the fossil ages



provide with respect to the regional stratigraphy. An attempt to reinterpret this evidence is made here.

#### *4.8.2 Mapping Observations*

A mapping transect was conducted along Coopers Brook, north of the Hunan Prospect. The brook exposes interbedded red to buff siltstone beds with brown limestone beds. Throughout the sequence, the limestone beds are boundinaged to form buff to white nodules (Plate 4.26, p. 157). No fossils were recovered, possibly due to the prevalent deformation in the immediate area caused by movement along the Coopers Brook fault as informally defined by Williams and Tallman (1995). The fault is a late dextral fault trending 100° that is outlined by geophysical surveys.

#### *4.8.3 Discussion*

Based upon a review of literature, coupled with mapping observations in the Coopers Brook and Hunan Prospect vicinities, several ideas are proposed. First, with respect to the fossil evidence presented by Williams and Tallman (1995), rather than disproving the case for a fault-bounded wedge of the Ordovician Davidsville group, it supports it. Williams and Tallman (1995) propose that the succession along Coopers Brook is a continuation of the Davidsville Group, however, the fossil evidence they presented suggests that the succession youngs to the southeast, in disagreement with the regional stratigraphy. Those authors also dated the fossils as ranging from Early to Middle Silurian and correlated the unit with the Davidsville Group to the east. Thus, it is

herein postulated that the succession is possibly part of a fault-bounded wedge of the group that was transported west, and subsequently rotated from its original orientation. The presence of Caradocian shale further supports the presence of the Davidsville Group here as it has been previously presented as the top unit of the group (see section 4.7.3). The deformation observed along Coopers Brook emphasizes the structural complexity of the area and further work is required to unravel the complexities of the stratigraphy of the Beaver Brook area. A MSc. thesis study on the geology and geochemistry of the Beaver Brook antimony deposit was initiated in 2005 and is being conducted by Justin Lake.

The suggestion that the Davidsville Group be extended further west to the MPIS is also discredited based on mapping observations east of the Beaver Brook deposit, in the vicinity of the Northwest Gander River. Sediments along transect are now mapped definitively as Indian Islands Group (Dickson, 1996).



**Plate 4.1:** Interlayered siltstone and limestone beds with laminations parallel to pencil. A fossiliferous layer where fossils have been weathered out, leaving impressions, is outlined in red.



**Plate 4.4:** Hand specimen JOD66 from the knobby gabbro exposure north of Duder Lake [Penny for scale]





**Plate 4.6:** Sample JOD08 photographed where it was removed from outcrop of the Bellman's Pond Conglomerate (sample is approximately 15 cm in length).

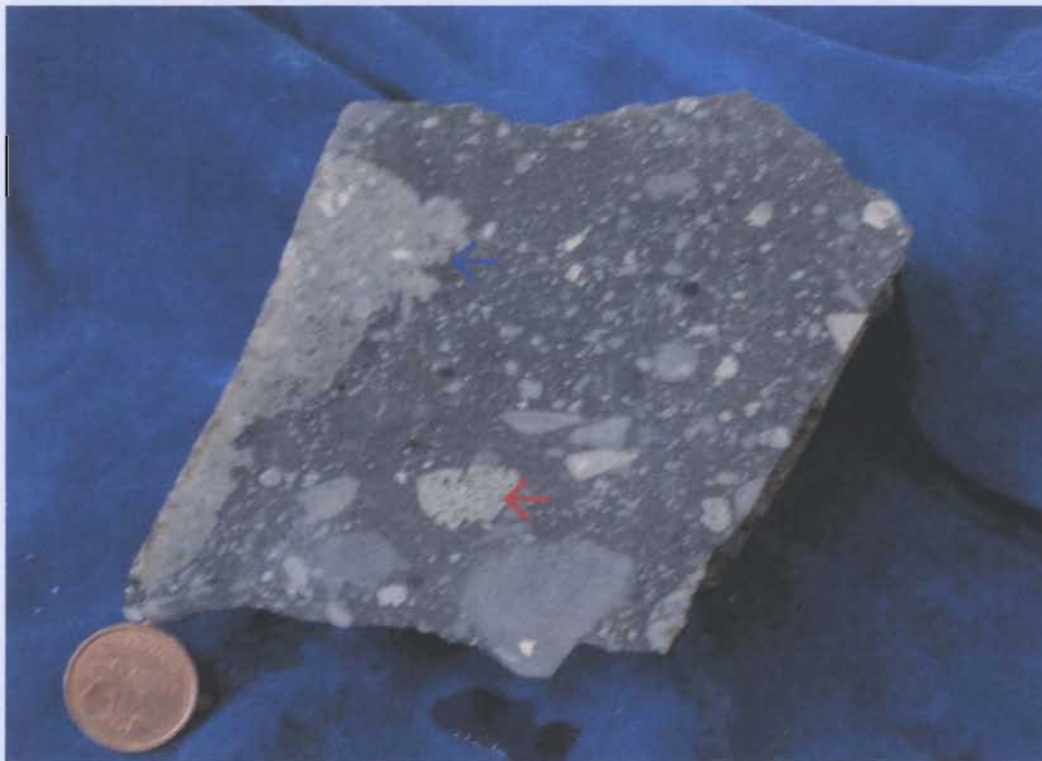


**Plate 4.7:** Cut section from sample JOD08 left over from removal of the volcanic clast. Several smaller volcanic clasts (red arrow) were identified in this section. The outline of the fragment is also noticeable on the left hand side (blue arrow) [penny for scale].



**Plate 4.9:** Gabbro exposure along Birchy Bay Resource road from which sample JOD57A was collected [S. Huelin for scale].



**Plate 4.10:** Gabbroic body along Birchy Bay Resource Road (southwest of Duder Lake) as mapped by Evans *et al.* (1992) and Currie (1995a). A) Rounded, weathered exposure of jointed gabbro [S. Heulin for scale], B) Sub-parallel quartz veins in gabbro [field book and rock hammer for scale].





**Plate 4.13:** Gabbro exposure of elongate ridge near Twin Ponds as mapped by Evans *et al.* (1992) [field notebook for scale].



**Plate 4.15:** Hand specimen (JOD04-12) bearing re-crystallized fossil casts. A re-crystallized crinoid column is outline in red [pencil for scale].





**Plate 4.16:** Re-crystallized, deformed limestone outcrop along Ten Mile Lake Resource Road from which sample JOD04-12 was collected [pencil for scale].



**Plate 4.18:** Hand Specimen (JOD04-14) bearing fossils. Re-crystallized crinoid columns are outlined in red [Penny for scale].



**Plate 4.19:** Ten Mile Lake Resource Road, purple fossiliferous bed from which sample JOD04-14 was collected [GPS for scale].

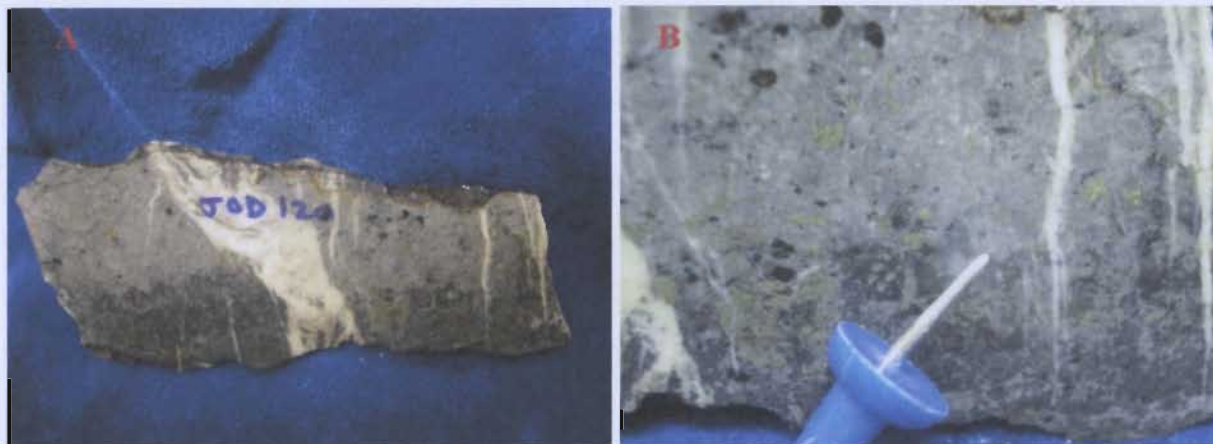


**Plate 4.20:** A) Hand sample 120, collected from dark, dense sedimentary interbeds in Davidsville group shale in the Appleton Pit. The sample is cut by a 4 cm wide quartz vein and exhibits sub-parallel quartz filled tension gashes. B) Close up of sample JOD120 showing disseminated sulphide mineralization in altered sediment [tack for scale].





**Plate 4.22:** A-B) Gabbro (Ga)- granite (Gr) contact at Salmon River. The outlined area in A illustrates a piece of gabbro stoped by the intruding granite [rock hammer for scale].

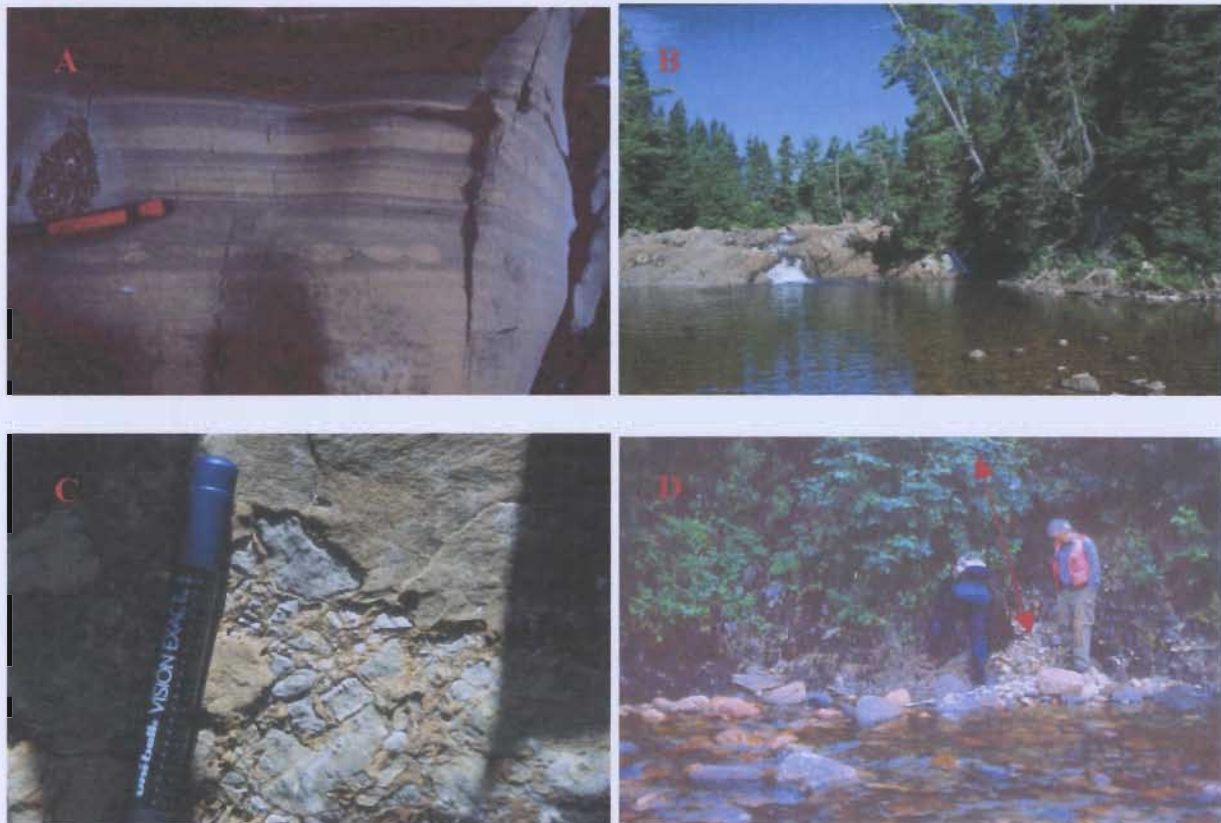


**Plate 4.24:** A) Load casts in Indian Islands Group siltstone [pencil for scale], B) View upriver, X marks fossil debris flow location, 3) close up of fossil local [pen for scale], 4) D. Wilton and S. Hinchey at contact of Indian Islands Group and Caradocian shale.





**Plate 4.26:** Cooper Brook outcrop exhibiting red and green interbedded siltstone with boudinaged limey beds [rock hammer for scale].

## CHAPTER 5

### WHOLE ROCK GEOCHEMISTRY

#### 5.1 Preamble

This chapter discusses the major and trace element geochemistry of various intrusive and sedimentary lithologies sampled throughout the Botwood Basin. These data are used for two main purposes: 1) to compare with previously derived geochemical data compiled for several intrusive lithologies throughout the basin (*i.e.*, Churchill, 1994) with particular emphasis on relationships, if any, between the extensive data set for the Mount Peyton Intrusive Suite derived by Dickson (1996), and 2) to better understand the petrology of sedimentary host lithologies in the region.

In terms of the first objective, Churchill (1994) had defined geochemical data for fresh volcanic rocks and altered gabbroic rocks at the Duder Lake showings, which he postulated, were Silurian-Devonian. He also presented data for a fresh gabbro sample from the Clutha Prospect and a fresh gabbro sample from near Dan's Pond to the immediate north and south of Duder Lake, respectively. Churchill's (1994) altered gabbro dataset was not utilized for comparison in the current study as it was compiled to determine alteration at the prospects rather than geochemical compositions of the original rocks. To the south, Dickson (1996) derived an extensive geochemical database for the Mount Peyton Intrusive Suite that cuts the Silurian rocks of the basin.

Conversely, there are no geochemical data for the gabbros mapped by Evans *et al.* (1992) and Currie (1995a) to the north of the Trans Canada Highway, intrusive into the

Late Silurian to Early Devonian Ten Mile Lake Formation. There was also no geochemical data available for gabbro and granite intrusives to the south at the Greenwood Pond #2 and LBNL Prospects, respectively, that intrude Ordovician Davidsville Group rocks.

The objective for the geochemical study of the intrusives, therefore, was to geochemically compare intrusive rocks from the region and to evaluate the petrogenesis of several host lithologies to gold mineralization. Due to the number of prospects and their extensive areal extents, the purpose was not to directly classify the various alteration systems related to gold mineralization, but rather to ascertain if there are geochemical relationships between the various intrusive bodies. Such relationships may provide links to common source areas and possibly the definition of a deep-rooted, areally extensive magma system.

The igneous samples will be discussed first to ascertain if there are definable relationships between the different intrusive bodies through the region. Secondly, the geochemical data for the sedimentary samples will be evaluated and combined with petrographic observations to better delineate host and country rock lithologies and to determine source rocks and the tectonic environments of origin and deposition.

Where possible, only "fresh" samples were used. Samples with intense alteration, weathering rims or veining, were not selected for analysis. A total of 34 whole rock samples (20 igneous and 14 sedimentary) were analyzed for major oxides and trace element compositions via pressed powder pellets using an X-Ray Fluorescence (XRF) spectrometer (after Longerich, 1995); sample numbers and locations are listed in table A3.1. All geochemical analyses were completed at the Department of Earth Sciences



laboratories, Memorial University of Newfoundland. The sampling protocol, analytical methods, as well as the precision and accuracy are outlined in Appendix 3 and the derived data are presented in Appendix 4.

## **5.2 Igneous Rocks**

### ***5.2.1 Sample Overview***

Table A3.1 lists the sample numbers, locations and detailed description of the igneous rock samples analyzed for this study.

Samples JOD21 and JOD22 were both collected from the Hurricane Prospect along the Salmon River. JOD21 is a fine-grained, slightly seritized, unmineralized diorite host, whereas JOD22 is an unaltered, albeit somewhat mineralized sample, from the same locale. Sample JOD25 was collected further upstream at the Corsair Prospect and contains trace amounts of disseminated sulphide. All three samples are mapped as part of the Mount Peyton Intrusive Suite (Dickson, 1992). Sample JOD04-20 was collected from a dyke (or sill) in Indian Islands Group sediments in a gravel pit just west of the town of Glenwood and east of the Salmon River Showings as mapped by Dickson (1992).

Samples JOD45A, JOD45B, JOD46B and JOD81A were collected from intrusive bodies into the Davidsville Group sedimentary rocks and host auriferous mineralization in the Paul's Pond area. Samples JOD45A and JOD45B were collected from the LBNL prospect host rock and consist of fine-grained leucogranite with a small amount of disseminated sulphide. The LBNL prospect has been previously mapped as a granitic

intrusion into the Davidsville Group (Evans, 1996). Sample JOD46B was collected from subcrop at the location of the Road Gabbro showing and comprises an unmineralized fine-grained gabbro. Sample JOD81A is from a small, fine-grained gabbro body at the Greenwood Pond #2 prospect that may have been altered by hydrothermal fluids but does not contain any sulphide mineralization in hand sample.

Sample JOD04-09 was collected from an elongate gabbro ridge (Evans *et al.*, 1992; Currie, 1995), west of Ten Mile Lake. The sample comprises an unmineralized fine-grained gabbro that intrudes green siltstone previously mapped as the Ten Mile Lake Formation (Currie, 1995a). Sample JOD04-13 is from an unmapped gabbro body, east of the aforementioned ridge, along the Ten Mile Lake Resource Road.

Samples JOD100, JOD101, and JOD102 were collected from gabbroic intrusions, possible dykes or sills (Evans *et al.*, 1992; Currie, 1995) intruding the Early Silurian to Early Devonian Ten Mile Lake Formation (Currie, 1995), north of the Trans Canada Highway. These outcrops were previously mapped as a single elongate gabbroic body, south west of the previously sampled intrusion (JOD04-09). These three samples appear to be geochemically unaltered.

Samples JOD90A and JOD90B were collected from Red Rock Brook. The granite samples, from different locations along the river, are fresh and represent the main body of Mount Peyton Intrusive Suite granite.

Sample JOD96D was collected from an exposed pink volcanic wedge, in the Duder Complex, south of the auriferous prospects at Duder Lake. Sample JOD97B is from the Corvette Prospect and samples JOD98 and JOD98A, which contain

disseminated sulphides, were collected from the Goldstash Prospect at Duder Lake (*cf.*, Churchill, 1994). Hydrothermal fluids may have affected these samples.

Sample W03-35 was collected from the Huxter Lane Prospect in the southern most Botwood Basin. The sample is a finely mineralized, felsic intrusive rock with a quartz breccia vein in the Coy Pond Complex. The vein was removed before geochemical analysis of the host lithology.

The geochemical data from this study were compared with a small representative data set from the northern Botwood Basin (Churchill, 1994) and a very extensive data set from the Mount Peyton Intrusive Suite (Dickson, 1996). Churchill's study mainly concentrated on the altered and mineralized gabbro intrusions. However, four regional, and presumably unaltered, igneous samples were reported as representative of the igneous lithologies in the northern region. Churchill had included these samples in an attempt to determine if there were any genetic relationships between igneous lithologies on a regional scale. He found that three of the samples had a calc-alkaline affinity but no direct conclusions about a genetic relationship between the samples were inferred. The data were collected for two volcanic samples (RC-92-04 and RC-91-62) which were presumed at the time to be from the Lawrenceton Formation, Botwood Group, one sample (DE-90-51) from the gabbroic host to the Clutha Prospect and one sample (JH-92-310) from a gabbroic body 25 km southwest of the Duder Lake Prospects, near Dan's Pond.

Since that study, the volcanic and intrusive rocks in the vicinity of the Duder Lake Prospects, including the host to the Clutha Prospect, have been remapped as tectonic blocks in the Duder Complex (Currie, 1995b). As already discussed (refer to chapter 2)



the inclusion of mappable volcanic and intrusive units in this complex has recently been questioned (*i.e.*, Churchill, 1994; Dickson, 1995). Because of this controversy, no inferences as to the petrogenetic origin of these rocks are made here and the geochemical data are evaluated to determine if there is any recognizable association with the other samples included in this study. The two volcanic samples collected near Duder Lake were defined by Churchill (1994) to comprise lower greenschist facies basalt. The intrusive gabbroic sample from the Clutha Prospect was described as a deformed, fine to medium-grained rock that may have been affected by Fe-carbonate alteration. The fourth sample from Dan's Pond was collected from a gabbroic body that intrudes the Ten Mile Lake Formation.

All samples contain S and some of the samples have very high S contents. The samples with the greatest S contents were collected from known Au occurrences. Some samples also had high Fe contents up to 23.6 wt. %  $\text{Fe}_2\text{O}_3$ , which reflects hydrothermal pyrite in the samples. In general, the oxide and trace element data show some variability within different lithological groups, due either to metamorphic overprinting or by the hydrothermal episode producing gold mineralization and it is thus assumed that original chemistry is not preserved.

### *5.2.2 Trace element discrimination diagrams for rock classification*

#### *5.2.2.1 Introduction*

The geochemical data were plotted on discrimination diagrams to group the samples according to rock type and magma series. These diagrams were created for

volcanic rocks and most samples in this study are intrusive plutonic, thus conclusions must be treated with caution. The diagrams do, however, provide a solid basis for distinguishing between different lithologies and recognizing common origins.

When dealing with metamorphosed or altered rocks, the plot of Nb/Y vs. Zr/TiO<sub>2</sub> of Winchester and Floyd (1977) is commonly used. The Zr/TiO<sub>2</sub> ratio indicates the extent of fractional crystallization as the ratio increases with fractionation due to the incompatibility of Ti. The Nb/Y ratio relates to the parent magma and the degree of alkalinity in the source since it rarely varies during fractionation (*i.e.*, Nb increases from tholeiitic to alkalic compositions (*cf.* Barrett and MacLean, 1994)).

A tertiary AFM plot and a bivariate alkalinity index plot of SiO<sub>2</sub> vs. alkalis (Irving and Barager, 1971) were used to determine the chemical affinity of the rocks. The alkali-silica diagram is one of the most useful classification schemes for volcanic rocks (Rollinson, 1993). However, these diagrams must be interpreted with caution as they are based on mobile elements, and the rocks from this study have undergone variable amounts of alteration related to ore-forming processes, as well as low-grade metamorphism. The total alkalis vs. silica diagram can be used to discriminate between two major magma series, alkaline and subalkaline (originally termed tholeiitic) (Rollinson, 1993).

#### *5.2.2.2 Results*

The SiO<sub>2</sub> contents in the samples from this study range from 33.0 to 70.7 wt. % (weight percent). Seven samples (JOD04-20, JOD04-09, JOD04-13, JOD100, JOD101,



JOD102 and JOD81A) had SiO<sub>2</sub> contents between 33.0 to 50 wt. % indicative of basaltic to basaltic andesite compositions. The lowest values (33.0 to 40.9 wt. %) were obtained from samples at the Duder Lake Prospects (JOD97B, JOD98 and JOD98A). Five samples (JOD21, JOD22, JOD25, JOD96D and W03-35B) had SiO<sub>2</sub> contents between 53.53 to 60.9 % indicating a rhyodacite to dacite composition, whereas another five samples (JOD45A, JOD45B, JOD90A and JOD90B) have SiO<sub>2</sub> contents ranging from 63.3 to 70.7 wt. % defining a rhyolitic composition.

The Winchester and Floyd (1977) plot of Nb/Y vs. Zr/TiO<sub>2</sub> (Figure 5.2, p. 195) defines three groups from this study. The first group with Zr/TiO<sub>2</sub> ratios between 0.008-0.02 and Nb/Y ratios between 0.1 and 0.3 plot as basalt to basaltic andesite. The samples that plot within this compositional range include the gabbro samples JOD46B, JOD81A, JOD97B, JOD98, JOD98A, JOD100, JOD101, JOD102 and JOD04-13, hence their plotting within or along the basalt field is expected.

Samples JOD100, 101, 102 and JOD04-09 from the linear gabbroic bodies southwest of Duder Lake (as mapped by Evans *et al.*, 1992) and JOD04-13 from the unmapped intrusion east of Ten Mile Lake plot near the dividing line of the andesite and andesitic basalt fields. This suggests that these mafic intrusive rocks in the north of the MPIS have similar compositions. The samples from the Duder Lake gabbros have slightly lower Nb/Y and Zr/TiO<sub>2</sub> ratios relative to the above gabbroic intrusions.

Samples in the second group have Zr/TiO<sub>2</sub> ratios ranging from 0.04 to 0.06 and Nb/Y ratios that vary between 0.2 and 0.5 placing them in the rhyodacite/ dacite compositional range. The samples in this group include JOD21, JOD22, JOD25, JOD96D, JOD04-20 and W03-35B. These samples, with the exception of JOD96D and



W03-35B were collected from, or immediately adjacent to, the MPIS near Glenwood. Sample W03-35B was collected from the south region and JOD96D was collected in the north.

The third group plot (Zr/TiO<sub>2</sub> ratios between 0.1 to 0.2 and Nb/Y ratios between 0.2 and 0.5) within the rhyolite compositional field. These samples include JOD45A and JOD45B, JOD90A and JOD90B. Samples JOD90A and JOD90B were collected from the granitic phase of the MPIS, sample JOD45A and JOD45B are from a leucogranitic intrusion in the Paul's Pond area and thus all four samples were expected to plot within this field.

For Dickson's (1996) extensive MPIS geochemical dataset the majority of the mafic rocks plot in the andesite field (Figure 5.2, p. 195). Some of the rocks plot in the rhyolite/ dacite field indicating a more intermediate phase of the suite and several samples plot in the upper andesitic basalt field. There are also outliers in other fields. The felsic intrusive rocks from this study plot within or near the dataset compiled by Dickson (1996) for the MPIS granitic phase.

The northern rock samples from Churchill (1994) range from sub alkaline basalt to andesite in composition on the Winchester and Floyd (1979) diagram. The Clutha Prospect sample plotted in the andesitic basalt field as did the samples from the Duder Lake Prospects from this study (Figure 5.2, p. 195). However, Churchill's sample collected from a gabbroic body near Dan's Pond plots with slightly higher Nb/Y vs. Zr/TiO<sub>2</sub> ratios on the dividing line between the andesite and dacite fields. Although this sample was collected from a gabbroic intrusion into the Ten Mile Lake Formation, the sample consistently plots away from the gabbroic intrusions that intrude that unit from

this study. In fact, the Churchill sample consistently plots with the MPIS diorite samples from the current study. The two volcanic samples from Churchill plot in different fields, one as andesitic basalt and another as subalkaline basalt.

The Irvine and Barager (1971) alkalinity plot for samples from this study indicates that they are mostly sub-alkaline with similar natural groupings to previous plots (Figure 5.3, p. 196). The exceptions are the two samples from the Duder Lake auriferous prospects, which plot with lower  $\text{SiO}_2$  contents and higher alkali contents. All samples from the previous studies plot as subalkaline.

Irvine and Barager's (1971) AFM plot indicates that the samples from this study plot in both the calc-alkaline and tholeiitic fields (Figure 5.4, p. 197). The calc-alkaline samples generally include the felsic samples JOD90A, JOD90B, JOD96D and W03-35B. The Huxter Lane sample (W03-35B) and the volcanic sample JOD96D from Duder Lake are distinctly different in that they clearly plot away from the other samples in the middle of the calc alkaline field. The samples that plot amid the two fields include intermediate JOD21, JOD22 and JOD25 and felsic JOD45A and JOD45B, and the samples that clearly plot in the tholeiitic field are mafic samples JOD46B, JOD81A, JOD97B, JOD98, JOD98A, JOD100, JOD101, JOD102, JOD04-09, JOD04-13 and JOD04-20. This indicates that the different groups identified in the AFM plot (Figure 5.2) still plot together. The exceptions are JOD45A and JOD45B as they plot slightly higher (in the tholeiite field) than the rest of the felsic group. Many of the samples from this study contained finely disseminated or invisible sulphides, which would have caused the samples to plot higher on this diagram due to an increased Fe content. Therefore, interpretation of this diagram must be treated with caution.



On the AFM plot (Figure 5.4), the felsic samples from Dickson (1996) plot in the calc alkaline field with a trend line towards and eventually crossing over into the tholeiitic field. The mafic samples from Dickson's (1996) dataset plot mainly in the calc-alkaline field but there is also some cross over and scatter into the tholeiitic field. In fact, the MPIS samples define a distinct trend line, which borders the tholeiitic-calc alkalic boundary defined by Irving and Barager (1971). Upon initial observation of this graph, one would assume that since the mafic samples from the current study plot distinctly in the tholeiitic field, apart from the MPIS dataset, that these intrusives are unrelated to the MPIS. However, as previously mentioned, several samples from the current study contained disseminated sulphides, which may cause them to plot in the tholeiitic field. This issue is further explored on a graph based on immobile elements by MacLean and Barrett (1993) in section 5.2.4.2. Churchill's (1994) samples plot among the MPIS dataset with the exception of one of the volcanic samples, which plots in the tholeiitic field.

On a Pearce and Cann (1973) tectonic discrimination diagram, the mafic rocks from this study plot mainly within two distinctive groups in fields C and D indicating that the samples represent calc-alkalic and within plate magmas, respectively (Figure 5.5, p. 198). There is minor overlap into the B (ocean floor field), but in general, the samples that plot there (JOD98A and JOD100) border on the boundary between the D and C fields respectively. The samples that plot in the calc-alkalic basalt field include JOD21, JOD22, JOD25, JOD46B, JOD81A and JOD04-13. The samples that plot within the within plate field are JOD97B, JOD98, JOD98A, JOD101, JOD102 and JOD04-09. The felsic group of samples, in addition to the diorite sample JOD04-20, plots with Dickson's



(1996) MPIS felsic samples, outside of the recognized fields. These samples display low Ti contents and, in general, the rocks from the northern portion of the Botwood Basin have slightly higher Ti than those from the central to southern Botwood Basin regions. The rocks from the northern region therefore plot as within plate basalts whereas those from the central to southern regions have lower Ti values and plot as calc-alkaline basalts.

Dickson's (1996) mafic dataset plot dominantly within the C and B fields on the Pearce and Cann (1973) diagram. This indicates that these rocks have calc alkaline affinities. The felsic rocks from that dataset plot in a linear trend below the recognized fields among the felsic rocks from the current study (JOD90A, JOD90B, JOD45A and JOD45B).

On a Pearce and Norry (1979) diagram of Zr vs.  $Zr/Y$ , the majority of felsic to mafic rocks from this study and previous studies plot as within plate basalts (Figure 5.6, p. 199). These samples show a continental influence as they all have  $Zr/Y$  ratios greater than 3. The exception to this are several samples from the Dickson (1996) dataset which plot within the mid ocean ridge and island arc basalt fields indicating an oceanic arc influence in those rocks.

The samples were also plotted on Meschedes (1986) tectonic discrimination plot to further assess the validity of results from the previous diagram (Figure 5.7, p. 200). This diagram is based on a ternary plot of Nb-Zr-Y and most of the samples from the three datasets plot within the C field (within plate tholeiite). Samples JOD97B and JOD98A plot within the D (N-MORB) field, however, it should be noted that they plot near the C field. Several of the mafic samples from Dickson (1996) also plot in D field.

Sample W03-35B from Huxter Lane plots within the AII (within plate alkalic basalt to tholeiite) field. Sample JOD45B plots on the dividing line between the AI and AII fields. Two samples, JOD04-20 and JOD96D plot outside all fields and are very enriched in Zr and depleted in Nb and Y in comparison with the other rocks.

The Meschedes (1986) tectonic discrimination diagram was also used to determine if the mafic intrusive rocks from the various studies implied similar paleotectonic environments (Figure 5.7). The two volcanic samples from Duder Lake and the gabbroic sample from Dan's Pond from Churchill's dataset plot in the C (arc) field as do the majority of the samples from the MPIS mafic dataset of Dickson. The sample from the Clutha Prospect plots close to the Duder Lake gabbro samples from the current study and plots in the D field, near the dividing line with the C field. Some of the samples from the current study, as well as the MPIS study, also plot in the D field indicating N-MORB affinities. The majority of samples from all studies plot in the C field and this implies that the majority of the samples from the all three datasets have within plate tholeiitic affinity. As this diagram uses immobile and incompatible elements, it is assumed to be more reliable than the AFM diagram previously discussed.

The samples were also plotted on a bivariate Ti/100 vs. V diagram (Shervais, 1982) (Figure 5.8, p. 201). Island Arc Tholeiites (IAT) typically exhibits Ti and Y depletions and this feature can be used to construct a discrimination diagram that separates them from Mid Ocean Ridge Basalts (MORB) and Within Plate Basalts (WPB). Ti has to be plotted against a compatible index of fractionation because evolved IAT can contain the same Ti contents as MORB or WPB due to the effects of fractional crystallization. V is used as this index and is plotted against Ti/1000 to distinguish

between volcanic arc tholeiites and alkali basalts (Shervais, 1982). The MPIS dataset from Dickson (1996) was added to this diagram to further illustrate the various amounts of fractionation present in the basin with respect to this large intrusive body. The Churchill (1994) dataset was not used because V content was not measured for that study. In general, the mafic samples from the southern and northern Botwood Basin are more enriched in V and Ti than those from the central Botwood Basin (*i.e.*, MPIS dataset [Dickson, 1996] and current study) initially suggesting that those intrusions further away from the MPIS are more fractionated. Samples JOD90A and JOD90B were both collected from the main granite phase of the MPIS and plot amongst the MPIS granite from Dickson (1996). The majority of the samples plot within the alkaline basalt field with the exception of mafic samples JOD98A, JOD46B, JOD81A, JOD101, JOD102 and JOD04-09. Sample JOD98A is the most depleted in Ti of the northern Botwood Basin samples, which may account for its plot away from the rest of the group. The samples collected from the linear gabbros in the north as mapped by Evans *et al.* (1992) are more enriched in Ti than any of the other samples from current and previous datasets and illustrate a trend of increasing Ti with respect to V.

### 5.2.3 Harker Bivariate Plots

#### 5.2.3.1 Introduction

Several major element bivariate plots were utilized to illustrate variation between samples and to determine trends. Harker variation diagrams are bivariate plots using SiO<sub>2</sub> along the X-axis and major oxides along the Y-axis. The major elements are plotted



against  $\text{SiO}_2$  because it is the most abundant oxide in igneous rocks and exhibits a wide variation in composition. These diagrams are particularly useful for large quantities of data and yield an approximation of inter-element variations for a group of samples. Thus, the samples from the current study were not assessed separate from previous data sets via this method.

As the following diagrams are built upon mobile elements, they must be viewed with caution as the rocks from the current study have been subjected to hydrothermal fluid and low-grade metamorphism. Rocks that are genetically related through fractional crystallization typically exhibit variation with: 1) decreases in  $\text{TiO}_2$ ,  $\text{FeO}$ ,  $\text{MgO}$  and  $\text{CaO}$ , and 2) increases in  $\text{K}_2\text{O}$  and  $\text{Na}_2\text{O}$  and  $\text{Al}_2\text{O}_3$  with increasing  $\text{SiO}_2$  content (Rollinson, 1993). Although these parameters are useful in determining fractionation trends, Harker diagrams cannot define a definite genetic link. As the MPIS dataset of Dickson (1996) is the most voluminous, the current study dataset and Duder Lake dataset (Churchill, 1994) will be compared against it in an attempt to define or disprove any genetic relationship between the rocks throughout the Botwood Basin.

#### *5.2.3.2 Results*

The three datasets were plotted on four Harker variation diagrams of  $\text{SiO}_2$  vs.  $\text{FeO}$ ,  $\text{MgO}$ ,  $\text{K}_2\text{O}$  and  $\text{TiO}_2$  (a symbol key for identifying the samples is presented in figure 5.1, p. 194). Generally, the Duder Lake gabbros have the lowest  $\text{SiO}_2$  contents of the mafic samples, indicating they may be different. On the plot of  $\text{SiO}_2$  vs.  $\text{FeO}$ , the MPIS data define a smooth, negative, slightly curvilinear trend of decreasing  $\text{FeO}$  content with

increasing  $\text{SiO}_2$  content reflecting fractional crystallization (Figure 5.9a, p. 202). In regards to the current study, the samples from the southern and central region generally plot along the trend but the samples from the north define a different trend line, suggesting a variation in fractionation away from the main pluton. Initially, one would assume that the increased Fe content in the Duder Lake samples was a reflection of the mineralization, however, several of the samples from the linear gabbroic bodies mapped by Evans *et al.* (1992) did not contain much sulphides, but also have higher Fe contents. In fact, this graph suggests that Fe contents increase to the north in proportion to distance from the MPIS pluton. Of the four samples from Churchill's (1994) dataset, three plot along the trend defined by the MPIS dataset. The mafic samples collected from the Clutha prospect or Dan's Pond did not contain the elevated Fe contents of the northern samples from the current study. One of the volcanic samples from Duder Lake did plot along the trend defined by higher Fe contents.

A plot of  $\text{SiO}_2$  vs. MgO defines a smooth, negative, curvilinear trend for the MPIS data, again indicating fractionation (Figure 5.9b, p. 202). The data from the current study generally agree with the trend, with the exception of the Duder Lake gabbros and to a lesser extent, the linear gabbros. In fact, these samples define a similar trend line, which is offset by decreased silica. The Duder Lake volcanic samples from Churchill (1994) lie along the trend defined by the MPIS intrusives, with the exception of the Clutha sample, which has lower MgO contents.

On a plot of  $\text{SiO}_2$  vs.  $\text{K}_2\text{O}$  a smooth linear positive trend is defined by the MPIS data (Figure 5.9c, p. 203). Most of the samples from the current study fall along, or slightly above the trend line with the exception of JOD97B and JOD98A from Duder



Lake, which are low in  $\text{SiO}_2$  and  $\text{K}_2\text{O}$  content and displaced to the left of the trend line. Sample JOD25 from the MPIS diorite and samples JOD45B (LBNL) and W03-35B (Huxter Lane), both felsic samples from the southern Botwood Basin, all have slightly elevated  $\text{K}_2\text{O}$  contents with respect to the main dataset. The Dan's Pond gabbro and the two volcanic samples from Churchill (1994) all have lower  $\text{K}_2\text{O}$  contents than the MPIS dataset, whereas the Clutha gabbro sample once again plots among the MPIS mafics.

A plot of  $\text{SiO}_2$  vs.  $\text{TiO}_2$  illustrates a negative, slightly hooked trend for the MPIS data (Figure 5.9d, p. 203). The samples from the current study show the greatest deviation from the MPIS dataset on this plot. Samples JOD90A, JOD90B, JOD21, 22 and 25, all collected from the MPIS, fall along the trend line defined by the Dickson (1996) MPIS data. The most significant deviation are the samples collected in the northern Botwood Basin. Samples JOD97B, JOD98A and JOD98 all demonstrate increasing  $\text{TiO}_2$  content with increasing  $\text{SiO}_2$  content. The samples from the linear gabbros have various elevations of  $\text{TiO}_2$  (2.0-3.7 wt. %) with similar  $\text{SiO}_2$  (48-52 wt. %) contents. The two gabbro samples from the Paul's Pond region (JOD81A and JOD46B) also have slightly elevated  $\text{TiO}_2$  with respect to the MPIS data, but lower concentrations than those of the northern intrusives. The samples from the Churchill (1994) study generally plot amongst the MPIS data with the exception of volcanic sample RC-92-04, which also has increased  $\text{TiO}_2$  contents. It should also be noted that the Clutha gabbro does not seem to contain such elevated contents, as it once again plots among the MPIS mafics.

One could attribute the increased  $\text{TiO}_2$  content of the northern linear gabbro samples to fractionation of the MPIS magma source. However, the samples do not have



increased  $\text{SiO}_2$ , which would be expected if the magma were more evolved. Thus, the linear gabbros probably are not genetically related to the MPIS through fractionation but could possibly be fractionated equivalents of a similar magma source. The Duder Lake gabbros have higher Fe and Ti contents than the MPIS dataset, but the very low  $\text{SiO}_2$  contents distinguish these gabbros from all of the other samples. Petrographical observations also show differences between the Duder Lake gabbro and the intrusives south of it.

Thus, Harker bivariate diagrams are useful in defining a fractionation trend for the MPIS dataset for a direct comparison against Churchill's (1994) Duder Lake dataset and the current study dataset. The plots show that the intermediate to felsic samples collected from the MPIS during the current study agrees with the previously compiled data from Dickson (1996). Although the Evans *et al.* (1992) gabbros generally fit the trends defined by the MPIS dataset they are more likely evolved from a fractionated equivalent rather than the MPIS magma source itself. The Duder Lake samples are distinct from the entire dataset.

#### *5.2.4 Bivariate trace element diagrams for magmatic affinity*

##### *5.2.4.1 Introduction*

Trace element data from the current study were combined with datasets from previous studies (Dickson, 1996; Churchill, 1994) and their magmatic affinity assessed on bivariate trace element diagrams (*i.e.*, Barrett and MacLean, 1994, 1999; MacLean and Barrett, 1993). These data are used to compare different rock suites, to arrange them

into tholeiitic, calc alkaline and transitional groups, and also to identify if any genetic relationships exist between intrusive lithologies throughout the region.

#### *5.2.4.2 Results*

The plot of Zr vs.  $\text{Al}_2\text{O}_3$  (Figure 5.10, p. 204) illustrates that the rocks in this study range from basalt to andesite in composition just as defined by the Winchester and Floyd (1977) diagram. This plot is interesting in that it seems to define two distinct fractionation trends with the MPIS dataset. If the pluton evolved successively, one would expect to see a straight linear fractionation trend, however, the felsic rocks seem to form a separate horizontal trend that may suggest that there was significant lag time between the evolution of the mafic and felsic phases respectively. This observation supports the conclusions of Strong (1979) and Strong and Dupuy (1982) that both phases of the MPIS evolved from separate sources in that the mafic rocks formed from mantle melts and the felsic rocks formed from crustal melts. The minor intermediate phase was postulated to form as a result of magma mixing or contamination. This plot indicates that the MPIS mafic dataset of Dickson (1996) may actually include a number of intermediate samples. Further evidence against coincident formation is presented in the geochronological results presented in chapter 8. This diagram does not indicate a significant mass gain/ loss in the samples from this study with the exception of JOD22 and JOD45B, which have experienced mass loss.

The plot of Zr vs.  $\text{TiO}_2$  illustrates a fractionation trend that has been defined by the MPIS dataset (Figure 5.11, p. 205). The MPIS granite samples from this study plot



among the Dickson's (1996) MPIS granite and the samples seem to define a linear alteration line. The intermediate samples from the current study also plot between the main mass of mafic MPIS and the felsic MPIS. However, the mafic samples from both the northern (JOD97B, JOD98, JOD98A, JOD100, JO101, JOD102, JOD04-09) and southern (JOD46B and JOD81A) Botwood Basin all have greater  $\text{TiO}_2$  than the MPIS region. The high  $\text{TiO}_2$  suggests that either the rocks are unrelated and formed from a different magmatic suite or that the rocks are related and the magma differentiated away from the main pluton. This graph again indicates that the MPIS mafic dataset of Dickson (1996) must be inclusive of a significant intermediate phase.

The plot of Zr vs. Y is very useful in determining the magmatic affinity of the igneous rocks, both in the current and previous studies. As earlier mentioned, the AFM diagram presented a complexity in that the mafic samples from this study seemed to be tholeiitic whereas the MPIS dataset of Dickson (1996) plotted on the boundary between calc alkaline and tholeiitic and the samples from Churchill (1994) plotted as calc alkaline. The bivariate graph of MacLean and Barrett (1993) is considered more reliable than the AFM plot because it is based on immobile elements. The graph illustrates that the samples from the current study are in fact transitional in nature and that the entire dataset inclusive of all three studies range from transitional to tholeiitic in nature (Figure 5.12, p. 206). This lends credence to the suggestion that the samples from the current study have increased Fe content due to sulphide mineralization, which caused them to plot as tholeiitic on the AFM diagram. The samples from Dickson's (1996) MPIS study are transitional to tholeiitic with some scatter into the calc alkaline field. The majority of the MPIS felsic samples plot in the transitional field whereas the mafic samples plot about



50:50 in the tholeiitic and transitional fields. The split in mafic rocks may reflect the presence of a significant intermediate phase in the MPIS that has been grouped with the mafic dataset. Although the mafic rocks from Churchill (1994) also plot as tholeiitic to transitional, the Duder Lake samples from the current study appear different from the MPIS because they plot between the transitional and calc alkaline fields. The Huxter Lane sample is also distinct as it plots away from the other datasets, down in the calc alkaline field.

### **5.3 Sedimentary Rocks**

#### *5.3.1 Sample Overview*

The sedimentary samples analyzed in this study include JOD15, JOD20, JOD39, JOD44A, JOD46A, JOD57B, JOD80A, JOD82A, JOD83A, JOD86B, JOD96G, JOD96J, JOD120A and JOD120B.

Samples JOD15 and JOD20 are from the Knob Hill and Third Pond Prospects, respectively, to the north of Glenwood. Both samples comprise least altered and unmineralized Davidsville Group greywacke. Sample JOD39 was collected from a contact between the Indian Islands Group and Caradocian shale along Careless Brook (see Chapter 4). The sample is dark grey, fine-grained, and dense, with little alteration. Sample JOD44A is of a sedimentary country rock to the LBNL prospect in the Paul's Pond region and is presumably from the Davidsville Group. Sample JOD80A was collected from the host rock to the Hornet Prospect in the Paul's Pond area. The host has previously been identified as a felsite (Evans, 1996) in Davidsville Group sedimentary

rocks. Samples JOD82A and JOD83A are Davidsville Group greywacke host rocks to the A-Zone Extension Prospect and the Knob Prospects, respectively. Both samples are mineralized and slightly altered by hydrothermal fluids. Sample JOD86B is Davidsville Group greywacke host rock collected from the vicinity of the Bowater Prospect.

Sample JOD57B is green siltstone from the Ten Mile Lake Formation (Currie, 1995) and was collected from where a gabbroic body as mapped by Evans *et al.* (1992) intrudes it.

Samples JOD96G and JOD96J are metasedimentary samples collected immediately south of the Duder Lake Prospects. The samples are slightly deformed due to their proximity to a shear zone that runs NE through the area. The sedimentary rocks to the west of this zone had previously been mapped as Botwood Group (Churchill, 1994), but have been reassigned to the Duder Complex by Currie (1995b) (see Chapter 2 and 4).

Samples JOD120A and JOD120B are shales collected from the Appleton gravel pit, due west of the Bowater prospect. Gerry Squires (pers. comm., 2003) had suggested that this was a possible intrusion into the Davidsville Group shale; however, geochemical and petrographic data (see chapter 4) suggest that these samples are actually sedimentary in nature. The samples are dark grey, fine-grained, very dense and exhibit disseminated sulphide. Both samples are from the same location.

O'Reilly (2005) collected samples ~40 km southwest of Glenwood and ~5 km northeast of the Beaver Brook Mine at the O'Reilly auriferous prospect. Altius Resources Inc. discovered this prospect in late 2002 along the Mustang Trend. The prospect is located within Indian Islands Group rocks in a northeast to southwest trending

dextral shear zone (O'Reilly, 2005). O'Reilly analyzed the sediment geochemistry of the various lithologies at the prospect. The main units present were fine-grained, tan to grey siltstone that had undergone intense silica alteration and minor hematite alteration and medium-grained interbedded siltstone/ sandstone. Data for both of these units are incorporated into the current study as representatives of the Indian Islands Group sedimentary rocks. One purpose of O'Reilly's study was to determine the tectonic setting of deposition for the host lithologies. He classified the host rocks as siliciclastic, calc-alkaline affinitive, sedimentary rocks of the Indian Islands Group. He also found them to have a continental margin provenance.

Churchill (1994) analyzed 12 sedimentary samples of what he presumed to be Davidsville Group sedimentary rocks from drill core at Duder Lake. His primary purpose was to evaluate the extent of sulphide present in the sedimentary rocks at Duder Lake. The rocks initially mapped as Davidsville group (*i.e.*, Evans *et al.*, 1992) have been reassigned to the Duder Complex by Currie (1995b). The samples include fine-grained argillaceous siltstones to coarser grained rocks such as sandstones and greywacke.

### *5.3.2 Trace element and petrographic discrimination diagrams*

All samples from the current study, with the exception of JOD57B (mapped as Ten Mile Lake Formation by Currie (1995)) and JOD96G and JOD96K (mapped as Botwood Group by Churchill (1994) but remapped as Duder Complex by Currie (1995b)) have been assigned to the Davidsville Group. Sample JOD39 is from Caradocian Shale, but this unit has been included as an upper unit of the Davidsville Group (*i.e.*, Williams,



1993). The petrography of samples JOD15, JOD20, JOD44A, JOD80A and JOD120 are discussed in chapter 3 and the petrography of sample JOD39 is presented in chapter 4. Geochemical data from the Duder Complex (Churchill, 1994) and Indian Islands Group sediments (O'Reilly, 2005) are also utilized to provide a larger dataset. These sedimentary samples are analyzed to determine: 1) what, if any, differences or similarities can be established between Davidsville and Indian Islands Group sedimentary host rocks throughout the Botwood Basin and 2) if tectonic environment and source rock environments can be established for the different groups. Several tectonic discrimination diagrams based on either element geochemistry or petrographical analysis were utilized during this study to aid in classifying the sedimentary rocks.

First, the elemental abundances of each sedimentary rock from this study were assessed. Most of the samples are enriched in Ba with values ranging from 92 to 1923 ppm. The normal range for Ba in siltstone is between 10 and 99 ppm and in sandstone, 580 ppm (Hsu *et al.*, 1995). Many of the samples are also enriched in As with values ranging from 18 to 9807 ppm. The exceptions are samples JOD39, JOD44A, JOD46A and JOD57A as As contents in these samples are below detection limits. Normal ranges for As in shale and sandstone are 10 ppm and 8 ppm respectively (Hsu *et al.*, 1995). Samples 120A and JOD120B are much more enriched in MnO than they other samples (generally < 1.0 wt. %) with values of 12.03 and 9.74 wt. % respectively.

Roser and Korsch (1986) and Hsu *et al.* (1995) have demonstrated that tectonic environments can be established for different sandstones, mudstones and sandstone-mudstone pairs based on SiO<sub>2</sub> contents and K<sub>2</sub>O/Na<sub>2</sub>O ratios. The authors have established three first-order tectonic categories for depositional settings. These

environments are Passive Continental Margin (PM), Active Continental Margin (ACM) and Oceanic Island Arc (ARC) (Figure 5.13, p. 207). It is important to note that when assessing the tectonic setting of sediments deposited in basins related to active plate boundaries, that they may be either related to either a continental magmatic arc (ACM) or an island arc (ARC).

The ARC field consists of low  $K_2O/Na_2O$  and  $SiO_2$  sedimentary rocks that are derived from volcanogenic sources in subduction related basins. Sediment sources from this category are derived from an island arc source and the rocks were subsequently deposited in a variety of settings including fore-arc, intra-arc, back-arc basins and trenches. The ACM field consists of mid  $K_2O/Na_2O$  and  $SiO_2$  sedimentary rocks that are derived from volcanogenic sources in subduction related basins, continental collision basins and pull apart basins. The PM field consists of quartz-rich sedimentary rocks deposited at stable continental margins or intracratonic basins. Roser and Korsch (1986) have suggested that the presence of silica cement and/ or a later episode in which silica rich fluids affected the rocks will cause the sediments to plot in the PM field.

The sedimentary rocks analyzed for this study plot within all three fields (Figure 5.13). The samples that plot within the ARC field are JOD20, JOD46A, JOD83A, JOD120A, JOD120B, JOD96G and JOD96J. Samples JOD20, JOD83A, JOD120A and JOD120B were all collected from the Davidsville Group near Glenwood in the central Botwood Basin region suggesting island arc sources for these sedimentary rocks. Samples JOD96J and JOD96G were collected from the Duder Complex and plot in the ARC field but it must be considered that these samples were collected adjacent to a shear



zone and therefore the elements on which this diagram has been constructed may have been mobilized.

The samples that plot within the ACM field include JOD57B, JOD80A, JOD82A, and JOD39. Samples JOD80A and JOD82A were both collected from Davidsville Group greywacke at auriferous occurrences in the Paul's Pond region, northern Botwood Basin. Sample JOD39 from the Caradocian shale and sample JOD57B from the Ten Mile Lake Formation, also plot within this field. The samples from the Duder Complex collected east of Duder Lake (Churchill, 1994) plot within the ACM and PM field.

Samples JOD15, JOD44A and JOD86B plot in the PM field. All three of these samples were collected from Davidsville Group fine-grained sandstone at auriferous occurrences that have undergone silicification. It is assumed that these samples were enriched in  $\text{SiO}_2$  due to variable amounts of silicification observed in hand sample.

The Indian Island Group samples from O' Reilly (2005) all plot within the PM field. Only two of the samples consist of altered siltstone so the plot is considered reliable. The Duder Complex samples plot in both the PM and ACM fields. The results of this graph are considered reliable because the rocks were not reported to be altered. The samples were, however, obtained from drill core at Duder Lake and it may be possible that the drill core actually contained Indian Islands Group rocks along with Duder Group rocks. Either the reports by Currie (1995b) that Indian Islands Group tectonic blocks are present in the complex or the suggestion of Dickson (2005) to extend the Indian Islands Group further west would support this.

Tectonic environments for different sedimentary rocks can also be determined from petrographic descriptions based on the work of Dickinson and Suczek (1979). Their



tertiary diagram uses modal abundances of quartz, feldspar and lithic fragments to define different tectonic environments. The diagram defines Continental Block Provenances, Recycled Orogen Provenances and Magmatic Arc Provenance, each of which are further subdivided into smaller divisions to further classify the tectonic processes that define each category. Only the 'least altered' samples from this study could be plotted on this tertiary diagram and include JOD15, JOD20, JOD39 and JOD044A (Figure 5.14, p. 209). Samples JOD15, JOD20 and JOD44A were variably silicified and may plot higher on the diagram than an unaltered equivalent. The rocks from the Davidsville Group and the sample from the Caradocian shale plot just below the Recycled Orogen Provenances field and have a high ratio of oceanic to continental components. The recycled orogen provenances represent zones of plate convergence. The samples that plot within this field can be related to subduction complexes, collisional orogens and foreland uplift. The source rocks are generally characteristic of uplifted suture zones and consist of sedimentary and metamorphosed sedimentary and igneous rocks. Generally, the sediments that are related to subduction will plot near the bottom of the field, whilst collision and uplift derived sediments will plot throughout (Boggs, 2001). The samples from this study show a high oceanic component.

Several of the Indian Islands Group samples from O' Reilly (2005) plot within the craton interior subdivision of the continental block provenance field. Interior craton sediments are considered to be quartz rich and contain very little feldspar (<10%) and plot near the quartz apex. Several other samples plot outside of the magmatic arc provenance field and O'Reilly (2005) attributed this to be a result of numerous obscure

clasts and the presence of unidentifiable altered fragments, which caused a shift to the lithic fragment corner.

Due to the observed alteration, both in hand sample and thin section, for the majority of the sedimentary samples from the current study, it is best to rely on elements with known low chemical mobility. The trace elements such as La, Ce, Nd, Y, Th, Zr, Hf, Nb, Ti and Sc are best used for provenance and tectonic studies because they have low chemical mobility during chemical processes and have a short residence time in seawater (Holland, 1978). These elements undergo very little chemical dissolution as they are transported into clastic sedimentary rocks and thus provide a representative example of parent material (Hsu *et al.*, 1995). The samples from the current study were plotted against the samples from the Indian Islands Group of O'Reilly (2005) and the Duder Complex of Churchill (1994).

On a Zr vs. Nb diagram, the samples show some variation that appears to be related to their respective locations in the Botwood Basin (Figure 5.15a, p. 209). For example, the Davidsville Group rocks from the southern and central region plot in separate groups. The Davidsville Group sediments collected from the southern Botwood Basin as part of the current study plot with the highest Zr and Nb contents, whereas the samples collected from the central region for the current study plot with the lowest contents of these elements. The Duder Complex samples are also elevated in Nb with respect to the samples aside from the southern Davidsville Group. The samples from the Ten Mile Lake Formation plot among O'Reilly's (2004) Indian Islands Group samples with intermittent values to the remaining dataset.

On a Zr vs. Y diagram the same trends as observed in the last diagram are noted (Figure 5.15b, p. 209). The southern Davidsville Group samples contain the highest Y contents. Two of the Indian Islands Group samples have high Y values but in general the samples plot together at median values. Once again the sample from the Ten Mile Lake formation plots with O' Reilly's (2004) Indian Islands Group samples. The central Botwood Basin Davidsville Group samples plot with lower values than the combined dataset and the northern Duder Complex samples plot with higher values than all samples with the exception of the southern Davidsville Group.

There was not any significant variation in  $\text{Al}_2\text{O}_3$  values on a plot of Zr vs.  $\text{Al}_2\text{O}_3$  (Figure 5.15c, p. 210). On a diagram of  $\text{TiO}_2$  vs. Zr, the Duder Complex samples, both from Churchill (1994) and the current study, display the highest  $\text{TiO}_2$  contents with variations in Zr values. The samples from the central Davidsville Group have the lowest  $\text{TiO}_2$  values whereas, the Davidsville Group samples from the southern region plot with values similar to the Duder Complex. The Indian Islands Group generally plots with median values and the Ten Mile Lake Formation sample has similar  $\text{TiO}_2$  contents to the Indian Islands group sediments from O' Reilly (2004).

These diagrams illustrate that there is a definable distinction between Davidsville Group sediments in the central and southern regions. The sediments from the south are generally more enriched in trace elements (Zr, Nb and Y) than those from the north and central regions respectively. The samples from the Duder Complex are the most enriched in Ti and the remaining samples and those from the southern region were more enriched in Ti than the sediments from the central region (Figure 5.15d, p. 210). The Indian Islands Group sediments exhibit values that are typically intermediate to those from the



Duder Complex and the central Davidsville Group and the Ten Mile Lake Formation consistently plots with that group. It is interesting to note that the intrusive lithologies from the northern and southern region also exhibited elevated Ti and Zr respectively. Since the southern Davidsville Group sediments also contained elevated Ti contents, it is valid to assume that the sediments are more enriched in Ti away from the central region.

Once the tectonic environment or potential origin or source rock has been determined, immobile elements can be used to determine the composition of source rocks. Potential source areas can be identified for sedimentary and metasedimentary rocks based on a ratio plot of  $\text{Al}_2\text{O}_3$ - $\text{TiO}_2$ -Zr as proposed by Fralick and Kronberg (1997) and Fralick (2003). The diagram is based on immobile elements and therefore the elemental ratios from the sedimentary rocks should reflect that of the source rocks. The diagram shows that the source rocks for the sedimentary samples from the Botwood Basin primarily have calc-alkaline volcanic to intrusive compositions (Figure 5.16, p. 211). Samples JOD15, JOD20, JOD39, JOD80A, JOD83A, JOD86B, JOD120A, JOD120B all plot within or immediately adjacent to the calc alkalic field. This field has been further subdivided into felsic and intermediate subfields and samples JOD20, JOD39 and JOD86B plot within the intermediate sub-field. All other samples plotted outside of both the calc alkaline and tholeiitic volcanic fields; however, due to their ratios it is presumed that the composition of the source rocks for these samples would more likely be calc-alkaline than tholeiitic. None of the samples from the study plotted within the tholeiitic field indicating that tholeiitic volcanic rocks were unlikely to have been source rocks for the sedimentary rocks.

A triangular quartz feldspar lithic fragment diagram of McBride (1986) was utilized in an attempt to classify the samples to identify the host rock (Figure 5.17, p. 212). This diagram is also based upon petrographic observations and plot in the same area as on figure 5.14. The diagram is divided into eight fields based upon modal abundance of quartz feldspar and lithic fragments. The samples from this study are dominantly feldspathic litharenite.

## **5.4 Discussion**

Most of the igneous and sedimentary rocks selected for geochemical study are variably affected by alteration associated with hydrothermal processes and low-grade metamorphism. However, several observations can be made based upon immobile elements that were not overly affected by these processes.

### *5.4.1 Igneous Rocks*

The igneous rocks assessed for this study range from mafic to intermediate to felsic in composition. The mafic rocks were collected from throughout the Botwood Basin including gabbroic dykes to the north, previously mapped by Evans *et al.* (1992), gabbroic bodies near Duder Lake in the north that host auriferous mineralization, and the hosts to the Greenwood Pond #2 and Paul's Pond prospects in the south.

Intermediate rocks include those from a diorite phase of the MPIS that hosts the Hurricane and Corsair auriferous prospects near Glenwood, a previously mapped dioritic

dyke near Glenwood (Dickson, 1996), an unknown volcanic unit at Duder Lake, subcrop from the Road Gabbro Prospect and the host to the Huxter Lane Prospect.

The felsic samples were collected from a volcanic unit as mapped by Evans (1992) south of Duder Lake, the granitic host to the LBNL Prospect near Paul's Pond and the felsic host to the Huxter Lane Prospect, which intrudes the Coy Pond Complex.

A direct comparison of the chemical affinities of the current geochemical data with previous datasets could not be achieved using an AFM plot because of the elevated levels of  $\text{Fe}_2\text{O}_3$  in the current samples. Alkali abundances were assumed to represent the original chemistry based upon an intergroup element abundance comparison but the elevated Fe contents, due to the presence of pyrite, caused those samples to plot higher on the tertiary plot. Although the samples from the current study plotted in the tholeiitic field on the AFM diagram, the samples from the MPIS dataset of Dickson (1996) appeared to border the boundary between, and also plot within, both the tholeiitic and calc alkaline fields. The samples from this study as well as from previous datasets are subalkaline in nature. A bivariate plot using the immobile elements Zr and Y (MacLean and Barrett, 1993) was considered more reliable for the determination of magmatic affinity because these elements are considered unaffected by alteration processes. This plot illustrated that the mafic samples from the current study are generally transitional in nature, which verifies the assumption that the AFM plot was influenced by elevated Fe contents. The samples from previous datasets plot as transitional to tholeiitic in nature. Interestingly, the mafic samples from Dickson's (1996) study plot 50: 50 in the tholeiitic and transitional fields whereas the majority of the MPIS felsic samples plot within the transitional field. This either illustrates the evolution of the magma from more primitive



to a more fractionated state or indicates the presence of an intermediate phase inclusive to the mafic dataset. The samples collected from the current study plot among the MPIS data suggesting a possible common magmatic affinity or an equivalent. The exception is the samples from Duder Lake, which plot along the boundary of the transitional to calc alkaline fields suggesting that these gabbros are more evolved and thus distinct from the MPIS mafics and the gabbroic samples mapped by Evans *et al.* (1992). Churchill (1994) also concluded that the Duder Lake gabbros are calc alkaline, further demonstrating that they are unrelated to the intrusives to the south.

On immobile element tectonic discrimination diagrams, the mafic samples from this study have within plate alkaline affinities and plot within the same fields as the Duder Lake and MPIS datasets. This suggests that there may be some geochemical relation between the MPIS and select intrusive lithologies throughout the Botwood Basin in that the tectonic environment of formation is similar. Although the samples plot suggest that been formed in similar tectonic environments, subtle differences were noted. For example, on the Pearce and Cann (1973) diagram the samples generally plotted as calc-alkalic and within plate magmas with minor overlap in the ocean floor field. The samples from the northern Botwood Basin, however, contain slightly elevated Ti with respect to the intrusives from the central and northern region. Thus, the northern samples plotted as within plate magmas whereas the central and southern samples plotted as calc-alkalic magmas. Other diagrams (Pearce and Norry (1979) and Meschedes (1986)) plot all samples as within plate magmas. A Shervais (1982) diagram suggests that the intrusives may have formed in the same tectonic environment, but that some intrusives are more fractionated than others. The samples from the northern Botwood Basin, and to

a lesser extent the southern Botwood Basin, contain more elevated V and Ti than the MPIS samples indicating either increased fractionation away from the MPIS or a fractionated magmatic equivalent from a similar magma source. The decreased SiO<sub>2</sub> content of the samples to the north indicates that a fractionated equivalent would be more plausible than increased fractionation of the same magma source.

Harker bivariate plots and trace element bivariate plots were utilized in conjunction with all three datasets to further demonstrate any fractionation trends and to evaluate the fit of the intrusive rocks collected away from the MPIS. The trace element plots were also useful in assessing the degree of alteration. These diagrams indicate that the samples collected in the north and to a lesser extent south are more fractionated with respect to the MPIS and that some of these samples have undergone mass loss or mass gain. This suggests that either the Duder Lake intrusives are genetically unrelated to the MPIS gabbro or that significant differentiation occurred as the magma traveled further away from the main chamber. As seen in section 5.3.2, the sediments from the Duder Lake Complex and to a lesser extent the Ten Mile Lake Formation, contain higher Ti levels than the sediments from the Davidsville Group in the central and southern region. This geochemistry might explain the presence of high Ti values in the gabbros from the north as more Ti must be available for sampling in that region.

The high levels of Fe and Ti have previously been recorded in the Duder Lake gabbros by Churchill and Evans (1992) who mapped the Duder Lake gabbros and defined two types: melanocratic and leucocratic. The melanocratic gabbros were more refractory and had an abundance of Fe and Ti rich minerals. Even though both the Duder Lake and gabbros mapped by Evans *et al.* (1992) contained high Ti contents, the intrusives seem

distinct from one another as the linear gabbros contain higher Ti and more SiO<sub>2</sub> than the Duder Lake gabbros and generally the two groups do not plot together.

#### *5.4.2 Sedimentary Rocks*

The sedimentary rocks analyzed for this study consist of black graphitic Caradocian shale, siltstone and sandstone of the Davidsville Group, and siltstone from the Ten Mile Lake Formation. Data for siltstone and sandstone of the Duder Complex and siltstone and metasediment from the Indian Islands Group from other authors was also compiled. Overall, the Davidsville Group samples from this current study are enriched in Ba and As which probably reflects proximity to Au bearing systems.

Petrographical analysis and discrimination plots indicate that the Davidsville Group greywacke may be classified as feldspathic litharenite, derived from volcanogenic sources in subduction related basins. The Davidsville Group and Caradocian shale both have high oceanic components with Recycled Orogen Provenances suggesting that these rocks were deposited at a zone of plate convergence with a relation to subduction, which is consistent with the tectonic history of the region. In fact, Blackwood (1982) and Scheuing and Jacobi (1990) both postulated that the sedimentary rocks of the Davidsville Group might have been derived from the island arc systems of the Notre Dame Bay subzone. The findings in the current study support these ideas.

The comparison of the different groups of sedimentary rocks illustrates that bivariate immobile plots can be utilized to differentiate between them. Although the differences are subtle, the groups did plot together and variations in trace element content



were related to the location from which the samples were collected (*i.e.*, higher trace element values such as V, Nb, Y and Zr in the south and higher TiO<sub>2</sub> in the north). Interestingly, some of these variations are also reflected in the igneous rocks. Major disparities between the Davidsville and Indian Islands groups and Caradocian shale were not strongly evident. However, this small dataset indicates that there may be small geochemical inconsistency between the Davidsville Group rocks in different sections of the Botwood Basin. Further, more detailed study would be required to delineate these differences. Also, a sample collected from the Ten Mile Lake Formation consistently plots with O' Reilly's (2004) Indian Islands Group samples. Based on field observations and the presence of Wenlock fossils, the author has suggested (refer to chapter 4) that the Indian Islands Group may extend westward and such an extension would also account for these samples plotting together.

✕	Duder Lake gabbroic dykes or sills (northern)
✕	Duder Lake pink volcanic (northern)
*	Linear gabbroic dykes or sills (northern)
+	MPIS diorite (central)
+	MPIS granite (central)
■	Paul's Pond mafic intrusions (southern)
□	Paul's Pond felsic intrusions (southern)
△	Huxter Lane felsic intrusion (southern)
* (green)	Churchill (1994) Dan's Pond gabbro (northern)
✕ (green)	Churchill (1994) Clutha Prospect gabbro (northern)
■ (green)	Churchill (1994) Duder Complex volcanics (northern)
■ (blue)	Dickson (1996) MPIS gabbro (central)
■ (red)	Dickson (1996) MPIS granite (central)

**Figure 5.1:** Symbol key for geochemical diagrams for igneous rocks. All samples in black were analyzed as part of the current study and the samples represented by colored symbols were taken from Churchill (1994) and Dickson (1996) as indicated.

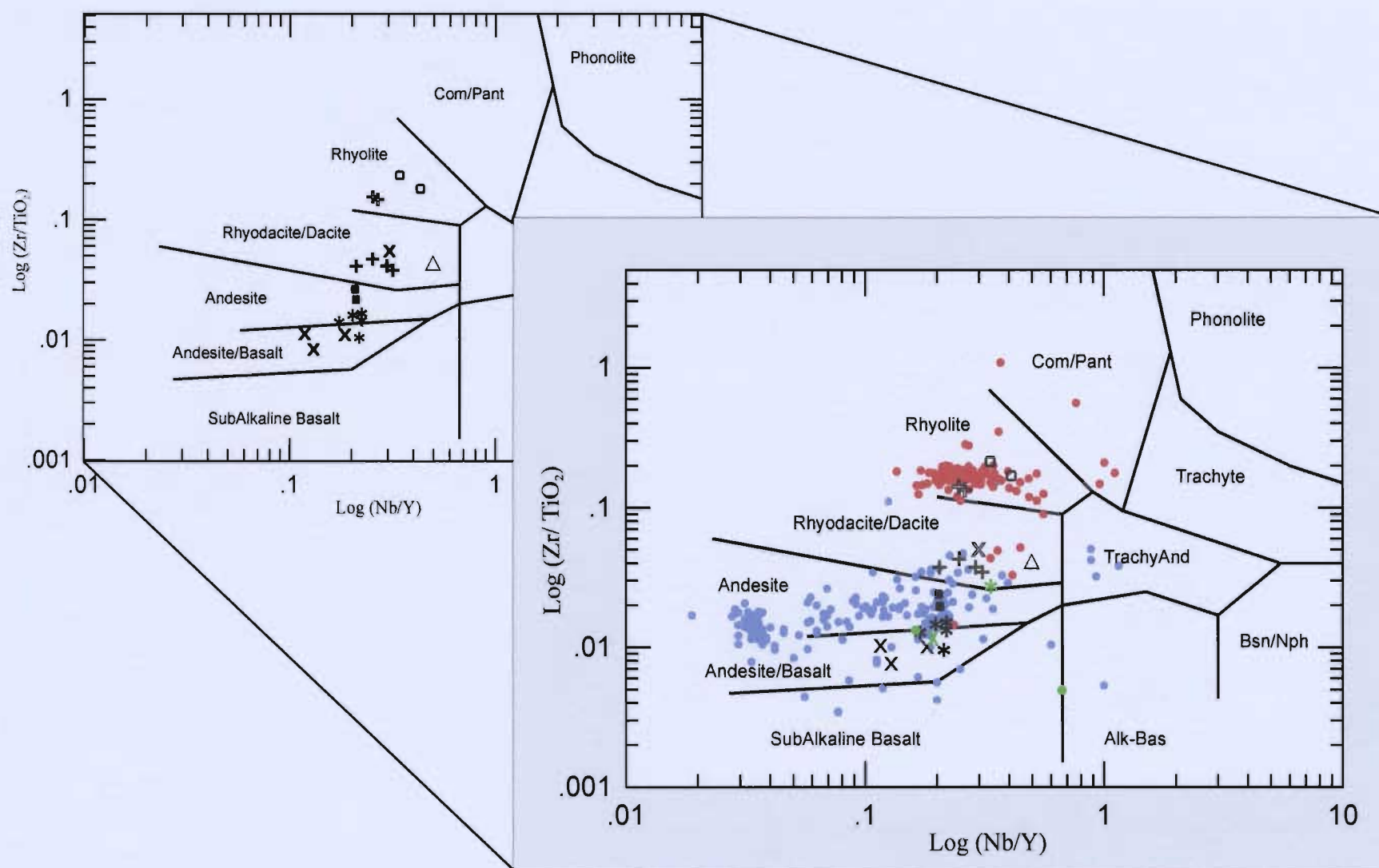


**Figure 5.2:** Nb/Y vs. Zr/TiO<sub>2</sub> discrimination diagram (Winchester and Floyd, 1977) which illustrates the compositions of the igneous rocks from the current study (black) in relation to pre-existing datasets from Duder Lake (Churchill, 1994) [green symbols] and MPIS (Dickson, 1996) [red and blue symbols] (refer to symbol key, figure 5.1).



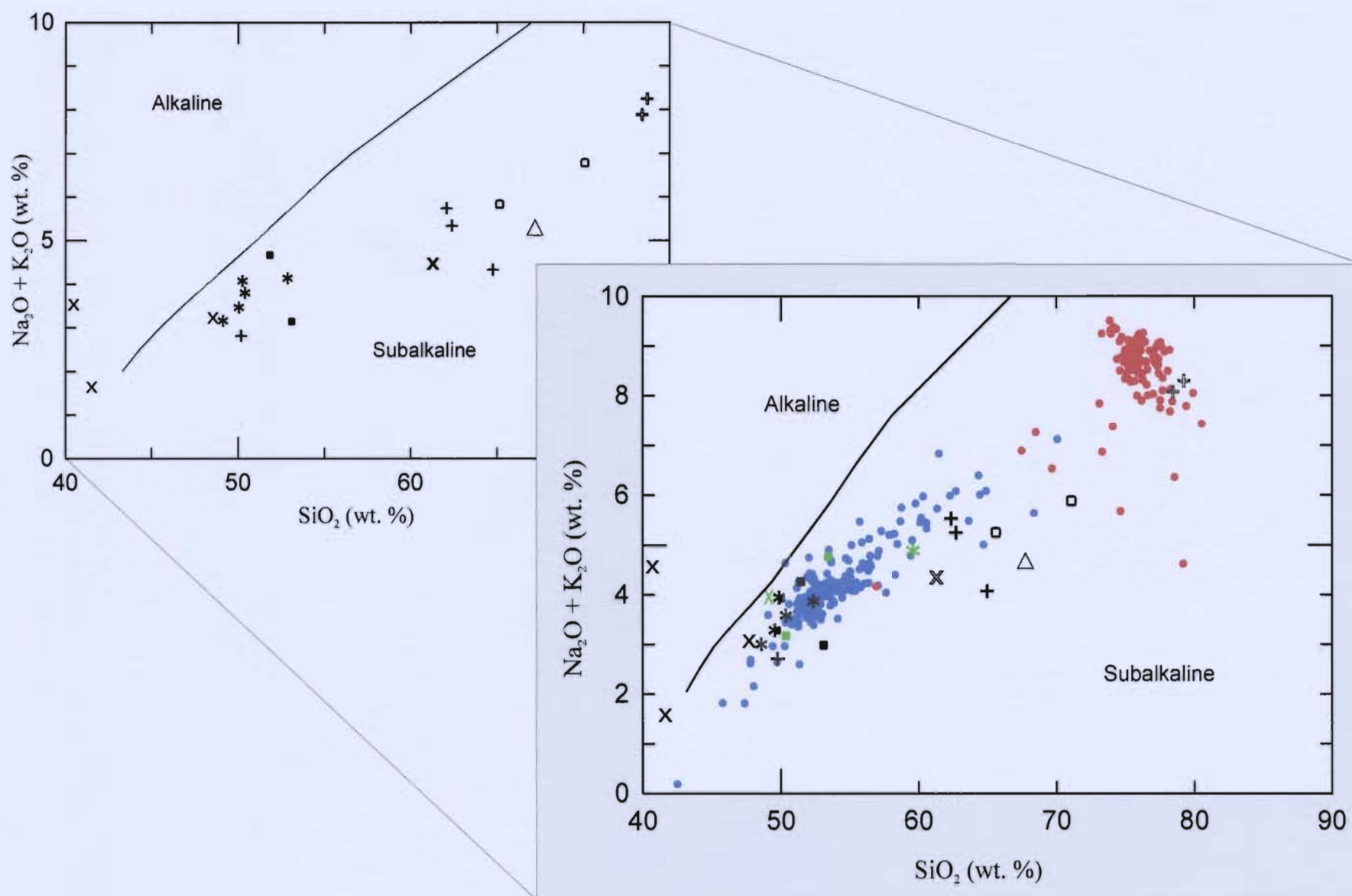


**Figure 5.3:** Irvine and Barager (1971)  $\text{Na}_2\text{O} + \text{K}_2\text{O}$  vs.  $\text{SiO}_2$  plot illustrating the sub-alkaline nature of the current study, Duder Lake (Churchill, 1994) and MPIS (Dickson, 1996) igneous rocks (refer to figure 5.1 for symbol key).

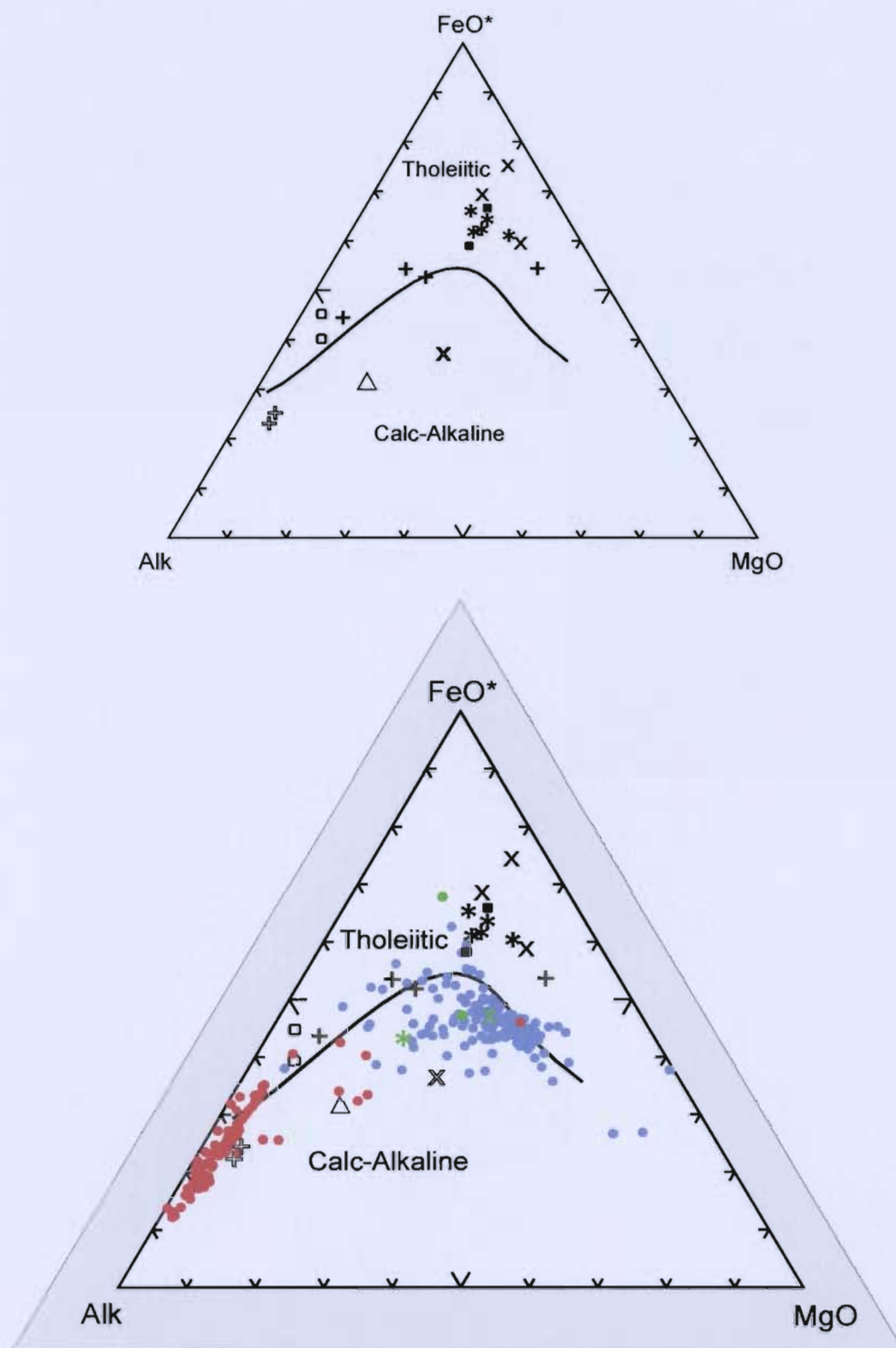


**Figure 5.4:** AFM plot of Irvine and Baragar (1971) indicating the chemical affinity of igneous rocks from the current study [black], Duder Lake (Churchill, 1994) [green], and MPIS (Dickson, 1996) [blue] (refer to figure 5.1 for symbol key).

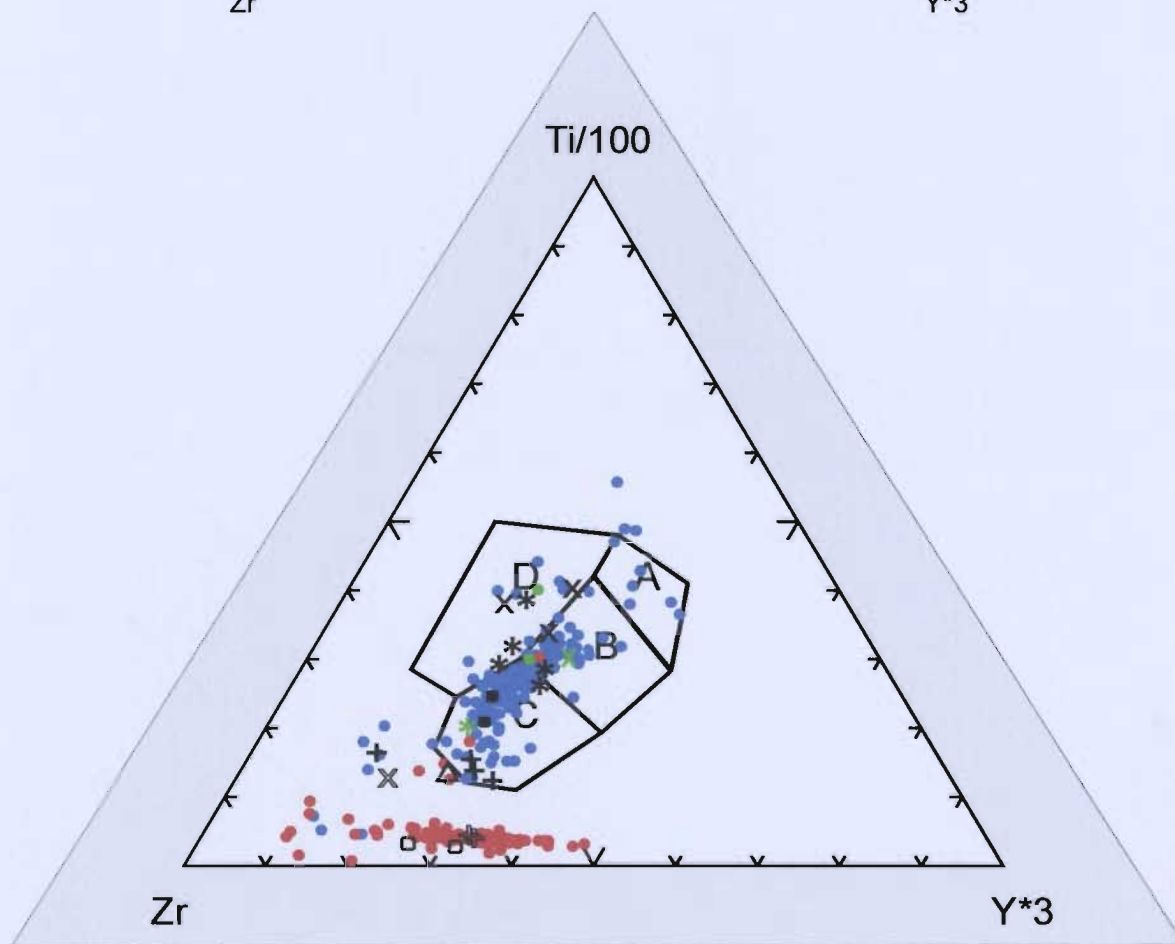
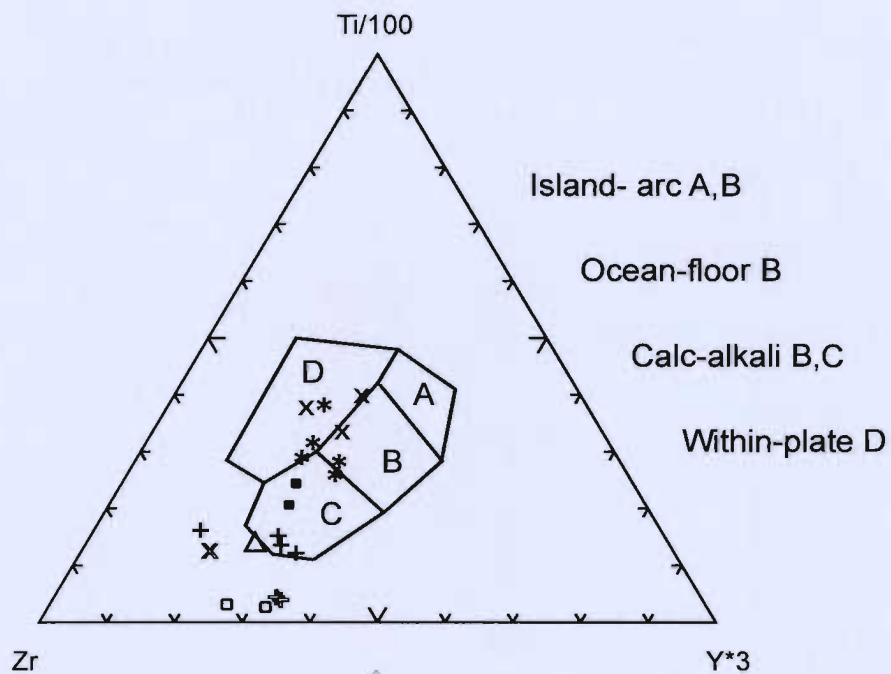


**Figure 5.5:** Ti-Zr-Y diagram (Pearce and Cann, 1973) illustrating the possible paleotectonic environments for the current [black], Churchill (1994) [green] and Dickson (1996) [blue and red] studies igneous rocks (refer to figure 5.1 for symbol key).



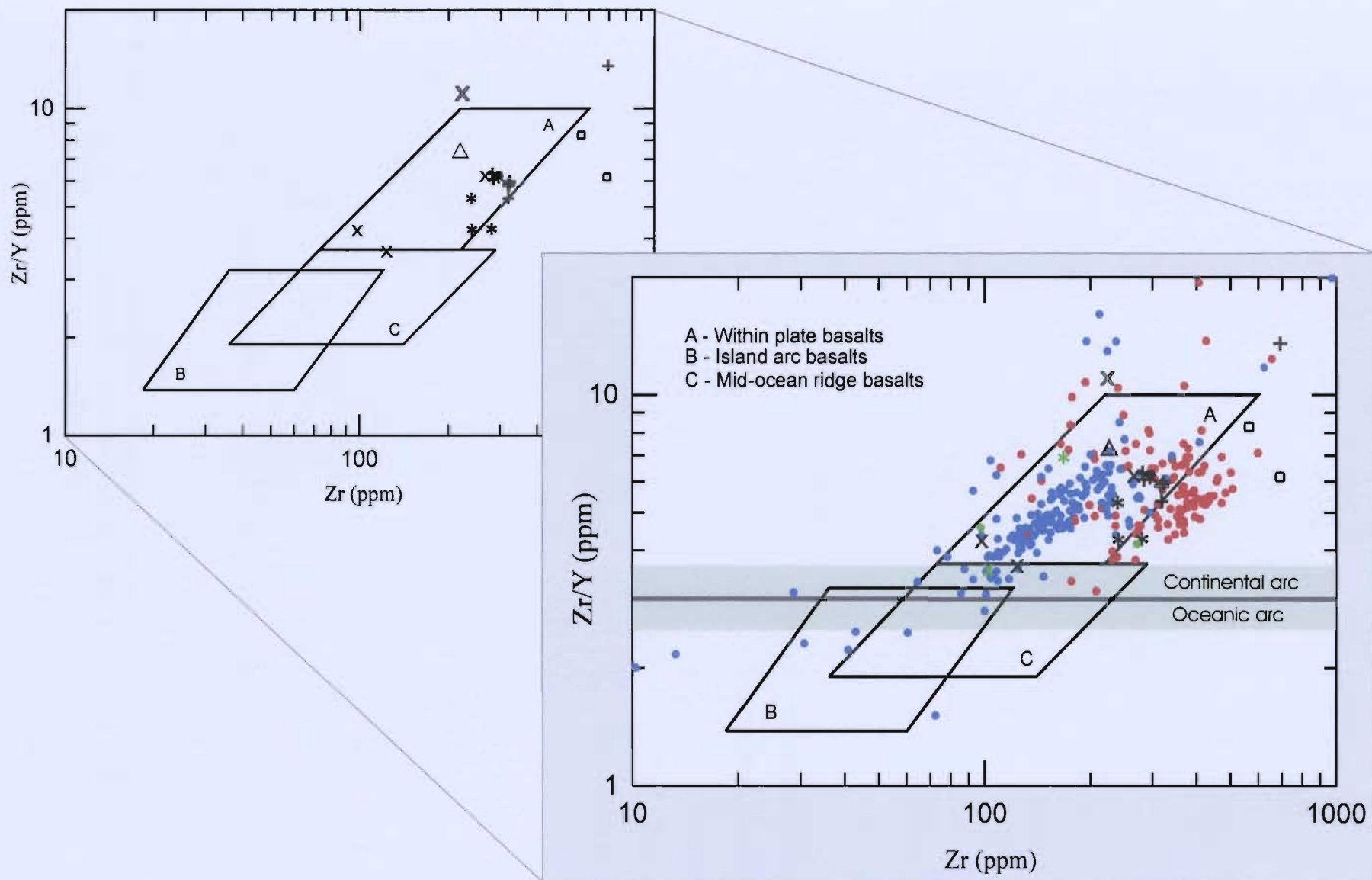


**Figure 5.6:** Zr vs. Zr/Y diagram (Pearce and Norry, 1979; Pearce, 1983) for igneous rocks from the current study, Dickson's (1996) dataset and Churchill's (1994) dataset illustrating a within plate, continental arc signature (refer to figure 5.1 for symbol key).

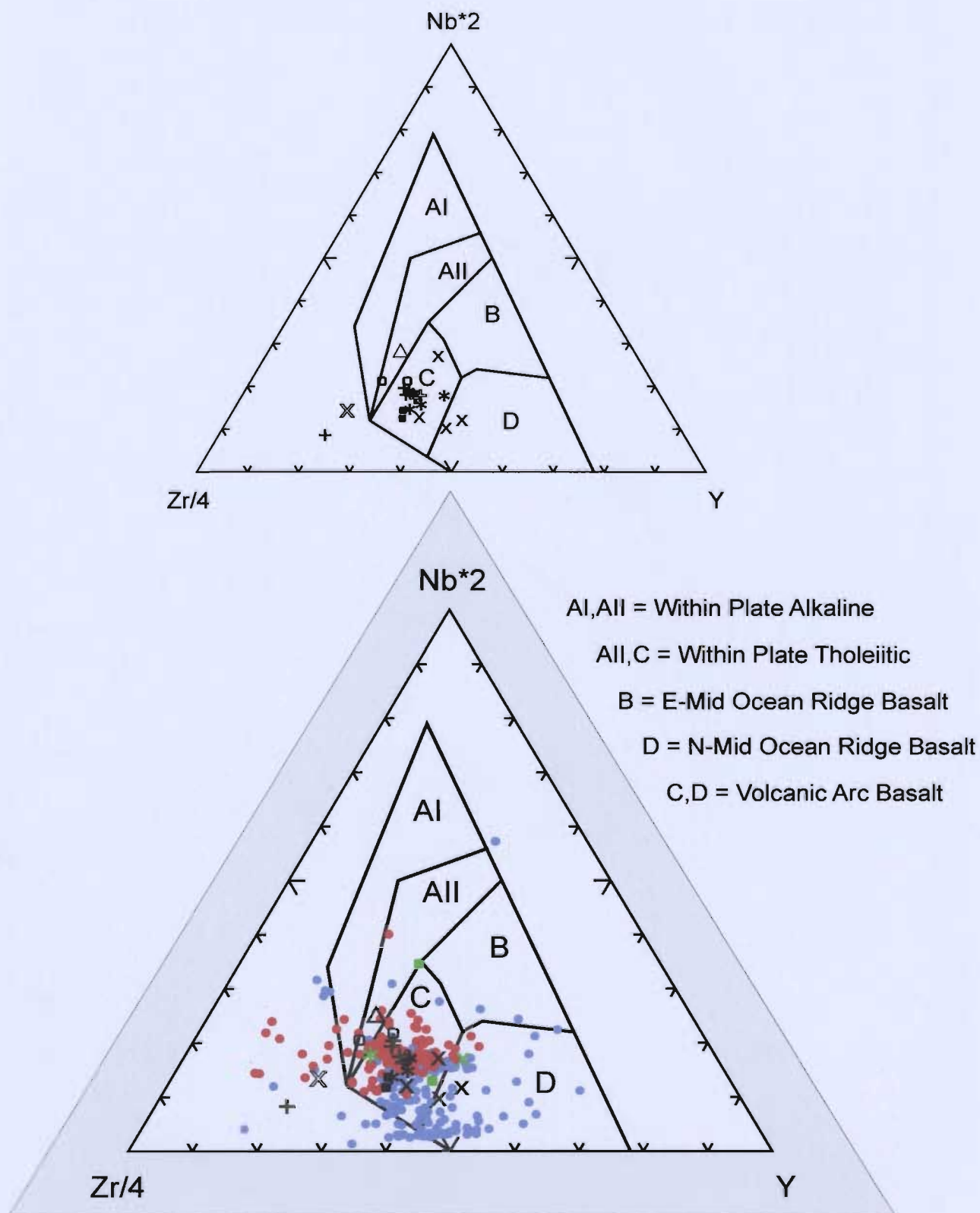


**Figure 5.7:** Tectonic discrimination diagram of Meschede (1986) indicating the tectonic affinity of igneous rocks from the current study [black], Churchill (1994) [green] and Dickson (1996) [red and blue] (refer to figure 5.1 for symbol key).

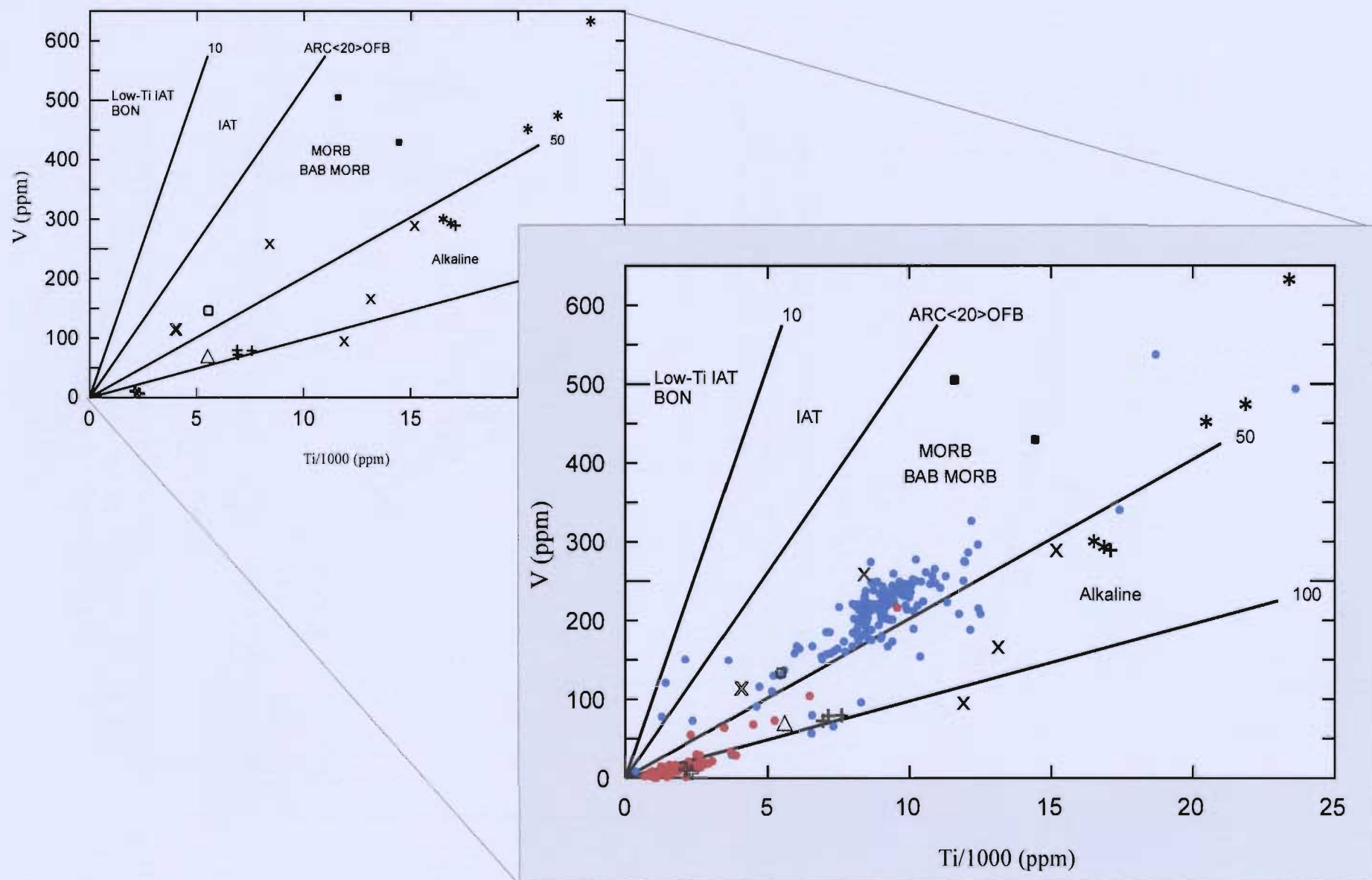


**Figure 5.8:** Ti vs. V diagram (Shervais, 1982) for igneous rocks from the current study [black] and Dickson (1996) [red and blue], illustrating a relative enrichment in Ti in the northern region (refer to figure 5.1 for symbol key).



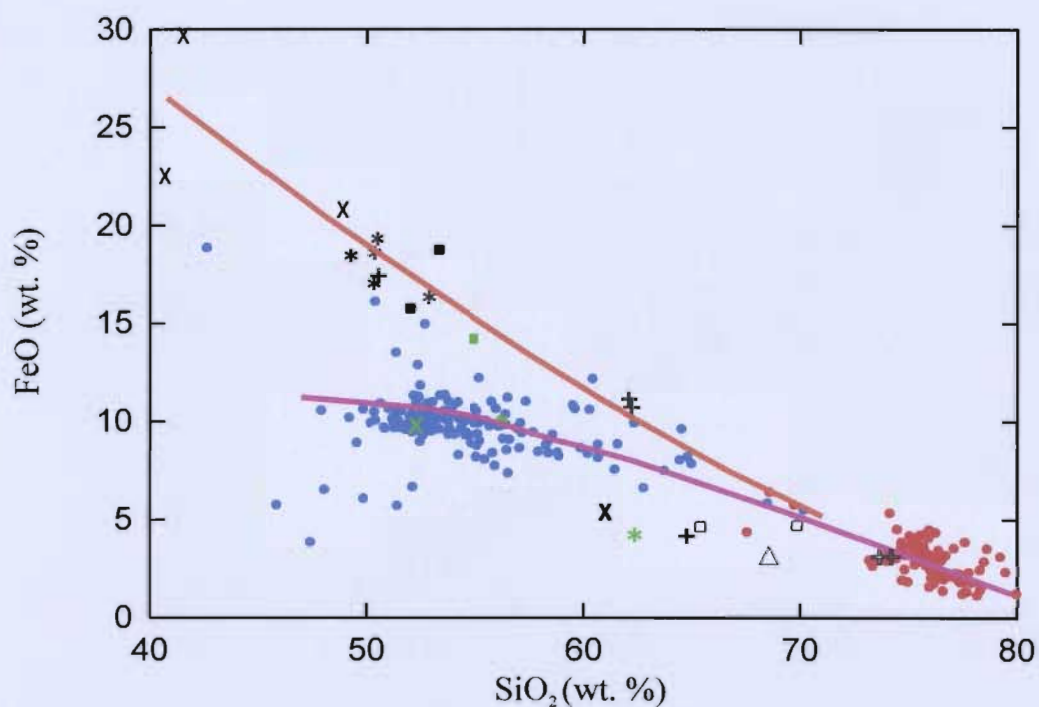


**Figure 5.9a:** Bivariate plot of SiO<sub>2</sub> vs. FeO illustrating a negative linear trend for the igneous rocks from the current study [black], Dickson (1996) and Churchill (1994) (refer to figure 5.1 for symbol key).

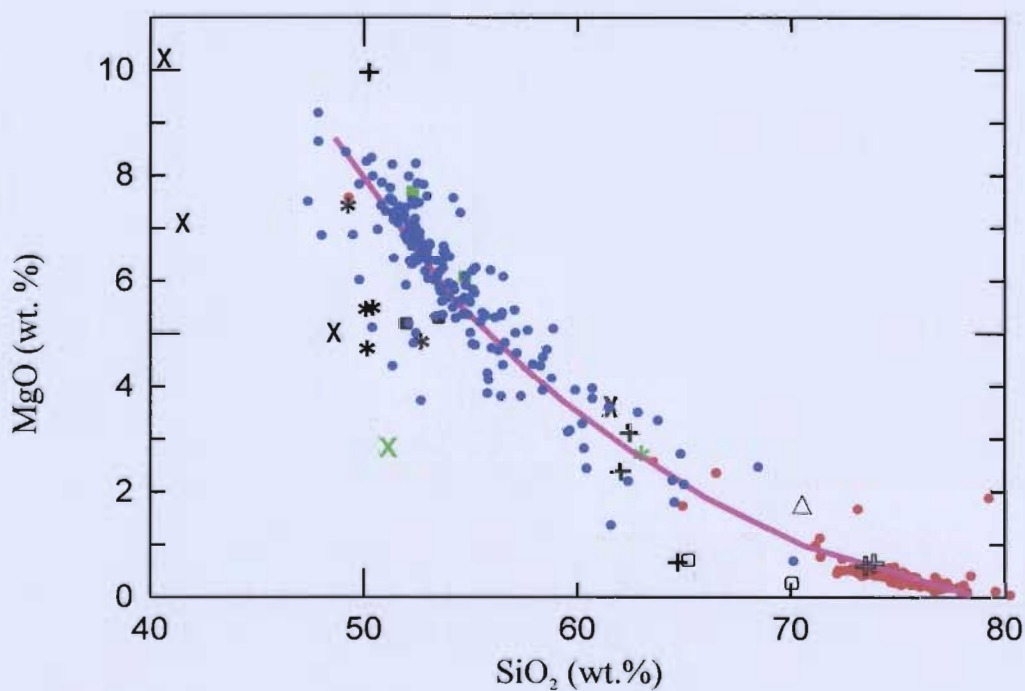


**Figure 5.9b:** Bivariate plot of SiO<sub>2</sub> vs. MgO illustrating a negative curvilinear trend for the igneous rocks from the current study [black], Dickson (1996) and Churchill (1994) (refer to figure 5.1 for symbol key).

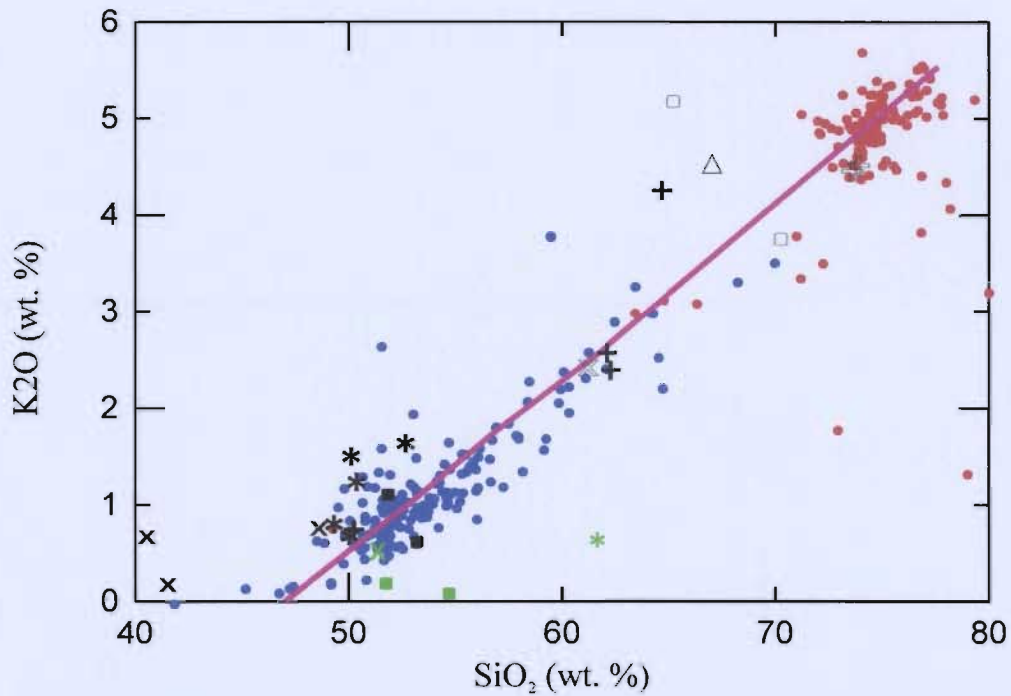


**Figure 5.9c:** Bivariate plot of SiO<sub>2</sub> vs. K<sub>2</sub>O illustrating a positive linear trend for the igneous rocks from the current study [black], Dickson (1996) and Churchill (1994) (refer to figure 5.1 for symbol key).

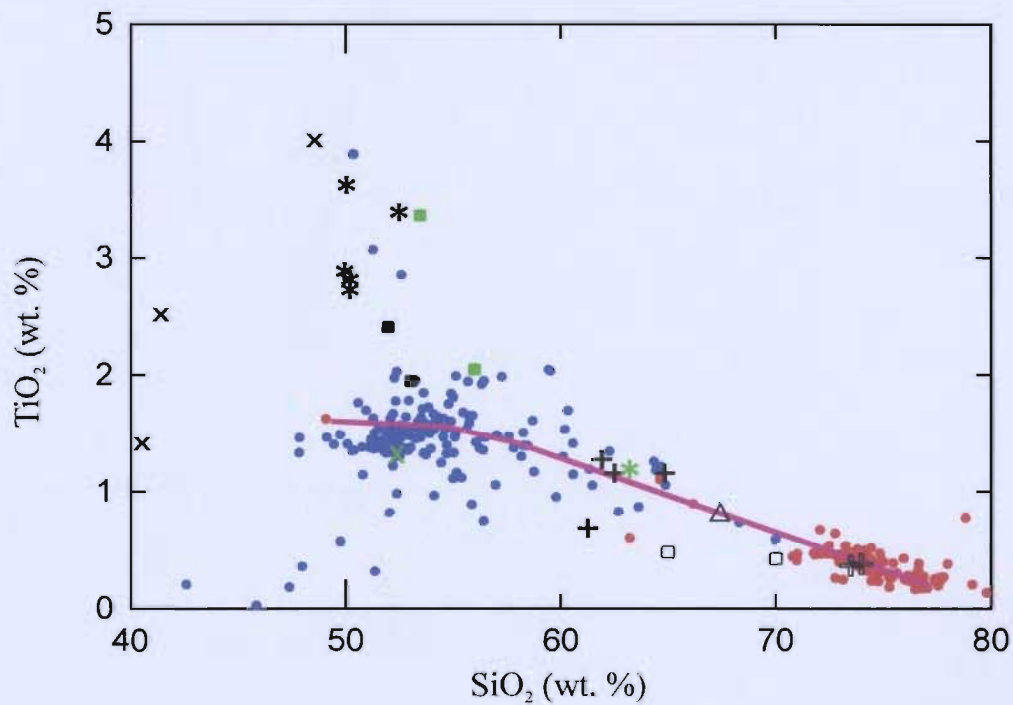


**Figure 5.9d:** Bivariate plot of SiO<sub>2</sub> vs. TiO<sub>2</sub> illustrating a negative linear trend for the igneous rocks from the current study [black], Dickson (1996) and Churchill (1994) (refer to figure 5.1 for symbol key).

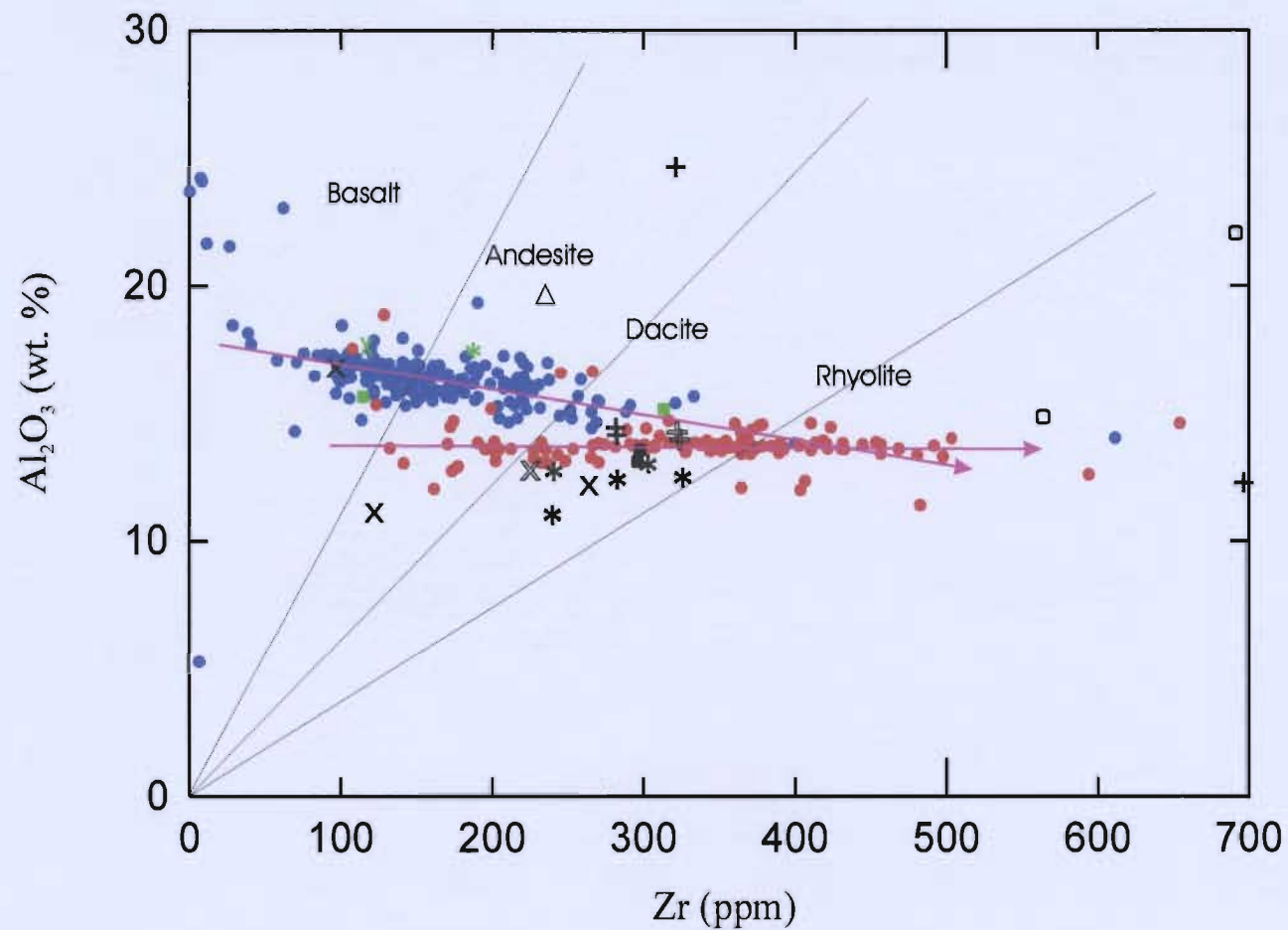


**Figure 5.10:** Zr vs.  $\text{Al}_2\text{O}_3$  bivariate plot (after MacLean and Barrett, 1993) illustrating a fractionation trend in the Botwood Basin igneous rocks. The mafic samples collected from the north for the current study either define a separate trend, or have experienced mass gain (refer to figure 5.1 for symbol key).



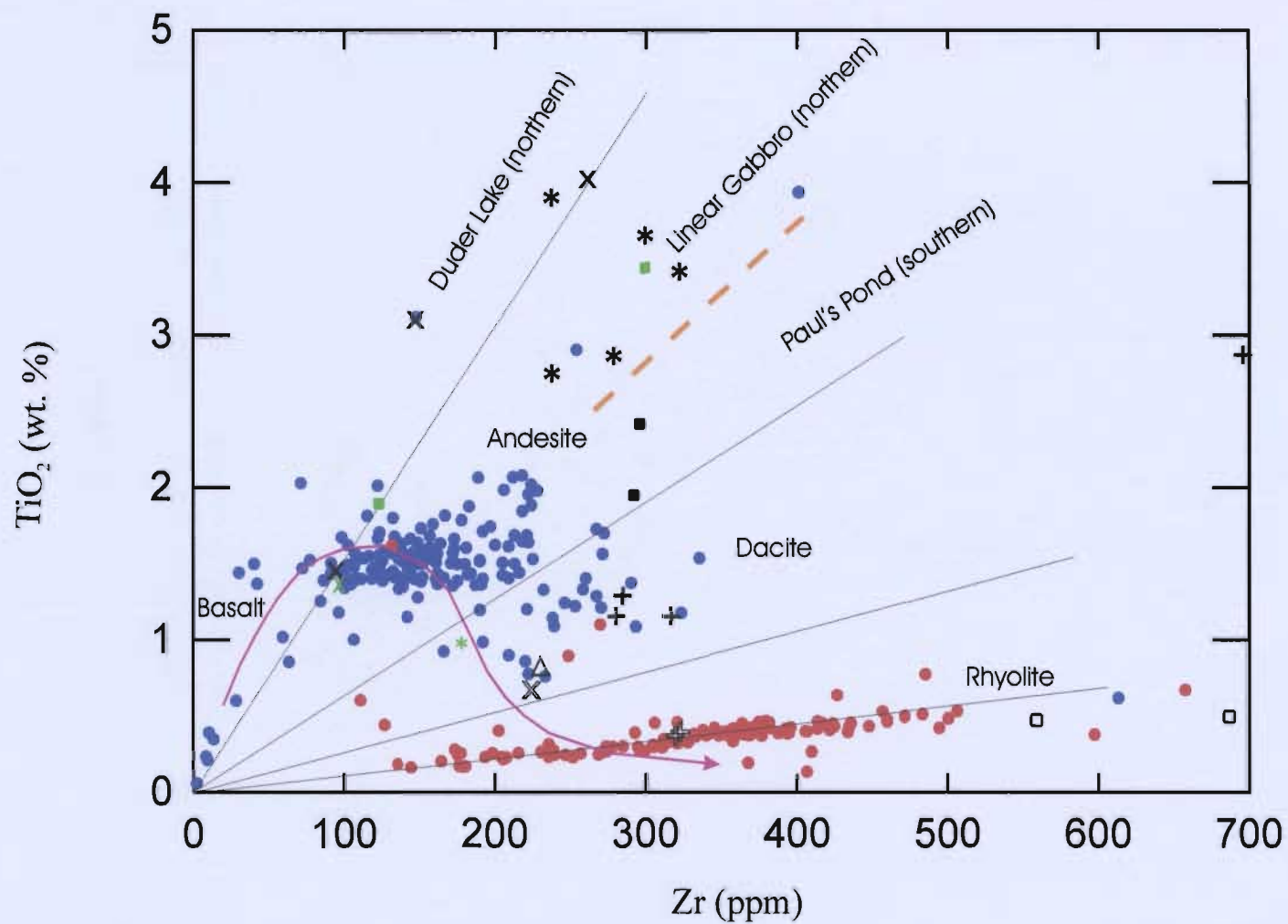


**Figure 5.11:** Zr vs.  $\text{TiO}_2$  bivariate plot ( after MacLean and Barrett, 1993) illustrating a fractionation trend in the Botwood Basin igneous rocks. The mafic samples from the current study have higher Ti values (refer to figure 5.1 for symbol key).

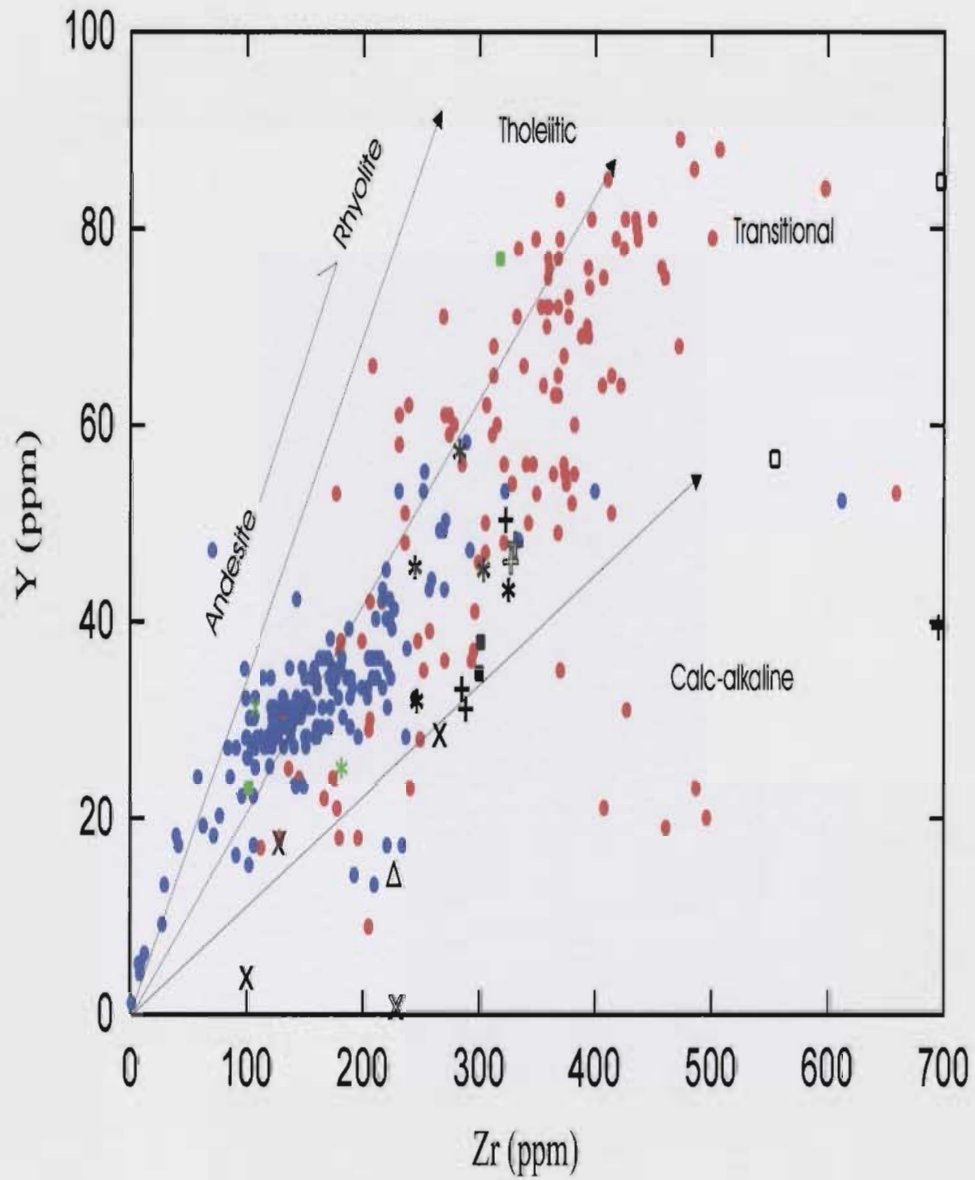


**Figure 5.12:** Zr vs. Y. diagram (after MacLean and Barrett, 1993) for igneous rocks in the Botwood Basin illustrating the transitional nature of the samples from the current study and the overall transitional to tholeiitic nature of all combined data (refer to figure 5.1 for symbol key).

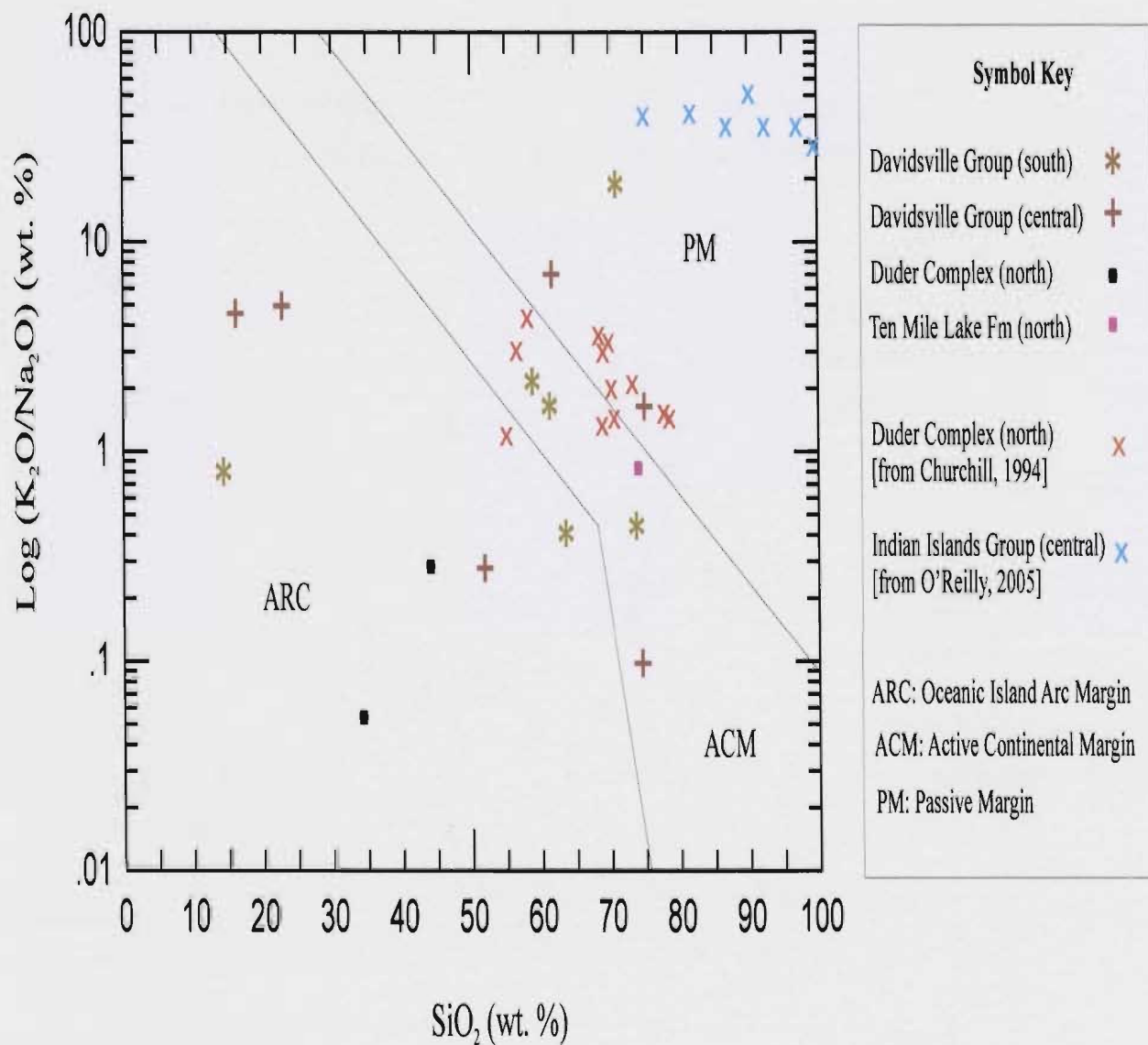


**Figure 5.13:** Roser and Korsch (1986) tectonic discrimination diagram for the Botwood basin sedimentary samples from the current study, Churchill's (1994) study at Duder Lake in the northern Botwood Basin and O'Reilly's (2005) study at the O'Reilly prospect in the central Botwood Basin.



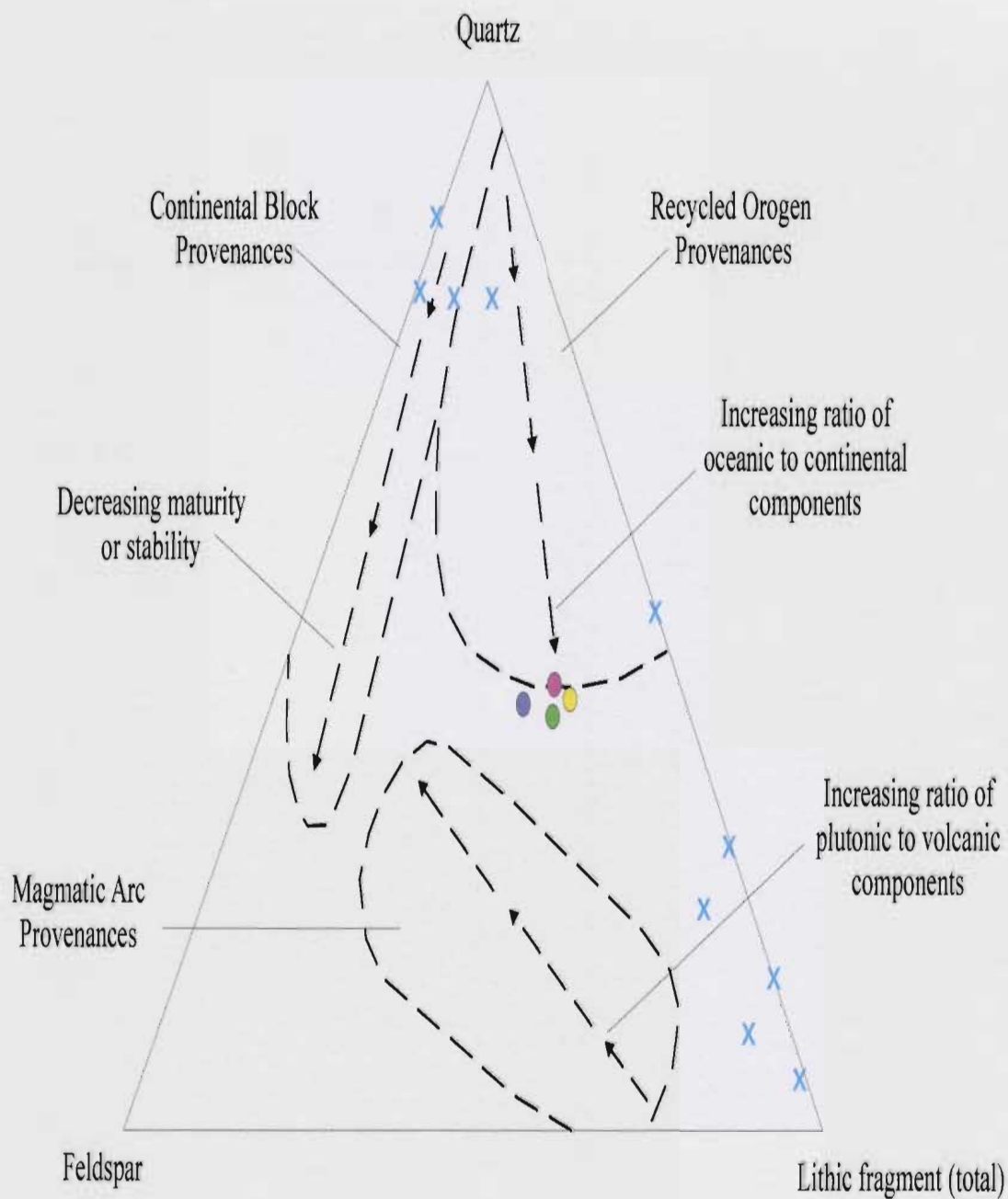


**Figure 5.14:** Dickinson and Suczec (1979) triangular quartz-feldspar-lithic fragment plot showing relationship between plate tectonics and the Davidsville Group (current study) [Red: JOD15 from central region; yellow: JOD20 from central; purple: JOD39 from central; green: JOD44A from southern region], and Indian Islands Group (O'Reilly, 2005) sedimentary rocks [blue].

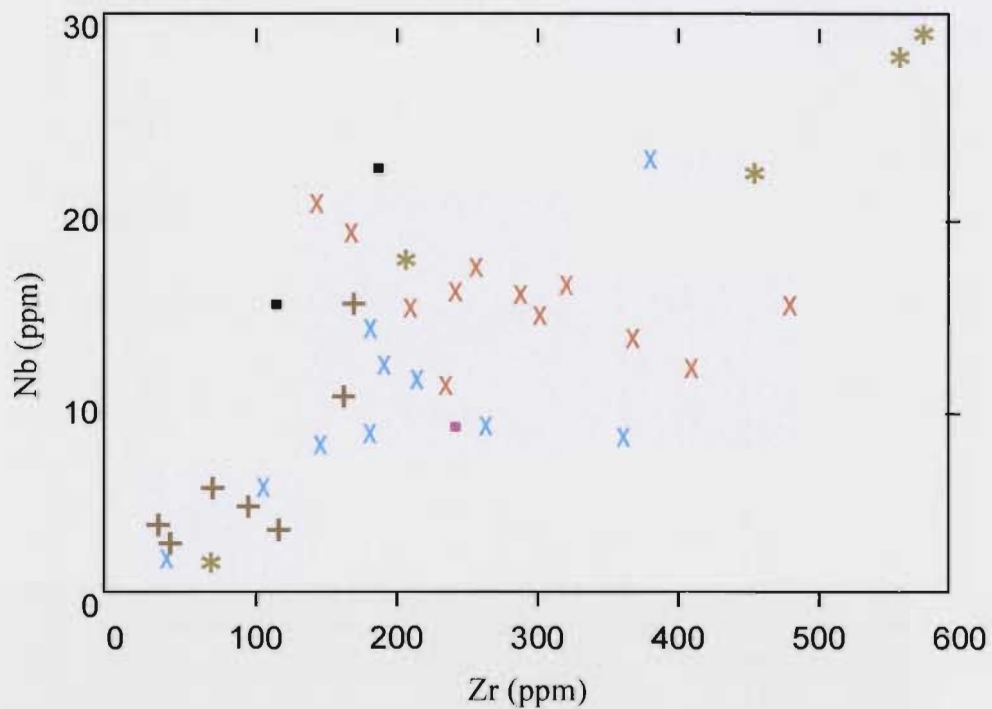


**Figure 5.15a:** Zr vs. Nb plot of sedimentary samples from the Botwood Basin (refer to figure 5.13 for symbol key).

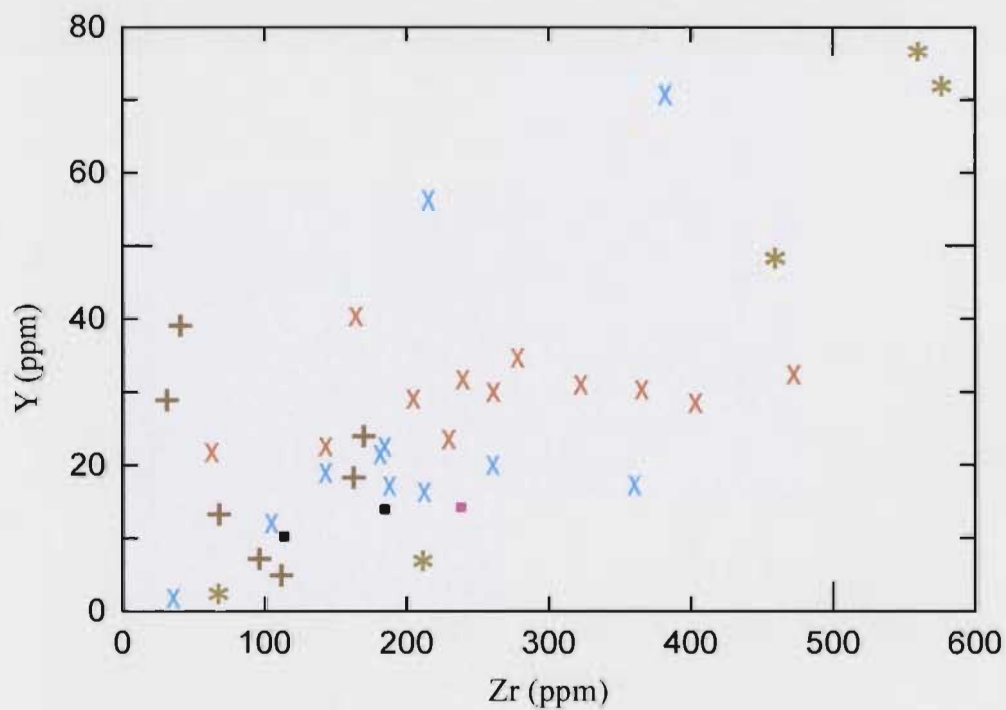


**Figure 5.15b:** Zr vs. Y plot of sedimentary samples from the Botwood Basin (refer to figure 5.13 for symbol key).

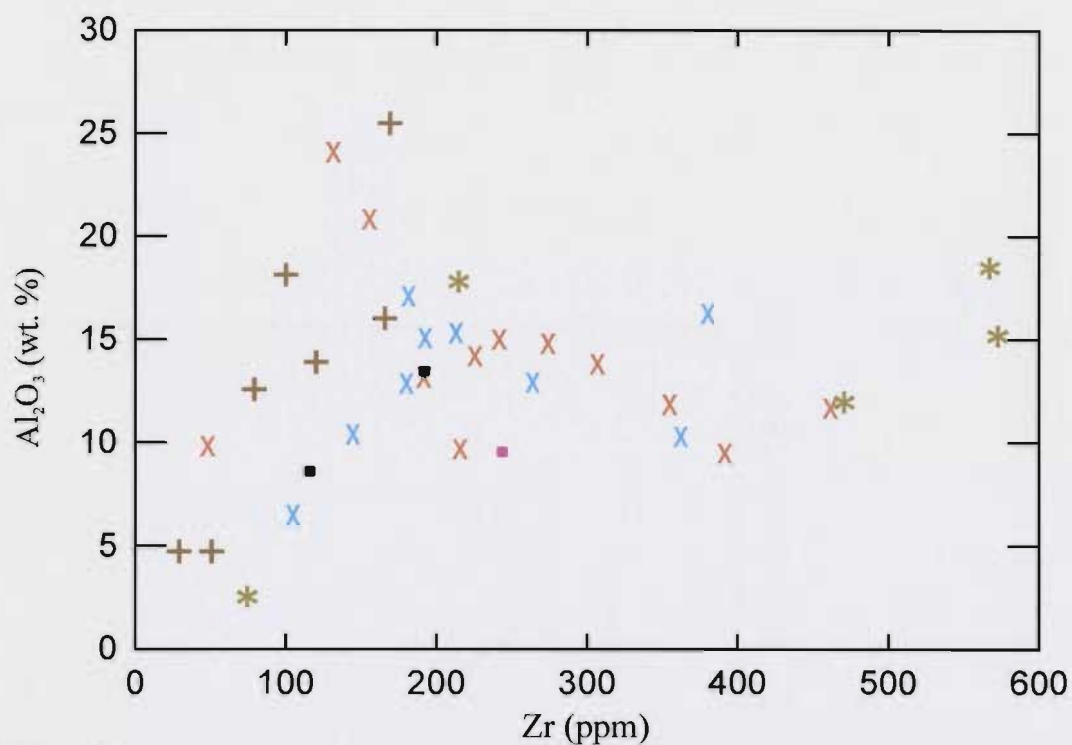


**Figure 5.15c:** Zr vs.  $\text{Al}_2\text{O}_3$  plot of sedimentary samples from the Botwood Basin (refer to figure 5.13 for symbol key).

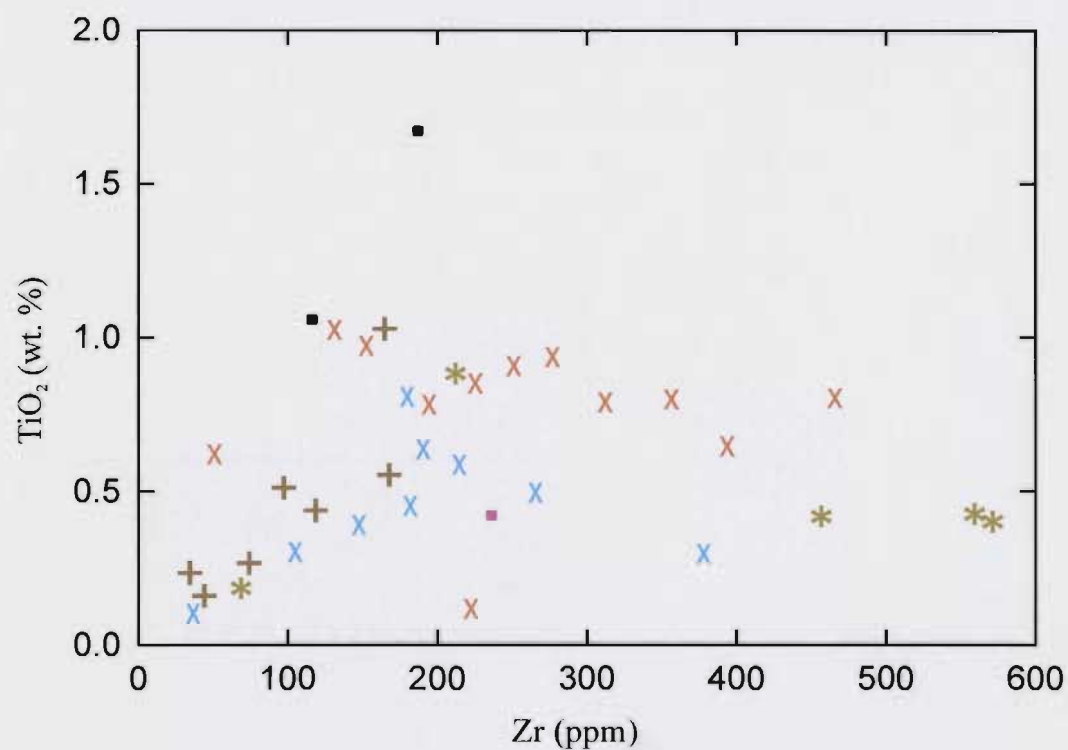


**Figure 5.15d:** Zr vs.  $\text{TiO}_2$  plot of sedimentary samples from the Botwood Basin (refer to figure 5.13 for symbol key).



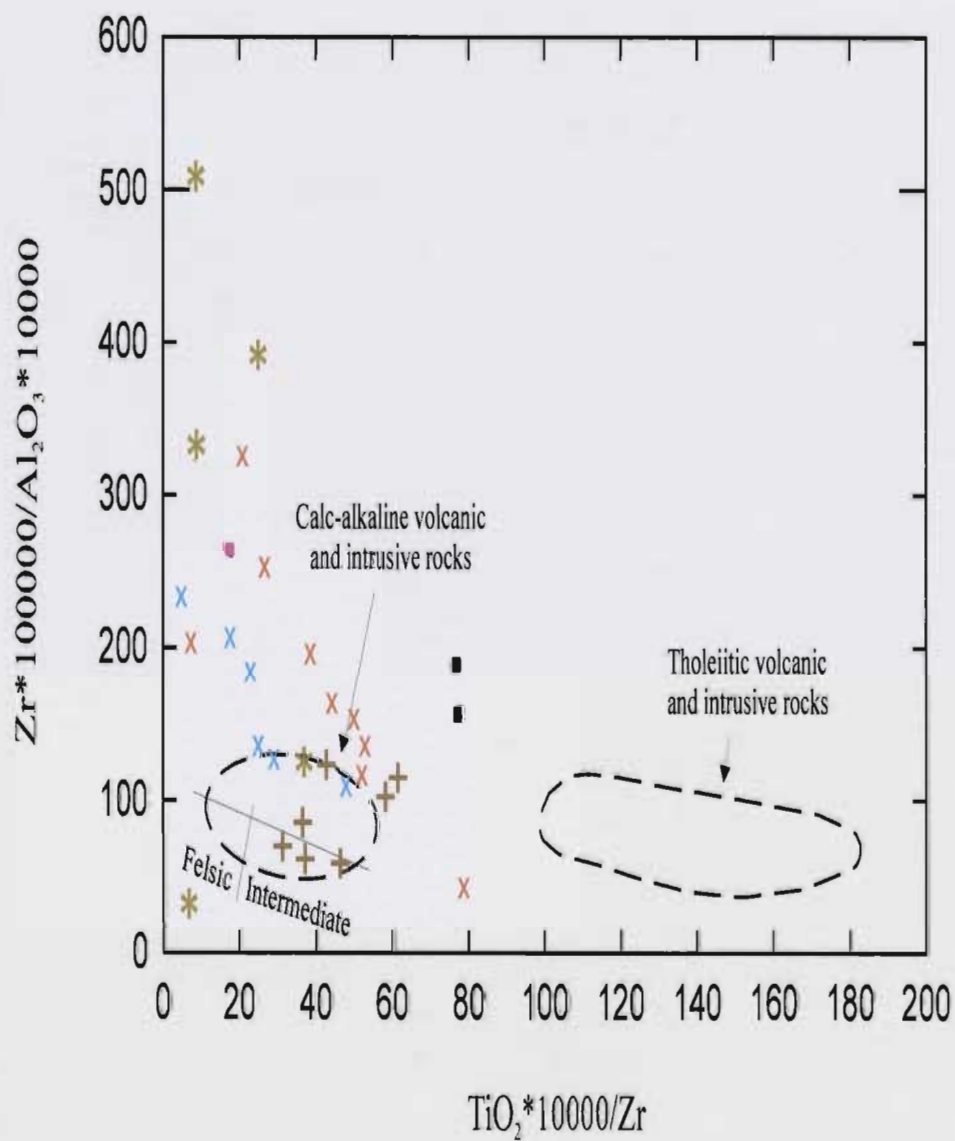


**Figure 5.16:** Fralick and Kronberg (1997)  $Al_2O_3$ - $TiO_2$ -Zr ratio diagram comparing Botwood Basin sedimentary samples with possible volcanic source terrains (refer to figure 5.13 for symbol key).

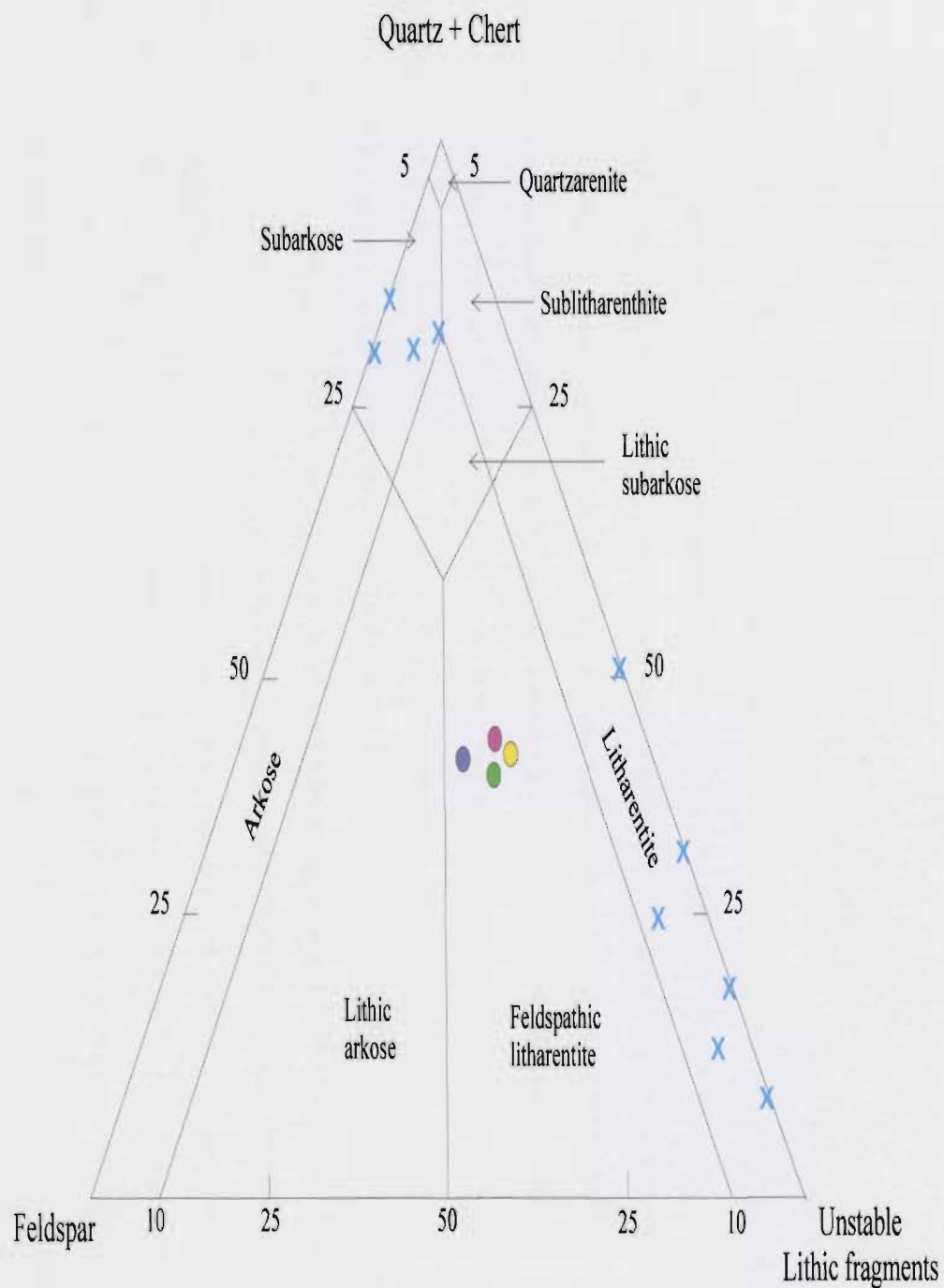


**Figure 5.17:** McBride (1963) triangular quartz-feldspar-lithic fragment classification diagram for the Davidsville (circles-see figure 4.14) and Indian Island (blue cross) Group rocks.

## CHAPTER 6

### SULPHUR ISOTOPE GEOCHEMISTRY

#### 6.1 Preamble

Light stable isotope systems (O, C, H, and S) are now commonly used to characterize, interpret, and explore for hydrothermal mineral deposits. Isotopic data alone cannot provide definitive answers because characteristics can vary in the same ore forming system depending on physio-chemical conditions. However, combined with geologic, mineralogic and geochemical analyses, these data provide information on several aspects of ore genesis including the characteristics of ore-forming fluids (Ohmoto, 1986). Sulphur isotope ratios are particularly useful for characterizing the ore forming fluids and mechanisms of ore precipitation.

When using sulphur isotope ratios, it is essential to consider that the interpretation of isotope ratios for sulphides associated with auriferous mineralization is fraught with difficulties unless the isotopic compositions of regional lithologies and local redox relationships are understood. For instance, different gold deposit types define wide ranges and/or non-diagnostic ratios. Bierlein and Crowe (2000, p. 121) suggest that while sulphides in most Phanerozoic orogenic lode gold deposits occurrences “cluster around 0 ‰”, sediment-hosted deposits such as the Meguma in Nova Scotia can have ratios of up to +10 to +30 ‰ (after Kontak and Smith, 1993).

In Carlin-type gold deposits, sulphur isotope variations can be even more extreme. A compilation of sulphur isotope data by Hofstra and Cline (2000) indicates



that ratios range from 0 to +17 ‰ in main ore stages of Carlin deposits, but can be as high as -32 ‰ in the distal edges of ore-forming systems (Figure 6.1, p. 224). Arehart (2003) defined pre-ore pyrite as having sulphur isotope ratios between -5 and +10 ‰, main ore pyrite as up to +20‰, and post-ore pyrite as -15 to -30 ‰. Ion microprobe analysis of individual pyrite grains from Carlin deposits (Arehart *et al.*, 1993) indicated that primary pyrite in host igneous rocks had isotope ratios of ~ 9 ‰, whereas primary sedimentary pyrite had ratios of -4 to -6 ‰. Auriferous arsenian overgrowths on ore zone pyrites had ratios up to +20 ‰ and in later non-auriferous arsenian overgrowths, the sulphur isotope ratios were -12 to -29 ‰. The sulphur isotope data derived to date for the Botwood Basin occurrences are too preliminary to develop any similar detailed paragenetic models (O' Driscoll and Wilton, 2005).

Sulphur isotope ratios for sulphides associated with the auriferous occurrences assessed for this project were compiled to determine whether there was any relation between the ore forming systems. Specifically, are there common sulphur sources, and if so, are these sources of primary magmatic origin, or derived from an external source (*i.e.*, seawater sulphate or biogenic sources).

## 6.2 Sulphur Isotope Systematics

Sulphur is both abundant and widely distributed throughout the lithosphere, biosphere, hydrosphere and atmosphere. There are four naturally occurring sulphur isotopes, and the natural terrestrial abundances of each are:  $^{32}\text{S}$  (95.02 %),  $^{33}\text{S}$  (0.75 %),  $^{34}\text{S}$  (4.21 %) and  $^{36}\text{S}$  (0.02 %). Isotope ratios between the two most abundant isotopes

$^{34}\text{S} / ^{32}\text{S}$  are measured more precisely than absolute abundances and are expressed in permil (‰) relative to a calibration standard. Troilite (FeS) from the Canon Diablo iron meteorite (CDT) is the standard for reporting  $\delta^{34}\text{S}$  values and has a  $^{34}\text{S} / ^{32}\text{S}$  ratio of 0.0450045. The CDT is used as a standard because it is believed to represent the composition of the bulk undifferentiated earth (Ohmoto and Rye, 1979). Isotopic composition is expressed in terms of  $\delta^{34}\text{S}$  defined as:

$$\delta^{34}\text{S} (\text{‰}) = [(^{34}\text{S}/^{32}\text{S}_{\text{sample}}/^{34}\text{S}/^{32}\text{S}_{\text{CDT}})-1]*1000$$

where  $^{34}\text{S} / ^{32}\text{S}_{\text{sample}}$  and  $^{34}\text{S} / ^{32}\text{S}_{\text{CDT}}$  are the  $^{34}\text{S} / ^{32}\text{S}$  ratios from the sample and the CDT respectively. Typical ranges of sulphur isotope compositions in geological systems are summarized in figure 6.2, p. 225.

It is reasonable to assume that there is no fractionation between mantle sulphur and magmatic sulphur, thus  $\delta^{34}\text{S}$  (magmatic sulphide)  $\approx \delta^{34}\text{S}$  (magma)  $\approx \delta^{34}\text{S}$  (parental rock)  $\approx 0$  ‰. Therefore, primary sulphur in magmas can be assumed to inherit the  $\delta^{34}\text{S}$  characteristics of their parent mantle melt and mantle source region and usually lie in the range of  $0 \pm 3$  ‰ (Ohmoto and Rye, 1979). The  $\delta^{34}\text{S}$  of any terrestrial sulphur is therefore representative of the amount of change in isotopic composition since derivation from its primary source reservoir. Sulphides in igneous rocks are isotopically similar to those in meteorites with average  $\delta^{34}\text{S}$  close to 0 ‰; sedimentary sulfates are enriched in  $^{34}\text{S}$  (+10 to +30 ‰); and sedimentary sulphides show a wide spread of  $\delta^{34}\text{S}$  values (+50 to -50 ‰) but are typically depleted (Ohmoto, 1972; Ohmoto and Rye, 1979; Hoefs, 1980).

Isotope variations in hydrothermal systems are related to mass and are produced by two different reactions: 1) kinematic isotope fractionation (*i.e.*, reduction of sulphate ions to hydrogen sulphides by anaerobic bacteria leading to  $^{32}\text{S}$  enrichment in the sulphide) (Taylor, 1974; Ohmoto and Rye, 1979), and 2) various chemical exchange reactions (ie: between sulfate and sulphides and between sulphides) where  $^{34}\text{S}$  is generally concentrated in those compounds with the highest oxidation strength or greatest bond strength (Faure, 1998).

Three isotopically distinct sulphur reservoirs are defined: 1) mantle-derived sulphur with  $\delta^{34}\text{S}$  values ranging from  $0 \pm 3 \text{ ‰}$  (Chaussidon and Lorand, 1990); 2) seawater sulphur with  $\delta^{34}\text{S}$  present day ratio of about  $\pm 20 \text{ ‰}$  (Claypool *et al.*, 1980); and 3) strongly reduced (sedimentary sulphur) with large negative  $\delta^{34}\text{S}$  ratios (Rollinson, 1993). Although the determination of the source reservoir for sulphur can be useful, when evaluating  $\delta^{34}\text{S}$  values it must be observed that mixing of sources may occur.

### 6.3 Sulphur Isotope Results

A total of 40 sulphide separates from Botwood Basin mineral occurrences as well as several select localities were analyzed on a Finnigan MAT 252 IR-MS at Memorial University of Newfoundland for their sulphur compositions including 31 pyrite samples, five arsenopyrite samples, two arsenopyrite + pyrite samples, one galena sample and one stibnite sample. The samples were derived from a variety of host lithologies including ultramafic (Gander River Complex, Great Bend Complex and Coy Pond Complex), mafic (dykes), intermediate and felsic (Mount Peyton Intrusive Suite) igneous rocks and deep



marine (Davidsville Group) sedimentary rocks. The results are presented in table A4.3 and on figure 6.3, p. 226 (along with previously compiled data) and are subdivided in terms of those with isotopically light ( $<0\text{‰}$ ), intermediate ( $\sim 0\text{‰}$ ) and isotopically heavy ( $>0\text{‰}$ ) ratios.

#### *6.3.1 Isotopically Light Sulphur Isotope Ratios*

The occurrences, which exhibit isotopically light ratios ( $<0\text{‰}$ ), include the Jonathon's Pond, Hunan, and the Outflow Prospects. Negative  $\delta^{34}\text{S}$  ratios typically indicate a reduced sedimentary source of sulphur. The Hunan and Outflow Prospects are both hosted by Davidsville Group rocks that have been postulated to have been thrust over Indian Islands Group sediments. These prospects have negative isotopic ratios from stibnite and pyrite separates of  $-6.43\text{‰}$  and  $-4.10\text{‰}$  respectively which suggests that the sulphur source may be from the deep marine turbiditic Davidsville Group. The exception in this instance is the Jonathon's Pond separates with a negative isotopic ratio range of  $-6.27\text{‰}$  to  $-8.20\text{‰}$  from pyrite separates. Such a negative ratio was not expected from a pyrite hosted in mafic to ultramafic lithologies of the Gander River Complex. A possible explanation for this ratio is the close proximity of the prospect to the Davidsville Group, hence, the sulphur in the sulphides may have derived from the turbidites. In fact, the Davidsville Group forms an imbricated cover sequence upon the complex immediately west of the occurrence.

### *6.3.2 Intermediate Sulphur Isotope Ratios*

Most of the sulphide separates analyzed fall within the intermediate ( $\sim 0\text{‰}$  to  $+3\text{‰}$ ) group which indicates a prevalent magmatic reservoir for sulphur within the Botwood Basin. Some of these prospects are hosted by mafic, intermediate and felsic intrusive lithologies such as the Greenwood Pond #2, LBNL, Hornet, Corsair, Hurricane, Slip and Duder Lake Prospects. The sedimentary-hosted prospects that fall into this category include the Linear, Knob, Jumper's Brook and A-Zone; intermediate values can be explained by the proximity of these prospects to intrusive units.

The separates analyzed for this study from Duder Lake included pyrite from the Flirt, Goldstash and Corvette prospects and the values obtained range from  $-0.02\text{‰}$  to  $+0.48\text{‰}$ . The values are consistent with a magmatic sulphur source that is expected since the prospects are hosted in gabbroic dykes, which intrude sedimentary rocks that are currently mapped as the Duder Complex matrix.

Separates were also analyzed from several prospects that are hosted by the Mount Peyton Intrusive Suite. The Hurricane and Corsair Prospects both occur in diorite along the Salmon River on the northern edge of the MPIS and pyrite separates from each returned values of  $3.80\text{‰}$  and  $1.21\text{‰}$  to  $2.18\text{‰}$  respectively; these values suggest a magmatic input of sulphur. The Slip Prospect is hosted in a granitic phase of the MPIS, northwest of the Salmon River Prospects. Pyrite, arsenopyrite and galena separates were collected from two samples collected from this prospect and returned values of  $1.02\text{‰}$ ,  $2.93\text{‰}$  and  $1.60\text{‰}$  respectively; these values indicate a magmatic sulphur input of sulphur.

The Greenwood Pond #2, LBNL and Hornet Prospects occur in the Paul's Pond region and are hosted by small gabbroic and granitic bodies that intrude the Davidsville Group. Pyrite separates from Greenwood Pond #2 returned ratios of 0.98 ‰, arsenopyrite separates from the LBNL returned values of 2.90 ‰ and 3.13 ‰ and pyrite separates from the Hornet returned values of 3.70 ‰ and 3.57 ‰, all of which indicate a magmatic sulphur input.

Pyrite separates were also analyzed from several intrusive bodies in the region to use as a comparison to the sulphides collected from the auriferous occurrences. Two samples, JOD04-09 and JOD04-13, were collected from gabbroic bodies intruding the Ten Mile Lake Formation as introduced in chapter 4 and two samples, JOD108 and JOD04-20, were collected from a diorite body intruding Indian Islands Group sediments in a gravel pit immediately west of Glenwood. The intrusions to the Ten Mile Lake Formation returned values of 1.26 ‰ and 0.26 ‰ and the intrusions in the Indian Islands Group returned values of 0.89 ‰ and 0.23 ‰, all of which reiterate that magmatic sulphides have intermediate  $\delta^{34}\text{S}$  values as suggested by Chaussidon and Lorand (1990).

The remaining intermediate samples are from prospects hosted in sedimentary rocks that occur either in the Paul's Pond or Glenwood areas, both of which lie directly west of the large MPIS. The A-Zone Prospect occurs in the Paul's Pond Region just west of the MPIS and immediate to the areas of the intrusive hosted Greenwood Pond #2, Hornet and LBNL prospects. The A-Zone pyrite separates returned values of 0.58 ‰ and 1.28 ‰ suggesting a magmatic sulphur source.

The Knob and Dome prospects occur in the Glenwood region and pyrite separates from each returned ratios of -0.07 ‰ to -0.95 ‰ and -0.35 ‰ to 0.81 ‰ respectively;



These values indicate a primarily magmatic sulphur source. The remaining sample in this group was collected from the Jumper's Prospect located within hornfelsed sedimentary rocks immediately NW of the MPIS. Pyrite separates from this prospect returned values of 2.81 ‰ and 3.93 ‰ indicating a magmatic source.

### 6.3.3 Isotopically Heavy Sulphur Isotope Ratios

The isotopically heavy group predominantly includes separates from prospects hosted in mafic to ultramafic rocks. Three samples that plot within this group were not collected from auriferous occurrences; sample JOD08 is a clast from the Bellman's Pond conglomerate, sample JOD39 is a sample from the contact between graphitic sediment (included in the Davidsville Group by Dickson *et al.* (1993) and Squires (2005)) and Indian Islands Group at Careless Brook, and sample JOD30 was a mineralized ultramafic sample of float collected from Gull River, just east of Breccia Pond in the Great Bend region.

Pyrite separates from the Bellman's Pond altered sedimentary clast returned a  $\delta^{34}\text{S}$  value of + 9.98 ‰ and the pyrite separate from Careless Brook returned a value of +18.67 ‰; the sulphur source for both these samples is assumed to be seawater sulphate as they both formed in marine environments.

Pyrite separates from the Gull River float returned a value of +7.47 ‰, which is similar to the values of +6.96 ‰ to 7.11 ‰ and +6.46 ‰ obtained from the Breccia Pond and Lizard Pond Prospect samples respectively. The sulphides in both latter samples are hosted in ultramafic rocks of the Great Bend Complex (Colman-Sadd and Swinden,

1984; Dickson, 1992). Arsenopyrite separates from the Huxter Lane Prospect, to the south of the Great Bend area, returned a  $\delta^{34}\text{S}$  value of +8.83 ‰. The sulphides from this prospect are hosted in igneous rocks intrusive to rocks to the Coy Pond Complex. As all of these occurrences are associated with igneous rocks of ultramafic ophiolitic complexes, the sulphur source is probably seawater sulfate, which would have been incorporated into the ophiolitic rocks during hydrothermal alteration on the seafloor. Many of the ultramafic rocks in the area exhibit intense magnesite and serpentinite alteration, indicating that these rocks were indeed in contact with seafloor fluids.

#### **6.4 Discussion**

The results from this study were combined with previously collected stable isotope data from various sources (Figure 6.3, p. 226) to determine whether the mineralized systems from within the Bowtood Basin had a dominant crustal or organic influence. The previously compiled data are discussed in comparison to the data collected for the current study.

Previous sulphur isotope data compiled for occurrences in the region suggest a very wide range in  $\delta^{34}\text{S}$  ratios for pyrite, arsenopyrite and stibnite. At the most simplistic level, the compiled data can be subdivided into three different groupings in terms of isotopic ratios as: (1) a group with negative (or isotopically light)  $\delta^{34}\text{S}$  ratios, (2) a group with ratios around 0 ‰, and (3) a group with slightly to moderately positive (isotopically heavy) ratios.

The isotopically light groups are mainly auriferous showings hosted within the dominantly sedimentary Baie d' Espoir Group (*i.e.*, Golden Grit, True Grit, Kim Lake and Little River), Botwood (*i.e.*, Aztec) and Davidsville Group (*i.e.*, Hunan and Outflow), thus these negative ratios probably reflect a reduced sedimentary source for the sulphur. The separates from the Aztec Showing have a wide range of ratios, up to and including slightly positive ratios. This particular showing is quite complex because it occurs at a faulted contact between the Indian Islands (shallow marine) and Davidsville (deep marine) groups and exhibits a wide range of sulphide paragenetic relationships (Wilton, 2003). The Jonathon's Pond occurrence, although located within ultramafic rocks of the Gander River Complex, is located immediately adjacent to the Davidsville Group zone and its noticeably isotopically light ratio (-8.2 ‰) presumably indicates that the sulphur was derived from a reduced sedimentary source (*i.e.*, the deep marine Davidsville Group sedimentary rocks).

The intermediate (around 0 ‰) group mostly represents showings hosted within the Mount Peyton Intrusive Suite, or adjacent to it, and thus may reflect S with a magmatic input from the intrusive suite. Several other occurrences, such as those in the Paul's Pond and Duder Lake region are also associated with gabbroic dykes or sills indicating an analogous magmatic sulphur source for these systems. All data collected for this study fall within the range of the previously derived intermediate data with the exception of the Duder Lake data. The new data did not indicate such a wide range in  $\delta^{34}\text{S}$  values, rather it clustered near 0 ‰ indicating that the sulphur was primary magmatic.



Sulphur in the mineral separates from the group with slightly to moderately positive (isotopically heavy) isotope ratios may at least in part be derived from the igneous host rocks (*e.g.*, Lizard Pond, Breccia Pond and Huxter Lane), which may have incorporated seawater sulphate during alteration. The Huxter Lane Occurrence is hosted in felsic intrusive rocks, but it occurs in rocks of the Ultramafic Coy Pond Complex. The Le Pouvoir separates, however, are hosted by the Baie d' Espoir Group sedimentary rocks, and plot with the slightly to moderately positive group.

Thus, the sulphur from the auriferous systems in the Botwood Basin is primarily magmatic, although some of the values reflect input from adjacent deep marine or ultramafic complexes. These data agree with previous S isotope studies within the basin by Churchill (1994) and Evans and Wilson (1994).

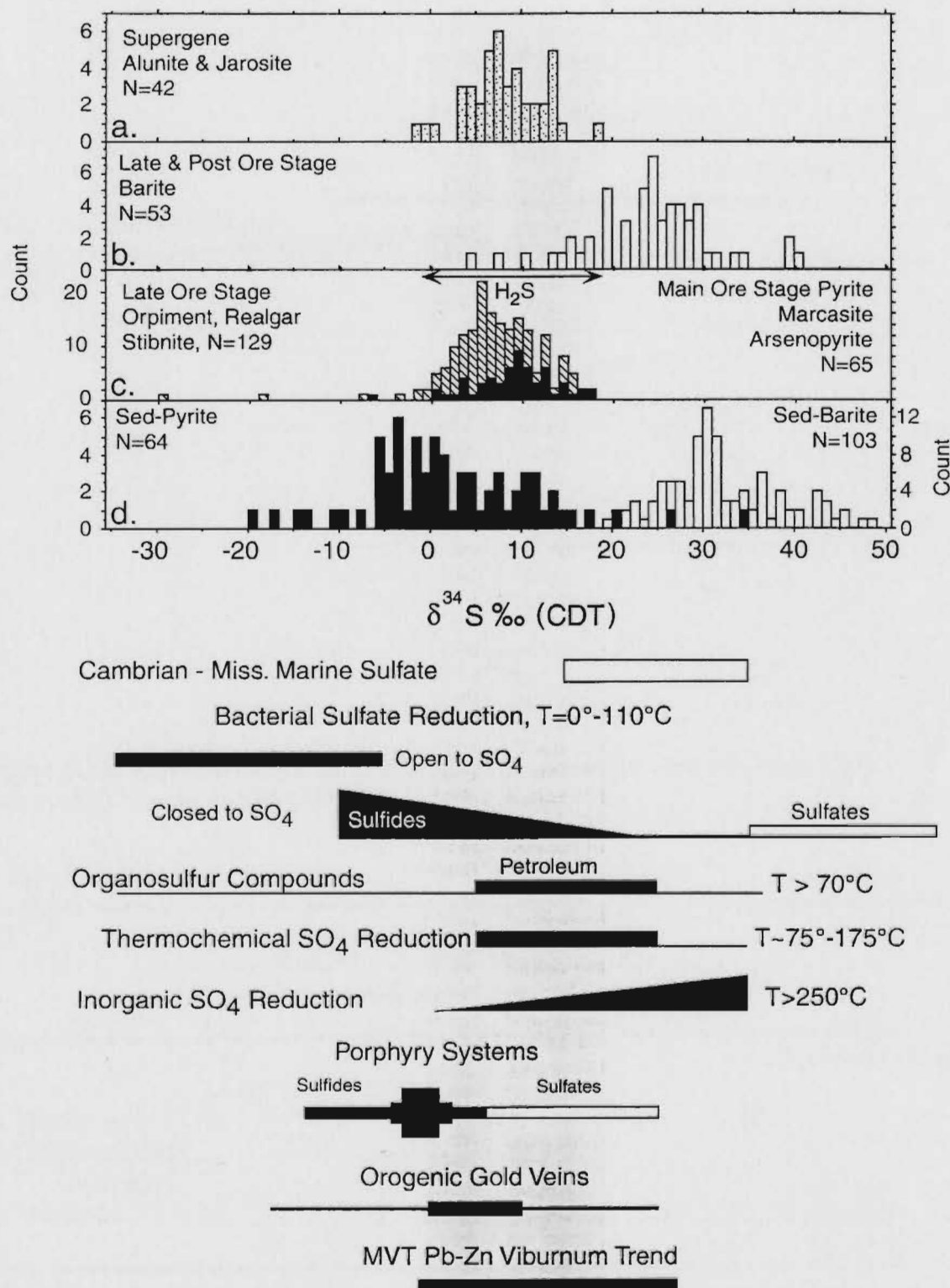


**Figure 6.1:** Sulphur isotope data from Carlin-type gold deposits relative to pertinent references from Ohmoto and Rye (1979) and Kerrich (1989). The isotopic composition of  $\text{H}_2\text{S}$  in ore fluids (shaded) was calculated using a temperature of  $200^\circ\text{C}$  and isotopic fractionations in Ohmoto and Rye (1979) (from Hofstra and Cline, 2000).

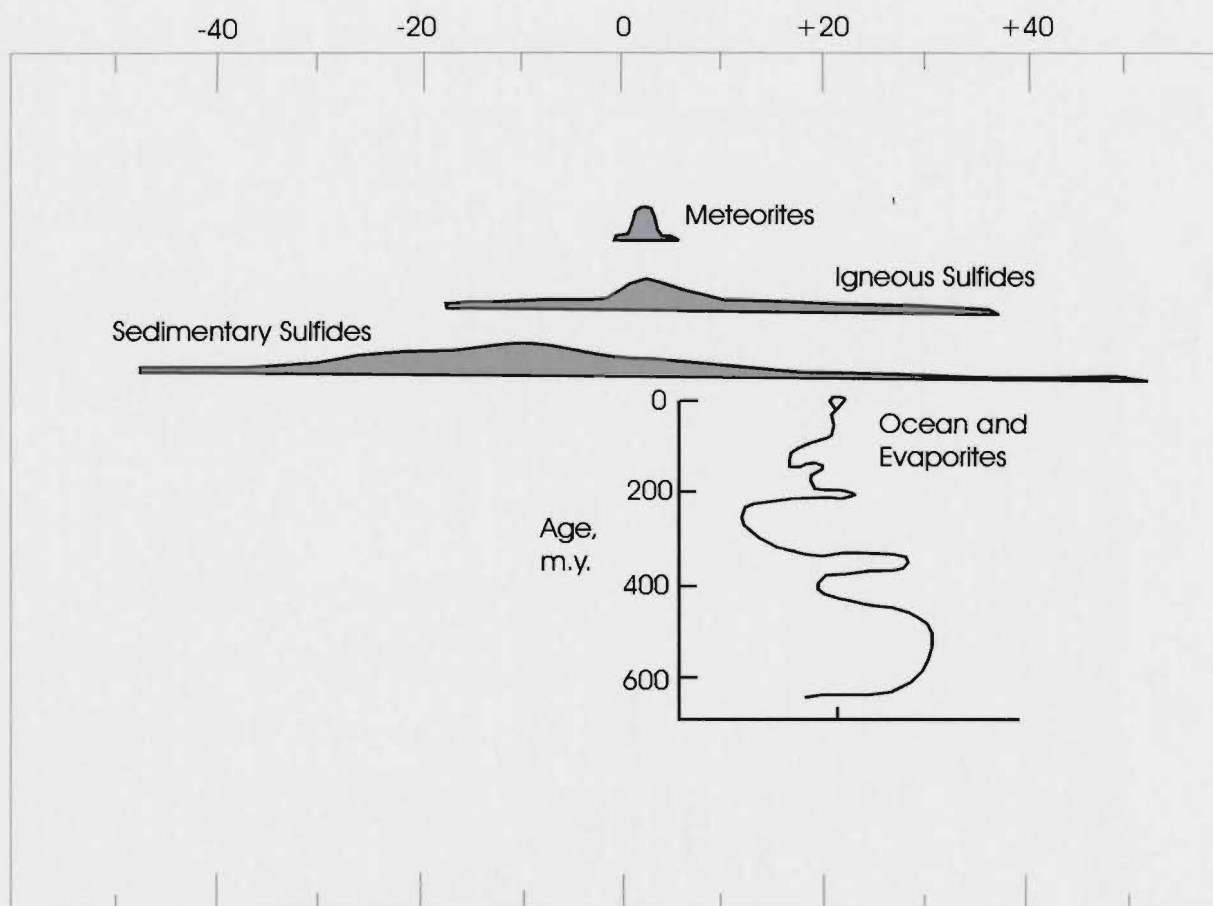


**Figure 6.2a:** The distribution of sulphur isotope values for common large earth reservoirs (Ohmoto and Rye, 1979).

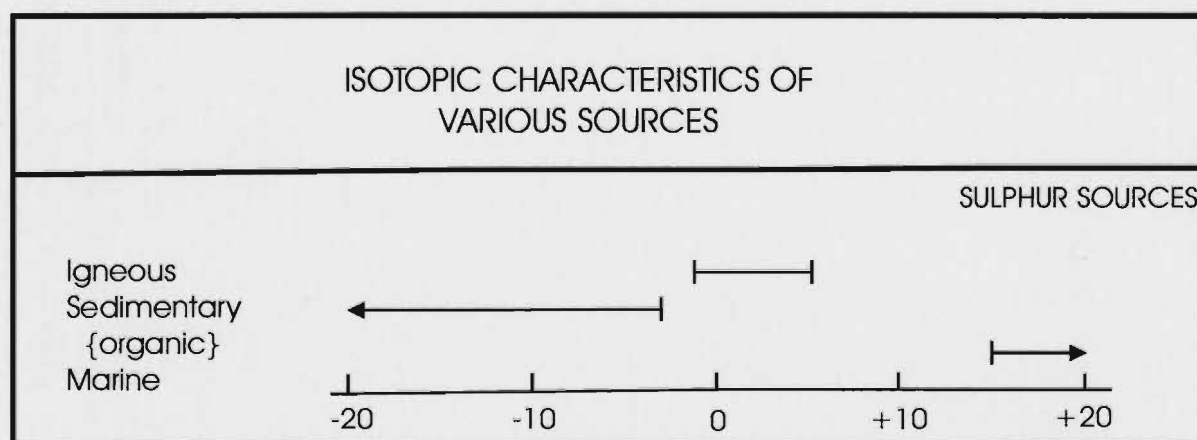


**Figure 6.2b:** Stable isotope composition of sulphur from different sources (Kyser, 1986; Kerrich, 1989).



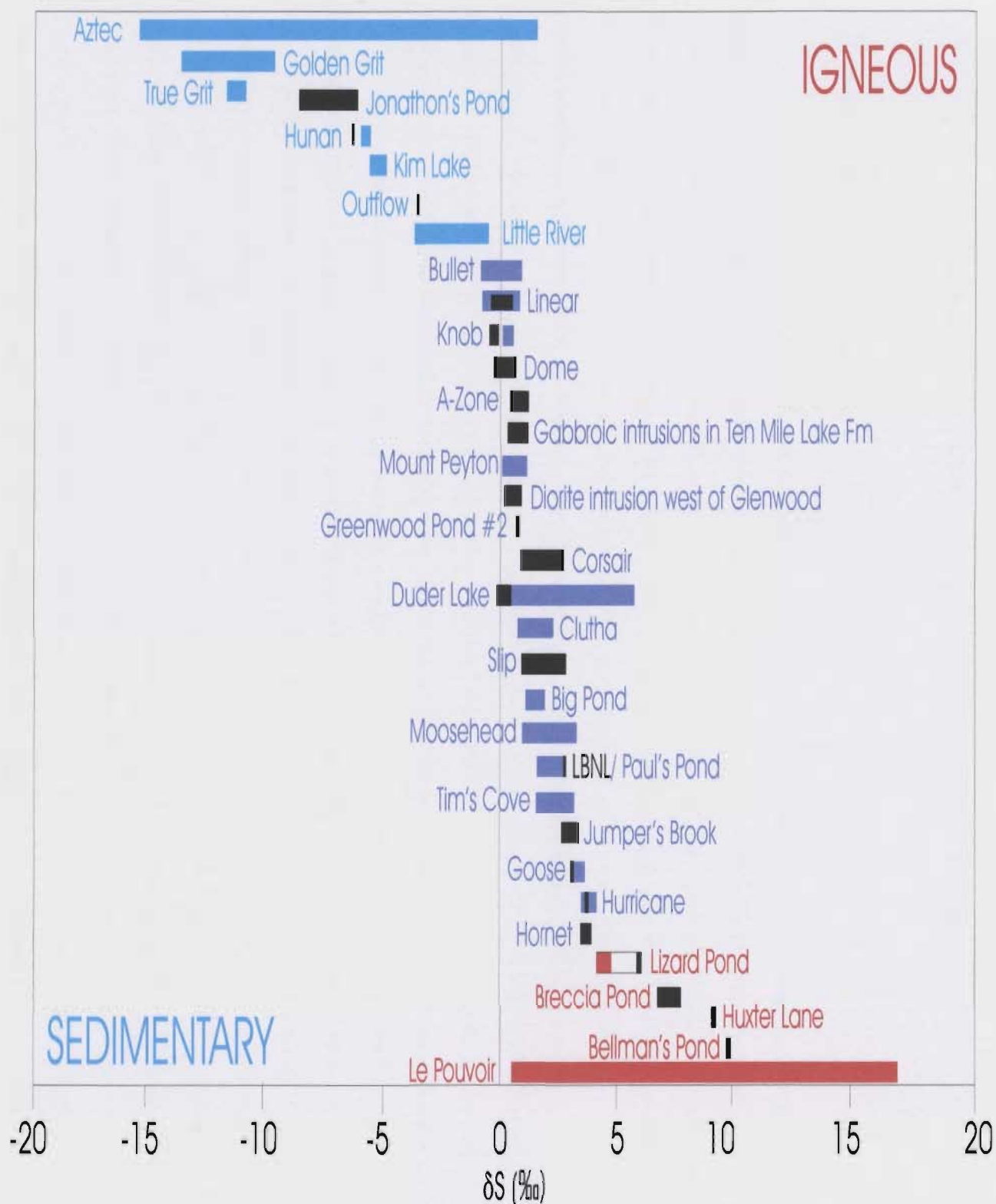


**Figure 6.3:** Compilation of sulphur isotope ratios for sulphide mineral separates from auriferous occurrences of the Botwood Basin; data compiled from Churchill (1994), Dalton (1998), Evans and Wilson (1994), D. Evans, (unpublished data, 2005), Greenslade (2002), unpublished data from D. Wilton and data from the current study (black) [blue=isotopically light; purple=intermediate ratios; red= isotopically heavy (modified from O' Driscoll and Wilton, 2005) .

## CHAPTER 7

### TRACE-ELEMENT CONTENT OF PYRITE

#### 7.1 Preamble

Trace element contents of pyrites from several auriferous occurrences were analyzed in an attempt to further define the styles of mineralization present in the Botwood Basin. One of the fundamental questions asked at the onset of this project was whether there are different types of auriferous systems present in the basin and environs such as orogenic (*cf.* Bierlein and Crowe, 2000; Groves *et al.* 1998, 2003), low-sulphidation epithermal (*cf.* Cooke and Simmons, 2000; Hedenquist *et al.*, 2000), intrusion-related (*cf.* Lang *et al.*, 2000; Thompson and Newberry, 2000) and/or Carlin-type (*cf.* Arehart, 1996, 2000, 2003; Hofstra and Cline, 2000), and, if present, how are these different types related to each other and the geological evolution of the region?

Previous workers have presented evidence in an attempt to classify these numerous pyrite  $\pm$  arsenopyrite-bearing gold occurrences, both individually (*i.e.*, Duder Lake Occurrences, Churchill, 1994) or regionally (*i.e.*, epigenetic occurrences of the eastern Dunnage Zone, Evans, 1996). Some of these occurrences, in Ordovician rocks, such as the Duder Lake Prospects (Churchill, 1994), are of mesothermal/ orogenic style with strong carbonate alteration and fluid inclusions (Flinch) containing CO<sub>2</sub>, T<sub>HOMO</sub>'s of 250-400°C and low salinities, whereas, others on the western and southern margins of the basin, such as the Moosehead (Dalton, 1998) and Rolling Pond (Turmel, 2000) are of low-sulphidation epithermal style with high-level brecciation and Flinch with T<sub>HOMO</sub>'s of

200-325°C and even lower salinities. A concept recently advanced by Altius Minerals Corp. (Butler, 2003) suggests that some of the occurrences on the eastern side of the basin are Carlin-style in that they are hosted by carbonaceous shales and limestones of the Indian Islands Group (IIG), which was overthrust by the Ordovician Davidsville Group.

Trace element data for pyrite grains from these auriferous occurrences could provide evidence for the classification of the mineralizing environments based on the fact that pyrite can incorporate characteristic trace elements into the crystal lattice. For example, Hofstra and Cline (2000) defined characteristic trace element suites in pyrite at Carlin-type deposits.

Trace element analyses were conducted on pyrite from seven different auriferous occurrences within the Botwood Basin. The derived data were compared to each other and also with pyrite data from two known auriferous occurrence types from elsewhere in Newfoundland.

The LAM-ICP-MS analytical technique used in this study is similar to that defined by Hinchey *et al.* (2003), which was originally designed to determine the nature and distribution of invisible gold in sulphide phases. O'Driscoll *et al.* (2005) presented preliminary results on the use of this technique for the classification of gold mineralization in the Botwood Basin.



## 7.2 Analytical Procedure and Sample Overview

The analyses were completed using the Laser Ablation Microprobe – Inductively Coupled Plasma – Mass Spectrometer (LAM-ICP-MS) in the Department of Earth Sciences, Memorial University of Newfoundland. Pyrite grains in single polished thin sections were analyzed. The technique has been described by Hinchey *et al.* (2003), except that in this case, an internal standard was used in some of the analyses, rather than an FeS standard. In several of the analysis (JOD23, JOD80A, JOD98A, JOD117 and JOD119), an acquired FeS standard was measured on an electron microprobe. A BSE image of one of the ablation pits produced by the laser is shown on plate 7.1. The internal standard used was MASS1, a United States Geological Survey pressed powder pellet. The analytical technique is described in detail in Appendix 3 and the resulting trace element data are presented in Appendix 4.

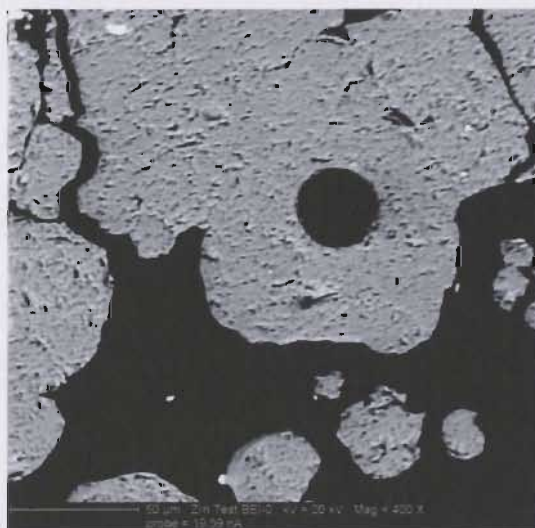


**Plate 7.1:** BSE image of an ablation pit in a pyrite grain from sample JOD23 collected from the Hurricane Prospect (image ~ 175  $\mu\text{m}$  wide).

From within the Botwood Basin, pyrite grains were analyzed from the Outflow (Mustang Zone), Bowater, Hurricane, Hornet, Goldstash and Jonathon's Pond properties in samples W90-49B, W90-48, JOD23, JOD80A, JOD98A and JOD117, respectively; Derek Wilton collected the Outflow (Mustang Zone) (W90-49B) and Bowater (W90-48) samples during fieldwork with D.T.W Evans in 1990. Each of the auriferous occurrences visited during this study and the petrography of each of the samples collected by the author have been described in chapter 3.

The Mustang and Bowater samples were chosen to represent possible so-called Carlin-style occurrences (Plates 7.2 and 7.3, p. 244). The Jonathon's Pond (as defined by Evans, 1996), Goldstash (as defined by Churchill, 1994) and Hurricane (as defined by Evans, 1996) samples (Plate 7.4, p. 244) were chosen to represent possible orogenic style occurrences, and the Hornet sample was selected to represent possible low-sulphidation epithermal style mineralization, as brecciation is present.

The Botwood Basin samples were also compared with pyrite from two auriferous prospects of known affinity from elsewhere in the Dunnage Zone. Sample W89-82 from the Stog'er Tight Prospect (Plate 7.5, p. 245), Baie Verte Peninsula (Ramezani *et al.*, 2000), was selected as a representative of orogenic (or mesothermal) lode gold occurrences. Sample KP-32-H1 is from the Gallery Resources Ltd. Bruce Pond epithermal system, ~ 15 km south of the Huxter Lane Showing. The bladed pyrite crystals in this sample were analyzed as examples of low-sulphidation epithermal systems (Plate 7.6, p. 245).

### 7.3 Results

The derived geochemical data indicate differences between the deposit-types. For instance, the Hurricane and Mustang Zone pyrites contain much higher Au and As contents, and in some grains higher Sb, than those from the other prospects (Figures 7.1, p. 237). In fact, the Hurricane Prospect pyrite grains are the most enriched in Au contents and the Mustang Zone pyrite contain the highest As contents. Several of the Mustang Zone pyrites are also more enriched in Hg and Pb.

The Bruce Pond (epithermal) pyrites are unique in that many of the grains contain the most enriched concentrations of Se (Figure 7.1h); the pyrite crystals in this sample also had very elevated local Ba concentrations that essentially tripped the LAM-ICP-MS detector. The Hornet Prospect pyrites, chosen to represent possible epithermal mineralization because of the brecciation observed at the prospect, had elevated concentrations of Au and As (Figure 7.1a), but were not enriched in any of the other elements. A few of the pyrite grains were somewhat elevated in Pb (Figure 7.1f), which was not unexpected as galena mineralization was also observed at this prospect.

The only elements in which the orogenic Stog'er Tight (orogenic) pyrite grains had elevated concentrations were Te, Se and W. Only one pyrite grain from the sample was enriched in both Te and W. Several grains were enriched in Se, although the concentrations of Se were not as high as that for the Bruce Pond samples. The pyrite grains from the other samples had lower concentrations for the Te and W elements with the exception of one grain from the Hurricane sample, which was enriched in W (Figures 7.1g and 7.1i). In fact, several grains from the Hurricane Prospect pyrites were variably



enriched in many of the elements tested, specifically As, Au, Sb and W. With respect to the samples apart from the Stog'er Tight and Hurricane, the Jonathon's Pond pyrite appear slightly more elevated in the W and Te, possibly due to the proximity of the MPIS. Most of the elements tested for in the pyrite grains from the Goldstash samples were under detection limits; Hg was slightly more elevated in these pyrites than the other samples with the exception of the Mustang pyrite (Figure 7.1b).

The above observations were made based on plotting the detected elements against Au concentrations. Several additional bivariate plots were constructed in an attempt to detect if any identifiable relationships existed between the analyzed elements (Figure 7.2, p. 242). A plot of Sb vs. W indicates that the some of the pyrite from Jonathan's Pond, Bruce Pond and the Mustang Zone have elevated Sb concentrations. A grain from the Jonathon's Pond also has elevated W. In general, the grains that contain elevated Sb do not contain elevated concentrations of W.

On a plot of As vs. Hg several interesting trends are noted. First, pyrite grains from the same occurrences generally plot together and the occurrences that are elevated in As are generally not elevated in Hg and vice versa, with the slight exception of some of the Mustang grains. The Hurricane, Jonathon's Pond, Mustang and Hornet pyrite are elevated in As and the Mustang and Goldstash are slightly elevated in Hg content.

On a plot of As vs. Sb, two plots are presented because of the extremely high As and Sb content in two of the grains from the Hurricane. On a plot with a reduced axis, several trends are again noted. First, some of the Bruce Pond pyrites are elevated in Sb but not in As. The Mustang and Jonathon's Pond pyrite are elevated in both elements

and in fact, the Mustang pyrite seems to define a trend of increasing Sb with increasing As content.

#### 7.4 Discussion

These data suggest that there are subtle differences between pyrite compositions predicated on the type of auriferous occurrence sampled. As, Sb, Tl, Hg, W, and Te, the so-called “*toxic element*” suite (Arehart, 2000, 2003), are typically associated with Carlin-style gold deposits and many of these elements are concentrated in pyrite grains at Carlin deposits (Hofstra and Cline, 2000). As defined by this preliminary study, pyrites from the Mustang Zone and to a lesser extent from the Bowater Prospect, have Carlin-like trace element signatures and are distinct from the orogenic and epithermal types sampled. More specifically, some of the Mustang pyrite was elevated in As, Au, Te, Sb, Hg and Pb whereas several of the Bowater pyrite was slightly elevated in As and Hg. In fact, many of the Mustang pyrite grains contained greater concentrations of Te, Hg and Pb than any of the other samples analyzed for this study.

Also of interest, is the fact that the pyrite grains with Hg did not contain elevated As, and vice versa. Several authors have conducted studies on auriferous prospects, usually with a specific emphasis on the relation of gold, pyrite and arsenopyrite (Wu and Delbove, 1989; Arehart *et al.*, 1993; Hinchey *et al.*, 2003). In general, the results show that Au increases with increasing As and decreases with increasing Fe. For the current study, the pyrite from the Hurricane Prospect and to a lesser extent the Mustang Zone, illustrates this trend. In previous studies, growth zoning was observed in most of the

crystals, but determinations of the specific trace element contents and possible zonation of these elements within the Fe sulphide crystals was not conducted. Although the results from this study are broad, and a larger dataset would be required to affirm postulations, Fe-sulphides from the Mustang Zone have elemental zonations as grains that are enriched in Hg are not enriched in As. Another explanation may be that the crystals that incorporate Hg in their lattices cannot incorporate As. This could be possible if the pyrite grains were produced from different hydrothermal events, which would produce different lattices.

Some workers in Phanerozoic fold belts have postulated that genetic models for Carlin-type Au deposits may also be applied to orogenic disseminated Au-type. For instance, Beirlein and Mahar (2001) suggested that orogenic disseminated gold deposits in Phanerozoic fold belts and some Carlin-type deposits of the western US have similar characteristics, which the authors attributed to a possible common ore fluid (*i.e.*, metamorphic). They concluded that caution must be applied, however, when relating sediment-hosted disseminated mineralization in orogenic systems to Carlin-type deposits.

Evidence for relating these deposits types, however, was subsequently presented by Bierlein and Smith (2003). They suggested that the two deposit types might coexist in an area where an intermittently active fault system would act as a feeder for both types. Further evidence for the relation is that both deposits have been associated with nearby granitoid plutonism and many authors favor a model of ore fluids derived by intrusion driven hydrothermal systems. Authors such as Berger and Bagby (1991) support a mixing model for Carlin type deposits whereby magmatic fluids mix with meteoric water to cause precipitation in favourable host rocks. Due to spatial proximity of the large



bimodal MPIS pluton, as well as the proximity of nearby occurrences of postulated orogenic (Hurricane), and Carlin or Sediment Hosted Disseminated Gold [SHDG] (Outflow) type occurrences to one another, a relation between the two deposit models may be suggested for the central Botwood Basin.

Hedenquist *et al.* (2000) suggest that both Se and Ba are associated with low-sulphidation epithermal gold deposits, in particular Se with samples from shallow depths. The pyrite grains from the Bruce Pond Epithermal occurrence contain appreciable Se and Ba contents that essentially distinguish them from the other pyrite samples and which also suggest a correlation between this occurrence and low-sulphidation epithermal models. However, the pyrites from the assumed epithermal Hornet Prospect did not exhibit elevated levels of these elements. They did however exhibit some elevated Au, As and Pb contents.

The Hurricane Prospect exhibited variable elevations of Au, As, Sb and W concentrations, whereas the Stog'er Tight sample had some elevated contents of W and Te. A study of the widespread orogenic gold deposits in the Yilgran Craton, western Australia showed that orogenic types of deposits are enriched in S, Sb, Si, Te and W and depleted in Na and Y with respect to the host rocks. The parameters that most consistently define dispersion haloes for these deposits are As, Au, Sb, Te and W, and carbonatization and seritization indices (Groves *et al.*, 2003).

The presence of W does not specifically define an orogenic type, as intrusion-related gold deposits are also associated with elevated W. Developing a clear determination about whether an occurrence is intrusion related or orogenic is often difficult as these deposit types typically exhibit many similarities (*i.e.*, metal associations,

wall rock alteration, ore fluids, *etc.*). In fact, different authors often place deposits with spatial associations to granitoid intrusions in both categories. One possibility for distinguishing the types is that the deposits that are distinctly classified as intrusion-related are located in cratonic settings, distal from subduction zones, when compared to orogenic. These provinces also typically contain Sn and/or W deposits (Grooves *et al.*, 2003). In relating this information to the geochemical signature of the MPIS prospects, the lack of recognized W occurrences in the immediate area, and the tectonic environment, suggest orogenic style as opposed to intrusion related style.

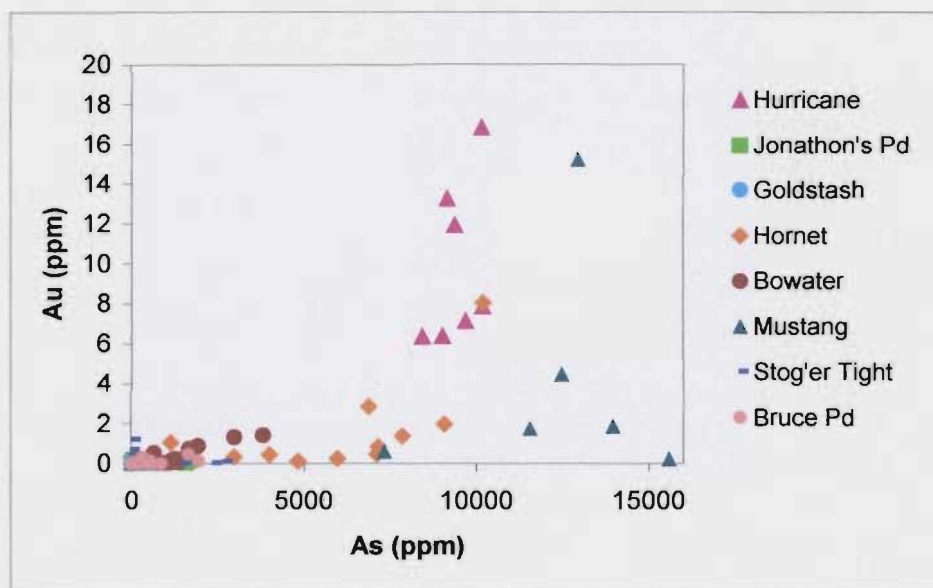


**Figure 7.1a:** Plot of As vs. Au illustrating that the Mustang, Hurricane and Hornet Prospect pyrites are elevated in Au and As contents relative to the other samples.

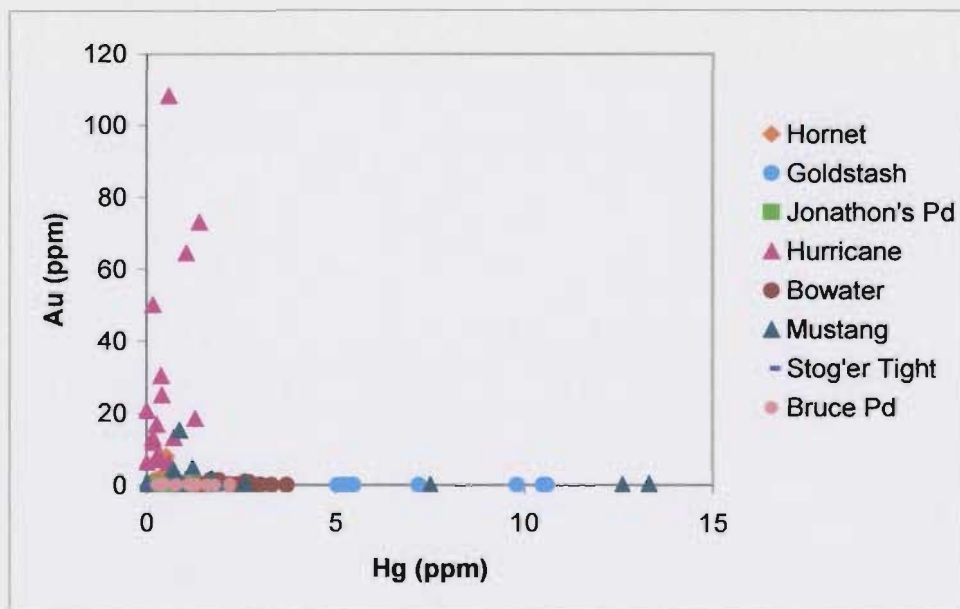


**Figure 7.1b:** Plot of Hg vs. Au illustrating that the Outflow (Mustang Trend) and Goldstash Prospect pyrites are elevated Hg contents relative to the other samples.



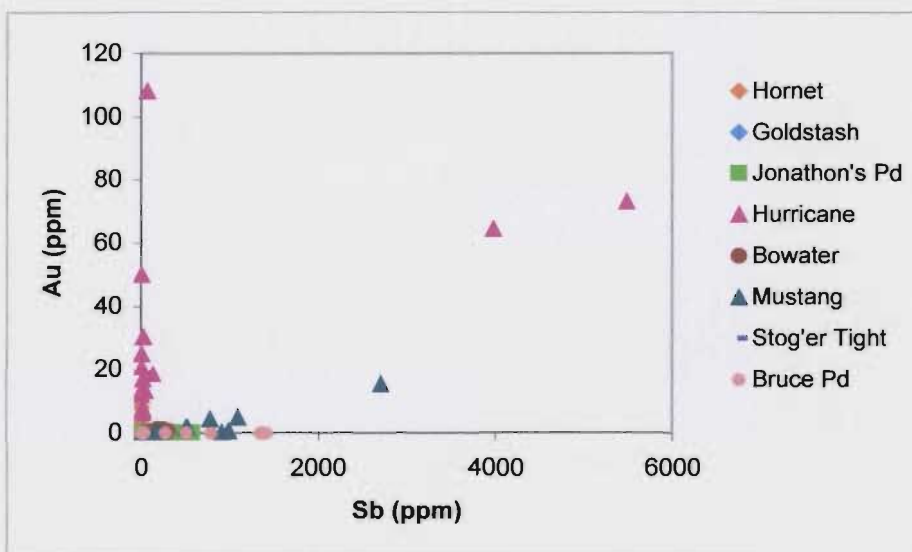


**Figure 7.1c:** Plot of Sb vs. Au illustrating that the Hurricane and Mustang Prospect pyrites are much more elevated in Sb contents relative to the other samples. The Bruce Pond pyrites has slightly elevated contents (see next chart).

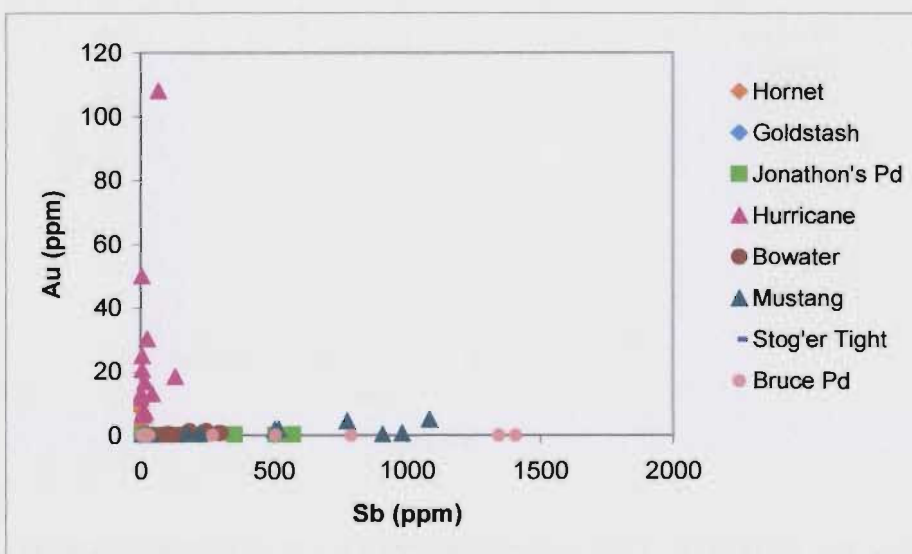


**Figure 7.1d:** Plot of Au vs. Sb (zoomed x-axis) illustrating that some of the Bruce Pond Prospect pyrites are more elevated in Sb contents than all samples except two Hurricane pyrite grains and one Mustang pyrite grain (refer also to figure 7.1c).

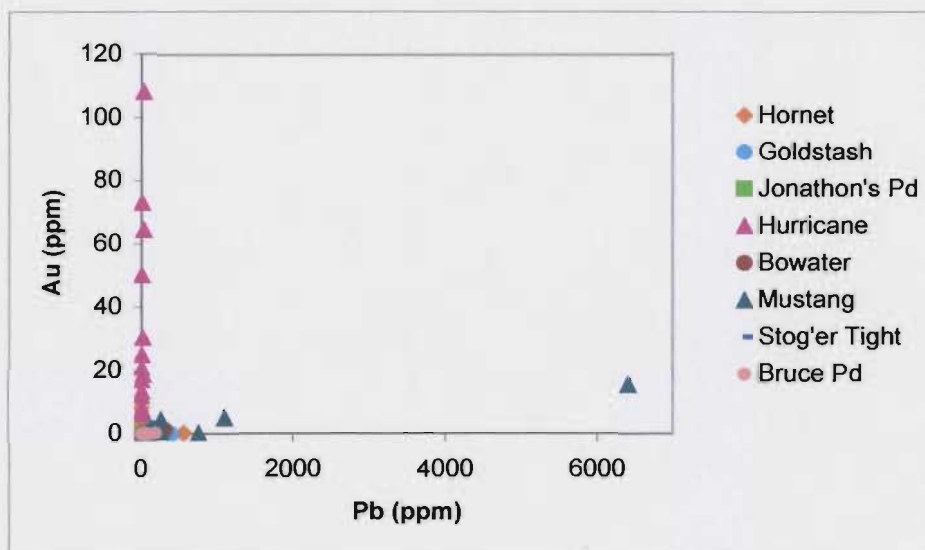


**Figure 7.1e:** Plot of Au vs. Pb illustrating that the Mustang Prospect pyrites are elevated in Pb contents relative to the other samples.

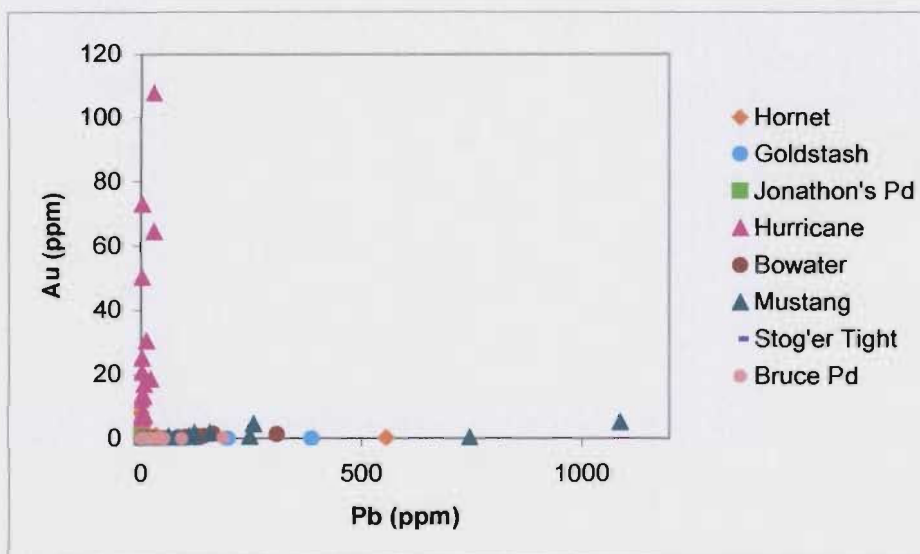


**Figure 7.1f:** Plot of Au vs. Pb (zoomed x-axis) illustrating that some pyrite from the Goldstash and Hornet Prospects are also slightly elevated in Pb contents relative to the other samples (refer also to figure 7.1e).

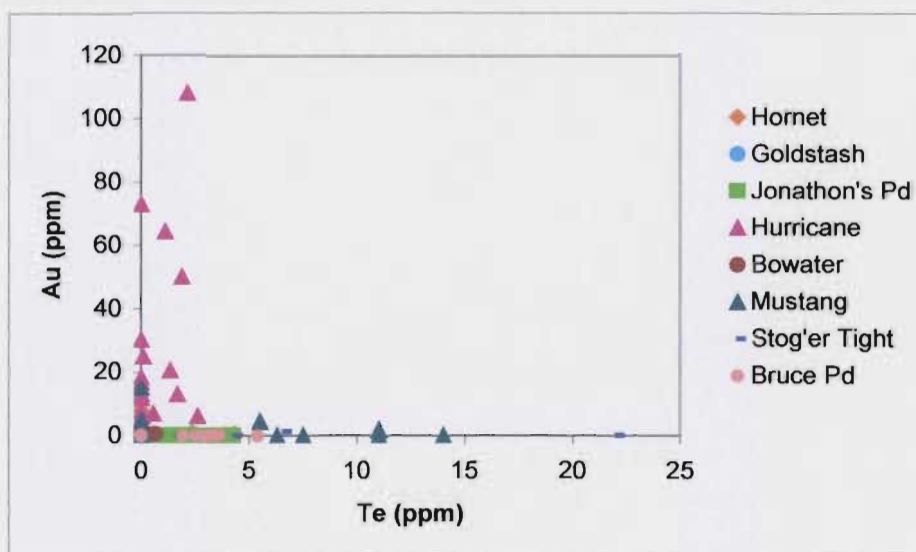


**Figure 7.1g:** Plot of Te vs. Au illustrating that the Mustang Prospect pyrites are elevated in Te contents relative to the other samples.

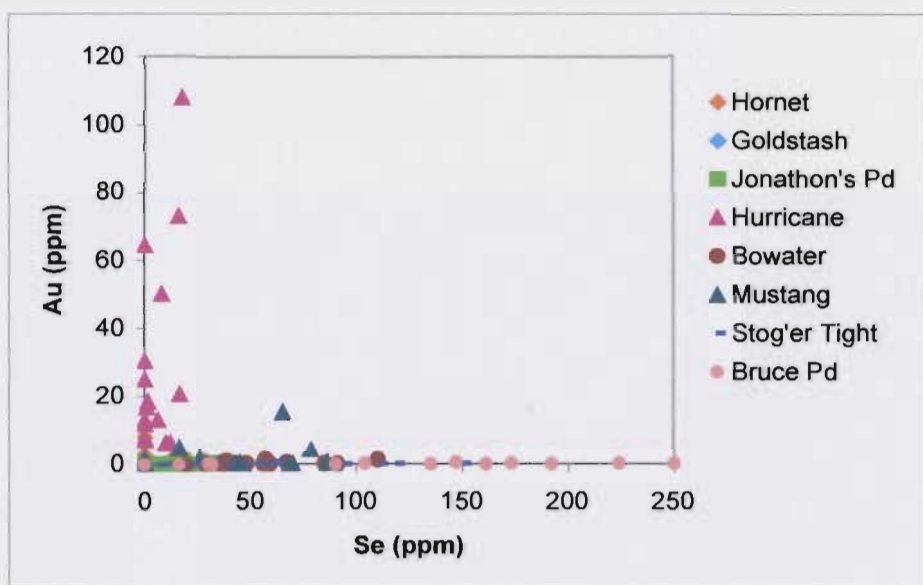


**Figure 7.1h:** Plot of Se vs. Au illustrating that the Bruce Pond Prospect pyrites are elevated in Se contents relative to the other samples.



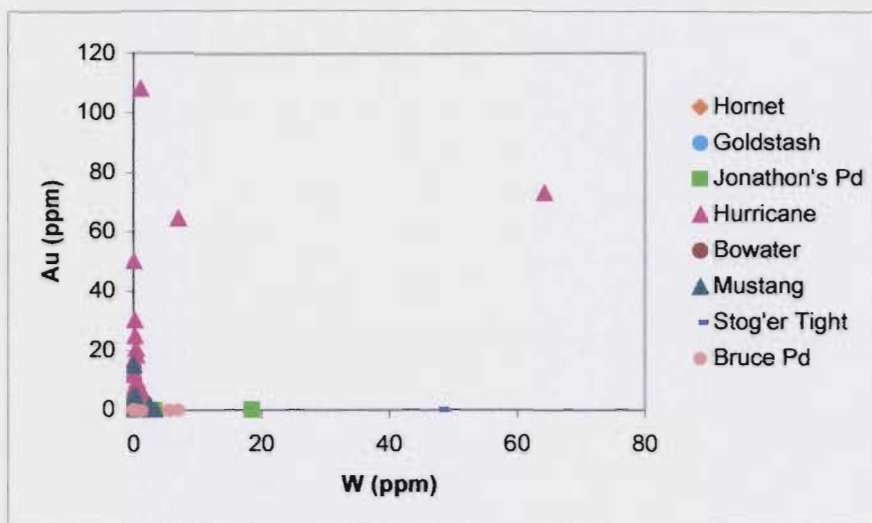


**Figure 7.1i:** Plot of W vs. Au illustrating that one Hurricane Pyrite and one Hornet Prospect pyrite are elevated in W contents relative to the other samples. One sample from Jonathon's Pond has a slightly elevated content.

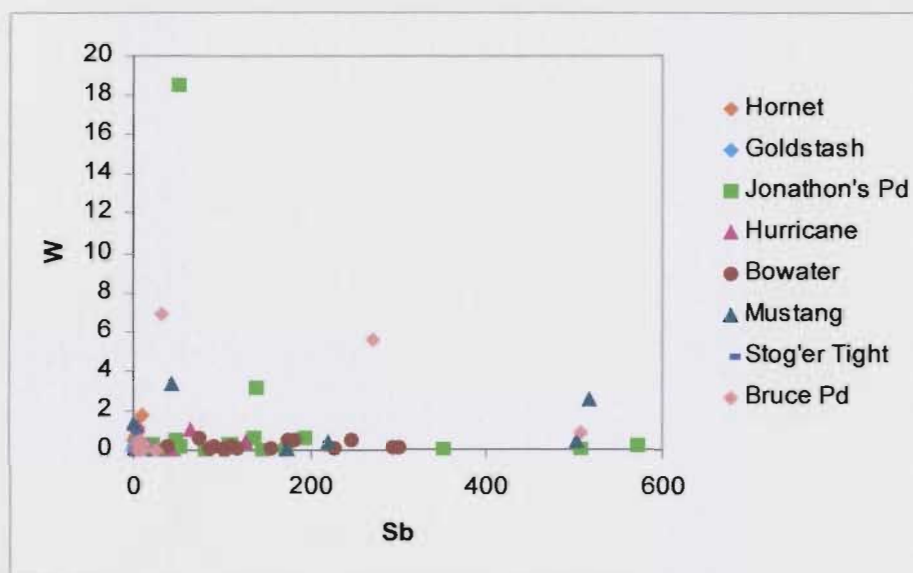


**Figure 7.2a:** Plot of Sb vs. W illustrating that the Jonathon's Pond and Bruce Pond Prospect pyrites are the most elevated in W contents relative to the other samples.

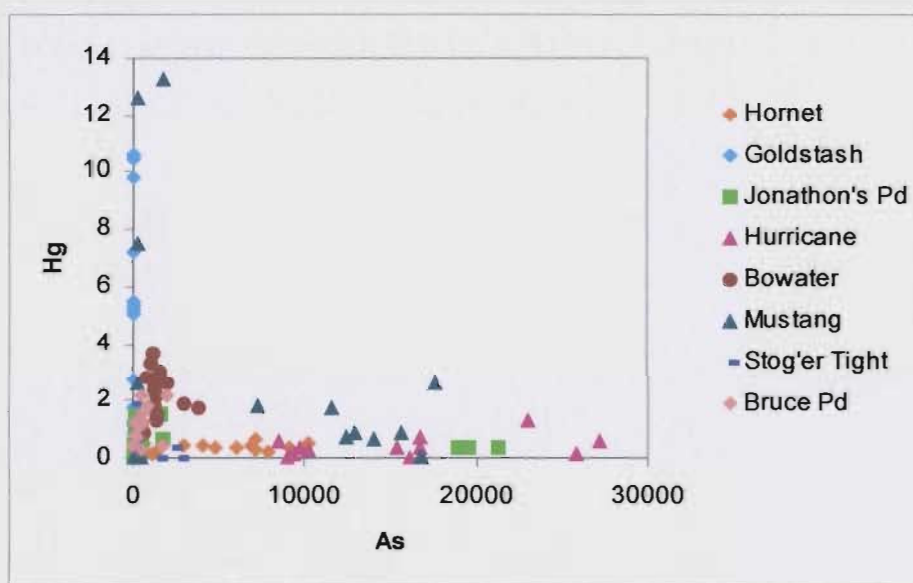


**Figure 7.2b:** Plot of As vs. Hg illustrating that the Mustang and Goldstash Prospect pyrites are the most elevated in Hg contents relative to the other samples. The Hurricane, Jonathon's Pond, Mustang and Hornet Prospects all have elevated As contents. The Mustang and Goldstash pyrite have elevated Hg contents. It should be noted that the grains from the Mustang that have elevated As do not have elevated Hg and vice versa.

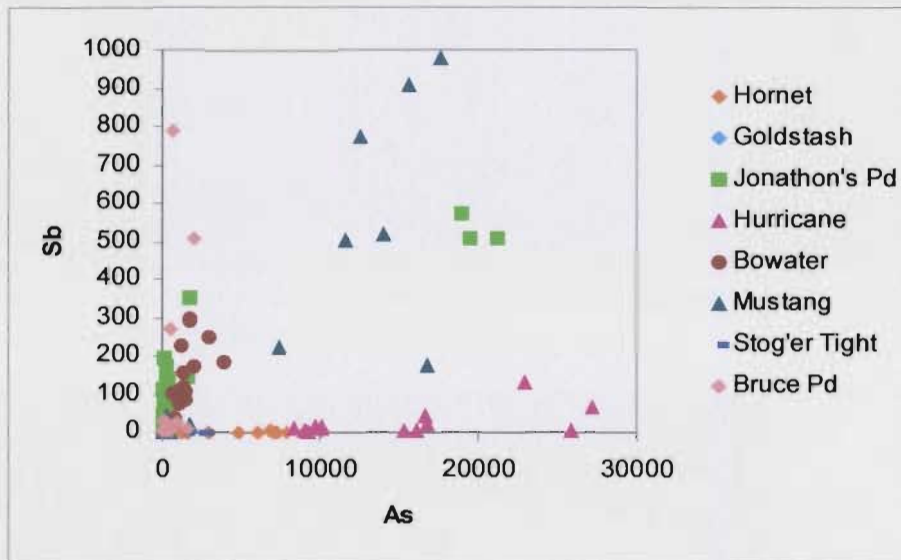


**Figure 7.2c:** Plot of As vs. Sb illustrating that the Mustang Prospect pyrites Sb content increase with As content. Also, Jonathon's Pond samples plot in two distinct groups indicating a possible element zonation in the pyrite grains.

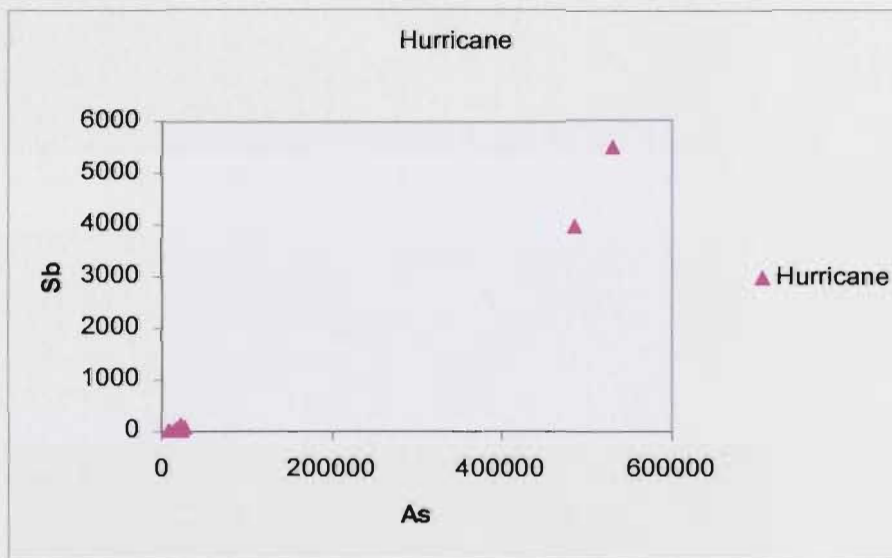


**Figure 7.2d:** Plot of As vs. Sb illustrating the elevated content of As and Sb in two of the Hurricane Prospect pyrites. The differences in concentrations may indicate that trace elements contents exhibit element zonations.





**Plate 7.2:** Outcrop at the Bowater Prospect exhibiting multiple quartz veining in Davidsville Group shale and greywacke.



**Plate 7.3:** Siliceous, quartz brecciated outcrop at the Mustang Zone, Outflow Prospect.



**Plate 7.4:** Conjugate quartz veining in diorite, approximately 100 m upriver from the Hurricane Prospect.



**Plate 7.5:** Outcrop at the Stog'er Tight prospect on the Baie Verte Peninsula, representative of orogenic (or mesothermal) lode gold occurrences. Quartz veins in gabbroic host.

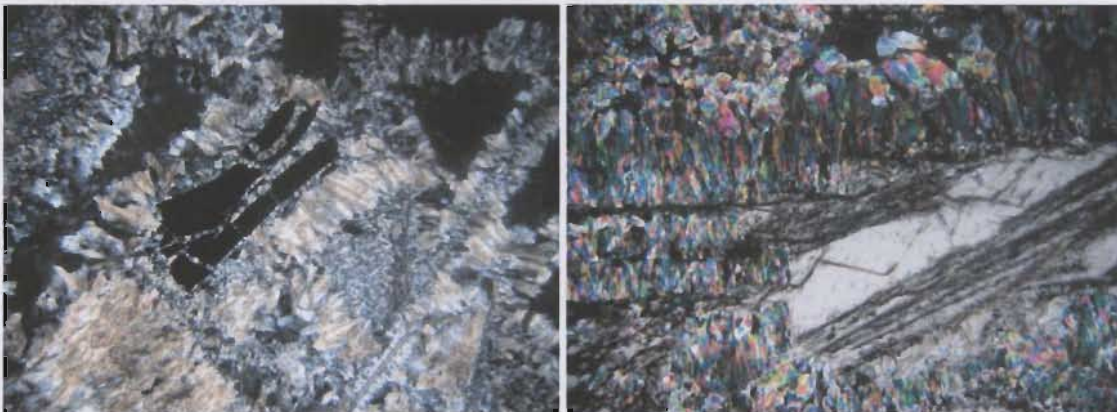


**Plate 7.6:** Photomicrographs of a sample from the Gallery Resources Ltd. Bruce Pond epithermal system. The bladed pyrite crystals in this sample were analyzed as examples of low-sulphidation epithermal systems.



## CHAPTER 8

### U-Pb GEOCHRONOLOGY

#### 8.1 Preamble

Geochronology is one of the primary uses of radiogenic isotope research. This chapter presents the systematics of the U-Pb radioactive decay system, followed by the application of the system to age determinations in the Botwood Basin. U-Pb data are presented for primary igneous zircon from several intrusive lithologies throughout the region and detrital zircon data are described for sedimentary sequences. These new data are compared with previously presented data (*i.e.*, Dunning *et al.*, 1990; Pollock *et al.*, in prep.) for some of these units.

A total of nineteen gabbro, granite, volcanic and sedimentary rock samples from throughout the study area were selected and prepared for U-Pb zircon geochronological studies (see Figure 8.1, p. 268 for locations); nine of these samples produced age determinations. These data will be used to determine if there is a correlation between the different intrusive lithologies within the basin and, in places, suggest maximum ages for the local epigenetic auriferous occurrences. The geochronological data may also define the actual ages of mineralization, for instance, according to Arehart (2003), Carlin-type auriferous systems are broadly synchronous with magmatism that provided heat and/or magmatic components. Furthermore, can different pulses of auriferous mineralizing fluids be differentiated and can the ages of different gabbros/granitoids and potential thermal engines, such as the Mount Peyton, be determined?



The analyses were completed at the Department of Earth Sciences, Memorial University of Newfoundland, LAM-ICP-MS facility following procedures described by Košler *et al.* (2002). To ensure the accuracy and reproducibility of the results, data were also consistently collected on zircon standards of known ages. Concordia and weighted average values were calculated for magmatic samples, whereas Concordia, cumulative frequency and weighted average values were calculated for detrital samples. Cumulative frequency plots are calculated for detrital samples to compare the range of age data from the different sedimentary packages to one another, as well as to assess similarities between the sample and the possible source terrains (Cox, 2002). The  $^{206}\text{Pb}/^{238}\text{U}$  age values were used to plot the cumulative frequency and weighted average plots. Refer to Appendix 4 for unknown sample data and known standard data tables.

## 8.2 Uranium-Thorium-Lead Isotope Systematics

There are four naturally occurring isotopes of lead. Of the four isotopes, three are the end products of complex decay schemes from parent isotopes. The parent isotopes  $^{238}\text{U}$  (99.2745%),  $^{235}\text{U}$  (0.7200%) and  $^{232}\text{Th}$  (100%) pass through a succession of intermediate radioactive daughters to produce stable isotopes of  $^{206}\text{Pb}$  (24.10%),  $^{207}\text{Pb}$  (22.10%) and  $^{208}\text{Pb}$  (52.40%), respectively. The fourth isotope (common lead),  $^{204}\text{Pb}$  (1.40%) is non-radiogenic (*i.e.*, abundance on earth not influenced by the decay of U or Th) and is treated as a stable reference isotope (Dickin, 1995).

The U-Th-Pb system is a valuable tool for age determination because the half-lives of these elements are extremely long and thus the isotopes can be applied over a

large expanse of geological time. The half-life of  $^{238}\text{U}$  is 4.47 Ga, similar to the age of the earth and the half-life for  $^{235}\text{Th}$  is 14.01 Ga, similar to the age of the universe. The half-life for  $^{235}\text{U}$  is much shorter than the other isotopes at 0.704 Ga, therefore almost all the primordial  $^{235}\text{U}$  in the Earth has decayed to  $^{207}\text{Pb}$  (Faure, 1986). The relationship between time, and initial and present day Pb isotopic compositions for the U-Th-Pb system can be expressed in three geochronometry equations as follows (Faure, 1986):

$$^{206}\text{Pb}/^{204}\text{Pb} = [^{206}\text{Pb}/^{204}\text{Pb}]_{\text{initial}} + [^{238}\text{U}/^{204}\text{Pb}] (e^{\lambda_{238}t} - 1)$$

$$\text{where } \lambda_{238} = (1.55125) * 10^{-10} \text{ a}^{-1} ; \text{ half-life} = 4.468 \text{ Ga}$$

$$^{207}\text{Pb}/^{204}\text{Pb} = [^{207}\text{Pb}/^{204}\text{Pb}]_{\text{initial}} + [^{235}\text{U}/^{204}\text{Pb}] (e^{\lambda_{235}t} - 1)$$

$$\text{where } \lambda_{235} = (9.8485) * 10^{-10} \text{ a}^{-1} ; \text{ half-life} = 0.704 \text{ Ga}$$

$$^{208}\text{Pb}/^{204}\text{Pb} = [^{208}\text{Pb}/^{204}\text{Pb}]_{\text{initial}} + [^{232}\text{U}/^{204}\text{Pb}] (e^{\lambda_{232}t} - 1)$$

$$\text{where } \lambda_{232} = (4.9475) * 10^{-11} \text{ a}^{-1} ; \text{ half-life} = 14.01 \text{ Ga}$$

If the U, Th and Pb isotope concentrations are measured and initial Pb is either small enough to be ignored, or can be effectively accounted for, the equations can be solved for t, in the form:

$$t^{206} = [1/\lambda_{238}] * \ln \{ [(^{206}\text{Pb}/^{204}\text{Pb}) - (^{206}\text{Pb}/^{204}\text{Pb})_{\text{initial}} / (^{238}\text{U}/^{204}\text{Pb})] + 1 \}$$

The equations for  $^{207}\text{Pb}$  and  $^{208}\text{Pb}$  can be solved in a similar form resulting in three independent age determinations for minerals or rocks containing both U and Th.

These independent chronometers can then be used to ascertain if the system has remained isotopically closed with respect to U, Th and Pb (Faure, 1986).

A Concordia diagram is a plot of  $^{207}\text{Pb}/^{235}\text{U}$  vs.  $^{206}\text{Pb}/^{238}\text{U}$ , which provides a visual assessment of concordancy (Figure 8.2, p. 269). The Concordia curve is defined by the locus of points where the  $^{238}\text{U}/^{206}\text{Pb}$  age is equal to the  $^{235}\text{U}/^{207}\text{Pb}$  age. All points (ages) that fall along this line are thus considered to be concordant (Dickin, 1995). The Concordia diagram is also useful in relaying information on systems that have not remained isotopically closed (*i.e.*, discordant). Discordant samples do not plot on the Concordia curve and the discordance of the analyses may be attributed to several factors including Pb loss, U loss or gain and mixing between new and old sections of minerals (Heaman and Parrish, 1991; Dickin, 1995). These factors may reflect metamorphism, constant diffusion of Pb, or loss of microcapillary water and chemical weathering near the Earth's surface (Richards and Noble, 1998). Discordant samples may be used to obtain additional information about the material in question, as discordant data will often form linear to sublinear arrays that define what is referred to as a 'discordia'. The upper and lower intercepts of the discordia with the Concordia curve are typically related to times of original crystallization and the subsequent isotopic system disturbance, respectively, that resulted in an open system (Dickin, 1995).

When determining the suitability of a material for U-Pb geochronology several factors are considered: 1) the material should concentrate U and contain minimal amounts of common lead at the time of formation, 2) the material must be correlated with the geological process to be dated (*i.e.*, crystallization, metamorphism, *etc.*), 3) the material must be resistant to isotopic diffusion after the time of formation, and 4) the material



should be relatively common in the crust and easily recoverable (Faure, 1986; Heaman and Parrish, 1991; Richards and Noble, 1998; Dickin, 1995). Thus, minerals are more suitable to these constraints than whole rock samples.

The minerals which best fit these requirements, and are thus commonly used for U-Pb geochronology, include zircon ( $\text{ZrSiO}_4$ ), titanite ( $\text{CaTi}[\text{SiO}_3]$ ), monazite ( $\text{CePO}_4$ ) and baddeleyite ( $\text{ZrO}_2$ ). For the current study, zircon crystals are used. Zircon is actually the most widely used accessory mineral for age determinations via this method for several reasons: 1) it is a common accessory mineral in many rocks as it can crystallize in a variety of different magma compositions and can grow during metamorphism, 2) it is resistant to mechanical weathering (due to a hardness of 7.5), 3) it is extremely resistant to chemical weathering and metamorphism, thus it is likely to remain a closed system, and 4) it concentrates U (and to a lesser extent Th) and excludes Pb typically resulting in high  $^{238}\text{U}/^{204}\text{Pb}$  ratios at the time of formation (Dickin, 1995). Zircon grains stay in the earth's crust almost indefinitely and thus, are easily recoverable (Mezger and Krogstad, 1997).

### **8.3 Sample Overview**

In total, 20 samples were processed for U-Pb geochronology including JOD08, JOD21, JOD25, JOD39, JOD57A, JOD66A, JOD81A, JOD90A, JOD97A, JOD98, JOD99, JOD100, JOD108, JOD04-01, JOD04-09, JOD04-13, JOD040-17, JOD04-20, W03-27 and W03-38 (refer to table A3.3 for sample description and ages and table A4.5 for processing results).

Sample JOD81A is from a least altered gabbroic dyke or sill that hosts auriferous mineralization at the Greenwood Pond #2 showing and sample W03-38 was collected from a felsic intrusive unit at the Huxter Lane Prospect in the southern Botwood Basin.

Samples JOD90A and JOD04-17 consist of unaltered granite from Red Rock Brook and a resource road northwest of Red Rock Brook, respectively. Samples JOD21 and JOD25 were both collected from a diorite phase of the bimodal MPIS along Salmon River. Sample JOD21 is unaltered diorite from the Hurricane Prospect and JOD25 is slightly altered diorite from the Corsair Prospect. The Salmon River and Red Rock Brook samples should provide ages for two phases of the MPIS batholith.

Samples JOD108 and JOD04-20 were collected from a dioritic dyke intruding Indian Islands Group sediments in a pit west of Glenwood which Dickson (1996) postulated to be related to the MPIS. Sample W03-27 was collected from the Charles Cove Pluton at the Tim's Cove Prospect, which is intrusive along the contact between the Davidsville and Indian Islands groups.

Sample JOD39 was collected along the contact between the Silurian Indian Islands Group and shale (presumably Caradocian); it consists of dark, dense material originally thought to be a mafic dyke, but later classified as sedimentary from petrography and geochemistry (refer to chapters 4 and 5, respectively). Determining in situ ages of detrital zircon from this sample may help to delineate possible source terrains for the upper Davidsville or lower Indian Islands groups.

Sample JOD08 is a volcanic fragment from the conglomerate near Bellman's Pond. This conglomerate has been variously mapped as either Davidsville Group or a later Devonian package (Currie, 1995), but has been reaffirmed as part of the Davidsville

Group in the current study (refer to chapter 4). This sample was analyzed to ascertain if definition of an age for a lithic fragment from within the conglomerate could help to resolve this debate.

Eight samples were collected from gabbroic rocks cutting the Ten Mile Lake Formation and Duder Group, north of the Trans Canada Highway as mapped by Evans *et al.* (1992) and Currie (1993 and 1995a). These include: (1) JOD100 from a gabbroic body north of Twin Ponds; some of the gabbro outcrops in this area contain disseminated sulfides, (2) JOD57A and JOD04-09, both from presumably the same gabbroic dyke intruding the Ten Mile Lake Formation to the west of Ten Mile Lake, and (3) JOD04-13 from a previously unmapped gabbroic dyke immediately east of Ten Mile Lake. The samples collected in the Duder Lake vicinity had been previously mapped as either gabbroic dykes or sills in Davidsville Group rocks (Evans and Churchill, 1992), or tectonic blocks in the Duder Complex (Currie, 1995b), and include: 1) JOD66A and JOD04-01 from a metamorphosed gabbro, similar to that which hosts the Duder Lake Prospects, collected from a knobby hill east of Birchy Bay and north of the Duder Lake Prospects, and 2) JOD97A, JOD98 and JOD99 from the gabbroic auriferous host rock at the Corvette, Goldstash and Flirt prospects, respectively.

Of the twenty samples prepared, only eleven contained zircon grains. The samples that did not contain zircon, JOD57A, JOD66A, JOD81A, JOD97A, JOD98, JOD99, JOD108, JOD04-01 and JOD04-20, were also examined for other dateable minerals such as baddeleyite or titanite, but the samples did not contain any. Extra material from these samples was processed but did not yield any datable minerals. Of the eleven samples that did contain variable amounts of zircon grains, nine (JOD08, JOD21,



JOD25, JOD39, JOD90A, JOD04-17, JOD100, W03-27 and W03-38) have been analyzed via LAM-ICP-MS.

## 8.4 Results

### 8.4.1 Hurricane Diorite (*Mount Peyton Intrusive Suite*)

Sample JOD21 is a slightly altered, unmineralized diorite from the Hurricane Prospect at UTM coordinates 645161/ 5425138. Approximately 40 zircon grains, ranging in size from 20 x 40µm to 30 x 60µm, were picked from the sample. The crystals are mostly elongate and euhedral and exhibit a brownish core (Plate 8.1, p. 254). The sample was analyzed in backscatter electron (BSE) mode on the electron microprobe (EMP) at the Earth Science Department labs, Memorial University, and the brown core was determined to be zircon and compositional zoning or evidence of inheritance was not observed in the grains. Laser ablation traverses were made across the brownish 'core' and surrounding clear 'rim', and the resulting data did not indicate any differences in age, which further disproves the existence of an inherited core in this sample. A Concordia age of  $405 \pm 11$  Ma was calculated for this phase of the intrusion (Figure 8.3, p. 270).

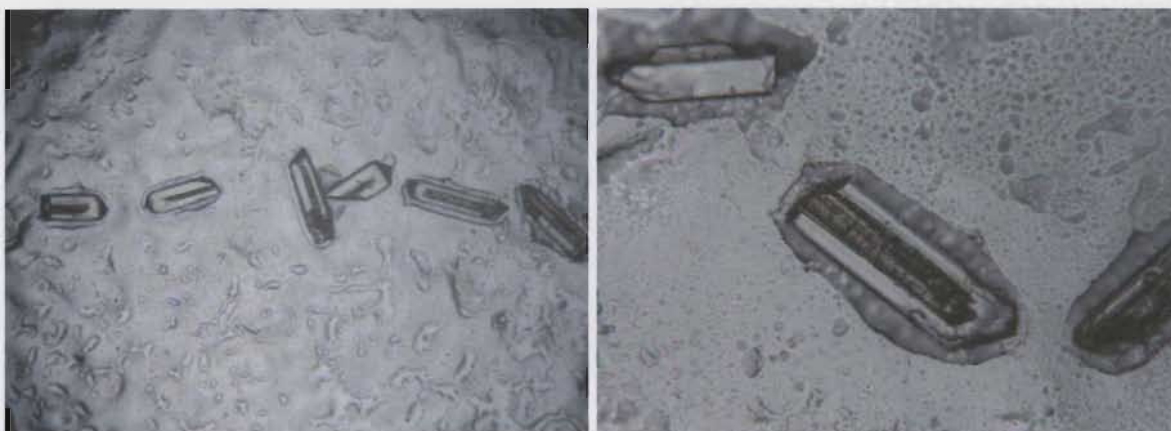


**Plate 8.1:** a) Row of prismatic zircon grains from sample JOD21 mounted in an epoxy resin puck [Field of view 7mm PPL]. B) Close up of zircon grain from mount exhibiting brownish core [Field of view 2mm, PPL].

#### 8.4.2 Corsair Diorite (*Mount Peyton Intrusive Suite*)

Sample JOD25 is of unaltered diorite from the Corsair Prospect at UTM coordinates 644408/ 5425289 and approximately 50 zircon grains were picked from the sample. The crystals are generally elongate, clear, and some are broken, ranging in size from 30 x 30 $\mu$ m to 50 x 120 $\mu$ m. A few grains are small and rounded and some have a slight yellow tint. The sample was analyzed in backscatter electron (BSE) mode on the scanning electron microprobe (SEM) at the Biology Department labs, Memorial University. The images so obtained indicate that the grains are similar in that they are generally euhedral and somewhat elongate (Plate 8.2, p. 255). No evidence of compositional zoning is indicated by the images. A Concordia age of  $427 \pm 4.2$  Ma was calculated for this phase of the intrusion (Figure 8.4, p. 271).



**Plate 8.2:** Backscatter Electron Microprobe images for sample JOD25 of the Corsair Prospect, MPIS diorite. The grains are generally elongate and homogenous with no apparent zoning.

#### 8.4.3 Twin Ponds Gabbro

Sample JOD100 was collected from a gabbroic dyke (Evans *et al.*, 1992) that intrudes the Ten Mile Lake Formation (Currie, 1995a) north of Twin Ponds at UTM coordinates 652973/ 5438288. There are several gabbro outcrops in this area (previously mapped as one intrusion) that appear to be a related unit. Approximately 40 zircon grains were picked from the sample and the grains were generally euhedral (some were broken) and some appeared to have small inclusions and slight elemental zoning. The grains range in size from 40 x 40µm to 80 x 120 µm and range in color from pale yellow to clear and a lesser amount of very pale pink. BSE electron microprobe images indicate that the grains have what appears to be oscillatory compositional zoning; but generally the grains are similar and no definable inherited cores or the like were detected (Plate 8.3, p. 256). A Concordia age of  $429.3 \pm 4.4$  Ma was obtained on the LAM-ICP-MS (Figure 8.5, p. 272), indistinguishable from the age obtained from the Corsair Prospect diorite.



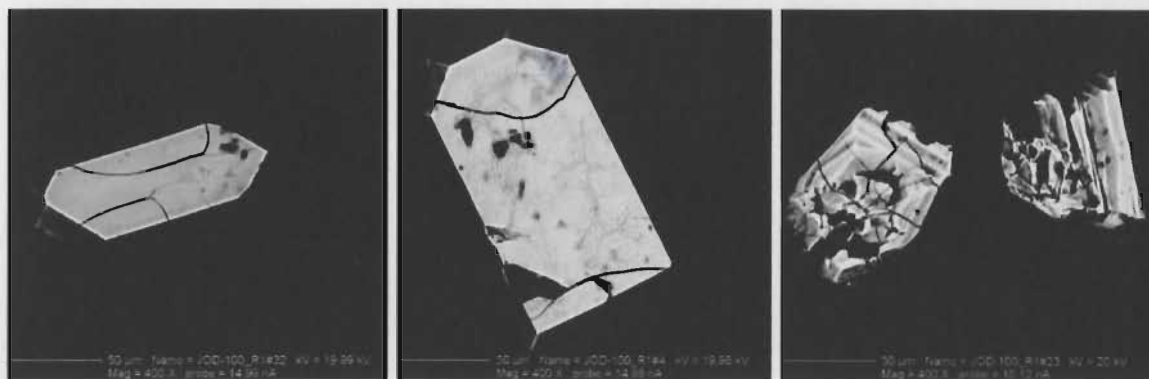


**Plate 8.3:** Backscattered electron microprobe images for Sample JOD100. The grains are mostly homogeneous but a few of the grains exhibit oscillatory compositional zoning.

#### 8.4.4 MPIS granite

Sample JOD04-17 was collected from the central portion of the exposed MPIS granite body along a newly constructed resource road. The sample is undeformed and fresh and approximately 35 grains were picked from the sample. The grains range in size from 20 x 30µm to 50 x 80µm in size but are generally small and subhedral. Most grains have impurities and appear dirty or fractured (Plate 8.4, p. 257). Two large round clear grains contained small prismatic pink zircon grains within their crystals. A Concordia age of  $409 \pm 4.5$  Ma with one discordant point at *ca.* 1800 Ma was obtained for this sample (Figure 8.6, p. 273).



**Plate 8.4:** Backscattered electron microprobe images for Sample JOD04-17. The grains are very fractured and contain small inclusions.

#### *8.4.5 Red Rock Brook Granite (Mount Peyton Intrusive Suite)*

Sample JOD90A was collected from Red Rock River and is a fresh piece of the pink Mount Peyton granite. Approximately 40 clear to pale pink, subhedral, elongate and broken zircon grains were picked from the sample. The grains range in size from  $40 \times 30 \mu\text{m}$  to  $60 \times 120 \mu\text{m}$  in size. BSE analyses did not reveal any evidence of inherited cores but some degree of compositional zoning and inclusions may be present in several grains (Plate 8.5). The data define a discordia age of  $381 \pm 18 \text{ Ma}$  (Figure 8.7, p. 274). The range in data suggests that the zircon grains contain mixed Pb contents with magmatic zircon from the actual granite magmatism and inherited older zircon. As previously indicated by Dunning and Manser (1993), the granite phase of the MPIS exhibits complex geochronological systematics and more work needs to be completed on this material in an attempt to better define the ages of the intrusion and inherited material.

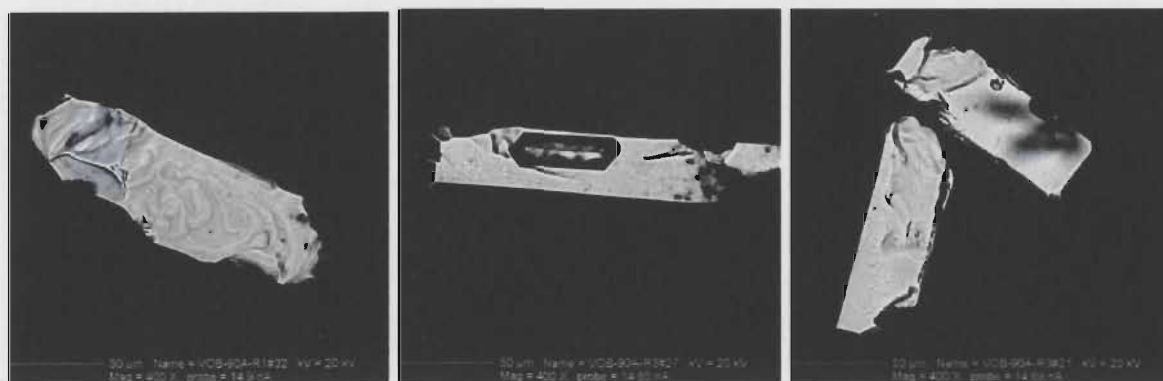


**Plate 8.5:** Backscattered electron microprobe images for Sample JOD90A, MPIS granite. Images reveal broken grains with mottled appearance and possible inclusions (the inclusions were not zircon).

#### 4.8.6 Charles Cove Pluton

The Charles Cove granodiorite (sample collected at the Tim's Cove Prospect) intruded both the Silurian Indian Islands Group and the Ordovician Davidsville Group along their mutual contact. There has been some debate as to the actual host unit to the granodiorite since Currie (1995) mapped the pluton as being surrounded by Davidsville Group rocks. Re-mapping of the area in 2003 indicated that the unit which Currie (*op cit.*) mapped as Indian Islands Group on the shoreline is the same unit along the eastern margin of the granodiorite. Wilton and Taylor (1999) indicated that granodiorite slightly hornfelsed the Indian Islands Group siltstones.

Geochronological analysis of this pluton was conducted because of its auriferous nature and because it is the single largest felsic intrusion in the region of the Botwood Basin, aside from the Mount Peyton Intrusive Suite. Sample W03-27 was collected at UTM coordinates 681434/ 5475798. The LAM-ICP-MS analyses of zircon separates from the granodiorite defined a late Silurian concordia age of  $429 \pm 19$  Ma (Figure 8.8, p.



275) with an upper intercept at 1850 Ma. The data define a discordia line which is suggestive of the presence of a mixture of young zircons from the *ca.* 429 Ma group to very old Proterozoic zircon. The low precision of this date is directly related to the discordance of the younger group indicating possible inheritance from the older grains (O' Driscoll and Wilton, 2005). This suggests that the granodiorite magma either inherited Proterozoic zircons enroute to intrusion or was derived as a partial melt of Proterozoic crust. More detailed work is required to refine the upper intercept and hence possible basement rocks to this part of the Dunnage Zone. Pollock *et al.* (in prep.) report a zircon with an age of 1843 Ma from the Indian Islands Group that they suggest may have been derived from the Makkovik Province, Laurentia.

#### 8.4.7 Huxter Lane

Sample W03-38 represents host rock from the so-called 'intrusion related', Huxter Lane auriferous showing in the Late Cambrian to Middle Ordovician Coy Pond Complex. The area, which hosts the prospect, was previously mapped as gabbro to diabase by Colman-Sadd (1985), however, trench mapping and petrographical analysis indicates that the host consists of a dacitic lithology.

Approximately 40 zircon grains ranging in size from 40 x 40µm to 50 x 120µm were picked from this sample and in general the grains were clear to very pale yellow and ranged from euhedral, needlelike to equi-dimensional grains. A couple of the smaller grains exhibit minor compositional zoning (Plate 8.6, p. 260). An age of  $497 \pm 7$  Ma was

obtained by the LAM-ICP-MS (Figure 8.9, p. 276), which is within the age range defined for the complex by Colman-Sadd (1985).

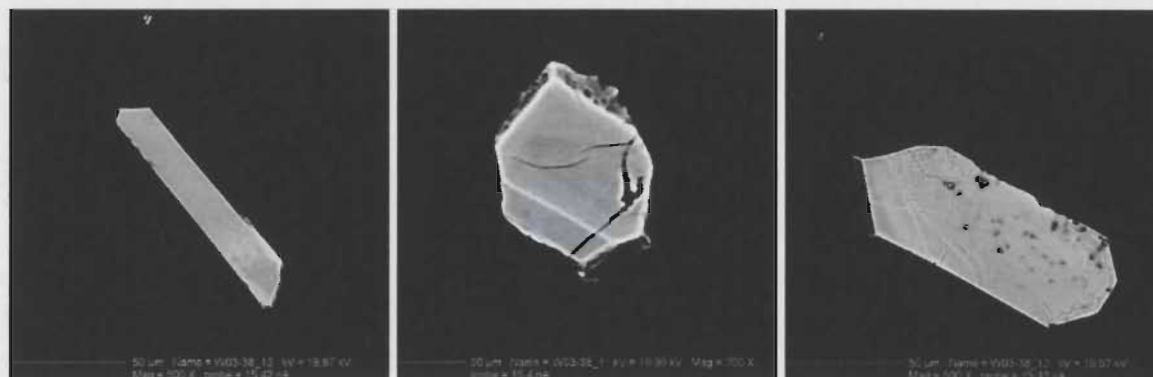


**Plate 8.6:** Backscatter Electron Microprobe images for Sample W03-38, Huxter Lane Intrusive.

#### *8.4.8 Contact between Davidsville and Indian Islands Groups*

Sample JOD39 was collected at the contact between the Silurian Indian Islands Group and shales (either the Davidsville Group or the Caradocian shale). The sample was collected from a massive, dark, dense rock within the shale unit originally thought to be a mafic dyke. Petrographical analysis indicates that the rock is actually a sedimentary rock composed of unaltered clast-supported sand-sized grains of carbonate, feldspar and quartz; the source appears to be gabbroic. Approximately 30 zircon grains were picked from the sample and in general the grains appear to be small and euhedral with some elongate crystals present. One of the grains was somewhat rounded and appeared to be compositionally zoned. The grains range in size from 20 x 20µm to 60x 100 µm. Minor compositional zoning was noted on some of the wider grains and a few of the grains had small inclusions. Two different ages were obtained from the analysis (Figure 8.10, p.

277). One group of grains yield average Concordia ages of  $472 \pm 8.5$  Ma and others were at *ca.* 900 Ma. Pollock *et al.* (in prep.) report detrital zircon ages from the Davidsville Group of 507 to 449 Ma and 964 to 886 Ma; thus the detrital sample is probably from the Davidsville Group in agreement with the mapping observations of Boyce *et al.* (1993).

#### 8.4.9 Bellman's Pond conglomerate clast

Sample JOD08 is a clast from the conglomerate at Bellman's Pond at UTM 670009/ 5447133. Originally the clast was thought to be a volcanic fragment. The clast has an intense green carbonate alteration and abundant sulfides. The sample was rather poor in zircon with only five very small, pink and rounded grains recovered. Petrographic examination indicates that the rock is actually an extremely altered felsic tuff (chapter 4). These grains yielded several very old ages from the mid Proterozoic *ca.* 1550 Ma to 1775 Ma (Figure 8.11, p. 278). These detrital ages far exceed the Paleozoic age of the host conglomerate, but forcefully illustrate the ancient crustal material available for sampling in the region, probably from the Gondwanan margin (*cf.* Pollock *et al.*, in prep.; Murphy *et al.* (in press)).

### 8.5 Discussion: Geochronology and the Mount Peyton Intrusive Suite in Relation to Previous Work

Two of the intrusive rocks analysed in this study (JOD25 and JOD100) define a *ca.* 430 Ma (mid-Silurian) age for magmatism in the central and northern Botwood Basin region. These dates suggest that at least some intrusive activity to the north coincided



with phases of MPIS magmatism. The MPIS magmatism was bimodal in nature as the rocks analysed range from gabbro through granodiorite and diorite to granite.

It has proven difficult to definitively pinpoint exact magmatic ages for the various phases of the MPIS. As seen in attempts to date both the granitic phase (JOD90A and JOD04-17) and the intermediate phase (JOD21 and JOD25), the zircon grains are small and some of the grains from the felsic phase contain evidence of inheritance. Thus undisputable Concordia ages were difficult to produce. Starting with the granitic phase, two ages were obtained from two samples collected at different localities. A very discordant age of  $381 \pm 18$  Ma was obtained from JOD90A collected near a presumed faulted contact with Indian Islands Group sediments and a concordant age of  $409 \pm 4.5$  Ma was obtained for a sample of the granite collected towards the centre of the intrusion, away from any known fault zones. The JOD90A age is considered less reliable due to the discordancy of the plot and the large error ellipses. The JOD04-17 age is considered more accurate because the points are concordant with smaller error ellipses, and cluster around one age. Both samples indicate that the granite phase of the MPIS contains inherited older zircon. In sample JOD90A, inheritance was suggested by the discordancy of the plot, whereas in sample JOD04-17, one grain actually yielded an inherited age of *ca.* 1800 Ma. The presence of inherited zircon in these samples further indicates that the MPIS granite was formed from crustal anatexis as was first suggested by Strong (1979). The data for the Charles Cove Pluton also lend credence to the suggestion that Silurian granitoids were generated as partial melts of old crust that contributes zircons to the melts. The discordant plot of the Charles Cove Pluton suggests the presence of inheritance and one grain yielded an age of *ca.* 1850 Ma indicating a possible common

crustal source for inherited zircon in Silurian granitoids.

The intermediate diorite phase also yields two conflicting ages. Sample JOD21 collected at the Hurricane Prospect yielded a Concordia age of  $405 \pm 11$  Ma and sample JOD25, collected 100 m up the Salmon River at the Corsair prospect, yielded a Concordia age of  $427.6 \pm 4.2$  Ma. The older age corresponds with the Concordia age of  $429.3 \pm 4.4$  Ma for the gabbro dyke to the north of the MPIS mapped by Evans *et al.* (1992). It was initially assumed that this proved a genetic relationship between the MPIS and intrusive dykes or sills to the north (*i.e.*, O' Driscoll and Wilton, 2005). However, this interpretation has become more difficult to sustain with the introduction of a younger age for the MPIS (it should be noted, however, that the 405 Ma age has considerably larger error). In fact, this data, as well as the data for the felsic portion of the MPIS suggest that central Botwood Basin magmatism was not simultaneous and that intrusion of the various felsic to intermediate phases was episodic over 30 Ma.

This episodic nature of MPIS magmatism also has been suggested in the Botwood Basin by a recent U-Pb SHRIMP geochronological study by McNicoll *et al.* (in press). This study produced an age of  $430.6 \pm 3.4$  Ma for an intrusive mafic body north of the MPIS and McNicoll *et al.* (in press) produced ages of  $411 \pm 5$  and  $381 \pm 5$  Ma for mafic dykes that both intrude the Indian Islands Group and host auriferous mineralization in the northern Botwood Basin. The disparities in these age results suggest that these units formed from different pulses of magma in the north from at least 430 to 381 Ma. Thus, magmatic pulses, at least in the central to northern Botwood Basin, continued over an extended period of time during the Middle Silurian to Middle Devonian.

Past attempts to define the age of the Mount Peyton Intrusive Suite have been

particularly difficult. Bell *et al.* (1977) defined a Rb-Sr age of  $390 \pm 15$  for the Mount Peyton Intrusive Suite (MPIS) granite. Reynolds *et al.* (1981), on the other hand, defined a  $420 \pm 8$  Ma Ar/Ar age for biotite and hornblende from the gabbro phases. Dunning (1992) dated a pegmatitic gabbro originally interpreted to be from the MPIS gabbro near Rolling Pond and defined a U-Pb zircon age of  $424 \pm 2$  Ma. Dunning (1994) dated a diorite phase of the northern MPIS from near Norris Arm with the same  $424 \pm 2$  Ma U-Pb zircon age. Mitchinson (2001), however, showed that the Rolling Pond pegmatite is actually part of the geochemically distinct Caribou Hills Intrusive Suite that was intruded by the MPIS gabbro.

In 1992 Lawson Dickson of the NLDNR (Geological Survey) collected a fine-grained, miarolitic granite at Red Rocks Brook, near the probable faulted contact with the Indian Islands Group (Dickson, 1993; Squires, 2005) siltstone and sandstone. Five zircon fractions were removed from the sample and analysed by Dunning and Manser (1993). The authors described the grains as numerous small crystals. Two possible age interpretations were obtained from the U-Pb isotope data (Dunning and Manser, *op cit.*) as: 1) fractions 1,2 and 3 defined a mixing line (37% probability to fit) that extended from  $419 \pm 2$  Ma to 2680 Ma, which the authors (*op. cit.*) dismissed as it required old inherited zircons to be present in all fractions to be correct and 2) fractions 1,3, and 5, which yielded a discordia line (56% probability to fit) that intersected Concordia at  $31 \pm 85$  Ma and  $439.5 \pm 9/-6$  Ma. Dunning and Manser (*op. cit.*) preferred this older age for the granite and noted that  $^{207}\text{Pb}$ - $^{206}\text{Pb}$  ages for the four fractions agreed within error.

L. Dickson (written communication, 2005) prefers the  $419 \pm 2$  Ma age for the granite based on geological observations as the MPIS gabbro phase is nowhere seen to



intrude the granite and Dunning (1992, 1994) had dated the gabbro phase at 424 Ma. Thus, a younger age for the granite would be more geologically accurate. The field observations, as well as geochronological results from this study support the theory that the gabbro phase is older than the granite phase.

Based on the problems encountered in previous studies (*i.e.*, Dunning and Manser, 1993; O' Driscoll and Wilton, 2005) and the current LAM-ICP-MS work it is obvious that zircon inheritance is an intrinsic feature of the Silurian granitoids. In fact, the data from the Charles Cove pluton (CCP) infers that Silurian granitoids rocks may have been generated as partial melts of old crust, from which old zircons became incorporated. The presence of these inherited zircons in the granitic phases of both the MPIS and CCP supports the model of Strong (1979) and Strong and Dupuy (1980) that the MPIS gabbroic rocks represent mantle melts and that the granites represent partial melts of lower crust by these mantle melts. Based on the results of this study, traditional Thermal Ionization Mass Spectrometry (TIMS) zircon dating (which is usually not done on single zircon crystals) should be used with caution when dating these Silurian granitoids as the technique would simply define average ages for the zircon separates.

This study has also shown that magmatic activity was prevalent from at least the Middle Silurian to Early Devonian in the central to northern Botwood Basin. Some of the northern magmatism does coincide with the MPIS magmatism but a definitive link that would define a common widespread magmatic event has not been identified.

## 8.6 Significance of Dates to Regional Metallogeny

Gabbro to granite intrusions in the central to northern Botwood Basin suggest that periodic episodes of high heat flow were prevalent from Middle Silurian to Early to Middle Devonian. The magmatism was bimodal as rocks ranging from gabbro through to minor granodiorite and diorite to granite were observed. The MPIS diorite and the Twin Ponds gabbro define a common *ca.* 430 Ma age for one of these pulses of magmatism. Geochemistry was utilized in chapter five in an attempt to determine if the intrusive units share a common magma source. The Twin Ponds gabbro is geochemically similar to the MPIS, however, gabbroic hosts to the mineralization at Duder Lake appeared to be geochemically distinct; an age for these latter bodies could not be obtained because they did not contain any dateable minerals. Linkage of the Twin Ponds gabbro with the MPIS indicates that at least some of the intrusives to the north share a common magma source with the MPIS and therefore, the spatial extent of the deep-seated magmatism is greater than previously realized. It is likely that even though magmatism was widespread, the intrusives to the extreme north (*i.e.*, Duder Lake) may have originated from a different magma source than the MPIS.

In all models suggested for Carlin-style gold deposits (*e.g.*, Arehart, 1996, 2000, 2003; Hofstra and Cline, 2000), and indeed epithermal and orogenic types of deposits, a large-scale heat flow system is a fundamental requirement. Since episodes of periodic magmatism in the central to northern Botwood Basin were prevalent from Middle Silurian to Early Devonian, it may have had some influence on mineralization systems at local scales. Several authors have illustrated that some of the mesothermal style

occurrences in the northern Botwood Basin are Early Devonian or younger (McNicoll *et al.*, in press; Squires 2005). However, age determinations have not been defined for the auriferous occurrences along the eastern edge of the MPIS. It is feasible that the early Devonian intrusion of the MPIS granite may have influenced mineralization at these locations. In chapter 7, it was suggested that the mixing model for genesis of Carlin-type deposits of Berger and Bagby (1991) may be applicable to some of the occurrences along the eastern margin of the MPIS. In that scenario, the MPIS granite acted as a driving force for mineralizing fluids. The Early Devonian age for the granite further enhances the applicability of such a model.



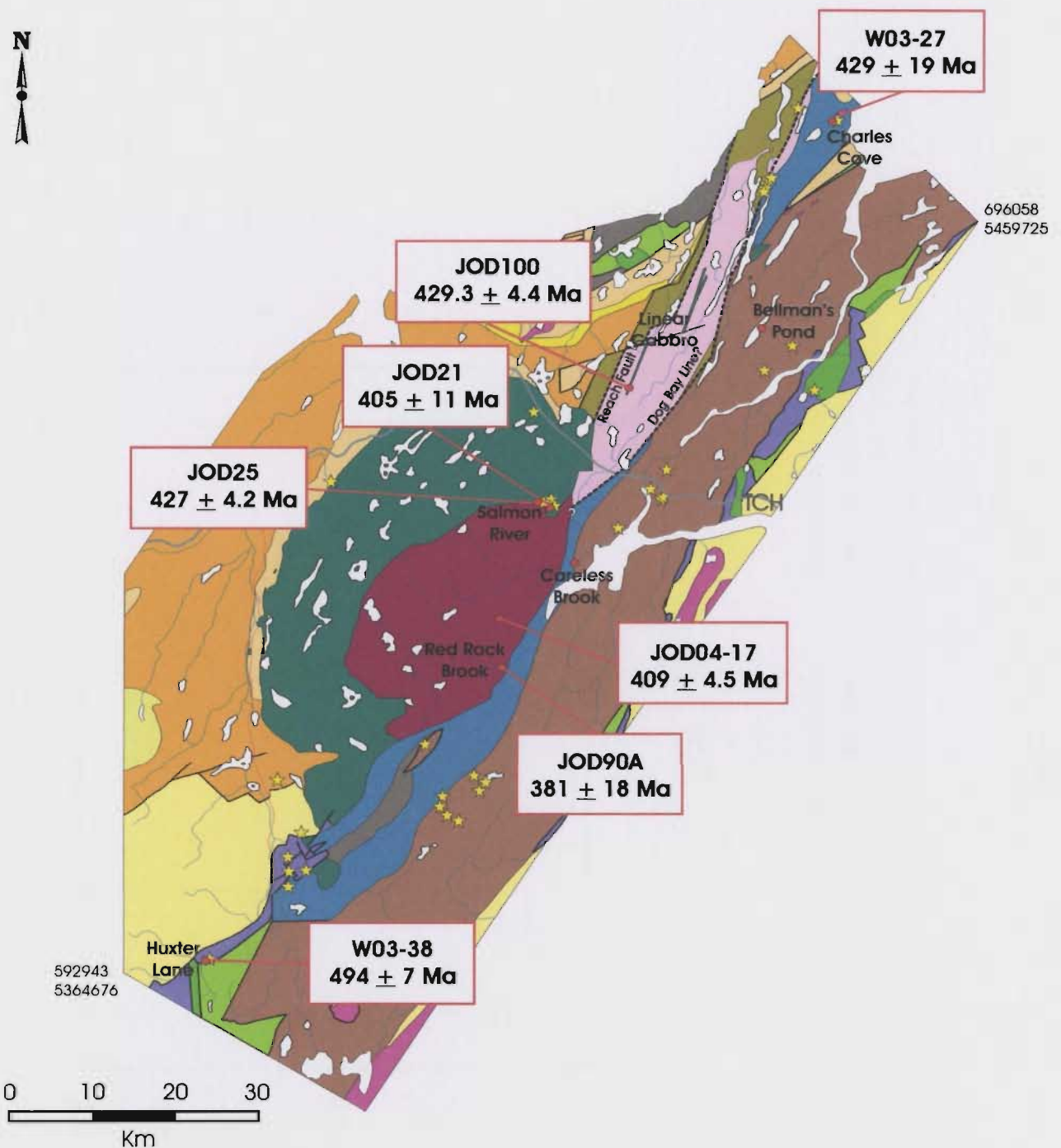


**Figure 8.1:** Generalized geology map of the Botwood Basin and environs, and specific locations of auriferous showings sampled for this study (yellow stars) and location of geochronological samples (red circles) from which U-Pb ages were obtained. Obtained ages for magmatic samples are indicated on map. Refer to figure 2.4 for corresponding legend (Geology modified from Colman-Sadd and Crisby-Whittle, 2002).

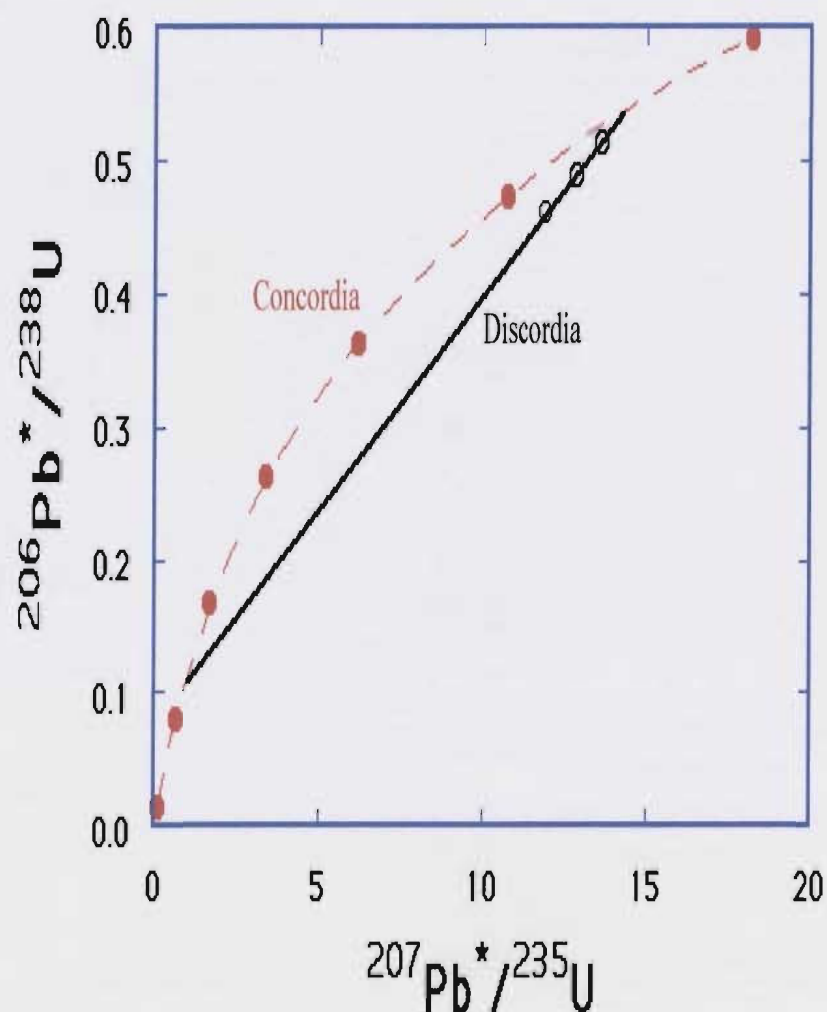


**Figure 8.2:** Concordia diagram illustrating the Concordia Curve and a line of discordia. Any point along the Concordia curve would produce a concordant or accurate date for the material being tested, whereas discordant points will result from either Pb loss or U loss/gain. Discordant points can be useful if they produce a linear or sublinear discordia as the upper intercept should represent time of formation and the lower intercept should represent the disturbance to the system.

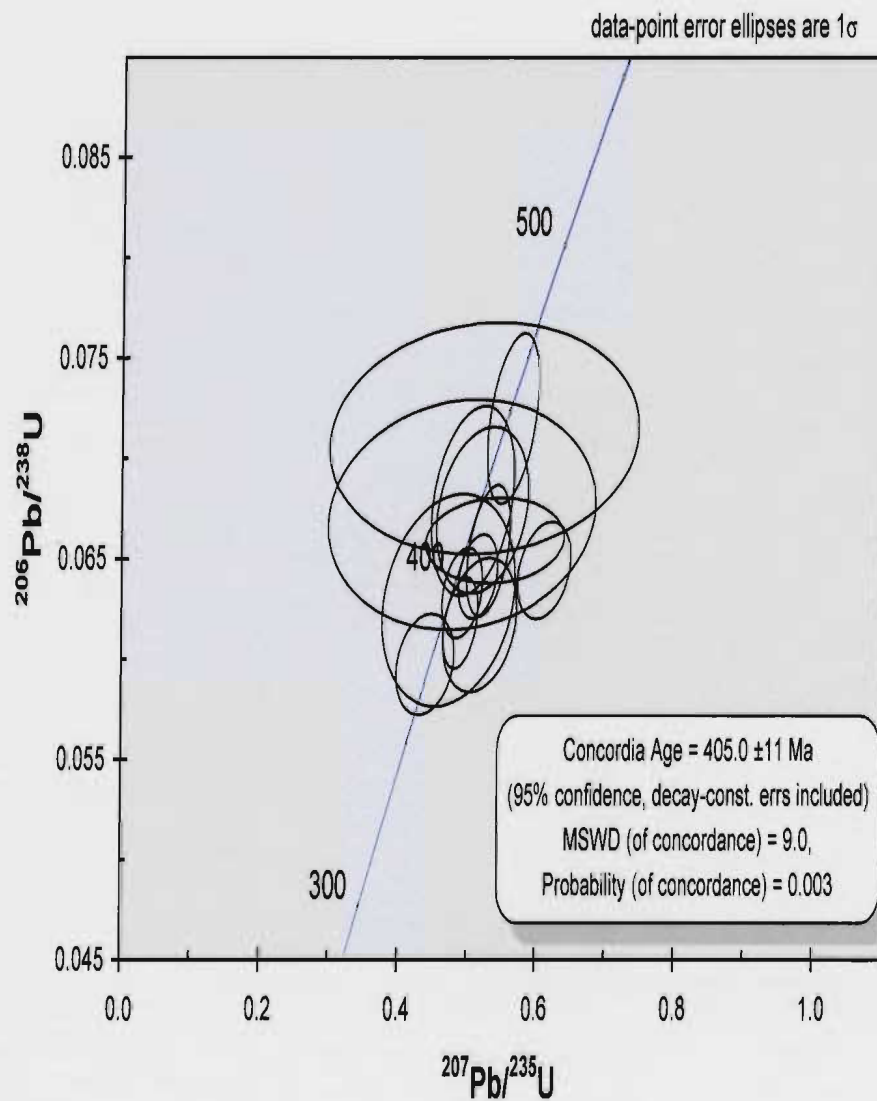


**Figure 8.3:** Concordia diagram for sample JOD21, Hurricane Prospect; the size of the ellipse represents the error measurement ( $1\sigma$ ) for that particular analysis [MSWD= Mean Square of Weighted Deviates indicating the goodness of fit].



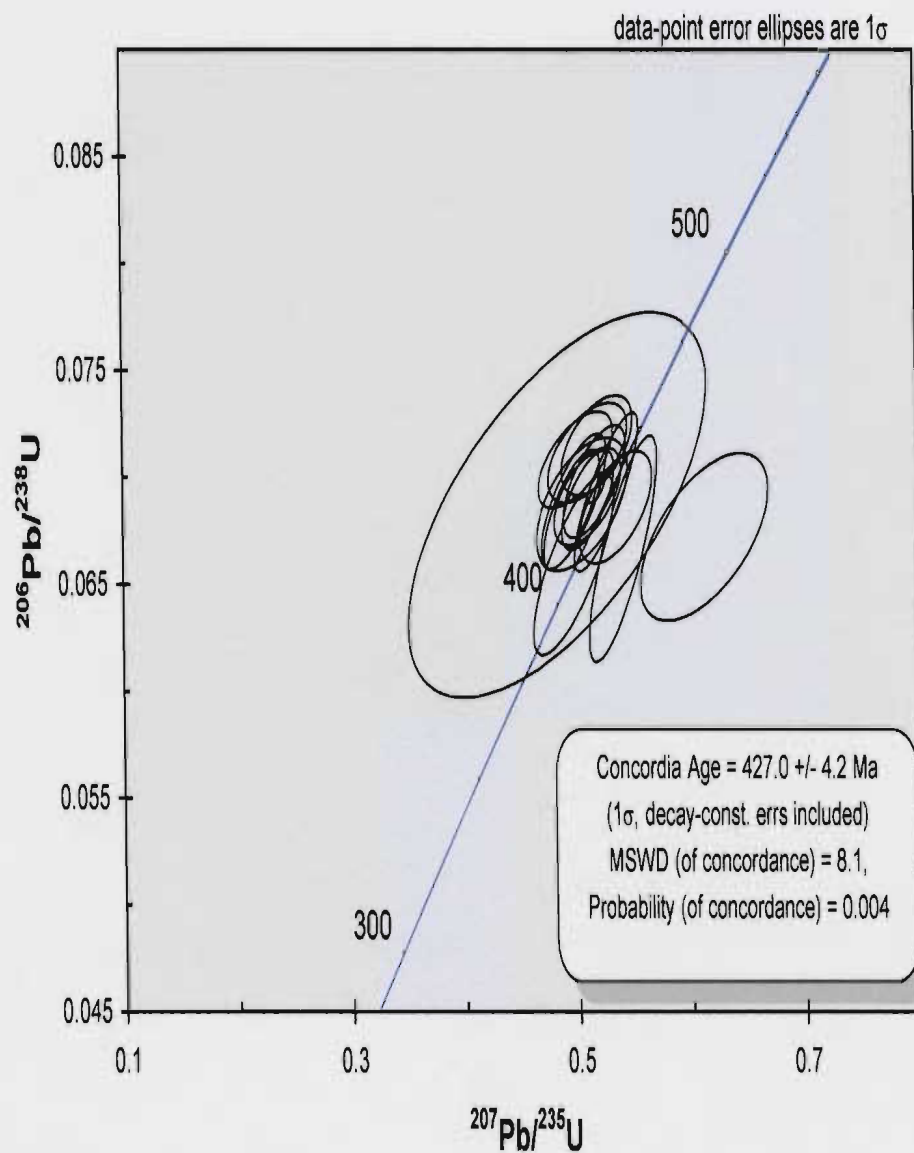


**Figure 8.4:** Concordia diagram for sample JOD25, Corsair Prospect; the size of the ellipse represents the error measurement ( $1\sigma$ ) for that particular analysis.

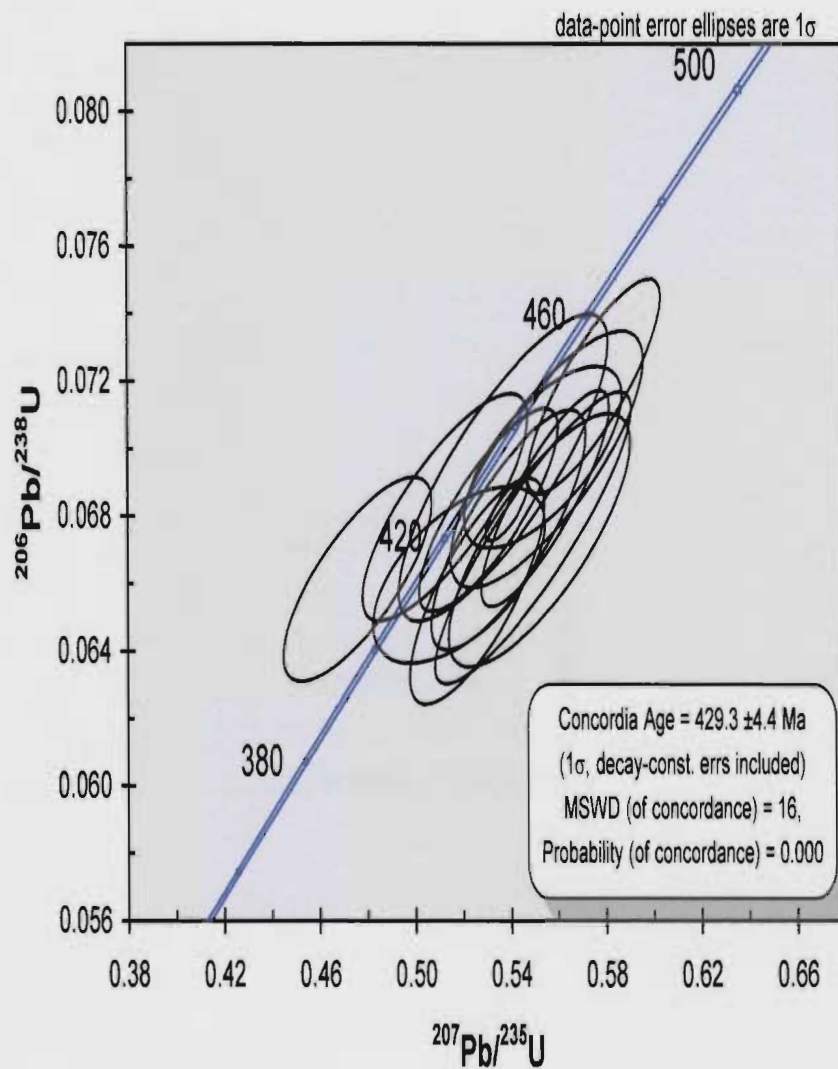


**Figure 8.5:** Concordia diagram for sample JOD100, Twin Ponds gabbro; the size of the ellipse represents the error measurement ( $1\sigma$ ) for that particular analysis.

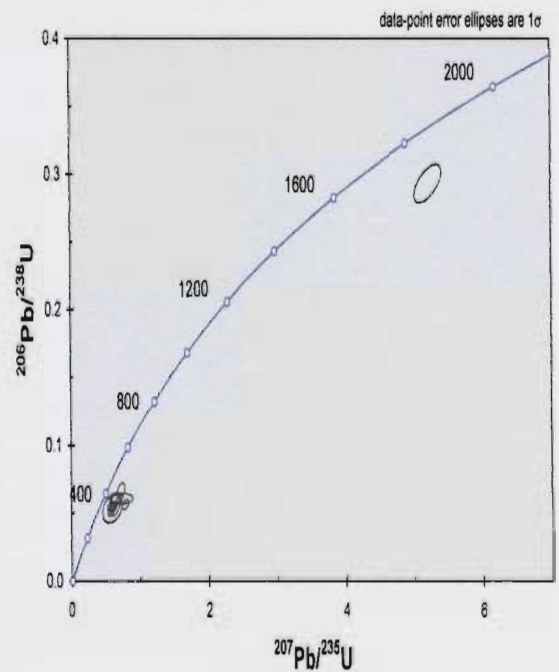
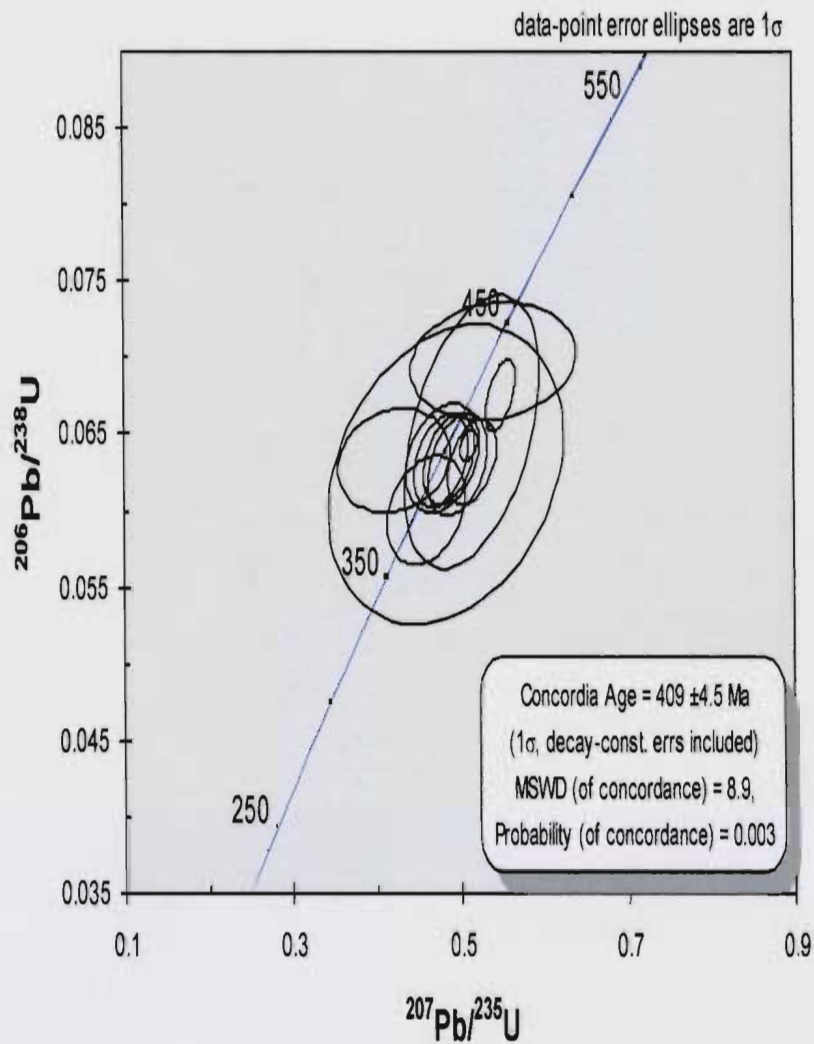


**Figure 8.6:** Concordia diagram for sample JOD04-17, MPIS granite; the size of the ellipse represents the error measurement (1 sigma) for that particular analysis.



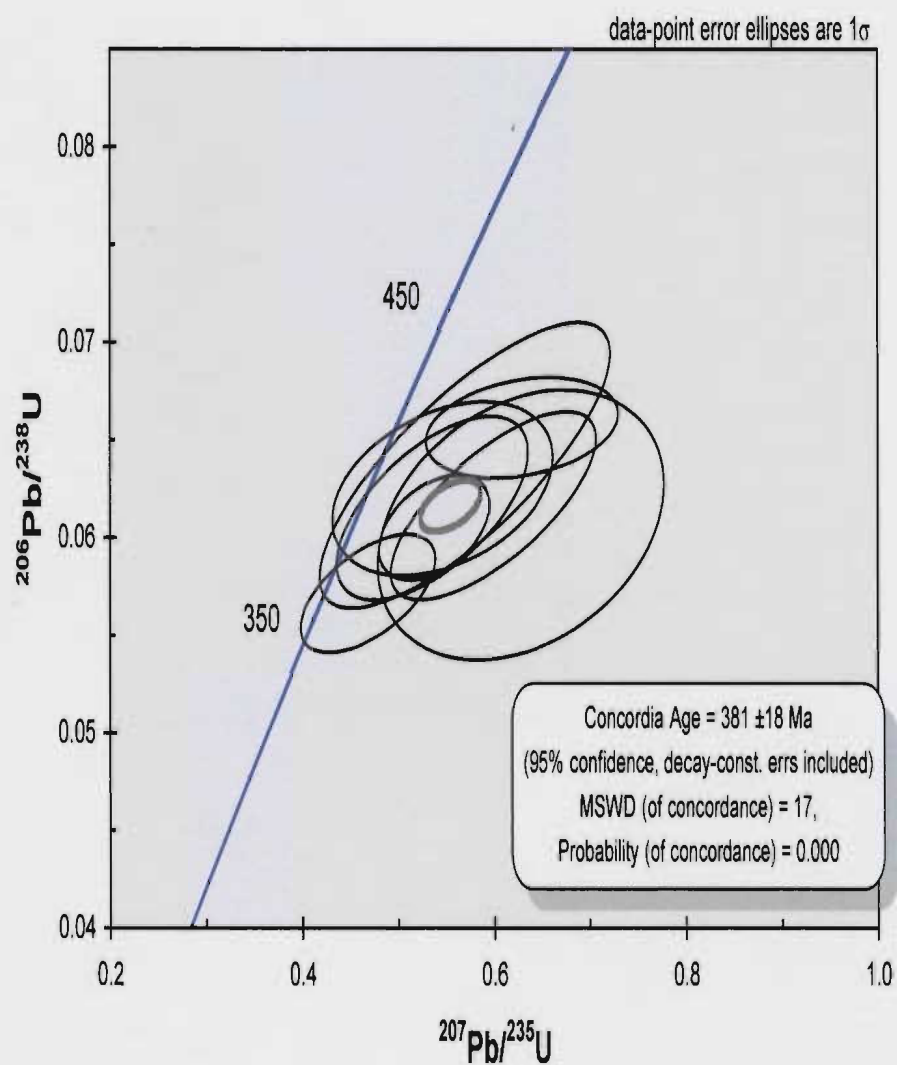


**Figure 8.7:** Concordia diagram for sample JOD90A, MPIS granite; the size of the ellipse represents the error measurement ( $1\sigma$ ) for that particular analysis.

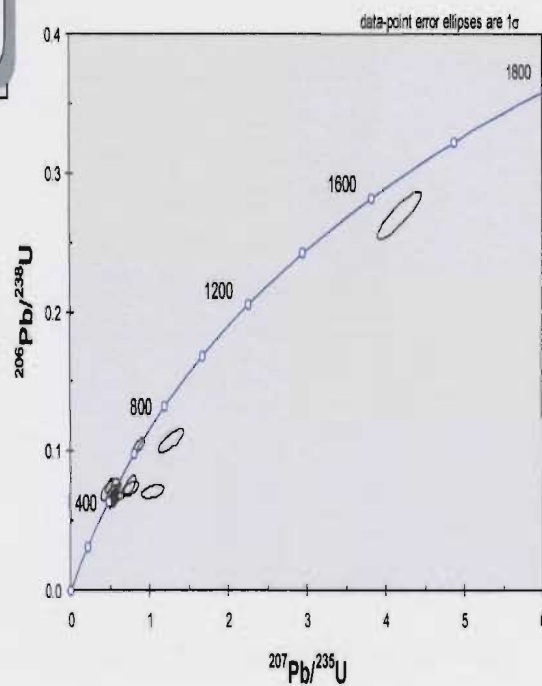
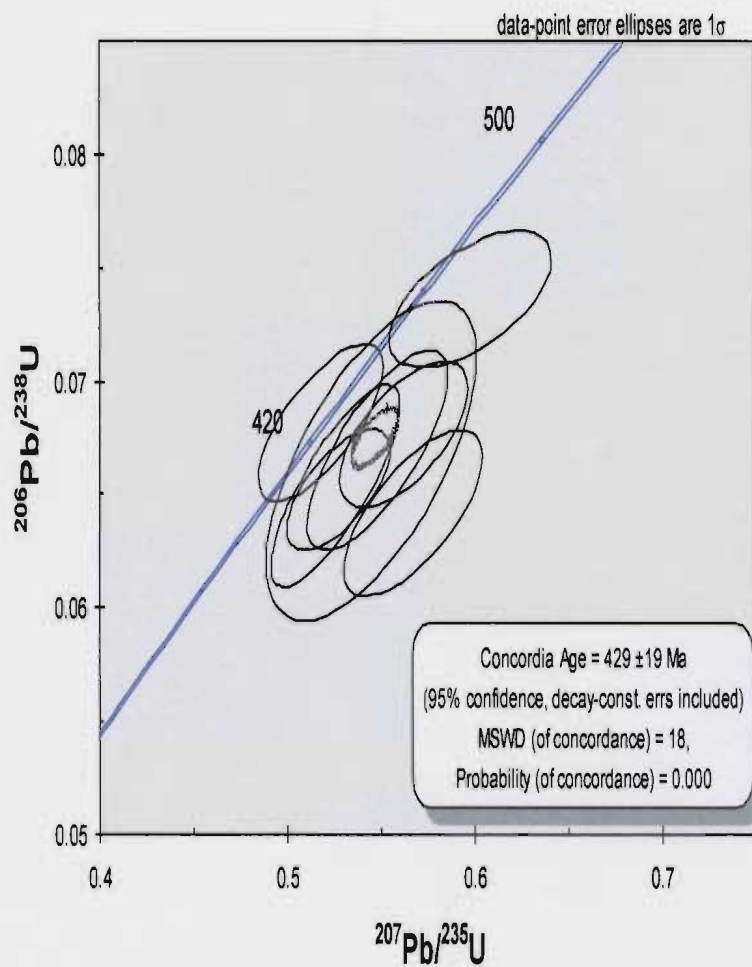


**Figure 8.8:** Concordia diagram for sample W03-27, Charles Cove pluton granite; the size of the ellipse represents the error measurement (1 sigma) for that particular analysis.

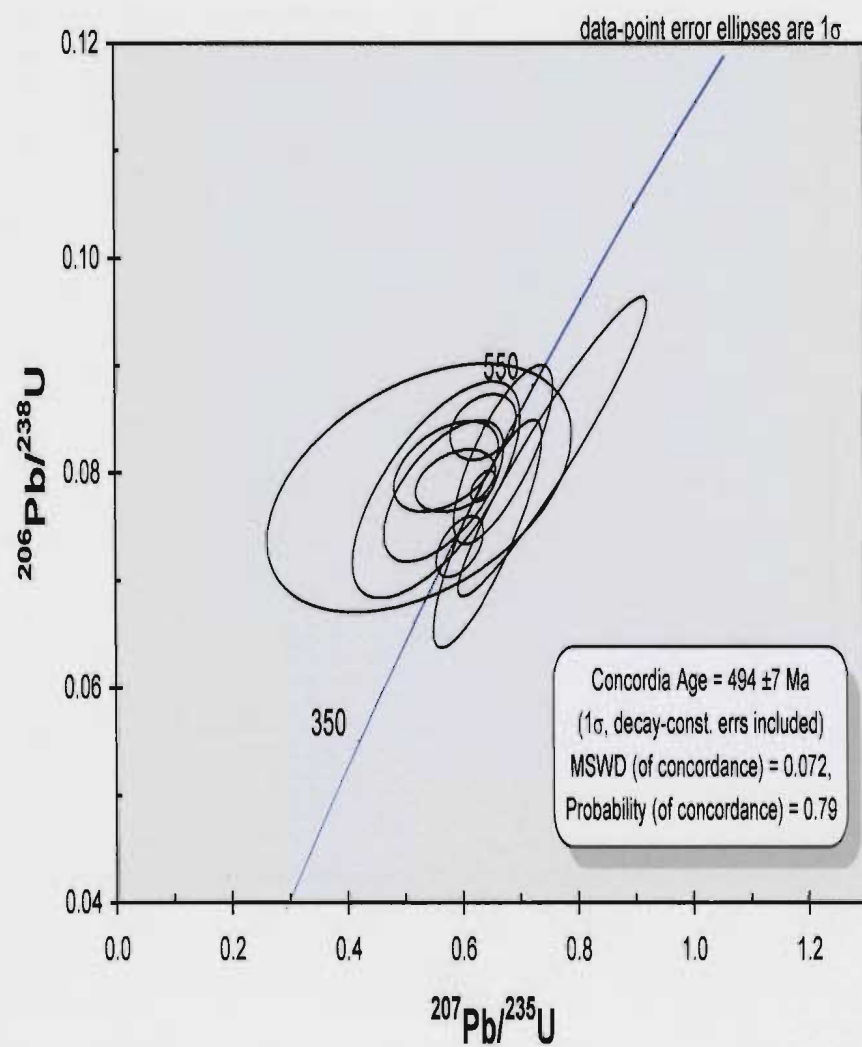


**Figure 8.9:** Concordia diagram for sample W03-38, Huxter Lane felsic intrusive; the size of the ellipse represents the error measurement ( $1\sigma$ ) for that particular analysis.



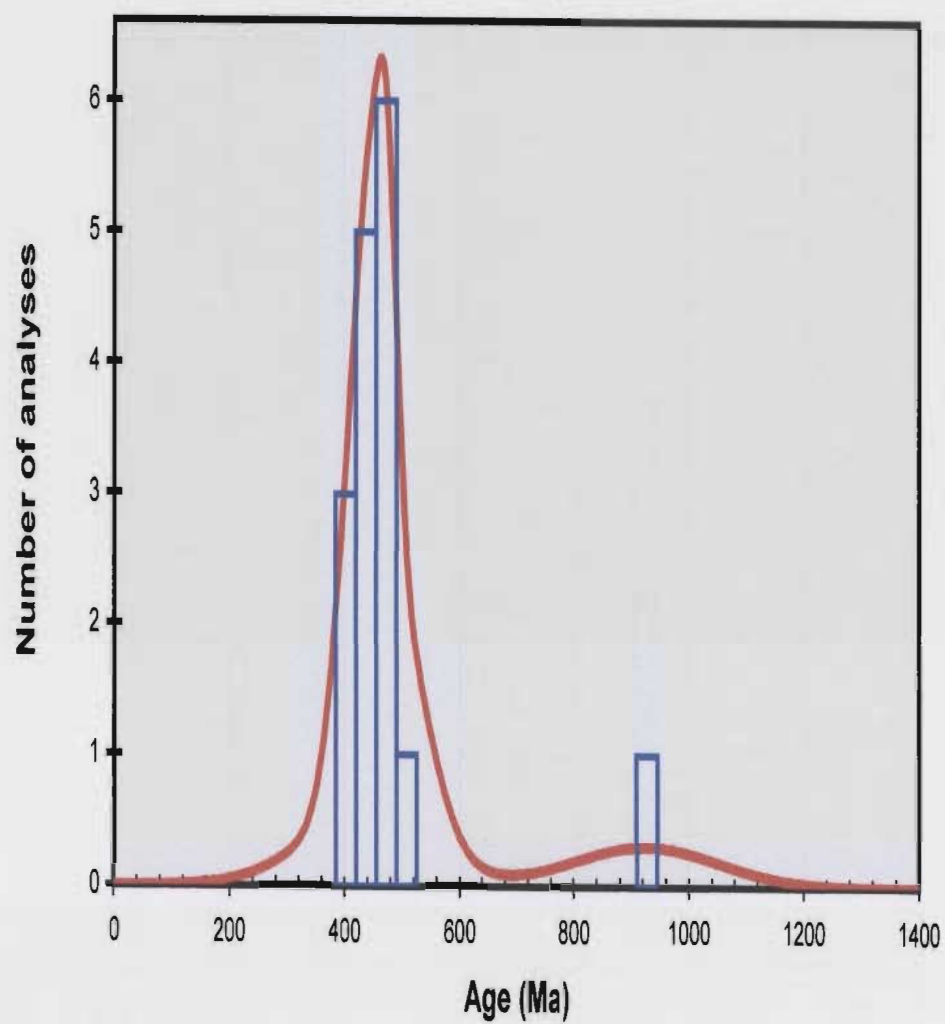


**Figure 8.10:** Histogram of detrital zircon  $^{206}\text{Pb}/^{238}\text{U}$  dates for sample JOD39.

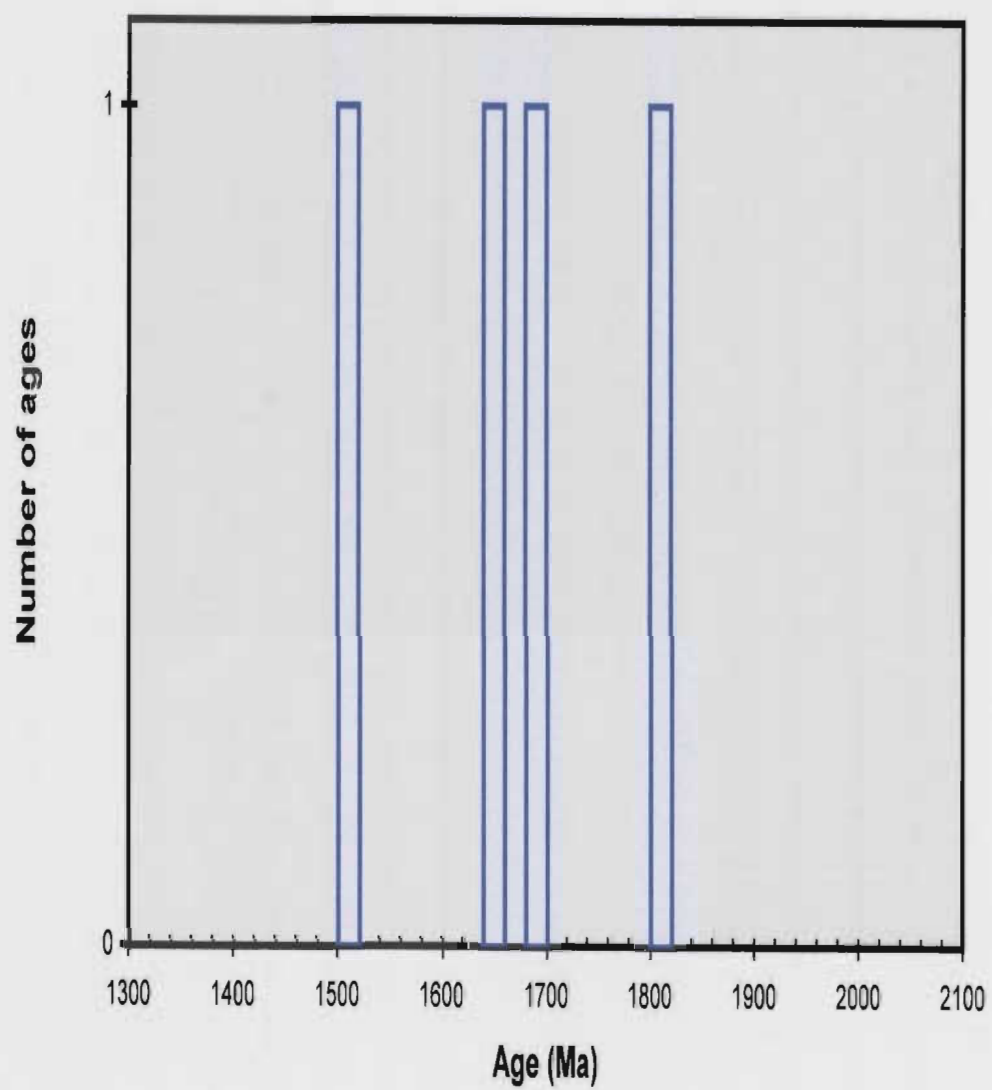


Figure 8.10: Histogram of zircon  $^{206}\text{Pb}/^{238}\text{U}$  dates for lithic tuff sample JOD08.

## CHAPTER 9

### CONCLUSIONS

#### 9.1 Preamble

This study was initiated to evaluate the auriferous occurrences throughout the region referred to as the 'Botwood Basin' in an attempt to better understand the different occurrences and their relationships to each other and regional lithologies. An attempt was also made to date various intrusive lithologies to determine whether there was a relation between these events and mineralization. The resulting compilation of field observations, major and trace element data, trace element data of pyrite, S-Isotope analyses, petrography and U-Pb geochronology has provided further insight into the nature of host and country rocks, as well as mineralization and intrusive events.

This thesis presents the results of an integrated geological, geochemical and geochronological study of the Botwood Basin, central Newfoundland. Reconnaissance mapping and fossil collection of previously reported localities (*i.e.*, Blackwood, 1982; Boyce *et al.*, 1993) along the eastern and southeastern margins of the MPIS have affirmed the presence of the Indian Islands Group rocks. Reconnaissance mapping in the northern Botwood Basin and the subsequent fossil identifications from previously unreported fossiliferous outcrop have provided evidence for a possible westward extension of the group into the area previously mapped as Ten Mile Lake Formation by Currie (1995). Geochemical and geochronological data have proven to be effective tools for linking the mafic phase of the MPIS to several smaller intrusive bodies in the northern



Botwood Basin. This suggests either the presence of a deep-rooted magmatic system with a greater extent than previously thought or several magmatic systems with similar geochemical characteristics and simultaneous activity. Geochronological data also provide evidence that suggests the intrusive events in the Botwood Basin were episodic from the Middle Silurian to Middle Devonian.

Geochemical data have proved important in identifying possible sources and tectonic environments of sedimentary lithologies throughout the study area. In fact, the geochemical data suggest that the different lithological units may be defined by abundances of immobile elements.

Sulphur isotope and trace element data from sulphide phases, coupled with field investigations, have aided in classifying the various auriferous occurrences throughout the basin. These studies have confirmed the presence of several mineralization styles and further portrayed the effect that the geological complexity of the region has had on the individual characteristics of these systems. Thus, although similarities between systems are recognized, a generalized 'Botwood Basin' style of mineralization does not apply.

## 9.2 Principal Results

Several key observations were made during reconnaissance mapping. First, new fossil localities are reported in the Duder Lake area interbedded with cherty siltstone. The fossils have been identified to include *Anthozoa* *Tabulata* *Favosites* (sp. undet.) and *Bryozoa* *Stictopora* *Scalpellum* (Lonsdale) (branching stick forms); both are common species of Wenlock (Middle Silurian) limestone. Thus the rocks are Indian Islands

Group. This area is currently mapped as the Ordovician Duder Complex (Currie, 1995b) and although fissile black shale (defined as complex matrix) was observed along the transect, green micaceous siltstone to red sandstone and pink volcanic lithologies were also observed in the area. The presence of fissile shale may be attributed to movement along a major regional fault.

A large shear zone transects the region and is reflected by a valley that runs NE. Some of the fossiliferous outcrops are adjacent to it. In fact, pieces of badly deformed fossiliferous material were observed in what appeared to be semi consolidated fault gouge which would suggest that movement along the fault was post Mid-Silurian. The mineralization in the area has been linked to second and third order structures related to this fault (*cf.* Churchill, 1994) and thus, mineralization would have had to occurred after Mid-Silurian time. This partly refutes the case for a Mid-Silurian magmatic event (related to the MPIS) acting as a heat source to drive mineralizing systems in the Duder Lake area specifically.

Also, if this fault is the Dog Bay Line and it cuts the Indian Islands Group rocks in the north, then it provides further evidence for extension of this fault system to the south and the possibility that it defines the faulted (or fault modified intrusive) contact between the Indian Islands Group and the MPIS. The puzzling point here is that if this fault does indeed cut the Indian Islands Group near Duder Lake, then sediments from this group should not occur to the west of it as observed in this study, for the Dog Bay Line has been defined as a major Silurian terrane boundary separating shallow marine sediments to the east from terrestrial sediments and volcanics to the west (*cf.* Williams *et al.*, 1993). Furthermore, even if the redefinition of sediments in the area as proposed by

Currie (*cf.* Currie, 1994; Currie, 1995a) holds true, then the question arises as to where do the Duder Complex and Ten Mile Lake Formation fit into the Botwood and Indian Islands Tectonostratigraphic belts? Currie (1995b) placed these units in the Duder Belt, which he mapped as lying spatially between the two previously defined belts. A recent study by Dickson (2005) has also questioned the incorporation of Indian Islands Group sediments as tectonic blocks within the Duder Complex. In fact, Dickson (2005) also questions the definition of the Dog Bay Line as a major terrane boundary.

New fossil localities and intrusive bodies were also mapped to the east of Ten Mile Lake in the region previously defined as the Ten Mile Lake Formation. The fossils collected from this area are somewhat deformed as they occur immediately west of a major regional fault. Despite the deformation, several fossil specimens were recoverable and identified as *Echinodermata-Crinozoa-Crinoidea* (Gen. Et sp (p). undet., *Brachiopoda-Articluata* (Gen et sp. undet.-heavily ribbed form), *Byrozoa* (Gen et sp. undet.), *Cnidaria-Anthozoa-Zoantharia-Tabulata-Favosites* (Gen et sp (p). undet.) and *Echinodermata-Crinoidea* (Gen et sp(p) undet.-columnals). Only broad identifications could be made for most of these specimens but again the presence of Stictopora Bryozoans of Wenlock age suggests a Middle Silurian age. Wenlock fossils have previously been reported from the Indian Islands Group (*i.e.*, Boyce *et al.*, 1993). The Ten Mile Lake Formation has been described as a Late Silurian to Early Devonian unit that conformably oversteps the Indian Islands Group and thus, one would not expect to find Wenlock fossils in this unit. Thus, the presence of these fossils again indicates that the Indian Islands Group, or a correlative unit, may actually exist to the west of the currently defined location of the Dog Bay Line.



Whole rock geochemical and sulphur isotopic data were presented for igneous and sedimentary lithologies throughout the Botwood Basin. Petrographical observations were combined with geochemical analysis of igneous lithologies to determine if the various intrusive units throughout the area were related to the large MPIS pluton. The geochemical data have shown that mafic, intermediate and felsic lithologies are present throughout the region. The small intrusive bodies to the north, excluding the Duder Lake gabbro, are mafic in nature and resemble the composition of the gabbroic phase of the MPIS petrographically, geochemically and geochronologically. Numerous attempts to date the mafic rocks in the Duder Lake and Paul's Pond area failed due to a lack of dateable minerals in those rocks. This is attributed to the generally small grain size of the intrusive lithologies throughout the region.

The petrographically most distinct intrusive bodies are those from the Duder Lake area. The gabbros were deformed and contain metamorphic and hydrothermal alteration assemblages. Several gabbroic dykes that intrude the Ten Mile Lake Formation north of the TCH and south of Duder Lake vary slightly in grain size and modal percentages, but do not exhibit any distinctive differences between them; they do, however, appear distinct from the Duder Lake gabbro.

A dioritic dyke collected west of Glenwood was compared with the diorite phase of the MPIS and was petrographically similar. This unit was initially correlated with the MPIS by Dickson (1996) and may provide evidence for intrusive plugs of the MPIS in the Indian Islands Group sediments. Lake and Wilton (2006) report another apparent intrusive relationship between the MPIS granite and Indian Islands Group sediments in the southeast, which provides further evidence for an intrusive relationship. A locality at

Red Rock Brook, along the southeast margin of the MPIS, indicates that the contact between the aforementioned units may be faulted, but as the contact was not actually visible, this postulation is only inferred. Thus, the possibility of a fault-modified intrusive contact cannot be ruled out.

Inherited zircon ages, both in the MPIS granite and the Charles Cove Pluton suggest inheritance of *ca.* 1800-1850 Ma. Pollock *et al.* (in prep.) report a zircon with an 1843 Ma age from the Indian Islands Group that they suggest may have been derived from the Makkovik Province, Laurentia. This could link the inherited zircon in Middle Silurian to Early Devonian Botwood Basin granitoids to the Indian Islands Group, implying an intrusive relationship.

The task of locating exposed geological contacts proved to be very difficult as till and vegetation cover in the region is quite extensive. A contact relationship was observed, however, between mafic and felsic phases of the MPIS along Salmon River. At certain localities, granite can be observed to stope gabbro blocks along fractures, which suggests that the granite is younger than the gabbro. This discredits the hybridization theory for the formation of the intermediate dioritic phase of gabbro, as a granite melt would not be of sufficient temperature to partially melt the cooled gabbro (lack of chill margins in the gabbro suggest that it was in fact cooled when the granite intruded). Further evidence against hybridization was provided in the geochronological studies of the MPIS, as the mafic phase has been dated at *ca.* 430 Ma and the granite phase at *ca.* 410 Ma.

The mafic rocks from this study are dominantly fine to medium-grained hornblende to pyroxene gabbro with varying amounts of chlorite. The presence of

chlorite indicates lower greenschist facies regional metamorphism. The intrusive lithologies have tholeiitic to transitional geochemical affinities and exhibit within plate magmatic signatures. The intrusive dykes or sills to the south and north of the MPIS appear to be more fractionated than the MPIS. Although the Duder Lake gabbros are assumed to be unrelated to the MPIS, apparent relations between the gabbroic bodies immediately north and south of the pluton may be attributed to fractionation of a similar magma source.

Sedimentary geochemistry illustrated that the various lithological groups contained varying amounts of trace elements dependant on their location in the Botwood Basin. For example, the sediments from the northern Botwood Basin were more Ti-rich. Increased Ti content was also observed in the northern intrusive bodies and thus, this may be indicative that the northern rocks have a more Ti-rich source region than those to the south.

Both geochemically and geochronologically, the MPIS granite displays characteristics of either a contaminated melt or a partial melt derived from lower crustal anatexis. Several bivariate trace element plots indicated this. For example, on the Zr vs.  $\text{Al}_2\text{O}_3$  diagram, Dickson's (1996) felsic dataset defined a different fractionation trend from that of the mafic dataset suggesting that they evolved independently. Geochronology of the Silurian granitoids in this region provides further evidence for magma contamination or partial melting as the data indicate that the zircon grains from these units may contain inherited cores from older crust.

Geochemical data for sedimentary lithologies indicate that different groups can be defined on immobile trace element diagrams. Intergroup differences can also be



identified on these plots. For example, the Davidsville Group rocks from the south (Paul's Pond area) consistently contained elevated trace element concentrations compared to those from the central region (Glenwood area) possibly reflecting input from local sources. In general, and with the exception of southern and central Davidsville Group rocks, all units plotted together on each graph. It can be assumed that the elemental characteristics of these units accurately reflect source material as these elements are considered immobile and would in most cases be unaffected by later processes. The main observations from these plots were that the sedimentary units to the north (Duder Complex) are enriched in Ti and the samples from the southern Botwood Basin are most enriched in Zr, Nb and Y. The northern and southern samples are more enriched in these elements than the central samples in general.

Tectonic environments for different sedimentary rocks were determined from petrographic descriptions. The rocks from the Davidsville Group and the sample from the Caradocian shale plot below the Recycled Orogen Provenances field, which represents zones of plate convergence. The samples that plot within this field can be related to subduction complexes, collisional orogens and foreland uplift. Several of the Indian Islands Group samples from O' Reilly (2005) plot within the craton interior subdivision of the continental block provenance field which includes quartz rich sediments that contain very little feldspar (<10%) and plot near the quartz apex. The source rocks for the sedimentary samples from the Botwood Basin primarily have calc-alkaline volcanic to intrusive compositions.

The sulphur isotope and trace element content of pyrite provided useful tools for further classifying some of the auriferous occurrences in the Botwood Basin. Three

distinct groups of sulphur isotope ratios were recognized, isotopically light (derived from a reduced sedimentary source), intermediate (derived from a primary magmatic source) and isotopically heavy (derived from a mafic to ultramafic magmatic source) indicating a wide variety of isotopic compositions throughout the area. Thus, the sulphur source for the systems studied is primarily crustal and the sulphur is of local derivation (*i.e.*, ratios reflect the host rock).

Trace element data for pyrite from several different auriferous occurrences define subtle differences between auriferous systems. Samples were selected from occurrences that had been classified as either orogenic, epithermal or postulated Carlin-style in order to determine if certain trace elements could be used to differentiate them. Previous studies (primarily with emphasis on Carlin-type deposits) indicated that pyrite incorporate distinctive trace element suites into their crystal lattices. Some of the pyrites did not contain elevated concentrations of the trace elements analysed and therefore could not be classified by this technique.

Some of the pyrite grains from the Mustang Zone (postulated Carlin-type) contained characteristic elements of the so-called 'toxic suite' of elements that are associated with Carlin-type deposits. Also, several of the pyrite grains from the Hurricane Prospect matched that from an orogenic style occurrence (Stog'er Tight) with elevated W and/or Te. Pyrite from a postulated epithermal occurrence (Bruce Pond) contained slightly elevated Se and Ba, typical of such deposits. Generally, the pyrite data within the individual occurrences were variable and more detailed studies are required to provide definitive links between the occurrences and deposit types.

In terms of regional metallogeny, this study has shown that several distinct styles

of auriferous mineralization are present throughout the Botwood Basin such as epithermal and orogenic. Furthermore, the possibility of Carlin –type mineralization could not be discredited. These occurrences are hosted in a variety of lithologies ranging from deep to shallow marine sedimentary and felsic to ultramafic igneous rocks. The mineralization generally consists of fine-grained disseminations of pyrite and arsenopyrite; gold is mostly invisible to the naked eye.

Past studies have suggested that the mineralization is Devonian as it straddles (Squires, 2005) or is younger than (Churchill, 1994) the currently defined Dog Bay Line. This study could not definitely link mineralization to the large bimodal MPIS due to difficulties in obtaining dateable minerals at auriferous occurrences, and in obtaining concordant ages due to the presence of inherited zircon. A Devonian age of *ca.* 405 Ma, however, may actually date the mineralizing event at the Salmon River Prospects rather than the diorite itself. If this age is reliable, it is within error of the *ca.* 410 Ma age defined for the MPIS granite. Orogenic styles of auriferous mineralization are often associated with granitoid plutonism, and as shown with the trace element concentrations of pyrite data, the Salmon River Prospects exhibit orogenic characteristics. Therefore, with the presently defined Early Devonian age, it is possible that the MPIS granite intrusion drove at least some of the spatially close auriferous mineralization.

This study did indicate that some of the magmatism in the north coincided with MPIS magmatism, indicating that an extensive heat flow system existed during the Middle to Late Silurian. Although mapping observations question the current definition of the Dog Bay Line, the presence of an extensive NE fault system cannot be disputed. Therefore, it is possible that the mobilization of the mineralizing fluids in some areas is



related to the various fault systems thought the Botwood Basin. Although there is no major fault system present, granitic and gabbroic dykes are host rocks at some of the Paul's Pond Prospects and thus mineralization in that area is possibly related to the intrusive events. In the Great Bend area, the mineralization is concentrated in areas of complicated and extensive fault systems, and thus, it is reasonable to assume that the mineralization is related to the local faulting episodes. In the Glenwood-Appleton area, the mineralization may be related to either the NE trending fault system that runs through the area or to the MPIS. Sulphur isotope studies indicate that the sulphides from these occurrences have a magmatic influence; therefore, the large intrusive body must have had some effect on these systems. Churchill (1994) had already linked the orogenic style Au occurrences at Duder Lake to the shearing events that he recorded in that area.

Thus, the 'Botwood Basin' auriferous occurrences, although exhibiting similarities locally, are generally distinct and cannot be grouped into a generalized mineralization model. Geochronology has shown that mineralization throughout the area has a very broad time range from at least 494 to 380 Ma. Through this time period, the region had undergone many phases of deformation and as seen in this study, episodic magmatic events at both local and regional scales.

### 9.3 Conclusions

Lithologies in the basin and environs were mapped and then sampled for geochemical and geochronological purposes. A number of conclusions have been reached, including:

- (1) Whole rock geochemical data indicate that intrusive lithologies throughout the Botwood Basin range from felsic to intermediate to mafic and generally exhibit tholeiitic to transitional geochemical affinities. The Duder Lake gabbros are dissimilar and have calc-alkalic affinities. Although the gabbroic units in the region north of the Trans Canada Highway and at Paul's Pond display some geochemical similarities to the Mount Peyton Intrusive Suite, the data suggest that these units evolved from separate magma sources. Petrographical data indicate that these units are petrographically similar and are typically fine-grained. The similarities between the intrusive bodies may indicate that they evolved from fractionated equivalents of similar magma sources. The unmineralized gabbroic bodies from the Duder Lake Prospect appear unrelated to the intrusive lithologies to the south as they are both petrographically and geochemically distinct.

- (2) Sulphur isotope ratio data for sulphide mineral separates indicate a very wide range in isotopic compositions throughout the region. The predominant distinction between samples from different occurrences seems to mainly indicate different sulphur sources related to the regional geology.
- (3) Pyrite crystals from different types of auriferous occurrences appear to exhibit distinctly different trace element compositions. Though the trace element database in the geological literature on pyrite compositions from gold deposits is limited (most information comes from Carlin studies, *e.g.*, Hofstra and Cline, 2000), it appears that some pyrite from the Mustang and Bowater prospects have the same compositions as pyrite from Carlin-type occurrences; most especially in terms of the “*toxic element*” suite so distinctive of the Carlin deposits. Trace element compositions of pyrite from the Stog’er Tight Prospect, a typical orogenic style occurrence, show low concentrations of most metals, but slightly elevated contents of Te and W in several grains. Some of the pyrite from the Hurricane Prospect, also defined as an orogenic style occurrence also have elevated W. These deposits are also generally spatially related to granotoid plutonism and the Hurricane Prospect occurs in a diorite phase of the bimodal MPIS.



- (4) Geochronological analysis of intrusive lithologies throughout the region proved difficult, as these intrusions are typically fine to medium-grained. Age determinations were made for the diorite and granite phases of the MPIS, a gabbroic intrusive immediately north of the MPIS, the Charles Cove pluton along the north coast and the Huxter Lane intrusive in the Coy Pond Complex to the south. The results of this study indicate that the gabbroic phase of the MPIS is older than the granitic phase and that the MPIS magmatism occurred around *ca.* 430-405 Ma. The data also suggest that the magmatism in the central to northern region was episodic. Both a gabbroic body north of the MPIS and the Charles Cove pluton were also dated at *ca.* 430 Ma, identifying at least one period of high heat flow beneath the central and northern Botwood Basin during Mid-Silurian time. In all models suggested for Carlin-style gold deposits (*e.g.*, Arehart, 1996, 2000, 2003; Hofstra and Cline, 2000), and indeed epithermal and orogenic types of deposits, a large-scale heat flow system is a fundamental requirement. The Early Devonian age defined for the granite phase of the MPIS makes this intrusion more feasible as the energy source for the auriferous mineralization hosted by at least the Silurian lithologies along its eastern margin. The *ca.* 494 Ma age obtained for the dacitic intrusion at the Huxter Lane Prospect forcefully illustrates that auriferous mineralization within the Botwood Basin and environs has a very extended time range of at least 100 Ma.

- (5) This study emphasized the influence of inherited zircon in Silurian granitoids. Both the MPIS granite and Charles Cove Pluton presented evidence for the incorporation of older, inherited zircon. The presence of inheritance further adds to the model proposed by Strong (1979) for crustal anatexis for the formation of the MPIS granite. The *ca.* 1800 to 1850 Ma age obtained from the inherited grains also suggests the incorporation of Indian Islands Group sediments into the magma.
- (6) Detrital age determinations were derived for a shale and conglomerate clast from the Davidsville Group. The conglomerate clast consisted of an extremely altered lithic tuff and yielded several very old ages from the Middle Proterozoic *ca.* 1550 Ma to 1775 Ma. As the host is Paleozoic, these data suggest that ancient crustal material was available for sampling in the region, probably from the Gondwanan margin (*cf.* Pollock *et al.*, in press). The shale was collected near a contact with the Indian Islands Group and two different groups of average ages were obtained from the analysis,  $472 \pm 8.5$  Ma and *ca.* 900 Ma. Pollock *et al.* (in prep) report detrital zircon ages from the Davidsville Group from 507 to 449 Ma and 964 to 886 Ma.
- (7) Although the various auriferous occurrences display some similarities in terms of style of mineralization and in some cases host rock, this

study has shown that a specific model for mineralization cannot be broadly applied to the Botwood Basin. The 494 Ma age of mineralization at the Huxter Lane Prospect and the 381 Ma age (McNicoll *et al.*, in press) for mineralization at the Titan Prospect illustrate that auriferous mineralization occurred over an extended period of time in the Botwood Basin. The local stratigraphic and tectonic environments also influenced mineralization and as these parameters vary throughout the region, so does the effect. The only broad generalization that can be commonly applied between occurrences is that the sulphur source is locally derived and dependent on local stratigraphy.

#### **9.4 Direction for Future Work**

The relationship between the MPIS and the sediments along its eastern and southern margin is still unclear, as no definite metamorphic aureoles have yet been identified. The Badger Group is intruded by the MPIS along the western margin and ranges from Late Ordovician to Early Silurian and is conformably overlain by the Silurian Botwood Group. If in fact the Stoney Lake volcanics are younger than the Botwood Group (*cf.* Anderson and Williams, 1970) and the *ca.* 423 Ma age for the volcanics is correct (*cf.* Dunning *et al.*, 1990), then deposition of the Botwood Group would have ranged from Early Silurian (*ca.* 440 Ma) to Late Silurian (*ca.* 424 Ma). The present study suggests that MPIS plutonism ranges from *ca.* 430-424 Ma (mafic to



intermediate phases) to *ca.* 410-380 Ma (felsic phase), suggesting that the intrusion coincided with some stages in the deposition of the Botwood Group. Along the eastern margin, several authors have postulated a possible faulted contact between the MPIS and the Indian Islands Group. This study suggests that the contact may actually be originally intrusive but fault modified. Thus, a detailed project with emphasis on defining this relationship should be conducted.

U-Pb geochronology proved to be a strong tool in defining a widespread magmatic system ranging from the central to coastal region. Further samples at more localities throughout the study area should be collected to provide a broader picture of the intrusive history of the region. The sampling focus should be on locating medium to coarser grained lithologies to improve the chance of obtaining dateable minerals.

Sulphur isotope studies and mapping projects should be conducted on a more localized scale. Sulphur isotopes for the region have been shown to be considerably variable and thus should be addressed at individual auriferous occurrences. New discoveries of significant auriferous occurrences have been made in the northern and north-central Botwood Basin since the onset of this study which reaffirm the potential of this area as a significant area for gold exploration and the need for a better understanding of the geological and structural history of this complex region.

Aside from a detailed mapping project along the eastern margin of the MPIS, the geology of the northern Botwood Basin, specifically the 'Duder Belt' that was defined by Currie (1995b), should be examined. The current study, along with recent observations presented by Dickson (2005), have produced questions concerning the current stratigraphy in this region.

## REFERENCES

- Anderson, F.D. and Williams, H. 1970. Gander Lake (west half), Newfoundland. Geological Survey of Canada, Map 195A, with descriptive notes.
- Arehart, G.B., Chryssoulis, S.L., and Kesler, S.E. 1993. Gold and arsenic in iron sulfides from sediment-hosted micron gold deposits: Implications for depositional processes *Economic Geology*, v. 88, pp. 171-185.
- Arehart, G.B. 1996. Characteristics and origin of sediment-hosted disseminated gold deposits: a review. *Ore Geology Reviews*, v.11, pp. 383-403.
- Arehart, G.B. 2000. Carlin type gold deposits of the North American cordillera: what are they and where are they? Mineral Deposit Research Unit, University of British Columbia, Short Course 27.
- Arehart, G.B. 2003. Giant Carlin-type gold deposits - Characteristics, origins and exploration methodology. Keynote talk at Geological Association of Canada, Newfoundland Branch, winter meeting, 2003. *Atlantic Geology*, v.39.
- Arehart, G.B., Chryssoulis, S.L. and Kesler, S.E. 1993. Gold and arsenic in iron sulphides from sediment hosted disseminated gold deposits; Implications for depositional processes. *Economic Geology*, v.88, pp.171-185.
- Arehart, G. B., Eldridge, C. S., Chryssoulis, S. L., and Kesler, S. E. 1993. Ion microprobe determination of sulfur isotope variations in iron sulfides from the Post-Betze sediment-hosted disseminated gold deposit, Nevada, USA. *Geochimica et Cosmochimica Acta*, v. 57, pp. 1505-1519.
- Ash, J.S. and Boyce, W.D. 1994. New Silurian-Devonian faunas from the Gander (NTS 2D/15) and Botwood (NTS 2E/3) map areas. *In* Current Research, Newfoundland and Labrador Department of Mines and Energy, Geological Survey Branch, Report 94-1, pp. 53-63.
- Baird, D.M. 1958. Fogo Island Map Area, Newfoundland (2E/9) mainly, Geological Survey of Canada, Memoir 301, 43 pages.
- Baird, D.M., Moore, J.C.G., Scott, H.S. and Walker, W. 1951. Reconnaissance survey of east-central Newfoundland between Sir Charles Hamilton Sound and Baie d'Espoir. Newfoundland Department of Natural Resources, Mineral Development Division, Newfoundland Geological Survey, Unpublished Report, 155 pages.
- Barbour, D.M. 1999. The Rolling Pond epithermal silica sinter. *In* Volcanogenic massive sulphide and gold mineralization, northern and central Dunnage Zone, Newfoundland. *Edited by* D.T.W. Evans, 1999 North Atlantic Minerals Symposium, 211 pages.
- Barbour, D.M., Churchill, R.A., Cole, D.J., Spurvey, P.E. and Scott, W.J. 1999. First year assessment report on geological, geochemical, geophysical and diamond drilling exploration for license 6101m on claims in The Outflow area, Gander Lake, central Newfoundland, 2 reports. Sulliden Exploration Incorporated and Altius Resources Incorporated, Newfoundland and Labrador Geological Survey, Assessment File 2D/15/0362, 121 pages.
- Barbour, D. M. and Churchill, R.A. 2000. First year assessment report on geological, geochemical, geophysical and diamond drilling exploration for licenses 6301M, 6479M-6483M and 6824M on claims in

the Rolling Pond area, central Newfoundland. Sulliden Exploration Incorporated and Altius Resources Incorporated. Newfoundland and Labrador Geological Survey, 146 pages.

Barbour, D. and Churchill, R.A. 2004. Second, third and sixth year assessment report on prospecting, trenching and geochemical sampling at the Mustang trend properties, map staked licenses 8252M, 8253M, 8354M, 6101M, 7677M, 8255M, 9649M, 9650M and 9788M; NTS sheets 02E02, 02E07, 02D05, 02D06, 02D11, 02D12, 02D13, 02D14 and 02D15, Botwood Basin, central Newfoundland. Confidential report for the Altius Resource Incorporated, Newfoundland and Labrador Department of Natural Resources, Geological Survey, Open File NFLD/2893.

Barrett, S. J. 2001. Structural analysis of the Moosehead Property, eastern Dunnage Zone, central Newfoundland Appalachians. Unpublished BSc. Thesis, Memorial University of Newfoundland, St. John's, Newfoundland, 111 pages.

Bazinet, J.P. 1980. Geology of the Gander Group, Gander River Ultramafic Belt and the Davidsville Group in the Jonathon's Pond-Weir's Pond Area, northeast Newfoundland. Unpublished MSc. Thesis, Brock University, St. Catharines, Ontario, 154 pages.

Bell, K and Blenkinsop, J. 1975. Geochronology of eastern Newfoundland. *Nature*, v. 254, pp. 410-411.

Bell, K., Blenkinsop, J. and Strong, D.F. 1977. The geochronology of some granitic bodies from eastern Newfoundland and its bearing on Appalachian evolution. *Canadian Journal of Earth Sciences*, v.14, pp. 454-476.

Berger, B.R., and Bagby, W.C. 1991. The geology and origin of Carlin-type gold deposits. *In* Gold metallogeny and exploration, *Edited by* R. P. Foster, Glasgow, Blackie and Son, pp. 210-248.

Bergstrom, S.M., Riva, J. and Kay, M. 1974. Significance of conodonts, graptolites and shelly fauna from the Ordovician of western and north-central Newfoundland. *Canadian Journal of Earth Sciences*, v.11, pp. 1625-1660.

Bierlein, F.P. and Crowe, D.E. 2000. Phanerozoic orogenic lode gold deposits. *Reviews in Economic Geology*, v.13, pp. 103-139.

Bierlein, F.P., and Maher, S. 2001. Orogenic disseminated gold in Phanerozoic fold belts - examples from Victoria, Australia, and elsewhere. *Ore Geology Reviews*, v. 18, pp. 113-148.

Bierlein, F.P., Arne, D.C. and Cartwright, I. 2004. Stable isotope (C, O, S) systematics in alteration haloes associated with orogenic gold mineralization in the Victorian gold province, SE Australia. *Geochemistry: Exploration, Environment, Analysis*, v. 4, no. 3, pp. 191-211.

Bird, J.M. and Dewey, J.F. 1970. Lithosphere plate-continental marginal tectonics and the evolution of the Appalachian Orogen. *Geological Society of America Bulletin*, v.81, pp. 1031-1060.

Blackwood, R.F. 1976. The relationship between the Gander and Avalon zones in the Bonavista Bay region, Newfoundland. Unpublished MSc. thesis, Memorial University of Newfoundland, St John's, Newfoundland, 346 pages.

Blackwood, R.F. 1978. Northeastern Gander Zone. *In* Report of Activities, Newfoundland Department of Mines and Energy, Mineral Development Division, Report 78-1, pp.72-79.

Blackwood, R.F. 1979. Geology of the Gander River area (2E/2) Newfoundland. *In* Report of Activities, Newfoundland Department of Mines and Energy, Mineral Development Division, Report 79-1, pp. 38-42.



- Blackwood, R.F. 1980. Geology of the Gander (west) area (2D/15), Newfoundland. *In* Current Research, Newfoundland and Labrador Department of Mines and Energy, Mineral Development Division, Report 80-1, pp. 53-61.
- Blackwood, R.F. 1981. Geology of the Gander Rivers area, Newfoundland. *In* Current Research, Newfoundland Department of Mines and Energy, Mineral Development Division, Report 81-1, pp.50-56.
- Blackwood, R.F. 1982. Geology of the Gander Lake (2D/15) and Gander River (2E/2) areas. Newfoundland Department of Mines and Energy, Mineral Development Division, Report 82-4, 56 pages.
- Blewett, R.S. and Pickering, K.T. 1988: Sinistral shear during Acadian deformation in north central Newfoundland based on transecting cleavage. *Journal of Structural Geology*, v.10, pp.125-127.
- Boggs, S. 2001. *Principles of Sedimentology and Stratigraphy*, 3rd edition, Prentice Hall, 726 pages.
- Boyce, W.D. 1987. Cambrian-Ordovician trilobite biostratigraphy in central Newfoundland. *In* Current Research, Newfoundland and Labrador Department of Mines and Energy, Mineral Development Division, report 87-1, pp.335-341.
- Boyce, W.D., Ash, J.S., O'Neill, P. and Knight, I. 1988. Ordovician biostratigraphic studies in the Central Mobile Belt and their implications for Newfoundland tectonics. *In* Current Research, Newfoundland and Labrador Mineral Development Division, Report No. 88-1, pp. 177-182.
- Boyce, W.D., Ash, J.S. and O' Brien, B. 1991. A new fossil locality in the Bay of Exploits, central Newfoundland. *In* Current Research, Newfoundland Department of Mines and Energy, Mineral Development Division, Report 91-1, pp. 79-81.
- Boyce, W.D. and Ash, J.S. 1992. Paleontological investigations in Newfoundland. *In* Report of Activities, Newfoundland Department of Mines and Energy, Geological Survey Branch, pp. 5-7.
- Boyce W.D. and Ash, J.S. 1994. New Silurian-Devonian [?] faunas from the Gander [NTS 2D/15] and Botwood [NTS 2E/3] map areas. *In* Current Research, Newfoundland and Labrador Department of Mines and Energy, Geological Survey Branch, Report No. 94-1, pp. 53-63.
- Boyce, W.D., Ash, J.S. and Dickson, W.L. 1993. The significance of a new bivalve fauna from the Gander map area (NTS 2D/15) and a review of Silurian bivalve-bearing fauna in central Newfoundland. *In* Current Research, Newfoundland Department of Mines and Energy, Geological Survey Branch, Report 93-1, pp. 187-194.
- Burton, W.B. 1987. First year assessment report on geological, geophysical and diamond drilling exploration for License 2738 on the Chiouk Brook prospect in the Great Bend area, Newfoundland. U.S. Borax Limited, unpublished report, 8 pages.
- Butler, A.J. and Davenport, P.H. 1981. Lake sediment survey of northeastern Newfoundland, NTS 2D, Gander Area. Department of Mines and Energy, Mineral Development Division, 28 pages.
- Butler, D.J. 1989. Report on geological and geochemical surveys on License 3292, Third Pond property, Newfoundland, NTS 2E/2. Falconbridge Nickel Mines Limited, unpublished report, 10 pages.
- Butler, R. 2003. The history of gold exploration in the Botwood Basin of central Newfoundland. Geological Association of Canada, Newfoundland Branch, winter meeting. *Atlantic Geology*, v.39.

- Butler, R. and Churchill, R. 2002. Second year assessment report on prospecting and geochemical exploration for license 8182M on claims in the Chiouk Brook area, central Newfoundland. Altius Resources Incorporated. Newfoundland and Labrador Geological Survey, Assessment File 2D/11/0415, 2002, 29 pages.
- Bradley, D.C., 1982. Subsidence in Late Paleozoic basins in the northern Appalachians. *Tectonics*, v.1, pp.107-123.
- Bruckner, W.D. 1972. The Gander Lake and Davidsville Groups of northeastern Newfoundland: new data and geotectonic implications: Discussion. *Canadian Journal of Earth Sciences*, v.9, pp. 1778-1779.
- Cawood, P.A. 1989. Acadian remobilization of a Taconic ophiolite, western Newfoundland. *Geology*, v.17, pp. 257-260.
- Chaussidon, M. and Lorand, J.P. 1990. Sulphur isotope composition of orogenic spinel lherzolite massifs from Ariege (north-eastern Pyrenees, France); an ion microprobe study. *Geochimica et Cosmochimica Acta*, v.54, no.10, pp.2825-2846.
- Churchill, R.A., 1994. An integrated study of epigenetic gold mineralization, Duder Lake area, northeastern Newfoundland. Unpublished MSc. thesis. Memorial University of Newfoundland, St. John's, Newfoundland, 305 pages.
- Churchill, R., Barbour, D. and Butler, R. Jr. 2001. First year assessment report on geological and geochemical exploration for licenses 7413M-7414M on claims in the Chiouk Brook area, near Great Bend, central Newfoundland. Altius Resources Incorporated, Newfoundland and Labrador Geological Survey, Assessment File 2D/11/0428, 33 pages.
- Churchill, R. and Butler, R. W. Jr. 2000. Third year assessment report on geological and geochemical exploration for license 4608m on claims in the Greenwood Pond area, central Newfoundland. Altius Resources Incorporated and Forex Resources. Newfoundland and Labrador Geological Survey, Assessment File 2D/11/0384, 32 pages
- Churchill, R., Clarke, E J and Butler, R. 1998a. First year assessment report on compilation, prospecting and geochemical exploration for license 5270m on claims in the Greenwood Pond area, central Newfoundland. Forex Resources and Butler, R, Jr. Newfoundland and Labrador Geological Survey, Assessment File 2D/11/0328, 1998, 36 pages
- Churchill, R., Clarke, E J and Butler, R. Jr. 1998b. First year assessment report on compilation, prospecting and geochemical exploration for license 5505m on claims in the Greenwood Pond area, near Northwest Gander River, central Newfoundland. Altius Resources Incorporated and Clarke, E. J. Newfoundland and Labrador Geological Survey, Assessment File 2D/11/0344, 38 pages.
- Churchill, R., Clarke, E. J. and Butler, R. 1998c. First year assessment report on compilation, and geological and geochemical exploration for license 4608m on claims in the Greenwood Pond area, near Northwest Gander River, central Newfoundland. Forex Resources and Butler, R. Jr. Newfoundland and Labrador Geological Survey, Assessment File 2D/11/0326, 41 pages.
- Churchill, R. A. and Evans, D.T.W. 1992. Geology and gold mineralization of the Duder Lake Gold showings, eastern Notre Dame Bay, Newfoundland. *In* Current Research, Newfoundland and Labrador Geological Survey Report No. 92-1, pp. 211-220

- Churchill R. A., Wilton, D.H.C. and Evans, D. T. W. 1993. Geology, alteration assemblages and geochemistry of the Duder Lake Gold showings, northeastern Newfoundland. *In* Current Research, Newfoundland and Labrador Geological Survey, Report No. 93-1, pp. 317-333.
- Claypool, G.E., Leventhal, J.S. and Goldhaber, M.B. 1980. Geochemical effects of early diagenesis of organic matter, sulfur and trace elements in Devonian black shales, Appalachian Basin. *American Association of Petroleum Geologists Bulletin*, v.64, no.5, p.692.
- Coish, R.A., Hickey, R. and Frey, F.A. 1982. Rare earth geochemistry of the Betts Cove ophiolite, Newfoundland: Complexities in ophiolite formation. *Geochemica et Cosmochimica Acta*, v.46, pp. 2117-2134.
- Collins, C.J. 1991. Fifth year assessment report for license 2821 and fourth year assessment report for license 3259, 1991 exploration and diamond drilling on the Glenwood project (66725) NTS 2D/15. Noranda Exploration Company Limited, confidential report, 25 pages.
- Collins, C.J. and Squires G. 1991. Report on assessment work over concession lands within the boundary of the Noranda-BP Canada Resources Limited joint venture (Reid Lot 229, 231, 235, and Charter) NTS 12A/7, 9, 10. Noranda Exploration Company Limited, unpublished report, 84 pages.
- Colman-Sadd, L.C. 1980. Geology of south central Newfoundland and evolution of the eastern margin of Iapetus. *American Journal of Science*, v.280, pp. 991-1017.
- Colman-Sadd, L.C. 1982. Two stage continental collision and plate driving forces. *Tectonophysics*, v.90, pp. 263-282.
- Colman-Sadd, S.P. 1985. Geology of the Burnt Hill Map area, Newfoundland (NTS 2D/5) at 1:50, 000 scale. Department of Mines and Energy, Mineral Development Division, Report 85-03, 1985, 108 pages.
- Colman-Sadd, S.P., 1989. Miquels Lake area 2D12: An update of the geology. *In* Current Research. Newfoundland Department of Mines, Geological Survey of Newfoundland, Report 89-01, pp. 47-53.
- Colman-Sadd, S.P. 1994. Silurian subaerial rocks near Lewisporte, central Newfoundland. *In* Current Research, Newfoundland Department of Mines and Energy, Geological Survey Branch, Report 94-1, pp. 65-76.
- Colman-Sadd, S. P., and Crisby-Whittle, L. V. J. (compilers) 2002: Partial bedrock geology dataset for the Island of Newfoundland (NTS areas 02E, 12H, 12G and parts of 01M, 02D, 02L, 11P, 12A, 12B, 12I). Newfoundland and Labrador Department of Mines and Energy, Geological Survey, Open File NFLD/2616.
- Colman-Sadd, S. P., Dunning, G. R. and Dec, T. 1992. Dunnage-Gander relationships and Ordovician orogeny in central Newfoundland: A sediment provenance and U/Pb age study. *American Journal of Science*, v. 293, pp. 317-55.
- Colman-Sadd, S.P., Hayes, J.P. and Knight, I. 1990. Geology of the Island of Newfoundland. Newfoundland Department of Mines and Energy. Geological Survey Branch, map 90-01, scale 1: 1, 000, 000.
- Colman-Sadd, S.P. and Russell, H.A.J. 1981. Miquels Lake, Newfoundland. Newfoundland Department of Mines and Energy, Mineral Development Division, Open File 2D/12/0121, [Map 81-108].



- Colman-Sadd, S.P. and Russell, H.A.J., 1982. Geology of the Miguel's Lake map area (2D/12), Newfoundland Department of Mines and Energy, Geological Survey of Newfoundland, Report 82-01, pp. 30-50.
- Colman-Sadd, S.P. and Russell, H.A.J. 1988. Miquels Lake (2D/12), Newfoundland. Newfoundland Department of Mines and Energy, Geological Survey Branch, Open File Map 88-50.
- Colman-Sadd, S.P. and Swinden, H.S. 1984. A tectonic window in central Newfoundland? Geological evidence that the Appalachian Dunnage Zone may be allochthonous. *Canadian Journal of Earth Sciences*, v.21, no. 12, pp. 1349-1362.
- Cooke, D. R. and Simmons, S. F. 2000. Characteristics and genesis of epithermal gold deposits. *Reviews in Economic Geology*, v. 13, pp. 221-244.
- Cooper, G.E. 1953. Tungsten occurrence-Gander Bay, Newfoundland. Unpublished Report, NALCO Ltd., 5 pages.
- Coyle, M. and Strong, D.F. 1987. Geology of the Springdale Group: a newly recognized Silurian epicontinental-type caldera in Newfoundland. *Canadian Journal of Earth Sciences*, v. 24, pp. 1135-1148.
- Currie, K.L. 1992. A new look at Gander-Dunnage relations in the Carmenville map area, Newfoundland. *In Current Research, Part D. Geological Survey of Canada, Paper 92-1D*, pp.27-33.
- Currie, K.L. 1993. Ordovician-Silurian stratigraphy between Gander Bay and Birchy Bay, Newfoundland. *In Current Research, Part D. Geologic Survey of Canada, Paper 93-1-D*, pp.11-18.
- Currie, K.L. 1994. Reconsidering parts of Comfort cove and Gander River map areas, Dunnage Zone of Newfoundland. *In Current Research 1994-D. Geological Survey of Canada*, pp.33-40.
- Currie K.L., 1995a. A tale of shale - stratigraphic problems in the Gander River map area, Newfoundland. *In Current Research, Geological Survey of Canada*, no. 1995-D, pp. 73-80.
- Currie, K.L. 1995b. The northeastern end of the Dunnage Zone in Newfoundland. *Atlantic Geology*, v. 31, pp. 25-38.
- Currie, K.L. 1997. Geology, Gander River-Gander Bay Region, Newfoundland (2E east half). *Geological Survey of Canada, Open File 3467*, scale 1:100, 000.
- Currie, K.L., Pajari, G.E. and Pickerill, R. K. 1979. Tectono-stratigraphic problems in the Carmenville area, northeastern Newfoundland. *In Current Research, Part A. Geological Survey of Canada, Paper 79-1A*, pp. 71-76.
- Currie, K.L., Pajari, G.E. and Pickerill, R.K., 1980. Comments on the boundaries of the Davidsville Group, northeastern Newfoundland. *In Current Research, Part A, Geological Survey of Canada, Paper 80-1A*, pp. 115-118.
- Currie, K.L., Pickerill, R.K., Pajari, G.E, Jacobi, R.D, Haworth, R.T, Lefort, J.P. and Miller, H.G. 1979. Geophysical evidence for an east-dipping Appalachian subduction. *Geology*, vol. 7, no. 10, pp. 469-470.
- Currie, K.L., Pickerill R.K. and Pajari G.E. 1983. Structural interpretation of the eastern Notre Dame Bay Area, Newfoundland: Regional post middle Silurian thrusting and asymmetrical folding: Discussion. *Canadian Journal of Earth Science*, v. 20, pp. 1351-1352.

- Currie, K.L. and Williams, H. 1995. Geology, Comfort Cove-Newstead (2E/07), Newfoundland. Geological Survey of Canada, Map, Open File 3161.
- Dalton, B., 1998. A descriptive and genetic study of mineralization and alteration at the Moosehead Prospect, central Newfoundland. Unpublished BSc. thesis, Memorial University of Newfoundland, St. John's, Newfoundland, 82 pages.
- Davenport, P.H. and Nolan, L.W. 1988. Gold and associated elements in lake sediment from regional surveys in the Botwood map area (2D): Newfoundland and Labrador Mineral Development Division Open File, 220 pages.
- Davenport, P.H. and Nolan, L.W., 1989. Mapping and regional distribution of gold in Newfoundland using lake sediment geochemistry. *In* Current Research, Newfoundland and Labrador Geological Survey, Report 89-01, pp. 259-266.
- Dean, P.L. 1977. Geology and metallogeny of the Notre Dame Bay area, Newfoundland to accompany metallogenic maps 12H/1,8,9 and 2E/3,4,5,6,7,9,10,11 and 12. Newfoundland Department of Mines and Energy, Mineral Development Division, Report 77-10, 17 pages.
- Dean, P.L. 1978. The volcanic stratigraphy and metallogeny of Notre Dame Bay. Unpublished MSc. thesis, Memorial University of Newfoundland, St. John's, 204 pages.
- Dean, P.L. and Strong, D.F. 1977. Folded thrust faults in Notre Dame Bay, central Newfoundland. *American Journal of Science*, v. 277, pp.97-108.
- Dickin, A.P. 1995. Radiogenic isotope geology. Cambridge University Press, Cambridge, 490 pages.
- Dickinson, W.R., and Suczek, C.A. 1979. Plate tectonics and sandstone composition. *American Association of Petroleum Geologists Bulletin* v.63, pp. 2164-2182.
- Dickson, W.L. 1991. Geology of the Eastern Pond (west half) map area (2D/11W), central Newfoundland. Newfoundland Department of Mines and Energy, Geological Survey of Newfoundland, Report of Activities, pp. 9-13.
- Dickson, W.L. 1992a. Mount Peyton (NTS 2D/14) map area, central Newfoundland, Newfoundland Department of Mines and Energy, Geological Survey Branch, Map 92-22.
- Dickson, W.L. 1992b. Ophiolites, sedimentary rocks, post-tectonic intrusions and mineralization in the Eastern Pond (NTS 2D/11, west half) map area, central Newfoundland. Newfoundland Department of Mines and Energy, Geological Survey Branch, Report 92-1, pp.97-118.
- Dickson, W. L. 1993. Geology of the Mount Peyton map area [NTS 2D/14], central Newfoundland. *In* Current research, Newfoundland and Labrador Geological Survey, Report No. 93-1, pp. 209-220.
- Dickson W. L. 1994. Geology of the southern portion of the Botwood map area [NTS 2E/3], north-central Newfoundland. *In* Current research, Newfoundland and Labrador Geological Survey, Report No. 94-1, pp. 101-116.
- Dickson, W.L. 1996. Whole rock geochemical and field data from the Mount Peyton Intrusive Suite, the Great Bend Complex and miscellaneous rocks, central Newfoundland (NTS Map areas 2D/11E, 2D/14, 2E/3 and parts of 2D/13 and 2D/15). Newfoundland and Labrador Department of Mines and Energy, Geological Survey, Open File NFLD/2614.

- Dickson, W.L. 2005. The Silurian Indian Islands Group, and its relationships to adjacent units, northeastern Newfoundland. *In* Report of Activities, Newfoundland and Labrador Department of Natural Resources, Minerals Deposits Section, pp.37-40.
- Dickson, W.L. and Colman-Sadd, S.P. 1993. Geology of the Botwood map area, central Newfoundland (NTS 2E/3); Newfoundland and Labrador Geological Survey, Map 93-99. Open File 002E/03/0864.
- Dickson, W.L., Colman-Sadd, S.P., and O' Brien, B.H. 2000. Geology of the Botwood map area (NTS 2E/3) central Newfoundland. Newfoundland and Labrador Department of Mines and Energy, Geological Survey, Map 2000-11, Open File 002E/03/1067.
- Donovan, S.K., Dickson, W.L., Boyce, W.D. and Ash, J.S. 1997. A new species of stalked crinoid (Echinodermata) of possible Late Silurian age from central Newfoundland. *Atlantic Geology*, v. 33, pp. 11-17.
- Dunning, G.R. 1992. U-Pb Geochronological research agreement final report for the Newfoundland and Labrador Mines and Energy, Newfoundland Mapping Section, unpublished report, NDME, Geological Survey Branch.
- Dunning, G.R. and Chourelton, L.B. 1985. The Annieopsquotch ophiolite belt of southwest Newfoundland: Geology and tectonic significance: *Geological Society of America Bulletin*, v.96, pp.1466-1476.
- Dunning, G.R. and Krogh, T.E. 1985. Geochronology of ophiolite of the Newfoundland Appalachians. *Canadian Journal of Earth Sciences*, v.22, pp. 1659-1670.
- Dunning, G.R. and Krogh, T.E. 1986. Geochronology of ophiolite of the Newfoundland Appalachians: Reply. *Canadian Journal of Earth Sciences*, v. 23 no. 11, pp. 1862-1864.
- Dunning, G.R. and Manser, K. 1993. U-Pb Geochronological Research Agreement; final report for the Newfoundland Department of Mines and Energy, Newfoundland Mapping Section, Unpublished report, Newfoundland Department of Mines and Energy, Geological Survey Branch.
- Dunning, G.R. O' Brien, S.J., Colman-Sadd, S.P., Blackwood, R.F., Dickson, W.L., O' Neill, P.P. and Krogh, T.E. 1990. Silurian orogeny in the Newfoundland Appalachians. *Journal of Geology*, v. 98, no. 6, pp. 895-913.
- Eastler, T.E. 1969. Silurian geology of Change Islands and eastern Notre Dame Bay. *In* North Atlantic Geology and Continental Drift. *Edited by* M. Kay, American Association of Petroleum Geologists, Memoir 12, pp.425-432.
- Eckstrand, O.R. and Cogulu, E.H. 1993. Geology of the Caribou Hill Intrusive, Mount Peyton Complex, central Newfoundland. *In* Report of Activities, Newfoundland Department of Mines and Energy, Geological Survey Branch Report, pp.116-118.
- Eilu, P. and Groves, D.I. 2001. Primary alteration and geochemical dispersion haloes of Archean orogenic gold deposits in the Yilgran Craton: the pre-weathering scenario. *Geochemistry: Exploration, Environment, Analysis*; v.1, no.3, pp.183-200.
- Elliot, C.G., Dunning, G.R., and Williams, P.F. 1991. New U/Pb zircon age constraints on the timing of deformation in north central Newfoundland and implication for early Palaeozoic Appalachian Orogenesis. *Geological Society of America Bulletin*, v.103, pp. 125-135.



- Elliot, C.G and Williams P.F. 1986. The tectonics and depositional history of the Ordovician and Silurian rocks of Notre Dame Bay, Newfoundland: Discussion. *Canadian Journal of Earth Sciences*, v.23, p. 586.
- Evans D. T. W., 1991. Gold metallogeny, eastern Dunnage Zone, central Newfoundland. *In Current Research, Newfoundland and Labrador Geological Survey, Report No. 91-1*, pp. 301-318.
- Evans D. T. W. 1992. Gold metallogeny of the eastern Dunnage Zone, central Newfoundland. *In Current Research, Newfoundland and Labrador Geological Survey Report No. 92-1*, pp. 231-243.
- Evans D. T. W. 1993: Gold mineralization in the eastern Dunnage Zone, central Newfoundland. *In Current Research, Newfoundland and Labrador Geological Survey Report No. 93-1*, pp. 339-349.
- Evans, D.T.W. 1996. Epigenetic gold occurrences, eastern and central Dunnage Zone, Newfoundland. Newfoundland Department of Mines and Energy, Geological Survey Branch, Mineral Resources Report. 9, 135 pages.
- Evans, D.T.W. 1999. Volcanogenic massive sulphide and gold mineralization, northern and central Dunnage Zone, Newfoundland. *Edited by D. T.W. Evans, North Atlantic Minerals Symposium, 1999*.
- Evans, D.T.W. 2005. Epigenetic gold occurrences, Baie Verte Peninsula (NTS 12H/09 and 12I/01). Newfoundland and Labrador Department of Natural Resources, Geological Survey, Mineral Resource Report 11, 159 pages.
- Evans, D.T.W., Hayes, J.P., and Blackwood, R.F. 1992. Gander River (NTS 2E/2), Newfoundland. Newfoundland Department of Mines and Energy, Geological Survey Branch, Map 92-21.
- Evans, D.T.W., Kean, B.F. and Dunning, G.R. 1990. Geologic studies, Victoria Lake Group, central Newfoundland. *In Current Research, Newfoundland Department of Mines and Energy, Geological Survey Branch, Report 90-1*, pp. 131-144.
- Evans, D.T.W. and Wilson, M. 1994. Epigenetic gold occurrences in the eastern Dunnage Zone, Newfoundland: Preliminary stable isotope results. *In Current Research, Newfoundland and Labrador Department of Mines and Energy, Geological Survey, Report 94-1*, pp. 211-223.
- Faure, G. 1986. Principles of isotope geology. John Wiley and Sons, New York, NY, 589 pages.
- Faure, G. 1998. Principles and applications of geochemistry: a comprehensive textbook for geology students. 2<sup>nd</sup> edition John Wiley and Sons, New York, NY, 600 pages.
- Fralick, P.W. 2003. Geochemistry of clastic sedimentary rocks: ratio techniques. *In Geochemistry of Sedimentary Rocks. Edited by D. Lentz, Geological Association of Canada, Geotext 4*, pp. 85-103.
- Fralick, P.W. and Kronberg, B.I. 1997. Geochemical discrimination of clastic sedimentary rock sources. *Sedimentary Geology*, v.113, pp. 111-124.
- Fryer, B.J., Kerr, A., Jenner, G.A. and Longstaffe, F.J. 1992. Probing the crust with plutons: regional isotopic geochemistry of granitoid intrusions across insular Newfoundland. *In Current Research, Newfoundland Department of Mines and Energy, Geological Survey Branch, Report 92-1*, pp.119-139.
- Gagnon, J. 1981. Report on geological, geochemical and geophysical exploration for license 1534 and 1638-1648 on the Jonathan's Pond claims in the Gander area, Newfoundland. Westfield Minerals Limited. Newfoundland and Labrador Geological Survey, Assessment File 2E/02/0410, 42 pages.

- Goodwin, L.B. and O'Neil, P. 1991. The structural evolution of the northern segment of the Dunnage Zone-Gander Zone Boundary, Newfoundland. *In* Current Research, Newfoundland and Labrador Department of Mines and Energy, Geological Survey Branch, Report 91-1, pp.97-107.
- Gower, D. and Tallman, P. 1988. Second year assessment report on geological mapping, prospecting, geophysical surveys, trenching, soil geochemistry and diamond drilling at Glenwood-White Bay project, Licenses 2821 and 3259, NTS 2D/15. Noranda Exploration Company Limited, unpublished report, 16 pages.
- Gower, D. and Tallman, P. 1989. Second and third year assessment report on soil geochemistry, geophysical surveys, trenching and diamond drilling at Glenwood-White Bay project, Licenses 2821 and 3259, NTS 2D/15. Noranda Exploration Company Limited, unpublished report, 12 pages.
- Grady, J.C. 1952. Report on southern ultrabasic party Gander River area, Newfoundland. Newfoundland and Labrador Geological Survey, Internal Report, Open File 002D/0054.
- Grady, J.C. 1953. The geology of the southern half of the Serpentine Belt in east-central Newfoundland. Newfoundland and Labrador Geological Survey, Internal Report, Open File 002D11/0005.
- Graham, D.R. 1989. A geochemical and geological assessment report on Great Bend-Murphy Option claims Licenses 3270, 3271, 3272, and 3563. BP Resources Canada Limited, confidential report, 15 pages.
- Graham, D.R. 1990. An assessment report on prospecting and geochemical surveys, trenching and diamond drilling performed at the Great Bend-Murphy option, central Newfoundland. BP Resources Canada Limited, unpublished report, 10 pages.
- Graves, G. 1991. First year assessment report on License 3968 Jumpers Brook (6796): Geochemistry, geophysics, geology, diamond drilling, NTS 2D/14. Noranda Exploration Company Limited, unpublished report, 9 pages.
- Green, K. 1989. First year assessment report on Licenses 3411, 3429, 3449, 3453, 3494, 3502, 3503, and 3504. NTS 2D/15, 2E/2 and 2E/7. Noranda Exploration Company Limited, unpublished report, 17 pages.
- Greenslade, S. 2002. Geochemical and Petrographical Analysis of the Tim's Cove Vein System, Gander Bay, Newfoundland. Unpublished B.Sc. thesis, Memorial University of Newfoundland, St. John's, Newfoundland, 102 pages.
- Groves, D.I., Goldfarb, R.J., Gebra-Mariam, M., Hagemann, S.G., and Robert, F. 1998. Orogenic gold deposits: a proposed classification in the context of their crustal distribution and relationships to other gold deposits types. *Ore Geology Reviews*, v.13, pp. 7-23.
- Groves, D.I., Richard, J., Goldfarb, F.R. and Hart, C.J.R. 2003. Gold Deposits in Metamorphic Belts: Overview of Current Understanding, Outstanding Problems, Future Research, and Exploration Significance. *Economic Geology*, v. 98, No.1, pp. 1-29.
- Hall, L.M. and Roberts, D. 1988. Timing of the Ordovician deformation in the Caledonian-Appalachian orogen. *In* The Caledonian-Appalachian orogen, *Edited by* A. L. Harris and D. J. Fettes, Geological Society Special Publication no. 38, pp. 291-309.
- Hammer, S. 1981. Tectonic significance of the northeastern Gander Zone, Newfoundland: An Acadia ductile shear zone, *Canadian Journal of Earth Sciences*, V.18, pp. 120-135.
- Harland W.B. and Gayer R.A. 1972. The arctic caledonides and earlier oceans. *Geological Magazine*, v. 109, pp. 289-314.

- Haworth, R.T. and Miller, H.G. 1982. The structure of Paleozoic oceanic rocks beneath Notre Dame Bay, Newfoundland. *In* Major structural zones and faults of the northern Appalachians. *Edited by* P. St. Julien and J. Beland, Geological Association of Canada, Special Paper no. 24, pp. 149-173.
- Heaman, L.M. and Parrish, R. 1991. U-Pb geochronology of accessory minerals. *In* Applications of isotope systems to problems in geology; short course handbook. Mineral Association of Canada, Short Course Handbook, v.19, pp. 59-102.
- Hedenquist, J.W., Arribas, A. and Gonzalez-Urien, E. 2000. Exploration for epithermal gold deposits. *Economic Geology Reviews*, v.13, Gold in 2000, pp. 245-277.
- Helwig, J.A. 1969. Redefinition of the Exploits Group, Lower Paleozoic, northeast Newfoundland. *In* North Atlantic: geology and continental drift. *Edited by* M. Kay. American Association of Petroleum Geologists, Memoir 12, pp. 408-413.
- Hinchey, J.G., Wilton, D.H.C and Tubrett, M. 2003. A LAM-ICP-MS study of the distribution of gold in arsenopyrite from the Iodestar Prospect, Newfoundland, Canada. *Canadian Mineralogist*, v. 41, pp.352-264.
- Hoefs, J. 1980. Stable isotope geochemistry. Springer-Verlag, Berlin, Federal Republic of Germany (DEU), 208 p.
- Hoffe, Crystal K., 2003. A detailed examination of the relationships between intrusive phases of the Neyles Brook Quarry, Mount Peyton. Unpublished BSc. thesis, Memorial University of Newfoundland, St. John's, Newfoundland, 87 pages.
- Hofstra, A.H. and Cline, J.S., 2000. Characteristics and models for Carlin-type gold deposits. *Economic Geology Reviews*, v.13, Gold in 2000, pp. 163-220.
- Holdsworth, R.E. 1982. The geology and structure of the Gander-Avalon Boundary zone in northeastern Newfoundland. *In* Current Research, Newfoundland Department of Mines and Energy, Report 82-1, pp. 99-108.
- Horne, G.S and Helwig, J. 1967. Ordovician stratigraphy of Notre Dame Bay, Newfoundland, Memoir 12. *In* North Atlantic geology and continental drift: A symposium. *Edited by* M. Kay, Proceedings of a conference held at Gander, Newfoundland, pp. 388-407.
- Hsu, L.C., Bonham, H.F., Price, J.G., Garside, L.J., Desilets, M.O. and Lechler, P.J. 1995. Geochemical characteristics of the Paleozoic sedimentary rocks in the Winnemucca Quadrangle, Nevada, U.S.A.- Background values for gold exploration. *Exploration Mining Geology*, v.4, no. 3, pp. 227-242.
- Hughes, C.J. 1970. The Late Precambrian Avalonian Orogeny in Avalon, southeast Newfoundland. *American Journal of Science*, v. 269, pp. 183-190.
- Hynes, G.F. 2001. A study of the metamorphic aureole of the Mount Peyton Intrusive, Dunnage Zone, central Newfoundland. BSc. thesis, Memorial University of Newfoundland, St. John's.
- Hynes, G.F and Rivers, T. 2002. A study of the metamorphic aureole of the Mount Peyton Intrusive, Dunnage Zone, central Newfoundland. *In* Current Research, Newfoundland Department of Mines and Energy, pp.53-65.
- Irvine, T.N. and Barager, W.R.A, 1971. A guide to the chemical classification of the common volcanic rocks. *Canadian Journal of Earth Sciences*, v.8, pp. 523-548.



Jackson, S.E., Longerich, H.P., Dunning, G.R. and Fryer, B.J. 1992. The application of laser-ablation microprobe-inductively coupled plasma-mass spectrometry (LAM-ICP-MS) to in situ trace element determination in minerals. *Canadian Mineralogist*, v. 30, pp.1049-1064.

Jenner, G.A. and Fryer, B.J. 1980. Geochemistry of the upper Snooks Arm Group basalts, Burlington Peninsula, Newfoundland: Evidence against formation in an island arc. *Canadian Journal of Earth Sciences*, v.17, pp.888-900.

Jenner, G.A. 1996. Trace element geochemistry of igneous rocks: geochemical nomenclature and analytical geochemistry. *In* Trace Element geochemistry of volcanic rocks: Application for Massive sulphide Exploration. *Edited by* D.A. Wyman. Geological Association of Canada, Short Course Notes, v.12, pp.51-77.

Jenness, S.E. 1958. Geology of the lower Gander River Ultrabasic Belt. Geological Survey of Newfoundland, Report 11, 58 pages.

Jenness, S.E. 1972. . The Gander Lake and Davidsville Groups of northeastern Newfoundland: new data and geotectonic implications: Discussion. *Canadian Journal of Earth Sciences*, v.9, pp. 1779-1781.

Johnston, D. 1992. The Noggin Cove Formation, Carmenville Map area, northeast Newfoundland: a backarc volcanic complex. *In* Current Research, Part E, Geological Survey of Canada, Paper 92-1E, pp.27-36.

Karlstrom, K.E., Van der Pluijm, B.A. and Williams, P.F. 1982. Structural interpretation of the eastern Notre Dame Bay Area, Newfoundland: Regional post middle Silurian thrusting and asymmetrical folding. *Canadian Journal of Earth Science*, v. 19, pp. 2325-2341.

Karlstrom, K.E., Van der Pluijm, B.A. and Williams, P.F. 1983. Structural interpretation of the eastern Notre Dame Bay Area, Newfoundland: Regional post middle Silurian thrusting and asymmetrical folding: Reply. *Canadian Journal of Earth Science*, v. 20, pp. 1353-1354.

Kay, M., 1951. North American Geosynclines. Geological Society of America, Memoir 48, 141 pp.

Kay, M. and Colbert, E.H. 1965. Stratigraphy and Life History. John Wiley and Sons Inc., New York, 736 pages.

Kay, M. 1967. Stratigraphy and structure of northeastern Newfoundland bearing on drift in North Atlantic. *American Association of Petroleum Geologists Bulletin*, v.51, pp. 579-600.

Kay, M. 1969. Silurian of northeast Newfoundland coast. *In* North Atlantic: geology and continental drift. *Edited by* M. Kay. American Association of Petroleum Geologists, Memoir 12, pp. 414-424.

Kay, M. 1975. Campbellton sequence, mangeriferous beds adjoining the Dunnage Melange, northeastern Newfoundland. *Geologic Society of America Bulletin*, v. 86, pp. 105-108.

Kean, B.F. 1974. Notes on the geology of the Great Bend and Pipestone Pond Ultramafic Bodies. *In* Report of Activities, Department of Mines and Energy, Government of Newfoundland and Labrador, Mineral Development Division, pp. 33-42.

Kean, B.F. 1977. Geological compilation of the Newfoundland central volcanic belt. Department of Mines and Energy, Government of Newfoundland and Labrador, Mineral Development Division, Map 77-030.

- Kean, B.F., Dean, P.L. and Strong, D.F. 1981. Regional geology of the central mobile belt of Newfoundland. *In* The Buchans orebodies: fifty years of geology and mining. *Edited by* E. A. Swanson, D. F. Strong and J. G. Thurlow, Geological Association of Canada, Special Paper 22, pp. 65-78.
- Keen, C.E., Keen, M.J., Nichols, B., Reid, I., Stockmal, G.S., Colman-Sadd, S.P., O'Brien, S.J., Miller, H., Quinlan, G., Williams, H. and Wright, J. 1986. Deep seismic reflection profile across the northern Appalachians. *Geology*, v. 4, pp.141-145.
- Kennedy, D.P. 1975. Repetitive orogeny in the northeast Appalachians-new plate models based upon Appalachian examples. *Tectonophysics*, v. 28, pp.39-87.
- Kennedy, D.P. 1976. The Fleur de Lys Supergroup: stratigraphic comparison of Moine and Dalradin equivalents in Newfoundland with the British Caledonides. *Geological Society of London*, v.131, pp. 305-310.
- Kennedy, M.J., Blackwood, R.F., Colman-Sadd, S.P., O' Driscoll, C.F. and Dickson, W.L. 1982. The Dover Hermitage Bay Fault: Boundary between the Gander and Avalon Zones, eastern Newfoundland. *In* Major Structural Zones and Faults of the northern Appalachians. *Edited by* P. St. Julien and J. Beland. Geological Association of Canada, Special Paper 24, pp. 231-248.
- Kennedy, M.J. and McGonigal, M.H. 1972a. The Gander Lake and Davidsville Groups of northeastern Newfoundland: new data and geotectonic implications. *Canadian Journal of Earth Sciences*, v.9 pp. 452-459.
- Kennedy M.J. and McGonigal, M.H. 1972b. The Gander Lake and Davidsville groups of northeastern Newfoundland: new data and geotectonic implications: Reply. *Canadian Journal of Earth Sciences*, v.9, pp.1781-83.
- Kerrick, R., 1989. Geochemical evidence on the sources of fluids and solutes for shear zone hosted mesothermal gold deposits. *In* Mineralization and Shear Zones. *Edited by* J. T. Bursnall. Geological Association of Canada, Short Course 6, pp. 129-198.
- Klassen, R.A. 1994. A preliminary interpretation of glacial history derived from glacial striation, central Newfoundland. *In* Current Research, Geological Survey of Canada, Paper 94-D, pp.13-22.
- Kontak, D.J. and Smith, P.K. 1993. A metaturbidite-hosted lode gold deposit; the Beaver Dam Deposit, Nova Scotia; I. Vein paragenesis and mineral chemistry. *Canadian Mineralogist*, v. 31, pp. 471-522.
- Kosler, J., Fonneland, H., Slyvester, P., Tubrett, M. and Peterson, R. 2002. U-Pb dating of detrital zircon for sediment provenance studies-a comparison of laser ablation ICPMS and SIMS techniques. *Chemical Geology*, v. 182, pp. 605-618.
- Kyser, T.K. 1986. Stable isotope variations in the mantle. *Reviews in Mineralogy*, v.16, pp.141-164.
- Lafrance, B. and Williams, P.F. 1989. Silurian-Devonian transcurrent movement deformation in the Canadian Appalachians: (Abstract). *Atlantic Geology*, v. 25, p.163.
- Lafrance, B. and Williams, P.F. 1992. Silurian deformation in eastern Notre Dame Bay, Newfoundland. *Canadian Journal of Earth Sciences*, v. 29, pp.1899-1914.
- Lake, J.W.L., 2004. Petrographic, geochemical and isotopic investigations of barite showings along the Mustang Trend, Botwood Basin, central Newfoundland. Unpublished BSc. thesis, Memorial University of Newfoundland, St. John's, 86 pages.

Lake, J.W.L and Wilton, D.H.C. 2006. Structural and stratigraphic controls on mineralization at the Beaver Brook antimony deposit, central Newfoundland. *In* Current Research, Newfoundland and Labrador Department of Natural Resources, Geological Survey, Report 06-01, pp. 135-146.

Lang, J.R., Baker, T., Hart, C. and Mortensen, J.K., 2000. An exploration model for intrusion-related gold systems. *Society of Economic Geologists Newsletter*, no. 40, pp. 6-14.

Lapointe, P.L. 1979. Paleomagnetism and orogenic history of the Botwood Group and Mount Peyton batholith, central Newfoundland. *Canadian Journal of Earth Sciences*, v. 16, pp. 866-876.

Longerich, H.P. 1995. Analysis of pressed pellets of geological samples using wavelength-dispersive X-ray fluorescence spectrometry. *X-ray Spectrometry*, v.24, pp. 123-136.

Lorenz, B.E. 1999. A study of the igneous intrusive rocks of the Dunnage melange, Newfoundland, Phd. thesis, Memorial University of Newfoundland, St. John's, 220 pages.

Ludwig, K.R. 2001. Users Manual for Isoplot/Ex Version 2.49: a geochronological toolkit for Microsoft excel. Berkeley Geochronology Centre, Special Publication, no. 1a, 55 pages.

MacKenzie, A.C. 1985. First year assessment report on geological, geochemical and geophysical exploration for licence 2472. Noranda Exploration Company Limited, unpublished confidential report, 19 pages.

MacLean, W.H. and Barrett, T.J. 1993. Lithogeochemical techniques using immobile elements. *Journal of Geochemical Exploration*, v.48, pp. 109-133.

MacNeil, R.J. and Cooper, G.E. 1953. Tungsten Occurrences, Gander Bay, Unpublished Report, NALCO Ltd, 3 pages.

Malpas, J. and Strong, D.F. 1975. A comparison of chrome spinels in ophiolites and mantle diapars in Newfoundland. *Geochimica et Cosmochimica Acta*, v. 39 no. 6/7, pp. 1045-1060.

Marillier, F., Keen, C.E., Stockmal, G.S., Quinlan, G. Williams, H., Colman-Sadd, S.P., O'Brien, S.J. 1989. Crustal structure and surface zonation of the Canadian Appalachians: Implications of deep seismic reflection data. *Canadian Journal of Earth Sciences*, v.26, pp.305-321.

McBride, E.F. 1986. Diagenesis of the Maxon Sandstone (Early Cretaceous), Marathon. Region, Texas: a diagenetic quartzarenite. *Journal of Sedimentary Petrology*, v.57, pp.98 -107.

McCann, A.M. and Kennedy, M.J. 1974. A probable glacio-marine deposit of Late Ordovician-Early Silurian age from the north central Newfoundland Appalachian belt; *Geological Magazine*, v.111, pp. 549-564.

McKerrow W.S. and Cocks, L.R.M. 1977. The location of the Iapetus Ocean Suture in Newfoundland. *Canadian Journal of Earth Sciences*, v.14, pp. 488-495.

McKerrow, W.S and Cocks, L.R.M. 1980. Conodonts from the Davidsville Group, northeast Newfoundland: Discussion. *Canadian Journal of Earth Sciences*, v.17, p.1599.

McKerrow, W.S. and Cocks, L.R.M. 1986. Oceans, island arcs and olistrostromes: the use of fossils in distinguishing sutures terranes and environments around the Iapetus ocean. *Journal of the Geological Society of London*, v.143, pp. 185-191.



- Mercer, B.J. 1988a. Assessment report on geological, geochemical, and geophysical exploration surveys in the Great Bend Area. A.C.A. Howe International Limited, unpublished report, 18 pages.
- Mercer, B.J. 1988b. Assessment report on diamond drilling from Chiouk Brook and Lizard Pond, Great Bend Area. A.C.A. Howe International Limited, unpublished report, 15 pages.
- Meschede, M. 1986. A method of discriminating between different types of mid-ocean ridge basalts and continental tholeiites with the Nb/Y diagram. *Chemical Geology*, v.56, pp.207-218.
- Mezger, K. and Krogstad, E.J. 1997. Interpretation of discordant U-Pb zircon ages: An evaluation. *Journal of metamorphic Geology*. v. 15, pp. 127-140
- Miller, H.G. 1970. A gravity survey of eastern Notre Dame Bay, Newfoundland. Unpublished MSc. thesis, Memorial University of Newfoundland, St. John's, Newfoundland, 83 pages.
- Miller, H.G. and Thakwalakwa, S.A.M. 1991. Geophysical and geochemical interpretation of the configuration of the Mount Peyton Complex, central Newfoundland. *Atlantic Geology*, v.28, pp. 221-223.
- Misra, K.C. 2000. *Understanding Mineral Deposits*. Kluwer Academic Publishers, 845 pages.
- Mitchell, G.A. 2001. A petrographical and geochemical comparison of two mesothermal gold prospects: The Romeo and Juliet, Prospect, Baie Verte, and the Appleton Linear Group Prospect, Appleton. Unpublished BSc. thesis, Memorial University of Newfoundland, St. John's, 102 pages.
- Mitchinson, Dianne. 2001. Petrography and Geochemistry of the Caribou Hill Intrusion, Central Newfoundland, and its discordant pegmatites. Unpublished BSc. thesis, Memorial University of Newfoundland, St. John's, 95 pages.
- Murchison, R.I. 1854. *Siluria: the history of the oldest known rocks containing Organic remains, with a brief sketch on the distribution of gold over the earth*. John Murray, London, 523 pages, Plates I to XXXVII.
- Murray, A. and Howley, J.P. 1881. Report for 1871. *In Geological Survey of Newfoundland*. Edward Stanford, London, 536 pages.
- Myers, R.E. and Bretkopf, H. 1989. Basalt geochemistry and tectonic settings: A new approach to relate tectonic and magmatic processes. *Lithos*, v.23, pp. 53-62.
- Najjarpour and Upadhyay, H.D. 1987. The closing of the Iapetus ocean in eastern Notre Dame Bay, Newfoundland: geochemical evidence. *Geological Society of America, Program with abstracts*, v.19, p 236.
- O'Brien, B.H. 1993. A mapper's guide to Notre Dame Bays folded thrusts: evolution and regional development. Newfoundland Geological Survey, Report 93-1, pp. 279-292.
- O'Brien, S.J., O'Driscoll, C.F. and King, A.F. 1996. Late Neoproterozoic evolution of Avalonian and associated peri-Gondwanan rocks of the Newfoundland Appalachians. *In Avalonian and related terranes of the Circum-North Atlantic*. Edited by M.D. Thompson and R.D. Nance. Geological Society of America, Special Paper 304, pp. 9-28.
- O'Driscoll, J.M. and Wilton, D.H.C. 2004. Studies of auriferous systems in the Botwood Basin and environs, central Newfoundland. *In Current Research*, Department of Natural Resources, Geological Survey, Report 05-01, pp.207-222.

- Ohmoto, H. 1972. Systematics of sulfur and carbon isotopes in hydrothermal ore deposits. *Economic Geology and the Bulletin of the Society of Economic Geologists*, v.67, pp.491-559.
- Ohmoto, H. 1986. Stable isotope geochemistry of ore deposits. *Reviews in Mineralogy*, v.16, pp. 491-559.
- Ohmoto, H. and Rye, R.O. 1979. Isotopes of sulfur and carbon. *In Geochemistry of Hydrothermal Ore Deposits*, John Wiley and Sons, New York, NY, pp. 509-567.
- O' Neill, P. 1987. Geology of the east half of the Weir's Pond [2E/1] map area, northeastern Newfoundland. *In Report of Activities, Mineral Development Division, Department of Mines and Energy, Government of Newfoundland and Labrador*, pp. 55-58.
- O'Neill, P.P. 1991. Geology of Davidsville Group and Gander River Complex, NW Weir's Pond area Map 90-004. Scale: 1:12, 500. *In Geology of the Weirs Pond area, Newfoundland (NTS 2E/1)*. Government of Newfoundland and Labrador, Department of Mines and Energy, Geological Survey Branch, Report 91-03, 164 pages.
- O'Neill P. and Blackwood, F. 1989. A proposal for revised stratigraphic nomenclature of the Gander and Davidsville Groups and the Gander River Ultrabasic Belt, of northeastern Newfoundland. *In Current Research, Newfoundland and Labrador Geological Survey Report No. 89-1*, pp. 127-130.
- O' Neill, P.P. and Colman-Sadd, S.P. 1993. Geology of the Eastern part of the Gander (NTS 2D/15) and western part of the Gambo (NTS 2D/16) map areas, Newfoundland. Newfoundland Department of Mines and Energy, Geological Survey Branch, Report 93-2, 42 pages.
- O' Toole, K.C. 1967. The Gander Bay tungsten prospect. NALCO unpublished report, 14 pages.
- O'Toole 1970. Preliminary report Gander Bay Tungsten diamond drilling and prospecting. NALCO unpublished report, 3 pages.
- Pajari, G.E. and Currie, K.L., 1978. The Gander Lake and Davidsville Groups of northeastern Newfoundland: a re-examination. *Canadian Journal of Earth Sciences*, v.13 pp.708-714
- Pajari, G.E., Pickerill, R.K. and Currie, K.L., 1979. The nature, origin and significance of the Carmenville ophiolitic mélange, northeastern Newfoundland. *Canadian Journal of Earth Science*, v. 16, pp.1439-1452.
- Papezik, V.S. 1972. Late Precambrian ignimbrites in eastern Newfoundland and their tectonic significance. *In Proceedings of the 24th international geological congress, Montreal, Section 1*, pp. 147-152.
- Patrick, T.O.H. 1953. Wolfram at Charles Cove, Gander Bay, Newfoundland. Geological Survey of Canada, unpublished manuscript, 2 pages.
- Patrick, T.O.H. 1956. Comfort Cove, Newfoundland. Geological Survey of Canada, Paper 55-31 (geology map with marginal notes).
- Pearce, J.A. 1982. Trace element characteristics of lavas from destructive plate boundaries. *In Andesites: Orogenic Andesites and Related Rocks. Edited by R.S. Thorpe*, John Wiley & Sons, Chichester, U.K., 548 pages.
- Pearce, J.A. 1996. A user's guide to basalt discrimination diagrams. *In Trace Element Geochemistry of Volcanic Rocks. Edited by D.A. Wyman*, Geological Association of Canada, Short Course Notes, v.12, pp. 79-114.

- Pearce, J.A., and Cann, J.R. 1973. Tectonic setting of basic volcanic rocks determined using trace element analyses. *Earth and Planetary Science Letters*, v.19, pp. 290-300.
- Pearce, J.A., and Norry, M.J., 1979. Petrogenetic implications of Ti, Zr, Y, and Nb variations in volcanic rocks. *Contributions to Mineralogy and Petrology*, v.69, pp. 33-47.
- Piasecki, M.A.J. 1992. Tectonics across the Gander-Dunnage Zone boundary in northeastern Newfoundland. *In Current Research, Part E, Geological Survey of Canada, Paper 92-1E*, pp. 259-268.
- Piasecki, M.A.J. 1995. Dunnage Zone Boundaries and some aspects of terrane development in Newfoundland. *In GAC Special Paper 41, Current Perspectives in the Appalachian-Caladonian Orogen*, St. John's, Newfoundland, pp. 324-325.
- Pickerill, R.K., Pajari, G.E., Currie, K.L. and Berger, A.R. 1978. Carmenville map area (2E/8): The northeastern termination of the Appalachians. *In Report of Activities, Part A, Geological Survey of Canada, Paper 78-1A*, pp. 209-216.
- Pickerill, R.K., Pajari, G.E. and Currie, K.L. 1979. Evidence of Caradocian glaciation in the Davidsville Group of northeastern Newfoundland. *In Current Research, Part C, Geological Survey of Canada, Paper 79-1C*, pp.67-72.
- Pickering, K.T., Bassett, M.G., and Siveter, D.J. 1988. Late Ordovician-early Silurian destruction of the Iapetus Ocean: Newfoundland, British Isles and Scandinavia- a discussion; *Transects of the Royal Society of Edinburgh, Earth Sciences*, v.79, pp.361-382.
- Pickett, J.W. 1990. Assessment report on Jumpers Brook Property, License 3463, Newfoundland, N.T.S. 2E/3, 2D/14. Lundrigan Consulting Services Ltd., unpublished report, 7 pages.
- Pollock, J.C., Wilton, D.H.C, van Staal, C.R. and Morrissey, K.D. in prep. The terminal closure of Iapetus: U-Pb zircon constraints on the Late Ordovician-Silurian collision of Ganderia and Laurentia along the Dog Bay Line, Newfoundland.
- Poulson, K.H., Robert, F. and Dube, B. 2000. Geological classification of Canadian gold deposits. *Geological Survey of Canada, Bulletin 540*, 106 pages.
- Quinlan, G. M. 1988. Deep crustal structure of the Newfoundland Appalachians. *Geological Association of Canada, program with abstracts*, v.26, p. A34.
- Quinlan, G.M., Hall, J., Williams, H. Wright, J.A., Colman-Sadd, S.P., O' Brien, S.J., Stockmal, G.S and Marillier, F. 1992. Lithoprobe onshore seismic reflection transects across the Newfoundland Appalachians. *Canadian Journal of Earth Sciences*, v.29, pp. 1865-1877.
- Ramezani, J, Dunning, G.R., and Wilson, M.R. 2000. Geologic Setting, Geochemistry of Alteration, and U-Pb Age of Hydrothermal Zircon from the Silurian Stog'er Tight Gold Prospect, Newfoundland Appalachians. *Canada Exploration and Mining Geology*, v.9, pp. 171-188.
- Rast, N., O' Brien, B.H. and Wardle, R.J. 1976. Relationships between Precambrian and lower Paleozoic rocks of the Avalon platform in New Brunswick, the northeast Appalachians and the British Isles. *Tectonophysics*, v. 30, pp. 315-338.
- Reynolds, P.H., Taylor, K.A., and Morgan, W.R. 1981.  $^{40}\text{Ar}/^{39}\text{Ar}$  ages from the Botwood/ Mount Peyton region, Newfoundland: possible paleomagnetic implications. *Canadian Journal of Earth Sciences*, v.18, no.12, pp.1850-1855.



- Richards, J.P. and Noble, S.R. 1998. Application of radiogenic isotope systems to the timing and origin of hydrothermal processes. *In* Techniques in hydrothermal ore deposits geology, Reviews in Economic Geology, v.10, pp.195-233.
- Rollinson H.R. 1993. Using geochemical data: evaluation, presentation and interpretation. Wiley and Sons Inc., New York, 352 pages.
- Roser, B.P. and Korsch, R.J. 1986. Determination of tectonic setting of sandstone-mudstone suites using SiO<sub>2</sub> content and K<sub>2</sub>O/Na<sub>2</sub>O ratio. *Journal of Geology*, v.94, no.5, pp.635-650.
- St. Croix, L. and Taylor, D.M. 1991. Regional striation survey and deglacial history of the Notre Dame Bay area, Newfoundland. *In* Current Research, Newfoundland Department of Mines and Energy, Geological Survey Branch, Report 91-1, pp.61-68.
- Scott, S. 1994. Surficial geology and drift exploration of Comfort Cove-Newstead and Gander River map areas (NTS 2E/7 and 2E/2). *In* Current Research, Newfoundland and Labrador Department of Mines and Energy, Geological Survey Branch, report 94-1, pp. 29-42.
- Seymour, C.R. 2003. Petrographical and geochemical analysis of the Reid Option Gold Property, south central Newfoundland. Unpublished BSc. thesis, Memorial University of Newfoundland, St. John's, 87 pages.
- Shervais, J.W. 1982. Ti-V plots and the petrogenesis of modern and ophiolitic lavas. *Earth and Planetary Science Letters*, v.59, pp. 101-118.
- Simpson, A. 1989. Report on fieldwork in the Jonathon's Pond Area, License 2472, Claim Blocks 3460, 3461, and 3463, License 2967, Claim Blocks 3468 and 3469, NTS 2E/2. Noranda Exploration Company Limited, unpublished report, 40 pages.
- Simpson, A. 1990. Report on fieldwork, geological, prospecting, trenching and diamond drilling in the Jonathon's Pond Area, License 2472, Claim Blocks 3460, 3461, and 3463, License 2967, Claim Blocks 3468 and 3469, NTS 2E/2. Noranda Exploration Company Limited, unpublished report, 20 pages.
- Smith, R., Butler, Jr. R., and Churchill, R., 2003. First, second and fifth year assessment reports on prospecting trenching and geochemical sampling at the Mustang Trend, Botwood Basin, central Newfoundland. Confidential report for Altius Resources Incorporated. Newfoundland and Labrador Department of Natural Resources, Geological Survey, Open File NFLD 2813.
- Snelgrove, A.K. 1934. Chromite deposits of Newfoundland. Department of Natural Resources, Geological Section. Bulletin No.1.
- Snelgrove, A.K., and Howse, C.K., 1934. Results of sampling Newfoundland gold prospects. Geological Survey of Newfoundland.
- Snelgrove, A.K., 1935. Geology of gold deposits of Newfoundland. Newfoundland Department of Natural Resources, Geology section, Bulletin, v.2, 46 pages.
- Snell, J. F. 2004. Bryozoa from the Much Wenlock Limestone (Silurian) Formation of the West Midlands and Welsh Borderland. Monograph of the Palaeontographical Society (London), 621 pages.
- Snow, P. 1988. First and fourth year assessment report on geological, geochemical, trenching and diamond drilling exploration for license 2472 on claim blocks 3460-3461 and 3463 and license 2965 on claim blocks 3438 and 3471 in the Jonathans Pond area, northeastern Newfoundland. Noranda Exploration Company Limited Newfoundland and Labrador Geological Survey, 111 pages.

- Squires, G.C. 2004. Gold and Antimony occurrences of the Exploits Subzone and Gander Zone: A review of recent discoveries and their interpretation. *In* Current Research, Newfoundland and Labrador Department of Natural Resources, Geological Survey, Report 05-1, pp. 223-237.
- Stearn, C. and Carroll, R. 1989. Paleontology: The Record of Life. John Wiley & Sons, Inc., 453 pages.
- Stevens, R.K. 1970. Cambro-Ordovician flysch sedimentation and tectonics in west Newfoundland and their possible bearing on a proto Atlantic Ocean. *In* Flysch Sedimentology in North America, *Edited by* J. Lajoie. Geological Association of Canada, Special Paper 7, pp.165-177.
- Stouge, S. 1980a. Conodonts from the Davidsville Group, northeastern Newfoundland. *Canadian Journal of Earth Science*, v.17, pp. 268-272.
- Stouge, S. 1980b. Conodonts from the Davidsville Group, northeastern Newfoundland: Reply. *Canadian Journal of Earth Science*, v.17, pp.1600-1601.
- Stouge, S. 1980. Lower and Middle Ordovician conodonts from central Newfoundland and their correlatives in western Newfoundland. *In* Current Research, Newfoundland and Labrador Mineral Development Division, Report no. 80-1, pp. 134-142.
- Strong, D.F. 1977. Volcanic regimes of the Newfoundland Appalachians. *In* Volcanic regimes in Canada. *Edited by* W.R.A. Barager, L.C. Colman and J.H. Hall, Geological Association of Canada, Special Paper 16, pp.61-90.
- Strong, D.F. 1979. The Mount Peyton Batholith, central Newfoundland, a bimodal calc-alkaline suite. *Journal of Petrology*, v.20, pp.119-138.
- Strong, D.F., Dickson, W.L., O' Driscoll, C.F., Kean, B.F. and Stevens, R.K. 1974. Geochemistry of eastern Newfoundland granitoid rocks. Newfoundland Department of Mines and Energy, Mineral Development Division, Report 74-3, 140 pages.
- Strong, D. F. and Dupuy, C. 1982. Rare earth elements in the bimodal Mount Peyton batholith: evidence of crustal anatexis by mantle derived magma. *Canadian Journal of Earth Sciences*, v.19, pp. 308-315.
- Swinden, H.S. 1987. Ordovician volcanism and mineralization in the Wild Bight Group, central Newfoundland: A geological, petrological, geochemical and isotopic study. Unpublished Phd. thesis, Memorial University of Newfoundland, St. John's, 452 pages.
- Swinden, H.S. 1988. Volcanogenic sulphide deposits of the Wild Bight Group, Notre Dame Bay. *In* Volcanogenic sulphide districts of central Newfoundland. *Edited by* H.S. Swinden and B.F. Kean. Mineral Deposits Division, Geological Association of Canada, pp. 178-192.
- Swinden, H.S. 1990. Regional geology and metallogeny of central Newfoundland. *In* Field Trip Guidebook, 8<sup>th</sup> IAGOD Symposium, Metallogenic Framework of Base and Metal Deposits, central and western Newfoundland. Newfoundland and Labrador Department of Mines and Energy, Geological Survey Branch, pp. 1-6.
- Swinden, S.H., Jenner, G.A. and Szybinski, A. 1997. Magmatic and tectonic evolution of the Cambrian - Ordovician Laurentian margin of Iapetus: geochemical and isotopic constraints from the Notre Dame Subzone, Newfoundland. Geological Society of America, Memoir 191, Nature of Magmatism in the Appalachian Orogen, pp. 337-365.

Swinden, H.S., Kean, B.F. and Dunning, G.R. 1988. Geological and paleotectonic settings of volcanogenic sulphide mineralization in central Newfoundland. *In* The volcanogenic sulphide districts of central Newfoundland, a guidebook and reference manual for volcanogenic sulphide deposits in the early Paleozoic oceanic volcanic terranes of central Newfoundland. *Compiled by* H. S. Swinden and B. F. Kean, Geological Association of Canada-Mineralogical Association of Canada-Canadian Society of Petroleum Geologists, Field Trip Guidebook, trips A2 and B5, pp. 5-26.

Swinden, H.S., and Thorpe, R.I. 1984. Variations in style of volcanism and massive sulphide deposition in Early to Middle Ordovician island arc sequences of the Newfoundland Central Mobile Belt. *Economic Geology*, v.79, pp.1596-1619.

Szybinski, Z.A., Swinden, H.S., O'Brien, F.H.C., Jenner, G.A. and Dunning, G.R. 1990. Correlation of Ordovician volcanic terranes in the Newfoundland Appalachians: Lithological, geochemical and age constraints. Geological Association of Canada, Program with Abstracts, 15, p. A128.

Tallman, P. 1989a. First year assessment report on License 3418 Noront –Paul's Pond (4716) NTS2D/11 Noranda exploration Company Limited, unpublished report, 5 pages.

Tallman, P. 1989b. First year assessment report on License 3361, 3468, 3536, 3480, 3418, 3547, 3539, 3549, 3537, 3538, 3559, NTS2D/11 Noranda exploration Company Limited, unpublished report, 19 pages.

Tallman, P. 1990a. First year assessment report on Licenses 3361, 3468, 3536, 3480, 3418, 3547, 3539, 3549, 3537, 3538, and 3550, NTS 2D/11, for the period April 12, 1988 to April 11, 1989. Noranda Exploration Company, unpublished report, 21 pages.

Tallman, P. 1990b. First year assessment report on License 3544 and 3856, Noront-Mount Peyton (4719), NTS 2D/14, 2D/15, 2E/2, 2E/3 Noranda Exploration Company Limited, unpublished report, 13 pages.

Tallman, P. 1990c. Second year assessment report on diamond drilling at Noront-Beaver Brook project (6723), License 4012, NTS 2D/11. Noranda Exploration Company Limited, unpublished report, 9 pages.

Tallman, P. 1990d. Second year assessment report on prospecting, geological mapping, diamond drilling at GRUB Line north and Duder Lake projects (6721), License 3989 (3851), NTS 2E/2 and 2E/7. Noranda Exploration Company Limited, unpublished report, 11 pages.

Tallman, P. 1991a. Second year assessment report on license 3544, geophysics, soils and diamond drilling, Noront-Mount Peyton (6719), NTS 2D/14. Noranda Exploration Company Limited, unpublished report, 13 pages.

Tallman, P. 1991b. The 'Hunan Line' discoveries: antimony mineralization in central Newfoundland. *In* Ore Horizons. *Edited by* H.S. Swinden and A. Hogan. Newfoundland Department of Mines and Energy, Geological Survey Branch, v.1, pp.11-21.

Tallman, P. and Evans, D.T.W. 1994. Geology of stibnite mineralization at the Hunan Line Prospects, central Newfoundland. *In* Current Research, Newfoundland and Department Mines and Energy, Geological Survey Branch, Report 94-1, pp. 263-271.

Tallman, P. and Williams, S.H. 1995. Graptolite-based evidence for a revised stratigraphic and structural setting of the Szechuan, Hunan and Xingchang antimony prospects, Exploits Subzone, central Newfoundland. *Atlantic Geology*, v. 31, no. 2, pp. 87-93.

Taylor, H.P. 1974. The application of oxygen and hydrogen isotopes studies to problems of hydrothermal alteration and ore deposition. *Economic Geology and the Bulletin of the Society of Economic Geologists*, v.69, no.6, pp.843-883.



Thakwalakwa, S.A.M. 1990. The surface and subsurface geology of the Mount Peyton Complex: an integrated geophysical, geological and geochemical approach. Unpublished BSc. thesis, Memorial University of Newfoundland, St. John's, Newfoundland, 47 pages.

Thompson, J.F.H. and Newberry, R.J. 2000. Gold deposits related to reduced granitic intrusions. *Economic Geology Reviews*, v.13, (Gold in 2000), pp.377-400.

Turmel, R.A., 2000. Petrography and geochemistry of alteration associated with the Rolling Pond Epithermal Gold Prospect, Newfoundland. Unpublished BSc. thesis, Memorial University of Newfoundland, St. John's, Newfoundland, 110 pages.

Twenhofel, W.H. and Shrock, R.R. 1937. Silurian strata of Notre Dame Bay and Exploits Valley, Newfoundland, *Bulletin of the geological society of America*, v.48, pp.1743-1772.

Twenhofel, W.H. 1947. The Silurian of eastern Newfoundland, with some data relating to physiography and Wisconsin glaciation of Newfoundland. *American Journal of Science*, v. 245, pp.65-122.

van der Pluijm, B.A., van der Voo, R. and Johnson, R.J.E. 1989. Middle Ordovician to Lower Devonian evolution of the northern Appalachians; The Acadian phase? (abstract). *Geological Society of America, Abstracts with Programs*, v.21, no.2, p. 72.

van Staal, C.R. 1994. Brunswick subduction complex in the Canadian Appalachians; record of the Later Ordovician to Late Silurian collision between Laurentia and the Gander margin of Avalon. *Tectonics*, v.13, no.4, pp. 946-962.

van Staal, C.R., Sullivan, R.W. and Whalen, J. 1996. Provenance and tectonic history of the Gander margin in the Caledonian/Appalachian Orogen: implications for the origin and assembly of Avalonia. In *Avalonian and related peri-Gondwanan terranes of the circum-North Atlantic*, Special Paper-Geological Society of America, v. 304, pp.347-367.

Wanless, R.K., Stevens, R.D., LaChance, G.R. and Edmonds, C.M. 1967. Age determinations and geological studies: K-Ar isotopic ages, report 7. *Geological Survey of Canada, report 66-17*, 120 pages.

Wasowski, J.J. and Jacobi, R.D. 1986. The tectonics and depositional history of the Ordovician and Silurian rocks of Notre Dame Bay, Newfoundland: Discussion. *Canadian Journal of Earth Sciences*, v. 23, pp. 583-585.

Whalen, J.B., Jenner, G.A, Longstaffe, F.J. and Hegner, E. 1996. Nature and evolution of the eastern margin of Iapetus: Geochemical and isotopic constraints from Siluro-Devonian granitoid plutons in the New Brunswick Appalachians: *Canadian Journal of Earth Sciences*, v.33, pp.140-155.

Whalen, J.B., Jenner, G.A, Longstaffe, F.J. and Gariépy, C. 1997. Implications of granitoid geochemical and isotopic (Nd, O, Pb) data from the Cambrian, Ordovician Notre Dame arc for the evolution of the Central Mobile Belt, Newfoundland Appalachians. In *The nature of magmatism in the Appalachian Orogen*. Edited by A. K. Sinha, J. B. Whalen and J. P. Hogan, Geological Society of America, Geological Society of America, Memoir 191. p. 367-395.

Williams, H. 1962. Botwood (west half) map area, Newfoundland. *Geological Survey of Canada, Paper 62-9*, 16 pages.

Williams, H. 1964a. The Appalachians in Newfoundland – a two-sided symmetrical system. *American Journal of Science*, v 262, pp.1137-1158.

- Williams, H. 1964b. Botwood, Newfoundland. Geological Survey of Canada, Map 60-1963 (geological map with descriptive notes).
- Williams, H. 1967a. Silurian rocks of Newfoundland. *In* Collected papers on Geology of the Atlantic Region – Hugh Lily Memorial Volume. *Edited by* E.R.W. Neale and H. Williams. Geological Association of Canada, Special Paper 4, pp.93-137.
- Williams, H. 1967b. Pre-carboniferous development of Newfoundland Appalachians. Memoir 12, *In* North Atlantic Geology and Continental Drift: A Symposium. *Edited by* M. Kay, Proceedings of a conference held at Gander, Newfoundland, August, 1967.
- Williams, H. 1970. Red Indian Lake (east half), Newfoundland. Geological Survey of Canada, Map 1196A (with descriptive notes).
- Williams, H. 1972. Stratigraphy of the Botwood map-area, northeastern Newfoundland. Geological Survey of Canada, Open File 113, 117 pages.
- Williams, H. 1975. Structural succession, nomenclature and interpretation of transported rocks in western Newfoundland. *Canadian Journal of Earth Sciences*, v.12, pp.1874-1894.
- Williams, H. 1978. Tectonic lithofacies map of the Appalachian Orogen. Memorial University of Newfoundland, Map No. 1, Scale 1: 1,000,000.
- Williams, H., 1978. Geological development of the Northern Appalachians: its bearing on the evolution of the British isles. *In* Crustal evolution in northwestern Britain and adjacent regions. *Edited by* D.R. Bowes and B.E. Leake. *Geological Journal*, Special Issue no.10, pp. 57-66.
- Williams, H., 1979. Appalachian Orogen in Canada. *Canadian Journal of Earth Sciences*, v. 16, pp. 792-807.
- Williams, H. 1982. Geology of the Canadian Appalachians. *In* Perspectives in Regional Geological Synthesis. *Edited by* A.R. Palmer, Decade of North American Special Issue no. 1, pp. 57-66.
- Williams, H. 1992. Mélanges and coticule occurrences in the northeast Exploits subzone, Newfoundland. *In* Current Research, Part D, Geological Survey of Canada, Paper 92-1D, pp. 121-127.
- Williams H. 1993. Stratigraphy and structure of the Dog Bay Line in northeastern Newfoundland. *In* Current Research, Part B. Geological Survey of Canada, Paper 03-1D pp.19-27.
- Williams, H. 1995. Geology of the Appalachian-Caledonian Orogen in Canada and Greenland. Geological Survey of Canada, Geology of Canada, no. 6, pp. 1-921.
- Williams, H., Colman-Sadd, S.P. and Swinden, H.S. 1988. Tectonic-stratigraphic subdivisions of central Newfoundland. *In* Current Research, Part B, Geological Survey of Canada, Paper 88-1B, pp. 91-98.
- Williams, H., Currie, K.L., and Piasecki, M.A.J. 1993. The Dog Bay Line: a major Silurian tectonic boundary in northeast Newfoundland. *Canadian Journal of Earth Sciences*, v. 30, pp. 2481-2494.
- Williams, H., Dickson, W.L., Currie, K.L., Hayes, J.P., and Tuach, J. 1989. Preliminary report on a classification of Newfoundland granitic rocks and their relations to tectonostratigraphic zones and lower crustal blocks. *In* Current Research, Part B, Geological Survey of Canada, pp. 47-53.

Williams, H., Dean, P.L. and Pickering, K.T. 1995. Botwood Belt; *In* Chapter 4 of Geology of the Appalachian Orogen in Canada and Greenland. *Edited by* H. Williams, Geological Survey of Canada, Geology of Canada, no. 6, pp. 413-420.

Williams, H. and Hatcher, R.D. 1983. Appalachian suspect terranes. *In* Contribution to the tectonics and geophysics of mountain chains. *Edited by* R.D. Hatcher, H. Williams, and I. Zeitz, Geological Society of America, Memoir 158, pp. 33-53.

Williams, H., Kennedy, M.J. and Neale, E.R. 1970. The Hermitage Flexure, the Cabot Fault, and the disappearance of the Newfoundland Central Mobile Belt. *Geological Society of America Bulletin*, v. 81, no. 5, pp.1563-1567.

Williams, H., Kennedy, M.J. and Neale, E.R.W., 1972. The Appalachian Structural Province. *In* Tectonic Styles in Canada. *Edited by* R.A. Price and R.J.W. Douglas, Geological Association of Canada, Special Paper 11, pp.181-261.

Williams, H., Kennedy, M.J. and Neale, E.R.W. 1974. The northwest termination of the Appalachian Orogen. *In* The Ocean Basins and Margins, v.2. *Edited by* A.E.M. Mairn and F.G. Stehli. Plenum Press, New York, NY, pp.70-123.

Williams, H. and Stevens, R.K. 1974. The ancient continental margin of eastern North America. *In* The Geology of Continental Margins. *Edited by* C.A. Burke and C.L. Drake. Springer-Verlag, New York, NY, pp. 781-796.

Williams, H. and St. Julien, P. 1982. The Baie Verte-Brompton Line: Early Paleozoic continental ocean interface in the Canadian Appalachians. *In* Major Structural Zones and Faults of the northern Appalachians. *Edited by* P. St. Julien and J. Beland. Geological Association of Canada, Special Paper 24, pp. 177-207.

Williams, S.H. 1988. Middle Ordovician graptolites from central Newfoundland. *In* Current Research, Newfoundland Department of Mines and Energy, Mineral Development Division, Report 88-1, pp. 183-188.

Williams S.H. 1989. New graptolite discoveries from the Ordovician of central Newfoundland. *In* Current Research, Newfoundland and Labrador Geological Survey, Report 89-1, pp. 149-157.

Williams, S.H. 1991. Stratigraphy and graptolites of the upper Ordovician Point Lemington Formation, central Newfoundland. *Canadian Journal of Earth Sciences*, v.28, pp. 581-600.

Williams, S.H. 1993. More Ordovician and Silurian graptolites from the exploits subzone. *In* Current Research, Newfoundland Department of Mines and Energy, Geological Survey Branch, Report 93-1, pp. 311-315.

Williams, S.H., Coleman-Sadd, S.P., O'Brien, B.H., Boyce, W.B. 1992. New discoveries of Ordovician (Arenig) and Silurian (Llandovery) graptolites from central Newfoundland and their paleographic implications. GAC-MAC-SEG Program with abstracts, v.16, p. A132.

Williams, S.H., Harper, D.A.T., Neuman, R.B., Boyce, W.D. and Mac Niocaill, C. 1996. Lower Paleozoic fossils from Newfoundland and their importance in understanding the history of the Iapetus Ocean. *In* Current Perspectives in the Appalachian-Caledonian Orogen, *Edited by* J.P. Hibbard, C.R. van Staal, P.A. Cawood, Geological Association of Canada, Special Paper 41, pp.115-126.



- Williams S.H. and O' Brien, B.H. 1991. Silurian (Llandovery) graptolites from the Bay of Exploits, north central Newfoundland, and their geological significance. *Canadian Journal of Earth Sciences*, v.28, pp. 1534-1540.
- Williams, S.H. and Tallman, P. 1995. Graptolite based evidence for a revised stratigraphic and structural setting of the Szechuan, Hunan, and Xingchang antimony prospects, Exploits subzone, central Newfoundland. *Atlantic Geology*, v. 31, pp. 87-93.
- Wilson, J.T. 1966. Did the Atlantic close and then re-open? *Nature*, v.211, pp. 676-681.
- Wilton, D.H.C. and Evans, D.T.W. 1991. Comparison of gabbro hosted mesothermal gold mineralization from opposite margins of the Dunnage zone. Geological Association of Canada, Program with abstracts, v.16, page A133.
- Wilton, D.H.C. 1997. Note on the Tim's Harbour (Charles Cove) prospect, north-central Newfoundland. St. John's, Newfoundland. Unpublished report for Copper Hill Resources Inc. 6 pages.
- Wilton, D.H.C. 1998: First year assessment report on geological, geophysical and prospecting surveys covering mineral claim license No's 5241M, 5299M, 5297M, and 5358M (NTS map sheets 2E/7, 8) the Tim's Cove property, Newfoundland, St. John's, Newfoundland, 10 pages.
- Wilton, D.H.C., 1998. *Geology 101: Carlin Type Gold Deposits, Part I and Part II. The Northern Miner.*
- Wilton, D.C.H. and Taylor, R.C. 1999. Second year assessment report on geological, geophysical, and prospecting surveys covering mineral claim license no.'s 5241M, 5297M, 5298M, 5299M, 5357M and 5358M (NTS mapsheet 2E/7, 8). The Tim's Cove Property, Newfoundland.
- Wilton, D.H.C. 2002. Unpublished report on Tim's Cove.
- Winchester, J.A. and Floyd, P.A. 1977. Geochemical discrimination diagrams on different magma series and their differentiation products using immobile elements. *Chemical Geology*, v. 20, pp.325- 343.
- Woldeabzghi, T. 1988. Second year assessment report on geological, geochemical, geophysical, trenching and diamond drilling exploration for license 2821 on claims in the Glenwood and Gander River Outflow areas, Newfoundland. Noranda Exploration Company Ltd., Newfoundland and Labrador Geological Survey, 18 pages.
- Wonderley, P.F. and Neuman, R.B. 1984. The Indian Bay Formation: fossiliferous Early Ordovician volcanogenic rocks in the northern Gander Terrane, Newfoundland, and their regional significance. *Canadian Journal of Earth Sciences*, v. 21, pp. 525-532.
- Wu, T.W. 1979. Structural, stratigraphic and geochemical studies of the Horwood Peninsula-Gander Bay area, northeast Newfoundland. MSc. thesis, Brock University, St. Catharines, Ontario, 185 pages.
- Wu, X. and Delbove, F. 1989. Hydrothermal synthesis of gold-bearing arsenopyrite. *Economic Geology*, v.84, pp.2029-2032.
- Zwicker, E.J. and Strong, D.F. 1986. The Great Bend Ophiolite, eastern Newfoundland. *In Current Research, Geological Survey of Canada, Paper 86-1A*, pp. 393-397.

**APPENDIX 1**

**PREVIOUS WORK**

**Table A1.1:** Brief description of previous work conducted within or adjacent to the Botwood Basin, central Newfoundland (Previous histories of paleontological and geochronological work are listed separately in tables A1.3 and A1.4, respectively).

<b>TECTONIC STUDIES</b>	
Kay (1951)	As an integral part of the geosynclinal theory that he applied to the Appalachian System, he postulated that an Ordovician chain of volcanic islands bordered the ancient North American continent.
Williams (1962)	Conducted reconnaissance mapping of the Botwood map area. Noted contrasts between subaerial volcanic rocks of Silurian age and marine rocks of Ordovician age. Assigned subaerial volcanics and interlayered redbeds near Botwood to the Botwood Group.
Williams (1964a)	Presented a summary of the sedimentary and tectonic features of northeastern Newfoundland, which demonstrated a two-sided system with a symmetrical Palaeozoic central mobile belt about a central axis. Concluded that the geology of northeastern Newfoundland contradicts the then widely accepted view that the Appalachian system formed as a Palaeozoic welt on the southeastern border of North America during Palaeozoic time.
Kay and Colbert (1965)	Made the first subdivision of the Canadian Appalachians based upon the northeastern Newfoundland cross section described by Williams (1964a). The subdivisions were the Western Platform, the Central Volcanic Belt and the Avalon Platform.
Wilson (1966)	Suggested that modern volcanic chains adjacent to continental margins are probably analogous to Ordovician volcanic-volcaniclastic sequences within the Appalachian System and that the evolution of the Appalachian-Caledonian Orogen was related to the opening and closing of a proto Atlantic Ocean.
Kay (1967)	Correlated the stratigraphic and tectonic belts of Newfoundland and the British Isles. Provided evidence to support either an original proximal relationship between opposing sides of the North Atlantic or continuity between the belts beneath the present day Atlantic Ocean basin.
Williams (1967b)	Outlined Pre-Carboniferous development of the Newfoundland Appalachians. Discussed the tripartite subdivision of Newfoundland into distinct geological provinces, the geology of each zone and the subsequent deformational events that affected the central Paleozoic mobile belt.



Table A1.1: *cont...*

Williams <i>et al.</i> (1972)	Subdivided the Appalachian structural province into nine zones (A-I) from West to East. Attributed deformation of central Newfoundland (zone D (Notre Dame Bay), zone E (Exploits), and zone F (Botwood Basin) to two Paleozoic Orogenic events: the Ordovician Taconic Orogeny and the mid Devonian Acadian Orogeny, but suggested that a more complex history was yet to be defined.
Williams and Stevens (1974)	Study of the western margin of the Appalachians or the ancient continental North American margin and its geological history in terms of the evolution of the Appalachian Orogeny.
McKerrow and Cocks (1977)	Proposed that the Long Reach Fault represents the suture point for the closure of the Iapetus Ocean at the end of the Early Devonian based on faunal evidence on opposing sides of the fault. Suggested that fauna from the west (i.e. middle Ordovician fauna on New World Island) have North American and Scottish affinities whereas those to the east (i.e. Ordovician fauna from the Gander region) do not have any affinities to known fauna provinces but are connected to those on the Avalon Peninsula, which have clear European affinities.
Strong (1977)	Broad study of volcanic regimes within the Newfoundland Appalachians. Author took the common approach of classifying the regimes based on geochemistry, but in this case put greater emphasis on geological observations. Concluded that the findings can be applied to the Wilson Cycle and therefore relates the entire Appalachian-Caledonian system to the birth, evolution and subsequent destruction of the proto Atlantic Ocean.
Pajari and Currie (1978)	Re-evaluated the three-fold subdivision that split northeastern Newfoundland into the Gneiss Complex, Gander Lake Group and the Davidsville Group and ascertained that this subdivision as suggested by Jenness (1963) and Kennedy and McGonigal (1972) is valid based on field observations and tectonic interpretations. Indicated that there is no evidence presented for or against a late Precambrian-early Phanerozoic orogeny. Determined that the observed tectonic relationships are consistent with the obduction of oceanic material during Ordovician time.
Williams (1978)	Correlated the zonal divisions of the Northern Appalachians to zones in the Caledonides of the British Isles.
Currie <i>et al.</i> (1979)	Suggested tectonic modeling indicates that the Carmenville map area rocks formed a continental slope and toe of slope to an eastern continent. Significant deformation occurred in Ordovician or Silurian time with a thermal climax in the Devonian. Postulated that transcurrent faulting occurred on a projection of the Avalonian continent subsequently placing it over a hot spot, which resulted in later magmatic and metamorphic activity.
Williams (1979)	Examined the history of the five broad zones in the Appalachian Orogen through an analysis of previous work. Provided a summary of work based on the evolution of plate tectonic theories with emphasis on the need for a broader look at the system as opposed to localized detailed work.

Table A1.1: *cont...*

Colman-Sadd (1980)	Studied the geology of south central Newfoundland and made correlations between the Bonavista Bay Gneiss Complex, the Gander and Davidsville Groups and granitoid intrusions. Observed relationships that suggest the Davidsville and Gander Groups are conformable. Concluded that the evidence suggests, in accordance with previous studies, that the Baie d'Espoir, Davidsville and Gander Groups were deposited in an Ordovician back arc basin.
Colman-Sadd (1982)	Discussion on plate tectonics, associated orogenies and plate driving forces in relation to the Newfoundland Appalachians.
Williams and Hatcher (1983)	Applied the suspect terrane concept to the Newfoundland Appalachians. Concluded that deformation, plutonic and metamorphic events were all related.
Colman-Sadd and Swinden (1984)	Stratigraphic, paleontological and structural examination of the Through Hill Area, which led to the conclusion that two layers of crust were superimposed in the area. The upper layer consists of Dunnage Zone rocks and the lower layer comprises the Mount Cormack Terrane (Gander Group). The authors suggested that this interpretation allows for the existence of two tectonically superimposed layers beneath the central mobile belt and therefore that the entire Dunnage Zone is allochthonous. The Gander Zone may be the upper overthrust sheet or part of the underlying crustal layer if the Dunnage Zone and Gander Zones are separated by an undefined structural discontinuity.
McKerrow and Cocks (1986)	Used faunal evidence to designate the Reach Fault as the suture for the closing Iapetus Ocean.
Najjarpour and Upadhyay (1987)	Determined that the Reach fault is the suture for the closing Iapetus Ocean based on contrasting major and trace element geochemical signatures on opposing sides of the fault.
Williams <i>et al.</i> (1988)	Revision of Newfoundland Appalachian Zonal divisions. Subdivided the Dunnage zone into the Notre Dame and Exploits subzones based on stratigraphic, structural, isotopic, geophysical and faunal evidence. The Red Indian Line, a faulted boundary separating geologically distinct Ordovician volcanic-sedimentary rocks, divides the zones.
Dunning <i>et al.</i> (1990)	Mapped and dated units in the Central Mobile Belt to better understand the tectonic evolution of the region. The majority of the units studied were in the extreme southern mobile belt and only one unit is relevant in this previous history evaluation, the Stoney Lake Volcanics. U-Pb date of the Stoney Lake rhyolitic tuff provided an estimated age of 423 $\pm$ 2 Ma. It was concluded that since previous workers ( <i>i.e.</i> Colman-Sadd and Russell (1982) and Anderson and Williams (1970)) suggested that an angular unconformity existed between the volcanics and the Botwood Group that their rhyolite age could possibly represent the lower Silurian deformation and cleavage event within the Silurian Botwood Group. The authors noted that such a contact is only inferred, as it was not observed in field studies.

Table A1.1: *cont...*

Currie (1995b)	Mapped the northeastern Dunnage Zone and presented a tectonic model for the development of the zone based on new field observations in relation to previous work.
Piasecki (1995)	Review of studies on the structural boundaries between the Gander, Dunnage and Humber Zones. Postulated that these complex zones exhibit ductile shearing followed by brittle movements and were subsequently reworked during successive tectono-metamorphic events.
Winchester and van Staal (1995)	Reassessed the tectonic evolution of the Appalachian orogen by correlating meta-volcanic and associated sedimentary assemblages between Newfoundland, New Brunswick and Maine based on lithology, tectonic setting, faunal provinciality and paleomagnetic data. Mainly used geochemical data to review the tectonic setting of volcanic suites and new data combined with previous work to reassess and compare the Appalachian and Caledonides.
Williams <i>et al.</i> (1995)	Definition of the Botwood Belt accompanied by an overview of previous work, nomenclature and stratigraphic relationships, lithology, correlation and age.
Cawood <i>et al.</i> (2001)	Presented a scenario for the opening of the Iapetus ocean based on geological, geochronological and paleomagnetic data from along the Iapetus margin of Laurentia.
<b>STRUCTURAL STUDIES</b>	
Dean and Strong (1977)	Correlated several of the large faults in the eastern area and provided an interpretation of the deformational history in relation to those faults (i.e. correlated the Lobster Cove fault in the western portion of the area to the Chanceport fault and suggested that they are thrust faults that were folded during Acadian deformation).
Karlstrom <i>et al.</i> (1982)	Correlated the Dunnage mélange to the Carmenville mélange as well as other mélanges in the area based on observed $f_2$ fabrics. Identified three fold generations that range in age from Ordovician to middle Silurian with the implication from this that the majority of the Dunnage Zone may be allochthonous.
Currie <i>et al.</i> (1983)	Discussion on Karlstrom <i>et al.</i> (1982). Suggested that the model that was presented would have to be reconsidered before it is applied on a regional scale.
Karlstrom <i>et al.</i> (1983)	Reply to Currie <i>et al.</i> (1983). Denoted that their model was not solely dependant on the points criticized by Currie <i>et al.</i> (1983) and presented macroscopic and microscopic structural evidence to reaffirm their conclusions.



Table A1.1: *cont...*

Blewett and Pickering (1988)	Suggested that the pattern of major sinistral transcurrent motions between Laurentia and colliding terranes observed in the British Caledonides are also present in north central Newfoundland.
Elliott <i>et al.</i> (1991)	Used U-Pb radiometric dating of felsic plutons in Notre Dame Bay to constrain the timing of deformation events within the Newfoundland Appalachians. Concluded that several tectonic elements were contemporaneously being generated, subducted or deformed and that deformation occurred continuously throughout the Late Cambrian to the end of the Palaeozoic.
Goodwin and O' Neil (1991)	Suggested that the present structural state of the Exploits-Gander Lake Boundary resulted from two episodes of strike slip and oblique slip motion.
Lafrance and Williams (1992)	Determined that Silurian deformation resulted from the thrusting of the Dunnage Zone over the Gander Zone, which resulted in dextral ductile faulting. Also concluded that the closure of Iapetus was oblique with a dextral, horizontal component.
Piasecki (1993)	Conducted a study of the Dog Bay Line structure and associated elements along the Port Albert Peninsula.
Williams (1993)	Determined that a major structure discontinuity was present near Duder Lake termed the Dog Bay Line. The structure has a dextral sense of movement with a possible offset of tens of kilometres.
Williams <i>et al.</i> (1993)	Examined the geology on either side of the Dog Bay Line, a Silurian terrane boundary, in an attempt to explore its significance. Recommended tectono-stratigraphic subdivision of a previously defined Botwood Belt (H. Williams, 1993) into the Botwood Belt for those rocks to the west of the Dog Bay Line and the Indian Islands Belt for the thin grouping of rocks to the southeast. Proposed redefinition of the Botwood Group in that the Late Ordovician marine greywacke-conglomerate sequence formerly included in the Botwood Grouping was redefined as the Badger Group following recommendations of previous workers. Therefore, the recognition of the Dog Bay Line led to a revision of nomenclature in the Exploits subzone and a revision of the tectonostratigraphic belts. Proposed the Dog Bay Line as a possible suture point for the closing Iapetus Ocean.
<b>REGIONAL GEOLOGY/ STRATIGRAPHIC STUDIES</b>	
Murray and Howley (1881)	Noted sandstone and conglomerate at both Peterview and Norris Arm and fossiliferous conglomerates at Martin Eddy Point. Highly folded sandstone and slate were observed along the Exploits River to Bishop Falls. Correlated fossils at Eddy's Point to fossils at Goldson's Sound. These fossils were assigned a Llandovrian age by Billings of the GSC.
Twenhofel and Shrock (1937)	First detailed regional study of the Silurian strata of Notre Dame Bay and the Exploits River Valley. The authors divided the geology into three lithological divisions, the Botwood Formation, the Goldson Formation and the Pike Arm

Table A1.1: *cont...*

	Formation and assigned them to the Notre Dame Series. They generally 1) mapped the extent of the Silurian strata and the structural overprinting present within units, 2) noted that dykes and sills were contemporaneous with a Silurian deformation event 3) defined stratigraphy, and 4) correlated fauna to eastern North American and European fauna.
Twenhofel (1947)	Proposed that the conglomerates at Martin Eddy Point are Devonian based on fossil evidence in clasts derived from Silurian strata.
Baird <i>et al.</i> (1951)	Briefly mentioned and described extensive gabbroic and granitic rocks that intruded sedimentary rocks in the eastern Dunnage Zone for the Photographic Survey Corporation.
Grady (1952, 1953)	Mapped and described the Great Bend Area for the GSC. Documented ultramafic and gabbroic rocks and defined their relationship to the surrounding sedimentary rocks. Contacts were interpreted to be faulted but originally intrusive. The sedimentary rocks were correlated with Ordovician rocks exposed in the Hamilton Sound of Notre Dame Bay and the intrusive rocks were linked to the Taconic orogeny. Identified magnesite within the ultramafic rocks as a possible exploration target and informally named many of the ponds in the area ( <i>i.e.</i> : Breccia Pond and Lizard Pond).
Patrick (1956)	Mapped the Comfort Cove-Newstead area and assigned rocks near Duder Lake to the Silurian-Devonian Springdale Group. Excluded shaley and calcareous rocks that were subsequently assigned to the Indian Islands Group from the Botwood Group.
Baird (1958)	Conducted a geological study on the rocks of the Fogo Island map area and proposed the name Indian Islands Group for Silurian rocks exposed on the Indian Islands.
Jenness (1958)	Mapped a narrow band of ultrabasic rocks north-northeast of Gander. Described the geology of these rocks and determined that they were not related to the gabbros or lavas within the Gander Lake Group. Determined a last Pleistocene ice movement of north to northeast.
Williams (1962)	Produced the first 1:250,000 scale map of the NTS/2E map area, west half. Introduced the term Botwood Group and included the Goldson Formation conglomerate of Twenhofel and Shrock (1937) within it. Defined the group as consisting of a basaltic volcanic component overlain by sedimentary strata. Fossils from the Exploits River shale that were included in the group indicated a mid Silurian age.
Williams (1964b)	Published a map of reconnaissance geological work in the Botwood Basin, which included a study of the geology of the Botwood map area, investigation of mineral occurrences, and completion of mapping started by Patrick (1956).

Table A1.1: *cont...*

Kay (1967)	Described the stratigraphy and structure of northeastern Newfoundland in an attempt to link the geology to the British Isles and southern New England as evidence for or against the theory of continental drift. Determined that if the stratigraphy and structure were once continuous, they have been offset by 500 miles via transcurrent faults in the North Atlantic. Decided that the similarity supports a case for either an original proximal relationship, or continuity beneath the ocean basin.
Williams (1967b)	Presented summary of results from reconnaissance mapping and previous work in central Newfoundland. Indicated that the current and previous studies suggest that the Silurian rocks of Llandoverly and early Wenlock age are widely distributed. Concluded that the Silurian rocks record a transition from deep-water marine to shallow water marine and then to a terrestrial environment and that Silurian deposition was restricted to troughs marked by one or more volcanic events.
Horne and Helwig (1969)	Examined an Ordovician chaotic melange in northeastern Notre Dame Bay and suggested that the melange records early Ordovician tectonic movement in the Appalachian belt that may have resulted from the onset of the Taconic Orogeny and correlated them to movements in western Ireland.
Kay (1969)	Renamed the Goldson Formation the Goldson Group and removed it from the Botwood Group.
Anderson and Williams (1970)	Produced a regional 1: 250, 000 scale geology map of the NTS/2D west half map area, Gander Lake.
Kennedy and McGonigal (1972a)	Re-evaluated the previously defined Gander Lake Group (Jenness, 1958) and determined that the group should be subdivided into three units based on structural evidence. Proposed the name Davidsville Group for the lowermost unit.
Bruckner (1972)	In response to Kennedy and McGonigal's (1972) redefinition of the Gander Group, suggested the name Gander Group for one of the newly defined units is in violation of the code of stratigraphic nomenclature because it was already in use by Jenness (1958) in reference to a previously defined unit.
Jenness (1972)	Questioned the use of structural evidence by Kennedy and McGonigal (1972) to redefine the Gander Lake Group (Jenness, 1958). Suggested that the field investigations to divide the group into three new units were lacking.
Kennedy and McGonigal (1972b)	In response to Jenness' discussion, provided further evidence to support their previous points that were questioned. Stood by the redefinition that the Gander Lake Group was actually composed of three distinct units.



Table A1.1: *cont...*

Williams, H. (1972)	Proposed a revision of the Botwood Group stratigraphy by introducing the Lawrenceton and Wigwam Formations. The new stratigraphy still included the Goldson Formation as a basal unit, overlain by the Lawrenceton and Wigwam units, respectively. The fossiliferous conglomerate from Eddys Point was included in the Wigwam Formation. Informally named the gabbro intrusion south of Norris Arm, the Mount Peyton Batholith.
Kean (1974)	Studied the geology of the Great Bend and Pipestone Pond ultramafic bodies. Suggested that the ultramafic and gabbroic rocks were mantle diapirs intruding the adjacent sedimentary rocks.
Strong <i>et al.</i> (1974)	Informally named the large gabbro-granite intrusion in the central region the Mount Peyton Batholith during a lithogeochemical survey of the northern portion of the intrusion. Geochemistry indicated that the pluton was bimodal with few intermediate silica values reported.
Kean (1977)	Produced a geological compilation of the Newfoundland central volcanic belt.
Blackwood (1978)	Reported on mapping during the 1978 field season in the northeastern Gander Zone. Mainly focused on unit relationships within the Gander Zone but also included a brief synopsis on observed Gander Group/ Davidsville relations in the Weir's Pond area.
Pickerill <i>et al.</i> (1978)	Conducted overview of units and tectonic relationships in the Carmenville map area (2E/8), which straddles both sides of a major tectonic boundary. Described the geology of the units present in the area and concluded that there is no evidence of subduction, which reinforces the symmetry of central Newfoundland as proposed by Williams (1964a). They also did not find evidence of a Precambrian orogeny or Cambro-Ordovician metamorphism, which contradicted the Ganderian Orogeny of Kennedy (1975). Nor did they find evidence for a major granitoid pluton emplacement prior to the Devonian, supporting the previous interpretations of Williams (1964a) and Jenness (1963).
Blackwood (1979)	Mapped the Gander River sheet (2E/2) as part of a larger Gander Rivers project that consisted of mapping along the Gander-Botwood Zone boundary. Defined five geological units in the area and presented a brief overview of mineralization (mainly in the Gander River Ultrabasic Belt).
Strong (1979)	Tried to explain the absence of an andesitic composition in the bimodal Mount Peyton Intrusive Suite using whole rock chemistry as it exhibited all other characteristics of a calc alkaline suite. Surface exposures of the bimodal suite exhibit very little per-aluminous intermediate composition, however geochemical classification of the suite produces calc alkaline variation patterns for both major and trace elements. Concluded that the results supported the view that the compositions appear unrelated by fractionation processes and that the gabbro was derived from the upper mantle, whereas the other compositions were derived by crustal anatexis.

Table A1.1: *cont...*

Bazinet (1980)	MSc. thesis project involving the mapping of the Gander Group, GRUB and Davidsville Group and the assessment of the relationships therein in the Jonathon's Pond-Weir's Pond area. Concluded that both the Gander and Davidsville Groups display different structural and metamorphic histories and that they were not conformable. Related the deformation in the Gander Group to the emplacement of the GRUB.
Currie <i>et al.</i> (1980)	Suggested that some units of the Davidsville-Gander Groups are diachronous and that the Silurian Indian Islands Group is unconformable upon the Davidsville Group. Based on these conclusions and on observations that the Indian Islands Group is equivalent to the Botwood Group and that the Davidsville Group is correlated to the Exploits Group, the authors concluded that the northeastern portion of the Dunnage is broadly synclinal.
Blackwood (1980)	Reported on the geology of the Gander (west) area (2D/15) and southeast Mount Peyton map area (2D/14) as part of the larger Gander Rivers project initiated in 1979. Mapped the area on a 1: 50, 000 scale.
Blackwood (1981)	Reported on the geology of the Great Bend-Paul's Pond area geology and produced a 1: 50, 000 scale map of the area as part of the NDME Gander Rivers project.
Blackwood (1982)	Mapped the Gander Lake (2D/ 15) and Gander River (2E/2) areas at a 1: 50, 000 scale for the NDME. Interpreted the Lower Ordovician, or younger, Gander Group as a shelf facies and the Middle Ordovician Davidsville Group as a turbidite sequence deposited on ophiolitic basement. Reported an unconformity between the GRUB and a conglomerate unit of the Davidsville Group. The author also noted regional deformation and mineralization and informally renamed the Mount Peyton Batholith (Williams, 1972), the Mount Peyton Intrusive Suite. Reported the Davidsville and Botwood Groups as conformable to faulted or conformable with fault modification based on observations made during regional mapping.
Colman-Sadd (1982)	Reconnaissance mapping at a 1:50, 000 scale of the Rolling Pond-Swan Lake areas.
Strong and Dupuy (1982)	Rare earth and trace element geochemical analysis of samples from the contrasting mafic and silicic portions of the Mount Peyton Intrusive Suite. Concluded that the rock types are not genetically related by crystal liquid fractionation. This supported earlier theories that the granite was derived by partial melting during the intrusion of a mantle-derived magma and that both compositions evolved independently. Study of mineral phases suggested intermediate compositions may have been somewhat evolved from partial melting but not in the absence of non-magmatic contamination.
Colman-Sadd and Swinden (1982, 1984)	Reconnaissance mapping in Great Bend Area. Determined that the Great Bend Complex was ophiolitic and part of the allochthonous Coy Pond Complex.

Table A1.1: *cont...*

Zwicker and Strong (1986)	Mapped the ultramafic and gabbroic rocks of the Great Bend Complex and adjacent rocks at a 1: 50, 000 scale for the GSC. Reported several mineralized areas of economic interest including the Chiouk Brook Au occurrence.
Coyle and Strong (1987)	Demonstrated three overlapping centers or calderas in west central Newfoundland and attributed their elongate distribution to northeast trending faults in basement rocks. Suggested a large caldera collapse model for the Springdale Group is consistent with the trapped heat and magma rising from the upper mantle at a weakened suture zone for a closing Iapetus ocean.
Colman-Sadd (1989)	Described the updated geology of the Miquel's Lake Area and included more precise dates for the Stoney Lake Volcanics and Spruce Brook Formation. Also documented new exposures of contact between the Botwood Group and Mount Peyton Group and Spruce Brook Formation, respectively.
O' Neill and Blackwood (1989)	Re-evaluation of the geology within the Weir's Pond map area, which contains rocks from the Gander and Davidsville Groups. Proposed a revised stratigraphic nomenclature for the Gander and Davidsville groups and the GRUB. Proposed a three-fold subdivision of the Davidsville Group and a two-fold subdivision of the Gander Group.
Dickson (1991)	Completed mapping as part of a project initiated by NDME to produce a more detailed mapping in the Great Bend-Paul's Pond area (NTS 2D/11 west half) at a 1:50, 000 scale to complement the work of Blackwood (1981) who mapped the NTS 2D/11 (east half).
O' Neill (1991)	Formally proposed a nomenclature change of the GRUB to the Gander River Complex. The change was suggested because although the GRUB is composed mostly of mafic and ultramafic rocks, felsic rocks form a significant portion.
Williams (1991)	Redefined the Point Lemington Formation of the Exploits Subzone. Correlated graptolite assemblages and stratigraphical succession of the unit to coeval rocks in southern Scotland, suggesting a relation between the areas in the late Ordovician.
Currie (1992)	Examination of the Gander-Dunnage Zones and relationships in the Carmenville map area.
Dickson (1992b)	Geological overview of ophiolites, sedimentary rocks, post-tectonic intrusions and mineralization in the Eastern Pond (NTS 2D/11, west half) map area. Determined that the composite Mount Peyton Intrusive Suite has intruded the Botwood Group and the Spruce Brook Formation based on metamorphic aureoles and that these units were deformed prior to the intrusion.
Boyce <i>et al.</i> (1993)	Identified fauna at Careless Brook and assigned a Late Silurian-Earliest Devonian age and suggested that this indicated Palaeozoic marine sedimentation continued later than previously suspected.



Table A1.1: *cont...*

Currie (1993)	A description of the Ordovician-Silurian stratigraphy between Gander Bay and Birchy Bay. Described stratigraphy to the east and west of the Dog Bay Line and stated that there was no known stratigraphic link across the Dog Bay Fault. Described movement along the Dog Bay Fault and the Reach Fault to the west and separated major units such as the Botwood Group into several formations based on lithological contrasts.
Eckstrand and Cogulu (1993)	Assessed a number of mafic intrusions in several terranes within Newfoundland for nickel and platinum potential. Assayed the Caribou Hill Intrusion for Pt potential and reported discoveries of several more ultramafic pipe-like bodies to the north and south and concluded that this increased the exploration viability of the area.
Dickson (1993)	Description of geology for the Mount Peyton Map area (NTS 2D/14). Noted mineralization and potential for dimension zone.
Dickson (1993)	Second of three projects aimed at mapping and obtaining geochemical samples from the three NTS map sheets, 2D/11, 2D14, and 2E/3 as well as areas containing segments of the Mount Peyton Intrusive Suite.
O' Brien (1993)	Described major thrusts in the Botwood map area NTS 2E/3. Indicated that the early Silurian Botwood Group is thrust against late Ordovician to early Silurian strata. Described major polyphase folding in the Botwood Group and older units. Informally renamed the Goldson Group, the Lewisporte Conglomerate. Also removed the grey sandstones from the Botwood Group and reassigned them to their own unit and informally called it the Campbellton Greywacke. This reassignment of units left the Botwood Group with no known fossil localities.
Williams (1993)	Reassigned fossiliferous strata from the Botwood Group near Glenwood to the Indian Islands Group.
Boyce and Ash (1994)	Assessment of additional fossils from Careless Brook and reexamination of previously recorded fossil localities. Fauna from Careless Brook indicate a Late Silurian upper age limit for the group at that locality and a possible correlation is made to the Wigwam Formation near Lewisporte where fauna indicate a late Silurian to Early Devonian age for the Botwood Group.
Currie (1994)	Discussed geology of the Comfort Cove and Gander map sheets and subdivided the map area into five regions. Concluded that a simplified stratigraphic column cannot be applied to this area and suggested that the model proposed by Colman-Sadd <i>et al.</i> (1992) of early Ordovician southeast directed thrusts and ophiolite obduction might accommodate the geology.
Dickson (1994)	Description of the geology of the southern part of the Botwood map area (NTS 2E/3). Observed significant mineralization along Jumpers Brook.

Table A1.1: *cont...*

Currie (1995a)	Re-examination of the Gander River Complex, Hamilton Sound Group, Davidsville Group, Indian Islands Group, Duder Complex and Ten Mile Lake Formation of the Gander River map sheet (2E/2) based on new exposures from forest access roads. Concluded that the GRC is extensively imbricated with sedimentary cover from the Davidsville Group and Weir's Pond Formation. Also postulated that the Duder Complex may form basement to the region between the Reach Fault and the Dog Bay Line and may be an accretionary prism of early Silurian affinity.
Currie (1995b)	Provided an overview of his geological and tectonic interpretation for the development of the northeastern end of the Dunnage Zone. Introduced the Duder Belt between the Botwood and Indian Islands Belts.
Dickson (1996)	Geochemical compilation for Mount Peyton Complex and associated surrounding intrusives.
Dickson (2000)	Compilation of a 1:50,000 scale geology map of the Botwood map area (NTS 2E/3) central Newfoundland.
Hynes (2001)	Described the aureole of the Mount Peyton Intrusive Suite as part of a BSc. thesis project. Proposed that the intrusion is a sheet like body or laccolith based on field relationships and that the body has a maximum thickness of 1-2 km with multiple sheet-like sub horizontal intrusions dipping gently to the SE.
Hynes and Rivers (2002)	Studied the metamorphic aureole of the Mount Peyton Intrusive Suite in order to determine the conditions for its development. Based on field relationships along Rattling Brook, authors conclude that the suite was emplaced as a laccolith or sheet like body, 1-2 km thick rather than a batholith as was previously reported. Report a granulite facies in a thermal aureole and indicate that this may be the first reported for Paleozoic rocks of the Newfoundland Appalachians.
Hoffe (2003)	Described the relationship between intrusive phases in the Mount Peyton Complex at Neyles Brook Quarry, location of the Slip Au occurrence, as part of a BSc. thesis project.
<b>METALLOGENY STUDIES</b>	
Snelgrove (1934)	Assessed seven known chromite occurrences in serpentinized belts of Newfoundland, including the region he termed the eastern belt, which occurs in the Botwood Basin. The project was initiated to provide a basic geological framework as well as to promote prospecting in an attempt to exploit the economic potential of Cr within the province.
Snelgrove and Howse (1934)	Conducted a study on known Au occurrences on the island of Newfoundland and reported assays. The project was initiated due to increasing market prices for the metal.
Snelgrove (1935)	Conducted additional work on the study of Au-only occurrences in Newfoundland. This project was aimed at delineating possible exploration targets, assessing known occurrences as well as the viability of producing known resources.

Table 1.1: *cont...*

Patrick (1953, 1956)	Discovered a large quartz vein near Charles Cove while working for the GSC and conducted a reconnaissance survey of the vein and surrounding area. Reported one showing of visible scheelite and two showings of fluorescent mineralization.
Copper (1953)	Examined the tungsten occurrence discovered by Patrick (1953). Observed one large vein and several smaller veins as well as tungsten mineralization at three localities.
Dean (1977, 1978)	Studied the stratigraphy and mineralization of Notre Dame Bay and produced a 1: 63, 360 scale map of the NTS 2E/3 map area and slightly modified William's (1972) interpretations. He removed the Goldson Formation from the Botwood Group. The report was compiled for the NDME on the geology and metallogeny of Notre Dame Bay as part of a MSc. thesis project.
Swinden and Thorpe (1984)	Determined that pre- Caradocian island arc sequences of the Newfoundland central mineral belt display progressive changes in styles of volcanism and in the nature of the associated VMS deposits. The variations reflect an increasing continental crust influence towards southern sequences. Island arc sequences in the northern and central belt were built upon oceanic crust, whereas those to the south have more of a continental crustal influence. Temporal and spacial details of middle Ordovician island arcs were not clear and the authors couldn't determine if the volcanic sequences were coeval or diachronous. Lead isotope isotopes suggest that the two sequences (northern and southern are distinct in terms of age and tectonic setting.
Tallman (1991b)	Summarized work to date on the geology, structure and antimony mineralization at the Hunan Property. Drilling indicated potential for economic mineralization at dept and potential for open pit reserves. Stream sediment and soil surveys were useful in delineating new targets, however, geophysical surveys were unsuccessful.
Evans (1991)	First systematic classification of Au mineralization in rocks of the eastern Dunnage zone. Identified the Botwood and Davidsville Groups as significant exploration targets for Au mineralization and presented preliminary results which indicated that two broad styles of mineralization are present; a mesothermal shear zone and epithermal style. Related the occurrences to a complex network of northeast, north-northeast and northwest trending structures and indicated these 'linears' as possible fluid conduits.
Wilton and Evans (1991)	Compared geology and geochemistry of two gabbro-hosted mesothermal Au showing from opposite margins of the Dunnage zone, the Stog'er Tight (west) and Clutha (east). Determined the mineralization style is similar and formed during late kinematic events but as expected from different tectonic and geological environments, the chemistries of the gabbros are distinct.
Churchill and Evans (1992)	Overview of the geology and Au mineralization at Duder Lake. Concluded that the mineralization is correlative to other gabbro hosted gold showings in the eastern Dunnage zone and that the alteration and mineralization is controlled by



Table A1.1: *cont...*

	structural parameters. Produced preliminary geology maps of the area.
Evans (1992)	Determined that the epigenetic gold mineralization in the eastern Dunnage Zone is structurally controlled and spatially associated with large-scale regional structures. Identified two broad mineralized belts and indicated that both may have had differing fluid source areas. The occurrences are related to a Late Silurian-Early Devonian mineralizing event during the Silurian Orogenesis. Identified the Gander Zone metamorphosed rocks as source rocks for mineralizing fluids. Further work presented on the Au metallogeny of the Dunnage zone.
Churchill <i>et al.</i> (1993)	Proposed a model for Au mineralization at the Duder Lake property based on geochemical, geological and structural relationships. Suggested that the mineralizing fluids were derived from metamorphic de-volatilization of a deep crustal source and inferred the source to be the Gander Zone Basement rocks. Assessed alteration and geochemistry associated with mineralized zones.
Evans (1993)	Continued gold metallogeny project ( <i>cf.</i> Evans 1991, 1992), which examined central Newfoundland au prospects. Presented an overview of the Au occurrences studied in the 1992 field season. Discussed the structurally controlled quartz veins of which he delineated four distinct types: 1) arsenopyrite rich, 2) pyrite rich, 3) antimony rich, and 4) base metal rich. Identified a zone of pervasive silicification, brecciation and quartz stockwork along the TCH near Gander, which provided evidence for an epithermal system in the area.
Tallman and Evans (1994)	Studied the stibnite mineralization at the Hunan Line Prospects. Concluded that structural evidence indicates that northeast-trending fault breccias (sub-parallel to bedding) are related to the loci of mineralization. Later faults disrupted the geology and geochemistry of the mineralized system. Indicated that a leuxocene-altered gabbro at depth may indicate exploration potential for Au although it was not observed with the stibnite at the surface.
Churchill (1994)	Conducted a study of epigenetic gold mineralization in Duder Lake area for an MSc. thesis project. Concluded that the fluids responsible for auriferous mineralization were derived from metamorphic de-volatilization reactions during a Silurian orogenic event and were subsequently concentrated in late structures transecting the crust. Au precipitated simultaneously with As and S and was incorporated into arsenopyrite (invisible Au). Concluded that the processes related to Au mineralization were possibly related to a regional event.
Evans and Wilson (1994)	Presented preliminary stable isotope results on epigenetic gold occurrences in the eastern Dunnage zone. Results indicate that there is variability in oxygen, carbon and sulfur isotopic compositions of quartz, carbonate and sulfur minerals from the gold occurrences and that such variability is atypical of Archean, Proterozoic or Mesozoic gold deposits.

Table A1.1: *cont...*

Williams and Tallman (1995)	Identified Late Arenig graptolites near the NW Gander River. Determined that fossiliferous units are associated with the antimony mineralization, which may be significant in delineating age of mineralization. The host greywacke was correlated to a fossiliferous greywacke that overlies the ophiolites of the Coy Pond Complex to the south, which indicate that turbiditic deposition was widespread during the Early Ordovician, possibly related to a major tectonic event.
Evans (1996)	Overall report on a series of papers presented on the Au mineralization in central Newfoundland as part of the NDME initiative to document the nature and setting of gold mineralization, initiated in 1989. Included documentation of epigenetic Au occurrences, a gold classification scheme, the geological setting of Au mineralization and selected S-isotopic analysis at some localities. Also included detailed deposit level studies of the Duder Lake Occurrences, (Churchill, 1994) and the Hunan Line antimony deposits (Tallman, 1995) and reconnaissance mapping of the NTS 2E/2 west half, map area (Evans <i>et al.</i> , 1992).
Wilton (1997)	Preliminary evaluation of the Tim's Harbor (Charles Cove) prospect for Copper Hill Resources Inc. Upon review of previous work, concluded that the vein at Tim's Harbor showing is an auriferous polymetallic vein system with an unknown aerial extent that should be further explored, not only in terms of its polymetallic nature but also in terms of high grade silica.
Dalton (1998)	Conducted a study on the mineralization and alteration at the Moosehead Property as part of a BSc. (honors) thesis project. Concluded that the mineralization was of LS epithermal type and that S and Pb isotopic determinations indicate that the mineralization shares genetic relationships with other gold occurrence in the eastern Dunnage zone.
Turnel (2000)	Studied the Rolling Pond epithermal gold prospect for a BSc. honors thesis project. Studied the petrography and alteration associated with mineralization even though rock microprobe analysis indicated a complicated alteration system. Concluded that the low precious and pathfinder elements are indicative that the system is at shallow depth and that the argillic alteration and open space textures all agree with this. Concluded that the property has excellent potential to contain ore grades at depth.
Barrett (2001)	Studied the structure of the Moosehead property for a BSc. Honors thesis project. Determined that macroscopic regional scale folds dominate the structure and contain smaller scale parasitic folds. Concluded that the property appears to lie within the southeast dipping limb of a south-southwest plunging regional scale anticline.
Mitchell (2001)	Compared two mesothermal Au prospects, the Romeo and Juliet Prospect, Baie Verte Peninsula and the Appleton Linear prospect, Appleton for a BSc. thesis project. Concluded that despite being hosted in differing lithologies in different tectonostratigraphic zones, the prospects display similar hydrothermal alteration zones. X-ray fluorescence, gold assays S-Isotope and fluid inclusion studies also delineated similarities. Noted that a significant difference was that arsenic was absent from the Romeo and Juliet prospect whereas the Linear prospect gold was associated with arsenopyrite.

Table A1.1: *cont...*

Greenslade (2002)	Geochemical and petrographical examination of the Tim's Cove Vein System for a BSc. (honors) thesis project. Concluded that the vein system exhibits some characteristic of both mesothermal and granophile systems.
Lake (2004)	Documented and characterized barite veins at the Barite Showing near Glenwood via fieldwork, petrography, fluid inclusion work, geochemistry and isotope data. Identified three possible stages of deposition. Pb isotope work indicated that the showing shares a common Pb source with the surrounding Au prospects and O and S isotope data indicated that the barite from the showing is distinct from barite at Carlin type deposits from Nevada. Concluded that the data are more applicable to a Creede deposit model than a Carlin model.
<b>GEOPHYSICAL STUDIES</b>	
Miller (1970)	Conducted a gravity survey of eastern Notre Dame Bay as part of a MSc. Thesis project.
Currie et al (1979)	Presented geophysical evidence for an east dipping Appalachian subduction.
Lapointe (1979)	First paleomagnetic study in the Paleozoic central belt. The author collected samples from the Botwood Group and the granite and diorite phases of the Mount Peyton batholith. Recognized two directions in the Mount Peyton in association with the two phases; one pole direction at 68° east, 15° south indicates an age of 420 Ma for the diorite and a second direction at 125° east, 63° south indicates an age of 380Ma for the granite. Two poles observed within the Botwood Group indicated that the Lawrenceton formation was probably of lower Silurian age whereas the overlying Wigwam Group was magnetized during a reversal event.
Reynolds <i>et al.</i> (1981)	Used biotite and hornblende from the latest gabbroic intrusive phase of the Mount Peyton batholith to obtain a $^{40}\text{Ar}/^{39}\text{Ar}$ age of 420 $\pm$ 8 Ma for the gabbro. Compared this to a previously obtained Rb/Sr age of 390 $\pm$ 15 Ma for the granite and concluded that the 400 Ma paleopole for Newfoundland may be different than other North American poles based on these new geochronological data on previously published paleomagnetic data.
Haworth and Miller (1982)	Compiled gravity and magnetic geophysical data on Notre Dame Bay to determine the structure of basement rocks.
Karlstrom (1983)	Re-examined gravity data for central Newfoundland and suggested that most of the Dunnage Zone is allochthonous and is representative of oceanic crust.
Keen <i>et al.</i> (1986)	Offshore deep seismic profiling across the Newfoundland Appalachians. Yielded information on terrane boundaries and the crustal basement to the different tectonostratigraphic zones.



Table A1.1: *cont...*

Hall <i>et al.</i> (1988)	Presented results of 6000 km of seismic profiling with gravity and aeromagnetic maps across the Appalachian Orogen in eastern Canada. Indicated that the central mobile belt has thinner crust than the adjacent zones. Traced a lower crustal fabric across the orogen and attributed it to a Silurian orogenesis. Suggested that the fabric is indicative of crustal thickening, erosion and subsequent isostatic readjustment.
Quinlan (1988)	Reported on geophysical work for the Lithoprobe East Program. Divided lower crust into three blocks across the island, the Grenville block in the west, a central block and the Avalon block to the east. Ascertained that the Dunnage zone is indeed allochthonous on the Grenville and central blocks
Williams <i>et al.</i> (1988)	Discussed the reasons for the proposed lithoprobe transect of central Newfoundland, Meelpaeg transect.
Todd and Ready (1989)	Conducted aeromagnetic total field, gradiometer and VLF-EM survey over part of the Dunnage Zone and produced maps of results. Aeromagnetism clearly outlined intrusive features, a series of folded sills and a thrust sheet.
Thakwalakwa (1990)	Conducted a geophysical, geological and geochemical study of the Mount Peyton Complex for a BSc. thesis project to try and redefine the lithological boundaries of the surface and subsurface. Two phases of deformation were identified. Remnant magnetism indicated that deformation and block faulting are associated with granite emplacement. Suggested that redefined boundaries indicated that granite comprised only 5% of the complex as opposed to 30% as mapped and that the batholith collapsed in the centre and the faulting is indicative of a tensional regime.
Miller and Thakwalakwa (1992)	Determined that the Mount Peyton batholith consists of a thin granitic phase and a thick gabbro phase based on geochemical, geochemical and geological analysis. Conducted the study to better understand the configuration of the intrusion at depth and to better define the extent of the phases and boundary relationships. Determined from aeromagnetic data that the batholith has undergone at least one phase of faulting. Proposed a model comprised of a number of inward dipping blocks that extend downward for 5 km.
Quinlan <i>et al.</i> (1992)	Reported onshore refraction seismic data collected from the onshore vibroseis profiles across the island as part of the Canadian Lithoprobe program. Used the data to discuss the Appalachian evolution and crustal scale deformations relative to the onshore Lithoprobe reflection transect results for Newfoundland. Results indicated that reflectors cut the Moho below surface and the upper crust exhibits ramp-flat style of deformation. The mid-lower crust is free of regional flats indicating a small homogeneous strain. Traced two crustal blocks, interpreted to represent the Laurentian and Gondwanan plates, that were juxtaposed during the closure of Iapetus. Proposed that the Gondwanan plate is underthrust westward beneath the Laurentian plate by as much as 200 km.

Table A1.1: *cont...*

Hall <i>et al.</i> (1998)	Presented a summary of results on 6000 km of crustal seismic profiling for the Appalachian Orogen of eastern Canada conducted between 1984 and 1992 as part of the Lihoprobe East program. Results indicated that the central mobile belt has thinner crust than the adjacent zones and underplating was found beneath the Laurentian continental margin.
<b>MISCELLANEOUS STUDIES</b>	
MacNeil and Cooper (1953)	Reported on the occurrence of tungsten minerals near Gander Bay for Newfoundland and Labrador Corporation Limited. Confirmed the presence of one or more long narrow quartz veins containing tungsten mineralization. Mineralization appeared to have limited horizontal extent and it was therefore concluded that this was unfavorable evidence for the presence of ore bodies.
O' Toole (1967)	Reported on the Gander Bay Tungsten Prospect for Newfoundland and Labrador Corp. Ltd.. Concluded that the granodiorite appears to be younger than adjacent intrusives and that insufficient exploration was conducted thus far. Recommended that economic potential is favorable and suggested further work be conducted on the area.
O'Toole (1970)	Preliminary report on detailed night mapping, drilling, grab sample assaying and field mapping of tungsten mineralization, Charles Cove. Seven areas of fluorescence were discovered, but only two were of interest. Drilling and assays concluded that the scheelite mineralization is confined to the vein footwall and the zone is less than 1 foot wide. Therefore, the scheelite is restricted to a narrow and discontinuous zone at the contact between the granodiorite and the footwall of the large quartz vein. Based on these results drilling was terminated.
Strong <i>et al.</i> (1974)	Obtained rock samples from 33 granitoid plutons across Newfoundland ranging in age from Precambrian to Devonian and assessed their geochemistry. Concluded that the Mount Peyton Intrusive Suite ranges in composition from syenite to granite and diorite. Observed that the pluton intruded the Botwood Group, and thus, was probably Devonian.
Malpas and Strong (1975)	Examined chromite occurrences in intrusive mantle diapirs of the Gander River Belt and in ophiolites of the Bay of Islands Complex of western Newfoundland. The intrusive mantle diapirs of the Gander Belt contain disseminated to podiform to banded chrome spinels occurring in a dunite fraction. In relation to the Bay of Islands chromite spinels they are relatively high in Cr:Al ratios.
Strong (1979); Strong and Dupuy (1982)	Regional geochemical survey of the Mount Peyton Intrusive Suite. Chemistry indicated a clear separation in SiO <sub>2</sub> values, which indicated a bimodal composition. Postulated that the gabbro from the MPIS is mantle derived whereas the granite composition is a result of partial melting of the continental crust from the heat generated by the intruding gabbro. Concluded that both phases derived independently in processes involving crystal fractionation and contamination with country rocks during ascent.
Gagnon (1981)	Assessment report on geological, geochemical and geophysical reconnaissance exploration in the Jonathan's Pond area.

Table A1.1: *cont...*

Butler and Davenport (1981)	Regional lake sediment geochemical survey in northeastern Newfoundland, map area 2D.
MacKenzie (1985)	Assessment report on the Jonathon's Pond claim area compiled for Noranda. Exploration initiated after a soil survey over the GRUB produced anomalous values resulting in 461 claims. The mafic rocks were found to have high level background gold and the NDME found 1 gold showing in the SW grid. Several conductors and magnetic anomalies, as well as copper and arsenic geochemical anomalies, form linear trends in the southern grid. Concluded that the Au mineralization appeared related to the zones of silicification associated with quartz veining. Recommended follow up work such as trenching and placing conductors near fault or shear zones that could have been conduits for quartz veins.
Burton (1987)	First year assessment report on geological, geophysical and diamond drilling at the Chiouk Brook Au showing compiled for U.S. Borax. Major regional faults were interpreted, through the drill program, to run parallel to Chiouk Brook. Two other general fault directions were determined. The discovery outcrop was described as altered sediment with up to 5 % disseminated (0.5-1mm) arsenopyrite crystals in a massive, very fine-grained matrix. Mineralized boulders were discovered along the brook consisted of a similar silicified rock and contained 5-20 % arsenopyrite. Bedrock was not untrenched due to a boulder till, however, several mineralized boulders were uncovered. Drilling wasn't successful due to broken sediments and over pressured faults.
Snow (1987)	Assessment report on grassroots exploration in the Jonathon's Pond area. Determined that there are two distinct groups of pyroxenites in the area. The sharp contact with surrounding gabbros and distinct chill margins indicate that the gabbro intruded the pyroxenite. The pyroxenites are thus thought to represent the oldest rocks in the GRUB Line. The serpentinites occur as a narrow outcrop in the NE and the gabbros appear to have two distinct modes of emplacement. The most significant structure is a NE trending, W dipping thrust contact between the Gander Group and the GRUB rocks, the Jonathon's Pond Fault, which was observed in drill hole as 20m wide, weakly pyritic, serpentinitic gouge zone.
Davenport and Nolan (1988)	Conducted a regional lake sediment survey for the NDME, which defined anomalous Au, Sb, and As concentrations in several regions in the eastern Dunnage zone.
Gower and Tallman (1988)	Second year assessment report on geological mapping, prospecting, trenching, soil geochemistry and diamond drilling at the Gander Outflow. Trenching of soil and VLF anomalies resulted in the discoveries of three zones of Au-Sb mineralization in silicified sedimentary rocks. Several mineralized zones were identified with the most important being the Mustang and Piper Zones.



Table A1.1: *cont...*

Gower and Tallman (1988)	Second and third year assessment reports on the Glenwood-White Bay Project for Noranda involving evaluation of the Bullet Showing. Channel samples returned Au values of 11.9 g/t over 0.5 m, 43.2 g/t over 0.8 m and 91.6 g/t over 1.1 m. The mineralized zone consisted of two or more quartz veins (2-10 cm wide) in friable sheared shale that is altered to hematite and siderite. Observed visible Au along vein margins and haloes of disseminated pyrite-arsenopyrite veinlets and disseminations extending up to 1 m from the veins.
Mercer (1988b)	Assessment report on diamond drilling at Chiouk Brook and Lizard Pond compiled for Atlantic Goldfields Ltd. and Jacan Resources through the consulting firm A.C.A. Howe International Ltd. There were no ore grade intersections on either property and further work was not recommended at Chiouk Brook. Further work was recommended at the Lizard Pond showing because of a reported favourable geological environment for auriferous mineralization.
Mercer (1988a)	Second year assessment report on geological, geophysical and geochemical exploration surveys in the Great Bend Area (west side of the Gander River) compiled for Atlantic Goldfields Inc. and Jacan Resources through the consulting firm of A.C.A International Ltd. Concluded that several areas have potential to host precious metal mineralization. Noted widespread Au occurrences and spatial association with carbonate alteration zones.
Snow (1988)	Assessment report on mapping, trenching and drilling and overview of previous work history in the Jonathon's Pond area during 1987. Concluded that the lack of surface exposure and thick overburden was problematic to exploration. Could not correlate main gold showing with Au in till to the east. Delineated the Jonathon's Pond fault as a viable exploration target in relation to the known applicable deposit model and recommended follow-up work.
Tallman (1988)	First year assessment report on grass roots exploration in the Noront-Paul's Pond area. Significant discoveries included epithermal style Au mineralization at the Aztec Showing and sericitic lode-Au type at Goose Showing as well as numerous other showings.
Bradley (1989)	Assessment report on a geophysical survey conducted over the Miquel Lake and Murphy Option along Great Rattling Brook and along the south side of the Northwest Gander River. The survey was conducted by Aerodat Ltd. for BP Resources Canada Ltd.
Butler (1989)	Assessment report on geochemical surveys at the Third Pond property for Falconbridge Ltd. Reported several significant Au anomalies in till and recommended further work on the property to determine the extent of mineralization.
Gower and Tallman (1989)	Second year assessment report on trenching at the Outflow Prospect for Noranda. Trenching of the Piper and Mustang zones traced the strike length of mineralization for over 5 km.

Table A1.1: *cont...*

Graham (1989)	Assessment report on geological mapping, deep overburden sampling, trenching, geophysics and diamond drilling of the Great Bend-Murphy option for BP Canada Ltd. The point of the exploration was to determine source of anomalous gold mineralization in soil and rock and to explore new areas for Au occurrences. Discovered mineralization at Lizard Pond, Swan Lake and Breccia Pond. Test pits and trenches were excavated at the showings and exposed silicified and mineralized ultramafic rocks. Diamond drilling at Lizard Pond and Breccia Pond were unsuccessful in determining the strike and dip of the anomalous Au values.
Green (1989)	First year assessment report on diamond drilling, prospecting and geochemical and geophysical surveys at the Duder Lake gold showings. Anomalous Au values were returned in soil samples, and the magnetic and VLF geophysical surveys outlined a number of geological structures and possible target areas for follow up trenching. Proposed till and soil sampling and prospecting along N-NE trending linears. Soil, magnetic and VLF surveys outlined trenching targets as possible extensions of the Goldstash and Corvette showings. Diamond drilling was proposed to test the Goldstash, Stinger and Corvette Showings
Simpson (1989)	Assessment report on fieldwork, geological mapping, prospecting, trenching and diamond drilling in the Jonathon's Pond area for Noranda. Three glaciation periods were identified via a 23-hole overburden drill program. Discovered two distinct tills through mapping of the overburden and gold grain analysis. This allowed for the delineation of four target areas as possible source areas for gold in till which coincided with MAG/VLF conductors. The magnetic survey may also outlined a large shear running through grid. Soil and geophysical surveys were also carried out and revealed additional target areas for follow up work in 1989. Concluded that the property held good potential for Au mineralization.
Tallman (1989a)	First year assessment report on licences owned by Noranda Exploration Limited in the Paul's Pond-Greenwood Pond area. Concluded that mineralization occurs over a broad area and that several styles appear to be present ranging from low grade, high tonnage to high grade, low tonnage lode styles. Recommended further work on properties.
Tallman (1989b)	First year assessment report on the Noront-Paul's Pond Property for Noranda. Concluded that the Au mineralization is hosted within Davidsville Group sediments at a Botwood-Davidsville Group fault contact in a large epithermal style alteration zone. Recommended further exploration at several areas including the Goose showing. Suggested winter geophysics over the Paul's Pond grid to identify the length of the Goose Showing mineralized structure.
Williams <i>et al.</i> (1989)	Examined Newfoundland granitic rocks (which were separated into 9 categories; one being the Mount Peyton). Determined that each distinct category occurred within discrete stratigraphic zones or coincided with lower crustal blocks. Suggested that the mid Paleozoic Mount Peyton granite is a post-accretionary pluton that transgresses a zonal boundary and shows preferences for a certain zone or block. Concluded that the Mount Peyton plutons are confined to the Exploits Subzone and central lower crustal block and post date Appalachian accretion because they cut zonal boundaries.

Table A1.1: *cont...*

Gower and Tallman (1990)	Second and third year assessment report on soil geochemistry, geophysical surveys, trenching and diamond drilling in the Glenwood-White Bay project for Noranda. Identified two narrow, high-grade Au zones. Suggested that the economic potential of the property was high and recommended further work.
Graham (1990)	Assessment report on prospecting, geochemical surveys, trenching and diamond drilling at the Great Bend Area-Murphy Option. 22 trenches and 22 test pits were excavated and Lizard Pond type mineralization was traced along strike 500 m east and 350 m southeast of the Lizard Pond Showing. Concluded that auriferous veins are narrow and too low grade to be economic. Au mineralization was postulated to be late, controlled by faults and fractures. The mineralized veins are associated with silicified zones associated with major thrust faults. The potential for mineralization at depth could not be determined due to faulted rock. Cambrian-Ordovician ophiolite rocks were found to be in non-conformable contact with overlying Silurian sediments.
Pickett (1990)	Assessment report on grassroots exploration work conducted on the Jumpers Brook Property in 1989.
Tallman (1990a, b)	First year assessment report on licenses owned by Noranda on the Noront-Mount Peyton property. Soil, geochemical surveys and magnetometer and VLF-EM surveys were conducted to test the extent of five showings (Hurricane, Corsair, Apache, Conache and Sabre) consisting of fracture controlled sericitic alteration with anomalous gold mineralization that were discovered during reconnaissance prospecting. Recommended extended IP survey to prioritize targets for diamond drilling and further prospecting on an extension of the grid.
Tallman (1990c)	Second year assessment report on the Beaver Brook antimony prospect.
Tallman (1990d)	Second year assessment report on diamond drilling, prospecting and mapping surveys on soil anomalies on the Duder Lake Grid in search of shear zone hosted lode gold deposits. Au mineralization was traced for 4 km along strike within a continuous shear zone. Mineralization was also recorded in secondary shear structures. Recommended drilling to evaluate the depth and extent of Goldstash showing and trenching along the mineralized zone to further delineate target areas.
Collins (1991)	Assessment report on trenching, geological mapping and geochemical surveys conducted in the Glenwood area in 1990. Trenching unveiled the Knob Prospect, a shear zone in greywacke with quartz veins hosting Au. Mineralization occurs in shale and greywacke, but is more abundant in greywacke and the highest values were returned from the quartz veins associated with shear zones.
Graves (1991)	First year assessment report on geochemistry, geophysics, geology and diamond drilling at Jumpers Brook for Noranda.



Table A1.1: *cont...*

St. Croix and Taylor (1991)	Mapped glacial striae and defined an early eastward flow that was successively followed by a northward flow, a north-eastward flow and finally an eastward flow.
Tallman (1991a)	Second year assessment report on Noront-Mount Peyton property for Noranda.
Fryer <i>et al.</i> (1992)	Conducted a temporal, isotopic study of Paleozoic plutonic suites across the Appalachians in Newfoundland, which subsequently helped to delineate and characterize major components of the Appalachians.
Klassen (1994)	Interpreted the glaciation history in central Newfoundland based on glacial striations. Concluded that striations and indicator erratics define four separate ice flow events.
Scott (1994)	A study of the surficial geology and drift exploration in the Comfort Cove-Newstead and Gander River map areas. Identified four ice flow events and concluded that the sediment dispersal is controlled by east-southeastward flow in the central region and by northeastward flow in the north. The source of Au in till was not identified.
Wilton (1997)	Preliminary evaluation on Tim's Cove Property for Copper Hill Resources. Upon a review of work history and an assessment of the property, determined that the vein system required further work and exhibited some features of a mesothermal lode gold system. Concluded that the property was worthy of more detailed examination and that the quartz vein should be considered as a potential source for high-grade silica.
Churchill <i>et al.</i> (1998a)	First year assessment report on geological and geochemical exploration in the Greenwood Pond area for Forex Resources (a syndicate of Newfoundland geologists and prospectors who evaluated a large concession of claims in the Beaver Brook area for Au mineralization). The report provides a compilation of all information on the Beaver Brook area in an attempt to better characterize the mineral potential of the area. The authors visited the site and re-evaluated past work and surveys. A grab sample collected in 1997 returned an encouraging assay value of 10.12 g/t Au. Recommended soil surveys in areas of in situ mineralization and mineralized float and IP surveys and additional mapping in the areas of contact between Silurian-Ordovician lithologies, especially near the Ricce, Shippin and Hornet showings.
Churchill <i>et al.</i> (1998b)	First year assessment report on compilation, prospecting and geochemical exploration in the Greenwood Pond area for Forex Resources. Concluded that several numerous gabbro dykes and sills and several granitoid plugs intrude Davidsville Group and Botwood Groups and that the spatial and temporal relationships suggest that they are genetically related to the MPIS. This implies that the MPIS could have acted as a heat source for epithermal systems in the Paul's Pond area. Suggested that the quality of Noranda stream and sediment survey was poor and recommended that it be redone properly.

Table A1.1: *cont...*

Churchill <i>et al.</i> (1998c)	First year assessment report on compilation, prospecting and geochemical exploration for the Aztec property. Evaluated re-processed regional aeromagnetic data that suggested that the reverse fault mapped in the Aztec zone might be part of a larger, regional structure that was controlled, or caused by, the placement of the MPIS. Assay values of 1.05 and 1.65 g/t Au were returned for the Aztec and A-zone extension, respectively. The authors recommended additional mapping, especially along the inferred faulted contact between Ordovician-Silurian rocks. They also suggested another IP survey be carried out over the NE trending anomalies, re-logging of drill core accompanied with petrographical and geochemical analysis and if further anomalies were identified, diamond drilling.
Wilton and Taylor (1999)	Second year mineral assessment report for Copper Hill Resources Ltd. on the Tim's Cove Property. A 1.5 km long quartz vein system ranging from 0.6 m to 2.5 m in width was studied and anomalous base metal or gold values in localized areas were determined. Authors suggested that the quartz vein was not thick at depth based on surface analysis and hence is not a good silica resource. Discovered two new styles of gold mineralization in bedrock and a broad alteration zone in the granodiorite host. Authors recommended localized trenching, a drill program to assess mineralization at depth and a follow-up to anomalous soil surveys.
Barbour and Churchill (1999)	First year assessment report on prospecting, sampling, IP surveying and diamond drilling at the Mustang Property for Altius Resources Inc. The old Noranda trenches were examined and re-sampled and an IP survey was conducted over 5 lines in the vicinity of the showings. Ten diamond drill holes were drilled to test mineralization and geophysical anomalies. Thin hydrobreccia units amongst quartz veined and locally silicified host rock were found at surface at the Piper and Mustang Zones. The best Au values were found in the breccia unit, which pinch out immediately along strike and downdip. Due to this lack of continuity it was determined that these zones have low potential to host economic Au concentrations. The best returned assay values were 1 to 2 g/t Au over 0.3 m in drill section.
Barbour and Churchill (2000)	First year assessment report of geology, prospecting, IP surveying and diamond drilling at the Rolling Pond Property for Altius Resources Inc. Prospecting and geological mapping delineated a major zone of epithermal mineralization with quartz flooded and vein breccias that exhibit LS epithermal features. The textural features present suggest a high level or bonanza zone. Five diamond drill holes were drilled into the quartz zone and the values returned from these near surface holes were up to 25 ppb Au. Au values were more elevated at depth (356 ppb) Au and the authors suggested that more work should be targeted at penetrating the zone at depth. The IP survey delineated quartz mineralization (zone of high resistivity). Concluded that potential for economic gold concentrations existed due to the large extent of the epithermal system and the consistency of Au values throughout. Recommended that further exploration be concentrated along the regional mineralized structures.
Churchill <i>et al.</i> (2001)	First year assessment report covering preliminary geological investigations at the Chiouk Brook Property in the Great Bend-Northwest River area. The authors visited the prospect, collected several samples and conducted a literature review to outline future exploration programs.

Table A1.1: *cont...*

Smith <i>et al.</i> (2003)	First, second and fifth year assessment reports on prospecting trenching and geochemical sampling at the Mustang Trend for Altius Resources Inc.
Barbour and Churchill (2004)	Second, third and sixth year assessment report on prospecting, trenching and geochemical sampling at the Mustang Trend properties for Altius Resources Inc.



**Table A1.2:** Brief descriptions of Botwood Basin auriferous prospects visited for the current study (descriptions modified from Evans (1996), unless otherwise noted).

Northern Botwood Basin Prospects		
Flirt	670596/ 5465115	Pyrite and arsenopyrite in 1-30 cm wide quartz-carbonate veins developed within brittly deformed, weakly carbonate and chlorite altered, gabbro. Veins have assayed values of 9.29 g/t (Green, 1989). Classified as mesothermal-style mineralization with shear controlled quartz-carbonate veins containing sulfides and minor gold (Churchill, 1994).
Goldstash	670488/ 5464542	Shear controlled disseminated sulfide restricted to gabbroic dykes and sills. Alteration ranges from moderate to strong silicification and red-brown carbonization with sericite and chlorite alteration surrounding the zone in weakly deformed gabbro. The gabbro has undergone lower greenschist metamorphism and mineralization consists of fine-grained pyrite and acicular arsenopyrite occurring as lens shaped boudinaged blocks ranging from 1-2 cm up to 2.5-3 m. Surface assays from trenching provided values of 13.5 g/t over 2.6 m (Green, 1989). Classified as mesothermal-style mineralization with shear-controlled sulphide disseminations in gabbro (Churchill, 1994).
Corvette	670326/ 5463622	Similar mineralization and alteration as Goldstash. Assays from trench grab samples returned values from 2.65 g/t Au over 3.6 m. Classified as mesothermal-style mineralization with shear-controlled sulphide disseminations in gabbro (Churchill, 1994).
Clutha	674900/ 5475350	Auriferous pyrite and arsenopyrite-bearing quartz carbonate veins that cut intensely Fe-carbonate altered and silicified, fine to medium-grained gabbros (Evans, 1991). The gabbros intrude a shale, siltstone and greywacke sequence supposedly of the Indian Islands Group. Channel sample assayed 0.146 oz/t Au over 4 m (Noront Resources Limited, Press Release, 1990). Classified as an altered wall rock-quartz-vein style of Au mineralization.
Charles Cove (Tim's Harbour)	681300/ 5475920	Pyrite-arsenopyrite rich quartz style of gold mineralization developed within the Charles Cove Pluton. Three generations of veining have been recognized: 1) white milky quartz, 2) dark grey dirty quartz, and 3) white glassy quartz (O' Toole, 1967, 1970). Mineralization consists of arsenopyrite-pyrite zones with minor molybenite, chalcopryite and galena and rare scheelite crystals; Au and Ag have been defined by assay. The mineralization primarily occurs within the quartz vein with minor occurrences noted in the adjacent granodiorite and underlying sedimentary unit. Assays of 1.2 and 5.76 g/t Au and 130 and 440 g/t Ag have been obtained from grab samples (Evans, 1991). Hydrothermal fluids have affected all host rocks and sericite alteration exists along quartz vein in both intrusive and sedimentary lithologies. Chlorite and epidote are present in the granodiorite, which classifies it as lower greenschist facies.

Table A1.2: *cont...*

Big Pond	657750/ 5441300	Fine to medium-grained gabbro, intruding red and green siltstone and sandstone. Au is hosted in shallow dipping extensional quartz veins and Fe-carbonate, sericitic and silicic alteration is present. Mineralization consists of fine-grained wispy bands of arsenopyrite and lesser pyrite and visible gold. The visible gold occurs as clusters in one of three exposed quartz veins. Assays up to 441.0 g/t Au (Evans, 1992) and 4.02 g/t Au (Tallman 1990) were returned from grab samples from the main quartz vein. Classified as arsenopyrite -rich quartz vein style Au mineralization.
Knob Hill	674259/ 5445813	Narrow quartz-pyrite veins in chloritic greywacke of Davidsville Group. An assay from trench grab sample returned a result of 2.7 g/t Au.
Third Pond	671020/ 5442038	Au in carbonate concentration and extensional quartz and quartz feldspar sulfide (pyrite, molybenite and galena) veins in a narrow zone of silicified and graphitic shale of the Davidsville Group. A grab sample from trenching assayed 4.6 g/t Au in 1987 and subsequent trenching revealed more concretions with the best value returned being 0.8 g/t Au (Butler, 1989).
Jonathon's Pond	677703/ 5440698	Pyrite and arsenopyrite bearing quartz veins in intensely sheared gabbro. Local concentrations of massive pyrite-arsenopyrite and cubic pyrite and rhombic arsenopyrite crystals. Au occurs in shear controlled and extensional fracture veins which contain pyrite and arsenopyrite bearing milky white locally vuggy quartz. Host is fine to medium grained gabbro and chloritized mafic volcanic rocks of the Gander River Complex. A grab sample assayed 6 g/t Au (Blackwood, 1982).
<b>Central Botwood Basin-Glenwood/Appleton Prospects</b>		
The Dome	658632/ 5428534	Quartz veining containing visible gold in primarily grey green to black argillites (shale) with minor greywacke close to the Appleton Linear. Pyrite, arsenopyrite, and minor chalcopyrite, boulangerite, malachite, galena and stibnite are associated with the Au mineralization. Alteration is characterized by Fe carbonate, green and brown sericite, clay alteration (possibly kaolinite) and chlorite. Green micas (fuchite) are also noted in the mineralized, carbonate-altered greywacke (Mitchell, 2001). Samples from the Dome showing produced drill assay values up to 18.46 g/t over 8.6m (Candente Press Release, 1999).
The Knob	657181/ 5425631	Auriferous quartz veins hosted in Davidsville Group greywacke. Two quartz vein types are present: 1) pyrite/arsenopyrite with low Au values, and 2) milky white massive and smaller sheet quartz veins containing coarse free Au, minor pyrite, chalcopyrite (Collins 1991). Fe-carbonate alteration is prevalent in the sheared greywacke and the immediate wall rock around the milky white veins is silicified and contain disseminated pyrite and arsenopyrite and deformed rusty zones occur locally. Au values of 6.26 g/t over 13 m were returned from channel samples and values up to 106 g/t over 2.3 m were obtained in drill core (Collins, 1991).



Table A1.2: *cont...*

The Bullet	657424/ 5425881	Milky white quartz veins (<15 cm wide) with disseminated pyrite, arsenopyrite, and boulangerite hosted by slightly graphitic shale and grey green siltstones of the Davidsville Group. Au occurs as specks and clusters of free Au in narrow quartz carbonate vein set. Channel and grab sample assays returned values of 11.9 g/t over 0.5m to 43.2 g/t Au over 0.8 m (Gower and Tallman, 1989). Trenches returned Au values from channel samples of 11.9g/t Au over 0.5 m, 43.2 g/t Au over 0.8 m and 91.6 g/t over 1.1 m.
The Outflow Prospect	653807/ 5422244	Au mineralization in greywacke lenses of Davidsville Group. Au associated with pyrite, arsenopyrite, stibnite and intense silicification. Three types: 1) hydrothermal stockwork 2) pervasive silicification 3) massive crystalline quartz + quartz carbonate veins (Gower and Tallman, 1988). Types 1 and 2 are mineralized with 1-3% disseminated stibnite, arsenopyrite, and pyrite with assays of up to 10 g/t Au, whereas Type 3 style alteration is typically barren. Quartz veining overprints styles 1 and 2 (Tallman, 1989). Stockwork type alteration is developed in slates and pervasive silicification is present in the sandstone units.
Bowater	656026/ 5426826	Pyrite-bearing quartz veins and quartz breccia developed within graphitic, and locally sericitic, black greywacke (Woldeabzghi, 1988). The extensional veins are composed of milky white, locally rusty, and vuggy quartz and are up to 10 cm wide with localized brecciation (Tallman, 1991). Mineralization consists of pyrite and lesser arsenopyrite in weakly seritized and carbonate altered, black, quartz-feldspar rich greywacke (Woldeabzghi, 1988). Au assays from the greywacke produced values less than 3 g/t (Evans 1991).
<b>Central Botwood Basin- Mount Peyton</b>		
Hurricane Prospect	645161/ 5425138	Sericitic, pyrite-bearing diorite cut by quartz-pyrite-arsenopyrite stockwork. Assays from drill core were up to 7.9 g/t over 1.0 m and a grab sample assayed 1.3 g/t Au (Tallman, 1990). Evans (1992) reports pyrite, arsenopyrite, silver, sphalerite, galena, chalcopyrite, and pyrrhotite in diorite.
Corsair Prospect	644408/ 5425289	Strongly seritized diorite with disseminated pyrite and arsenopyrite associated with quartz veins. Pyrite and arsenopyrite occur as disseminated euhedral crystals and also as coarse patches locally concentrated along quartz carbonate veins (Tallman, 1990, 1991). IP and VLF-EM geophysical surveys identified a strong NE-SW trend (Tallman, 1991).
Slip	643541/ 5438244	Au associated with miarolitic granitic dykes. Galena, pyrite and arsenopyrite in granitic dykes.
Jumper's Brook	617185/ 5428579	Pyrite and arsenopyrite in quartz vein bearing sandstone hornfels along Jumper's Brook; exhibits slightly elevated Au values (Pickett, 1990).



Table A1.2: *cont...*

<b>Southern Botwood Basin-Paul's Pond Area</b>		
Hunan	629855/ 5395490	Fracture controlled stibnite veins hosted in lower greenschist-grade pebble greywacke of the Davidsville Group. Classified as Acadian, epithermal-style mineralization in which mineralization is controlled by an array of fractures in greywacke and brecciation was noted locally (Tallman, 1991).
LBNL	636504/ 5391062	Silicified granitic intrusion into Davidsville Group with quartz-arsenopyrite veins. The best results obtained from assay were 1.80 g/t Au over 1.0 m (Tallman, 1989a).
Goose	635743/ 5390002	Numerous quartz veins and veinlets in seritized and weakly silicified greywacke of Davidsville Group. Arsenopyrite and pyrrhotite occur as disseminations in wall rock and as coarse patches in the veins. Arsenopyrite also occurs as randomly oriented needles and pyrite as aligned elongate grains. Classified as an arsenopyrite-rich, quartz vein style mineralization (Tallman, 1989a). assays of 7540 ppb/ 1.0 m from drill core.
Road Gabbro	635216/ 5391238	Pyrite-arsenopyrite in quartz veins within silicified and carbonized gabbro that intruded the Davidsville Group. The best assay obtained by Noranda from a grab sample at the prospect was 2.24 g/t and 7.9 g/t over 1.0m (Tallman 1989a).
Aztec	6306041/ 5388967	Alteration at, or near, presumed contact between Davidsville and Indian Islands Groups. Locally silicified, pyrite conglomerate or breccia with breccia above silica scinter. Classified as epithermal, low grade Au mineralization. Au mineralization is associated with the conglomerate (typically less 1g/t Au) and the silica sinter is comprised of multi phase hydrothermal breccia and pervasive silicification. A 70 km thick zone of argillic alteration underlies the sinter, and is variably developed in fine-grained siltstone and sandstone (Tallman, 1989a).
Hornet	628844/ 5388101	Small quartz-pyrite stringers and 1-2 m wide quartz veins in locally silicified, fractured and brecciated felsite or k-feldspar granite intrusive to Davidsville Group. The best assays from channel samples were 9.9 g/t over 1.0 m and 2.86 g/t Au over 1.0 m (Tallman, 1989a).
Greenwood Pond #2	630400/ 5387150	Disseminated pyrite and arsenopyrite hosted by weakly chlorite-altered, small gabbroic intrusion in Davidsville Group. Assay of 23.2 and 5.27 g/t in grab sample.
A-Zone	631150/ 5388800	Small discontinuous pyrite and arsenopyrite extensional quartz-carbonate veins and veinlets in chloritized, potassically altered Davidsville Group greywacke. The greywacke unit is a 15-20 m wide bed within grey-green siltstone. A value of 2.60 g/t Au over 1.0 m was obtained from assay from channel sample (Tallman, 1989a).

Table A1.2: *cont...*

Southern Botwood Basin-Great Bend Region		
Rolling Pond	611423/ 5391239	Classified as epithermal style Au mineralization exhibiting extensive silicification, hydrobrecciation and quartz veining within sedimentary and volcanic host rocks. Arrays of distinctive epithermal textures are present including cockade textures, quartz rosettes (silica scinter) and silica-replaced carbonate lattice blades (Barbour <i>et al</i> , 1999).
Chiouk Brook	616099/ 5383976	Disseminated arsenopyrite needles, pyrite and chalcopyrite in grey-black brecciated slate. Assays ran as high as 18 ppm and the mineralization appears to be associated with an east-northeast trending fault (Mercer, 1988a).
Breccia Pond	616675/ 5380345	Silica and magnesite-altered ultramafic rocks of the Great Bend Complex cut by narrow fracture controlled quartz-carbonate veins and stockwork. Hematite and silicification are associated with veining and mineralization consists of pyrite, arsenopyrite, and millerite. Assays from the core were not as good as at surface (Graham, 1990); a channel sample assayed 3.24 g/t Au over 1.0 m (Evans, 1992).
Swan Lake	613387/ 5378508	Silicified shear zone with disseminated arsenopyrite and quartz breccia veins in Indian Island Group sedimentary rocks. Grab sample assayed 1.38 g/t Au. The prospect consists of a silicified shear zone in sedimentary rocks containing arsenopyrite and a 2 m wide quartz vein breccia (Graham, 1990).
Lizard Pond South	614200/ 5379550	Sporadic, fault controlled, quartz breccia veins in grey-brown, siliceous, locally brecciated magnesite altered serpentinite of the Great Bend Complex. Veins contain fine-grained disseminated arsenopyrite and pyrite. The veins, up to 1.5 m wide and 9 m long, contain fine-grained disseminated arsenopyrite and pyrite and yielded assays of up to 12.58 g/t Au over 0.4 m (Graham, 1989).
Lizard Pond North	613612/ 5380831	Fault brecciated magnesite-altered peridotite with disseminated pyrite and arsenopyrite of the Great Bend Complex. Assays from channel sample returned 960 ppb Au over 1 m.
Huxter Lane	603859/ 5367584	Disseminated pyrite and arsenopyrite in dacite and massive arsenopyrite rimming quartz brecciated dacite and quartz veins.



**Table A1.3:** Brief description of previous paleontological studies from within the Botwood Basin and environs.

Author(s)	Description
Bergstrom <i>et al.</i> (1974)	Assessed known Ordovician fossil collections in an attempt to provide a better biostratigraphic framework for north-central Newfoundland and assigned graptolite fauna to European affinities.
Stouge (1980)	Assigned conodonts from limestone in basal Davidsville Group (east of the Reach Fault) at Weirs Pond to Late Llandovery to Early Llandeilo and correlated the fauna to conodonts from Cobb's Arm limestone at New World Island (west of the Reach Fault). Based on this correlation the author suggests that McKerrow and Cocks (1977) interpretation of the suture for the Iapetus Ocean is insignificant.
McKerrow and Cocks (1980)	In response to Stouge (1980) the authors argue that similar conodont fauna on either side of the Reach Fault does not dismiss the fault as a suture point because middle Ordovician conodont distributions could occur on both sides of the Iapetus Ocean.
Stouge (1980)	In response to McKerrow and Cocks (1980) the authors argue that since the faunal provinces are not restricted to plates, benthic fauna cannot be used solely as arguments for delineating plate boundaries.
Stouge (1980)	Processed further samples collected from Weir's Pond in 1977 (Blackwood, 1978) for conodonts and assign the fauna an Upper Llanvirn-Lower Llandeilo age, which confirms the age provided for the group by Blackwood (1978).
Boyce <i>et al.</i> (1988)	Presented new trilobite discoveries from within Davidsville Group rocks ranging in age from late Arenig to early Llandeilo in argument against McKerrow and Cocks (1977) interpretation that suggests the Reach Fault represents a suture point for the Iapetus Ocean closure.
Williams (1988)	Conducted systematic fossil collection and taxonomic identification (graptolite fauna) of Middle Ordovician black shale of the Shoal Arm Formation and Lawrence Harbor shale.
Williams (1989)	Reported findings on a study of graptolite assemblages in central Newfoundland primarily to provide a biostratigraphic and taxonomic revision on the widespread middle Ordovician black shale unit as described by Williams (1988) and found much earlier shale units. Thus, based on a review of faunal assemblages in the Dunnage zone, he ascertained that there is no geographically widespread lower Ordovician black shale unit as opposed to the known widespread mid Ordovician unit.



Table A1.3: *cont...*

Boyce <i>et al.</i> (1991)	Discussed the discovery of shelly, trilobite fauna from limestone lenses in the Botwood Group on Upper Black Island. The fauna indicate a probable late Ordovician Ashgill age.
Williams and O' Brien (1991)	Discussion on the graptolite discovery at Upper Black Island. It is the first positively identified specimen of Silurian taxa from Newfoundland and provides evidence that there was Silurian oceanic sedimentation in the Dunnage Zone. This suggests that at least part of the Iapetus ocean was still open in central Newfoundland during the early Silurian because the graptolite assemblage with European affinities suggests open ocean conditions or deep marginal basins during the Llandovery.
Williams (1991)	Redefined the Point Lemington Formation (overlying the Lawrence Harbor Formation) to comprise a thick sequence of siliciclastic turbidites containing occasional Upper Ordovician graptolites. Correlated the unit to rocks in southern Scotland suggesting a relation between these areas during the Late Ordovician.
Williams <i>et al.</i> (1992)	Discussed new fossil discoveries from the Coy Pond Complex, south central Newfoundland and Lawrence Harbor Formation Graptolites from north central Newfoundland. The trilobite from the Coy Pond Complex yields an upper age constraint of Late Arenig to the complex. Correlated the fauna to fossils from England and South Wales suggesting that this section of central Newfoundland lay on the northern oceanic margin of eastern Avalonia during the Lower Ordovician. The graptolites are Silurian indicating that at least part of the Iapetus ocean was open in central Newfoundland during early Silurian time.
Boyce <i>et al.</i> (1993)	Discovered a new bivalve fauna at Careless Brook from latest Silurian-early Devonian implying a later termination to the Paleozoic marine sedimentation than was previously thought.
Williams (1993)	Identified biostratigraphically diagnostic graptolite sequences from the Exploits subzone of a middle Ordovician age. These represent outcrops of the Lawrence Harbor Formation and its correlatives. First reported graptolites of Cardoc age from shale along Careless Brook. Suggested that the unit itself is unlike the typical Lawrence Harbor Formation and that the shale may represent the top of a black shale unit passing into sandstone gradually or an argillite lens in a coarser sandstone sequences. Another sequence along stream may contain fauna from the <i>D. clingani</i> zone. He also identified faunal assemblage along Great Gull River Forest access road indicating presence of a <i>D. clingani</i> zone.
Boyce and Ash (1994)	Suggested a possible correlation between the Wigwam Formation (Botwood Group) and the Indian Islands Group at Careless Brook based on additional fossil collection and identification. A late Silurian to early Silurian age for the Wigwam Formation was proposed based on species of <i>Goniophora</i> from a fossil local near Lewisporte. Reinvestigated Careless Brook bivalve locality of Boyce <i>et al.</i> (1993) and the fossils from Indian Islands Group of Williams (1993). These were obtained upstream (west of the logging road) from buff to yellow weathered fine-grained

Table A1.3: *cont...*

	sandstone. Additional collections of the bivalves confirmed an upper age limit of Late Silurian to early Devonian for the Indian Islands Group at that locality.
Williams and Tallman (1995)	Re-examined the Beaver Brook mine area because of disparities in previous geology reports on the age of the strata. Authors collected a graptolite assemblage from along Beaver Brook (from locality reported by Dickson, 1992) and confirmed the Middle Ordovician (Carodoc) age originally assigned to the unit here and correlated it to the Lawrence Harbour Formation. The authors assigned a graptolite assemblage in nearby Cooper Brook an early Ordovician (late Arenig) age in a unit that was initially considered to be Middle to Late Ordovician and concluded that the previously proposed stratigraphy would have to be revised.
Donovan <i>et al.</i> (1997)	Determined a unit previously assigned to Middle Ordovician Baie d'Espoir Group is actually Late Silurian based on a new fossil locality. The fauna were correlated with bivalve bearing strata to the northeast, which led the authors to suggest that a major unconformity exists above the Early-Middle Ordovician fossiliferous strata and Early Ordovician ophiolite complexes.

**Table A1.4:** Brief summary of previous geochronological studies from within the Botwood Basin.

Author(s)	Description
Wanless <i>et al.</i> (1965 and 1967)	Provided the first age dates for Mount Peyton. Dated a diorite from Burnt Lake, NTS 2D/14 using the K-Ar biotite method and obtained an age of 418 +/- 21 Ma. They also dated granodiorite at this time collected SW of Glenwood using the K-Ar hornblende method and obtained a date of 270 +/- 52 Ma. Dated granodiorite from Rattling Lake, NTS 2E/3, using the K-Ar biotite method and obtained an age of 369 +/- 21 Ma.
Anderson and Williams (1970)	Reported a K-Ar mica age of 265 +/- 52 Ma for granite phase of MPIS and a K-Ar biotite age of 410 +/- 21 Ma for the gabbro phase of the MPIS.
Bell and Blenkinsop (1975)	Dated various granitiferous intrusions in eastern Newfoundland using whole rock Rb/ Sr isochron method and assigned the Mount Peyton batholith a 375 +/- 15 Ma age.
Bell <i>et al.</i> (1977)	Obtained whole rock Rb-Sr isochron ages for granitic plutons across Newfoundland, including foliated granites from the GRUB, central Newfoundland. Obtained three dates for foliated granites within the Gander Zone and concluded that granites from the Gander Zone are younger than 420 +/- 20 Ma. Indicated that as of yet no geochronological evidence existed for a Precambrian basement in the central mobile belt. Obtained two Rb-Sr whole rock ages for the granite of the Mount Peyton Intrusive Suite at the north end of the pluton of 380 +/- 30 Ma and 390 +/- 15 Ma. Bell and Blenkinsop later revise these dates as published by Reynolds <i>et al.</i> (1981).
Reynolds, P.H., Taylor, K.A., and Morgan, W.R. (1981)	Used biotite and hornblende from the latest gabbroic intrusive phase of the MPIS to obtain a $^{40}\text{Ar}/^{39}\text{Ar}$ age of 420 +/- 8 Ma. Compared this to a previously obtained Rb/Sr age of 390 +/- 15 Ma (Bell and Blenkinsop revision of previously reported age via personal communication) for the granite phase and concluded that the 400 Ma paleopole for Newfoundland may be different than other North American poles based on these new geochronological data on previously published paleomagnetic data.
Dunning and Krogh (1985)	Dated four ophiolitic complexes within the Newfoundland Appalachians. The complexes of interest to this study were the Pipestone Pond Complex and the Coy Pond Complex. The authors obtained an age from a coarse grained trondhjemite from a pod within the gabbro of 493.9 +/- 2.5/-1.9 Ma. They dated the Coy Pond Complex via trondhjemite from a small pod in the gabbro, which was similar in composition to that from the previous complex. A minimum slightly discordant age of 207/206 Pb age of 489 Ma was recorded. Suggested that the Coy Pond and Pipestone Pond Complexes are equivalent in age based both on this study and on field relationships observed by Colman-Sadd and Swinden (1984).
Dunning <i>et al.</i> (1990)	Mapped and dated units in the Central Mobile Belt to better understand the tectonic evolution of the region. The majority of the units studied were in the extreme southern mobile belt and only one unit is relevant in this previous history evaluation, the Stoney Lake Volcanics. U-Pb date of the Stoney Lake rhyolitic tuff provided an estimated age of 423 +/- 2 Ma. It was concluded



Table A1.4: *cont...*

	that since previous workers ( <i>i.e.</i> Colman-Sadd and Russell (1982) and Anderson and Williams (1970)) suggested that an angular unconformity existed between the volcanics and the Botwood Group that the rhyolite age could possibly represent the lower Silurian deformation and cleavage event within the Silurian Botwood Group. The authors noted that such a contact is only inferred, as it was not observed in field studies.
Elliot <i>et al.</i> (1991)	Used U-Pb radiometric dating (TIMS) of felsic plutons in Notre Dame Bay to constrain the timing of deformation events within the Newfoundland Appalachians. Concluded that several tectonic elements were contemporaneously being generated, subducted or deformed and that deformation occurred continuously throughout the Late Cambrian to the end of the Palaeozoic. They obtained an age of 422 $\pm$ 2 Ma for a composite felsic/ mafic dyke on the Port Albert Peninsula.
Colman-Sadd <i>et al.</i> (1992)	Established a Dunnage Zone (specifically the Exploits Subzone)-Gander Zone Silurian-Devonian interaction history through U-Pb radiometric dating of important units and provenance studies of sediments in key fossil locals.
Dunning (1992)	Dated a pegmatite south of the MPIS about 1 km south of Rolling Pond at 424 $\pm$ 2 Ma using the U-Pb (TIMS) method.
Dunning, and Manser (1993)	U-Pb geochronological report on analysis done on granite for the MPIS for the NDME. Reported numerous small prismatic zircon grains and separated five zircon fractions. Two possible age dates of 2680 Ma to 419 $\pm$ 2 Ma and 439.5 $\pm$ 9/-6 Ma were obtained. The authors preferred the older age of 439 Ma because four fractions are within error for that age, they did however note the lack of a concordant point provides questionability to the results.
Mitchinson (2001)	Defines the Caribou Hill Intrusive to be a geochemically and petrologically distinct unit from the MPIS, thus the 424 Ma age of Dunning (1992) could not be applied to the MPIS.

**APPENDIX 2**

**GOLD DEPOSIT MODELS**

## **APPENDIX 2**

### **GOLD DEPOSIT MODELS**

#### **A2.1 Gold Exploration within the Dunnage Zone**

Gold production in Newfoundland has historically been as a by-product from mining VMS deposits. The first recorded gold production is reported from the Cross Cove and Stewarts Mine at Moretons Harbour, eastern Notre Dame Bay during the late 1890's (Snelgrove, 1935). The Newfoundland Department of Natural Resources commissioned an appraisal of known gold occurrences within the island in the early 1930's, which was undertaken, by Snelgrove and Howse in 1934. Snelgrove published the results of this study in the "Geology of Gold Deposits of Newfoundland, Bulletin no.2" in 1935. The author reported 29 named occurrences as well as several minor occurrences on the island. Gold exploration waned following this report as only 29 gold only occurrences were reported for the island in 1976 as part of a mineral occurrences list (Douglas, 1976).

Gold exploration on the island surged after the discovery of the Hope Brook Deposit on the south coast in 1984. The Hope Brook Mine was in production for the most part from 1986 to 1997 and produced 752, 162 ounces of gold (Evans, 1999). The new surge in exploration was focused on the Baie Verte and GRUB lines due to the structural complexities of the areas and the comparison of each to the Californian Mother Lode Belt (Evans, 1999). The model for exploration concentrated on mesothermal or metamorphogenic styles of mineralization although epithermal style mineralization and associated alteration were discovered as well (*e.g.*, the Aztec and the Outflow prospects)



(Evans, 1996). After more than 200 Au occurrences were discovered, this new surge in exploration activity declined during the late 1980's. The interest slowly rebounded in the late 1990's and Richmont Mines opened the Nugget Pond gold mine in 1997. New discoveries by prospectors and junior exploration companies continued to attract attention and in 2000 a new exploration surge erupted in central Newfoundland when Altius Minerals attracted Barrick Gold to the scene.

Around 60 additional gold occurrences were documented in the eastern Dunnage Zone (east of the Red Indian line and west of the Gander Zone) since 1980. During the early to mid 1990s a study of the nature and setting of the gold mineralization in the eastern Dunnage Zone was conducted by D.W. Evans under the NDME. The study produced a complete documentation of the existing occurrences and included trench mapping and diamond drill core logging as well as sample collection for assay. A preliminary gold classification scheme was produced for the eastern Dunnage zone similar to the one devised by Dube (1990) for western Newfoundland occurrences (Figure A2.1).

The ages for the known gold mineralization in the Newfoundland Appalachians ranges from Late Neo-Proterozoic to the Silurian-Devonian (Evans, 1999). As discussed, both syngenetic and epigenetic styles of gold mineralization have been documented in Newfoundland. Syngenetic gold is present as an accessory to VMS deposits in the Dunnage Zone whereas epigenetic occurrences consist of structurally controlled mesothermal and epithermal style gold mineralization (refer to figure A2.1 for the classification of prospects included in this study).

## **A2.2 Overview of Applicable Gold Deposit Models**

### **A2.2.1 Syngenetic**

Syngenetic deposits are formed during country rock formation and occur as accessory gold associated with VMS in the Dunnage Zone of Newfoundland. The mineralization is associated with VMS deposits with the oldest being dated at  $513 \pm 2$  Ma (Evans *et al.*, 1990) for the Tally Pond volcanics and the youngest deposits predating the deposition of the Llandeilo-Caradoc shales. For the area and occurrences discussed and studied within this project, this model is not applicable.

### **A2.2.2 Epigenetic**

#### *A2.2.2.1 Orogenic Lode*

This deposit type has been referred to in literature as ‘Archean gold’, ‘mesothermal gold’, ‘gold only’, or ‘lode gold’ but today they are commonly referred to as orogenic gold deposits. Orogenic type deposits are generally associated with regional structures and include all Au (-Ag) vein deposits in metamorphic rocks regardless of age and metamorphic grade (Misra, 2000). This model indicates that deposits form along localized major regional fault and fracture systems in secondary and tertiary structures. The vein deposits generally form from hydrothermal fluids originating from a deep crustal origin at temperatures ranging from 250-300° C. Mineralization precipitates with quartz vein material when fluid traveling along a conduit reacts due to changing conditions. The host rocks are normally affected by faults or fracture systems and can range from mylonites to fault gouge depending on the depth of vein formation. Typical

host types include basalts, greenstones, gabbros and turbiditic shale. The mineralization generally consists of Au, pyrite and arsenopyrite in quartz veins with the Au occurring as solitary grains or intergrown with arsenopyrite or electrum. The alteration is typically dominated by Fe carbonate assemblages, which form alteration haloes in the host rock adjacent to the veins. Sulphide haloes and K-metasomatism alteration is also associated with the Au mineralization (Wilton, 1998).

The Dunnage Zone presents a possible exploration target for this deposit type as it exhibits the required large-scale regional structures (*i.e.*, Baie Verte and Dog Bay Lines) in lower greenschist facies units. The prospects tend to be concentrated in regions where the structure has been disrupted, such as flexures (*i.e.*, Hermitage Flexure). In the Dunnage Zone the orogenic lode type occurrences have been subdivided into different classes: 1) vein hosted with gold occurring within the quartz veins and 2) altered wall rock or replacement style mineralization in which gold is disseminated through the altered wall rock (Evans, 1996). The vein-hosted class has been further subdivided by Evans (1999) into 1) quartz-gold veins, 2) quartz-pyrite/ arsenopyrite veins, 3) base metal-rich quartz veins, and 4) barite rich veins. The altered wall rock, replacement class has also been subdivided into 1) carbonate-quartz pyrite, 2) silica-sulphide, 3) talc-magnesite-magnetite, and 4) red albite-ankerite-pyrite. For a complete description of each if the aforementioned subtypes refer to Evans (1999).

The age of structurally controlled or mesothermal gold mineralization in the Eastern Dunnage Zone has not yet been well defined by radiometric dating methods, though field observations suggest that the age is constrained at Early Silurian to Devonian. It is not yet known if the mineralization is constrained to one specific event or



several localized events. The oldest constrained age for this type of mineralization within the zone is 437 Ma and comes from the Hammerdown deposit whereas the youngest constrained age is 374 Ma and comes from the Nugget Pond Deposit. These dates are coincidental with the Salinian and Acadian Orogenies, which were periods of deformation, metamorphism and plutonism. During the Salinic Orogeny (*ca.* 430 to 415 Ma; Dunnng *et al.*, 1990) extensive reactivation of fault systems occurred (Karlstrom *et al.*, 1982; Tauch, 1987; Szybinski, 1988). The Salinic orogeny appears to be the most significant post Taconic event to have affected the Dunnage Zone (Evans, 1999) and Swinden (1990) suggest that the Salinic orogeny may have been a climatic metallogenic event. The Acadian Orogeny also affected the Dunnage Zone, but the reactivation of structures to produce mesothermal style mineralization occurred on a more regional scale. The Acadian and subsequent carboniferous deformation events may have remobilized pre-existing mineralization (Evans, 1999).

#### *A2.2.2.2 Epithermal*

The term epithermal was first introduced by Lindgren (1933) and was used to define deposits that formed near surface in an extensional tectonic environment exhibiting a well developed fracture system and normal faulting. The deposits are thought to be generated from relatively dilute, near neutral to weakly alkaline chloride waters that underwent boiling, mixing and oxidation at temperatures between 200 and 300° C. The maximum ore depth is about 1000 m. However, the ore strike length can be considerable. Veins are the most common ore host and tend to form an upward branching cone or wedge-like structure complete with breccia zones, stockworks and fine

grained bedding replacement zones (Figure A2.2). The associated mineralization is common in volcanic related hydrothermal and geothermal systems generally exhibiting well-differentiated subaerial pyroclastic rocks and small subvolcanic intrusions (Misra, 2000).

These deposits can contain gold, silver  $\pm$  base metal sulphides and gangue minerals such as quartz, calcite, adularia, barite and fluorite. Alteration is characteristic and minerals in the zones of alteration include quartz, adularia, illite, chlorite and kaolinite. The mineralization and the location of these deposits is dependant on the permeability of host lithologies. The ore and mineralization are typically deposited as open spaces resulting in banded, crustiform, vuggy, drusy, colloform and cockscomb textures. The zone may also show evidence of replacement textures such as pseudomorphs after calcite. The main economic minerals are typically Au and Ag (with widely varying ratios), which are associated with Hg, As, Sb, and less often Ti, Se and Te. The main ore minerals include native Au and Ag, electrum, acanthite and silver bearing arsenic-antimony sulphosalts. Cinnabar, stibnite, tetrahedrite and selenides can be important in some deposits. The main gangue minerals include quartz and calcite with minor bearing on fluorite, barite and pyrite and lesser chlorite, hematite, dolomite, rhodonite and rhodochrosite. An epithermal deposit is characterized by dominant hydrothermal alteration of wallrock and precious metal mineralization closely associated with silicification. The silicification zones may be flanked by zones of illite, sericite and clay alteration, all which occur in a larger zone of propylitic alteration. Some zones may exhibit adularia associated with quartz veins at surface and argillic alteration near surface (Panteleyev, 1988).

Mineralization may occur in repeated cycles and is typically fine grained with coarse-grained well-crystallized gangue mineral overgrowths (Misra, 2000). The fluid origin is mostly meteoric waters derived from a deep magmatic source and the metals are from either a deep magmatic source or leached from host lithologies that range from volcanics to sediments. These deposits are generally formed as veins, breccia and disseminations (Misra, 2000). This type of mineralization has been discovered at several localities in the eastern Dunnage Zone including the Aztec, Outflow and Moosehead Prospects (Evans, 1996; Dalton, 1998). The amount and type of mineralization is dependent on the characteristics of the carrying solution, which have been divided into two classes: low and high sulfidation.

#### *Low Sulfidation*

Low sulfidation fluids are reduced and have a near neutral pH resulting from the mixing of subsurface water (ie: rainwater) and magmatic water (from a deep molton source) that has migrated to the surface. The economic minerals are deposited when the carrying solution reaches the surface and boils. Au mineralization is generally hosted in cavity filling veins and stockwork and is associated with Ag, and minor Pb, Zn and Cu. Common minerals include quartz (chalcedony), carbonate, pyrite, sphalerite and galena. Deposits formed from this fluid type are characterized by high Zn and Pb, low Cu values and a high Ag/Au ratio (Wilton, 1998).

The deposits are generally found in caldera or complex volcanic environments consisting of a rhyolite to andesite volcanic host with associated intrusions and sediments. The ore has high gold and silver values with variable copper and is situated



outside of the heat source. Mineralization also tends to postdate that of the host rock by >1 Ma and alteration is argillic to adularia. The meteoric fluid develops a varied elemental composition from the surrounding lithologies, as it is heated by the intrusion it joins a convective cell and rises to the surface, moving within the plane of major fracture system it cools, causing precipitation of its metals and the formation of a deposit (Misra, 2000).

### *High Sulfidation*

High sulfidation fluids are more oxidized and acidic and are mainly derived from a magmatic source. The gold mineralization is deposited near surface, as the solution is cooled or diluted by mixing with rainwater. In this type of deposit the mineralization occurs in veins but is more concentrated in surrounding host rock containing economic amounts of Cu and some Ag. Deposits formed from this fluid type have a low Ag/Au ratio, contain greater amounts of As and Cu and are typically lower grade (Wilton, 1998).

These deposits are usually located in calderas or silicic domes and are hosted mainly by rhyodacite forming domes and ash flows. The ore has variable gold and silver values with high levels of copper and is situated within the heat source. Mineralization and host rock are generally of similar age and alteration near and around the ore body is argillic with alunite and kaolinite without adularia alteration. With the convective circulation of meteoric and magmatic waters, elements are leached from the surrounding host rocks and upon cooling are deposited near the surface forming a deposit within the heat source (Misra, 2000).

Evans (1999) outlines central Newfoundland to exhibit high potential to develop into a major epithermal gold district based on several factors. First, the occurrence of fossil epithermal systems appear to be widely developed and preserved throughout with most known occurrences located in Ordovician and Silurian sequences surrounding the Mount Peyton Intrusive Suite. He suggests that the Mount Peyton may have acted either as a heat source for these systems or as a homogeneous mass that intruded into the Silurian-Ordovician sequences causing widespread focused deformation and extension (Evans, 1999). The age of epithermal systems, as like mesothermal systems, is not well constrained. The mineralized zones are associated with brittle fault systems rather than ductile systems which primarily affect Silurian sequences and are thus considered to be Late Devonian (corresponding to the Acadian Orogeny) or maybe as young as Carboniferous (Evans, 1999).

#### *A2.2.2.3 Sediment Hosted Disseminated (Carlin Type)*

Altius Minerals first applied the Carlin type deposit model to central Newfoundland at their outflow property along the Mustang Trend in 2002, attracting gold mogul Barrick to the scene and effectively creating a staking rush within the 'Botwood basin'.

Sediment Hosted Disseminated Gold (SHDG) or Carlin Type Au deposits form in complex terranes at depths of 2-4 km and have a spatial association with high angle normal faults and permeable horizons, generally with a spatial relationship to igneous granitic rocks. These disseminated auriferous pyrite deposits are characterized by carbonate dissolution, argillic alteration, sulfidation and silicification of typically calcitic

sedimentary rocks (Hoftra and Cline, 2000). Micron Au mineralization occurs within arsenic bearing pyrite and quartz and has associated elevated concentrations of antimony, mercury, barium and thallium. Host rocks are typically thickly bedded silty carbonaceous rocks such as limestones, dolomites, shales, and silica rich intrusive igneous rocks and breccias. Ore bearing host rocks are extremely altered and exhibit decarbonization, silicification, and argillization alteration assemblages which may not always be fully developed and all of which can contain Au. Zones of jasperoid are characteristic and can extend up to 30 m from the fault (Figure A2.3). Depths range anywhere from 1.5 to 4 km and temperature is generally  $> 225^{\circ}\text{C}$  (Wilton, 1998). Theories exist for both magmatic and meteoric fluid, which circulates through rocks and remobilizes minerals along linear trends, with fault lines acting as fluid pathways. Some deposit models suggest that magmatic fluids mix with those of meteoric origin. The deposits are either tabular or irregular in form, however some develop within breccias formed as a result of the faulting.

These deposits commonly have a low Ag content and are of low grade and large tonnage (Wilton, 1998). Mineralization consists of S and Au with associated As, Sb, Ti, Ag  $\pm$  W and  $\pm$  Te. The deposits typically exemplify the following sequence of events: 1) a main ore stage distinguished by acid attack and replacement of host rocks 2) a late ore stage distinguished by quartz, calcite, orpiment, realgar or stibnite, 3) a peripheral stage of botroidal pyrite  $\pm$  marcasite, 4) a post ore stage of mainly calcite and 5) a supergene stage of dissolution and minerals formed as result of weathering and oxidation of the ores" (table A2.1) (Hoftra and Cline, 2000).



# STYLES OF GOLD MINERALIZATION EASTERN DUNNAGE ZONE, CENTRAL NEWFOUNDLAND

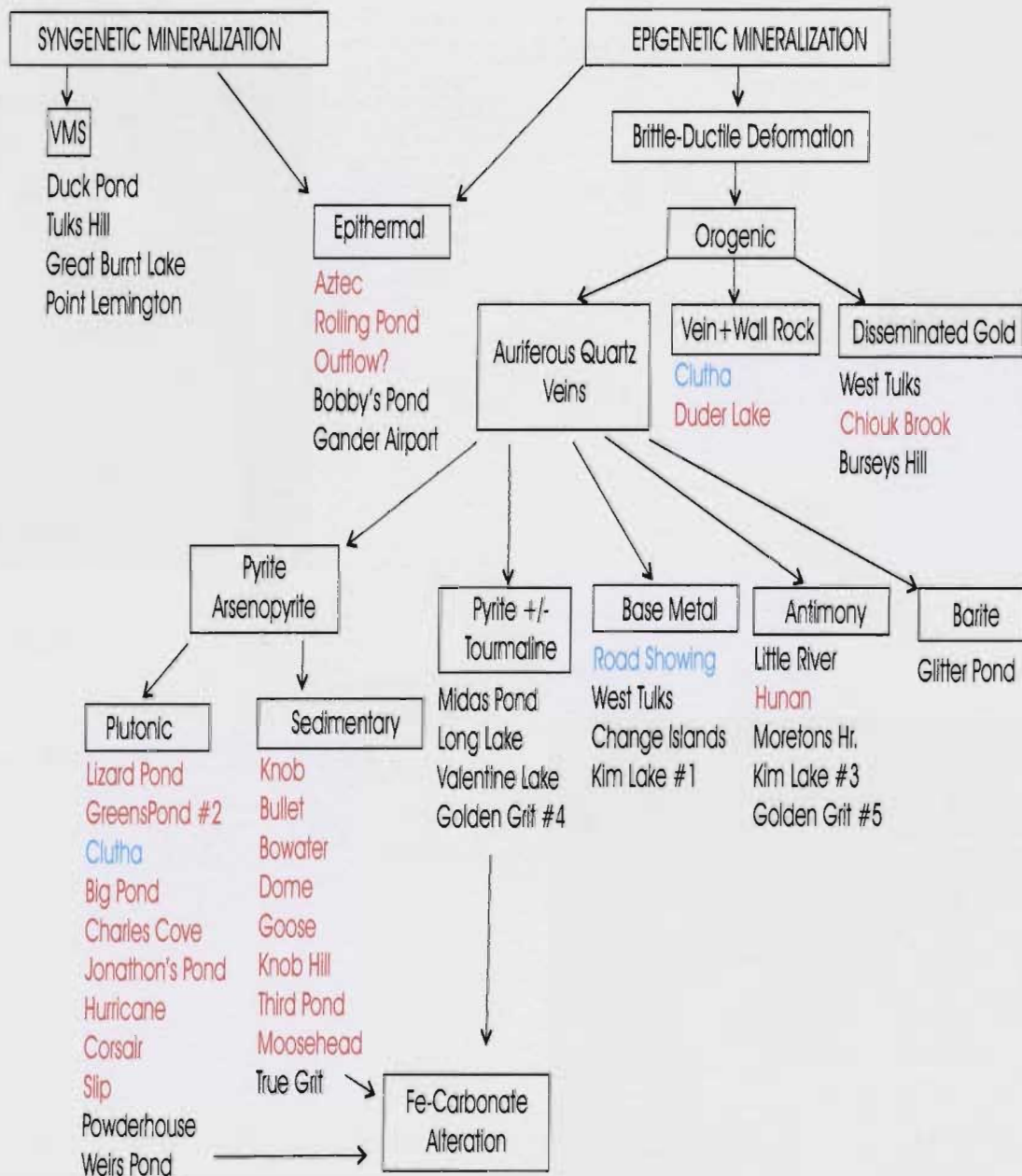


**Figure A2.1:** Classification scheme for gold mineralization within the eastern Dunnage Zone. Prospects in red were visited and assessed during the current project and those in blue were visited but have been backfilled since last documentation (modified from Evans, 1993).

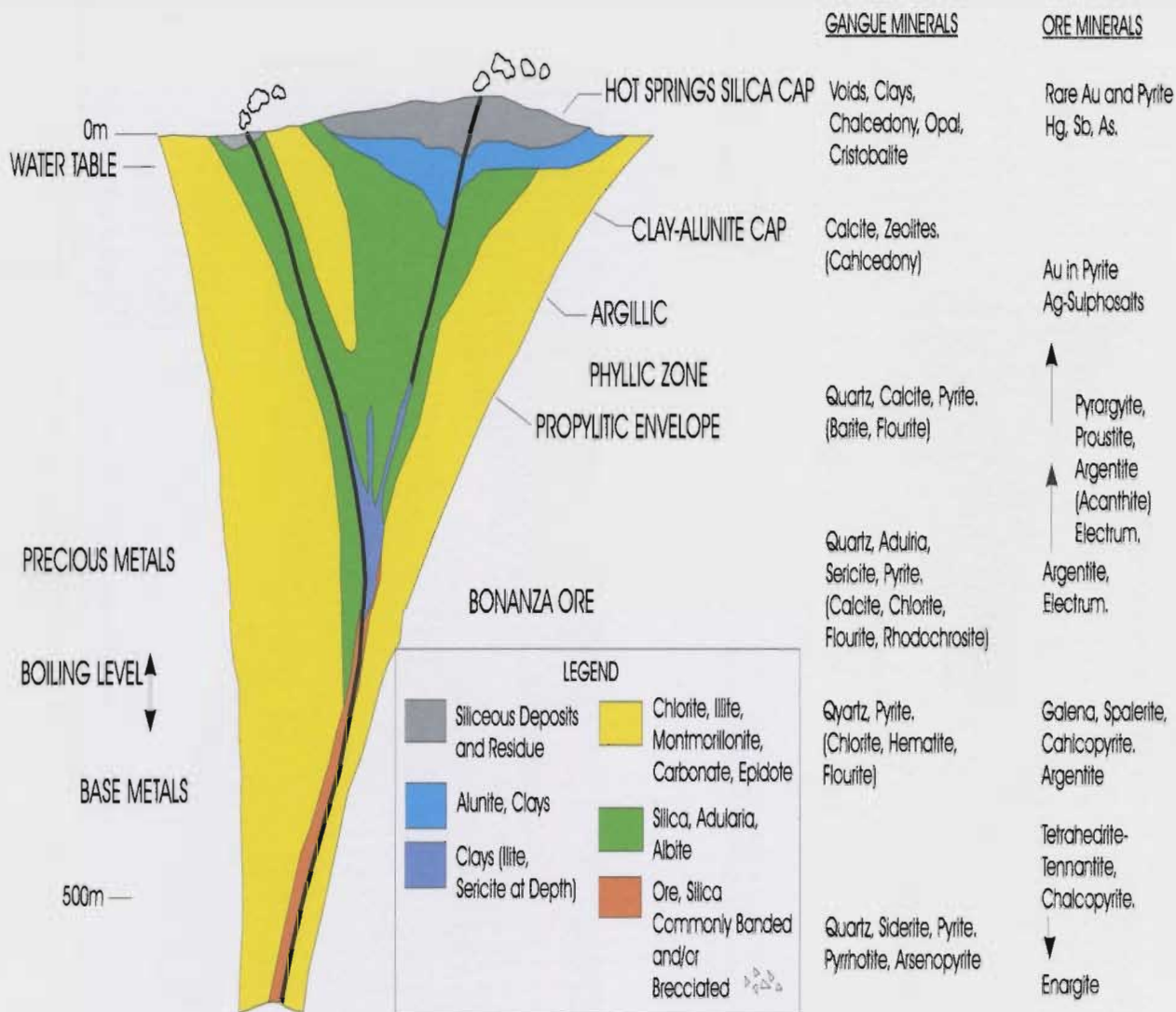
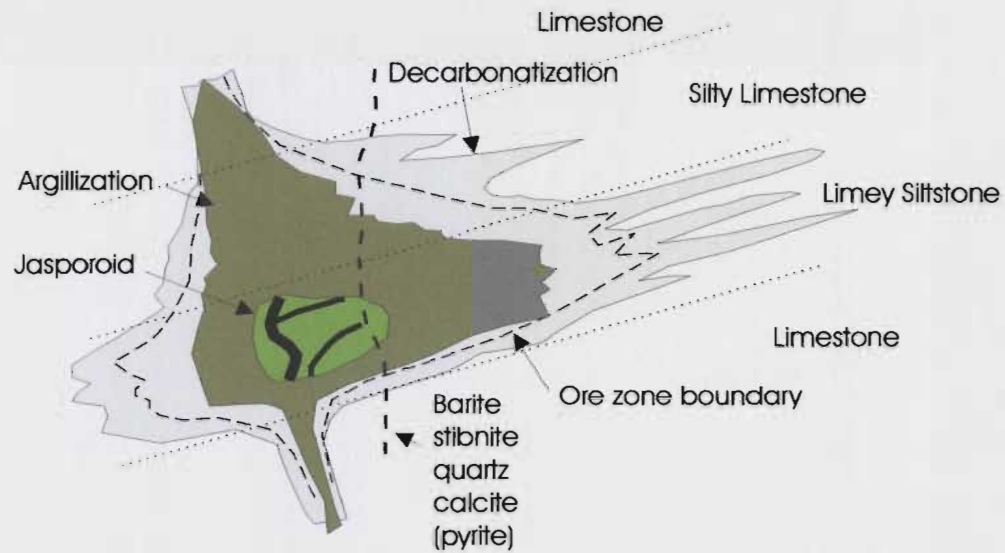
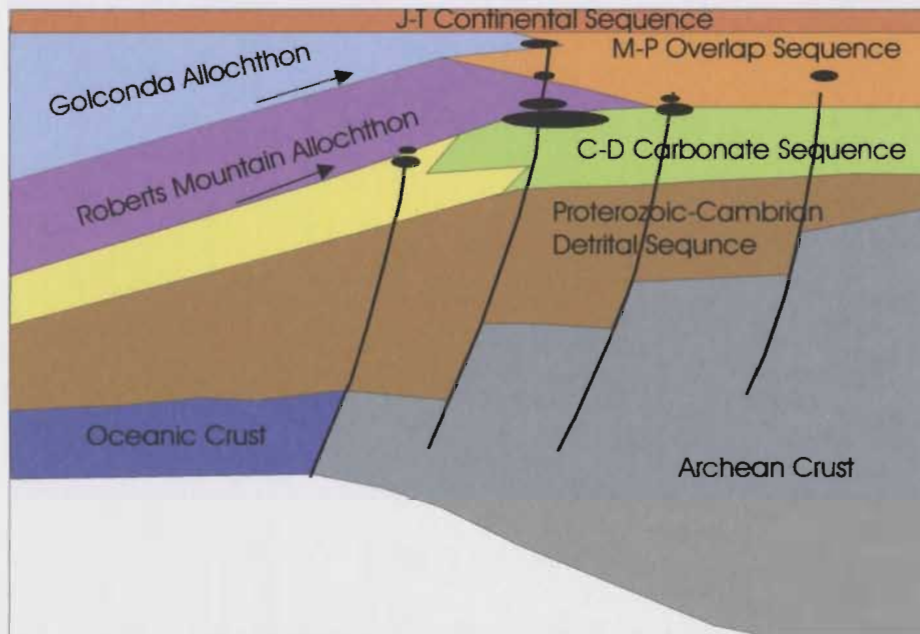


Figure A2.2: Idealized section of a bonanza epithermal deposit (after Buchanan, 1981).



**Figure A2.3a:** Schematic cross section through a SHDG deposit showing major alteration and mineralization features adjacent to a fluid feeder (*after* Arehart, 1996).



**Figure A1.3b:** Schematic cross section of northern Nevada and northwest Utah, showing attenuated Archean crust, oceanic crust, overlying stratigraphic sequences and allochthons, fault zones and locations of Carlin-type gold deposits (black) (*after* Hofstra and cline, 2000).



Main Ore Stage	Late Ore Stage	Perithermal Stage	Postore Stage	Supergene Stage
<b>Decarbonation</b> <b>decalcification,</b> dedolomitization  <b>Silicification</b> <b>quartz, chalcedony</b>  <b>Argillization of silicates</b> <b>kaolinite, illite,</b> <b>illite-smectite, smectite</b> chlorite-smectite  <b>Sulfidation of Fe minerals</b> <b>As pyrite,</b> As marcasite arsenopyrite <b>submicron gold</b>  Carbonation <i>calcite, dolomite,</i> <i>ankerite, siderite</i>  K metasomatism <i>adularia, illite</i>	<b>Open Space minerals</b> <b>quartz, clacite,</b> dolomite <i>barite, fluorite, adularia</i> <b>orpiment, realgar, arsenic</b> <b>stibnite,</b> As pyrite, As marcasite, <i>cinnabar,</i> <i>galkhaite, Ti Sulfides,</i> <i>tellerides, native gold</i>  <b>Silicification</b> <b>quartz, chalcedony</b>	<b>Open-space minerals</b> <b>As pyrite-marcasite</b> alunite, kaolinite, barite, <i>sphalerite,</i> <i>realgar, stibnite,</i> <i>native gold</i>  Argillization <i>kaolinite, alunite</i>	<b>Open-space minerals</b> <b>calcite, barite</b>  Decarbonation vugs, decalcification, Dedolomitization  Epithermal overprints <i>Opaline silica +/- Hg</i> <i>Au-Ag veins</i>	Decarbonation karst cavities, decalcification  Argillization of silicates alunite, kaolinite, halloysite, smectite  Oxidation of sulfides goethite, hematite, jarosite, alunite, stibiconite, scorodite, <i>kermesite,</i> <i>native gold</i>  Open-space minerals goethite, jarosite, alunite, kaolinite, halloysite, smectite, calcite, aragonite gypsum, <i>celestite</i> melanterite phosphates

**Table A2.1:** Generalized Mineral Paragenesis in Carlin Type Gold Deposits. Common alteration types and minerals are in **bold** and rare minerals are in *italics* (after Hofstra and Cline, 2000)

**APPENDIX 3**  
**ANALYTICAL TECHNIQUES**

## **APPENDIX 3**

### **ANALYTICAL TECHNIQUES**

#### **A3.1 Sample Collection**

Bulk sampling of grab samples from the prospects, as well as regional host and intrusive units, was implemented in the 2003 and 2004 field seasons. Where possible, a minimum of three samples were collected from each prospect with the aim towards having an unaltered host, altered host and mineralized host rock. Samples collection was restricted to surface outcrops because the number of prospects assessed during the study was too large to consider bulk sampling of drill core.

Sedimentary, intrusive and host rock samples ranged in size from 5 to 40 cm wide depending on the availability of outcrop to provide sufficient material. Samples were selected for processing for lithogeochemical, isotopic, geochronological and petrographical studies. All samples were prepared for analysis at the Memorial University of Newfoundland, Earth Sciences laboratories. First, weathered and/or altered pieces, which could alter the chemistry data, were removed, where possible, with a diamond tipped saw. Large pieces (size was dependant on the analytical method) were cut for whole rock geochemical, geochronological and isotopic analyses and small pieces were kept for hand specimens and thin sections.



## **A3.2 Whole Rock Geochemical Analysis *via* X-Ray Fluorescence (XRF)**

### *A3.2.1 Introduction*

The XRF is a multi element instrumental technique for the high precision determination of major elements and trace elements and involves simple sample preparation. Major elements are determined on powders that are fused with a suitable flux and cast as glass discs and trace elements are determined on pressed powder pellets (Riddle, 1993). A complete list of the samples prepared for this analysis, along with sample location and description is presented in table A3.1.

### *A3.2.2 Sample Preparation and Data Collection for XRF Analysis*

Slabs cut for whole rock geochemistry (~4 cm x 4 cm x 2 cm) were crushed in a steel jaw crusher to rock chips about 1-2 cm<sup>2</sup>. Approximately ½ cup of this material was put into a tungsten-carbide bowl-puck assembly to grind them into a very fine powder (~200 mesh). Rocks of similar lithologies were crushed as groups to reduce inter-group contamination between samples. Between each sample, the jaw crusher was extensively cleaned with a pressurized air gun, paper towels and alcohol, and a steel brush. The mill assembly was also extensively cleaned between each sample and silica sand was intermittently powdered in the bowl-puck-mill to further reduce the possibility of cross contamination between samples. The powders were placed in vials, labeled and submitted to the XRF laboratory where they were pressed into disc-like pellets.

The use of the pressed powder pellet technique allows for limits of detection below 1ppm for trace elements. The pressed pellets were prepared by a method as described by Longerich (1995). 5.00 g ( $\pm$  0.05 g) of sample powder is combined with 0.70 g of BRP-5933 bakelite phenolic powder binding resin and placed in a glass jar with two stainless steel ball bearings which is subsequently rotated for ten minutes on a roller mixer. The resulting mixture is placed within a pellet press where it is pressed for 5 seconds at 20 tonnes to make it compact. Finally, the samples are placed in an oven and baked at 500° C for 15 minutes.

Qualitative and quantitative determinations of elements were determined from the pressed pellets using a Fisons/Applies Research Laboratories model 8420+ sequential wavelength-dispersive x-ray spectrometer. The data was collected by an automated computer system attached to the XRF. Four quality control reference standards and five internal standards were also analyzed intermittently with the samples from this study. The values for the reference materials are published by Potts *et al.* (1992), Jenner *et al.* (1990) and Longerich *et al.* (1990).

The elements determined are K, Ca, Sc, Ti, V, Cr, Mn, Fe, Ni, Cu, Zn, Ga, As, Rb, Sr, Y, Zr, Nb, Ba, Ce, Pb, Th, U. The light major elements and S and Cl were also determined on a semi-quantitative basis.

#### *A3.2.3 Precision and Accuracy*

Precision and accuracy are determined by using a standard reference material and analyzing this material intermittently with study samples. The reference used was standard DNC-1 and five replicate analysis were conducted between September 2000 and

November 2002. Precision is typically excellent (0-3% RSD) for all major oxides. Precision of trace element data was excellent (0-3% RSD) with the exceptions of S, Sc, Ba, Rb and Nb. Long term precision is variably between 2 (Rb, Sr) to 5% (Ba, Nb, Zr, Y) RSD. These elements typically have low concentrations in the standard, thereby explaining the lower precision values. The limits of detection for these elements varies from 0.6ppm Nb and Y, 0.7 ppm for Rb, 1.1 ppm for Sr and Zr, and 21 ppm for Ba (Longerich, 1995).

Accuracy is usually excellent (RD's from 0-3%) with the exception of P<sub>2</sub>O<sub>5</sub>, Al<sub>2</sub>O<sub>3</sub>, Sr and Zr. This once again attributed to lower concentrations of these elements in the standard material (Longerich, 1995).

### **A3.3: Sulphide Isotope Geochemical Analysis *via* Inductively Coupled Plasma-Mass Spectrometry (ICP-MS)**

#### *A3.3.1 Introduction*

The majority of naturally occurring elements are combinations of at least two isotopes. The variation in the profusion of these isotopes is caused by radioactive decay in unstable isotopes and by fractionation in stable isotopes. In the case of S the variation is a result of fractionation, as isotopes of this stable element partition into different phases in response to minute differences in chemical and physical properties related to mass. This difference is most evident in the light elements H, C, O and N because the disparities in mass between isotopes of these elements are large. Measuring isotopic compositions of these stable elements is useful for recognizing sources and/or determining chemical reactions. In this case, SO<sub>2</sub> gas extractions from single crystals of



sulphide material are used to measure the abundance ratios to delineate possible sources of mineralizing fluids. A table listing the location and description of samples prepared for sulphur isotope analyses is presented in table A3.2.

#### *A2.3.2 Sample Preparation and Data Collection for S-Isotope Analysis*

Mineralized samples were selected for analysis and small pieces (~3 x 3 cm) of the samples were pulverized using hand tools. Single crystals of pyrite, arsenopyrite, stibnite or galena were hand picked from the crushed material using tweezers and a hand lens and placed in small, labeled glass vials. In some instances, the material was too fine grained to separate and was analyzed as a pyrite + arsenopyrite mixture. The workspace and tools were thoroughly cleaned with alcohol between each sample to avoid cross contamination. The sulphide separates were crushed in a ceramic mortar and pestle assembly into a sulphide powder (4-9 mg), and were once again stored in labeled glass vials. Approximately 0.95 mg of pyrite, .250 mg of arsenopyrite, 0.4 mg of galena or 0.175 mg stibnite (amount is dependant on the specific sulphide being analyzed) was measured out on a calibrated electronic scale and placed in high quality, 7 x 7 mm tin vessels with 0.200 mg of vanadium pentoxide ( $V_2O_5$ ).

The tins containing the dry mixture were closed and loaded into a Carlo Erba Automatic Gas Chromatographic Elemental Analyzer carousel and the sample details were entered into an auto run file in the machine. The auto run program is then started and drops each sample into a combustion region of the elemental analyzer.  $SO_2$  gas is extracted from single sulphide crystals from which isotopic abundances are measured on a Finnigan MAT 252 and compared with those of international standards.

### **A3.4 U-Pb Geochronological Analysis *via* Laser Ablation Microprobe-Inductively Coupled Plasma-Mass Spectrometer (LAM-ICP-MS)**

#### *A3.4.1 Introduction*

Laser Ablation ICP-MS is an efficient and suitable method for sediment provenance studies where many analyses are required to define the age of a population (Kosler *et al.*, 2002). The LAM-ICP-MS technique consists of a laser-ablation sampling device, LAM (Laser Ablation Microprobe) and an inductively coupled torch-mass spectrometer (ICP-MS). The combination of these two devices provides a relatively simple, efficient, and inexpensive technique for the determination of the direct elemental and isotope ratio analysis of solid samples. Sample preparation is also relatively simple. The method for geochronology involves the in situ analysis of single zircon grains, thus allowing for the determination of growth zonation and overgrowth ages. Such considerations are significant concerns in material with inherited cores, and the problem is not overcome using standard TIMS geochronological determinations (Cox, 2002).

The benefit of using this technique as a geochronometer is the efficiency to produce high quality data for a large number of samples relatively quickly compared to other techniques such as TIMS (Thermal Ionization Mass Spectrometer). The technique has been shown to be an efficient geochronometer using detrital zircon U-Pb geochronology (Kosler *et al.*, 2002). A table listing the location and description of samples prepared for U-Pb geochronology is presented in table A3.3.

#### *A3.4.2 Sample Preparation and Data Collection*

The collected samples were individually crushed by a jaw crusher into rock chips up to 2 cm in diameter, and then ground into medium-coarse sand using a disk mill. The laboratory and machinery were thoroughly cleaned between each sample to avoid sample contamination.

The medium-coarse sand was put through several heavy mineral separation processes. First, heavy minerals were separated from light minerals using a Wilfley table. The remaining 'heavy' and 'light' minerals were rinsed thoroughly with ethanol and dried out using a hot plate and heat lamp. The 'heavies' were taken to the mineral separation laboratories where they were sieved through a 40- $\mu$ m mesh. Magnetic minerals and metal filings were removed from the sieved grains using a hand held magnet. The next step in the separation process was *Heavy Liquid Separation* using MI (Methylene Iodide). Minerals with a density greater than the MI fell through the solution and were collected, rinsed with acetone, and dried under a heat lamp. This material was then put through the *Frantz Magnetic Separator*, which separates minerals based on magnetic susceptibility. The strength of the magnet was gradually increased, and minerals with high magnetic susceptibility such as zircon and corundum were collected as the end result.

The final step in the preparation was hand picking zircon grains in nanopure ethanol with a binocular microscope. The zircon grains were mounted in epoxy resin in a round ring assembly, polished, and analyzed using an electron microprobe and LAM-ICP-MS.



The U-Pb dating technique used here is described in detail by Kosler *et al.* (2002). A VG Plasma Quad II + “S” ICP-MS, coupled with an in-house-custom-built Q-switched ND: YAG, 266nm ultraviolet laser is used for LAM-ICP-MS analysis in the Department of Earth Sciences laboratories at Memorial University of Newfoundland. An ultraviolet laser beam is directed into the focusing objective lens, enters a transparent sample cell and ablates the polished sample surface. The ablated material is then transported in a helium gas stream to the ICP-MS for chemical analysis. Zircons were ablated using a laser repetition rate of 10Hz and a laser energy of 0.8 mJ/pulse. The beam was focused 100  $\mu\text{m}$  above the sample surface. A sample cell is mounted on a motorized stage on the microscope and is controlled by a computer. The stage was moved beneath the stationary laser beam to produce a 20-40  $\mu\text{m}$  raster pit (depending on the size of the grain) in the sample. The depth of the pit ranges from ca 10 to 50  $\mu\text{m}$  depending on the width of the pit and ablation time. The ancillary equipment allows one to safely view the sampling site while the laser beam is rastering on the sample surface.

A He carrier gas transports the ablated material to the plasma by acid washed plastic tubing via the mixing chamber at the rear of the plasma torch. The mass spectrometer measures the U/Pb and Pb isotopic ratios of the zircon samples as well as the Tl/Bi/Np tracer solution that is nebulized along with the laser ablated sample material. The tracer solution should contain natural Tl,  $^{209}\text{Bi}$  and  $^{237}\text{Np}$  at concentrations of 10.6 ppb for each isotope.

The data are acquired using Fisons time-resolved software; this software allows for the acquisition of multiple elements using multiple channels. Data are acquired for approximately 60 s prior to ablation to obtain a background of the He gas blank and

tracer solution signals. Once ablation is started, U and Pd signals for the sample, along with the continuing tracer solution are acquired for 180-200 s. Data are periodically collected from a zircon standard of known age to ensure reproducibility and accuracy of the analysis. The standards used in this study include the  $295 \pm 1$  Ma (Ketchum *et al.*, 2001) pegmatitic zircon standard (02123). Data was acquired in time resolved- peak jumping-pulse counting mode with 1 point measured per peak using commercial PQVision v.4.30 software. In total masses 201 (flyback), 203 (Tl), 204 (Pb), 205 (Tl), 206 (Pb), 207 (Pb), 209 (Bi), 237 (Np) and 238 (U) were measured in total masses. Np and U oxides were also measured to monitor minor changes in the solution over time of the analysis. Quadruple settling time was 1 ms for all masses and the dwell time was 8.3 ms for all masses except for mass 207 where it was 24.9 ms. Over the 240 seconds of measurement approximately 1600 data acquisition cycles (sweeps) were collected. A typical analysis takes approximately 3 minutes to complete.

#### *A3.4.3 Data Reduction*

The raw data was collected for electron multiplier dead time (20ns) and downloaded to a PC for processing using an in house spreadsheet utility program to integrate signals from each sequential set of ten sweeps.  $^{207}\text{Pb}/^{206}\text{Pb}$ ,  $^{208}\text{Pb}/^{206}\text{Pb}$ ,  $^{206}\text{Pb}/^{238}\text{U}$  and  $^{207}\text{Pb}/^{235}\text{U}$  were calculated for each analysis using a natural  $^{238}\text{U}/^{235}\text{U}$  ratio of 137.88. Signal intervals for the background and ablation were selected for each sample and harmonized with similar intervals for the standards. The calculated isotope ratios were then corrected for gas blank and the small contribution of Pd and U from the

tracer solution. Using  $^{233}\text{U}$  in the tracer solution allowed for a real-time instrument mass bias correction with the  $^{205}\text{Tl}/^{233}\text{U}$  value measured while the sample was being ablated.

### **A3.5 Electron Microprobe**

#### *A3.5.1 Introduction*

The electron microprobe microanalyzer is the “definitive” technique for the nondestructive, accurate determination major and trace elements from small volumes (3-4  $\mu\text{m}$  diameter) of *in situ* solid materials down to detection limits of typically 50-200  $\mu\text{g/g}$  (Riddle, 1993). The instrument is used for several applications including the determination of mineral identification and composition, mineral zoning, chemical reactions, etc. For this study, the instrument was employed for determining the composition of pyrite grains to establish an internal FeS standard for the trace element analysis of pyrite and also, to determine if any zoning was present in zircon grains that were mounted for U-Pb geochronology analysis. The instrument was also utilized for micrograph imaging of the zircon grains and of an ablation pit on a pyrite grain.

The machine identifies and measures x-rays that are characteristic of the samples composition. A high-energy electron beam is focused on the surface of the sample and as the beam penetrates into the sample, inner shell orbital electrons are removed and the replacement of the resulting vacancies by outer orbital electrons produces x-rays. The source of electrons in the electron gun is typically a tungsten filament bent into a hairpin shape. A High voltage potential is applied across the gun to accelerate the electrons through the potential of typically 15-25 kV. The beam then passes down an electron column,



which focuses the beam to a pinpoint of minimum diameter 0.1-1  $\mu\text{m}$ . Two electromagnetic lenses are used for focusing, the condenser lens control the total probe reaching the sample and the objective lens allows the operator to focus the electron beam on the surface of the sample. An element can be identified and its abundance measured as mass fractionation via measuring the x-rays energy (determined relative to either energy or wavelength) and intensity (Riddle, 1993). A ray of electrons exits the sample and secondary X-rays are analyzed according to the wavelength. It has excellent spatial resolution and emits an electron beam 1 and 2  $\mu\text{m}$  in diameter meaning that very small samples areas can be used (Rollinson, 1993).

Image data can be achieved by scanning the electron beam across the surface of the sample in a raster pattern. As the beam scans t surface, the intensity of the backscattered electrons is measured a detector that is mounted above the sample in the specimen chamber. The spot on the electron ray tube (CRT) is scanned at the same time as the probe beam and its strength is adjusted in proportion to that of the measured backscattered electron signal. The resulting display on the CRT is the resultant electron micrograph mage of the sample (Riddle, 1993).

#### *A3.5.2 Sample Preparation and Microanalysis*

Specimens that are analyzed using this instrument must be prepared as thin sections or blocks that have highly polished flat surfaces. The petrographic thin sections that were prepared for the pyrite trace element analyses and the puck mounts that were prepared for the U-Pb analyses were both highly polished and ready for carbon coating. The surfaces of the specimens must be coated with a thin film (20nm) of carbon to enable

the electron beam to conduct to earth (Riddle, 1993). The thin sections and pucks were analyzed on separate occasions.

The specimens were loaded into a *Cameca* SX-50 microprobe that is configured with three wavelength discriminating (WD) spectrometers and an *Oxford Instruments* energy dispersive (ED) detector. The laboratory at MUN utilizes Samx software to control the instrument. The specimen surface has to be adjusted to lie on the plane of focus of the X-ray spectrometers. This is achieved by examining the specimen through an integral binocular microscope and adjusting the height until it comes into sharp focus.

The thin sections for the trace element of pyrite analysis were analyzed using the WD x-ray spectrometer, which allows the precise and accurate measurement of minor and major elements at concentrations typically as low as 0.01 wt %. The stage was moved around to locate the pyrite grains. Once a grain was located, the electron beam was focused above the sample and the analysis was implemented to produce the precise Fe and S concentrations of the grains. The resulting data was used as an internal FeS standard. The pucks for the U-Pb analysis were imaged in backscattered electron mode to determine if any chemical or compositional zoning was evident in the zircon grains.

### **A3.6 Trace Element Geochemical Analysis of Pyrite *via* LAM-ICP-MS**

#### *A3.6.1 Introduction*

Quantitative analysis of mineral chemistry via LAM-ICP-MS is useful because it enables the measure of a wide range of trace elements using only a small sample with very low detection limits and good accuracy and precision (Jenner *et al.*, 1990).

### *A3.6.2 Sample preparation and data collection for pyrite chemistry*

Samples with visible sulphides from different areas within the Central Mobile Belt were selected for analysis. Polished thin sections were cut from the samples, which were subsequently studied to ascertain the mineralogy. Samples W90-48, W90-49A, KP-32-H1 and W89-82 were not collected by the author and an internal standard was used for those cases. The internal standard was MASS1, a United States Geological Survey pressed powder pellet. Samples JOD23, JOD80A, JOD98A, JOD117 and JOD119 were collected by the author for this study and the pyrite grains from each sample were analyzed using an electron microprobe to obtain acquired independent FeS standards. The method for quantitative analysis of pyrite by LAM-ICP-MS as described below was obtained from Hinchey *et al.* (2003).

The naturally occurring internal standard, usually a major element that is present in the calibration standard and the unknown mineral, is calibrated using an external calibration. Using an internal standard corrects for the multiplicative effects of matrix, drift and, specifically for laser ablation, the amount of sample ablated (e.g. Longerich, 2001). It also allows for calibration of different mineral matrixes in regards to one another and for the use of changing energies of the laser to optimize signals from matrix to matrix. The internal standard for the samples collected by the author was sulphur (Sylvester, 2001) and the concentration of this element was determined by electron-microprobe analyses (EMPA) of pyrite in each sample. Refer to Longerich *et al.* (1996) for a detailed discussion on the equations for calibration and sample concentration calculations that were used in this study.



**Table A3.1:** List of igneous and sedimentary samples with location and description for XRF analysis.

Sample	Location (UTM)	Description	Nomenclature
JOD15	674259/ 5445813	Fine-grained, white to grey, greywacke host to auriferous mineralization at the Knob Hill Prospect.	Davidsville Group (Blackwood, 1982)
JOD20	671020/ 5442038	Fine-grained, quartz rich greywacke host to auriferous mineralization at the Third Pond Prospect.	Davidsville Group (Blackwood, 1982)
JOD21	645161/ 5425138	Slightly sericitized, fine-grained diorite host rock to auriferous mineralization at the Hurricane Prospect along Salmon River.	MPIS (Tallman, 1990b, 1991a; Dickson, 1992)
JOD22	645161/ 5425138	Sericitized, mineralized diorite host to the Hurricane Prospect along Salmon River.	MPIS (Tallman, 1990b, 1991a; Dickson, 1992)
JOD25	644408/ 5425289	Slightly sericitized diorite host rock with <5% disseminated sulphide at the Corsair Prospect along Salmon River.	MPIS (Tallman, 1990b, 1991a; Dickson, 1992)
JOD39	647570/ 5418043	Dense, dark grey to black, fine-grained sedimentary rock at a sheared contact zone at Careless Brook.	Caradocian Shale (Boyce <i>et al.</i> , 1994)
JOD44A	636504/ 5391062	Silicified, dark grey siltstone with minute quartz filled tension gashes adjacent to the LBNL Prospect.	Davidsville Group (Blackwood, 1981; Tallman, 1989a)
JOD45A	636504/ 5391062	Fine-grained, white to grey leucogranitic host to the LBNL auriferous Prospect in Paul's Pond region	Davidsville Group Unnamed granitic intrusion (Blackwood, 1981; Tallman, 1989a)
JOD45B	636504/ 5391062	Fine-grained, white to grey leucogranitic host to the LBNL auriferous Prospect in Paul's Pond region	Davidsville Group Unnamed granitic intrusion (Tallman, 1989a)
JOD46A	635216/ 5391238	Angular sedimentary float collected from trench float at the Roadside Gabbro Showing in the Paul's Pond region.	Davidsville Group Greywacke (Tallman, 1989a)

Table A3.1 *cont...*

JOD46B	635216/ 5391238	Angular, unmineralized, fine-grained gabbroic float from a dirt mound at the Roadside Gabbro Showing in the Paul's Pond region.	Davidsville Group Unnamed gabbroic intrusion (Tallman, 1989a)
JOD57B	662766/ 5450790	Green siltstone adjacent to gabbroic intrusion.	Ten Mile Lake Formation (Currie, 1995a)
JOD81A	630400/ 5387150	Fine-grained gabbro with disseminated sulphides, host to the Greenwood Pond #2 auriferous prospect.	Davidsville Group Small gabbroic intrusion (Tallman, 1989a)
JOD82A	631150/ 5388800	Fine-grained greywacke host with disseminated sulphides, host to the A-Zone Extension auriferous prospect.	Davidsville Group (Blackwood, 1981; Tallman, 1989a)
JOD83A	657181/ 5425631	Medium grained greywacke host to the auriferous Knob Prospect in Appleton.	Davidsville Group (Blackwood, 1982; Collins, 1991)
JOD86B	656026/ 5426826	Fine grained greywacke host with <3% sulphide disseminations and small quartz veins Collected near the Bowater Prospect.	Davidsville Group (Blackwood, 1982; Woldeabzghi, 1988)
JOD90A	641210/ 5408962	Red, unaltered granite from Red Rock River.	MPIS (Dickson, 1992)
JOD90B	641195/ 5408973	Red, unaltered granite from Red Rock River:	MPIS (Dickson, 1992)
JOD96D	669906/ 5462509	Medium grained, red volcanic from south of the Duder Lake Prospects.	Duder Complex (Currie and Williams, 1995)
JOD96G	669996/ 5462812	Metasedimentary rock with no apparent Fe carbonate alteration or mineralization collected near a faulted contact immediately south of the Duder Lake Prospects.	Duder Complex (Currie, 1995b);
JOD96J	670004/ 5462834	Metasedimentary rock collected from the faulted contact (shear zone) immediately south of the Duder Lake Prospects.	Duder Group (Currie, 1995b)

Table A3.1 *cont...*

JOD97	670326/ 5463622	Medium grained gabbro collected from the auriferous Corvette Prospect.	Gabbro dyke or sill (Churchill and Evans, 1992); Tectonic block, Duder Complex (Currie and Williams, 1995)
JOD98	670488/ 5464542	Mineralized medium-grained gabbro from Goldstash. Prospect	Gabbro dyke or sill (Churchill and Evans, 1992); Tectonic block, Duder Complex (Currie and Williams, 1995)
JOD98A	670476/ 5464573	Medium grained gabbro from the Goldstash Prospect.	Gabbro dyke or sill (Churchill and Evans, 1992); Tectonic block, Duder Complex (Currie and Williams, 1995)
JOD100	652973/ 5438288	Fine-grained, dark grey to black gabbro with <5 % disseminated pyrite.	Gabbro dyke or sill (Evans <i>et al.</i> , 1992), intrusive to Ten Mile Lake Formation (Currie, 1995a)
JOD101	652926/ 5438456	Fine-grained, dark grey, silicified gabbro.	Gabbro dyke or sill (Evans <i>et al.</i> , 1992), intrusive to Ten Mile Lake Formation (Currie, 1995a)
JOD102	654346/ 5439266	Fine-grained, dark grey, silicified gabbro.	Gabbro dyke or sill (Evans <i>et al.</i> , 1992), intrusive to Ten Mile Lake Formation (Currie, 1995a)
JOD118	617183/ 5428664	Fine-grained, medium to dark grey, mica rich boulder with small sulfide veinlets and 5 mm round blebs of pyrite collected from Jumpers Brook. Pyrite and arsenopyrite-bearing sandstone hornfels.	Botwood Group (Pickett, 1990; Dickson, 1994)
JOD120A	656077/ 5426977	Fine-grained, dark grey, very dense, Mn rich shale interbed with disseminated sulphide from Appleton pit.	Davidsville Group
JOD120B	656077/ 5426977	Fine-grained, dark grey, very dense Mn rich shale or siltstone with disseminated sulphide from Appleton pit.	Davidsville Group
JOD04-09	662775/ 5450772	Fine-grained, black gabbro intrusive to interbedded green and red siltstone.	Gabbro dyke or sill (Evans <i>et al.</i> , 1992), intruding Ten Mile Lake Formation (Currie, 1995a)



Table A3.1 *cont...*

JOD04-13	667551/ 5456465	Fine-grained, black gabbro intrusive to green siltstone with fossiliferous interbeds.	Indian Islands Group (currently mapped as Ten Mile Lake Formation, Currie, 1995a) Gabbro dyke or sill
JOD04-20	649599/ 5425395	Medium-grained, buff diorite from pit just west of Glenwood.	Gabbro dyke or sill (Dickson, 1992)
W03-35	603859/ 5367584	Fine-grained, light grey to green, extrusive volcanic with disseminated pyrite and arsenopyrite.	Rhyolite

**Table A3.2:** Description and location of samples processed for sulphur isotope chemistry.

Sample	Prospect or Outcrop/ UTM	Sample Description	Mineral (# analyses)
JOD08	Bellman's Pond: 670009/5447133	Pyrite rich, altered, felsic tuff clast (10cm wide) in Bellman's Pond conglomerate. Pyrite grains were separated out by the <i>Frantz magnetic separator</i> at 1.7 A/ 10° during processing for U-Pb geochronology.	Pyrite
JOD23	Hurricane: 645161/5425138	Fine-grained diorite host with semi-massive sulphide veins up to 1 cm in width and small patches of pyrite. Pyrite separates were picked from the veins and patches.	Pyrite
JOD25	Corsair: 644408/5425289	Fine-grained diorite host with fine pyrite disseminations. Two separate vials of pyrite separates were picked from crushed material.	Pyrite (2)
JOD26A	Slip: 643541/5438244	Rusty, granite host with abundant sulphide mineralization. Arsenopyrite and pyrite occur as disseminations and could not be separated because of fine grain size so were analyzed together.	Pyrite + Arsenopyrite
JOD26B	Slip: 643541/5438244	Rusty, granite host with abundant sulphide mineralization. Disseminated pyrite and rare cubic grains and patches were picked from crushed material.	Pyrite
JOD26B	Slip: 643541/5438244	Rusty, granite host with abundant sulphide mineralization. Galena occurred as abundant large black cubic grains that were easily separated from grab sample.	Galena

Table A3.2: cont ...

JOD26B	Slip: 643541/5438244	Rusty, granite host with abundant sulphide mineralization. Arsenopyrite occurred as needles and disseminations and exhibited twinning on some faces.	Arsenopyrite
JOD30	Gull River 616723/5380287	Sub-rounded float with semi-massive sulphides in a hematite altered ultramafic rock downriver from Breccia Pond. Pyrite is cubic and easily picked from sample.	Pyrite
JOD36	Breccia Pond 616723/5380287	Semi massive pyrite in hematized ultramafic. Two vials of pyrite separates were picked from the sample.	Pyrite (2)
JOD39	Careless Brook 647570/5418043	Very fine-grained, dark, dense unit at contact between Caradocian shale and Indian Islands Group. Pyrite grains were separated out by the <i>Frantz magnetic separator</i> at 1.7 A/ 10° during processing for U-Pb geochronology.	Pyrite
JOD41A	Hunan 629855/5395490	Quartz breccia of grey silicified greywacke containing massive stibnite. Stibnite separates were picked from hand sample.	Stibnite
JOD45A	LBNL: 636504/5391062	Mineralized granite with abundant needle-like arsenopyrite grains up to 1 cm x 2 mm in size. Grains were picked from hand sample.	Arsenopyrite
JOD45B	LBNL: 636504/5391062	Mineralized granite with abundant needle-like arsenopyrite grains up to 1 cm x 2 mm in size. Grains were picked from hand sample.	Arsenopyrite
JOD51B	Lizard Pond: 613387/5378508	Hydrothermally altered and sheared ultramafic unit with some original chromite up to 5 mm. Variable amounts of magnesite and serpentinite alteration. Pyrite is disseminated and picked from crushed material.	Pyrite



JOD80A	Hornet: 629810/5388130	Felsite (Evans, 1996) host rock with pyrite occurring along quartz vein margins. Two vials of pyrite separates were picked from hand sample.	Pyrite (2)
JOD81A	Greenwood Pond #2: 630400/5387150	Fine-grained gabbro with minor rusting from disseminated sulfide. Pyrite grains were separated out by the <i>Frantz magnetic separator</i> at 1.7 A/ 10° during processing for U-Pb geochronology.	Pyrite
JOD82A	A-Zone: 631180/5388800	Mineralized greywacke host with semi massive pyrite vein (~2 cm wide). Some grains are cubic with surface striations. Pyrite picked from hand sample.	Pyrite (2)
JOD83B	Knob: 657156/5425610	Vuggy quartz in greywacke with VG. Disseminated arsenopyrite in greywacke picked from crushed material.	Arsenopyrite
JOD83B	Knob: 657156/5425610	Vuggy quartz in greywacke with VG. Disseminated pyrite in quartz picked from vein hand sample.	Pyrite
JOD84B	Knob: 657156/5425610	Shale next to large vuggy quartz vein with large ocubic pyrite mineralization. Pyrite picked from hand sample.	Pyrite
JOD97B	Corvette: 670488/5464542	Altered, coarse-grained gabbro with disseminated pyrite throughout. Pyrite grains were picked from crushed material.	Pyrite
JOD98	Goldstash: 670488/5464515	Altered, coarse-grained gabbro with disseminated pyrite. Pyrite grains were separated out by the <i>Frantz magnetic separator</i> at 1.7 A/ 5° during processing for U-Pb geochronology.	Pyrite

Table A3.2: *cont...*

JOD99	Flirt: 670596/5465115	Metamorphosed, seritized gabbro with cubic pyrite grains (1mm wide). Pyrite and arsenopyrite occur but mostly pyrite. Pyrite grains were separated out by the <i>Frantz magnetic separator</i> at 1.7 A/ 1° during processing for U-Pb geochronology.	Pyrite
JOD108	Diorite intrusion west of Glenwood: 649599/5425295	Fine-grained diorite intrusion in Indian Islands group sediments. Sulphide mineralization not visible in hand sample. Pyrite grains were separated out by the <i>Frantz magnetic separator</i> at 1.7 A/ 5° during processing for U-Pb geochronology.	Pyrite
JOD110	Dome: 658632/5428534	Quartz breccia with pyrite grains (up to 1 mm) in pieces of brecciated Davidsville siltstone. Grains are mostly cubic and striated at surface. Some arsenopyrite but finer grained and less abundant. Two vials of pyrite separates picked from hand sample.	Pyrite (2)
JOD110A	Dome: 658632/5428534	Quartz breccia with pyrite grains (up to 1 mm) in pieces of brecciated Davidsville siltstone. Pyrite picked from hand sample.	Pyrite
JOD110A	Dome: 658632/5428534	Quartz breccia with pyrite grains (up to 1 mm) in pieces of brecciated Davidsville siltstone. Fine grained pyrite and arsenopyrite picked from crushed material.	Pyrite + Arsenopyrite
JOD117	Jonathon's Pond: 676938/5441002	Serpentinized ultramafic with quartz veining. Disseminated and needle like sulfide at vein margins and small veinlets. Pyrite picked from hand sample.	Pyrite (2)
JOD118	Jumper's Brook: 617183/5428664	Small sulfide veinlets and patches (5 mm wide) in medium-grained, mica rich, light grey to green sub angular boulders. Pyrite picked from hand sample.	Pyrite (2)

Table A3.2: *cont...*

JOD119A	Outflow: 653807/5433344	Pyrite occurs in quartz-brecciated siltstone and veins. Mineralization is very finely disseminated in sedimentary unit. Some very small arsenopyrite needles occur in siltstone. Pyrite separates were picked from quartz veins.	Pyrite
JOD04-13	Gabbro intrusion in Ten Mile Lake Formation: 667551/5456465	Fine-grained, dark grey to black gabbro. Mineralization not obvious in hand sample. Pyrite grains were separated out by the <i>Frantz magnetic separator</i> at 1.7 A/ 3° during processing for U-Pb geochronology.	Pyrite
JOD04-20	Diorite intrusion west of Glenwood: 649599/5425295	Fine-grained diorite intrusion in Indian Islands group sediments. Sulphide mineralization not visible in hand sample. Pyrite grains were separated out by the <i>Frantz magnetic separator</i> at 1.7 A/ 5° during processing for U-Pb geochronology.	Pyrite
W03-35	Huxter's Lane: 603859/5367584	Semi-massive arsenopyrite in quartz brecciated dacite. Arsenopyrite separates picked from hand sample.	Arsenopyrite



**Table A3.3:** Sample location and description for U-Pb Geochronology.

Sample #	Location	Description	# Zircon Grains	Age
JOD08	670009 5447133/ Bellman's Pond/ Davidsville Group?	Pyrite rich, chlorite altered felsic tuff clast, 10 cm wide.	5	1600-1800 Ma
JOD21	645161 5425138/ Salmon River/ Hurricane Prospect/ MPIS	Fine grained, unaltered, unmineralized, diorite host rock.	40	$405 \pm 11$ Ma
JOD25	644408 5425289/ Salmon River/ Corsair Prospect/ MPIS	Fine grained, slightly mineralized, diorite host rock.	50	$430.6 \pm 3.4$ Ma
JOD39	647570 5418043/ Careless Brook/ Davidsville Group?	Dense, dark grey to black very fine-grained shale.	20	$472 \pm 8.5$ Ma and <i>ca.</i> 520 and 900 Ma
JOD90A	Red Rock Brook/ MPIS	Fine to medium grained pink granite.	25	389-423 Ma
JOD04-17	641210 5408962/ MPIS	Fine to medium grained pink granite.	35	$409 \pm 4.5$ Ma and <i>ca.</i> 1800 Ma
JOD100	652973 5438288/ Twin Ponds	Fine grained, dark grey gabbro with fine disseminated pyrite.	40	$429.3 \pm 4.4$ Ma
W03-27	681434 5475798/ Charles Cove Pluton/ Tim's Cove Prospect	Granodiorite	40	$429 \pm 19$ Ma with an upper intercept at 1850 Ma
W03-38	603859 5367584/ Coy Pond Complex/ Huxter Lane Prospect	Mineralized dacite	40	$494 \pm 7$ Ma

**APPENDIX 4**  
**COMPILED DATA TABLES**

**Table A4.1:** Paleontological sample location, description and fossil assemblages for samples collected from the Botwood Basin and environs.

Sample Number	NLDNR Number	UTM (NAD27)	Description	Fossil Assemblage	Age Range
JOD-37A	2004F002	647491E 5418269N	Careless Brook fossiliferous limestone from a debris flow. Rusty weathering, micaceous fine-grained, dark grey calcareous sandstone.	<i>Cnidaria-Tabulata-?Favosites</i> (sp. undet.) <i>Echinodermata-Crinoid</i> (gen. et sp. undet.)	Silurian
JOD-86D	2004F003	656026E 5426826N	Appleton Pit graptolites in graptolitic black slate.	<i>Hemichordata-Graptolithina-Climacograptus bicornis</i> (Hall) <i>Climacograptus</i> (sp (p).)	Ordovician (Caradoc)
JOD96E	2004F004	670020E 5462754N	Fossil bearing limestone from fossiliferous beds from south of Duder Lake Au Prospects.	<i>Cnidariaa-Tabulata-?Favosites</i> (sp. undet.) Bryozoa-Ptilodictya scalpillum (Lonsdale) [branching stick forms]	Wenlock
JOD96I	2004F005	670004E 5462834N	Fossiliferous beds from Duder Lake. Small, badly deformed (in big cobble)	<i>Brachiopoda-Articulata</i> (gen. et sp. undet.)	Middle Cambrian- Upper Permian
JOD113	2004F006	654920E 5430998N	North Salmon Pond Access Road fossiliferous limestone from wood ship pit.	Bryozoa-Ptilodictya scalpillum (Lonsdale) [branching stick forms (abundant)] <i>Echinodermata-Crinoid</i> (gen. et sp. undet.) [abundant] <i>Mollusca-Cephalopoda?</i> (gen. et sp. undet.) [straight form]	Silurian (Wenlock)



JOD114	2004F007	654515E 430031N	North Salmon Pond Road fossiliferous limestone.	<i>Anthozoa-Tabulata-?Favosites</i> (sp. undet.) <i>Bryozoa-Ptilodictya scalpellum</i> (Lonsdale) [branching stick forms] <i>Echinodermata-Crinoid</i> (gen. et sp. undet.)	Silurian
JOD04-12	2004F045	664908E 5449784N	Re-crystallized fossiliferous outcrop from Ten Mile Lake Resource Road	<i>Echinodermata-Crinoidea</i> (gen. et sp(p). undet.) [columnals (recrystallized)]	Middle Cambrian- Upper Permian
JOD04-14	2004F046	666223E 5452666N	Medium to coarse-grained pebbly sandstone (or conglomerate). 1x1m purple fossiliferous outcrop or boulder.	<i>Brachiopoda-Articulata</i> (Gen. et sp. undet.) [heavily ribbed form] <i>?Bryozoa</i> (Gen. et sp. undet.) <i>Cnidaria-Anthozoa-Zoantharia-Tabulata- Favosites</i> (sp. undet.) <i>Echinodermata-Crinoidea</i> (gen. et sp(p). undet.) [columnals]  Note: Fossils are poorly preserved	Middle Cambrian- Upper Permian
JOD04-15	2004F047	665602E 5451534N	Large piece of very hard, fossil rich, red, sandy siltstone or mudstone.	<i>Bryozoa-Ptilodictya scalpellum</i> (Lonsdale)	Wenlock

**Table A4.2:** Pressed pellet X-Ray Fluorescence (XRF) data for intrusive and sedimentary rocks from the Botwood Basin.

	Sample	JOD15	JOD20	JOD21	JOD22	JOD25	JOD39	JOD44A	JOD44B	JOD45A	JOD45B
SiO <sub>2</sub>	wt%	71.12	46.14	58.52	60.89	57.77	67.97	70.52	63.33	64.69	69.62
Al <sub>2</sub> O <sub>3</sub>	wt%	13.24	16.37	13.26	23.15	13.4	11.23	17.78	21.58	13.75	18.96
Fe <sub>2</sub> O <sub>3</sub>	wt%	4.13	8.37	9.9	4.18	9.98	3.13	5.08	4.65	5.58	2.74
TiO <sub>2</sub>	wt%	0.41	0.44	1.08	1.09	1.18	0.25	0.41	0.48	0.42	0.44
MnO	wt%	0.17	0.16	0.15	0.01	0.15	0.06	0.1	0.12	0.13	0.02
MgO	wt%	0.3	6.82	2.96	0.63	2.21	1.82	0.44	0.64	0.35	0.49
CaO	wt%	3	3	3.81	0.3	3.79	1.82	0.29	1.1	1.57	0.26
Na <sub>2</sub> O	wt%	1.23	3.74	2.79	0.09	3.01	5.08	<LD	0.57	2.64	2.85
K <sub>2</sub> O	wt%	1.99	1.99	2.26	4	2.38	0.49	4.25	5.1	3.55	3.17
P <sub>2</sub> O <sub>5</sub>	wt%	0.06	0.08	0.24	0.22	0.24	0.08	0.17	0.15	0.21	0.14
Total	wt%	95.9	90.81	95.19	100.32	94.33	91.93	99.76	100.94	93.18	102.17

All elements were recalculated to 100% anhydrous

**Table A4.2:** Pressed pellet X-Ray Fluorescence (XRF) data for intrusive and sedimentary rocks from the Botwood Basin.

	Sample	JOD15	JOD20	JOD21	JOD22	JOD25	JOD39	JOD44A	JOD44B	JOD45A	JOD45B
S	ppm	51	375	134	22389	165	399	1134	5551	145	5916
Rb	ppm	50.4	37.5	105.5	148	124.6	12.5	134.5	152.3	92	82.9
Sr	ppm	68.2	402.2	193.9	11.2	139.2	157.9	30.8	66	148.8	69.3
Y	ppm	5.9	7.1	46.3	59.8	44.7	13.3	76.7	111.2	68.4	84.1
Zr	ppm	113.5	95.2	281.9	319.5	283.1	70.1	563.8	690.6	564	608.2
Nb	ppm	4	5.5	13.7	15.2	14	6.5	28.5	37.8	28	30.1
Ba	ppm	302	221	434	77	402	169	495	890	786	609
Cr	ppm	686	424	16	11	31	36	<LD	<LD	11	<LD
Ni	ppm	27	38	17	13	14	12	6	8	6	<LD
Cu	ppm	10	58	13	8	6	0	14	10	32	8
Zn	ppm	<LD	21	39	24	24	4	24	41	31	<LD
Ga	ppm	8	18	22	28	22	10	22	33	21	34
As	ppm	64	18	<LD	233	<LD	0	<LD	10159	21<LD	11871
Ce	ppm	<LD	<LD	80	165	106	0	159		176	2005
Cl	ppm	51	62	175	49	211	0	52	87	3.55	<LD
Sc	ppm	<LD	30	31	29	24	10	31	39	28	34
V	ppm	77	222	78	73	80	19	<LD	<LD	<LD	<LD
Pb	ppm	<LD	14	14	11	11	20	16	13	36	12
Th	ppm	<LD	7	11	6	10	5	17	20	15	15
U	ppm	<LD	<LD	<LD	<LD	<LD	0	7	8	<LD	6

All elements were recalculated to 100% anhydrous

**Table A4.2:** Pressed pellet X-Ray Fluorescence (XRF) data for intrusive and sedimentary rocks from the Botwood Basin.

	Sample	JOD46A	JOD46B	JOD57A	JOD80A	JOD81A	JOD82A	JOD83A	JOD86B	JOD90A	JOD90B
SiO <sub>2</sub>	wt%	10.75	47.97	71.23	72.19	47.99	48.76	58.94	57.08	69.76	70.7
Al <sub>2</sub> O <sub>3</sub>	wt%	1.63	11.91	9.15	14.81	12.53	9.98	14.6	23.81	13.64	13.29
Fe <sub>2</sub> O <sub>3</sub>	wt%	1.19	17.03	3.46	2.97	14.67	23.3	7.31	2.49	3	2.82
TiO <sub>2</sub>	wt%	0.15	1.75	0.41	0.38	2.23	0.33	0.96	0.51	0.35	0.34
MnO	wt%	0.14	0.29	0.06	0.12	0.26	0.18	0.14	0.06	0.04	0.05
MgO	wt%	0.98	4.81	2.92	0.19	4.81	0.26	6.57	2	0.61	0.62
CaO	wt%	60.39	4.98	5.6	0.75	6.87	0.26	0.52	0.66	0.3	0.36
Na <sub>2</sub> O	wt%	0.34	2.26	2.14	4.3	3.27	0.68	3.04	0.74	3.25	3.56
K <sub>2</sub> O	wt%	0.28	0.57	1.91	1.86	1.03	1.52	1.28	5.19	4.22	4.3
P <sub>2</sub> O <sub>5</sub>	wt%	0.04	0.44	0.1	0.23	0.37	0.15	0.14	0.06	0.05	0.05
Total	wt%	76.08	92.39	97.21	99.22	94.03	98.9	93.79	93.11	95.22	96.09

All elements were recalculated to 100% anhydrous



**Table A4.2:** Pressed pellet X-Ray Fluorescence (XRF) data for intrusive and sedimentary rocks from the Botwood Basin.

	Sample	JOD46A	JOD46B	JOD57A	JOD80A	JOD81A	JOD82A	JOD83A	JOD86B	JOD90A	JOD90B
S	ppm	352	661	78	4624	319	48596	261	869	59	39
Rb	ppm	8.1	19.4	52	50	35.1	44.6	42.1	165.4	202.2	200.4
Sr	ppm	392	162	197.7	106	232.5	36.6	170.1	53.4	39.9	42.3
Y	ppm	2.9	47.7	14.2	70.7	49.9	47.8	18.3	25.2	56	57.8
Zr	ppm	64.2	294.5	236.5	571.7	296.5	460.8	159.4	166.2	323.2	326.4
Nb	ppm	2	10	9.5	29.9	10.4	22.5	11	15.7	14.9	14.7
Ba	ppm	92	152	629	427	220	445	446	1923	491	512
Cr	ppm	41	<LD	157	<LD	25	<LD	316	53	14	0
Ni	ppm	<LD	22	24	5	21	<LD	82	22	4	5
Cu	ppm	5	32	<LD	5	31	23	22	<LD	0	0
Zn	ppm	<LD	78	<LD	16	76	<LD	21	<LD	14	25
Ga	ppm	<LD	26	8	19	24	33	14	23	20	20
As	ppm	<LD	39	<LD	464	22	9807	21	32	0	0
Ce	ppm	<LD	<LD	65	262	62	981	100	73	155	126
Cl	ppm	337	<LD	85	<LD	0	<LD	54	56	141	179
Sc	ppm	35		11	27	53	20	28	<LD	10	0
V	ppm	22	505	60	11	430	13	161	41	8	11
Pb	ppm	5	6	9	15	7	700	16	7	12	14
Th	ppm	<LD	<LD	6	14	0	12	8	12	20	22
U	ppm	<LD	<LD	<LD	6	0	<LD	<LD	9	8	9

All elements were recalculated to 100% anhydrous

**Table A4.2:** Pressed pellet X-Ray Fluorescence (XRF) data for intrusive and sedimentary rocks from the Botwood Basin.

Sample		JOD96D	JOD96G	JOD96J	JOD97B	JOD98	JOD98A	JOD100	JOD101	JOD102
SiO <sub>2</sub>	wt%	53.53	37.23	28.17	33	40.93	33.2	45.27	45.82	46.94
Al <sub>2</sub> O <sub>3</sub>	wt%	11.2	11.34	6.94	5	10.36	13.81	11.41	10.16	11.89
Fe <sub>2</sub> O <sub>3</sub>	wt%	4.67	13.67	11.79	23.57	17.4	18.35	11.79	17.06	15.35
TiO <sub>2</sub>	wt%	0.6	1.42	0.87	2.02	3.39	1.16	0.87	3.63	3.23
MnO	wt%	0.13	0.18	0.41	0.35	0.23	0.33	0.41	0.31	0.25
MgO	wt%	3.18	15.8	13.11	5.66	4.26	8.39	4.94	6.92	4.67
CaO	wt%	10.54	4.24	20.42	6.93	6.52	5.35	7.13	7.42	6.59
Na <sub>2</sub> O	wt%	1.82	1.34	1.26	1.17	2.04	2.38	2.39	2.17	2.38
K <sub>2</sub> O	wt%	2.12	0.37	0.07	0.16	0.68	0.55	1.11	0.75	1.55
P <sub>2</sub> O <sub>5</sub>	wt%	0.17	0.26	0.24	0.14	0.38	0.11	0.88	0.42	0.51
Total	wt%	87.96	86.18	83.28	83.24	86.19	85.6	86.2	95.2	93.36

All elements were recalculated to 100% anhydrous

**Table A4.2:** Pressed pellet X-Ray Fluorescence (XRF) data for intrusive and sedimentary rocks from the Botwood Basin.

Sample		JOD96D	JOD96G	JOD96J	JOD97B	JOD98	JOD98A	JOD100	JOD101	JOD102
S	ppm	4262	123	1427	4441	2464	6916	1045	1281	812
Rb	ppm	43.9	12	3.3	3.2	28.5	23	49.4	28.9	59.2
Sr	ppm	142.7	105.6	223.5	144.7	191.2	262	201.5	213.2	225.7
Y	ppm	20.3	13.8	10.7	33.8	42.4	23.1	56.3	45.2	54.6
Zr	ppm	224.4	184.3	113.8	123.4	264.3	97.3	240.8	240.6	325.3
Nb	ppm	6.2	23	15.4	4.4	7.8	2.7	12.7	9.8	11.2
Ba	ppm	199	154	155	61	134	257	192	275	205
Cr	ppm	234	580	669	30	27	332	50	82	31
Ni	ppm	25	235	191	26	19	103	26	36	23
Cu	ppm	4	20	31	86	27	72	33	43	17
Zn	ppm	15	103	42	62	68	34	86	97	50
Ga	ppm	9	21	14	18	21	19	25	22	27
As	ppm	141	121	47	23	0	59	0	0	0
Ce	ppm	97	207	154	<LD	0	<LD	0	0	62
Cl	ppm	0	65	80	<LD	104	46	556	980	495
Sc	ppm	20	24	37	46	37	55	45	44	48
V	ppm	112	276	244	289	664	259	303	632	451
Pb	ppm	13	<LD	32	<LD	10	<LD	12	8	6
Th	ppm	4	16	10	<LD	0	<LD	6	0	4
U	ppm	0	<LD	0	<LD	0	<LD	5	0	0

All elements were recalculated to 100% anhydrous

**Table A4.2:** Pressed pellet X-Ray Fluorescence (XRF) data for intrusive and sedimentary rocks from the Botwood Basin.

Sample		JOD120A	JOD120B	JOD04-09	JOD04-13	JOD04-20
SiO <sub>2</sub>	wt%	12.61	18.41	45.49	44.97	44.61
Al <sub>2</sub> O <sub>3</sub>	wt%	3.68	3.84	11.93	11.25	10.93
Fe <sub>2</sub> O <sub>3</sub>	wt%	8.21	9.04	16.64	17.4	15.07
TiO <sub>2</sub>	wt%	0.18	0.14	3.31	2.56	2.51
MnO	wt%	12.03	9.74	0.27	0.31	0.23
MgO	wt%	10.24	10.48	4.99	4.24	8.86
CaO	wt%	29.45	28.07	6.19	5.87	5.04
Na <sub>2</sub> O	wt%	0.2	0.2	2.55	2.35	1.82
K <sub>2</sub> O	wt%	0.96	0.98	0.62	1.35	0.67
P <sub>2</sub> O <sub>5</sub>	wt%	0.98	0.73	0.5	1.13	0.61
Total	wt%	78.54	81.63	92.97	91.91	90.92

All elements were recalculated to 100% anhydrous



**Table A4.2:** Pressed pellet X-Ray Fluorescence (XRF) data for intrusive and sedimentary rocks from the Botwood Basin.

Sample		JOD120A	JOD120B	JOD04-09	JOD04-13	JOD04-20
S	ppm	20391	24978	730	1114	921
Rb	ppm	27.8	27.2	23.8	51.2	27.4
Sr	ppm	851.4	1019.5	250.5	276.1	283.5
Y	ppm	28.7	39.2	55.8	65.3	51.2
Zr	ppm	31	38.3	301.5	281.9	696.4
Nb	ppm	4.5	3.3	9.6	14.6	10.7
Ba	ppm	801	614	522	298	850
Cr	ppm	28	56	27	16	23
Ni	ppm	438	206	23	20	37
Cu	ppm	74	62	25	29	32
Zn	ppm	41	21	78	88	58
Ga	ppm	7	4	20	24	23
As	ppm	216	66	20	0	0
Ce	ppm	120	159	77	97	95
Cl	ppm	0	105	140	139	113
Sc	ppm	13	0	39	50	49
V	ppm	55	70	475	291	293
Pb	ppm	31	24	7	13	6
Th	ppm	0	0	0	6	4
U	ppm	7	0	0	0	0

All elements were recalculated to 100% anhydrous

**Table A4.3:** Sulphur isotope values for Botwood Basin sulphide separates.

Sample Number	Location	Prospect/ Name	Host Rock	Mineral	VCDT
JOD08	670009/5447133	Bellman's Pond	Tuff?	pyrite	9.98
JOD23	645150/5425150	Hurricane	Diorite	pyrite	3.8
JOD25	644408/5425289	Corsair	Diorite	pyrite	1.21
JOD25	644408/5425289	Corsair	Diorite	pyrite	2.18
JOD26A	643541/5438244	Slip	Granite	pyrite + arsenopyrite	1.69
JOD26B	643541/5438244	Slip	Granite	arsenopyrite	2.93
JOD26B	643541/5438244	Slip	Granite	pyrite	1.02
JOD26B	643541/5438244	Slip	Granite	galena	1.6
JOD30	620899/5379987	Gull River Float	peridotite	pyrite	7.47
JOD36	616723/5380287	Breccia Pond	serpentinite	pyrite	6.96
JOD36	616723/5380287	Breccia Pond	serpentinite	pyrite	7.11
JOD39	647570/5418043	Careless Brook	shale	pyrite	18.67
JOD41A	629855/5395490	Hunan	greywacke	stibnite	-6.43
JOD45A	636504/5391062	LBNL	granite?	arsenopyrite	2.9
JOD45B	635748/5390002	LBNL	granite	arsenopyrite	3.13
JOD51B	613387/5378508	Lizard Pond	magnesite	pyrite	6.46
JOD80A	629810/5388130	Hornet	flesite?	pyrite	3.17
JOD80A	629810/5388130	Hornet	flesite?	pyrite	3.57
JOD81A	630400/5387150	Greenwood Pond #2	gabbro	pyrite	0.98
JOD82A	631150/5388800	A-Zone	greywacke	pyrite	0.58
JOD82A	631150/5388800	A-Zone	greywacke	pyrite II	1.28
JOD83B	657156/5425610	Knob	greywacke	pyrite	-0.56
JOD83B	657156/5425610	Knob	greywacke	arsenopyrite	-0.95
JOD84B	6573341/5425531	Knob	shale	pyrite	-0.07

**Table A4.3:** Sulphur isotope values for Botwood Basin sulphide separates (*cont...*).

Sample Number	Location	Prospect	Host Rock	Mineral	VCDT
JOD97B	670346/5463748	Corvette	gabbro	pyrite	-0.02
JOD98	670488/5464542	Goldstash	gabbro	pyrite	0.48
JOD99	670596/5465115	Flirt	gabbro	pyrite	-0.1
JOD108	649599/5425395	Diorite Intrusion	diorite	pyrite	0.89
JOD04-20	649599/5425395	Diorite Intrusion	diorite	pyrite	0.23
JOD110	658632/5428534	Dome	siltstone	pyrite	0.57
JOD110	658632/5428534	Dome	siltstone	pyrite	0.41
JOD110A	658632/5428534	Dome	siltstone	pyrite	0.81
JOD110A	658632/5428534	Dome	siltstone	pyrite + arsenopyrite	-0.35
JOD117	676938/5441002	Jonathon's Pond	serpentinite	pyrite	-8.2
JOD117	676938/5441002	Jonathon's Pond	serpentinite	pyrite	-6.27
JOD118	617183/5428664	Jumper's Brook	metapelite	pyrite	2.81
JOD118	617183/5428664	Jumper's Brook	metapelite	pyrite	3.93
JOD119A	653807/5433344	Outflow	siltstone	pyrite	-4.1
W03-35	603859/5367584	Huxter's Lane	rhyolite	arsenopyrite	8.83
JOD04-09	662775/5450772	Gabbro intrusion	gabbro	pyrite	1.26
JOD04-13	667551/5456465	Gabbro intrusion	gabbro	pyrite	0.26

**Table A4.4a:** Trace element content of pyrite grains from the Hornet Prospect.

Sample JOD80A							
Au ppm	As ppm	Se ppm	Sb ppm	Te ppm	W ppm	Hg ppm	Pb ppm
0.162	672.999	0.000	0.956	0.000	0.000	0.514	556.515
2.834	6865.006	0.000	0.101	0.000	0.000	0.423	0.053
0.000	370.549	0.000	0.000	0.000	0.000	0.629	0.626
0.824	7142.952	28.924	0.171	0.000	0.261	0.305	0.063
8.040	10180.659	0.000	0.016	0.000	0.530	0.517	0.591
0.249	5968.817	0.000	12.752	3.884	0.046	0.346	9.681
1.360	7837.038	20.121	2.953	0.000	0.000	0.249	2.536
1.946	9077.856	13.213	9.257	0.048	1.765	0.354	11.936
0.471	7099.622	0.655	2.858	4.354	0.735	0.615	3.365
0.119	4824.075	20.678	0.441	0.000	0.000	0.379	0.291
1.046	1156.146	20.458	5.234	2.328	1.198	0.147	34.369
0.184	1538.110	0.000	1.320	0.000	0.342	0.331	2.030
0.326	2978.815	0.000	2.102	0.000	0.627	0.423	2.345
0.443	3997.460	0.000	0.667	2.565	0.000	0.448	0.945

**Table A4.4b:** Trace element content of pyrite grains from the Goldstash Prospect.

Sample JOD98A							
Au ppm	As ppm	Se ppm	Sb ppm	Te ppm	W ppm	Hg ppm	Pb ppm
0.000	0.287	10.238	0.584	1.607	0.000	5.343	6.773
0.046	6.562	1.871	16.298	0.000	0.000	5.227	196.905
0.000	2.281	0.000	25.193	0.000	0.000	10.486	386.763
0.000	0.351	0.283	0.041	0.000	0.000	5.044	1.074
0.034	1.758	0.000	1.572	0.000	0.309	10.583	14.797
0.033	0.000	10.327	0.059	0.000	0.147	9.798	2.109
0.000	0.000	1.064	0.171	0.909	0.070	1.153	1.920
0.000	0.202	10.759	0.000	0.000	0.239	0.670	0.527
0.000	0.254	0.000	2.156	1.276	0.000	1.205	1.336
0.013	0.000	0.000	0.413	1.055	0.000	0.894	3.135
0.073	20.706	14.829	5.799	0.928	0.000	1.258	5.357
0.019	0.851	0.317	2.167	1.956	0.256	5.470	2.180
0.114	0.000	13.440	0.325	0.000	0.093	0.873	1.766
0.034	10.436	14.039	5.682	1.532	0.520	2.721	15.793
0.000	0.000	4.757	0.067	0.000	0.196	7.204	1.266
0.000	12.747	1.556	7.145	0.000	0.000	1.751	129.251



**Table A4.4c:** Trace element content of pyrite grains from the Outflow Prospect (Piper Zone).

Sample JOD119

Au ppm	As ppm	Se ppm	Sb ppm	Te ppm	W ppm	Hg ppm	Pb ppm
0.036	17.049	0.000	111.003	0.000	0.337	0.154	0.215
0.069	58.129	7.913	51.038	0.000	18.517	0.176	1.161
0.066	270.757	5.768	19.915	0.777	0.039	0.582	0.263
0.000	229.929	13.504	137.265	1.412	0.597	1.093	0.417
0.051	21218.702	19.848	506.553	1.329	0.000	0.361	0.077
0.000	19522.099	26.732	507.965	0.000	0.000	0.367	0.424
0.000	60.397	22.846	26.405	2.420	0.000	0.464	0.533
0.090	91.454	32.132	53.159	0.000	0.214	0.761	0.360
0.157	1689.018	0.000	352.484	1.311	0.031	0.634	0.042
0.107	86.294	5.315	107.815	0.000	0.276	1.247	0.943
0.189	88.404	0.000	14.713	1.892	0.295	1.429	0.325
0.000	121.912	22.360	82.275	4.257	0.000	0.285	0.148
0.156	268.142	38.343	7.704	0.000	0.000	0.474	0.217
0.066	322.358	6.199	47.250	0.000	0.489	0.725	0.133
0.132	288.280	0.000	18.044	0.000	0.000	0.152	0.067
0.055	248.946	0.000	12.675	0.000	0.121	0.579	0.076

**Table A4.4d:** Trace element content of pyrite grains from the Jonathon's Pond Prospect.

Sample JOD117

ppm	ppm	ppm	ppm	ppm	ppm	ppm	ppm
0.160	18911.462	14.869	571.321	1.242	0.225	0.342	0.057
0.000	325.467	0.000	170.941	0.000	0.000	0.843	0.089
0.099	386.019	0.000	14.773	0.000	0.175	0.572	0.190
0.000	337.855	5.862	30.034	0.000	0.000	0.262	0.324
0.050	1588.137	8.336	145.589	0.000	0.000	1.545	0.109
0.000	299.150	16.520	18.739	0.552	0.147	0.378	0.189
0.000	433.023	21.998	41.753	0.401	0.000	0.531	0.484
0.027	141.265	0.000	46.442	0.000	0.011	0.663	0.219
0.000	144.341	1.466	11.994	2.785	0.000	0.341	0.238
0.000	515.490	25.177	21.552	3.402	0.317	0.872	0.245
0.034	226.203	16.508	38.345	0.000	0.000	0.492	0.103
0.171	347.492	0.000	23.637	0.603	0.023	0.534	0.173
0.153	428.135	0.000	138.614	2.058	3.190	0.709	0.764
0.090	81.518	0.000	192.827	0.505	0.619	0.826	1.084

**Table A4.4e:** Trace element content of pyrite grains from the Hurricane Prospect.

sample JOD23

Au ppm	As ppm	Se ppm	Sb ppm	Te ppm	W ppm	Hg ppm	Pb ppm
6.355	8434.274	9.670	9.601	2.585	0.162	0.578	4.512
6.380	9009.750	11.819	4.064	0.043	1.225	0.000	0.775
13.234	9141.273	6.113	0.705	1.665	0.000	0.165	0.705
7.131	9671.945	0.000	16.579	0.543	0.208	0.355	8.081
7.856	10161.063	0.000	10.249	0.000	0.119	0.261	3.854
16.864	10147.837	1.017	15.364	0.000	0.000	0.255	6.298
30.424	16763.947	0.000	24.014	0.000	0.143	0.374	11.168
11.929	9359.155	0.000	0.396	0.000	0.000	0.176	0.306
25.049	15309.997	0.000	5.667	0.088	0.187	0.394	1.723
13.208	16722.562	0.000	42.132	0.000	0.000	0.706	5.719
18.522	22990.093	1.412	127.145	0.000	0.406	1.264	20.484
72.977	531244.400	15.634	5477.800	0.000	64.326	1.368	2.579
64.419	484849.400	0.000	3976.791	1.095	6.879	1.026	28.452
50.121	25811.456	7.844	4.418	1.855	0.000	0.164	1.741
108.099	27188.653	17.262	64.090	2.104	1.047	0.576	28.017
20.751	16159.601	16.052	4.762	1.330	0.376	0.000	1.313

**Table A4.4f:** Trace element content of pyrite grains from the Bowater Prospect.

Sample W90-48

Au ppm	As ppm	Se ppm	Sb ppm	Te ppm	W ppm	Hg ppm	Pb ppm
0.04	1085	19	74	0	0.63	3.7	25
0.01	760	29	39	0	0.17	2.8	2.4
0.08	1257	56	116	0	0.12	2.6	21
0.1	1359	45	103	0	0.11	1.5	58
0.18	1189	48	226	0	0.15	2.4	25
0.03	956	37	92	0	0.18	3.3	32
0.87	1941	39	175	0	0.57	2.6	142
0.72	1680	38	294	0.65	0.14	2.7	126
0.73	1698	38	300	0.61	0.14	2.7	128
0.23	1278	85	156	0	0.12	1.8	83
0.22	1333	43	117	0	0.06	2.2	29
0.53	662	67	102	0	0	0.85	100
1.4	3817	57	182	0	0.51	1.7	164
0.13	1420	59	109	0	0.25	3	47
0.09	1405	91	85	0	0.07	1.3	40
1.3	2984	110	246	0	0.48	1.9	308

**Table A4.4g:** Trace element content of pyrite grains from the Outflow Prospect (Mustang Zone).

Sample W90-49A

Au ppm	As ppm	Se ppm	Sb ppm	Te ppm	W ppm	Hg ppm	Pb ppm
0.66	16779	0	173	0	0	0	108.5
0.66	16801	0	174	0	0	0	109.5
0.6	17564	0	981	0	0	2.6	247
15.2	12942	65	2699	0	0	0.85	6412
4.4	12473	78	774	5.5	0.44	0.69	255
0.57	7301	86	220	0	0.43	1.8	63
0.09	187	0	16	14	0	2.6	80
0.28	1730	45	24	0	0	13.3	85
0	281	68	42	0	3.4	7.5	66
0	194	43	5.5	11	0	12.6	65
1.8	13960	0	517	11	2.5	0.66	121
1.7	11547	26	502	0	0.41	1.7	156
0	540	70	1	6.3	1.4	0	13
0	7.8	0	2.6	7.5	0	0	4.9
0.18	15575	0	907	0	0	0.88	745
4.9	31028	38	1084	0	0	1.2	1086

**Table A4.4h:** Trace element content of pyrite grains from the Stog'er Tight Prospect.

Sample W89-82

Au ppm	As ppm	Se ppm	Sb ppm	Te ppm	W ppm	Hg ppm	Pb ppm
0.02	1479	5.8	0.05	4.3	0.14	0	2.1
0.1	2686	8.4	0.07	22	0	0	0.47
0	16	111	0	1.6	0	0.33	1.2
0.19	21	60	0.39	3	0.2	0.21	9.2
0.07	97	119	0.55	5.2	0.12	0.23	2.8
1.2	45	32	0.32	6.6	0	0.92	17
0.7	15	62	0.48	2.8	0	0.31	5.5
0.04	2384	23	0.04	3.2	0	0.34	0.88
0.04	33	94	0.1	2.7	0	1	4.6
0	24	47	0.08	1.8	0.09	0.59	0.59
0.02	20	55	0	0	0	1.1	0.46
0.06	26	150	0	2.3	0	0.7	2.3
0.02	18	39	0	3.3	0	1.3	0.33
0.11	32	53	1.19	3	48	0.44	10
0.02	5.6	16	0	0	0	1.9	0.12
0.42	0	13	0.54	0	0.96	0.85	1.4

**Table A4.4i:** Trace element content of pyrite grains from the Bruce Pond Prospect.

Sample KP-32-H1

Au ppm	As ppm	Se ppm	Sb ppm	Te ppm	W ppm	Hg ppm	Pb ppm
0	882	90	25	0	0	1.8	93
0	306	192	12	5.4	0	0.75	51
0.46	1663	147	13	0	0	0.45	41
0	171	135	8.9	2.9	0	1.2	53
0.17	402	173	11	3.6	0	1.3	7.9
0.09	289	250	6.7	1.9	0.51	1.3	37
0.2	313	104	12	0	0.33	1.1	45
0	3.2	161	4.5	0	0	0.4	20
0	557	32	1345	0	1	1.6	0.86
0.06	509	30	270	0	5.5	1.2	3.3
0.06	84	0	32	0	6.9	0.79	0.18
0.14	1945	16	506	3.2	0.89	2.2	0
0	535	0	1407	0	1.3	2.2	0.12
0	658	0	790	0	0.85	1.2	0.09
0.32	320	327	27	0	0	1.3	187
0.15	545	224	5	2.5	0.27	0.26	23



**Table A4.5a:** LAM-ICP-MS U-Pb data for magmatic zircons from the MPIS diorite (sample JOD21) collected on December 19, 2005.

JOD21	CONCORDIA COLUMNS					2 s %	2 s %	AGES Ma			
spot #	$^{207}\text{Pb}/^{235}\text{U}$	$^{207}\text{Pb}/^{235}\text{U}$ err	$^{206}\text{Pb}/^{238}\text{U}$	$^{206}\text{Pb}/^{238}\text{U}$ err	Rho	$^{207}\text{Pb}/^{235}\text{U}$	$^{206}\text{Pb}/^{238}\text{U}$	$^{207}\text{Pb}/^{235}\text{U}$ age	1 sigma	$^{206}\text{Pb}/^{238}\text{U}$ age	1sigma
	I N T E R C E P T V A L U E S										
de19a06	0.5288	0.0255	0.0654	0.0027	0.42	9.66	8.20	431.0	17.0	408.4	16.2
de19a07	0.5165	0.0436	0.0617	0.0027	0.26	16.88	8.91	422.8	29.2	385.8	16.7
de19a08	0.5200	0.0541	0.0674	0.0034	0.24	20.79	10.15	425.2	36.1	420.5	20.7
de19a09	0.5386	0.0825	0.0659	0.0017	0.09	30.62	5.31	437.5	54.4	411.4	10.6
de19a10	0.5228	0.1836	0.0710	0.0047	0.09	70.25	13.32	427.0	122.4	442.2	28.5
de19a11	0.4903	0.1582	0.0672	0.0047	0.11	64.54	13.94	405.1	107.8	419.2	28.3
de19a14	0.4906	0.0239	0.0633	0.0018	0.30	9.73	5.79	405.3	16.3	395.6	11.1
de19a15	0.4374	0.0341	0.0597	0.0021	0.22	15.59	6.91	368.4	24.1	373.9	12.5
de19a16	0.5051	0.0491	0.0679	0.0039	0.29	19.44	11.38	415.1	33.1	423.3	23.3
de19a18	0.6101	0.0323	0.0644	0.0020	0.29	10.58	6.19	483.6	20.4	402.3	12.1
de19a19	0.4888	0.0203	0.0618	0.0019	0.36	8.31	6.02	404.1	13.9	386.3	11.3
de19a20	0.4712	0.0782	0.0629	0.0043	0.21	33.20	13.79	392.0	54.0	393.4	26.3
de19a21	0.5633	0.0306	0.0720	0.0035	0.44	10.88	9.67	453.7	19.9	448.3	20.9

**Table A4.5b:** LAM-ICP-MS U-Pb data for magmatic zircons from the MPIS diorite (sample JOD25) collected on March 2, 2004.

JOD25	CONCORDIA COLUMNS					2 s %	2 s %	AGES Ma			
spot #	207/235	7/5 err	206/238	6/8 err	Rho	207/235	206/238	7/5 age	1 sigma	6/8 age	1sigma
	I N T E R C E P T V A L U E S										
mr02c03	0.4977	0.0297	0.0659	0.0035	0.7779	11.94	10.61	410.2	20.1	411.7	21.1
mr02c04	0.5169	0.0226	0.0698	0.0022	0.6794	8.73	6.24	423.1	15.1	435.2	13.1
mr02c05	0.5272	0.0233	0.0694	0.0031	0.8487	8.83	8.81	430.0	15.5	432.2	18.4
mr02c06	0.4987	0.0238	0.0689	0.0026	0.7444	9.54	7.55	410.8	16.1	429.5	15.7
mr02c07	0.4966	0.0205	0.0685	0.0023	0.7532	8.27	6.67	409.4	13.9	427.3	13.8
mr02c08	0.6139	0.0466	0.0672	0.0032	0.5848	15.17	9.56	486.0	29.3	419.5	19.4
mr02c09	0.5418	0.0249	0.0667	0.0043	0.8083	9.20	13.02	439.6	16.4	416.2	26.2
mr02c13	0.5004	0.0270	0.0709	0.0019	0.6258	10.80	5.23	412.0	18.3	441.4	11.2
mr02c14	0.5196	0.0257	0.0715	0.0019	0.5445	9.89	5.38	424.9	17.2	445.3	11.6
mr02c16	0.5052	0.0332	0.0688	0.0026	0.5551	13.14	7.49	415.2	22.4	428.8	15.5
mr02c17	0.5354	0.0264	0.0686	0.0022	0.5788	9.87	6.35	435.4	17.5	427.9	13.1
mr02c20	0.5105	0.0242	0.0691	0.0019	0.5851	9.50	5.48	418.8	16.3	430.9	11.4
mr02c21	0.4835	0.1089	0.0687	0.0074	0.6357	45.05	21.55	400.4	74.5	428.4	44.7
mr02c22	0.5110	0.0285	0.0712	0.0019	0.5671	11.16	5.43	419.1	19.2	443.1	11.6
mr02c23	0.4290	0.0493	0.0676	0.0023	0.3848	23.00	6.77	362.5	35.1	421.5	13.8
mr02c24	0.5109	0.0187	0.0690	0.0019	0.6689	7.34	5.61	419.1	12.6	430.0	11.7

**Table A4.5c:** LAM-ICP-MS U-Pb data for magmatic zircons from the Twin Ponds gabbro (sample JOD100) collected on March 1, 2 and 24, 2004.

JOD100	CONCORDIA COLUMNS					2 s %	2 s %	AGES Ma			
spot #	207/235	7/5 err	206/238	6/8 err	Rho	207/235	206/238	7/5 age	1 sigma	6/8 age	1sigma
	I N T E R C E P T V A L U E S										
mr01b04	0.5496	0.0338	0.0674	0.0035	0.8883	12.29	10.51	444.7	22.1	420.3	21.4
mr01b05	0.5522	0.0312	0.0673	0.0031	0.7728	11.31	9.12	446.5	20.4	419.8	18.5
mr01b06	0.5554	0.0331	0.0697	0.0031	0.7809	11.92	8.92	448.6	21.6	434.3	18.7
mr01b07	0.5394	0.0266	0.0676	0.0029	0.7977	9.88	8.59	438.0	17.6	421.7	17.5
mr01b10	0.5539	0.0271	0.0698	0.0022	0.6799	9.78	6.32	447.5	17.7	434.7	13.3
mr01b11	0.5310	0.0239	0.0682	0.0025	0.8165	9.02	7.21	432.5	15.9	425.2	14.8
mr01b12	0.5753	0.0228	0.0719	0.0026	0.8356	7.93	7.24	461.5	14.7	447.3	15.6
mr01b13	0.5548	0.0221	0.0685	0.0026	0.8481	7.95	7.64	448.1	14.4	427.3	15.8
mr01b14	0.5128	0.0284	0.0683	0.0028	0.7959	11.08	8.07	420.4	19.1	425.7	16.6
mr02a10	0.4760	0.0254	0.0661	0.0025	0.7597	10.68	7.47	395.3	17.5	412.8	14.9
mr02a11	0.5261	0.0232	0.0658	0.0027	0.7666	8.83	8.33	429.2	15.4	410.7	16.6
mr02a12	0.5373	0.0360	0.0694	0.0037	0.8186	13.40	10.70	436.6	23.8	432.8	22.4
mr02a14	0.5186	0.0295	0.0663	0.0021	0.5733	11.39	6.45	424.2	19.7	413.6	12.9
mr24a06	0.5978	0.0354	0.0736	0.0025	0.5916	11.86	6.72	475.9	22.5	457.9	14.9
mr24a09	0.5273	0.0226	0.0652	0.0022	0.6638	8.56	6.62	430.0	15.0	407.4	13.1
mr24a14	0.5482	0.0307	0.0670	0.0036	0.7462	11.19	10.79	443.8	20.1	417.8	21.8
mr24a22	0.5257	0.0280	0.0654	0.0036	0.8065	10.65	11.09	428.9	18.6	408.2	21.9
mr24a24	0.5449	0.0458	0.0665	0.0058	0.6527	16.83	17.35	441.6	30.1	415.0	34.9
mr24a27	0.5669	0.0303	0.0642	0.0030	0.6911	10.70	9.33	456.0	19.7	401.0	18.1
mr24a28	0.5180	0.0272	0.0682	0.0028	0.7178	0.0023	8.31	8.06	18.2	425.2	17.1
mr24a29	0.5621	0.0280	0.0677	0.0026	0.6288	0.0029	7.70	9.52	18.2	422.1	15.7



**Table A4.5d:** LAM-ICP-MS U-Pb data for magmatic zircons from the MPIS granite (sample JOD204-17) collected on December 19, 2005.

JOD04-17	CONCORDIA COLUMNS					2 s %	2 s %				
spot #	207/235	7/5 err	206/238	6/8 err	Rho	207/235	206/238	7/5 age	1 sigma	6/8 age	1sigma
	I N T E R C E P T V A L U E S										
de19a25	0.4607	0.0380	0.0602	0.0029	0.29	16.49	9.49	384.8	26.4	376.8	17.4
de19a26	0.4799	0.0362	0.0636	0.0029	0.30	15.09	9.06	398.0	24.8	397.7	17.5
de19a27	0.4841	0.1148	0.0625	0.0080	0.27	47.42	25.61	400.9	78.5	391.0	48.6
de19a28	0.5158	0.0659	0.0653	0.0073	0.44	25.56	22.53	422.3	44.2	407.5	44.5
de19a29	0.4873	0.0253	0.0635	0.0025	0.37	10.37	7.74	403.1	17.3	396.7	14.9
de19a30	0.5411	0.0811	0.0699	0.0031	0.15	29.96	9.00	439.2	53.4	435.7	19.0
de19a31	0.4982	0.0292	0.0631	0.0027	0.37	11.72	8.68	410.5	19.8	394.5	16.6
de19a34	0.5497	0.0143	0.0676	0.0019	0.55	5.22	5.75	444.8	9.4	421.9	11.7
de19a35	0.4228	0.0552	0.0634	0.0028	0.17	26.10	8.86	358.1	39.4	396.4	17.0
de19a36	0.6185	0.1403	0.0690	0.0031	0.10	45.35	8.99	488.9	88.0	430.2	18.7
de19a37	5.1303	0.1571	0.3020	0.0115	0.62	6.12	7.59	1841.1	26.0	1701.4	56.8
de19a38	0.4774	0.0260	0.0634	0.0025	0.35	10.90	7.74	396.3	17.9	396.0	14.9
de19a39	0.6077	0.0480	0.0763	0.0040	0.33	15.78	10.47	482.1	30.3	474.0	23.9
de19a40	0.6680	0.0339	0.0653	0.0032	0.49	10.14	9.91	519.5	20.6	407.7	19.6
de19a41	0.5152	0.0235	0.0633	0.0023	0.40	9.10	7.25	422.0	15.7	395.6	13.9



**Table A4.5e:** LAM-ICP-MS U-Pb data for magmatic zircons from the MPIS granite (sample JOD90A) collected on March 2, 2004.

JOD90A	CONCORDIA COLUMNS					2 s %	2 s %	AGES Ma							
spot #	207/235	7/5 err	206/238	6/8 err	Rho	207/235	206/238	7/5 age	1 sigma	6/8 age	1sigma				
	I	N	T	E	R	C	E	P	T	V	A	L	U	E	S
mr02d07	0.5992	0.0877	0.0616	0.0039	0.7181	29.26	12.78	476.7	55.7	385.6	23.9				
mr02d08	0.5464	0.0941	0.0625	0.0036	0.3664	34.45	11.64	442.6	61.8	390.9	22.1				
mr02d11	0.5354	0.0815	0.0615	0.0038	0.6136	30.44	12.47	435.4	53.9	384.8	23.3				
mr02d19	0.5697	0.1239	0.0637	0.0060	0.7836	43.48	18.77	457.9	80.1	398.2	36.2				
mr02d20	0.6291	0.0821	0.0656	0.0021	0.2807	26.10	6.42	495.5	51.2	409.8	12.7				
mr02d21	0.6278	0.1221	0.0607	0.0056	0.3032	38.89	18.62	494.7	76.1	379.7	34.3				
mr02d25	0.5371	0.0469	0.0605	0.0022	0.4339	17.46	7.31	436.5	31.0	378.9	13.5				
mr02d26	0.4683	0.0572	0.0572	0.0025	0.5855	24.44	8.65	390.0	39.6	358.3	15.1				

**Table A4.5f:** : LAM-ICP-MS U-Pb data for magmatic zircons from the Charles Cove granodiorite (sample W03-27) collected on March 24, 2004.

W03-27	CONCORDIA COLUMNS					2 s %	2 s %	AGES Ma							
spot #	207/235	7/5 err	206/238	6/8 err	Rho	207/235	206/238	7/5 age	<sup>1</sup> sigma	6/8 age	1sigma				
	I	N	T	E	R	C	E	P	T	V	A	L	U	E	S
mr24a06	0.5978	0.0354	0.0736	0.0025	0.5916	11.86	6.72	475.9	22.5	457.9	14.9				
mr24a09	0.5273	0.0226	0.0652	0.0022	0.6638	8.56	6.62	430.0	15.0	407.4	13.1				
mr24a14	0.5482	0.0307	0.0670	0.0036	0.7462	11.19	10.79	443.8	20.1	417.8	21.8				
mr24a22	0.5257	0.0280	0.0654	0.0036	0.8065	10.65	11.09	428.9	18.6	408.2	21.9				
mr24a24	0.5449	0.0458	0.0665	0.0058	0.6527	16.83	17.35	441.6	30.1	415.0	34.9				
mr24a27	0.5669	0.0303	0.0642	0.0030	0.6911	10.70	9.33	456.0	19.7	401.0	18.1				
mr24a28	0.5180	0.0272	0.0682	0.0028	0.7178	10.52	8.31	423.8	18.2	425.2	17.1				
mr24a29	0.5621	0.0280	0.0677	0.0026	0.6288	9.96	7.70	452.9	18.2	422.1	15.7				

**Table A4.5g:** LAM-ICP-MS U-Pb data for magmatic zircons from the Huxter Lane dacite (sample W03-38) collected on February 20, 2004.

W03-38	CONCORDIA COLUMNS					2 s %	2 s %	AGES Ma			
spot #	207/235	7/5 err	206/238	6/8 err	Rho	207/235	206/238	7/5 age	1 sigma	6/8 age	1sigma
	I N T E R C E P T V A L U E S										
fe20a12 1	0.6387	0.0780	0.0753	0.0087	0.8549	24.42	23.21	14.08	501.5	48.3	467.7
fe20a05 1	0.6658	0.0710	0.0827	0.0068	0.7701	21.33	16.54	13.70	518.1	43.3	512.0
fe20a06 1	0.5632	0.0848	0.0792	0.0054	0.6206	30.12	13.58	17.16	453.6	55.1	491.5
fe20a09 1	0.5835	0.0576	0.0802	0.0024	0.3553	19.74	5.89	15.49	466.7	36.9	497.3
fe20a13 1	0.5209	0.2165	0.0795	0.0095	0.4328	83.10	23.96	49.90	425.8	144.5	493.3
fe20a16 1	0.5666	0.0746	0.0815	0.0034	0.4578	26.32	8.38	16.28	455.8	48.3	505.2
fe20a17 1	0.5492	0.1205	0.0793	0.0083	0.6751	43.88	20.87	22.81	444.4	79.0	492.2
fe20a24 1	0.5898	0.0340	0.0740	0.0023	0.5143	11.53	6.24	10.40	470.8	21.7	460.5
fe20a25 1	0.7521	0.1350	0.0834	0.0115	0.9534	35.91	27.46	8.69	569.4	78.3	516.5
fe20a27 1	0.6315	0.0475	0.0852	0.0025	0.3112	15.04	5.89	18.00	497.0	29.6	527.2

**Table A4.5h:** LAM-ICP-MS U-Pb data for magmatic zircons from the Bellman's Pond Conglomerate clast (sample JOD08) collected on February 25, 2004.

JOD08	CONCORDIA COLUMNS					2 s %	2 s %	AGES Ma			
spot #	207/235	7/5 err	206/238	6/8 err	Rho	207/235	206/238	7/5 age	1 sigma	6/8 age	1sigma
	I N T E R C E P T V A L U E S										
fe25a06	3.7351	0.2340	0.2919	0.0198	0.8995	12.53	13.54	1578.9	50.2	1650.8	98.6
fe25a07	4.1437	0.2597	0.2621	0.0130	0.6475	12.53	9.89	1663.0	51.3	1500.5	66.2
fe25a08	4.0866	0.1721	0.3007	0.0102	0.9424	8.42	6.77	1651.6	34.4	1695.0	50.5
fe25a09	4.7549	0.2047	0.3241	0.0132	0.7909	8.61	8.12	1777.0	36.1	1809.8	64.1



**Table A4.5i:** LAM-ICP-MS U-Pb data for detrital zircons from the Davidsville Group (sample JOD39) collected on February 20, 23 and March 23, 2004.

JOD39	CONCORDIA COLUMNS					2 s %	2 s %	AGES Ma			
spot #	207/235	7/5 err	206/238	6/8 err	Rho	207/235	206/238	7/5 age	1 sigma	6/8 age	1sigma
	I N T E R C E P T V A L U E S										
mr23a09	0.5932	0.0394	0.0711	0.0067	0.8239	13.29	18.93	472.9	25.1	442.6	40.5
mr23a12	0.5924	0.0933	0.0667	0.0063	0.6553	31.50	18.76	472.4	59.5	416.0	37.8
mr23a13	0.5727	0.0360	0.0731	0.0039	0.6702	12.57	10.81	459.8	23.2	454.6	23.7
fe23a07	0.4744	0.2602	0.0658	0.0182	0.9287	109.69	55.33	394.2	179.2	410.9	110.1
fe23a09	0.6569	0.0773	0.0844	0.0072	0.5394	23.53	17.01	512.7	47.4	522.3	42.7
fe23a10	0.5808	0.0378	0.0747	0.0033	0.6249	13.03	8.95	465.0	24.3	464.3	20.0
fe23a11	0.5745	0.0318	0.0711	0.0047	0.9004	11.08	13.11	460.9	20.5	442.8	28.1
fe20b04	0.7828	0.0926	0.0778	0.0097	0.9020	23.65	24.83	587.1	52.7	483.2	57.8
fe20b05	0.6711	0.0511	0.0687	0.0052	0.8753	15.23	15.14	521.4	31.1	428.3	31.4
fe20b07	0.5511	0.0418	0.0761	0.0027	0.5598	15.17	7.06	445.7	27.4	472.8	16.1
fe20b11	0.6203	0.0221	0.0697	0.0034	0.8133	7.12	9.86	490.0	13.8	434.2	20.7
fe20b12	0.7434	0.0459	0.0778	0.0055	0.6391	12.35	14.12	564.4	26.7	483.3	32.9
fe20b13	0.7302	0.0648	0.0770	0.0028	0.3843	17.76	7.31	556.6	38.1	478.3	16.8
fe20b15	1.3652	0.3223	0.1541	0.0230	0.9501	47.22	29.90	874.1	138.4	923.8	128.7
fe20b19	0.6195	0.0334	0.0648	0.0048	0.8716	10.80	14.76	489.6	21.0	404.5	28.9
fe20b20	0.7883	0.2522	0.0764	0.0145	0.9491	63.98	37.91	590.2	143.2	474.5	86.7

**Table A4.6a:** LAM-ICP-MS U-Pb data for zircon standard samples 91500 and Kosler obtained on December 19, 2005\*.

SAMPLE			CONCORDIA COLUMNS					2 s %	2 s %	AGES Ma			
spot #	Standard	file	207/235	7/5 err	206/238	6/8 err	Rho	207/235	206/238	7/5 age	1 sigma	6/8 age	1sigma
I N T E R C E P T V A L U E S													
1	Kosler	de19a03	0.4026	0.0181	0.0550	0.0015	0.31	9.01	5.50	343.5	13.1	344.9	9.2
2	Kosler	de19a04	0.3882	0.0156	0.0546	0.0016	0.36	8.06	5.78	333.1	11.4	342.7	9.6
3	Kosler	de19a13	0.3968	0.0178	0.0536	0.0018	0.37	8.97	6.65	339.3	12.9	336.5	10.9
4	Kosler	de19a33	0.3706	0.0214	0.0528	0.0017	0.28	11.56	6.44	320.1	15.9	331.7	10.4
5	Kosler	de19a45	0.3937	0.0146	0.0533	0.0019	0.47	7.43	7.02	337.1	10.7	334.5	11.4
6	Kosler	de20a01	0.3945	0.0180	0.0548	0.0021	0.41	9.11	7.54	337.6	13.1	343.8	12.6
7	Kosler	de20a02	0.4087	0.0188	0.0466	0.0022	0.50	9.22	9.28	347.9	13.6	293.8	13.3
8	Kosler	de20a11	0.4204	0.0430	0.0530	0.0039	0.36	20.46	14.60	356.3	30.7	332.6	23.7
9	Kosler	de20a22	0.4058	0.0138	0.0543	0.0019	0.51	6.80	6.93	345.9	10.0	341.0	11.5
10	Kosler	de20a29	0.4231	0.0146	0.0552	0.0015	0.38	6.88	5.29	358.3	10.4	346.2	8.9
1	91500	de19a01	1.8603	0.0972	0.1796	0.0057	0.31	10.45	6.40	1067.1	34.5	1064.9	31.4
2	91500	de19a12	1.7930	0.1702	0.1792	0.0081	0.24	18.99	9.09	1042.9	61.9	1062.4	44.5
3	91500	de19a23	1.8233	0.0985	0.1802	0.0053	0.27	10.80	5.84	1053.9	35.4	1067.9	28.8
4	91500	de19a32	1.8726	0.0889	0.1784	0.0060	0.35	9.49	6.70	1071.4	31.4	1058.1	32.7
5	91500	de19a42	1.8705	0.2268	0.1810	0.0092	0.21	24.25	10.14	1070.7	80.2	1072.5	50.1
6	91500	de20a03	1.9506	0.1234	0.1850	0.0053	0.23	12.65	5.73	1098.6	42.5	1094.5	28.8
7	91500	de20a04	1.9464	0.2567	0.1796	0.0128	0.27	26.38	14.23	1097.2	88.5	1064.9	69.8
8	91500	de20a12	1.8200	0.1013	0.1786	0.0071	0.36	11.13	8.01	1052.7	36.5	1059.2	39.1
9	91500	de20a21	1.8131	0.1321	0.1837	0.0061	0.23	14.57	6.62	1050.2	47.7	1087.0	33.1
10	91500	de20a23	1.8818	0.1077	0.1777	0.0047	0.23	11.45	5.26	1074.7	37.9	1054.5	25.6
11	91500	de20a30	1.7747	0.1173	0.1759	0.0069	0.30	13.22	7.85	1036.2	42.9	1044.5	37.9
12	91500	de20a30	1.8161	0.1330	0.1770	0.0075	0.29	14.65	8.45	1051.3	48.0	1050.5	40.9

**Table A4.6b:** LAM-ICP-MS U-Pb data for zircon standard samples 02123, Kosler and 91500 obtained on February 20, 2004\*\*.

SAMPLE			CONCORDIA COLUMNS					2 s %	2 s %	AGES Ma			
spot #	Standard	file	207/235	7/5 err	206/238	6/8 err	Rho	207/235	206/238	7/5 age	1 sigma	6/8 age	1sigma
I N T E R C E P T V A L U E S													
1	02123	fe20a04	0.3370	0.0160	0.0481	0.0022	0.6977	7.84	9.09	294.9	11.5	303.1	13.5
2	02123	fe20a11	0.3295	0.0169	0.0461	0.0017	0.6282	9.14	7.28	289.2	12.5	290.4	10.3
3	02123	fe20a20	0.3335	0.0212	0.0476	0.0014	0.4740	11.34	5.81	292.2	15.7	299.9	8.5
4	02123	fe20a21	0.3471	0.0397	0.0426	0.0020	0.4676	17.78	9.47	302.5	27.9	269.2	12.5
5	02123	fe20a22	0.3322	0.0129	0.0437	0.0012	0.4850	9.15	5.61	291.2	10.2	275.8	7.6
6	02123	fe20b10	0.3548	0.0174	0.0479	0.0019	0.6794	9.79	7.85	308.3	13.0	301.4	11.6
7	02123	fe20b18	0.3581	0.0166	0.0469	0.0016	0.6294	9.27	6.74	310.8	12.4	295.3	9.7
1	Kosler	fe20b03	0.3952	0.0238	0.0496	0.0051	0.7226	12.04	20.75	338.1	17.3	312.0	31.6
1	91500	fe20a01	1.9615	0.4101	0.1800	0.0102	0.3110	41.82	11.34	1102.4	140.6	1066.7	55.7
2	91500	fe20a02	1.7473	0.0910	0.1755	0.0064	0.7061	10.42	7.31	1026.2	33.6	1042.2	35.2
3	91500	fe20a03	1.8789	0.0756	0.1742	0.0052	0.5869	8.05	5.93	1073.7	26.7	1035.3	28.4
4	91500	fe20a10	1.8460	0.0619	0.1725	0.0046	0.6263	6.71	5.36	1062.0	22.1	1025.8	25.4
5	91500	fe20a19	1.8773	0.0957	0.1735	0.0101	0.6918	10.20	11.63	1073.1	33.8	1031.6	55.4
6	91500	fe20a23	2.0052	0.1841	0.1794	0.0066	0.4355	18.36	7.33	1117.3	62.2	1063.8	36.0
7	91500	fe20a29	2.0054	0.0965	0.1849	0.0080	0.8557	9.62	8.65	1117.3	32.6	1093.9	43.5
8	91500	fe20b01	1.7816	0.0839	0.1785	0.0076	0.7665	9.98	8.50	1038.8	31.8	1058.8	41.5
9	91500	fe20b02	1.8339	0.1260	0.1857	0.0060	0.4884	13.74	6.51	1057.7	45.2	1097.9	32.9
10	91500	fe20b09	1.8490	0.1200	0.1902	0.0140	0.8520	12.98	14.73	1063.1	42.8	1122.5	75.9
11	91500	fe20b17	1.8906	0.0837	0.1693	0.0065	0.6235	8.86	7.69	1077.8	29.4	1008.2	35.9

**Table A4.6c:** LAM-ICP-MS U-Pb data for zircon standard samples 02123, Kosler and 91500 obtained on February 25, 2004\*\*.

SAMPLE			CONCORDIA COLUMNS					2 s %	2 s %	AGES Ma			
spot #	Standard	file	207/235	7/5 err	206/238	6/8 err	Rho	207/235	206/238	7/5 age	1 sigma	6/8 age	1sigma
I N T E R C E P T V A L U E S													
1	02123	fe25a04	0.3522	0.0166	0.0483	0.0018	0.6147	9.41	7.62	306.4	12.4	303.8	11.3
2	02123	fe25a05	0.3690	0.0203	0.0477	0.0022	0.6782	10.98	9.06	318.9	15.0	300.3	13.3
3	02123	fe25a14	0.3210	0.0208	0.0443	0.0022	0.47	12.94	10.14	282.7	16.0	279.5	13.9
4	02123	fe25a15	0.3549	0.0227	0.0448	0.0028	0.38	12.82	12.58	308.4	17.0	282.4	17.4
1	Kosler	fe25a06	0.3781	0.0181	0.0485	0.0018	0.5662	9.55	7.33	325.6	13.3	305.3	10.9
1	91500	fe25a01	1.8477	0.0844	0.1820	0.0082	0.7008	9.14	9.05	1062.6	30.1	1077.8	44.9
2	91500	fe25a02	1.8464	0.0817	0.1760	0.0050	0.5536	10.60	5.68	1062.1	32.6	1045.0	27.4
3	91500	fe25a03	1.8793	0.0662	0.1753	0.0050	0.6600	7.45	5.75	1037.9	24.2	1041.3	27.6
4	91500	fe25a11	1.9499	0.1810	0.1788	0.0161	0.53	18.57	18.03	1098.4	62.3	1060.5	88.2
5	91500	fe25a13	1.8432	0.1408	0.1782	0.0096	0.64	16.16	10.78	1024.6	52.1	1056.9	52.6
6	91500	fe25a21	1.8228	0.0784	0.1646	0.0066	0.44	8.60	7.98	1053.7	28.2	982.5	36.4



**Table A4.6d:** LAM-ICP-MS U-Pb data for zircon standard samples 02123, 91500 and Kosler obtained on March 24, 2004\*\*.

SAMPLE			CONCORDIA COLUMNS					2 s %	2 s %	AGES Ma			
spot #	Standard	file	207/235	7/5 err	206/238	6/8 err	Rho	207/235	206/238	7/5 age	1 sigma	6/8 age	1sigma
I N T E R C E P T V A L U E S													
1	02123	mr24b11	0.3521	0.0370	0.0512	0.0027	0.6697	20.99	10.53	306.3	27.8	321.7	16.5
1	Kosler	mr24b03	0.4065	0.0179	0.0535	0.0021	0.7098	8.82	7.77	346.3	12.9	336.2	12.7
2	Kosler	mr24b18	0.4039	0.0172	0.0528	0.0018	0.6374	8.54	6.99	344.4	12.5	331.8	11.3
3	Kosler	mr24b25	0.3704	0.0219	0.0519	0.0017	0.6134	11.84	6.39	319.9	16.2	326.4	10.2
4	Kosler	mr24b32	0.4260	0.0179	0.0531	0.0019	0.6702	8.40	7.28	360.3	12.7	333.7	11.8
5	Kosler	mr24b39	0.3947	0.0189	0.0530	0.0017	0.6477	9.58	6.47	337.8	13.8	333.2	10.5
1	91500	mr24b02	1.8548	0.1021	0.1740	0.0109	0.7671	11.00	12.53	1065.2	36.3	1034.1	59.8
2	91500	mr24b17	1.8146	0.1397	0.1836	0.0082	0.5141	16.94	8.89	1050.7	53.5	1086.8	44.5
3	91500	mr24b24	1.8724	0.0961	0.1796	0.0082	0.6099	11.50	9.09	1071.4	36.5	1064.9	44.6
4	91500	mr24b31	1.9338	0.1209	0.1851	0.0075	0.5801	12.51	8.08	1092.9	41.9	1095.0	40.7
5	91500	mr24b38	1.8628	0.1375	0.1722	0.0082	0.6391	14.76	9.50	1068.0	48.8	1024.0	45.0

Calculated TIMS ages for the zircon standards are as follows:

02123: 295 Ma

91500: 1065 Ma

Kosler: 337 Ma

\*Weighted averages for standards for December 2005 analyses are as follows:

91500:  $1065 \pm 8.8$  Ma

Kosler:  $339 \pm 3.1$  Ma

\*\* Weighted averages for standards for February and March 2004 analyses are as follows:

02123:  $293.4 \pm 3.1$  Ma

91500:  $1061 \pm 6.7$  Ma

Kosler:  $331.8 \pm 4.3$  Ma





